INTERNATIONAL REVIEW OF CELL AND MOLECULAR BIOLOGY

Edited by
Kwang W. Jeon

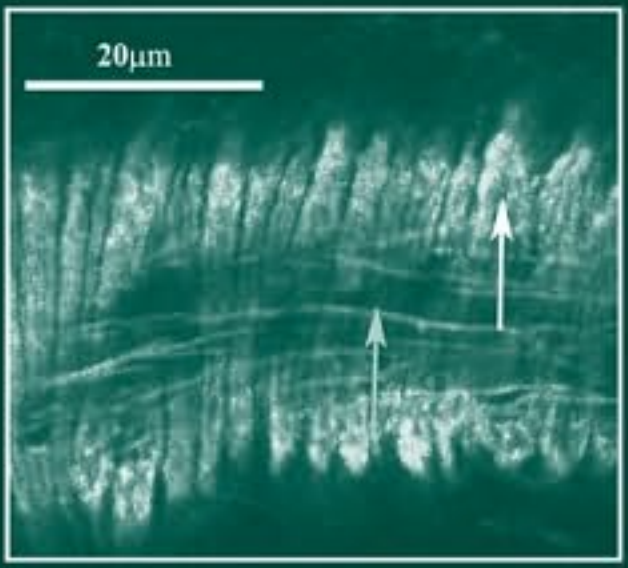

Volume 278

VOLUME TWO SEVENTY EIGHT

International Review of CELL AND MOLECULAR BIOLOGY

INTERNATIONAL REVIEW OF CELL AND MOLECULAR BIOLOGY

Series Editors

GEOFFREY H. BOURNE *1949–1988*
JAMES F. DANIELLI *1949–1984*
KWANG W. JEON *1967–*
MARTIN FRIEDLANDER *1984–1992*
JONATHAN JARVIK *1993–1995*

Editorial Advisory Board

ISAIAH ARKIN
PETER L. BEECH
ROBERT A. BLOODGOOD
DEAN BOK
KEITH BURRIDGE
HIROO FUKUDA
RAY H. GAVIN
MAY GRIFFITH
WILLIAM R. JEFFERY
KEITH LATHAM
WALLACE F. MARSHALL
BRUCE D. MCKEE
MICHAEL MELKONIAN
KEITH E. MOSTOV
ANDREAS OKSCHE
MANFRED SCHLIWA
TERUO SHIMMEN
ROBERT A. SMITH

VOLUME TWO SEVENTY EIGHT

International Review of CELL AND MOLECULAR BIOLOGY

EDITED BY

KWANG W. JEON
Department of Biochemistry
University of Tennessee
Knoxville, Tennessee

ELSEVIER

AMSTERDAM • BOSTON • HEIDELBERG • LONDON
NEW YORK • OXFORD • PARIS • SAN DIEGO
SAN FRANCISCO • SINGAPORE • SYDNEY • TOKYO
Academic Press is an imprint of Elsevier

Front Cover Photography: Cover figure by Brant Isakson

Academic Press is an imprint of Elsevier
525 B Street, Suite 1900, San Diego, CA 92101-4495, USA
30 Corporate Drive, Suite 400, Burlington, MA 01803, USA
32 Jamestown Road, London NW1 7BY, UK
Radarweg 29, PO Box 211, 1000 AE Amsterdam, The Netherlands

First edition 2009

Copyright © 2009, Elsevier Inc. All Rights Reserved.

No part of this publication may be reproduced, stored in a retrieval system or transmitted in any form or by any means electronic, mechanical, photocopying, recording or otherwise without the prior written permission of the publisher

Permissions may be sought directly from Elsevier's Science & Technology Rights Department in Oxford, UK: phone (+44) (0) 1865 843830; fax (+44) (0) 1865 853333; email: permissions@elsevier.com. Alternatively you can submit your request online by visiting the Elsevier web site at http://elsevier.com/locate/permissions, and selecting *Obtaining permission to use Elsevier material*.

Notice
No responsibility is assumed by the publisher for any injury and/or damage to persons or property as a matter of products liability, negligence or otherwise, or from any use or operation of any methods, products, instructions or ideas contained in the material herein. Because of rapid advances in the medical sciences, in particular, independent verification of diagnoses and drug dosages should be made.

British Library Cataloguing in Publication Data
A catalogue record for this book is available from the British Library

Library of Congress Cataloging-in-Publication Data
A catalog record for this book is available from the Library of Congress

For information on all Academic Press publications
visit our website at elsevierdirect.com

ISBN: 978-0-12-374809-6

PRINTED AND BOUND IN USA
09 10 11 12 10 9 8 7 6 5 4 3 2 1

Working together to grow
libraries in developing countries
www.elsevier.com | www.bookaid.org | www.sabre.org
ELSEVIER BOOK AID International Sabre Foundation

Contents

Contributors *ix*

1. Macromolecular Trafficking and Immune Evasion in African Trypanosomes **1**
Mark C. Field, Jennifer H. Lumb, Vincent O. Adung'a, Nicola G. Jones, and Markus Engstler

1. General Overview of the Trypanosome Life Cycle 3
2. Immune Evasion Mechanisms 5
3. Endocytic Pathways 16
4. Developmental Remodeling and Signaling 27
5. Sorting Signals 28
6. Secretory Protein Folding and Exocytosis 32
7. Golgi Apparatus; Functions and Replication 39
8. Ubiquitylation and Endocytosis of *Trans*-Membrane Domain Proteins 42
9. Evolution of the Trypanosome Endomembrane System 46
10. Conclusions and Future Perspectives 50

Acknowledgments 51
References 52

2. Biological and Biophysical Properties of Vascular Connexin Channels **69**
Scott Johnstone, Brant Isakson, and Darren Locke

1. Introduction 71
2. The Vasculature 72
3. Connexin Channels 75
4. Gap Junctional Communication Pathways in the Vasculature 82
5. Permeability of Vascular Connexin Channels 87
6. Involvement of Connexins in Vascular Diseases 101
7. Concluding Remarks 104

Acknowledgments 105
References 105

3. Genotype–Phenotype Mapping: Developmental Biology Confronts the Toolkit Paradox **119**
Joel Atallah and Ellen Larsen

1. Introduction 120
2. Understanding the Genotype–Phenotype Relationship 121
3. From Sequence to Form 125
4. Beyond Sequence 135
5. Case Study for Parsing Gene, Cell and Self-Organizing Roles in Morphogenesis 138
6. Conclusion 142

Acknowledgments 142
References 142

4. Role of Spindle Asymmetry in Cellular Dynamics **149**
Yves Barral and Dimitris Liakopoulos

1. Introduction 150
2. Spindle Asymmetry and Control of Cell Cycle 152
3. Spindle Asymmetry During Asymmetric Cell Divisions 174
4. Concluding Remarks 201

References 203

5. Cell Adhesion in Amphibian Gastrulation **215**
Rudolf Winklbauer

1. Introduction 216
2. Characteristics of Amphibian Gastrulation 217
3. Gastrula Tissue as a Liquid: Cell Adhesion, Cell Sorting, Boundary Formation, and Tissue Positioning 223
4. Collective Cell Migration, Cell Rearrangement, and Intercellular Migration 249
5. Conclusion 260

Acknowledgments 261
References 261

6. Molecular and Cell Biology of Testicular Germ Cell Tumors **277**
Paolo Chieffi, Renato Franco, and Giuseppe Portella

1. Introduction 278
2. Epidemiology and Risk Factors 279
3. Histopathology 280
4. Prognostic and Diagnostic Markers 294

5. Therapy 297
6. Conclusions and Perspectives 301
Acknowledgments 301
References 302

7. Polarity Proteins and Cell–Cell Interactions in the Testis 309
Elissa W.P. Wong and C. Yan Cheng

1. Introduction 310
2. Rho GTPases and Cell–Cell Interactions in the Testis: Cdc42 315
3. Polarity Proteins and Cell–Cell Interactions in the Testis 327
4. The Apical ES-BTB-Basement Membrane Functional Axis in the Seminiferous Epithelium that Coordinates the Cellular Events of Spermiation and BTB Restructuring During the Seminiferous Epithelial Cycle of Spermatogenesis: The Role of Polarity Proteins in Mediating the Apical ES-BTB-Basement Membrane Axis 335
5. Roles of Polarity Proteins in Coordinating the Opposing Effects of Cytokines and Testosterone in Primary Preleptotene Spermatocyte Transit at the BTB 339
6. Concluding Remarks and Future Perspectives 341

Acknowledgment 342
References 342

Index *355*

Contributors

Vincent O. Adung'a
Department of Pathology, University of Cambridge, Cambridge CB2 1QT, United Kingdom

Joel Atallah
Department of Cell and Systems Biology, University of Toronto, Toronto, Ontario M5S 3G5, Canada

Yves Barral
Institute of Biochemistry, ETH Hönggerberg, HPM, CH-8093 Zurich, Switzerland

C. Yan Cheng
Mary M. Wohlford Laboratory for Male Contraceptive Research, Center for Biomedical Research, Population Council, New York, New York 10065, USA

Paolo Chieffi
Dipartimento di Medicina Sperimentale, II Università di Napoli, 80138 Naples, Italy

Markus Engstler
Lehrstuhl für Zell- und Entwicklungsbiologie, Biozentrum der Universitaet Wuerzburg, Am Hubland, 97074 Wuerzburg, Germany

Mark C. Field
Department of Pathology, University of Cambridge, Cambridge CB2 1QT, United Kingdom

Renato Franco
Area Funzionale di Anatomia Patologica, Istituto Nazionale dei Tumori "Fondazione G. Pascale," 80131 Naples, Italy

Brant Isakson
Robert M. Berne Cardiovascular Research Center, University of Virginia School of Medicine, Charlottesville, Virginia 29908, USA; and Department of Molecular Physiology and Biological Physics, University of Virginia School of Medicine, Charlottesville, Virginia 29908, USA

Scott Johnstone
Robert M. Berne Cardiovascular Research Center, University of Virginia School of Medicine, Charlottesville, Virginia 29908, USA

Nicola G. Jones
Lehrstuhl für Zell- und Entwicklungsbiologie, Biozentrum der Universitaet Wuerzburg, Am Hubland, 97074 Wuerzburg, Germany

Ellen Larsen
Department of Cell and Systems Biology, University of Toronto, Toronto, Ontario M5S 3G5, Canada

Dimitris Liakopoulos
Biochemie Zentrum Heidelberg, Im Neuenheimer Feld 328, D-69120 Heidelberg, Germany

Darren Locke
Department of Pharmacology and Physiology, New Jersey Medical School, University of Medicine and Dentistry of New Jersey, Newark, New Jersey 07103, USA

Jennifer H. Lumb
Department of Pathology, University of Cambridge, Cambridge CB2 1QT, United Kingdom

Giuseppe Portella
Dipartimento di Biologia e Patologia Cellulare e Molecolare, Università di Napoli "Federico II," 80131 Naples, Italy

Rudolf Winklbauer
Department of Cell and Systems Biology, University of Toronto, Toronto, Ontario M5S 3G5, Canada

Elissa W.P. Wong
Mary M. Wohlford Laboratory for Male Contraceptive Research, Center for Biomedical Research, Population Council, New York, New York 10065, USA

CHAPTER ONE

Macromolecular Trafficking and Immune Evasion in African Trypanosomes

Mark C. Field,* Jennifer H. Lumb,* Vincent O. Adung'a,* Nicola G. Jones,† *and* Markus Engstler†

Contents

1. General Overview of the Trypanosome Life Cycle 3
2. Immune Evasion Mechanisms 5
   2.1. VSG and antigenic variation 5
   2.2. Membrane dynamics and antibody clearance 7
   2.3. Cellular immune responses 11
   2.4. Innate immunity 13
3. Endocytic Pathways 16
   3.1. Clathrin-mediated endocytosis 16
   3.2. Cargo adaptors and sorting 18
   3.3. Early and recycling endocytic compartments 20
   3.4. Multivesicular bodies and late endocytosis 21
   3.5. Lysosome 22
   3.6. Involvement of the cytoskeleton in endocytosis 24
   3.7. Complexity of endsomal sorting 25
   3.8. Surface receptors and endocytic pathways 25
4. Developmental Remodeling and Signaling 27
5. Sorting Signals 28
   5.1. Targeting at the ER 28
   5.2. Endocytic and lysosomal targeting signals 29
   5.3. Endomembrane sorting based on posttranslational modification 30
   5.4. Sorting to the flagellum 30
   5.5. Sorting to the glycosome 31

* Department of Pathology, University of Cambridge, Cambridge CB2 1QT, United Kingdom
† Lehrstuhl für Zell- und Entwicklungsbiologie, Biozentrum der Universitaet Wuerzburg, Am Hubland, 97074 Wuerzburg, Germany

International Review of Cell and Molecular Biology, Volume 278
ISSN 1937-6448, DOI: 10.1016/S1937-6448(09)78001-3
© 2009 Elsevier Inc.
All rights reserved.

6. Secretory Protein Folding and Exocytosis 32
6.1. Membrane protein biosynthesis 32
6.2. Polypeptide delivery 32
6.3. Polypeptide folding and maturation 35
6.4. ER exit to the Golgi complex or ER-associated degradation (ERAD) 37
7. Golgi Apparatus; Functions and Replication 39
7.1. Golgi replication by binary fission 39
7.2. Role of the cytoskeleton in Golgi complex replication 40
7.3. Cell-cycle and life-cycle coordination of Golgi complex replication and function 41
7.4. Retrograde transport 42
8. Ubiquitylation and Endocytosis of *Trans*-Membrane Domain Proteins 42
8.1. The VSG sorting problem 42
8.2. Ubiquitylation and endocytosis 43
8.3. ISGs are ubiquitylated 44
8.4. Late endocytosis and the multivesicular body 45
9. Evolution of the Trypanosome Endomembrane System 46
9.1. Changing views of the eukaryotic tree of life 46
9.2. Comparative genomics 47
9.3. G-protein signaling complexity and evolution 48
9.4. Convergent evolution 49
9.5. Evolutionary exploitation of the flagellar pocket 49
10. Conclusions and Future Perspectives 50
Acknowledgments 51
References 52

Abstract

Intracellular trafficking is a major mechanism contributing to maintenance of the surface composition in most eukaryotic cells. In the case of unicellular eukaryotic pathogens, the surface also represents the host–parasite interface. Therefore, the parasite surface is both a critical player in immune recognition, from the host's point of view, or in immune evasion, from the pathogen's point. The African trypanosomes are remarkable in dwelling throughout their period in the mammalian host within the bloodstream and tissue spaces, and have evolved several mechanisms that facilitate chronic infection. Here, we discuss current understanding of intracellular trafficking pathways of trypanosomes, and relate these processes to immune evasion strategies by the parasite and avoidance of immune responses from the host.

Key Words: Antigenic variation, Immune evasion, Intracellular trafficking, Protein sorting, Trypanosome. © 2009 Elsevier Inc.

1. General Overview of the Trypanosome Life Cycle

The lifestyle of *Trypanosoma brucei,* the African trypanosome, is venturesome, and unlike the vast majority of endoparasites, has exploited mechanisms allowing survival without sequestration within host cells. While thriving in the body fluids of vertebrate hosts, the parasites are continuously attacked by the immune system and also endure harsh physicomechanical conditions that prevail in the mammalian circulation.

The mammalian host is infected when a tsetse fly carrying trypanosomes (*Glossina* spp.) takes a blood meal (Vickerman, 1985; Vickerman et al., 1988) (Fig. 1.1). The insect's bite inoculates the parasites into the host's subcutaneous tissue, where they rapidly proliferate. Metabolic products, or other undefined factors, cause local inflammation of the skin at the bite site, producing a so-called chancre, which is the first sign of infection. From here, rapidly dividing cells enter the draining lymphatic system and are

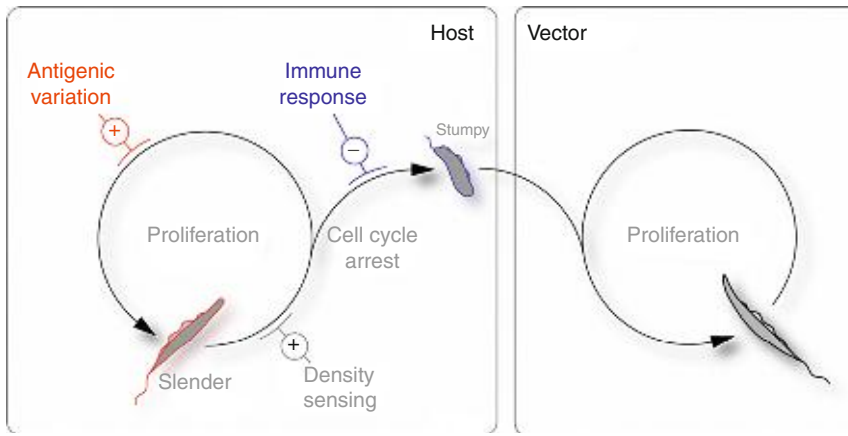

Figure 1.1 Partial life cycle of trypanosomes, emphasizing the transition from the mammalian host to the insect vector. Left box (host): Proliferative slender forms (gray) survive within the host bloodstream, lymphatics, and issue spaces. These cells exhibit antigenic variation as the primary route to immune evasion, facilitating chronic infection. Additionally, a density sensing mechanism, mediated by stumpy induction factor, causes the slender forms to exit from the cell cycle, preventing overgrowth of the host by excessively high parasite numbers. Cell cycle exit is accompanied by morphological changes, resulting in the stumpy form, as well as additional underlying metabolic and proteome changes, preadapting the parasite to life in the tsetse fly. These cells are sensitive to immune killing and do not exhibit antigenic variation. Right box (vector): On entry to the tsetse midgut, stumpy form parasites reenter the cell cycle and begin to proliferate. A fuller version of the parasite life cycle is detailed in Vickerman (1969).

flushed into the circulation. An early symptom of infection is enlarged cervical lymph nodes of the neck, the Winterbottom's sign, but both of these symptoms fade rapidly and have limited diagnostic use (Ormerod, 1991).

The parasites are well prepared for life in the mammalian host. The quiescent, nondividing metacyclic stage, which awaits transmission in the insect salivary glands, expresses a special version of the most conspicuous weapon that trypanosomes have evolved to defend against host attack: A dense layer of a single protein species, the variant surface glycoprotein (VSG), shields the entire cell surface (Pays, 2006). In the skin tissue, following injection the metacyclic trypanosomes reenter the cell cycle and proliferate as long slender trypomastigotes (Fenn and Matthews, 2007). Energy metabolism in this form is simplified and relies completely on nonoxidative consumption of glucose, which is constantly provided by the host. In the bloodstream, the trypanosome population oscillates between proliferative slender forms and cell cycle-arrested stumpy forms. The parasites secrete an, as yet, undefined low-molecular-weight factor which triggers differentiation to the stumpy stage in a cell-density-dependent manner. As parasitemia rises, more stumpy induction factor (SIF) accumulates and the cells become quiescent (Reuner et al., 1997). Thereby, population density is limited, allowing the parasites to persist for significant periods without killing the host. Thus, one could argue that the stumpy stage acts altruistically in sacrificing itself for the sake of population survival. In fact, stumpy forms survive only for a rather short period (a few days) and appear to be efficiently eliminated by the humoral immune response. However, the stumpy stage is crucial for life-cycle progression as only they can successfully establish an infection in the transmitting insect vector (Fig. 1.1). Stumpy forms are preadapted to a life within the fly, including increased mitochondrial activity, reorganization of the endomembrane system, and hypersensitivity to environmental cues such as cold shock and citrate/*cis*-aconitate (Engstler and Boshart, 2004).

When the fly ingests stumpy form trypanosomes, the parasites immediately encounter a loss of temperature homeostasis. This has been suggested to cause upregulation of the major insect stage surface proteins, procyclins (Engstler and Boshart, 2004). The expression of procyclins is accompanied by rapid loss of the VSG coat. How exactly the VSG is lost is not fully understood, but the participation of both a metalloprotease and phospholipase appears likely (Gruszynski et al., 2003). The expression of distinct procyclins during the process of adaptation to the insect environment has also been described in a series of elegant experiments, however, the function of the new cell-surface coat remains unclear (Acosta-Serrano et al., 2001). In fact, procyclins appear to be dispensable both *in vitro* and their expression is not essential for successful passage through the tsetse fly (Vassella et al., 2009).

In the insect, trypanosome metabolism switches from glycolysis to cytochrome-mediated oxidative respiration. After establishing a midgut infection, trypanosomes migrate to the fly salivary glands, to complete the life cycle. Little is known about this journey and how trypanosomes navigate through the fly. Having reached the salivary glands, the epimastigote parasites attach to the microvilli of epithelial cells (Urwyler et al., 2007). This anchoring is mediated by the trypanosome flagellum through an, as yet, unknown mechanism. The density of the actively dividing epimastigotes within the salivary glands can become rather high. Finally, the attached epimastigotes give rise to quiescent (i.e., nondividing) metacyclic trypanosomes, which reacquire the VSG coat. This completes the trypanosome life cycle.

Although this basic itinerary for *T. brucei* transmission through host and vector has been known for decades, the signals and molecular responses underlying the alterations between proliferative and quiescent stages remain enigmatic. While considerable effort and progress in understanding the slender-to-stumpy and stumpy-to-procyclic differentiation events has been made recently, and a molecular marker, PAD1, has now been identified for the stumpy stages, very little is known about transition between fly stages (Dean et al., 2009). This is in part due to the fact that fly resources are limited and few laboratories are experienced in maintaining and manipulating tsetse. This extensive research effort should be devoted to understanding the fly–parasite interaction and development stages within the tsetse fly is underlined by exciting recent findings showing that meiosis and the exchange of genetic material occurs only within the fly; hence the tsetse fly is formally the definitive host.

2. Immune Evasion Mechanisms

2.1. VSG and antigenic variation

The ability to survive in the vasculature of the mammalian host, despite constant exposure to a highly sophisticated immune response, was a major challenge to understanding of trypanosome virulence mechanisms. It is now 30 years since seminal work identified the VSG surface coat as the basis for antigenic variation (Cross, 1977).

A 15 nm thick layer of 5×10^6 identical VSG homodimers covers each trypanosome cell. This amazingly high concentration of a single species of plasma membrane protein is unprecedented, and represents $\sim 90\%$ of cell-surface protein. The spacing between individual VSG dimers is 3–5 nm, which effectively shields most of the VSG epitopes from antibody recognition (Overath and Engstler, 2004). The classical view proposes that other

surface proteins are buried within the VSG coat and that the plasma membrane is virtually untouchable by the immune system. However, a full description of the mammalian host immune response remains to be achieved and it is possible that additional determinants are recognized.

Evolution may have shaped the molecular structure of VSG for maximum efficiency as an immunological shield. Two extended α-helices project perpendicular to the cell surface and provide the molecule with an extended conformation (Freymann et al., 1990). VSG proteins generally comprise two domains, a larger externally disposed N-terminus of 350–400 residues and a smaller C-terminal domain 40–80 residues that is proximal to the plasma membrane (Chattopadhyay et al., 2005). Once packed into the surface coat, only a restricted number of amino acids are accessible to external probes. The exposed amino acid positions are highly variable, while more conserved sites, especially several cysteines required for disulfide bond formation and hence secondary structure, are less accessible (Field and Boothroyd, 1996). While the crystal structure of two N-terminal domains was solved some 20 years ago, the structure of the relatively conserved C-terminal was described only recently (Chattopadhyay et al., 2005). NMR analyses revealed that C-terminal domains display related core structures consisting of two α- or 3_{10}-helices and two antiparallel β-sheets. However, the length of the secondary structure elements and the loops connecting these elements vary between different C-terminal domains. Up to now no complete VSG structure has been solved, and the structure of the connection between the two domains remains unknown. More importantly, we still have little structural appreciation of the linkage between the VSG C-terminal domain and the hallmark of VSGs, the glycosylphosphatidylinositol (GPI) anchor.

The GPI anchor is rapidly added posttranslationally to the C-terminus of VSG and ultimately anchors the protein to the outer leaflet of the plasma membrane (Martin and Smith, 2006). The lipid anchoring of VSG has many important implications for the physicochemistry of the trypanosome cell surface and VSG sorting. A great many GPI-anchored proteins (GPI-APs) with various functions have been described in many organisms (Field and Menon, 1993). However, compared to *trans*-membrane proteins, GPI-APs are rare or of low abundance in most taxa. As the insect stage dominant antigens, procyclins and BARP, are also GPI anchored, African trypanosomes link all dominant surface proteins via a GPI anchor to the plasma membrane independent of the life-cycle stage (Engstler et al., 2004; Urwyler et al., 2007).

The unique structure of VSG and its ability to support an extreme form of molecular crowding on the cell surface would not help the parasites to survive in the mammalian bloodstream unless coupled to antigenic variation. In fact, the immune system would actually become hyperactivated by an almost crystalline array of protein epitopes, accurately displayed on the

surface of the trypanosome cell, and VSG is known to be an effective immunogen. During rising parasitemia the majority of trypanosomes belong to a particular antigenic type, giving rise to a strong antibody response, which kills the large majority of trypanosomes bearing that VSG. These parasites are apparently cleared from the bloodstream. However, antigenic variation replaces the VSG on the cell surface of a small proportion of trypanosomes with another, and immune selection determines if these parasites expressing a new VSG can survive. Laboratory strains switch rarely, with a rate of 10^{-6}–10^{-7} per cell generation. Recent work suggests that the antigenic switching rate in natural isolates is much higher, up to 10^{-2}–10^{-3} (Lythgoe et al., 2007). A repertoire of hundreds of different VSGs that can potentially be expressed on the cell surface indicates that the host immune response always lags behind, allowing trypanosomes to survive for prolonged periods.

VSGs are transcribed from one of 20 telomeric expression sites (ESs) (Cross, 1996; McCulloch, 2004; Pays, 2006). The VSG gene is located at the end of a long polycistronic transcriptional unit, and transcribed by RNA polymerase I. This transcription unit contains more than 10 genes, which are termed as expression site associated genes (ESAGs). The function of many ESAGs is still unknown. The active ES is localized to an extranucleolar structure that is known as the ES body (Navarro and Gull, 2001). Besides the ES-linked copies, the majority of VSG genes locate as nontranscribed basic copies to either large arrays in central regions of megabase chromosomes or as single copies on mini chromosomes. The basic copies are abundantly flanked by repeats that facilitate homologous recombination with the active ES.

Multiple mechanisms for mobilizing VSG genes have been described. Activation of a silent ES displaying another VSG is known as an *in situ* switch. This form of switching not only activates another VSG, but also a new array of ESAGs. It has been postulated that activation of alternative ESAGs could be involved in adaptation to various host environments (Gerrits et al., 2002). Telomere exchange between ESs or gene conversions that introduce all or part of a basic copy VSG into the active ES are also known. The potential for creation of mosaic VSG sequences from multiple basic copy ORFs extends the repertoire hugely, while gene conversion most probably dominates in field infections, and provides access to this near limitless repository.

2.2. Membrane dynamics and antibody clearance

The VSG coat is endocytosed with unprecedented speed and fidelity (Engstler et al., 2004). An area equivalent to the entire plasma membrane is internalized and recycled once every 10 min. Compared to membrane recycling in other organisms this is amazingly fast kinetics, especially when

taking into account that all membrane traffic is routed via the tiny flagellar pocket, which only accounts for ~2% of surface membrane (Field and Carrington, 2009). In trypanosomes, internalization of plasma membrane and embedded proteins is restricted to clathrin-mediated endocytosis (CME). Comparatively large clathrin vesicles, termed CCV class I, abundantly bud from the flagellar pocket. Every second six new CCVs are rapidly transported by an actin-dependent mechanism to early endosomes, which are located between 2 and 4 μm away from the pocket. About 60–70 CCV class I can be found in the posterior part of the cell. CCV I fuse to early endosomes that are easily detectable in trypanosomes as mostly circular cisternal structures (Grünfelder et al., 2002). In bloodstream forms this also appears independent of dynamin, but in the procyclic it is possible that dynamin is required (Morgan et al., 2004; Chanez et al., 2006).

The next step on the itinerary of endocytosed membrane is the recycling endosome, which appear to be the main sorting station of GPI-APs. However, unlike yeast or mammalian cells, trafficking through recycling endosomes in *T. brucei* is not rate limiting. In fact, the delivery from early endosomes follows biphasic kinetics, with one part of VSG or reporter proteins being delivered very rapidly to the recycling endosome, while the other half arrives significantly later. The reason for this is a detour of part of the internalized membrane and embedded proteins to late endosomes. Interestingly, this material is not delivered to the lyosome but is redirected to recycling endosomes, albeit with comparatively slow kinetics (Engstler et al., 2004). In trypanosomes, recycling endosomes are most prominent endomembrane structures. In this "recycling factory," ligands uncouple from their receptors and are sorted together with endocytosed fluid-phase cargo into smaller clathrin-coated vesicles (CCV class II), which abundantly bud from the rims of the cisternal recycling endosome (Grünfelder et al., 2003). CCV class II have two destinations within the cell: late endosomes and the lysosome. They are devoid of VSG, transferrin receptor (TfR), and some *trans*-membrane proteins (e.g., invariant surface glycoproteins (ISGs)). Thus, by a negative mechanism, namely withdrawal of membrane, GPI-APs are passively (i.e., by default) concentrated (Overath and Engstler, 2004). How GPI-proteins are excluded from entry into budding vesicles remains to be elucidated. The subregion of the recycling endosome that carries the concentrated VSG eventually gives rise to small, disk or cup-shaped carriers that fuse with the flagellar pocket. These exocytic carriers (EXCs) are profusely found within the posterior part of the cell (Grünfelder et al., 2003).

Why have trypanosomes evolved such a sophisticated and highly active plasma membrane recycling machinery? The selective pressure for uptake of sufficient nutrients from host blood is one obvious answer. However, it has been shown that the vast majority of fluid-phase cargo is actually not transported to the lysosome, but is excreted by the cells (Engstler et al., 2004).

More than 20 years ago, it was reported that antibodies bound to the trypanosome cell surface are internalized and most probably routed to the lysosome. These early studies suggested that host antibodies are cleared from the cell surface of bloodstream trypanosomes within 15–30 min (Russo et al., 1993). A more recent report has revealed that VSG-bound IgGs (VSG-IgG) accumulate at the flagellar pocket region within 20–40 s. VSGs and bound antibodies are rapidly internalized via CME (Allen et al., 2003; Engstler et al., 2007). 3D-fluorescence microscopy and quantitative colocalization analyses with organelle-specific marker proteins have confirmed that a significant amount of antibody is routed via late endosomes to the lysosome, while VSG is recycled to the cell surface.

The internalization of antibody-bound VSG from the trypanosome cell surface comprises three consecutive steps, each displaying distinct temperature sensitivities. Initially, VSG–IgG complexes accumulate at the posterior pole of the cell. The kinetics of this process is comparatively independent of temperature; even at 12 °C rapid antibody accumulation is observed. In contrast, the rate of entry of VSG–IgG complexes into the flagellar pocket is significantly decelerated at 24 °C, and at 12 °C the process almost halts. Once arrived in the flagellar pocket, VSG–IgG is internalized by bulk membrane uptake. The endocytosis of IgG-bound VSG exhibits similar temperature sensitivity as the entry into the flagellar pocket. Hence, the three-step antibody clearance process involves posterior accumulation of antibodies as immediate event and passage through the flagellar pocket as rate-limiting step. Posterior accumulation of VSG–IgG does not result from VSG shedding and is independent of endocytosis.

Downregulation by RNAi of clathrin heavy chain causes a block of all endocytic traffic. Although in clathrin-depleted cells endocytosis is stalled, VSG–IgG accumulates at the flagellar pocket in a similar manner as in control cells. Posterior accumulation of VSG–IgG requires energy as the glycolytic inhibitor 2-deoxyglucose decreases posterior accumulation of VSG–IgG complexes. When cellular motility is stalled by ATP depletion, no antibody accumulation is observed, but cells remained uniformly coated with immunoglobulin, suggesting a correlation between cellular motility and antibody clearance (Engstler et al., 2007).

Bloodstream forms of *T. brucei* swim with an average speed of 20 $\mu m\, s^{-1}$. A directional, spiral trajectory is mediated by a single flagellum, which emerges from the flagellar pocket, attaches to the cell body, and extends beyond the anterior pole of the cell (Fig. 1.2). FlaI is required for the connection of the flagellum to the cell body, and downregulation of FlaI results in detachment of the flagellum and loss of directional motility. FlaI-depleted trypanosomes retain their VSG coat and VSG-bound antibodies are internalized from the flagellar pocket with similar kinetics as in control cells. Strikingly, obstruction of directional swimming coincides with a loss of accumulation of antibody-bound VSG at the posterior cell surface.

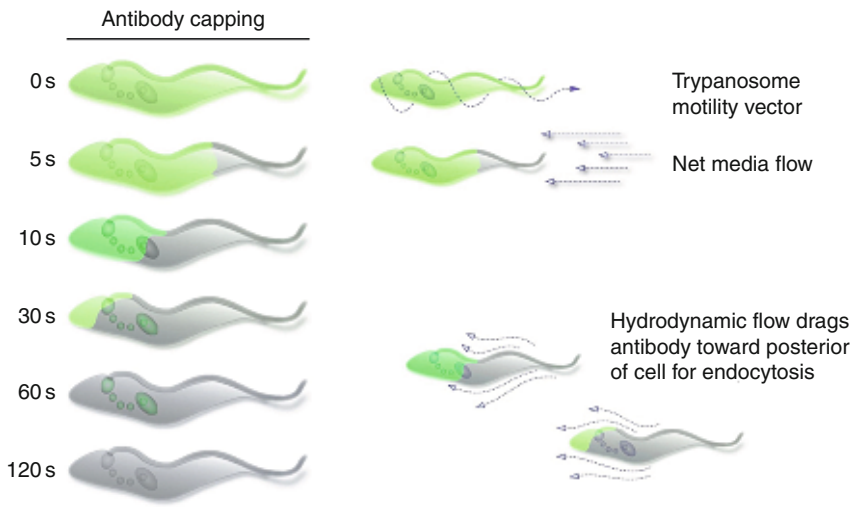

Figure 1.2 Immune evasion by antibody capping; a role for hydrodynamic flow. Left column: Antibody recognizing the surface variant surface glycoprotein (VSG) is rapidly capped toward the posterior of the cell. The high rate of endocytosis facilitates efficient uptake of the antibody, which is ultimately degraded; the uptake process, even in the presence of high antibody titers, can be completed within 2 min. Right column: Trypanosomes continuously swim, and thereby generate directional flow fields on their cell surface. These flow forces become more significant when the surface VSG is recognized by immunoglobulins. Antibody–VSG complexes are pulled by hydrodynamic forces toward the rear of the cell, where they are endocytosed. This implies that purely physical forces can sort proteins in the plane of the plasma membrane. The schematic shows antibody in green coating VSG in gray. Note that the mechanism for capping, or delivery of antibody to the flagellar pocket, is likely distinct from that which operates in metazoan cells.

Conversely, a marked reduction in antibody concentration is observed in the flagellar pocket area, which is explained by continuing membrane recycling in the absence of antibody accumulation. Clearly, there is direct involvement of cell motility and endocytosis in antibody clearance (Engstler et al., 2007).

The size, but not the nature of the protein bound to VSG, is critical for accelerated removal from the cell surface; for example, IgM is removed much more rapidly than Fab fragments. Mammals respond to trypanosome infections with elevated levels of VSG-specific IgM rather than IgG. Both immunoglobulins are internalized in a concentration-dependent manner but the overall kinetics of IgM-uptake is significantly faster. This observation is difficult to explain on the basis of specific recognition of antibody-bound VSGs by cytoplasmic adapter proteins as VSG is anchored via a GPI-anchor.

A provocative alternative possibility is that hydrodynamic flow acts on swimming trypanosomes and specifically drags VSG–Ig complexes toward the flagellar pocket (Fig. 1.2). The most direct evidence for

hydrodynamic drag arises from downregulation of the dynein arm intermediate chain DNAI1, which reverses the trypanosome swimming direction. Hydrodynamic drag predicts that the immunoglobulins would be pushed toward the other cell pole in the DNAI1-supressed cells, and is exactly what is observed (Engstler et al., 2007).

However, the role of antibody clearance for parasite survival *in vivo*, that is, in the natural host, remains to be elucidated. Antibody removal could be crucial for parasite survival during early parasitemia, when antibody titers are still low, after differentiation to the cell cycle-arrested stumpy stage, which is critically required for the successful completion of the parasite life cycle or for removal of immunoglobulins recognizing invariant epitopes. All of these possibilities remain to be fully investigated.

2.3. Cellular immune responses

The trypanosome lifestyle is provocative in its complete exposure to the mammalian host, yet, at the population level they prosper in the face of massive immune attack. VSG is highly immunogenic and trypanosomes produce it in huge amounts. The immune system, when confronted with a wave of parasites, aims at rapidly clearing the trypanosomes, and paradoxically this mechanism is essential for chronic infection. Rapid growth of trypanosomes can overwhelm the host within days, and one mechanism to avoid this is the continuous secretion of SIF, triggering differentiation from long slender to stumpy stage. The importance of SIF is underscored by the observation that strains that have become unresponsive to SIF kill their host within a few days. Further, generation of VSG-specific antibodies is crucial to early host survival and B cell-deficient mice poorly control trypanosome infections (Baral et al., 2006).

Antibody-opsonized trypanosomes will be phagocytosed and destroyed by hepatic Kupffer cells. The paracrystalline structure of the VSG coat, with homogeneously organized epitopes, may explain why the early immune response is largely T cell independent (Mansfield, 1994). The VSG-specific antibody response is crucially insufficient for efficient protection during early phases of infection and IFN-γ appears to be required. The majority of IFN-γ is produced after T cell stimulation through antigen presenting cells (Magez et al., 2006). The absence of MHC-II diminishes IFN-γ production and parasite control. Also natural killer cells have been proposed to be involved in the production of IFN-γ (Mansfield and Paulnock, 2005).

In the beginning, it was believed that IFN-γ would bind directly to trypanosomes stimulating their proliferation. Now it appears clear that *in vivo* IFN-γ is responsible for a proinflammatory reaction, which attacks the parasites (Namangala et al., 2001). Mice deficient of either IFN-γ or IFN-γ receptor reveal high-level parasitemia and die earlier than control animals. The IFN-γ-mediated control involves classic macrophage

activation. The effector cells produce a range of antitrypanosome compounds, including tumor necrosis factor alpha (TNF-α) as well as reactive oxygen species, which cause the so-called host oxidative burst. Reactive nitrogen, NO, is also involved. Interestingly, the role of NO as inflammatory effector appears to be distinct for infections with different trypanosome species (Vincendeau et al., 1992). Toll-like receptors are thought to be involved in the activation of macrophages by T cell-derived IFN-γ and endogenous TNF-α. The toll-like receptors represent a steadily growing family of proteins that can recognize conserved pathogen signatures, such as the bacterial lipopolysaccharide, nonmethylated DNA, or GPI structures (Coller et al., 2003). During the cyclical destruction of large trypanosome populations, massive amounts of these molecules are released into the bloodstream. Consequently, parasite control involves toll-like receptors that recognize the VSG-GPI and free nonmethylated CpG DNA sequences.

Highly inflammatory reactions govern the initial phase of infections with African trypanosomes. The long-lasting type I immune response leads to many of the pathological signs associated with sleeping sickness, such as anemia, fever, splenomegaly, liver damage and neurological disorder and cachexia, from which any infected human or animal will finally die. Therefore, having survived the first wave of parasitemia, the infected host needs to remodel its immunological landscape to enhance survival chances. Although TNF-α knockout mice are not able to control parasitemia efficiently, they reveal prolonged survival (Magez et al., 1999). This is also true for mice treated with anti-IFN-γ antibodies. The initial proinflammatory phase ends by secretion of cytokines and generation of alternatively activated macrophages. Interleukin 10 inhibits classically activated macrophages. The alternatively activated macrophages display anti-inflammatory properties and could dampen the pathological consequences of type I immune response.

In addition to the induction of various immune pathological damage in different tissues, immunosuppression is yet another consequence of trypanosome infection and T cell suppression is severe. Obviously, this leads to frequent opportunistic superinfections, which additionally weaken the host. Early on, immunosuppression appears to be mediated by NO, prostaglandin E2, and TNF-α from classically activated macrophages (Mansfield and Paulnock, 2005; Sternberg and Mabbott, 1996). At later stages, the immunosuppression is mediated by alternatively activated macrophages, but our knowledge about the mechanisms behind this process is rudimentary.

African trypanosomes are capable of manipulating and controlling the highly sophisticated immune system of their vertebrate host. Apparently, this hijacking can occur at very different levels. While some trypanosome species kill their host rather quickly, other infections can last for months or even years. In any case, most hosts will not survive their encounter with trypanosomes.

2.4. Innate immunity

Fascinating exceptions to the fatal outcome are humans and primates, which are fully protected against most trypanosome species. Human innate immunity against African trypanosomes has been known for more than a century. However, only recent extensive work of several laboratories has finally shed light on the molecular mechanisms behind the trypanosome resistance.

Normal human serum (NHS) *in vitro* is cytotoxic for *T. brucei*. Neither immunoglobulins, the complement activation pathway nor the blood clotting system are responsible. Furthermore, NHS is not activated by trypanosome-derived factors. Many different substances and macromolecules have been put forward as candidate trypanosome lytic factor (TLF), one of which, high-density lipoprotein (HDL), was postulated as early as 1960 to be involved in trypanosome killing. The first systematic study on the nature of TLF, demonstrated the involvement of HDL and revealed that trypanosome lysis is a two-step process (Rifkin, 1978). Initially trypanosomes are motile and intact but start swelling. After about an hour, lysis commences. The kinetics of trypanosome killing depends on human serum concentration and temperature; at 4 °C the process is totally inhibited but is optimal at ~37 °C (Rifkin, 1984). Although this key concept of trypanosome lysis by TLF was formulated in the mid-1980s, it required 20 years to identify TLF, to understand the molecular mechanism of lysis and to unravel the secret of resistance to TLF by human pathogenic trypanosomes, namely *T. brucei rhodesiense*.

Since it was known that TLF was an HDL component, the obvious candidate for the toxic factor was the major constituent of HDL itself, namely apoA-1 (Gillett and Owen, 1991; Hajduk et al., 1989). However, biochemical characterization of HDL revealed that TLF is only a minor subset of human HDL. Furthermore, transgenic mice expressing human apoA-1 were not significantly protected against trypanosome infection (Rifkin, 1991). Fractionation of HDL and reconstitution revealed that more than one protein was required for the assembly of the lytic particle, suggesting that distinct TLF components may act cooperatively (Hajduk et al., 1989). A more detailed analysis of TLF proteins suggested paraoxonase–arylesterase and haptoglobin-related protein (Hpr) as potential toxins. Since paraoxonase–arylesterase is present in nonlytic human HDL, it could be excluded. The haptoglobin-related protein, on the other hand, was selectively enriched in TLF and antibodies directed against the protein were shown to inhibit lysis in a dose-dependent manner (Smith and Hajduk, 1995).

Hpr is restricted to primates (Maeda, 1985). Although the physiological function is unknown, it is evolutionarily derived from haptoglobin, an abundant acute-phase protein forming a high-affinity complex with free hemoglobin. Haptoglobin is critically involved in clearance of hemoglobin

from the circulation after intravascular hemal lysis. The haptoglobin–hemoglobin complex is recognized by macrophage surface receptors and then degraded. Hpr is a dimer, and in contrast to haptoglobin, is associated with apoA-1. Interestingly, although it was generally accepted that TLF was part of HDL, reports suggesting an additional trypanolytic activity appeared.

This second lytic factor had a higher molecular mass than TLF and was termed TLF-2 (Tomlinson et al., 1997). It was reported to be a lipid-poor complex containing mainly IgM together with apoA-1 and Hpr, while TLF-1 contained essentially apoA-1 and Hpr. Haptoglobin is a potent inhibitor of TLF-1, but does not interfere with TLF-2-meditated lysis. Apparently, the specific lytic activity of TLF-1 was much higher than that of TLF-2 (Raper et al., 1999). Confusingly, haptoglobin levels below physiological concentrations were shown to be sufficient to completely inhibit TLF-1. However, purified TLF-1 protected mice in a dose-dependent manner against trypanosome infections, and it was generally accepted that Hpr was the actual toxin. Further, phylogenetic analyses of the primate lineage revealed a direct correlation between the presence of Hpr and trypanolytic potential. While sera from several old world monkeys contained trypanolytic activity, this was not the case for chimpanzee serum. The Hpr gene of chimpanzees was thought to be a pseudogene, but recent data suggest that the coding region is intact (Lugli et al., 2004).

Trypanosome lysis by TLF/TLF-2 was initially believed to be initiated at the plasma membrane (Rifkin, 1984). However, a detailed cellular study showed that TLF rather affects the endocytic pathway after receptor-mediated endocytosis (Hager et al., 1994). There are about 350 high-affinity TLF binding sites within the flagellar pocket, and electron microscopy revealed that gold-labeled TLF is endocytosed and transported to the lysosome, where it accumulates and causes disintegration of the organelle. The release of lysosomal proteases into the cytoplasm would be lethal to the parasite. It was also suggested that free radical generation through the Fenton reaction at low pH could cause peroxidation of lysosomal membrane lipids, contributing to membrane disruption (Bishop et al., 2001). A further mechanism was proposed whereby Hpr, or part of it, disrupted the membrane directly (Molina Portela et al., 2000). The generation of transgenic mice expressing Hpr added yet another level of complexity to the problem. Although Hpr was properly incorporated into HDL, those mice were not protected against trypanosomes (Hatada et al., 2002).

Two *T. brucei* subspecies are resistant against TLF and are the causative agents of human sleeping sickness. It was known that TLF-resistant strains become susceptible when maintained for long periods in mice, and when exposed to human serum, resistant parasites arise from sensitive populations at low frequency. This apparent high-frequency reversal was difficult to reconcile with classical genetic views of resistance. In fact, it appears that antigenic variation and resistance to human serum are linked processes.

The underlying gene responsible for TLF resistance was identified and termed serum resistance associated gene (SRA) (de Greef and Hamers, 1994). Curiously, the SRA sequence closely resembles VSG, although the region encoding surface exposed loops was deleted from SRA. Thus, SRA is likely a truncated VSG (Campillo and Carrington, 2003). However, unlike VSG, SRA is not expressed on the cell surface, but appears to be restricted to endosomes and lysosome (Vanhamme et al., 2003). The exact localization within the endosomes and the rate of recycling remains to be elucidated. Importantly, when SRA was expressed in human serum sensitive trypanosomes, the parasites became human infective (Xong et al., 1998).

SRA is expressed from just one expression site as an ESAG. The exact mechanism by which SRA confirms human serum resistance is still not unambiguously clear. Mutation analyses suggest that an N-terminal helix could be involved in neutralizing the TLF toxin (Vanhamme et al., 2003). Through interaction with immobilized SRA a fraction from normal human serum was isolated. Surprisingly, Hpr did not bind to SRA, but apoL-1 revealed specific and strong binding. ApoL-1 is associated with HDL and its physiological function is still unclear. Recombinant apoL-1 revealed an SRA-dependent trypanolytic potential. ApoL-1 is found in both TLF-1 and TLF-2, and consequently, this lipoprotein was suggested to be the only trypanosome toxin in human serum (Shiflett et al., 2005). Like Hpr, apoL-1 can be found in many primates, but is absent from the chimpanzee genome (Poelvoorde et al., 2004).

It remains an open question whether apoL-1 and Hpr have to act synergistically for full protective immunity, but reconstitution experiments suggest that both proteins contribute to human serum resistance. While apoL-1 is necessary and sufficient for lysis, Hpr may mediate binding of TLF to a cognate receptor at the trypanosome cell surface. This receptor has recently been identified as a glycoprotein modified by poly-*N*-acetyllactosamine (pNAL) residues and located in the flagellar pocket (Vanhollebeke et al., 2008). In mice, the receptor binds the haptoglobin–hemoglobin (Hp–Hb) complex with high affinity and is responsible for the uptake of sufficient heme for incorporation into trypanosome hemoproteins. *T. brucei* apparently cannot discriminate between Hp–Hb and TLF1–Hpr–Hb complexes. Consequently, in human blood Hb-charged TLF1 complexes are targeted to the trypanosome cell. Thus, it appears that Hpr is required for high-affinity TLF-receptor binding, while apoL-1 is the actual toxin.

The exact mode of apoL-1-mediated lysis is still a matter of debate. However, it appears likely that it acts by generating pores in the lysosome membrane (Perez-Morga et al., 2005; Vanhollebeke et al., 2007). ApoL-1 reveals surprising homology to the pore-forming domain of bacterial colicins. In fact, it was shown that the N-terminal domain of apoL-1 can generate ionic pores *in vitro* and *in vivo*. Furthermore, a pH-sensitive domain is thought to be involved in membrane targeting. Thus, a possible scenario

for trypanolysis by human serum can be summarized as follows. In the flagellar pocket, TLF1–Hpr–Hb particles bind to the TLF-receptor via Hpr. Passage of the internalized complex through the endocytic pathway is accompanied by progressive acidification. This induces conformational changes in the apoL-1 membrane-tethering domain, which could facilitate sequestration of apoL-1 from the HDL carrier. Free apoL-1 inserts into the membrane of the acidic lysosome. Within the membrane, the two central hydrophobic helices of the apoL-1 pore-forming domain open a pore, leading to depolarization of the lysosomal membrane. Influx of chloride ions from the cytoplasm into the lysosome generates osmotic pressure that triggers lysosome swelling. The depletion of cytoplasmic chloride results in compensatory chloride uptake from the extracellular environment. Eventually, the developing intracellular pressure compromises the plasma membrane and the trypanosome is killed. While there are certain aspects of the model that still await experimental confirmation, it provides the so far most complete explanation of trypanolysis in human serum.

3. Endocytic Pathways

The endocytic system is an important component of the intracellular trafficking system that modulates the composition of the cell surface through the sorting of internalized proteins, lipids, and glycoconjugates into recycling or degradative pathways, and thus play a crucial role in many biological functions, including maintenance of the cell surface, immune modulation, signal transduction, and nutrition (Piper and Katzmann, 2007). Study of the uptake of various ligands and surface proteins, coupled with development of subcompartment-specific markers has allowed considerable delineation of the major endocytic routes in *T. brucei* and the organism probably has the best characterized endocytosis apparatus of any protist. Light and electron microscopy have revealed the presence of morphologically distinct populations of early and late endosomes, based on the kinetics in which they are loaded with material and the specific sets of markers they contain (Engstler et al., 2004; Grünfelder et al., 2002, 2003). Further, the later endocytic compartments, the multivesicular body and lysosome have also been defined, and in part functionally investigated (Leung et al., 2008; Peck et al., 2008).

3.1. Clathrin-mediated endocytosis

All endocytosis in African trypanosomes is CME and occurs solely at the flagella pocket (FP; Allen et al., 2003; Overath et al., 1997) (Fig. 1.3). CME involves assembly of receptor-bound cargo and GPI-anchored membrane

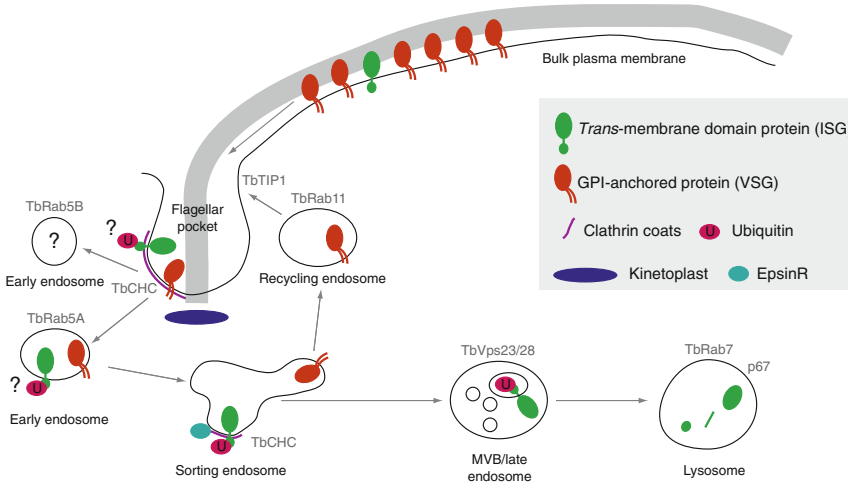

Figure 1.3 A model of sorting of GPI-anchored and *trans*-membrane domain proteins in trypanosomes. *Trans*-membrane domain proteins such as ISGs (green) are present at low density at the cell surface in comparison to the dominant GPI-anchored VSG (red). There is presently no evidence that there is selective partitioning of GPI versus *trans*-membrane anchored proteins at the cell surface. Endocytosis requires the function of clathrin (purple) at the flagellar pocket, and for ISG65 and VSG, this serves to target the molecules to the Rab5A-positive early endosome. VSG is segregated at the sorting endosome, and is excluded from a clathrin-tagged membrane microdomains; it is hypothesized that clathrin may actively sort *trans*-membrane domain proteins at this location, via recognition of ubiquitylated cargo (pink lozenge); this may involve the trypanosome epsin-related protein, which interacts with clathrin (cyan lozenge). Recycled molecules are returned to the cell surface via a Rab11-dependent pathway that also involves a coiled-coil Rab11-interacting protein that likely serves as a docking site at the flagellar pocket. *Trans*-membrane domain cargo is delivered to the lysosome via the multivesicular body, and degraded. This latter pathway depends on functioning of the ESCRT complex, including TbVps23. The site(s) where ubiquitin is added are unknown. Also the model assumes that all GPI-anchored proteins are recycled and all *trans*-membrane domain proteins are directed to the lysosome—this is unlikely to be the case, but data concerning trafficking of additional factors are not available at this time. Finally, the function of the Rab5B endosome remains mysterious as besides the presence of lactosamine-repeat determinants, the identity of the molecules transported via this route are unidentified.

components into clathrin-coated pits, which are formed at the site of endocytosis by recruitment and polymerization of assembly units of the cytoplasmic protein, clathrin, composed of three heavy chains (CHC), each tightly associated with a single light chain (CLC; Kirchhausen and Harrison, 1981). This structural organization results in a basket-like polyhedral lattice (Brodsky et al., 2001) that assists in deformation of the underlying membrane (Conner and Schmid, 2003) into coated pits. Subsequently, these pits invaginate and pinch off, forming class I CCVs (Engstler et al., 2004;

Grünfelder et al., 2003; Overath and Engstler, 2004). Class I CCVs rapidly shed their coat and the resulting vesicles dock and fuse with an early endosomal compartment. Subsequent intracellular sorting of components designated for degradation occurs via a negative sorting mechanism (Overath and Engstler, 2004). Here, class II CCVs containing components for lysosomal degradation bud from early and recycling endosomes while VSGs are concentrated in Rab11-positive, flat, disc-like structures designated EXCs that fuse with the FP (Grünfelder et al., 2003).

Mammalian forms of African trypanosomes exhibit extremely rapid endocytosis and recycling compared to the insect forms. This upregulation of ~10-fold (Natesan et al., 2007) is suspected to be involved in immune evasion in bloodstream forms (Morgan et al., 2002). A similar variation is exhibited in clathrin expression levels (Morgan et al., 2001; Natesan et al., 2007), evidence for developmental regulation of endocytosis. Clathrin ablation is lethal due to a direct arrest of vesicular traffic from the FP leading to an enlarged FP or "BigEye" phenotype (Allen et al., 2003; Hung et al., 2004). This underscores the unique role of clathrin and CME as the sole endocytic mechanism in African trypanosomes.

CCV-formation machinery in *T. brucei* is unusual (Fig. 1.4). First, pit formation does not involve a concentration step (Grünfelder et al., 2003), a hallmark of CME in other eukaryotes. Second, since the *T. brucei* genome does not code for the key adaptor protein, AP-2 (Morgan et al., 2002), the mechanism of clathrin recruitment to the plasma membrane is unknown, despite clear ultrastructural evidence of clathrin-coated pits and CCVs (Engstler et al., 2004). AP-2 is a heterodimeric complex that binds cargo receptors and recruits clathrin in addition to providing a platform for assembly of accessory proteins that stabilize the activated receptor/AP-2/clathrin coat interaction. Reasons of this loss or its replacement are unknown but its loss may be due to the extremely high levels of cell-surface VSG (Field et al., 2007b) precluding further concentration. Significantly, the absence of AP-2 is common to all salivarian trypanosomes, that is, those possessing a VSG-mediated antigenic variation mechanism.

3.2. Cargo adaptors and sorting

In the absence of an AP-2 complex, it is unclear how clathrin is specifically targeted to the flagellar pocket membrane or how the system interacts with cargo (Fig. 1.4). One candidate for the latter is the trypanosome epsinR. Various epsin isoforms have been characterized (Chen et al., 1998; Rosenthal et al., 1999; Spradling et al., 2001) and epsinR or epsin-related proteins (Ford et al., 2002; Hirst et al., 2003), also called *cl*athrin *int*eracting protein, Clint (Kalthoff et al., 2002) or enthroprotin (Wasiak et al., 2002) are also implicated in transport processes. The epsin family shares a similar domain organization and mainly interacts with membrane lipids, clathrin,

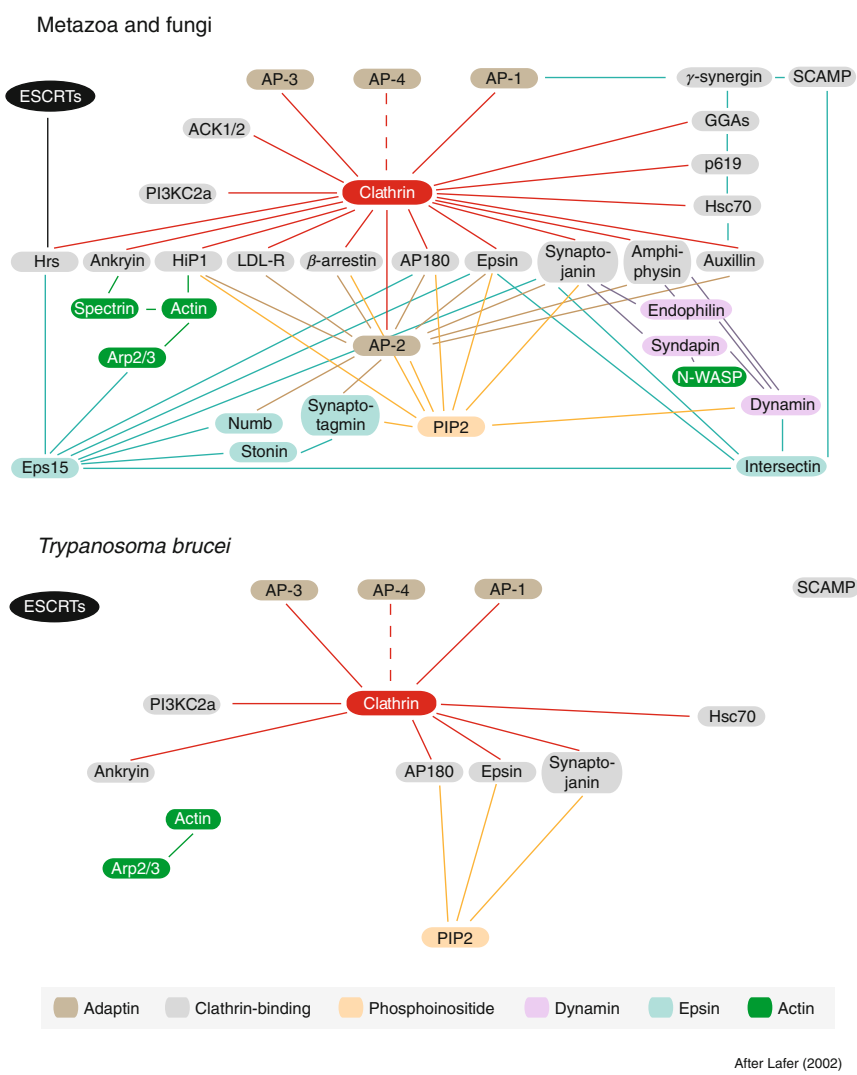

After Lafer (2002)

Figure 1.4 Presence and connectivity between gene products in trypanosomes and metazoa. In metazoan cells clathrin mediates only one of several endocytosis routes, while in trypanosomes all evidence indicates exclusive use of the clathrin pathway. A clear extensive level of connectivity is evident between the polypeptides of the clathrin endocytosis pathway in metazoa, and many of these factors also participate in additional clathrin-independent processes. In trypanosomes, the majority of these factors are absent from the genome, or experimental evidence also precludes a direct role in clathrin-mediated endocytosis. Moreover, the majority of connections shown are hypothetical and have not been experimentally determined. Red, clathrin; black, ESCRTs; brown, adaptins; gray, direct clathrin-binding partners; green, actin; orange, phosphoinositide phosphates; purple, others. The diagram is based on the data originally given by Lafer (2002).

and recruits additional proteins. At the N-terminus is a phosphatidylinositol (4,5)-bisphosphate ($PtdInsP_2$) binding epsin N-terminal homology (ENTH) domain of ~150 amino acids (de Camilli et al., 2002). The remaining largely unstructured region includes an ubiquitin-interacting motif (UIM), clathrin-binding box, and AP/GGA-binding motifs in the central region. The epsinR forms lack the UIM but retain most of the other sequence features.

The *T. brucei* genome has one ENTH-family gene, TbEpsinR; the sequence has conserved lipid-binding residues in the ENTH domain, lacks NPF and UIM motifs and multiple DPW motifs are replaced by DxF, and together with phylogenetic reconstruction, placing this clearly as an epsinR subfamily member (Gabernet-Castello et al., 2008). Like other endocytic factors, it is located between the kinetoplast and nucleus, and ablation is lethal. RNAi knockdown indicates a clear role in endocytosis, turnover of ISGs, and a conserved interaction with clathrin. However, knockdown of TbEpsinR does not prevent clathrin recruitment to the membrane or emergence of a BigEye, which suggests that while TbEpsinR and clathrin clearly function together in endocytosis, it is probable that other factors help load clathrin onto the membrane. Further, TbEpsinR is not a player in the mechanism of endocytosis *per se*, and clearly implicated as a cargo adaptor. A related ENTH/ANTH domain protein, TbAP180, has so far not been studied, and there is essentially no data on roles or locations of phosphoinositides in trypanosomes.

3.3. Early and recycling endocytic compartments

Endocytic compartments progressively mature into degradative of recycling pathways with a concomitant change in the markers they possess. Much work in higher eukaryotes has focused on using Rab GTPases of the Ras superfamily as such markers due to their integral roles in the regulation of vesicle transport, thereby allowing the spatial coordination of vesicle targeting, docking, and possibly budding (Zerial and McBride, 2001). A similar approach has also been applied to trypanosomes.

While endoyctosis in trypanosomes has a single mode of entry for material, that is, CME (Allen et al., 2003; Overath and Engstler, 2004), up to 16 Rabs are present in the *T. brucei* genome, reflecting an inherent level of sophistication within the trafficking system (Ackers et al., 2005). Sorting of material most likely occurs within internal endocytic compartments and not at the plasma membrane. This is supported by the presence of distinct, punctuate, early endocytic structures differentiated by the presence of two Rab5 homologues, TbRab5A and TbRab5B, and containing distinct cargo molecules (Field et al., 1998; Pal et al., 2002a). Selectivity is apparent at this initial stage of uptake as the Rab5A endosome contains IgG, transferrin, VSG, and ISG65, a type I *trans*-membrane protein

(Chung et al., 2004; Field et al., 1998; Hall et al., 2004a,b; Pal et al., 2002a). In contrast, the only cargo to be localized to the TbRab5B compartment is recognized by polyclonal antisera to ISG100, suggesting a differential function between the two endosomal populations (Field et al., 1998). How this discrimination occurs is unclear, but the mode of membrane attachment may function to direct cargo to specific early endosome compartments, and is supported by the presence of carbohydrate-mediated endocytic targeting in trypanosomes (Nolan et al., 1999; Pal et al., 2002a). Both TbRab5A and 5B clearly participate in endocytosis, levels of TbRab5A and 5B protein correlate with clathrin expression levels and knockdown leads to loss of clathrin expression and the BigEye enlarged flagellar pocket phenotype, suggesting a direct interaction between these factors (Hall et al., 2004a; Koumandou et al., 2008).

Rab5-positive early endosomes interface with components of the recycling systems, predominantly controlled by TbRab11 (Field et al., 1998; Hall et al., 2004a,b; Jeffries et al., 2001; Pal et al., 2003). VSG and the TfR are extensively recycled in BSF and quickly enter a highly fenestrated, TbRab11-positive compartment after uptake, separating them from soluble fluid-phase cargo (Overath and Engstler, 2004; Pal et al., 2002a, 2003) (Fig. 1.3). The recycling pathway appears to be under extensive developmental regulation as TbRab11 is rather more highly expressed in BSF, and while TbRab4 is involved in fluid-phase lysosomal transport, its participation in recycling appears restricted to procyclic culture forms (PCFs) (Hall et al., 2004b, 2005a,b). Importantly, PCF cells do not separate fluid-phase cargo from surface proteins in the same manner as BSF, and the endocytic system appears to be less diversified in the insect life stage, supported by the fact that in PCF TbRab5A and TbRab5B are located on the same vesicular structures (Field et al., 1998; Hall et al., 2005a,b). More emphasis is placed on recycling pathways in the BSF, whereas in PCFs the endocytic system is committed to lysosomal routes (Hall et al., 2005a,b). Undoubtedly, differences in the regulation of endocytosis between life stages are indicative of altered requirements for survival in the insect and mammalian host (Natesan et al., 2007).

3.4. Multivesicular bodies and late endocytosis

In higher eukaryotes, multivesicular bodies (MVBs) receive input from both the endocytic pathway, and also the post-Golgi network. Membranes intended for lysosome degradation are incorporated into intralumenal vesicles (ILV) that bud from the MVB-limiting membrane. Fusion of these vesicles with the lysosome results in degradation of the vesicles along with their contents. The pathway is proposed to mediate the degradation of damaged proteins, perhaps including exocytic cargo misprocessed in the Golgi complex, and also proteins that require efficient downregulation, for

example, activated receptor-type tyrosine kinases (Katzmann et al., 2002; Piper and Katzmann, 2007).

At the ultrastructural level, MVB architecture appears conserved in *T. brucei* and the similarity extends to positioning of the organelle in terms of relationships with the early endosome and the lysosome (Allen et al., 2007). At present, the highly dynamic structure is undefined; however, trypanosomes do posses the signals and molecular machinery necessary to direct cargo into MVB via ubiquitylation and action of the ESCRT complexes, albeit with some lineage-specific differences (Leung et al., 2008) (Figs. 1.3 and 1.5). Although purely speculative, one could assume that the extensive remodeling of the cell surface during parasite differentiation might be accompanied by a massive expansion in MVB activity. Analysis of MVB function during differentiation could be informative and studies in PCF are warranted, especially due to the apparent lack of sorting within the earlier endocytic compartments.

In addition, MVB internal vesicles do not always mark proteins for degradation and different ILV may be cordoned off into distinct endosomal carrier vesicles in mammalian cells (Chow and Mellman, 2005; Gu and Gruenberg, 1999; van Niel et al., 2006). Whether this occurs in *T. brucei* is unknown, but could go some way to explain the pleiotropic effects upon knockdown of proteins involved in the endocytic system, for example, clathrin and AP-1 (Allen et al., 2003, 2007).

3.5. Lysosome

Juxtaposed to Rab5 endosomes in an area close to the terminal endocytic compartment are the morphologically distinct late endosomes. Rab7 defines these structures and mediates delivery of material to the lysosome

	Trans-membrane	Cytoplasmic
ISG64 (Tb927.5.1410)	ILM **AVLIPVAILAIITAVVLVFV**	RRRRGNAEDVIDEKGEAVSSPDKKGGATSPCYRKE
ISG65 (Tb927.2.3320)	TAM **IILAVLVPAIILAAAVAFFI**	MVKRRRNSSQDVDTGKAEGGVSSVKVVM
ISG75 (Tb927.5.370)	EAK **SGWIGTTKVLVFLIPLLLLLLGLLVFFVI**	RGRRKAEVKDDINIEEGGAKSKNTKTAAGLDSDI

Figure 1.5 Putative ubiquitylation sites in trypanosome *trans*-membrane domain surface proteins. The extreme predicted C-terminal domain sequences of representative members of three of the invariant surface glycoproteins, ISG64, ISG65, and ISG75, are shown. The hydrophobic *trans*-membrane domain is shown underlined, and lysine residues in the short cytoplasmic domains are highlighted in red. Note the rather short length of these cytoplasmic domains and the absence of a canonical dileucine or tyrosine-based endocytosis motif. Only the two C-terminal-most lysine residues in ISG65 have been experimentally shown to be capable of covalent modification by ubiquitin *in vivo* (Chung et al., 2008), while the three C-terminal lysines in ISG75 are implicated empirically in endocytosis and turnover (K.F. Leung and MCF, manuscript in preparation). Accession numbers are given in parenthesis.

(Overath and Engstler, 2004). Protein degradation occurs within the lysosome via the concerted action of acid hydrolases (Kornfeld and Mellman, 1989), and the organelle plays a central role in nutrient acquisition and immune evasion, directly contributing to parasite pathogenesis. Internalized immune complexes are rapidly trafficked to the lysosome for degradation, and the structure is the site at which the antiparasitic effect of TLF is manifested in susceptible species (Balber et al., 1979; Barry, 1979; Hager et al., 1994; Pal et al., 2003; Pays et al., 2006; Raper et al., 2001; Shimamura et al., 2001).

In trypanosomes, the lysosome is a single-membrane-bound vacuole-like organelle, and is in a constant state of flux due to the dual flow of material from the cytosol and from other endocytic compartments (Liu et al., 2000; Pal et al., 2003; Shimamura et al., 2001). Studies on a resident glycoprotein of the trypanosome lysosome, the p67 protein, have furthered our understanding of lysosomal function, but its role in maintaining the integrity of the lysosomal membrane was uncovered only recently (Peck et al., 2008). p67 is potentially analagous to the LAMP and LAMP-like proteins of mammalian lysosomes, and shares the type I topology and extensive *N*-glycosylation of the mammalian proteins as well as a dileucine-based cytoplasmic targeting signal (Allen et al., 2007). However, there is no evidence for sequence similarity or common ancestry between p67 and higher eukaryote LAMPs. Precisely how p67 participates in maintaining the lysosome remains unclear, but evidence suggests the protein may play a role in recycling or export of proteins across the lysosomal membrane (Peck et al., 2008).

Most work has focused on the transport and processing of p67, revealing the conservation of dileucine signal-based lysosomal targeting and some evidence for a saturable cytosolic component (Allen et al., 2007; Tazeh and Bangs, 2007). Trafficking of p67 is regulated in a stage-specific manner and occurs independently of AP-1 complex action, signifying the presence of divergent lysosomal trafficking mechanisms in trypanosomes (Alexander et al., 2002; Allen et al., 2007).

The stage-specific trafficking of p67 and the potent phenotype following ablation in BSFs correlate with higher lysosomal activity in this life stage, and serves to illustrate that lysosome morphology and activity is developmentally regulated (Alexander et al., 2002; Kelley et al., 1995; Langreth and Balber, 1975; Mackey et al., 2004; Pamer et al., 1989; Peck et al., 2008). However, there is no evidence for significant alterations in the expression level of the p67 protein or alterations to lysosome morphology or positioning in any life stage (Natesan et al., 2007). However, endocytosis and lysosomal activity in trypanosomes are coupled; downregulation of nutrient acquisition in the insect life stage is associated with downregulation of the major thiol protease, trypanopain (Caffrey et al., 2000; Mbawa et al., 1992). Hence, while the overall structure as defined

by p67 may appear equivalent throughout the life cycle, functionality is likely to be developmentally controlled.

In other eukaryotic systems, transient and stable fusion of endosomes with the lysosome can result in the generation of hybrid organelles (Bright et al., 2005). Formation of such hybrids is dependent on the presence of Syntaxins 7 and 8, Vti1B, NSF, SNAPs, and Rab7 (Antonin et al., 2000a,b, 2002; Mullock et al., 1998; Pryor et al., 2004), while lysosomal reformation is probably mediated by the retromer complex (Arighi et al., 2004; Seaman, 2004). Trypanosomes have orthologues of all of these factors, indicating potential conservation of the machinery required to direct these restructuring events despite the fact that direct fusion of MVB/late endosomes and lysosomes has not yet been reported (Berriman et al., 2005; J.B. Dacks, MCF, and V. Koumandou, unpublished data).

3.6. Involvement of the cytoskeleton in endocytosis

In higher eukaryotes, the actin and tubulin cytoskeletons have clear roles in endocytosis and movement of vesicles. In trypanosomes, the apparent absence of a cytoplasmic tubulin population, apart from the subpellicular corset, raises the issue of how the various structures are positioned, and the mechanisms by which vesicles move between them. This remains an unaddressed area at the present time. Rather more is known concerning the role of actin. Endocytosis requires cell cortex remodeling (Engqvist-Goldstein and Drubin, 2003; Qualmann et al., 2000), and hence actin is implicated. The involvement of actin polymerization in endocytosis has been very clearly demonstrated but varies between cell types (Fujimoto et al., 2000). Though there is distinct variation between organisms and study is almost exclusively of Opitstokhonta (Lanzetti et al., 2004; Merrifield, 2004), African trypanosomes present a specifically interesting case. In BSFs actin is essential for efficient endocytosis, evident in polarized localization at the endocytic site and an enlarged FP observed on knockdown (García-Salcedo et al., 2004); the phenotype is remarkably similar to that obtained by RNAi against clathrin (Allen et al., 2003; Hung et al., 2004), Rab5 (Hall et al., 2004a,b), Rab 11 (Hall et al., 2005a,b), and ARF1 (Price et al., 2007), suggestive of endocytic blockade.

The precise role of actin in trypanosome endocytosis has not been determined but addressing certain questions could improve our understanding of the process greatly. Firstly, how does actin polymerization occur in the two forms? The actin-related protein Arp2/3 complex, which is important in driving actin polymerization, is present in the trypanosome genome (Berriman et al., 2005), but the Arp2/3 activators and eps15 are lacking, suggesting that a novel process or scaffold protein could be involved. Secondly, how do endocytic factors influence or initiate actin polymerization or F-actin promote endocytosis? A possible candidate involved in actin

remodeling, and which is developmentally regulated, is Rab5 (Lanzetti et al., 2004; Pal et al., 2002a) and in higher eukaryotes possibly acts through an actin-binding effector molecule; significantly Rab5 expression levels influence clathrin protein copy number (Koumandou et al., 2008), suggestive of direct control of endocytosis through Rab5. However, a large number of other candidates are also present in the genome, and many could aid cross-linking of soluble actin into an F-actin network at the plasma membrane facilitating endocytosis in BSF. Recent data from our laboratory has implicated a myosin IB in endocytosis, based on colocalization with clathrin and emergence of an enlarged flagellar pocket on RNAi knockdown (VOA and MCF, unpublished data). A better understanding of the role of actin, and the overall control of endocytic activity will likely require direct characterization of the protein–protein interactions that subtend this system.

3.7. Complexity of endsomal sorting

The extent of Rab protein functional complexity and hence the potential number of independent transport steps within the trypanosome endocytic system remains unknown, and is further complicated by the fact that additional potential endocytic Rab proteins have recently been discovered (JHL, M. Ali, and MCF, unpublished data). Promiscuity is evident as the activity of several Rabs can likely be modulated by a single GTPase activating protein (GAP) (Field and O'Reilly, 2008). This suggests a level of integration within the endosomal system comparable to other eukaryotes. Furthermore, orthologues of several proteins involved in retrograde trafficking pathways in higher eukaryotes can be found within the genome. The presence of syntaxin 16 and Vps45 indicate the probable presence of a highly developed endosome to *trans*-Golgi network trafficking pathway (Dacks and Doolittle, 2004; Koumandou et al., 2007) and the retention of the COPI trafficking coat complex suggests functionality of both an intra-Golgi anteriograde and Golgi to endoplasmic reticulum (ER) retrograde route (Berriman et al., 2005). However, the presence and functional importance of retrograde transport in trypanosomes has yet to be addressed experimentally.

3.8. Surface receptors and endocytic pathways

As true parasites, trypanosomes are reliant on the host for many metabolic needs, and these have to be acquired. This poses a specific problem to the bloodstream stage trypanosomes, as they have to shield receptors and transporters from the immune system. Only low-molecular-weight molecules can pass across the surface coat and thus reach plasma membrane channels, receptors, or transporters. Macromolecules, however, must be

recognized by conventional receptors, and many are thought to be restricted to the flagellar pocket. Critically, the flagellar pocket is occluded from the surface and hence not accessible to many immune effectors, including lymphocytes (Overath et al., 1997). Further, rapid uptake and degradation, as discussed earlier for immunoglobulins, likely extends to additional factors, including complement.

Very few trypanosome receptor proteins have been characterized. The TfR is vital for trypanosomes since it provides the parasites with iron. In vertebrates, TfRs are *trans*-membrane proteins, but the trypanosome receptor is an example of convergent evolution and is unrelated to the metazoan receptor. The trypanosome TfR is a heterodimer, and the product of two ESAG genes, 6 and 7 (Salmon et al., 1994). The complex is anchored to the plasma membrane via a single GPI-anchor attached to ESAG6, and has structural similarity to VSG. *S*witching between ESs allows expression of different TfRs with distinct binding properties, which may facilitate adaptation to the distinct transferrin proteins encountered in different hosts (Gerrits et al., 2002). However, the biological significance of transferrin-based selective pressure to antigenic variation is a matter of debate, and the comparatively high concentrations of transferrin in mammalian sera also question the significance of comparatively small differences in affinity. Significantly, the ESAG repertoire itself is quite variable between different ESs, with the exception that all contain ESAG6 and 7, underscoring the importance of this receptor to the trypanosome.

Despite structural similarity between the trypanosome TfR and VSG, TfR appears not to be expressed on the cell surface (Mussmann et al., 2004). Instead most is retained by the flagellar pocket and the endosomal system, which may assist in ensuring that the TfR is not recognized by the immune system. While this may also be true for other receptor molecules, few have been identified unambiguously. Both the HbHp receptor and SRA, which are also GPI-anchored, appear to share a similar location to the TfR; it remains to be seen how general this phenomenon will be.

The mechanism by which receptors are sequestered to the flagellar pocket remains to be addressed. The number of lipid anchors has been suggested to play a role in TfR localization; while the ESAG6/7 dimer contains one GPI anchor, VSGs have two and are readily routed to the cell surface (Schwartz et al., 2005a). However, it is unclear how such a mechanism would operate, and importantly overexpression of TfR leads to the receptor spilling out onto the surface. The exclusive use of short GPI anchors (myristate, C14:0), which should more easily flip out of the membrane, is a bloodstream stage-specific feature. The exact roles of the GPI anchor, ectodomain sequences, and possibly also N- and O-glycans in flagellar pocket retention of proteins remain to be systematically evaluated.

Accumulation of host steroids is essential for trypanosomes, as they have a limited synthetic capacity. Bloodstream stage trypanosomes take up

low-density lipoprotein (LDL) significantly faster than fluid-phase cargo and this process is saturable and inhibitable. Two classes of receptor-binding site have been described, a low-copy high-affinity and a high-copy low-affinity site (Coppens et al., 1991). These sites are likely manifestations of the same receptor as manipulation of copy number has equivalent effects on both high- and low-affinity copy number. The LDL receptor itself has not been identified.

Appreciation of the organization, identity, and chemical nature of trypanosome flagellar pocket proteins remains in its infancy, and the absence of a validated flagellar pocket or endosomal proteome presents a considerable barrier to further investigation. Most significantly, high-molecular-weight pNAL-type N-glycans fill the pocket lumen and most probably contribute considerably to the gel-like matrix that fills the structure (Atrih et al., 2005). Many pNAL-containing proteins are clearly residents of the trypanosome endosomal system, which includes the flagellar pocket membrane (Nolan et al., 1999). It is likely that these high-molecular-weight glycans contribute to the trafficking of the glycoproteins that bear them, but again, until a full list of pNAL-bearing factors is forthcoming, it remains difficult to evaluate the full importance of this posttranslational modification to trypanosome endocytosis.

4. Developmental Remodeling and Signaling

In the transition between hosts the parasite must adapt to very different conditions, including nutrient sources, defense requirements, and temperature. This is facilitated by a differentiation program including at least two distinct phases. A preadaptation step involves differentiation to nonproliferative forms, metacyclic, or stumpy stages, which exhibit partial or full expression of final differentiated stage proteins. Differentiation is completed by full remodeling of gene expression and reentry to the cell cycle.

In terms of macromolecular trafficking, two features stand out that accompany these transitions. First is exchange of the major surface antigens, VSG expressed in the bloodstream form, and procyclins in the procyclic stage. A further surface switch also accompanies the transition to epimastigotes within the tsetse fly, where the procyclin coat is exchanged for BARP. Interestingly all of these proteins possess GPI anchors (Roditi and Lehane, 2008; Urwyler et al., 2007). The second aspect is the very large difference in endocytic capacity between the high rate in the bloodstream form and the much lower level in the procyclic stage.

At least in general terms, changes to the surface coat can be meaningfully interpreted. VSG is required for antigenic variation, and indeed is reactivated in the metacyclic stage in readiness of introduction into a

vertebrate host. Procyclins are highly charged and with a repetitive protease-resistant C-terminus. These proteins were proposed to mediate defense against trypanolytic factors in the tsetse fly, and while the ability of procyclin-null parasites to complete the insect portion of the life cycle clearly indicates that they are nonessential, it is likely that an important contribution is made, and that these procyclin-nulls are at a selective disadvantage (Vassella et al., 2009).

The augmentation of endocytic activity in the bloodstream stage is presumed to be an important component of immune evasion (Overath and Engstler, 2004; Field and Carrington, 2004), and this is supported both by the clear ability of the system to remove and degrade immune effectors from the surface (Engstler et al., 2007; Field and Carrington, 2004), as well as the observation that reactivation of the high endocytic rate is a component of metacyclogenesis, that is, part of the preadaptation of insect stage parasites (Natesan et al., 2007).

Developmental regulation of trypanosome trafficking does appear mainly restricted to endocytic pathways, and there is little evidence for changes to expression of factors associated with either ER exit, anterograde Golgi transport, or late exocytic factors between the two life stages, albeit with restriction of such analysis to mRNA levels only (Koumandou et al., 2008). While several endocytic factors are upregulated, including clathrin, Rab11 and RME8, a clear view of how the endocytic pathway is controlled does not emerge from transcriptome analysis. This may reflect the absence of transcriptional control, but is also likely a result of regulation by control of protein levels (Koumandou et al., 2008) and the participation of multiple enzymes and transient complexes in modulation of membrane transport. Significantly, the unfolded protein response, a pathway stimulated by increased concentrations of unfolded nascent chains in the ER, and which is mediated by increased transcription of key ER chaperones, including BiP, is also absent from *T. brucei* (Koumandou et al., 2008). Clearly, this is an area where further exploration is warranted.

5. Sorting Signals

5.1. Targeting at the ER

Retention of lumenal ER-resident proteins in higher eukaryotes requires the presence of a conserved C-terminal tetrapeptide sequence motif, mediating interaction with the Erd2 receptor (Lewis et al., 1990). The precise sequence varies in a species- and protein-specific manner, and in African trypanosomes the motif is divergent from the canonical XDEL motif, where X is any amino acid (Bangs et al., 1996). For example, the retention signal of TbBiP is MDDL and that of an ER-located protein disulfide isomerase

(PDI) is KQDL. Mutant forms of BiP where the native MDDL signal is replaced by KQDL or the mammalian signal sequence KDEL are efficiently retained in the trypanosome ER, indicating considerable flexibility in the sequence requirements for recognition by the trypanosome Erd2. The significance of this is unclear.

Trypanosome ER membrane proteins of trypanosomatids, for example, the ER Ca^{2+}-ATPase, also contain a C-terminal motif directing ER localization (McConville et al., 2002). This is also highly related to the higher eukaryote signal, and consists of the sequence KKXX in the cytosolic domain. While full exploration of the sequence requirements/restrictions for retention of either lumenal or membrane-spanning ER proteins in trypanosomes has not been achieved at this point, it is significant that the systems are so similar to higher eukaryotes, indicating a very early establishment of these mechanisms in eukaryotic evolution.

5.2. Endocytic and lysosomal targeting signals

In higher eukaryotes, several categories of sorting signal have been identified and include dileucine-based [DE]XXXL[LI] signals that promote interaction with adaptins, together with tyrosine-based NPXY/YXXØ motifs, lysine residues that provide sites for the addition of ubiquitin and addition of mannose-6-phosphate as a lysosomal marker (Braulke and Bonifacino, 2009). It appears that only part of this system of signals is conserved in trypanosomes. Most prominently, the mannose-6-phosphate system is absent, and no evidence for the residue, enzymatic activity for its synthesis, or genes corresponding to the biosynthetic enzymes is present.

Sorting of proteins to the lysosome can occur via a [DE]XXXL[LI]-related signal. However, whereas the dileucine motif in higher eukaryotes consists of an acidic cluster, with no specified amino acid sequence, followed by two leucine residues, the trypanosomal lysosomal protein p67 requires the two acidic amino acids DE to immediately precede the dileucine. The DELL sequence is both necessary and sufficient for lysosomal targeting as shown by the generation of a chimeric protein in which the C-terminus of the major lysosomal protein p67 was added to the ER-resident BiP, followed by mutagenesis of the DE or the LL motifs (Allen et al., 2007).

Endocytosis of *trans*-membrane proteins from the cell surface remains comparatively unexplored, and a full understanding of this topic remains to be achieved. A small selection of surface *trans*-membrane proteins have been studied, principally the ISG65 and 75 families and TbMBAP1, a membrane-bound acidic phosphatase (Chung et al., 2004; Engstler et al., 2005). ISG65 resides both on the cell surface and within early endosomes, but lacks dileucine or tyrosine-based signals. Targeting is instead achieved through ubiquitylation of cytoplasmic lysine residues (Fig. 1.5). TbMBAP1

localizes mainly to the endosomal compartment of *T. brucei*, where it is readily found in early, late as well as recycling endosomes. Stepwise localization to the flagellar pocket, the flagellum, and the pellicular cell surface can be achieved by increasing expression levels. It is unclear how sorting of this protein is achieved as again classical sorting signals are absent (Engstler et al., 2005).

5.3. Endomembrane sorting based on posttranslational modification

Two additional mechanisms may be operating in trypanosomes, and it is unclear if, or how, these are related to higher eukaryotic systems. pNAL N-glycans have been discussed earlier, and suggested to act as a sorting signal for endocytosis (Nolan et al., 1999); this is likely a rather unique mechanism specific to trypanosomes, but these high-molecular-weight N-glycans do resemble those found on many metazoan lysosomal membrane glycoproteins. Interaction with a specific, but yet unidentified, protein with pNAL-binding specificity in the flagellar pocket or endosomes could explain the retention of pNAL-containing proteins in the flagellar pocket thus restricting access to the cell surface. Secondly, GPI anchors have been implicated as sorting signals in African trypanosomes with protein localization dependent on GPI valence, whereby proteins containing two GPI anchors show a cell-surface localization, proteins with one GPI anchor are localized in the flagellar pocket and proteins with no GPI anchor are rapidly degraded in the lysosome (Schwartz and Bangs, 2007; Schwartz et al., 2005b). Full evaluation of these mechanisms must await further and more systematic study, and it is unclear how general either of these processes may be in terms of the range of trypanosome proteins that are sorted using one or other of these mechanisms.

5.4. Sorting to the flagellum

While not *sensu stricto* a component of the endomembrane system, it is becoming increasingly apparent that there is both a mechanistic and evolutionary connection between the endomembrane system and flagellar biogenesis. Targeting of flagellar proteins can occur via a tripeptide sequence comprising the amino acid residues HLA (Ersfeld and Gull, 2001). Deletion of this signal in the flagellar proteins PFRA and ARP severely compromises flagellar targeting of these proteins. However, not all flagellar proteins contain this tripeptide signal, and may reflect the presence of different pathways for import into the flagellum or of preformed protein complexes that require only one protein of the complex to carry the HLA signal. As many nonflagellar as flagellar proteins contain the HLA motif, suggesting

that the sequence is not sufficient for exclusive transport to the flagellum and that the structural context of the HLA motif likely makes an important contribution to function as a flagellar targeting signal. A further signal for targeting of proteins to the flagellum was discovered when two flagellar adenylate kinases, TbADKA and TbADKB, present in *T. brucei* were studied (Pullen et al., 2004). These two proteins contain an additional 55 amino acids at their N-terminus compared to other known adenylate kinases that are usually localized in the cytoplasm or mitochondria. Deletion of the N-terminal extension from the adenylate kinase and addition of the 55 amino acids to GFP demonstrated that the sequence is both necessary and sufficient for flagellar targeting. The extension contains a conserved motif comprised of the amino acids $YLX_4IPXLXE$, followed by two conserved proline residues. The receptor proteins that recognize these motifs have yet to be identified.

5.5. Sorting to the glycosome

In trypanosomes, enzymes of the glycolytic pathway are targeted to a peroxisome-related organelle, the glycosome (Sommer and Wang, 1994). This compartment is abundant within the cytoplasm of the bloodstream form, and retains an import system that is clearly derived from classical peroxisomal targeting pathways. Glycosomal import is mediated by two main peptide targeting signals, PTS1 and PTS2, that are well characterized and conserved across species (Hettema et al., 1999). PTS1 is a C-terminal tripeptide motif. In *T. brucei* functional tripeptides conform to the motif [S/A][K/S/H/R]L. This is comparable to the first C-terminal tripeptide motif SKL identified in firefly luciferase, which mediates peroxisomal targeting (Sommer et al., 1994). PTS2 is a nonameric peptide found at or in close proximity to the N-terminus. The consensus sequence is [R/K][L/V/I]X_5[H/Q][L/A/F] and *T. brucei* aldolases are imported into the glycosome via PTS2 (Chudzik et al., 2000). Additional targeting signals that work independently or in conjunction with PTS1 or PTS2 have been suggested. Studies on *T. brucei* PEPCK suggested the possibility of an additional internal signal about 40 amino acids upstream of the C-terminal SRL signal sequence (Sommer et al., 1994). Again, the level of conservation of these sequence motifs between trypanosomes and higher eukaryotes is remarkable, reflecting a common mechanism that has likely been maintained under strong evolutionary selective pressure. Significantly, while peroxisome/glycosome targeting signals are highly conserved, the function of the peroxisome has been dramatically altered in trypanosomes, and glycosomes appear to be restricted to the trypanosomatids, and clearly not present in metazoa or fungi.

6. Secretory Protein Folding and Exocytosis

6.1. Membrane protein biosynthesis

Production of the protein molecules that constitute the cell surface is initiated at the ER, and hence in this context the trypanosome ER is responsible for synthesis of the VSG coat, antigenic variation, and the host parasite interface. The ER is the site of *N*-glycosylation, disulfide bond formation, addition of GPI anchors, and protein folding into appropriate tertiary and quaternary structures. In addition, the ER possesses a mechanism for sorting appropriately folded proteins from incompletely or malfolded polypeptides and resident ER proteins, a process generally called quality control (Ellgaard et al., 1999; Sitia and Braakman, 2003). Recent work has unexpectedly found that if synthesis of the VSG polypeptide is interrupted by RNAi, then trypanosomes rapidly fall out of the cell cycle (Sheader et al., 2005). This is of particular interest, as one possible explanation is that the trypanosome possesses a specific checkpoint or quality control sensor that is able to monitor ongoing VSG synthesis, potentially placing a novel burden on the trypanosome ER.

6.2. Polypeptide delivery

Sorting of secretory and most membrane protein residents of the endomembrane system begins with targeted import into the ER. Translocation into the ER lumen or membrane is mediated by a cleavable N-terminal signal peptide (SP) or an internal signal sequence and occurs by either of two pathways. Interaction of the SP of the nascent protein with the signal recognition particle (SRP) leads to the ribosome complex being targeted to the translocon, through which the protein traverses the ER membrane cotranslationally. In the second SRP-independent pathway proteins are translocated posttranslationally from the cytoplasm into the ER. Here the SEC complex, that spans the ER membrane, interacts with the translocon to facilitate engaging of the signal sequence thus guiding the nascent polypeptide through the translocon. Both pathways require the active participation of the major ER-resident chaperone and ATPase BiP, which ensures directional movement of the protein into the ER.

In higher eukaryotes, nascent polypeptide delivery to the ER can be cotranslational or posttranslational (Abell et al., 2004; Kutay et al., 1995; Stefanovic and Hedge, 2007). In mammalian cells, SP-containing proteins are translocated exclusively by either one of these two pathways with the SRP pathway being predominant. In *Saccharomyces cerevisiae* posttranslational translocation is likely as prominent as the SRP-dependant translocation. In the former, entry is initiated by binding of a ribonucleoprotein complex,

composed of the 7SL RNA and six polypeptides comprising the SRP, to the SP of the nascent chain in an active ribosome (RNC) forming a SRP–RNC complex (Schwartz and Blobel, 2003; Walter and Johnson, 1994) in which translation is slowed or arrested. In a GTPase-dependent cycle (Bacher et al., 1996), the SRP–RNC complex is targeted to a membrane-bound SRP receptor (SR; Keenan et al., 2001; Seiser and Nicchitta, 2000) and SRP subsequently released. Translation resumes and the polypeptide is translocated through a translocation pore/translocon composed of three proteins forming the Sec61 complex, Sec61α, β, and γ (Rapoport et al., 1996). In posttranslational translocation, extensive folding and aggregation of the nascent polypeptide must be prevented and delivery of ribosome-free preproteins is by a cytosolic chaperone pathway, mainly involving the Hsp70 family (Egger et al., 1997; Wickner and Schekman, 2005; Yam et al., 2005). For proteins whose carboxy-terminal hydrophobic *trans*-membrane domains act as a signal, delivery is via multiple pathways (Rabu and High, 2007).

Downregulation of key components of each of these two pathways by RNAi in *T. brucei* indicates that most SP-containing proteins can be translocated by either pathway, though subsequent processing may be influenced by the pathway taken. Exceptions to this promiscuity are polytopic proteins, which are solely translocated by the cotranslational pathway, and GPI-APs, which are predominantly imported using an SRP-independent pathway. The preference of GPI-APs may be due to a less hydrophobic SP, mirroring the situation found in *S. cerevisiae*. However, studies here are at an early stage, and RNAi is an indirect method for characterizing such processes; the recent demonstration of reconstitution of ER translocation in a fully *in vitro* system in *T. brucei* will likely facilitate further biochemical dissection of this system. Significantly, although many eukaryotic signal sequences function in heterologous systems, the exact nature of the interaction between the SP and the translocation machinery may retain species-specific features. In particular, kinetoplastid signal sequences, though reliably predicted using standard *in silico* algorithms, frequently fail to direct translocation of secretory and membrane proteins when expressed in higher eukaryotic systems.

Polypeptide ER delivery, maturation, and quality control in the kinetoplastids is of evolutionary interest, and not simply due to divergence. These organisms have surfaces dominated by GPI-anchored molecules. While *T. brucei* has VSG, procyclin, and a heterodimeric TfR (Schell et al., 1991), the American trypanosome *T. cruzi* has abundant surface GPI-anchored mucins (Di Noia et al., 1998; Pollevick et al., 2000). In *Leishmania* lipophosphoglycan (LPG), free GPI lipids (GIPLs; Beverley and Turco, 1998) and GPI-anchored glycoproteins (Bahr et al., 1993) all contribute to surface architecture. These molecules are efficiently and rapidly synthesized and translocated to the surface, hence protein

maturation and ER function may be endowed with unique features in these organisms.

Trypanosomastids do have an unusual SRP complex. First, in addition to the ubiquitous 7SL RNA, they possess a short tRNA-like molecule, sRNA-76 in *T. brucei* (Béjà et al., 1993), and sRNA-85 in *Leptomonas collosoma* (Liu et al., 2003). Second, of the six polypeptides (Srp9/21, 14, 19, 54, 68, 72) of the higher eukaryote SRP, only Srp19, 54, 68, and 72 are present in *T. brucei* (Liu et al., 2003; Rosenblad et al., 2004). Interestingly, sRNA-76 binds the Alu domain or domain I of the 7SL RNA to which the absentees (Srp9/21 and 14) bind in other systems (Lustig et al., 2005). Knockdown of individual trypanosome SRP proteins is lethal and results in mislocalization due to sorting defects, but nascent polypeptides still transverse the ER (Liu et al., 2003; Lustig et al., 2005) possibly by a posttranslational chaperone pathway. In common with mammalian and yeast systems, the SRP is assembled in the nucleolus, but Srp68 and Srp72 are also involved in XPO1 assisted nuclear export (Biton et al., 2006). Putative genes encoding subunits of the nascent polypeptide-associated complex (NAC), a factor that works in concert with SRP in maintenance of high fidelity in ER targeting (Lauring et al., 1995; Wiedmann et al., 1994), are present in the trypanosomatid genomes, suggesting that this aspect is common between trypanosomes and higher organisms.

Data mining for members of the protein translocation apparatus in the *T. brucei* genome suggests multiple missing factors. For example, while the mammalian system has a heterodimeric SR (SRα and SRβ; Schwartz and Blobel, 2003; Tajima et al., 1986), only an SRα homologue is clearly present in *T. brucei,* inferring a minimal requirement for SR as in prokaryotes. However, the distant similarity of SRβ to GTPases of the Sar1/ARF family (Miller et al., 1995) may suggest that other uncharacterized trypanosome GTPases could fill the role of SRβ. Recently, Lustig et al. (2007) showed that RNAi of TbSRα caused accumulation of SRP–RNC complexes and inhibition of spliced-leader RNA synthesis, subsequently resulting in decreased mRNA levels. The trypanosome also encodes only two of the three Sec61 ER-translocon subunits (Sec61α and Sec61γ), while of the accessory proteins that function with the Sec61 complex in the higher eukaryote chaperone-dependent pathway, Sec62p, 63p, 71p, and 72p, only Sec63p and Sec71p are present in trypanosomes (Goldshmidt et al., 2008). However, several of these factors possess the Sec7 domain and several novel Sec7 domain-containing proteins are also present in the trypanosome genome, rising the possibility that a divergent factor or factors could function in concert with the translocon. While our knowledge here remains rather fragmentary, these highlighted variations suggest significant divergence between ER-targeting mechanisms in kinetoplastids and higher eukaryotes and could explain the poor translocation competence of *T. brucei* proteins when expressed in heterologous systems (Al-qahtani et al., 1998).

6.3. Polypeptide folding and maturation

Oligosaccharyltransferase (OST) is a multimeric enzyme complex that transfers a preassembled dolichol-linked core glycan, $Glc_3Man_9GlcNAc_2$, to asparagine residues exclusively within NXS/NXT glycosylation sequons within the nascent polypeptide during translocation (Chavan et al., 2005; Helenius and Aebi, 2001, 2004; Moremen and Molinari, 2006). The process is thus a component of both cotranslational and posttranslational pathways. The glycan moiety imposes a conformational constraint that retains the polypeptide in solution (Braakman, 2001) and its modification by the concerted action of numerous factors is important in subsequent folding and sorting events (Helenius and Aebi, 2001; Trombetta and Parodi, 2005).

Folding of the glycosylated polypeptides is carried out by ER-resident chaperones and other proteins such as lectins including; calnexin (CNX) and calreticulin (CRT), binding protein (BiP/GRP78), endoplasmin (GRP94), PDI, peptidyl-prolyl *cis-trans* isomerase (PPI), ERp72 and ERp57. In a CNX–CRT chaperon pathway, glucosidase I and II (GI and GII), sequentially remove the first and second glucose residues of the polypeptide-bound glycan (Moremen and Molinari, 2006). The resultant $GlcMan_9GlcNAc_2$ is recognized by membrane-bound CNX and/or its soluble homologue CRT forming a complex that prevents aggregation, premature oligomerization, and formation of nonnative disulfide bonds. While bound to CNX–CRT, the glycoprotein is presented to a thiol oxidoreductase homologue of PDI, ERp57, forming short-lived disulfide bonds, and consequently catalyzes folding through formation and reshuffling of intra- and intermolecular disulfide bonds before the monoglucosylated glycan–polypeptide intermediate is released (Cai et al., 1994; Hebert and Molinari, 2007). Based on biophysical properties such as exposed hydrophobic patches, unpaired cysteines, immature glycans (Meusser et al., 2005), a folding sensor UDP-glucose:glycoprotein glucosyltransferase (UGT1) scans through the glycoprotein directing nearly native misfolded intermediates for reglucosylation and into another CNX–CRT cycle, while misfolded intermediates are transported to the cytosol for degradation by the proteasome (Caramelo and Parodi, 2007; Hebert and Molinari, 2007). Conformers are finally deglucosylated by GII prior to aided selection by a type I lectin, ERGIC-53 (Appenzeller et al., 1999; Klumperman et al., 1998) and exported to the Golgi apparatus. BiP is a master ER regulator involved in multiple functions (Hebert and Molinari, 2007) and acts at least in two ways in the folding process. First, sequentially through binding and preventing aggregation and secondly through delivery of nascent polypeptides to additional chaperones such as glucose-regulated protein 94 (GRP94), a glycoprotein involved in late folding steps. BiP recognition of the hydrophobic domains of nascent polypeptides and subsequent release is

mediated through repetitive cycles of ATP hydrolysis and ADP exchange (Gething, 1999) while participation in complexes composed of Grp94, ERdj3, Grp170, lectins, and additional factors serves to bring such factors into proximity with folding polypeptides (Shen and Hendershot, 2005; Tatu and Helenius, 1997; Zhang et al., 1997).

The domination of the trypanosome surface by GPI-anchored molecules and the emphasis on a limited number of superabundant antigens prompts expectations of evolution of highly selective and efficient folding pathways, modification, and export mechanisms. Indeed, some clear differences with higher eukaryotes do exist, starting with the missing gene products discussed earlier. Further, the otherwise universal dolichol-linked N-glycan precursor varies from other eukaryotes (Labriola et al., 1999), among trypanosomatids and between life stages (de la Canal and Parodi, 1987; Parodi, 1993). Trypanosomes transfer an unglucosylated glycan, $Man_{9–5}GlcNAc_2$ and additional highly unusual biantennary mannose-based structures; specifically $Man_{3–4}GlcNAc_2$ in *T. brucei* (Jones et al., 2005; Zamze et al., 1991), $Man_{7–9}GlcNAc_2$ in *T. cruzi*, and $Man_{6–7}GlcNAc_2$ in *Leishmania* spp. as opposed to $Glc_3Man_9GlcNAc_2$. This appears to be due, at least in part, to an inability to synthesize the glucosyl donor dolichol-P-Glc (de la Canal and Parodi, 1987) and is possibly due to loss of biosynthetic gene products (Manthri et al., 2008) while intraspecies variation may be an aspect of developmental regulation.

The subunit composition of OST ranges from one to eight polypeptides across the eukaryota; trypanosomastids retain a single subunit, the catalytic Stt3p (Kelleher and Gilmore, 2006). The absence of OST compositional complexity is suggested as a reason for the accumulation and transfer of a single dominant glycan moiety (Castro et al., 2006). The unglucosylated glycan-polypeptide is first bound by BiP, an essential protein in *T. brucei* (Subramaniam et al., 2006). BiP's cochaperone, a GRP94 homologue, is also present, while additional BiP cofactors, including ERdj3, have homologues present in *T. brucei*. Some of the over 20 putative DnaJ chaperone proteins encoded in the genome could also be involved in folding of nascent polypeptides in the trypanosome ER.

The trypanosome lectin chaperone system has only CRT (Labriola et al., 1999). Though CRT and CNX share a common ancestry through gene duplication (Navazio et al., 1998), the presence of only CRT in trypanosomes suggests CRT as a minimal requirement for protein folding. A recent study demonstrated variation in glycoprotein dependence on CNX/CRT in higher eukaryotes and importantly, the ability of CRT to effectively substitute for CNX in certain circumstances (Molinari et al., 2004). Moreover, the observation that loss of either lectin alone did not compromise protein folding supports the model that CRT represents a fully functional system in trypanosomes. Interestingly, protein folding in CRT-deficient cells is compromised only for specific proteins (Knee et al., 2003); this could

suggest that evolutionary selection may have been sufficient to remove the need for both CNX and CRT from the trypanosomatid lineage.

Polypeptide disulfide bonds can be formed by both class I and II PDIs and several PDI-like proteins are present in trypanosome genomes. Earlier studies showed downregulation of a class II TbPDI in PCF. Similarly observations on both class I and II PDIs as well as an unexpected endosomal localization and inessentiality on knockdown have also been made (Hsu et al., 1989; Rubotham et al., 2005). Since cysteine residues that form disulfide bonds in mature VSGs are highly conserved (Carrington et al., 1991), PDI knockdown could be expected to result in anomolous VSG folding; the lack of such a phenotype potentially implicates other PDI-like proteins and/or oxidoreductases present in the genome as being capable of assisting VSG to fold.

Partially folded proteins are detected by trypanosome UGT and subsequently glucosylated into monoglucosylated polypeptide intermediates for refolding (Conte et al., 2003; Trombetta et al., 1989). Consequently, trypanosomastids lack GI activity but have retained GII for deglucosylation of fully folded polypeptides. Functional analysis of *T. brucei* GII revealed unique features in trypanosome folding and possible roles for the variant N-glycan dolichol-linked precursors (Jones et al., 2004; Jones et al., 2005). Trimming of high mannose forms could be carried out by any of several α-mannosidase I proteins in *T. brucei* (Tb927.82910-40) while a putative mannose-specific lectin (Tb11.02.1680) could have a role in recognition of specific oligomannosyl structures. Appropriately folded/assembled proteins are subsequently trafficked to post-ER compartments.

6.4. ER exit to the Golgi complex or ER-associated degradation (ERAD)

Precision in sorting and export of nonresident ER proteins and retrieval of escaped resident factors is key to maintenance of a constant ER composition. Defects in these processes can be catastrophic and are associated with specific disease states in mammals (Castro-Fernández et al., 2005). Natively folded proteins and/or appropriately assembled multimeric complexes are selectively segregated from resident ER proteins at organized membrane domains called ER exit sites (ERES) or transitional ER. Here, cargo molecules are packaged and trafficked in COPII coated vesicles to the Golgi complex (Antonny and Schekman, 2001; Barlowe, 2002). Sar1p, a small GTPase, coordinates cargo and COPII cytosolic coat complexes recruitment at the ERES. Sar1p is initially activated by conversion from the GDP- to GTP-bound state by an ER-bound *trans*-membrane guanine nucleotide exchange factor (GEF) Sec12p (Barlowe and Schekman, 1993; Nakano et al., 1988). Sar1p-GTP inserts into the ER membrane (Huang et al., 2001), recruits the Sec23/24p heterodimer, forming a cargo selecting

prebudding complex (Kuehn et al., 1998) that recognizes export signals. The Sec13/31p subcomplex, a driver for coat polymerization, membrane curvature, and activator of the Sec23p GTPase activity, is subsequently added to the cargo complex (Barlowe, 2002; Kuehn et al., 1998; Lederkremer et al., 2001) generating coated vesicles. Other factors have also been implicated in this assembly (Sato and Nakano, 2007).

Irreversibly misfolded proteins are destined for ERAD. Some are quiescently retained by the ER or transported to the Golgi and later retrieved to the ER (Hammond and Helenius, 1994; Kincaid and Cooper, 2007; Klausner and Sitia, 1990; Young et al., 1993) while others are retrotranslocated to the cytosolic proteasome or vacuole (Hong and Kaiser, 1996). Selection is based on exposed hydrophobic peptide patches, signal sequences, or *trans*-membrane domains. Distinction from folding intermediates is achieved by a slow-acting enzyme, mannosidase I which removes terminal mannose residue (Jacob et al., 1998) and trims only persistently misfolded proteins (Ellgaard and Helenius, 2001). The resultant intermediate is recognized by a further lectin, ER degradation-enhancing α-mannosidase-like protein (EDEM), that also interacts with CNX and possibly releases aberrant proteins from the cycle (Molinari et al., 2003; Oda et al., 2003; Wang and Hebert, 2003). Other mechanisms of segregation have been proposed (Caramelo and Parodi, 2008). BiP and two interacting partners, Scj1 and Jem1, are also involved in directing misfolded soluble proteins for degradation (Nishikawa et al., 2001; Plemper et al., 1997). Retro-translocation occurs through the Sec61 channel (Pilon et al., 1997; Tsai et al., 2002; Wiertz et al., 1996).

Homologues of the COPII exit machinery are clearly present in trypanosomes (He et al., 2004). As in other eukaryotes, the trypanosome translocon could be involved in retro-translocation of misfolded proteins. A functional ERAD system most likely is also functioning since four homologues of mannose-binding proteins, potentially representing mannosidase I and EDEM, are present in the genome. In addition, ER retention and subsequent degradation of structurally faulty VSGs (Böhme and Cross, 2002; McDowell et al., 1998; Wang et al., 2003) or mistargeting (Triggs and Bangs, 2003) are clear indications of an active ER-based quality control and ERAD machinery. DnaJ domain-containing proteins, potential cochaperones of BiP including Scj1 and Jem1 are also present.

The high abundance and rates of synthesis and traffic of many surface proteins and extensive previous work on protein traffic make further exploration of trypanosome exocytosis feasible. With most candidates of this system experimentally uncharacterized, much more investigation is required to fully understand trypanosome protein folding, and especially on the possible roles this process may play in parasite survival in the mammalian host.

7. Golgi Apparatus; Functions and Replication

The Golgi apparatus is a highly organized and dynamic structure, reflected by the role of the Golgi complex as a site for glycan elaboration and macromolecular sorting, producing a huge array of glycan structures essential for parasite cell survival, but whilst also receiving constant input from anterograde and retrograde trafficking pathways. *T. brucei* contains a single Golgi apparatus comprising flattened cisternal membranes arranged in a stacked configuration, proximate to an ERES (Grab et al., 1997). The overall architecture of the organelle is instantly recognizable by electron microscopy and is highly similar to the structure as described for higher eukaryotes. The entry face of the organelle, the *cis*-Golgi network, most likely receives the entire cohort of proteins and majority of lipids derived from the trypanosome ER. Material is then processed before being sorted to final destinations from the exit face, the *trans*-Golgi network, again homologous to the higher eukaryote structure (Mellman and Warren, 2000). However, our understanding of the detailed functions resident within the trypanosome Golgi apparatus is not very advanced, and certainly we cannot yet evaluate the presence and importance of any trypanosome-specific functions or organizational features.

7.1. Golgi replication by binary fission

The environment encountered by trypanosomes in the mammalian host appears to dictate that a fully functional exocytic system is required, exemplified by a block in cytokinesis upon knockdown of VSG expression (Lillico et al., 2003; Sheader et al., 2005). It is unclear if this is a direct result of sensing of loss of VSG molecules, emptying of the exocytic pathway (VSG accounts for the major bulk of biosynthetic exocytic polypeptide), or some more complex mechanism unrelated to exocytosis. Evidence from higher eukaryotes indicates that the Golgi complex cannot arise completely *de novo* (Shorter and Warren, 2002), and hence the presence of a single Golgi apparatus in the trypanosome has the consequence that faithful replication and segregation during mitosis is essential to avoid creation of daughter cells lacking the Golgi organelle. Contrary to mammalian cells, Golgi biogenesis in trypanosomes occurs early in the cell cycle (Field et al., 2000) and probably by binary fission; fragmentation as observed in mammalian cells is never seen (Shorter and Warren, 2002). The process occurs in a highly coordinated and regulated manner, just after basal body (BB) duplication. The signals for initiation of replication are currently unknown, however, the order in which the trypanosome Golgi complex is assembled and the mode of inheritance

have recently been elucidated in considerable detail, and may indicate some novel aspects to Golgi biogenesis in trypanosomes.

Visualizing a GFP fusion of the trypanosome paralogue of the Golgi reassembly stacking protein, GRASP55/65, revealed that the new Golgi apparatus appears independently of the preexisting Golgi complex concurrent with emergence of a new ERES during early stages of mitosis. Interestingly, although the new Golgi appears *de novo*, photobleaching experiments using the Golgi-resident enzyme *N*-acetylglucosamine transferase B as a probe show that the ERES is not the sole source of new Golgi material (He et al., 2004). Membrane components traffic from the old to the new Golgi complex highlighting the role of the old organelle and raising the question as to the identity of the transfer carriers. More recent work using additional markers indicates that growth of the new Golgi complex is at least a two-stage process; structural and enzymatic components are laid down first, followed by those necessary to move and sort cargo in transit (Ho et al., 2006).

7.2. Role of the cytoskeleton in Golgi complex replication

Centrins, calcium-binding proteins associated with microtubule organizing centers including the BB, are also implicated in trypanosome Golgi biogenesis. The trypanosome orthologue of centrin-2 marks a bilobed Golgi-associated structure throughout the cell cycle, and is essential for Golgi duplication. This centrin-2 containing structure partially overlaps the new ERES and may serve to position the exit site in a process coupled to microtubule dynamics. A further possibility is that the structure defines a physical link between the new Golgi apparatus and the associated ERES, thus defining the location where Golgi biogenesis occurs (He, 2007; He et al., 2005). Indeed, depletion of polo-like kinase (TbPLK), essential for replication of the centrin-2 structure, results in a malformed bilobe and numerous dispersed Golgi-like structures throughout the cell. However, although their exact structure and function remains obscure, the appearance of satellite Golgi-like structures without an associated centrin-2 bilobe are normal parts of the trypanosome cell cycle, and the multiple structures present in TbPLK depleted cells therefore could represent an enlarged population of satellite Golgi-like organelles, implying a role for centrin-2 in determining Golgi size (de Graffenried et al., 2008; He et al., 2004). Certainly, studies of this process in trypanosomes should be especially informative due to the smaller and more compact nature of the Golgi complex compared to higher eukaryotes.

There is also evidence for developmental aspects of Golgi complex regulation, that is, that the organelle in procyclic forms may be regulated in a manner distinct from the BSF. For example, the PCF Golgi apparatus is

almost double in size and contains more cisternae compared to the BSF. This may reflect differential demands on the secretory system, and specifically an altered requirement for polypeptide-associated glycan elaboration (discussed in Field and Carrington, 2004). However, the presence of very large *N*-acetyllactosamine repeat N-glycans in a subset of BSF endosomal proteins and the presence of similar structures on the procyclin GPI-anchor may indicate a comparatively constant level of Golgi-mediated carbohydrate synthesis between life stages. However, developmental alterations are supported by a much increased expression of TbRab18 in the PCF and altered distributions of additional Golgi-resident Rab proteins (Dhir et al., 2004; Field et al., 2000; Jeffries et al., 2002). Moreover, knockdown of the ARL1 GTPase involved in maintenance of Golgi integrity only causes cell death in BSF and not PCF (Price et al., 2005). The functional consequences of these developmental differences between life stages and their implications for mechanisms of Golgi biogenesis remains unknown.

7.3. Cell-cycle and life-cycle coordination of Golgi complex replication and function

During the G2 phase of the cell cycle, duplicated BB and kinetoplasts separate in a microtubule-dependant manner (Robinson and Gull, 1991), and several lines of evidence now show that this is essential for Golgi complex segregation. Pharmacological inhibition of BB separation also inhibits Golgi segregation (He et al., 2004), and a pool of BB-associated centrin-2 may serve to connect duplication of these organelles in a manner similar to mammalian cells (He, 2007). Furthermore, centrin-1 is implicated in the spatial positioning of multiple organelles required for the initiation of cytokinesis in *T. brucei*. In addition, centrin-1 also localizes to the BB and a bilobed structure in close proximity to the Golgi complex. However, the two centrins do have distinct functions, as only centrin-1-depleted cells possess multiple BB and Golgi complexes suggesting that centrin-1 may function in organelle segregation rather than duplication *per se* (Selvapandiyan et al., 2007). Finally, a novel role for the class III PI-3-kinase Vsp34 in Golgi segregation has been demonstrated in trypanosomes. Attenuation of TbVsp34 levels severed the spatial connection between BB and Golgi complex replication and positioning; the two cisternae replicate but fail to segregate, resulting in considerably enlarged Golgi stacks with an increased number of cisternae (Hall et al., 2006). Employing interconnected duplication in this manner appears to facilitate coordinated biogenesis of multiple trypanosome organelles and hence their accurate partitioning at cytokinesis.

7.4. Retrograde transport

It is well established in yeast and mammalian cells that retrograde transport pathways are vital for correct functioning of the Golgi complex (Pavelka et al., 2008; Sannerud et al., 2003). However, the mechanism of delivery of material, and the extent to which this occurs, remains unresolved, and the role of retrograde transport pathways in organelle biogenesis remains an open question. As *T. brucei* contains orthologues of both retromer and COPI complex subunits, both of which participate in retrograde transport in higher eukaryotes, this is likely indicative of some functional conservation of these pathways (Berriman et al., 2005; J.B. Dacks, MCF, and V. Koumandou, unpublished data). Direct functional studies are clearly required to establish if such retrograde pathways are indeed operational in trypanosomes and what role, if any, they play in Golgi complex biogenesis and maintenance.

8. Ubiquitylation and Endocytosis of *Trans*-Membrane Domain Proteins

A fundamental issue in protein sorting is defining the mechanism by which the endomembrane system machinery is able to discriminate between different cargo. A comparatively limited set of polypeptide signals, together with diverse physicochemical properties dependent on the mode of membrane attachment, appears to account for this process. In trypanosomes, and especially the bloodstream stages, the sheer bulk of VSG at the surface possesses a considerable challenge for faithful sorting of any non-VSG polypeptides.

8.1. The VSG sorting problem

VSG is present at $\sim 10^7$ copies per cell, overwhelmingly as dimeric forms, representing $\sim 90\%$ of cell-surface glycoprotein. The turnover of VSG is extremely slow; loss of VSG from the cell occurs with a half-life in excess of 36 h, and detailed analysis of the fate of VSG suggests that the vast majority of this loss is via slow shedding, such that if all degradation were by internalization and proteolysis, the half-life of VSG would be in excess of 250 h (Seyfang et al., 1990), more than 30 cell generation times. Therefore, VSG is recycled with extreme efficiency, and any degradation of the polypeptide is a minor pathway. Knockdown analysis indicates that maintenance of the expression level of VSG is essential for viability and continued normal morphology (Sheader et al., 2005), suggesting

that even in the absence of antigenic variation there is a considerable burden to the trypanosome cell to maintain the surface VSG density at correct levels.

In sharp contrast, the major families of type I *trans*-membrane domain proteins, the ISGs, are represented at more modest copy number; both ISG65 and ISG75 are at $\sim 10^4$ copies per cell (Ziegelbauer and Overath, 1992), that is, a 1000-fold lower than VSG. Moreover, these ISG polypeptides are actively degraded with half-lives of ~ 4 h (ISG65) and ~ 2 h (ISG75) (Chung et al., 2004, K.F. Leung and MCF, manuscript in preparation). Therefore, for the ISGs, degradation represents the major fate of the protein, and recycling makes a comparatively modest contribution to the itinerary. Given that all endocytosis is mediated by a single clathrin-mediated mechanism, this is independent of AP-2 (Morgan et al., 2002), and both VSG and ISG are dependent on TbEpsinR as discussed earlier, how is such selectivity achieved? At least part of the process appears to be due to posttranslational ubiquitylation of the ISG proteins.

8.2. Ubiquitylation and endocytosis

In higher eukaryotes, the contribution of ubiquitylation to endocytosis has been well characterized (Williams and Urbé, 2007). Several surface receptors, including the growth hormone and epidermal growth factor receptors are modified by ubiquitin at the cell surface; this process requires the action of highly specific plasma membrane E3 ubiquitin ligases that transfer the ubiquitin to the target molecule (Katzmann et al., 2002, 2004); at least two, c-*cbl* and Rsp5, have been described that carry out this function in metazoa and yeast. Both monoubiquitylation and oligoubiquitylation appear to take place, which contrasts with the polyubiquitylation that occurs on soluble cytoplasmic proteins destined for degradation by the proteasome, and presumably confers specificity in recognition. Ubiquitylated endocytic cargo molecules are recognized by a number of factors, most of which utilize a conserved UIM to facilitate the interaction; UIM–ubiquitin interactions are low affinity (Babst, 2005), but the large number of the UIMs present in the system likely facilitate sequential handing off of ubiquitylated molecule as it progresses through the endosomal pathway. Further, several UIM-containing proteins, for example epsin, also interact with both the lipid bilayer and clathrin, providing a mechanism for recognition and incorporation of ubiquitylated cargo into clathrin-coated pits. Ubiquitylated cargo is ultimately handled by the ESCRT system, a supercomplex that in higher eukaryotes, at least, contains ~ 20 distinct polypeptides. Final disposal of the ubiquitylated protein requires the action of a deubiquitylation peptidase, Doa4p, that removes the ubiquitin and allows the cargo molecule to be further degraded by the lysosome (Clague and Urbé, 2006).

8.3. ISGs are ubiquitylated

Until recently, this entire system was uncharacterized in trypanosomes. While a clear role for ubiquitylation in protein turnover, and hence cell-cycle progression, has been demonstrated by knockdown of individual components of the trypanosome proteasome, as well as via inhibition with proteasome blocking compounds (Li and Wang, 2002; Mutomba et al., 1997), a role in intracellular trafficking has not been defined. Interestingly, the cytoplasmic domains of the ISGs are rather short, between 28 and 35 amino acids (Fig. 1.3). The absence of dileucine or tyrosine-based canonical endocytosis signals, which are represented on the lysosomal protein p67, for example (Allen et al., 2007; Tazeh and Bangs, 2007), but the conservation of a high proportion of lysines within these sequences (11–15%) is suggestive of ubiquitylation. Further, in contrast to earlier reports, it is apparent that the ISGs have a substantial endosomal presence in addition to their expression at the cell surface (Chung et al., 2004).

The *trans*-membrane and cytoplasmic domains of ISG65 or ISG75 are sufficient and necessary for targeting to endosomes and the plasma membrane (Chung et al., 2004, 2008; K.F. Leung and MCF, unpublished data), and precludes a major role for the ISG ectodomain in targeting. Further, deletion mutants demonstrate a role for the cytoplasmic domain of ISG65 in anterograde transport as removal of the 16 very C-terminal residues traps the protein within the ER. Mutagenesis demonstrates a role for the cytoplasmic lysine residues in endocytosis, turnover, and ubiquitylation of both ISG65 and ISG75 (Chung et al., 2008; K.F. Leung and MCF, unpublished data). Moreover, the reporter protein is oligoubiquitylated, with up to five ubiquitin chains. Remarkably, this is identical to the situation in higher eukaryotes, indicating a very ancient evolutionary origin and retention of this process (Williams and Urbé, 2007).

Significantly, these observations indicate a hierarchy in the importance of cytoplasmic lysine residues, with those at the C-terminus bearing a predominant role as ubiquitin acceptors (Chung et al., 2008). However, there is also sequence context at work, and this hierarchy is not just the result of proximity to the C-terminus and/or distance from the cell membrane. C-terminal fusion of the ubiquitin-like polypeptide, NEDD8, does not support additional ubiquitylation, despite presenting a number of new sites for modification. However, at variance with the system in higher eukaryotes is the finding that the trypanosome lacks clear homologues of Rsp5 or c-Cbl (Chung et al., 2008), and at present the ubiquitin ligases remain unknown.

Internalization of ISGs is presumed nonselective (Field and Carrington, 2009; Grünfelder et al., 2003), but there is a clear compartment where such a sorting could take place, post the early endosome, and which also contains clathrin coats on the cytoplasmic membrane face (Grünfelder et al., 2003).

In this structure, VSG clearly segregates into the central regions of cisternae and away from clathrin, which is localized to peripheral budding profiles. It is possible that ubiquitylated cargo is separated via preferential incorporation into clathrin-rich membrane domains.

8.4. Late endocytosis and the multivesicular body

The final steps in turnover of ubiquitylated molecules are also broadly homologous to higher eukaryotes, with at least one important distinction. *In silico* analysis demonstrates that the ESCRT system is highly conserved, and in trypanosomes the majority of the ESCRT subunits are represented in the genome (Leung et al., 2008 and table 1). Representatives of ESCRT I-complex factors can be localized to the endosomal system and are juxtaposed to Rab5 early endosomes and the lysosome, a position closely paralleling higher eukaryote MVBs. Knockdown of TbVps23, one of the ESCRT I factors, leads to partial inhibition of ISG65 degradation, while treatment with weak bases suggests that degradation requires the function of low pH compartments, strongly indicative of a role for ESCRTs and MVBs in this process (Chung et al., 2008; Leung et al., 2008). The major difference between higher eukaryotes and trypanosomes, which is in fact shared with all non-Opistokhont taxa, is the absence of the ESCRT 0 complex (Fig. 1.6). ESCRT 0 is a heterodimer that has been implicated in several processes, including recognition of ubiquitylated cargo via a UIM motif in Vps23/HRS, membrane attachment through a PIP3-binding FYVE domain in Hse1/STAM, and also in recruitment of the ESCRT I complex (Babst, 2005). The latter is present in higher eukaryotes as both soluble and membrane-bound populations, a property shared with the trypanosomes. These data suggest that a distinct mechanism must exist in trypanosomes for both initiation of ESCRT assembly at the endosomal membrane and also for recognition and delivery of ubiquitylated cargo into that compartment. It is formally possible that a divergent ESCRT 0 complex, that has not been detected *in silico,* is present but restriction to animals and yeasts strongly suggest this is a lineage-specific innovation. Rather, the possibilities that either ESCRT I directly binds endosomes or that a completely distinct mechanism is acting are attractive and aspects that require further analysis.

Overall, the identification of ubiquitylation as a mechanism for internalization of ISGs explains many facts. Firstly, absence of canonical endocytosis motifs from these proteins, but their efficient internalization is now explained. Secondly, these insights also show how endocytosis can function in the absence of AP-2, and further that sorting probably does not take place at the plasma membrane. Further, the involvement of the ESCRT complexes also explains the presence of MVB profiles as seen by ultrastructure, and suggests a mechanism for segregation of GPI-anchored and *trans*-membrane domain proteins. It is currently unknown if other *trans*-membrane domain

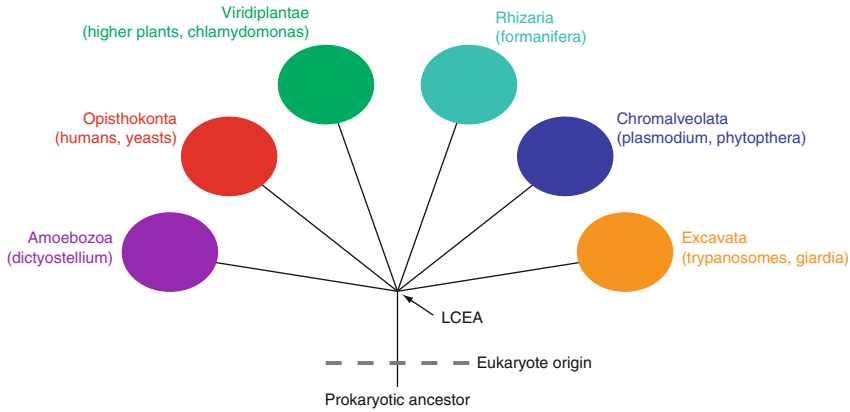

Figure 1.6 Simplified eukaryotic phylogeny. Each supergroup is represented by a colored lollipop, and representative species are indicated by each. An unresolved root, corresponding in the last common eukaryotic ancestor (or LCEA) is shown. The detailed implications of this view of eukaryotic lineages are discussed elsewhere, but the relevant point for this discussion is the absence of a primitive versus modern lineage. However, trypanosomes are highly derived organisms due to their parasitic lifestyle and coevolution with vertebrate hosts for tens of millions of years.

proteins enter this pathway. Finally, the possibility that ubiquitylation could be exploited for therapeutic gain is raised. Significant differences in the E3 ligases appear to be present, with the exciting possibility that if the factors responsible for modification of ISGs can be identified, then specific inhibitors may be designed.

9. Evolution of the Trypanosome Endomembrane System

9.1. Changing views of the eukaryotic tree of life

Our views of the evolution of the eukaryotes, and hence the position of trypanosomes within this history, have been revolutionized in the last 5 years (Adl et al., 2005). A reexamination of taxon relationships, facilitated by major advances in DNA sequencing technology and hence the quantity of molecular data, together with recognition of technical issues with earlier topologies based on rRNA data (Dacks et al., 2008b) has led to a redrawing of the tree of life (Fig. 1.6). Principal implications of this new topology are that a rapid explosion of eukaryotic lineages occurred early in evolutionary history, and that this radiation was so fast as to preclude robust resolution of branching

order at the deepest levels (Embley and Martin, 2006). The result is a view of eukaryotes as comprised of at least six supergroups, all originating at approximately equivalent times. The major consequences are that protistan lineages can no longer be considered as ancient (or metazoa and yeast as modern), nor is there evidence for long periods of common evolutionary history between the members of different supergroups. Experimentally, this means that trypanosomes are no closer to the last common eukaryotic ancestor (LCEA) than yeasts, plants, or amebae. A further consequence is that one cannot extrapolate, with any degree of accuracy, across supergroups, unless there is additional good evidence to do so. Trypanosomes and *Plasmodium*, for example, do not share an early origin, and hence are not especially related. It is, therefore, essential that model organisms representative of individual supergroups are carefully selected, so that a broader understanding of the diversity of the eukaryota can be obtained (Dacks et al., 2008a,b). Fortunately, the African trypanosome is well placed in this regard, being very experimentally tractable, and as a result has attracted considerable attention as a model system for evolutionary cell biology.

9.2. Comparative genomics

The application of comparative genomics to trypanosomes has uncovered a significant level of divergence between these organisms and the higher eukaryotes. Many of these are examples of lineage-specific features that appear restricted to the Opisthokont, and therefore are not unique features of trypanosomes. The list of absences includes ESCRT0, caveolin (suggesting the absence of large stable lipid rafts), the GGA and stonin sorting adaptors, some GRASPs, UIM-containing ENTH-domain proteins (true epsins), and numerous factors that are part of the clathrin interactome (Field et al., 2007a,b; Gabernet-Castello et al., 2008; MCF and J.B. Dacks, unpublished data). Some uncertainty remains concerning the absence of specific factors, that is, if these are true absences or just undetectable, but overall it is clear that trypanosomes lack a considerable number of trafficking factors. These observations do suggest, however, that while trypanosomes cannot be considered as ancient, the absence of many Opisthokont-specific factors indicates that they may be more representative of the vast majority of lineages, and, in this context at least, that they are perhaps more similar to the LCEA. However, there have been few successful attempts to identify trypanosome trafficking factors that do not directly depend on a knowledge of Opisthokont systems, and hence any truly novel factors likely remain to be described, the "asymmetry" problem (Dacks and Field, 2007).

9.3. G-protein signaling complexity and evolution

Exploration of the potential signaling complexity that subtends and integrates the trypanosome trafficking system is also relatively uncharted, and our lack of information concerning molecular pathways remains a major challenge. The kinome is of relative high complexity, but the functions of the vast majority of these factors are unexplored (Parsons et al., 2005). Significantly several kinases are implicated in control of endocytosis, which may suggest some similarity with higher eukaryotes (Koumandou et al., 2008; Pelkmans et al., 2005) and there is clear evidence for a role for phosphoinositide-based signal transduction (Hall et al., 2005a,b; Rodgers et al., 2007). The ratio of the numbers of Rab to Rab GAPs genes is comparable to that found in many unicellular systems distributed across the eukaryota (Field and O'Reilly, 2008) and the level of connectivity within the Rab and GAP interactome is also remarkably similar between trypanosomes and *S. cerevisiae* (C. Gabernet-Castello and MCF, unpublished data); while very preliminary, these observations are suggestive of a conserved level of integration between trafficking in trypanosomes and other unicellular organisms.

However, several lineage-specific factors have been uncovered. For example, three of the trypanosome Rab proteins, X1, X2, and X3, appear to be restricted to the Excavata. At the time of writing, it is unclear what the functions of these three proteins may be, although double gene knockout has shown that X1 and X2 are nonessential *in vitro* or *in vivo,* and a specific role in trafficking has so far eluded characterization, despite a clear location for RabX1 and RabX2 on exocytic compartments (Field et al., 1999, 2000; S. Natesan et al., submitted for publication). Comparisons of the Rab gene repertoire between *T. brucei* and *Leishmania* and *T. cruzi* has demonstrated the presence of likely secondary losses in *T. brucei* as both of the other kinetoplastida genomes encode additional Rabs, some of which are shared across the eukaryota, suggestive of a presence in the LCEA (Ackers et al., 2005; Berriman et al., 2005). The selective pressure that has molded the Rab repertoire is unclear, but the trivial explanation that the simpler system in *T. brucei* is due to loss of cell-invasive forms can be confidently rejected as the ancestral kinetoplastid was almost certainly free-living, and the intracellular stages of *Leishmania* and *T. cruzi* are the later adaptation. A final insight from the Rab gene family is that the division of endocytic pathways is also lineage specific. In particular, Rab5 plays an intimate role in control of the early stages of endocytosis, and this is common between trypanosomes and higher eukaryotes (Pal et al., 2002a,b; Zerial and McBride, 2001). Further, most species possess more than one Rab5 (*T. brucei* possesses two, 5A and 5B) and there is good evidence that this represents division of early endocytosis pathways. Unexpectedly, phylogenetic analysis indicates that the Rab5 subfamilies arose following the radiation of the supergroups

(Dacks et al., 2008a,b); significantly this suggests independent evolution of multiple Rab5 isoforms, and hence the selective pressure for such differentiation has been separately exerted on the individual supergroups. But, this also indicates that the precise manner in which division of labor between the Rab5 subfamily members is likely distinct to each lineage. However, the Rab5 subclasses were established prior to separation of *T. brucei* and *Leishmania* and hence the functions within the kinetoplastida are likely conserved (Dacks et al., 2008a,b).

9.4. Convergent evolution

Two potent examples of convergent evolution are provided by the TfR and the lysosomal protein p67. The former is a heterodimer consisting of the ESAG6 and ESAG7 gene products, and binds mammalian apo-transferrin with high affinity (Steverding et al., 1994). Most significantly ESAG6/7 is restricted to the flagellar pocket, anchored to the plasma membrane by a GPI-anchor and serves to facilitate efficient endocytosis of transferrin via the common clathrin pathway. However, both subunits are clearly related to VSG and hence have a completely distinct evolutionary origin from the host TfR. ESAG6 and 7 are the only ESAGs that are present in all expression sites, underscoring an absolute requirement for transferrin accumulation in the bloodstream stage (Berriman et al., 2002). It has been suggested that the presence of multiple and different copies of ESAG6/7 may facilitate an increased host range (van Luenen et al., 2005) but other data suggest that any one heterodimer may be sufficiently efficient in transferrin accumulation to fulfil the parasite's iron requirements (Salmon et al., 2005).

9.5. Evolutionary exploitation of the flagellar pocket

The flagellar pocket represents an evolutionary adaptation that many workers have proposed is exploited for the sequestration of surface receptors. For example, the ESAG6/7 complex is restricted to this membrane subdomain, which likely has the dual advantage of increased endocytic efficiency and also removal from the bulk surface and hence recognition by the host. However, it needs to be recognized that these observations remain correlative or ''just-so'' stories, and that a flagellar pocket-like invagination predates antigenic variation or parasitism; a similar structure is present in many free-living kinetoplastids and even in the more distant photosynthetic *Euglena*. This does not, however, prevent the exploitation of a preexisting structure for new functions, and potentially facilitating the acquisition of new ecological niches.

A recent study demonstrated elegantly how the flagellar pocket is now indispensable for trypanosomes. Ablation of expression of Bilbo-1, a component of the hemi-desmosomal flagellar pocket collar complex mediating

flagellum and flagellar pocket membrane adhesion results in loss of the pocket, but also major failures to vesicular transport, resulting in secretory cargo becoming trapped within accumulating cytoplasmic transport vesicles (Bonhivers et al., 2008). The resulting cells also exhibit major cytokinesis defects. It is tempting to speculate that this trafficking defect results from dilution of factors that mark the flagellar pocket membrane and that mis-sorting then results in defective cell division. However, the polarity of the trypanosome cell and hence faithful cytokinesis, is strongly dependent on flagellum positioning, so it is likely that this aspect of Bilbo-1 function also contributes. Regardless of the mechanism that leads to lethality, this work is an important reminder that whatever advantages the flagellar pocket may bring to the African trypanosome, there are additional and essential aspects that dictate retention beyond any role in protein sorting or immune evasion.

10. Conclusions and Future Perspectives

The last decade or so has seen a revolution in the depth of analysis that is possible for trypanosomes. In multiple areas, including cell-cycle control, differentiation, cytoskeletal function, and membrane transport, advances have been considerable (e.g., Broadhead et al., 2006; Fenn and Matthews, 2007; Hammarton et al., 2007). Completion of the genome sequence of *T. b. brucei*, partial sequences for additional African trypanosomes and complete sequences for *Leishmania* and *T. cruzi* have facilitated rapid analysis, comparative approaches, and much else. The recent reworking of the eukaryotic tree of life (Adl et al., 2005) may have displaced trypanosomes as putative ancient systems, but the new topology more than underscores their importance for understanding the range of eukaryotic diversity. In short, trypanosomes have emerged as an important model for cell and evolutionary biology, while retaining their preeminence for understanding of antigenic variation, immune evasion, virulence, and for design of antikinetoplastid therapeutics (Barrett et al., 2007). This optimism in laboratory or molecular-based science is somewhat tempered by limited progress in disease control, but there is also a basis for a positive outlook even here, with new funding approaches and postgenomics programs (Barrett et al., 2007). Drug resistance, ongoing difficulties with bridging the gap between bench and bedside and current political, agricultural and economic turmoil in Africa, however, caution against misplaced optimism (The Economist, 2008).

What are the priorities for ongoing work, in terms of macromolecular transport? There are at least three areas which require addressing at this time; systematic exploration of the cell biology, more thorough investigations of

therapeutic intervention and direct assessment of the contributions to immune evasion. All of these are clearly aspects of the same overall question.

Much of the progress in study of macromolecular transport has relied on mapping the functions of homologues of higher eukaryote factors into trypanosomes. This has served well, and demonstrated deep evolutionary connections for many pathways. Further, lineage-specific features have also been documented (Field et al., 2007a,b). However, an absence of a direct analysis by forward genetics or other approaches leads to an asymmetry; specifically we are ignorant of the level that trypanosome- or excavate-specific factors play in intracellular transport. Given that $\sim 40\%$ of trypanosome open reading frames remain unassigned, the likelihood of a contribution of trypanosome-specific factors is high. Clearly, identification of such factors and pathways to which they contribute would provide deep insights into kinetoplastid-specific processes, parasitism, and also evolution of the endomembrane system.

Such a deeper exploration of the protein networks participating in trypanosome macromolecular transport are of direct practical application. Specifically, it is clear that endocytosis is essential as multiple knockdown experiments attest. However, the factors investigated so far are both homologous to the host system, and also nondruggable at present; small GTPases and structural elements like clathrin are unappealing targets. But, identification of potential differences in the endocytic ubiquitylation enzymology, importance of the PI-3-kinase TbVps34 and likely participation of additional kinases and phosphatases all suggest that factors with enzymatic roles are present, and potentially much more accessible.

Finally, the role that the endomembrane system plays in immune evasion remains incompletely understood. Copious *in vitro* evidence has been accumulated; essentiality of endocytosis and VSG expression, correlation of high endocytic activity with mammalian infectivity, active antibody capping mechanisms coupled to extensive proteolysis within the endocytic/recycling system, and roles for various transport factor in these processes have all been reported. However, it remains that a detailed understanding of how the host immune system interfaces with trypanosome macromolecular transport in an *in vivo* context has not been forthcoming, and remains a challenge for the future.

ACKNOWLEDGMENTS

We are grateful to the following members of our laboratories for comments, suggestions, and sharing unpublished data; Ka-Fai Leung, Carme Gabernet-Castello, and Senthil Natesan. The Cambridge laboratory receives financial support from the Wellcome Trust, the Commonwealth Commission, the Bill and Melinda Gates Foundation, and the Medical Research Council (UK), all of which is gratefully acknowledged.

REFERENCES

Abell, B.M., Pool, M.R., Schlenker, O., Sinning, I., High, S., 2004. Signal recognition particle mediates post-translational targeting in eukaryotes. EMBO J. 23, 2755–2764.

Ackers, J.P., Dhir, V., Field, M.C., 2005. A bioinformatic analysis of the RAB genes of *Trypanosoma brucei*. Mol. Biochem. Parasitol. 141, 89–97.

Acosta-Serrano, A., Vassella, E., Liniger, M., Kunz Renggli, C., Brun, R., Roditi, I., et al., 2001. The surface coat of procyclic *Trypanosoma brucei*: programmed expression and proteolytic cleavage of procyclin in the tsetse fly. Proc. Natl. Acad. Sci. USA 98, 1513–1518.

Adl, S.M., Simpson, A.G., Farmer, M.A., Andersen, R.A., Anderson, O.R., Barta, J.R., et al., 2005. The new higher level classification of eukaryotes with emphasis on the taxonomy of protists. J. Eukaryot. Microbiol. 52, 399–451.

Alexander, D.L., Schwartz, K.J., Balber, A.E., Bangs, J.D., 2002. Developmentally regulated trafficking of the lysosomal membrane protein p67 in *Trypanosoma brucei*. J. Cell Sci. 115, 3253–3263.

Allen, C.L., Goulding, D., Field, M.C., 2003. Clathrin-mediated endocytosis is essential in *Trypanosoma brucei*. EMBO J. 22, 4991–5002.

Allen, C.L., Liao, D., Chung, W.L., Field, M.C., 2007. Dileucine signal-dependent and AP-1-independent targeting of a lysosomal glycoprotein in *Trypanosoma brucei*. Mol. Biochem. Parasitol. 156, 175–190.

Al-qahtani, A., Teilhet, M., Mensa-Wilmot, K., 1998. Species-specificity in endoplasmic reticulum signal peptide utilization revealed by proteins from *Trypanosoma brucei* and *Leishmania*. Biochem. J. 331, 521–529.

Antonin, W., Holroyd, C., Fasshauer, D., Pabst, S., Von Mollard, G.F., Jahn, R., 2000a. A SNARE complex mediating fusion of late endosomes defines conserved properties of SNARE structure and function. EMBO J. 19, 6453–6464.

Antonin, W., Holroyd, C., Tikkanen, R., Höning, S., Jahn, R., 2000b. The R-SNARE endobrevin/VAMP-8 mediates homotypic fusion of early endosomes and late endosomes. Mol. Biol. Cell 11, 3289–3298.

Antonin, W., Dulubova, I., Arac, D., Pabst, S., Plitzner, J., Rizo, J., et al., 2002. The N-terminal domains of syntaxin 7 and vti1b form three-helix bundles that differ in their ability to regulate SNARE complex assembly. J. Biol. Chem. 277, 36449–36456.

Antonny, B., Schekman, R., 2001. ER export: public transportation by the COPII coach. Curr. Opin. Cell Biol. 14, 417.

Appenzeller, C., Andersson, H., Kappeler, F., Hauri, H.P., 1999. The lectin ERGIC-53 is a cargo transport receptor for glycoproteins. Nat. Cell Biol. 1, 330–334.

Arighi, C.N., Hartnell, L.M., Aguilar, R.C., Haft, C.R., Bonifacino, J.S., 2004. Role of the mammalian retromer in sorting of the cation-independent mannose 6-phosphate receptor. J. Cell Biol. 165, 123–133.

Atrih, A., Richardson, J.M., Prescott, A.R., Ferguson, M.A., 2005. *Trypanosoma brucei* glycoproteins contain novel giant poly-*N*-acetyllactosamine carbohydrate chains. J. Biol. Chem. 280, 865–871.

Babst, M., 2005. A protein's final ESCRT. Traffic 6, 2–9.

Bacher, G., Lütcke, H., Jungnickel, B., Rapoport, T.A., Dobberstein, B., 1996. Regulation by the ribosome of the GTPase of the signal-recognition particle during protein targeting. Nature 381, 248–251.

Bahr, V., Stierhof, Y., Lig, T., Demar, M., Quinten, M., Overath, P., 1993. Expresssion of lipophosphoglycan, high molecular weight phosphoglycan and glycoprotein 63 in promastigotes and amastigotes of *Leishmania mexicana*. Mol. Biochem. Parasitol. 58, 107–121.

Balber, A.E., Bangs, J.D., Jones, S.M., Proia, R.L., 1979. Inactivation or elimination of potentially trypanolytic, complement-activating immune complexes by pathogenic trypanosomes. Infect. Immun. 24, 617–627.

Bangs, J.D., Brouch, E.M., Ransom, D.M., Roggy, J.L., 1996. A soluble secretory reporter in *Trypanosoma brucei*. Studies on endoplasmic reticulum targeting. J. Biol. Chem. 271, 18387–18393.

Baral, T.N., Magez, S., Stijlemans, B., Conrath, K., Vanhollebeke, B., Pays, E., et al., 2006. Experimental therapy of African trypanosomiasis with a nanobody-conjugated human trypanolytic factor. Nat. Med. 12, 580–584.

Barlowe, C., 2002. COPII-dependent transport from the endoplasmic reticulum. Curr. Opin. Cell Biol. 14, 417–422.

Barlowe, C., Schekman, R., 1993. SEC12 encodes a guanine nucleotide exchange factor essential for transport vesicle budding from the ER. Nature 365, 347–349.

Barrett, M.P., Boykin, D.W., Brun, R., Tidwell, R.R., 2007. Human African trypanosomiasis: pharmacological re-engagement with a neglected disease. Br. J. Pharmacol. 152 (8), 1155–1171.

Barry, J.D., 1979. Capping of variable antigen on *Trypanosoma brucei*, and its immunological and biological significance. J. Cell Sci. 37, 287–302.

Béjà, O., Ullu, E., Michaeli, S., 1993. Identification of a tRNA-like molecule that copurifies with the 7SL RNA of *Trypanosoma brucei*. Mol. Biochem. Parasitol. 57, 223–230.

Berriman, M., Hall, N., Sheader, K., Bringaud, F., Tiwari, B., Isobe, T., et al., 2002. The architecture of variant surface glycoprotein gene expression sites in *Trypanosoma brucei*. Mol. Biochem. Parasitol. 122, 131–140.

Berriman, M., Ghedin, E., Hertz-Fowler, C., Blandin, G., Renauld, H., Bartholomeu, C.D., et al., 2005. The genome of the African trypanosome *Trypanosoma brucei*. Science 309, 416–422.

Beverley, S.M., Turco, S.J., 1998. Lipophosphoglycan (LPG) and the identification of virulence genes in the protozoan parasite *Leishmania*. Trends Microbiol. 6, 35–40.

Bishop, J.R., Shimamura, M., Hajduk, S.L., 2001. Insight into the mechanism of trypanosome lytic factor-1 killing of *Trypanosoma brucei brucei*. Mol. Biochem. Parasitol. 118, 33–40.

Biton, M., Mandelboim, M., Arvatz, G., Michaeli, S., 2006. RNAi interference of XPO1 and Sm genes and their effects on the spliced leader RNA in *Trypanosoma brucei*. Mol. Biochem. Parasitol. 150, 132–143.

Böhme, U., Cross, G.A.M., 2002. Mutational analysis of the variant surface glycoprotein GPI-anchor signal sequence in trypanosome. J Cell Sci. 115, 805–816.

Bonhivers, M., Nowacki, S., Landrein, N., Robinson, D.R., 2008. Biogenesis of the trypanosome endo-exocytotic organelle is cytoskeleton mediated. PLoS Biol. 6, e105.

Braakman, I., 2001. A novel lectin in the secretory pathway. An elegant mechanism for glycoprotein elimination. EMBO Rep. 2, 666–668.

Braulke, T., Bonifacino, J.S., 2009. Sorting of lysosomal proteins. Biochim. Biophys. Acta 1793, 605–614.

Bright, B.A., Gratian, M.J., Luzio, J.P., 2005. Endocytic delivery to lysosomes mediated by concurrent fusion and kissing events in living cells. Curr. Biol. 15, 360–365.

Broadhead, R., Dawe, H.R., Farr, H., Griffiths, S., Hart, S.R., Portman, N., et al., 2006. Flagellar motility is required for the viability of the bloodstream trypanosome. Nature 440 (7081), 224–227.

Brodsky, F.M., Chen, C.Y., Knuehl, C., Towler, M.C., Wakeham, D.E., 2001. Biological basket weaving: formation and function of clathrin-coated vesicles. Annu. Rev. Cell Dev. Biol. 17, 517–568.

Caffrey, C.R., Scory, S., Steverding, D., 2000. Cysteine proteinases of trypanosome parasites: novel targets for chemotherapy. Curr. Drug Targets 1, 155–162.
Cai, H., Wang, C., Tsou, C., 1994. Chaperon-like activity of protein disulfide isomerase in the refolding of a protein with no disulfide bonds. J. Biol. Chem. 269, 24550–24552.
Campillo, N., Carrington, M., 2003. The origin of the serum resistance associated (SRA) gene and a model of the structure of the SRA polypeptide from *Trypanosoma brucei* rhodesiense. Mol. Biochem. Parasitol. 127, 79–84.
Caramelo, J.J., Parodi, A.J., 2007. How sugars convey information on protein conformation in the endoplsmic reticulum. Semin. Cell Dev. Biol. 18, 732–742.
Caramelo, J.J., Parodi, A.J., 2008. Getting in and out from calnexin/calreticulin cycles. J. Biol. Chem. 283, 10221–10223.
Carrington, M., Miller, N., Blum, M., Roditi, I., Wiley, D., Turner, M., 1991. Variant surface glycoprotein of *Trypanosoma brucei* consists of two domains each having an independently conserved pattern of cysteine residues. J. Mol. Biol. 221, 823–835.
Castro, O., Movsichoff, F., Parodi, A.J., 2006. Preferential transfer of complete glycan is determined by the oligosaccharyltransferase complex and not by the catalytic subunit. Proc. Natl. Acad. Sci. USA 103, 14756–14760.
Castro-Fernández, C., Maya-Núñez, G., Conn, P.M., 2005. Beyond the signal sequence: protein routing in health and disease. Endocr. Rev. 26, 479–503.
Chanez, A., Hehl, A.B., Engstler, M., Schneider, A., 2006. Ablation of the single dynamin of *T. brucei* blocks mitochondrial fission and endocytosis and leads to a precise cytokinesis arrest. J. Cell Sci. 119, 2968–2974.
Chattopadhyay, A., Jones, N.G., Nietlispach, D., Nielsen, P.R., Voorheis, H.P., Mott, H.R., et al., 2005. Structure of the C-terminal domain from *Trypanosoma brucei* variant surface glycoprotein MITat1.2. J. Biol. Chem. 280, 7228–7235.
Chavan, M., Yan, A., Lennarz, W.J., 2005. Subunits of the translocon interact with components of the oligosaccharyl transferase complex. J. Biol. Chem. 280, 22917–22924.
Chen, H., Fre, S., Slepnev, V.I., Capua, M.R., Takei, K., Butler, M.H., et al., 1998. Epsin is an EH-domain-binding protein implicated in clathrin-mediated endocytosis. Nature 394, 793–797.
Chow, A.Y., Mellman, I., 2005. Old lysosomes, new tricks: MHC II dynamics in DCs. Trends Immunol. 26, 72–78.
Chudzik, D.M., Michels, P.A., de Walque, S., Hol, W.G., 2000. Structures of type 2 peroxisomal targeting signals in two trypanosomatid aldolases. J. Mol. Biol. 300, 697–707.
Chung, W.L., Carrington, M., Field, M.C., 2004. Cytoplasmic targeting signals in *trans*-membrane invariant surface glycoproteins of trypanosomes. J. Biol. Chem. 279, 54887–54895.
Chung, W.-L., Leung, K.-F., Carrington, M., Field, M.C., 2008. Position-specific ubiquitylation is required for internalisation and degradation of *trans*-membrane surface proteins in trypanosomes. Traffic 9, 1681–1697.
Clague, M.J., Urbé, S., 2006. Endocytosis: the DUB version. Trends Cell Biol. 16, 551–559.
Coller, S.P., Mansfield, J.M., Paulnock, D.M., 2003. Glycosylinositolphosphate soluble variant surface glycoprotein inhibits IFN-gamma-induced nitric oxide production via reduction in STAT1 phosphorylation in African trypanosomiasis. J. Immunol. 171, 1466–1472.
Conner, S.D., Schmid, S., 2003. Regulated portals of entry into the cell. Nature 422, 37–44.
Conte, I., Labriola, C., Cazzulo, J.J., Docampo, R., Parodi, A.J., 2003. The interplay between folding-facilitating mechanisms in *Trypanosoma cruzi* endoplasmic reticulum. Mol. Biol. Cell 14, 3529–3540.
Coppens, I., Bastin, P., Courtoy, P.J., Baudhuin, P., Opperdoes, F.R., 1991. A rapid method purifies a glycoprotein of Mr 145, 000 as the LDL receptor of *Trypanosoma brucei brucei*. Biochem. Biophys. Res. Commun. 178, 185–191.

Cross, G.A., 1977. Antigenic variation in trypanosomes. Am. J. Trop. Med. Hyg. 26, 240–244.
Cross, G.A., 1996. Antigenic variation in trypanosomes: secrets surface slowly. Bioessays 18, 283–291.
Dacks, J.B., Doolittle, W.F., 2004. Molecular and phylogenetic characterization of syntaxin genes from parasitic protozoa. Mol. Biochem. Parasitol. 136, 123–136.
Dacks, J.B., Field, M.C., 2007. Evolution of the eukaryotic membrane-trafficking system: origin, tempo and mode. J. Cell Sci. 120, 2977–2985.
Dacks, J.B., Poon, P.P., Field, M.C., 2008a. Phylogeny of endocytic components yields insight into the process of nonendosymbiotic organelle evolution. Proc. Natl. Acad. Sci. USA 105, 588–593.
Dacks, J.B., Walker, G., Field, M.C., 2008b. Implications of the new eukaryotic systematics for parasitologists. Parasitol. Int. 57, 97–104.
Dean, S., Marchetti, R., Kirk, K., Matthews, K.R., 2009. A surface transporter family conveys the trypanosome differentiation signal. Nature 459, 213–217.
De Camilli, P., Chen, H., Hyman, J., Panepucci, E., Bateman, A., Brunger, A.T., 2002. The ENTH domain. FEBS Lett. 513, 11–18.
de Graffenried, C.L., Ho, H.H., Warren, G., 2008. Polo-like kinase is required for Golgi and bilobe biogenesis in *Trypanosoma brucei*. J. Cell Biol. 181, 431–438.
De Greef, C., Hamers, R., 1994. The serum resistance-associated (SRA) gene of *Trypanosoma brucei* rhodesiense encodes a variant surface glycoprotein-like protein. Mol. Biochem. Parasitol. 68, 277–284.
de la Canal, L., Parodi, A.J., 1987. Synthesis of dolichol derivatives in trypanosomatids: characterization of enzymatic patterns. J. Biol. Chem. 262, 11128–11133.
Dhir, V., Goulding, D., Field, M.C., 2004. TbRAB1 and TbRAB2 mediate trafficking through the early secretory pathway of *Trypanosoma brucei*. Mol. Biochem. Parasitol. 137, 253–265.
Di Noia, J.M.D., D'Orso, I., Åslund, L., Sánchez, D.O., Frasch, A.C.C., 1998. The T*rypanosoma cruzi* mucin family is transcribed from hundreds of genes having hypervariable regions. J. Biol. Chem. 273, 10843–10850.
Egger, D.K., Welch, W.J., Hansen, W.J., 1997. Complexes between nascent polypeptides and their molecular chaperons in the cytosol of mammalian cells. Mol. Biol. Cell 8, 1559–1573.
Ellgaard, L., Helenius, A., 2001. ER quality control: towards an understanding at the molecular level. Curr. Opin. Cell Biol. 13, 431–437.
Ellgaard, L., Molinari, M., Helenius, A., 1999. Setting the standards: quality control in the secretory pathway. Science 286, 1882–1888.
Embley, T.M., Martin, W., 2006. Eukaryotic evolution, changes and challenges. Nature 440, 623–630.
Engqvist-Goldstein, A.E., Drubin, D.G., 2003. Actin assembly and endocytosis: from yeast to mammals. Annu. Rev. Cell Dev. Biol. 19, 287–332.
Engstler, M., Boshart, M., 2004. Cold shock and regulation of surface protein trafficking convey sensitization to inducers of stage differentiation in *Trypanosoma brucei*. Genes Dev. 18, 2798–2811.
Engstler, M., Thilo, L., Weise, F., Grünfelder, C.G., Schwarz, H., Boshart, M., et al., 2004. Kinetics of endocytosis and recycling of the GPI-anchored variant surface glycoprotein in *Trypanosoma brucei*. J. Cell Sci. 117, 1105–1115.
Engstler, M., Weise, F., Bopp, K., Grünfelder, C.G., Günzel, M., Heddergott, N., et al., 2005. The membrane-bound histidine acid phosphatase TbMBAP1 is essential for endocytosis and membrane recycling in *Trypanosoma brucei*. J. Cell Sci. 118, 2105–2118.
Engstler, M., Pfohl, T., Herminghaus, S., Boshart, M., Wiegertjes, G., Heddergott, N., et al., 2007. Hydrodynamic flow-mediated protein sorting on the cell surface of trypanosomes. Cell 131, 505–515.

Ersfeld, K., Gull, K., 2001. Targeting of cytoskeletal proteins to the flagellum of *Trypanosoma brucei*. J. Cell Sci. 114, 141–148.

Fenn, K., Matthews, K.R., 2007. The cell biology of *Trypanosoma brucei* differentiation. Curr. Opin. Microbiol. 10 (6), 539–546.

Field, M.C., Boothroyd, J.C., 1996. Sequence divergence in a family of variant surface glycoprotein genes from trypanosomes: coding region hypervariability and downstream recombinogenic repeats. J. Mol. Evol. 42, 500–511.

Field, M.C., Carrington, M., 2004. Intracellular membrane transport systems in *Trypanosoma brucei*. Traffic 5, 905–913.

Field, M.C., Carrington, M., 2009. The trypanosome flagellar pocket; a multifunctional organelle for membrane transport and cell architecture. Nat. Rev. Micro. (in press).

Field, M.C., Menon, A.K., 1993. Glycolipid anchoring of cell surface proteins. In: Schlesinger, M. (Ed.), CRC Handbook of Lipid Modifications of Proteins. CRC Press, Boca Raton, Florida, pp. 83–134.

Field, M.C., O'Reilly, A.J., 2008. How complex is GTPase signaling in trypanosomes? Trends Parasitol. 24, 253–257.

Field, H., Farjah, M., Pal, A., Gull, K., Field, M.C., 1998. Complexity of trypanosomatid endocytosis pathways revealed by Rab4 and Rab5 isoforms in *Trypanosoma brucei*. J. Biol. Chem. 273, 32102–32110.

Field, H., Ali, B.R., Sherwin, T., Gull, K., Croft, S.L., Field, M.C., 1999. TbRab2p, a marker for the endoplasmic reticulum of *Trypanosoma brucei*, localises to the ERGIC in mammalian cells. J. Cell Sci. 112, 147–156.

Field, H., Sherwin, T., Smith, A.C., Gull, K., Field, M.C., 2000. Cell-cycle and developmental regulation of TbRAB31 localisation, a GTP-locked Rab protein from *Trypanosoma brucei*. Mol. Biochem. Parasitol. 106, 21–35.

Field, M.C., Gabernet-Castello, C., Dacks, J.B., 2007a. Reconstructing the evolution of the endocytic system: insights from genomics and molecular cell biology. Adv. Exp. Med. Biol. 607, 84–96.

Field, M.C., Natesan, S.K.A., Garbernet-Castello, C., Koumandou, V.L., 2007b. Intracellular trafficking in the trypanosomatids. Traffic 8, 629–639.

Ford, M.G.J., Mills, I.G., Peter, B.J., Vallis, Y., Praefcke, G.J.K., Evans, P.R., et al., 2002. Curvature of clathrin-coated pits driven by epsin. Nature 419, 361–366.

Freymann, D., Down, J., Carrington, M., Roditi, I., Turner, M., Wiley, D., 1990. 2.9 Å resolution structure of the N-terminal domain of a variant surface glycoprotein from *Trypanosoma brucei*. J. Mol. Biol. 216, 141–160.

Fujimoto, L.M., Roth, R., Heuser, J.E., Schmid, S.L., 2000. Actin assembly plays a variable, but not obligatory role in receptor-mediated endocytosis in mammalian cells. Traffic 1, 161–171.

Gabernet-Castello, C., Dacks, J.B., Field, M.C., 2008. The single ENTH domain protein of trypanosomes; functional and evolutionary relationship with the epsins. (submitted).

García-Salcedo, J.A., Pérez-Morga, D., Gijón, P., Dilbeck, V., Pays, E., Nolan, D.P., 2004. A differential role for actin during the life cycle of *Trypanosoma brucei*. EMBO J. 23, 780–789.

Gerrits, H., Mussmann, R., Bitter, W., Kieft, R., Borst, P., 2002. The physiological significance of transferrin receptor variations in *Trypanosoma brucei*. Mol. Biochem. Parasitol. 119, 237–247.

Gething, M.J., 1999. Role and regulation of the ER chaperone BiP. Semin. Cell Dev. Biol. 10, 465–472.

Gillett, M.P., Owen, J.S., 1991. *Trypanosoma brucei brucei*: differences in the trypanocidal activity of human plasma and its relationship to the level of high density lipoproteins. Trans. R. Soc. Trop. Med. Hyg. 85, 612–616.

Goldshmidt, H., Sheiner, L., Bütikofer, P., Roditi, I., Uliel, S., Günzel, M., et al., 2008. Role of protein translocation pathways across the endoplasmic reticulum in *Trypanosoma brucei*. J. Biol. Chem. 283 (46), 32085–32098.

Grab, D.J., Webster, P., Verjee, Y., Lonsdale-Eccles, J., 1997. Golgi-associated phosphohydrolases in *Trypanosoma brucei brucei*. Mol. Biochem. Parasitol. 86, 127–132.

Grünfelder, C.G., Engstler, M., Weise, F., Schwarz, H., Stierhof, Y.D., Boshart, M., et al., 2002. Accumulation of a GPI-anchored protein at the cell surface requires sorting at multiple intracellular levels. Traffic 3, 547–559.

Grünfelder, C.G., Engstler, M., Weise, F., Schwarz, H., Stierhorf, Y., Morgan, G.W., et al., 2003. Endocytosis of a glycosylphosphatidylinositol-anchored protein via clathrin-coated vesicles, sorting by default in endosomes, and exocytosis via RAB11-positive carriers. Mol. Biol. Cell 14, 2029–2040.

Gruszynski, A.E., DeMaster, A., Hooper, N.M., Bangs, J.D., 2003. Surface coat remodeling during differentiation of *Trypanosoma brucei*. J. Biol. Chem. 278, 24665–24672.

Gu, F., Gruenberg, J., 1999. Biogenesis of transport intermediates in the endocytic pathway. FEBS Lett. 452, 61–66.

Hager, K.M., Pierce, M.A., Moore, D.R., Tytler, E.M., Esko, J.D., Hajduk, S.L., 1994. Endocytosis of a cytotoxic human high density lipoprotein results in disruption of acidic intracellular vesicles and subsequent killing of African trypanosomes. J. Cell Biol. 126, 155–167.

Hajduk, S.L., Moore, D.R., Vasudevacharya, J., Siqueira, H., Torri, A.F., Tytler, E.M., et al., 1989. Lysis of *Trypanosoma brucei* by a toxic subspecies of human high density lipoprotein. J. Biol. Chem. 264, 5210–5217.

Hall, B., Allen, C.L., Goulding, D., Field, M.C., 2004a. Both of the Rab5 subfamily small GTPases of *Trypanosoma brucei* are essential and required for endocytosis. Mol. Biochem. Parasitol. 138, 67–77.

Hall, B.S., Pal, A., Goulding, D., Field, M.C., 2004b. Rab4 is an essential regulator of lysosomal trafficking in trypanosomes. J. Biol. Chem. 279, 45047–45056.

Hall, B.S., Pal, A., Goulding, D., Acosta-Serrano, A., Field, M.C., 2005a. *Trypanosoma brucei*: TbRAB4 regulates membrane recycling and expression of surface proteins in procyclic forms. Exp. Parasitol. 111, 160–171.

Hall, B.S., Smith, E., Langer, W., Jacobs, L.A., Goulding, D., Field, M.C., 2005b. Developmental variation in Rab11-dependent trafficking in *Trypanosoma brucei*. Eukaryot. Cell 4, 971–980.

Hall, B.S., Gabernet-Castello, C., Voak, A., Goulding, D., Natesan, S.K., Field, M.C., 2006. TbVps34, the trypanosome orthologue of Vps34, is required for Golgi complex segregation. J. Biol. Chem. 281, 27600–27612.

Hammarton, T.C., Monnerat, S., Mottram, J.C., 2007. Cytokinesis in trypanosomatids. Curr. Opin. Microbiol. 10 (6), 520–527.

Hammond, C., Helenius, A., 1994. Quality control in the secretory pathway: retention of a misfolded viral membrane glycoprotein involved cycling between the ER, intermediate compartment and Golgi apparatus. J. Cell Biol. 126, 41–52.

Hatada, S., Seed, J.R., Barker, C., Hajduk, S.L., Black, S., Maeda, N., 2002. No trypanosome lytic activity in the sera of mice producing human haptoglobin-related protein. Mol. Biochem. Parasitol. 119, 291–294.

He, C.Y., 2007. Golgi biogenesis in simple eukaryotes. Cell Microbiol. 9, 566–572.

He, C.Y., Ho, H.H., Malsam, J., Chalouni, C., West, C.M., Ullu, E., et al., 2004. Golgi duplication in *Trypanosoma brucei*. J. Cell Biol. 165, 313–321.

He, C.Y., Pypaert, M., Warren, G., 2005. Golgi duplication in *Trypanosoma brucei* requires Centrin2. Science 310, 1196–1198.

Hebert, D.H., Molinari, M., 2007. In and out of the ER: protein folding, quality control, degradation and related diseases. Physiol. Rev. 87, 1377–1408.
Helenius, A., Aebi, M., 2001. Intracellular functions of N-linked glycans. Science 291, 2364–2369.
Helenius, A., Aebi, M., 2004. Roles of N-linked glycans in the endoplasmic reticulum. Annu. Rev. Biochem. 73, 1019–1049.
Hettema, E.H., Distel, B., Tabak, H.F., 1999. Import of proteins into peroxisomes. Biochim. Biophys. Acta 1451, 17–34.
Hirst, J., Motley, A., Harasaki, K., Chew, S.Y.P., Robinson, M.S., 2003. EpsinR: an ENTH domain-containing protein that interacts with AP-1. Mol. Biol. Cell 14, 625–641.
Ho, H.H., He, C., de Graffenried, C.L., Murrells, L.J., Warren, G., 2006. Ordered assembly of the duplicating Golgi in *Trypanosoma brucei*. Proc. Natl. Acad. Sci. USA 103, 7676–7681.
Hong, A.K.D., Kaiser, C.A., 1996. A pathway for targeting misfolded proteins to the yeast vacuole. J. Cell Biol. 135, 623–633.
Hsu, M.P., Muhich, M.L., Boothroyd, J.C., 1989. A developmentally regulated gene of trypanosomes encodes a homologue of rat protein-disulphide Isomerase and phosphoinositol-phospholipase C. Biochemistry 28, 6440–6446.
Huang, M., Weissman, J.T., Beraud-Dufour, S., Luan, P., Wang, C., Chen, W., et al., 2001. Crystal structure of Sar1-GDP at 1.7A resolution and the role of the NH2 terminus in ER export. J. Cell Biol. 155, 937–948.
Hung, C., Qiao, X., Lee, P., Lee, M.G., 2004. Clathrin-dependent targeting of the flagella pocket of procyclic-form *Trypanosoma brucei*. Eukaryot. Cell 3, 1004–1014.
Jacob, C.A., Burda, P., Toth, J., Aebi, M., 1998. Degradation of misfolded endoplasmic reticulum glycoproteins in *Saccharomyces cerevisiae* is determined by a specific oligosaccharide structure. J. Cell Biol. 142, 1223–1233.
Jeffries, T.R., Morgan, G.W., Field, M.C., 2001. A developmentally regulated Rab11 homologue in *Trypanosoma brucei* is involved in recycling processes. J. Cell Sci. 114, 2617–2626.
Jeffries, T.R., Morgan, G.W., Field, M.C., 2002. TbRAB18, a developmentally regulated Golgi GTPase from *Trypanosoma brucei*. Mol. Biochem. Parasitol. 121, 63–74.
Jones, D., Mehlert, A., Fergusin, M.A.J., 2004. The N-glycan glucosidase system in *Trypanosoma brucei*. Biochem. Soc. Trans. 32, 766–768.
Jones, D.C., Mehlert, A., Güther, M.L.S., Ferguson, M.A.J., 2005. Deletion of the glucosidase II gene in *Trypanosoma brucei* reveals novel *N*-glycosylation mechanisms in the biosynthesis of variant surface glycoprotein. J. Biol. Chem. 280, 35929–35942.
Kalthoff, C., Groos, S., Kohl, R., Mahrhold, S., Ungewickell, E.J., 2002. Clint: a novel clathrin-binding ENTH-domain protein at the Golgi. Mol. Biol. Cell 13, 4060–4073.
Katzmann, D.J., Odorizzi, G., Emr, S.D., 2002. Receptor downregulation and multivesicular-body sorting. Nat. Rev. Mol. Cell Biol. 3, 893–905.
Katzmann, D.J., Sarkar, S., Chu, T., Audhya, A., Emr, S.D., 2004. Multivesicular body sorting: ubiquitin ligase Rsp5 is required for the modification and sorting of carboxypeptidase S. Mol. Biol. Cell 15, 468–480.
Keenan, R.J., Freymann, D.M., Stroud, R.M., Walter, P., 2001. The signal recognition particle. Annu. Rev. Biochem. 70, 755–775.
Kelleher, D.J., Gilmore, R., 2006. An evolving view of the eukaryotic oligosaccharyltransferase. Glycobiology 16, 47R–62R.
Kelley, R.J., Brickman, M.J., Balber, A.E., 1995. Processing and transport of a lysosomal membrane glycoprotein is developmentally regulated in African trypanosomes. Mol. Biochem. Parasitol. 74, 167–178.

Kincaid, M.M., Cooper, A.A., 2007. Misfolded proteins traffic from the endoplasmic reticulum (ER) due to ER export signal. Mol. Biol. Cell 18, 455–463.
Kirchhausen, T., Harrison, S.C., 1981. Protein organization in clathrin trimers. Cell 23, 755–761.
Klausner, R.D., Sitia, R., 1990. Protein degradation in the endoplasmic reticulum. Cell 62, 611–614.
Klumperman, J., Schweizer, A., Clausen, H., Tang, B.L., Hong, W., Oorschot, V., et al., 1998. The recycling of protein ERGIC-53 and dynamics of the ER-Golgi intermediate compartment. J. Cell Sci. 111, 3411–3425.
Knee, R., Ahsan, I., Mesaeli, N., Kaufman, R.J., Michalak, M., 2003. Compromised function in calreticulin-deficient cells. Biochem. Biophys. Res. Commun. 304, 661–666.
Kornfeld, S., Mellman, I., 1989. The biogenesis of lysosomes. Annu. Rev. Cell Biol. 5, 483–525.
Koumandou, V.L., Dacks, J.B., Coulson, R.M., Field, M.C., 2007. Control systems for membrane fusion in the ancestral eukaryote; evolution of tethering complexes and SM proteins. BMC Evol. Biol. 7, 29.
Koumandou, V.L., Natesan, S.K., Sergeenko, T., Field, M.C., 2008. The trypanosome transcriptome is remodelled during differentiation but displays limited responsiveness within life stages. BMC Genomics 9, 298.
Kuehn, M.J., Herrmann, J.M., Schekman, R., 1998. COPII-cargo interactions direct protein sorting into ER-derived transport vesicles. Nature 391, 187–190.
Kutay, U., Ahnert-Hilger, G., Hartmann, E., Wiedenmann, B., Rapoport, T.A., 1995. Transport route for synaptobrevin via a novel pathway of insertion into the endoplasmic reticulum membrane. EMBO J. 14, 217–223.
Labriola, C., Cazzulo, J.J., Parodi, A., 1999. *Trypanosoma cruzi* calreticulin is a lectin that binds monoglucosylated oligosaccharide but not protein moieties in glycoproteins. Mol. Biol. Cell 10, 1381–1394.
Lafer, E., 2002. Clathrin-protein interactions. Traffic 3, 513–520.
Langreth, S.G., Balber, A.E., 1975. Protein uptake and digestion in bloodstream and culture forms of *Trypanosoma brucei*. J. Protozool. 22, 40–53.
Lanzetti, L., Palamidessi, A., Areces, L., Scita, G., Di Fiore, P.P., 2004. Rab5 is a signaling GTPase involved in actin modeling by receptor tyrosine kinases. Nature 429, 309–314.
Lauring, B., Sakai, H., Kreibich, G., Wiedmann, M., 1995. Nascent polypeptide-associated complex protein prevents mistargeting of nascent chains to the endoplasmic reticulum. Proc. Natl. Acad. Sci. USA 92, 5411–5415.
Lederkremer, G.Z., Cheng, Y., Petre, B.M., Vogan, E., Springer, S., Schekman, R., et al., 2001. Structure of the Sec23p/24p and Sec13p/31p complexes of COPII. Proc. Natl. Acad. Sci. USA 98, 10704–10709.
Leung, K.F., Dacks, J.B., Field, M.C., 2008. Evolution of the multivesicular body ESCRT machinery; retention across the eukaryotic lineage. (submitted).
Lewis, M.J., Sweet, D.J., Pelham, H.R., 1990. The ERD2 gene determines the specificity of the luminal ER protein retention system. Cell 61, 1359–1363.
Li, Z., Wang, C.C., 2002. Functional characterization of the 11 non-ATPase subunit proteins in the trypanosome 19 S proteasomal regulatory complex. J. Biol. Chem. 277, 42686–42693.
Lillico, S., Field, M.C., Blundell, P., Coombs, G.H., Mottram, J.C., 2003. Essential roles for GPI-anchored proteins in African trypanosomes revealed using mutants deficient in GPI8. Mol. Biol. Cell 14, 1182–1194.
Liu, J., Qiao, X., Du, D., Lee, M.G., 2000. Receptor-mediated endocytosis in the procyclic form of *Trypanosoma brucei*. J. Biol. Chem. 275, 12032–12040.

Liu, L., Ben-Slomo, H., Xu, Y., Stern, M.Z., Goncharov, I., Zhang, Y., et al., 2003. The trypanomastid signal peptide recognition particle consists of two RNA molecules, a 7SL RNA homologue and a novel tRNA-like molecule. J. Biol. Chem. 278, 18271–18280.

Lugli, E.B., Pouliot, M., Portela Mdel, P., Loomis, M.R., Raper, J., 2004. Characterization of primate trypanosome lytic factors. Mol. Biochem. Parasitol. 138, 9–20.

Lustig, Y., Goldshmidt, H., Uliel, S., Michaeli, S., 2005. The *Trypanosoma brucei* signal recognition particle lacks the Alu-domain-binding proteins: purification and functional analysis of its binding proteins by RNAi. J. Cell Sci. 118, 4551–4562.

Lustig, Y., Scheiner, L., Vagima, Y., Goldshmidt, H., Das, A., Bellofatto, V., et al., 2007. Spliced-leader RNA silencing: a novel stress-induced mechanism in *Trypanosoma brucei*. EMBO Rep. 8, 408–413.

Lythgoe, K.A., Morrison, L.J., Read, A.F., Barry, J.D., 2007. Parasite-intrinsic factors can explain ordered progression of trypanosome antigenic variation. Proc. Natl. Acad. Sci. USA 104, 8095–8100.

Mackey, Z.B., O'Brien, T.C., Greenbaum, D.C., Blank, R.B., McKerrow, J.H., 2004. A cathepsin B-like protease is required for host protein degradation in *Trypanosoma brucei*. J. Biol. Chem. 279, 48426–48433.

Maeda, N., 1985. Nucleotide sequence of the haptoglobin and haptoglobin-related gene pair. The haptoglobin-related gene contains a retrovirus-like element. J. Biol. Chem. 260, 6698–6709.

Magez, S., Radwanska, M., Beschin, A., Sekikawa, K., De Baetselier, P., 1999. Tumor necrosis factor alpha is a key mediator in the regulation of experimental *Trypanosoma brucei* infections. Infect. Immun. 67, 3128–3132.

Magez, S., Radwanska, M., Drennan, M., Fick, L., Baral, T.N., Brombacher, F., et al., 2006. Interferon-gamma and nitric oxide in combination with antibodies are key protective host immune factors during trypanosoma congolense Tc13 infections. J. Infect. Dis. 193, 1575–1583.

Mansfield, J.M., 1994. T-cell responses to the trypanosome variant surface glycoprotein: a new paradigm? Parasitol. Today 10, 267–270.

Mansfield, J.M., Paulnock, D.M., 2005. Regulation of innate and acquired immunity in African trypanosomiasis. Parasite Immunol. 27, 361–371.

Manthri, S., Güther, M.L.S., Izquierdo, L., Acosta-Serrano, A., Ferguson, M.A.J., 2008. Deletion of the TbALG3 gene demonstrates site-specific *N*-glycosylation and N-glycan processing in *Trypanosoma brucei*. Glycobiology 18, 367–383.

Martin, K.L., Smith, T.K., 2006. The glycosylphosphatidylinositol (GPI) biosynthetic pathway of bloodstream-form *Trypanosoma brucei* is dependent on the *de novo* synthesis of inositol. Mol. Microbiol. 61, 89–105.

Mbawa, Z.R., Gumm, I.D., Shaw, E., Lonsdale-Eccles, J.D., 1992. Characterisation of a cysteine protease from bloodstream forms of *Trypanosoma congolense*. Eur. J. Biochem. 204, 371–379.

McConville, M., Mullin, K., Ilgoutz, S., Teasdale, R., 2002. Secretory pathway of trypanosomatid parasites. Microbiology and Molecular Biology Reviews: MMBR 66, 122–154.

McCulloch, R., 2004. Antigenic variation in African trypanosomes: monitoring progress. Trends Parasitol. 20, 117–121.

McDowell, M.A., Ransom, D.M., Bangs, J.D., 1998. Glycosylphosphatidylinositol-dependent secretory transport in *Trypanosoma brucei*. Biochem. J. 335, 681–689.

Mellman, I., Warren, G., 2000. The road taken: past and future foundations of membrane traffic. Cell 100, 99–112.

Merrifield, C.J., 2004. Seeing is believing: imaging actin dynamics at single sites of endocytosis. Trends Cell Biol. 14, 352–358.

Meusser, B., Hirsch, C., Jaroch, E., Sommer, T., 2005. ERAD: the long road to destruction. Nat. Cell Biol. 7, 766–772.

Miller, J.D., Tajima, S., Lauffer, L., Walter, P., 1995. The β subunit of the signal recognition particle receptor is a transmembrane GTPase that anchors the α subunit, a peripheral membrane GTPase, to the endoplasmic reticulum membrane. J. Cell Biol. 128, 273–282.

Molina Portela, M.P., Raper, J., Tomlinson, S., 2000. An investigation into the mechanism of trypanosome lysis by human serum factors. Mol. Biochem. Parasitol. 110, 273–282.

Molinari, M., Calanca, V., Galli, C., Lucca, P., Paganetti, P., 2003. Role of EDEM in the release of misfolded glycoprotein from the calnexin cycle. Science 299, 1397–1400.

Molinari, M., Eriksson, K.K., Calanca, V., Galli, C., Cresswell, P., Michalak, M., et al., 2004. Contrasting functions of calreticulin and calnexin in glycoprotein folding and ER quality control. Mol. Cell 13, 125–135.

Moremen, K.W., Molinari, M., 2006. N-linked glycan recognition and processing: the molecular basis of endoplasmic reticulum quality control. Curr. Opin. Struct. Biol. 16, 592–599.

Morgan, G.W., Goulding, D., Field, M.C. 2004. The single dynamin-like protein of *Trypanosoma brucei* regulates mitochondrial division and is not required for endocytosis. J. Biol. Chem. 279 (11), 10692–10701.

Morgan, G.W., Allen, C.L., Jeffries, T.R., Hollonshead, M., Field, M.C., 2001. Developmental and morphological regulation of clathrin-mediated endocytosis in *Trypanosoma brucei*. J. Cell Sci. 114, 2605–2615.

Morgan, G.W., Hall, B.S., Denny, P.W., Carrington, M., Field, M.C., 2002. The endocytic apparatus of the kinetoplastida. Part I: A dynamic system for nutrition and evasion of host defences. Trends Parasitol. 18, 491–496.

Mullock, B.M., Bright, N.A., Fearon, C.W., Gray, S.R., Luzio, J.P., 1998. Fusion of lysosomes with late endosomes produces a hybrid organelle of intermediate density and is NSF dependent. J. Cell Biol. 140, 591–601.

Mussmann, R., Engstler, M., Gerrits, H., Kieft, R., Toaldo, C.B., Onderwater, J., et al., 2004. Factors affecting the level and localization of the transferrin receptor in *Trypanosoma brucei*. J. Biol. Chem. 279, 40690–40698.

Mutomba, M.C., To, W.Y., Hyun, W.C., Wang, C.C., 1997. Inhibition of proteasome activity blocks cell cycle progression at specific phase boundaries in African trypanosomes. Mol. Biochem. Parasitol. 90, 491–504.

Nakano, A., Brada, D., Schekman, R., 1988. A membrane glycoprotein, Sec12p, required for protein transport from the endoplasmic reticulum to the Golgi apparatus in yeast. J. Cell Biol. 107, 851–863.

Namangala, B., De Baetselier, P., Noel, W., Brys, L., Beschin, A., 2001. Alternative versus classical macrophage activation during experimental African trypanosomosis. J. Leukoc. Biol. 69, 387–396.

Natesan, S.K.A., Peacock, L., Matthews, K., Gibson, W., Field, M.C., 2007. Activation of endocytosis as an adaptation to the mammalian host by trypanosomes. Eukaryot. Cell 6, 2029–2037.

Navarro, M., Gull, K., 2001. A pol I transcriptional body associated with VSG mono-allelic expression in *Trypanosoma brucei*. Nature 414, 759–763.

Navazio, L., Nardi, M.C., Pancaldi, S., Dainese, P., Baldan, B., Ftchette-Lainé, A., et al., 1998. Functional conservation of calreticulin in *Euglena gracilis*. J. Eukaryot. Microbiol. 45, 307–313.

Nishikawa, S.I., Fewell, S.W., Kato, Y., Brodsky, J.L., Endo, T., 2001. Molecular chaperones in yeast endoplasmic reticulum maintain the solubility of proteins for retrotranslocation and degradation. J. Cell Biol. 153, 1061–1070.

Nolan, D.P., Geuskens, M., Pays, E., 1999. N-linked glycans containing linear poly-*N*-acetyllactosamine as sorting signals in endocytosis in *Trypanosoma brucei*. Curr. Biol. 9, 1169–1172.

Oda, Y., Hosokawa, N., Wada, I., Nagata, K., 2003. EDEM as an acceptor of terminally misfolded glycoproteins released from calnexin. Science 299, 1394–1397.

Ormerod, W.E., 1991. Hypothesis: the significance of Winterbottom's sign. J. Trop. Med. Hyg. 94, 338–340.

Overath, P., Engstler, M., 2004. Endocytosis, membrane recycling and sorting of GPI-anchored proteins: *Trypanosoma brucei* as a model. Mol. Microbiol. 53, 735–744.

Overath, P., Stierhof, Y.D., Wiese, M., 1997. Endocytosis and secretion in trypanosomatid parasites—tumultuous traffic in a pocket. Trends Cell Biol. 7, 27–33.

Pal, A., Hall, B.S., Field, M.C., 2002a. Evidence for a non-LDL-mediated entry route for the trypanocidal drug suramin in *Trypanosoma brucei*. Mol. Biochem. Parasitol. 122, 217–221.

Pal, A., Hall, B.S., Nesbeth, D.N., Field, H.I., Field, M.C., 2002b. Differential endocytic functions of *Trypanosoma brucei* Rab5 isoforms GPI-specific endosomal pathway. J. Biol. Chem. 272, 9529–9539.

Pal, A., Hall, B.S., Jeffries, T.R., Field, M.C., 2003. Rab5 and Rab11 mediate transferrin and anti-variant surface glycoprotein antibody recycling in *Trypanosoma brucei*. Biochem. J. 374, 443–451.

Pamer, E.G., So, M., Davis, C.E., 1989. Identification of a developmentally regulated cysteine protease of *Trypanosoma brucei*. Mol. Biochem. Parasitol. 33, 27–32.

Parodi, A.J., 1993. *N*-glycosylation in trypanosomatid protozoa. Glycobiology 3, 193–199.

Parsons, M., Worthey, E.A., Ward, P.N., Mottram, J.C., 2005. Comparative analysis of the kinomes of three pathogenic trypanosomatids: *Leishmania major*, Trypanosoma brucei and Trypanosoma cruzi. BMC Genomics 6, 127.

Pavelka, M., Neumuller, J., Ellinger, A., 2008. Retrograde traffic in the biosynthetic-secretory route. Histochem. Cell Biol. 129, 277–288.

Pays, E., 2006. The variant surface glycoprotein as a tool for adaptation in African trypanosomes. Microbes Infect. 8, 930–937.

Pays, E., Vanhollebeke, B., Vanhamme, L., Paturiaux-Hanocq, F., Nolan, D.P., Pérez-Morga, D., 2006. The trypanolytic factor of human serum. Nat. Rev. Microbiol. 4, 477–486.

Peck, R.F., Shiflett, A.M., Schwartz, K.J., McCann, A., Hajduk, S.L., Bangs, J.D., 2008. The LAMP-like protein p67 plays an essential role in the lysosome of African trypanosomes. Mol. Microbiol. 68, 933–946.

Pelkmans, L., Fava, E., Grabner, H., Hannus, M., Habermann, B., Krausz, E., et al., 2005. Genome-wide analysis of human kinases in clathrin- and caveolae/raft-mediated endocytosis. Nature 436, 78–86.

Perez-Morga, D., Vanhollebeke, B., Paturiaux-Hanocq, F., Nolan, D.P., Lins, L., Homble, F., et al., 2005. Apolipoprotein L-I promotes trypanosome lysis by forming pores in lysosomal membranes. Science 309, 469–472.

Pilon, M., Schekmam, R., Römisch, K., 1997. Sec61p mediates export of a misfolded secretory protein from the endoplasmic reticulum to the cytosol for degradation. EMBO J. 16, 4540–4548.

Piper, R.C., Katzmann, D.J., 2007. Biogenesis and function of multivesicular bodies. Annu. Rev. Cell Dev. Biol. 23, 519–547.

Plemper, R.K., Bohmler, S., Bardallo, J., Sommer, T., Wolf, D.H., 1997. Mutant analysis links the translocon and BiP to retrograde protein transport for ER degradation. Nature 388, 891–895.

Poelvoorde, P., Vanhamme, L., Van Den Abbeele, J., Switzer, W.M., Pays, E., 2004. Distribution of apolipoprotein L-I and trypanosome lytic activity among primate sera. Mol. Biochem. Parasitol. 134, 155–157.

Pollevick, G.D., Di Noia, J.M., Salto, M.L., Lima, C., Leguizamón, M.S., de Lederkremer, R.M., et al., 2000. *Trypanosoma cruzi* surface mucins with exposed variant epitopes. J. Biol. Chem. 275, 27671–27680.

Price, H.P., Panethymitaki, C., Goulding, D., Smith, D.F., 2005. Functional analysis of TbARL1, an *N*-myristoylated Golgi protein essential for viability in bloodstream trypanosomes. J. Cell Sci. 118, 831–841.

Price, H.P., Stark, M., Smith, D.F., 2007. *Trypanosoma brucei* ARF1 plays a central role in endocytosis and golgi-lysosome trafficking. Mol. Biol. Cell 18, 864–873.

Pryor, P.R., Mullock, B.M., Bright, N.A., Lindsay, M.R., Gray, S.R., Richardson, S.C., et al., 2004. Combinatorial SNARE complexes with VAMP7 or VAMP8 define different late endocytic fusion events. EMBO Rep. 5, 590–595.

Pullen, T.J., Ginger, M.L., Gaskell, S.J., Gull, K., 2004. Protein targeting of an unusual, evolutionarily conserved adenylate kinase to a eukaryotic flagellum. Mol. Biol. Cell 15, 3257–3265.

Qualmann, B., Kessels, M.M., Kelly, R.B., 2000. Molecular links between endocytosis and the actin cytoskeleton. J. Cell Biol. 150, F111–F116.

Rabu, H., High, S., 2007. Membrane protein chaperones: a new twist in the tail. Curr. Biol. 17, R472–R474.

Raper, J., Fung, R., Ghiso, J., Nussenzweig, V., Tomlinson, S., 1999. Characterization of a novel trypanosome lytic factor from human serum. Infect. Immun. 67, 1910–1916.

Raper, J., Portela, M.P., Lugli, E., Frevert, U., Tomlinson, S., 2001. Trypanosome lytic factors: novel mediators of human innate immunity. Curr. Opin. Microbiol. 4, 402–408.

Rapoport, T.A., Jungnickel, B., Kutay, U., 1996. Protein transport across the eukaryotic endoplasmic reticulum and bacterial inner membranes. Annu. Rev. Biochem. 65, 271–303.

Reuner, B., Vassella, E., Yutzy, B., Boshart, M., 1997. Cell density triggers slender to stumpy differentiation of *Trypanosoma brucei* bloodstream forms in culture. Mol. Biochem. Parasitol. 90, 269–280.

Rifkin, M.R., 1978. *Trypanosoma brucei*: some properties of the cytotoxic reaction induced by normal human serum. Exp. Parasitol. 46, 189–206.

Rifkin, M.R., 1984. *Trypanosoma brucei*: biochemical and morphological studies of cytotoxicity caused by normal human serum. Exp. Parasitol. 58, 81–93.

Rifkin, M.R., 1991. *Trypanosoma brucei*: cytotoxicity of host high-density lipoprotein is not mediated by apolipoprotein A-I. Exp. Parasitol. 72, 216–218.

Robinson, D.R., Gull, K., 1991. Basal body movements as a mechanism for mitochondrial genome segregation in the trypanosome cell cycle. Nature 352, 731–733.

Rodgers, M.J., Albanesi, J.P., Phillips, M.A., 2007. Phosphatidylinositol 4-kinase III-beta is required for Golgi maintenance and cytokinesis in *Trypanosoma brucei*. Eukaryot. Cell 6, 1108–1118.

Roditi, I., Lehane, M.J., 2008. Interactions between trypanosomes and tsetse flies. Curr. Opin. Microbiol. 11 (4), 345–351.

Rosenblad, M.A., Zwieb, C., Samuelsson, T., 2004. Identification and comparative analysis of components from the signal recognition particle in protozoa and fungi. BMC Genomics 5, 5.

Rosenthal, J.A., Chen, H., Slepnev, V.I., Pellegrini, L., Salcini, E.A., Di Fiore, P.P., et al., 1999. The epsins define a family of proteins that interact with components of the clathrin coat and contain a new protein module. J. Biol. Chem. 274, 33959–33965.

Rubotham, J., Woods, K., Garcia-Salcedo, J.A., Pays, E., 2005. Characterization of two protein disulfide isomerases from the endocytic pathway of bloodstream forms of *Trypanosoma brucei*. J. Biol. Chem. 280, 10410–10418.

Russo, D.C., Grab, D.J., Lonsdale-Eccles, J.D., Shaw, M.K., Williams, D.J., 1993. Directional movement of variable surface glycoprotein-antibody complexes in *Trypanosoma brucei*. Eur. J. Cell Biol. 62, 432–441.

Salmon, D., Geuskens, M., Hanocq, F., Hanocq-Quertier, J., Nolan, D., Ruben, L., et al., 1994. A novel heterodimeric transferrin receptor encoded by a pair of VSG expression site-associated genes in *T. brucei*. Cell 78, 75–86.

Salmon, D., Paturiaux-Hanocq, F., Poelvoorde, P., Vanhamme, L., Pays, E., 2005. *Trypanosoma brucei*: growth differences in different mammalian sera are not due to the species-specificity of transferrin. Exp. Parasitol. 109, 188–194.

Sannerud, R., Saraste, J., Goud, B., 2003. Retrograde traffic in the biosynthetic-secretory route: pathways and machinery. Curr. Opin. Cell Biol. 15, 438–445.

Sato, N., Nakano, A., 2007. Mechamisms of COPII vesicle formation and protein sorting. FEBS Lett. 581, 2076–2082.

Schell, D., Evers, R., Preis, D., Ziegelbauer, K., Kiefer, H., Lottspeich, F., et al., 1991. A transferrin-binding protein of *Trypanosoma brucei* is encoded by one of the genes in the variant surface glycoprotein gene-expression site. EMBO J. 10, 1061–1066.

Schwartz, K.J., Bangs, J.D., 2007. Regulation of protein trafficking by glycosylphosphatidylinositol valence in African trypanosomes. J. Eukaryot. Microbiol. 54, 22–24.

Schwartz, T., Blobel, G., 2003. Structural basis for the function of the β subunit of the eukaryotic signal recognition receptor. Cell 112, 793–803.

Schwartz, K.J., Peck, R.F., Tazeh, N.N., Bangs, J.D., 2005a. GPI valence and the fate of secretory membrane proteins in African trypanosomes. J. Cell Sci. 118, 5499–5511.

Schwartz, K.J., Peck, R.F., Tazeh, N.N., Bangs, J.D., 2005b. GPI valence and the fate of secretory membrane proteins in African trypanosomes. J. Cell Sci. 118, 5499–5511.

Seaman, M.N., 2004. Cargo-selective endosomal sorting for retrieval to the Golgi requires retromer. J. Cell Biol. 165, 111–122.

Seiser, R.M., Nicchitta, C.V., 2000. The fate of membrane-bound ribosomes following termination of protein synthesis. J. Biol. Chem. 275, 33820–33827.

Selvapandiyan, A., Kumar, P., Morris, J.C., Salisbury, J.L., Wang, C.C., Nakhasi, H.L., 2007. Centrin1 is required for organelle segregation and cytokinesis in *Trypanosoma brucei*. Mol. Biol. Cell 18, 3290–3301.

Seyfang, A., Mecke, D., Duszenko, M., 1990. Degradation, recycling, and shedding of *Trypanosoma brucei* variant surface glycoprotein. J. Protozool. 37, 546–552.

Sheader, K., Vaughan, S., Minchin, J., Hughes, K., Gull, K., Rudenko, G., 2005. Variant surface glycoprotein RNA interference triggers a precytokinesis cell cycle arrest in African trypanosomes. Proc. Natl. Acad. Sci. USA 102, 8716–8721.

Shen, Y., Hendershot, L.M., 2005. ERdj3, a stress-inducible endoplasmic reticulum DnaJ homologue, serves as a coFactor for BiP's interactions with unfolded substrates. Mol. Biol. Cell 16, 40–50.

Shiflett, A.M., Bishop, J.R., Pahwa, A., Hajduk, S.L., 2005. Human high density lipoproteins are platforms for the assembly of multi-component innate immune complexes. J. Biol. Chem. 280, 32578–32585.

Shimamura, M., Hager, K.M., Hajduk, S.L., 2001. The lysosomal targeting and intracellular metabolism of trypanosome lytic factor by *Trypanosoma brucei brucei*. Mol. Biochem. Parasitol. 115, 227–237.

Shorter, J., Warren, G., 2002. Golgi architecture and inheritance. Annu. Rev. Cell Dev. Biol. 18, 379–420.
Sitia, R., Braakman, I., 2003. Quality control in the endoplasmic reticulum protein factory. Nature 426, 891–894.
Smith, A.B., Hajduk, S.L., 1995. Identification of haptoglobin as a natural inhibitor of trypanocidal activity in human serum. Proc. Natl. Acad. Sci. USA 92, 10262–10266.
Sommer, J.M., Wang, C.C., 1994. Targeting proteins to the glycosomes of African trypanosomes. Annu. Rev. Microbiol. 48, 105–138.
Sommer, J.M., Nguyen, T.T., Wang, C.C., 1994. Phosphoenolpyruvate carboxykinase of *Trypanosoma brucei* is targeted to the glycosomes by a C-terminal sequence. FEBS Lett. 350, 125–129.
Spradling, K.D., McDaniel, A.E., Lohi, J., Pilcher, B.K., 2001. Epsin 3 is a novel extracellular matrix-induced transcript specific to wounded epithelia. J. Biol. Chem. 279, 29257–29267.
Stefanovic, S., Hedge, R.S., 2007. Identification of a targeting factor for posttranslational membrane protein insertion into the ER. Cell 128, 1147–1159.
Sternberg, M.J., Mabbott, N.A., 1996. Nitric oxide-mediated suppression of T cell responses during *Trypanosoma brucei* infection: soluble trypanosome products and interferon-gamma are synergistic inducers of nitric oxide synthase. Eur. J. Immunol. 26, 539–543.
Steverding, D., Stierhof, Y.D., Chaudhri, M., Ligtenberg, M., Schell, D., Beck-Sickinger, A.G., et al., 1994. ESAG 6 and 7 products of *Trypanosoma brucei* form a transferrin binding protein complex. Eur. J. Cell Biol. 64, 78–87.
Subramaniam, C., Veazey, P., Redmand, S., Hayes-Sinclair, J., Chambers, E., Carrington, M., et al., 2006. Chromosome-wide analysis of gene function by RNA interference in the African trypanosome. Eukaryot. Cell 5, 1539–1549.
Tajima, S., Lauffer, L., Rath, V.L., Walter, P., 1986. The signal recognition particle receptor is a complex that contains two distinct polypeptide chains. J. Cell Biol. 103, 1167–1178.
Tatu, U., Helenius, A., 1997. Interactions between newly synthesized glycoproteins, calnexin and a network of resident chaperones in the endoplasmic reticulum. J. Cell Biol. 136, 555–565.
Tazeh, N.N., Bangs, J.D., 2007. Multiple motifs regulate trafficking of the LAMP-like protein p67 in the ancient eukaryote *Trypanosoma brucei*. Traffic 8, 1007–1017.
The Economist, Stability in Africa Economist Intelligence Unit ViewsWire, May 22nd 2008. http://www.economist.com/agenda/displaystory.cfm?story_id=11412430.
Tomlinson, S., Muranjan, M., Nussenzweig, V., Raper, J., 1997. Haptoglobin-related protein and apolipoprotein AI are components of the two trypanolytic factors in human serum. Mol. Biochem. Parasitol. 86, 117–120.
Triggs, V.P., Bangs, J.D., 2003. Glycosylphosphatidylinositol-dependent protein trafficking in bloodstream stage *Trypanosoma brucei*. Eukaryot. Cell 2, 76–83.
Trombetta, E.S., Parodi, A.J., 2005. Glycoprotein reglucosylation. Methods 35, 328–337.
Trombetta, S.E., Bosch, M., Paroji, A.J., 1989. Glucosylation of glycoproteins by mammalian, plant, fungal, and trypanosomatid protozoa microsomal membranes. Biochemistry 28, 8108–8116.
Tsai, B., Ye, Y., Rapoport, T.A., 2002. Retro-translocation of proteins from the endoplasmic reticulum in the cytosol. Nat. Rev. Mol. Cell Biol. 3, 246–255.
Urwyler, S., Studer, E., Renggli, C.K., Roditi, I., 2007. A family of stage-specific alanine-rich proteins on the surface of epimastigote forms of *Trypanosoma brucei*. Mol. Microbiol. 63 (1), 218–228.

Vanhamme, L., Paturiaux-Hanocq, F., Poelvoorde, P., Nolan, D.P., Lins, L., Van Den Abbeele, J., et al., 2003. Apolipoprotein L-I is the trypanosome lytic factor of human serum. Nature 422, 83–87.

Vanhollebeke, B., Lecordier, L., Perez-Morga, D., Amiguet-Vercher, A., Pays, E., 2007. Human serum lyses *Trypanosoma brucei* by triggering uncontrolled swelling of the parasite lysosome. J. Eukaryot. Microbiol. 54, 448–451.

Vanhollebeke, B., De Muylder, G., Nielsen, M.J., Pays, A., Tebabi, P., Dieu, M., et al., 2008. A haptoglobin-hemoglobin receptor conveys innate immunity to *Trypanosoma brucei* in humans. Science 320, 677–681.

van Luenen, H.G., Kieft, R., Mussmann, R., Engstler, M., ter Riet, B., Borst, P., 2005. Trypanosomes change their transferrin receptor expression to allow effective uptake of host transferrin. Mol. Microbiol. 58, 151–165.

van Niel, G., Wubbolts, R., Ten Broeke, T., Buschow, S.I., Ossendorp, F.A., Melief, C.J., et al., 2006. Dendritic cells regulate exposure of MHC class II at their plasma membrane by oligoubiquitination. Immunity 25, 885–894.

Vassella, E., Oberle, M., Urwyler, S., Renggli, C.K., Studer, E., Hemphill, A., et al., 2009. Major surface glycoproteins of insect forms of *Trypanosoma brucei* are not essential for cyclical transmission by tsetse. PLoS One 4 (2), e4493.

Vickerman, K., 1969. On the surface coat and flagellar adhesion in trypanosomes. J. Cell Sci. 5 (1), 163–193.

Vickerman, K., 1985. Developmental cycles and biology of pathogenic trypanosomes. Br. Med. Bull. 41, 105–114.

Vickerman, K., Tetley, L., Hendry, K.A., Turner, C.M., 1988. Biology of African trypanosomes in the tsetse fly. Biol. Cell 64, 109–119.

Vincendeau, P., Daulouede, S., Veyret, B., Darde, M.L., Bouteille, B., Lemesre, J.L., 1992. Nitric oxide-mediated cytostatic activity on *Trypanosoma brucei gambiense* and *Trypanosoma brucei brucei*. Exp. Parasitol. 75, 353–360.

Walter, P., Johnson, A.E., 1994. Signal sequence recognition and protein targeting to the endoplasmic reticulum membrane. Annu. Rev. Cell Biol. 10, 87–119.

Wang, T., Hebert, D.N., 2003. EDEM an ER quality control receptor. Nat. Struct. Biol. 10, 319–321.

Wang, J., Böhme, U., Cross, G.A.M., 2003. Structural features affecting variant surface glycoprotein expression in *Trypanosoma brucei*. Mol. Biochem. Parasitol. 128, 135–145.

Wasiak, S., Legendre-Guillemin, V., Puertollano, R., Blondeau, F., Girard, M., de Heuvel, E., et al., 2002. Enthoprotin: a novel clathrin associated protein identified through subcellular proteomics. J. Cell Biol. 158, 855–862.

Wickner, W., Schekman, R., 2005. Protein translocation across biological membranes. Science 310, 1452–1456.

Wiedmann, B., Sakai, H., Davis, T.A., Wiedmann, M., 1994. A protein complex required for signal sequence-sorting and translocation. Nature 370, 434–440.

Wiertz, E.J., Tortorella, D., Bogyo, M., Yu, J., Mothes, W., Jones, T.R., et al., 1996. Sec61-mediated transfer of a membrane protein from the endoplasmic reticulum to the proteasome for destruction. Nature 384, 432–438.

Williams, R.L., Urbé, S., 2007. The emerging shape of the ESCRT machinery. Nat. Rev. Mol. Cell Biol. 8, 355–368.

Xong, H.V., Vanhamme, L., Chamekh, M., Chimfwembe, C.E., Van Den Abbeele, J., Pays, A., et al., 1998. A VSG expression site-associated gene confers resistance to human serum in *Trypanosoma rhodesiense*. Cell 95, 839–846.

Yam, A.Y., Albanèse, V., Lin, H.T., Frydman, J., 2005. Hsp110 cooperates with different cytosolic HSP70 systems in a pathway for *de novo* folding. J. Biol. Chem. 280, 41252–41261.

Young, J., Kane, L.P., Exley, M., Wileman, T., 1993. Regulation of selective degradation in the endoplasmic reticulum by redox potential. J. Biol. Chem. 268, 19810–19818.

Zamze, S.E., Ashford, D.A., Wooten, E.W., Rademacher, T.W., Dwek, R.A., 1991. Structural characterization of the asparagine-linked oligosaccharides from *Trypanosoma brucei* type II and type III variant surface glycoproteins. J. Biol. Chem. 266, 20244–20261.

Zerial, M., McBride, H., 2001. Rab proteins as membrane organizers. Nat. Rev. Mol. Cell Biol. 2, 107–117.

Zhang, J.X., Braakman, I., Matlack, K.E.S., Helenius, A., 1997. Quality control in the secretory pathway: the role of calreticulin, calnexin and BiP in the retention of glycoproteins with C-terminal truncations. Mol. Biol. Cell 8, 1943–1954.

Ziegelbauer, K., Overath, P., 1992. Identification of invariant surface glycoproteins in the bloodstream stage of *Trypanosoma brucei*. J. Biol. Chem. 267, 10791–10796.

CHAPTER TWO

Biological and Biophysical Properties of Vascular Connexin Channels

Scott Johnstone,* Brant Isakson,*,† *and* Darren Locke‡

Contents

1. Introduction 71
2. The Vasculature 72
   2.1. Homocellular gap junctions 74
   2.2. Heterocellular gap junctions 74
3. Connexin Channels 75
   3.1. Connexins 75
   3.2. Hemichannels 79
   3.3. The gap junction channel 82
4. Gap Junctional Communication Pathways in the Vasculature 82
   4.1. Between endothelial cells in large vessels 83
   4.2. Between vascular smooth muscle cells 84
   4.3. In resistance vessels 85
   4.4. In capillaries and veins 86
5. Permeability of Vascular Connexin Channels 87
   5.1. Ion permeability 90
   5.2. Molecular permeability 92
   5.3. Posttranslational modifications 98
   5.4. Interaction of connexin with other proteins 99
   5.5. Pharmacological block 100
6. Involvement of Connexins in Vascular Diseases 101
   6.1. Hypertension 101
   6.2. Atherosclerosis 102

* Robert M. Berne Cardiovascular Research Center, University of Virginia School of Medicine, Charlottesville, Virginia 29908, USA
† Department of Molecular Physiology and Biological Physics, University of Virginia School of Medicine, Charlottesville, Virginia 29908, USA
‡ Department of Pharmacology and Physiology, New Jersey Medical School, University of Medicine and Dentistry of New Jersey, Newark, New Jersey 07103, USA

International Review of Cell and Molecular Biology, Volume 278
ISSN 1937-6448, DOI: 10.1016/S1937-6448(09)78002-5
© 2009 Elsevier Inc.
All rights reserved.

7. Concluding Remarks 104
Acknowledgments 105
References 105

Abstract

Intercellular channels formed by connexin proteins play a pivotal role in the direct movement of ions and larger cytoplasmic solutes between vascular endothelial cells, between vascular smooth muscle cells, and between endothelial and smooth muscle cells. Multiple genetic and epigenetic factors modulate connexin expression levels and/or channel function, including cell-type-independent and cell-type-specific transcription factors, posttranslational modifications, and localized membrane targeting. Additionally, differences in protein–protein interactions, including those between connexins, significantly contribute to both vascular homeostasis and disease progression. The biophysical properties of the connexin channels identified in the vasculature, those formed by Cx37, Cx40, Cx43 and/or Cx45 proteins, are discussed in this chapter in the physiological and pathophysiological context of vessel function.

Key Words: Connexin, Endothelial cells, Hemichannel, Heterocellular communication, Myoendothelial junction, Smooth muscle cells. © 2009 Elsevier Inc.

Abbreviations

A350	Alexa350 dye
A488	Alexa488 dye
A594	Alexa594 dye
ADP	adenosine diphosphate
AMP	adenosine monophosphate
ATP	adenosine triphosphate
BFA	brefeldin A
CA	calcein
$Ca^{2+}/[Ca^{2+}]_i$	calcium ion/intracellular concentration of
cAMP	adenosine 3′,5′-cyclic monophosphate
CF	6-carboxyflourescein
cGMP	guanosine 3′,5′-cyclic monophosphate
CL	cytoplasmic loop domain
CT	carboxyl-terminal domain
Cx	connexin
Cx37	connexin37
Cx40	connexin40
Cx43	connexin43

Cx45	connexin45
DAPI	4,6-diamidino-2-phenyl-indole dihydrochloride
E1/E2	first/second extracellular loop domains
EB	ethidium bromide
EC	endothelial cell
ECM	extracellular matrix
IEL	internal elastic lamina
IP_3	inositol triphosphate
IP_3-R	receptor for IP_3
LY	Lucifer yellow
M1/M2/M3/M4	connexin transmembrane domains
MEJ	myoendothelial junction
NB	neurobiotin
NBD-TMA	2-(4-nitro-2,1,3-benzoxadiazol-7-yl)-aminoethyl trimethylammonium
NO	nitric oxide
NT	amino-terminal domain
P_0	"nonphosphorylated" Cx43
P_1 and P_2	phosphorylated Cx43
Panx	pannexin
Panx1	pannexin1
Panx2	pannexin2
Panx3	pannexin3
PI	propidium iodide
pS	picoSiemens
siRNA	silencing/antisense RNA
$t_{1/2}$	half-life
TGN	trans-Golgi network
V_{i-o} or V_m	transmembrane voltage
V_j	transjunctional voltage
VSMC	vascular smooth muscle cell
ZO-1	zonula occludens-1

1. Introduction

The coordination of vascular responses is essential for normal vessel function. Long-distance communication networks in the vessel wall achieve the dynamic modulation of vascular resistance and blood flow to match different tissue oxygen requirements. Morphologically distinct gap junctions are a vital component in this process.

While ionic coupling by gap junctions enables changes in membrane potential to be propagated electrotonically between adjacent cells, they

uniquely allow the cellular exchange of metabolites, ions, and other small molecules, such as second messengers, which play important roles in transverse and longitudinal signaling in the vascular bed, and processes including angiogenesis, vascular cell growth, cell differentiation and development (Chadjichristos et al., 2008; Coutinho et al., 2003; Liao et al., 2007).

The expression of different gap junction proteins is dynamically regulated throughout different types of vascular bed in healthy vessels and in vascular disease states such as atherosclerosis and hypertension (Brisset et al., 2009; Kwak, 2002).

2. The Vasculature

Direct electrical (ionic) coupling between cells has been observed for over half a century (Holland and Dunn, 1954), a process requiring intimate focal contact structures bridging intermembrane "gaps" (Dewey and Barr, 1964). The nature of these interactions was resolved by thin section and freeze fracture electron microscopy of heart and nonexcitable liver tissue. En face views of the focal plaque-like regions showed there to be densely packed hexagonal intramembrane particles in the membranes of both apposing cells where two cells remained separated by a uniform gap of ~ 2 nm. These particles had diameters of ~ 7 nm and an electron opaque region of ~ 1 nm at their center (Revel and Karnovsky, 1967). Such observations, having subsequently been structurally refined by biochemical, biophysical, and crystallographic study, support the working/current model of "gap junction" structure as an array of aqueous intercellular channels directly connecting the cytoplasms of adjacent cells.

Gap junctions can be morphologically identified within the vasculature at sites of endothelial cell (EC), vascular smooth muscle cell (VSMC), and EC and VSMC contact, the latter a specialized region referred to as the "myoendothelial junction" (MEJ) (de Wit et al., 2006a,b; Isakson and Duling, 2005; Rhodin, 1967; Simionescu et al., 1976) (Fig. 2.1).

The involvement of gap junctions, and their constituent connexin (Cx) proteins, is vital to the coordination of cellular activities within the wall of the vasculature (Figueroa and Duling, 2008; Segal and Jacobs, 2001) and most other tissues (Harris and Locke, 2009).

A total of 21 human connexin genes and 20 mouse connexin genes have been identified, with each cell generally containing multiple connexin isoforms. Each isoform contributes a particular set of functional and regulatory properties to a gap junction channel that is essential, either intact or as modified by interaction with other connexins, for normal cellular development and function (Harris and Locke, 2009).

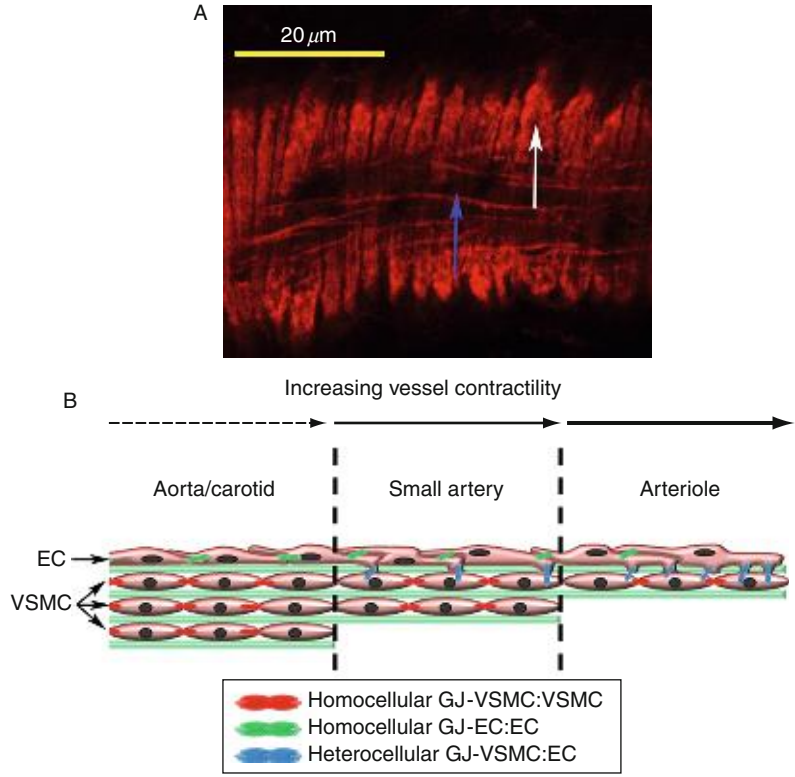

Figure 2.1 Vessel composition and functional interactions. (A) A mouse cremasteric arteriole is stained with phalloidin. Endothelial cells align in the direction of flow (blue arrow) and vascular smooth muscle cells align perpendicular to the endothelial cells (white arrow). (B) Gap junctions form homocellular (green and red symbols) and heterocellular (blue) contact points between VSMC and EC in the vasculature depending on the vessel bed studied.

In most tissues, including the vasculature, functional deletion of a connexin isoform produces distinct and severe pathophysiology, and genetic knock-in replacement of one connexin by another isoform fails to fully compensate for the loss (Winterhager et al., 2007; Zheng-Fischhofer et al., 2006); specifically, this reflects the need for different intercellular signaling pathways mediated by the different connexin channels.

The vasculature can be divided into large conduit vessels (macrovessels; e.g., veins, aorta or carotid arteries) and smaller highly contractile vessels (microvessels; e.g., venules, mesenteric arteries or cremasteric arterioles). Anatomically, EC line the lumen of all vessels and align with the direction of blood flow (Brisset et al., 2009). EC are separated by extracellular matrix (ECM), termed the "internal elastic lamina" (IEL), from layers of VSMC

patterned perpendicularly and arranged helically to the EC on the outside of the vessel (Cornhill et al., 1980; Hirano et al., 2007; Ohtani et al., 1983; Wolinsky and Glagov, 1967). This assembly permits efficient flow within the vessel across the EC and control of vessel tone by VSMC.

In the larger vessels, ECM separates VSMC layers into ''lamellar units'' that vary in number, proportionate to vessel size and flow rate, for example, eight in the ascending and four in the descending aorta (Hirano et al., 2007). Here, the VSMC are important in maintenance of tone, whereas in the smaller vessels, such as the arterioles, single layers of EC and VSMC are more responsive to contractile stimuli and so play an integral role in the maintenance of blood pressure.

2.1. Homocellular gap junctions

Gap junctions facilitate the movement of small molecules and ions at homocellular contact points, that is, EC:EC or VSMC:VSMC (Beny and Gribi, 1989; Ebong et al., 2006; Figueroa et al., 2003; Hoffmann et al., 2003; Isakson et al., 2006a; Ko et al., 1999; Little et al., 1995a; Rummery and Hill, 2004; Sandow et al., 2003; Segal and Beny, 1992).

Macrovessel EC are extensively coupled by these intercellular connections, as shown by laying out the vessel en face (an exposed luminal face) and microinjecting a single EC with a gap junction-permeable fluorescent dye that quickly diffuses to surrounding cells (Ebong et al., 2006; Segal and Duling, 1986). Homocellular dye transfer between VSMC *in vivo* has been demonstrated (Little et al., 1995a; Straub et al., 2009), though not to the same extent as between EC, due in large part to the orientation of the VSMC making these experiments difficult.

2.2. Heterocellular gap junctions

At perforations of the IEL in microvessels, EC and VSMC make heterocellular contact at MEJ (Rhodin, 1967). These unique structures are widely distributed throughout the vasculature, though are less abundant in the larger arteries and veins than in the arterioles and venules, where they are numerous (Heberlein et al., 2009). It is estimated that one MEJ is found every ~ 5 μm along the length of first-order arterioles, which represents six MEJ for every EC or three MEJ for every VSMC (Heberlein et al., 2009; Sokoya et al., 2007). The MEJ are small, ~ 0.5 μm wide by ~ 0.5 μm in length, making their detection by light microscopy extremely difficult.

The complexity of the MEJ environment has also made difficult and limiting any standard *in vivo* techniques, and as such has required innovative new approaches, which have only recently begun to show some interesting results. Evolving experimental evidence shows gap junctions at the MEJ play a

pivotal role in coordinating microvessel function (Duling et al., 2003; Haddock et al., 2006; Heberlein et al., 2009; Isakson, 2008; Isakson et al., 2008).

3. Connexin Channels

Only four connexin proteins, Cx37, Cx40, Cx43 and Cx45, have been robustly documented within the different layers of the vasculature (Brisset et al., 2009; Hill et al., 2001; Isakson et al., 2006a, 2008) (Table 2.1). Prior to the realization that there was more than one connexin isoform, morphological studies had shown that the size and abundance of gap junctions varied in different regions of the vascular tree and changed during disease. The distribution of connexins is currently known to vary between individual vascular beds of one species, between the same vascular bed of different species as well as during embryological development and progression of disease (Figueroa et al., 2004; Severs, 2001).

The primary role for connexin proteins is the formation of intercellular gap junctions, which are unique in the type of intercellular signaling they mediate. However, connexins may also be involved in a regulated non-junctional permeability pathway, one allowing ions and some (notably larger) molecules to passively cross the plasma membrane (Spray et al., 2006). Additionally, gap junctions are now realized to be focal sites for interaction with accessory proteins, these often linked to the cytoskeleton (Giepmans, 2004); such nonchannel behavior is a common feature of other membrane channels and transporters, and provides mechanisms for both "outside-in" and "inside-out" signaling.

3.1. Connexins

In the absence of a clear understanding of the functional differences between different connexins, a logical nomenclature for distinguishing the various members of the gene family was to add the molecular weight of each protein variant as a suffix to the descriptor "Cx". Hence, a protein composing gap junctions in heart that runs at ~ 43 kDa by reducing SDS–PAGE is known as Cx43.

Connexins may be further subclassified based on their phylogenetic origins (Eastman et al., 2006). Of the four vascular connexins, three belong to the alpha (α) subgroup (Cx37, Cx40 and Cx43) while Cx45 is a member of the gamma (γ) subgroup (Saez et al., 2003). Subgroup designation plays a major role in determining the ability of these proteins to interact with one another (Beyer et al., 2000; Gemel et al., 2004) (Table 2.2).

Irrespective of such differences, all connexins share the same overall protein topology. There are four transmembrane domains (M1–M4), two

Table 2.1 Physical properties of vascular gap junctions

	Cx37	Cx40	Cx43	Cx45
	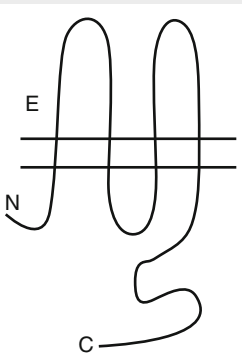	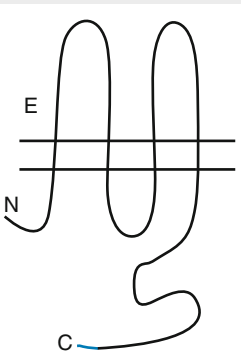	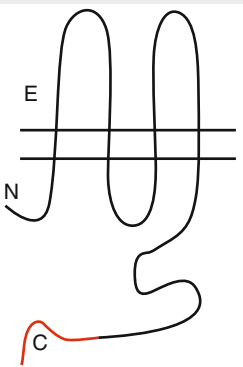	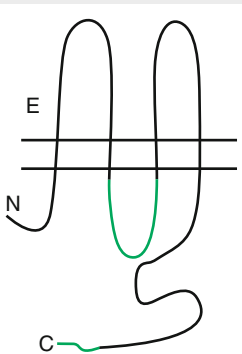
Chromosome	1p35.1	1q21.1	6q22–q22.3	17q21.31
Gene	GJA4	GJA5	GJA1	GJC1
Subgroup	α	α	α	γ
Protein (kDa)	37	40	43	45
Protein (aa)	332	357	382	396

NT domain (aa)[a]	19	18	12	22
CL (aa)[a]	49	67	55	80
CT domain (aa)[a]	103	132	159	148
Pore diameter (Å)	10–14 Å (Veenstra et al., 1994b)	6.6 Å (Beblo and Veenstra, 1997)	10 Å[b] (Heyman and Burt, 2008)	10 Å (Veenstra et al., 1994a)
Pore length (Å)	ND	ND	160 Å (Heyman and Burt, 2008)	ND
Protein expression	EC/VSMC (Krattinger et al., 2007; Yeh et al., 2000b)	EC/VSMC	VSMC/EC (Krattinger et al., 2007; Yeh et al., 2000b)	VSMC/EC

[a] Sizes and approximate regions were determined from data available in http://www.uniprot.org/.
[b] Radius ~6 Å has been determined, but is inconsistent with dye transfer so is thus inferred to be ~10 Å (Heyman and Burt, 2008).
Vascular Cx37, Cx40, C43, and Cx45 show significant sequence homology. Major sequence divergence is observed primarily in the cytoplasmic loop (CL) and tail (CT) domains. Images are characterizations of membrane topology with light grey highlighting the regions at which there are significant differences in amino acid sequence or length. The amino terminus in most α subgroup connexins is ~23 aa, but is shorter in Cx45 at ~18 aa. The CL of Cx45 is elongated compared to Cx37, Cx40, or Cx43. The lengths of the CT domains are based on hydropathy plots. ND, not demonstrated.

Table 2.2 Vascular gap junction channel assembly

	Cx37	Cx40	Cx43	Cx45
Cx37	Y	Y (Rackauskas et al., 2007)	Y (Brink et al., 1997)	Y (Elfgang et al., 1995)
Cx40	–	Y	Y/N[a] (Cottrell et al., 2002; Rackauskas et al., 2007; Valiunas et al., 2000)	Y (Martinez et al., 2002)
Cx43	–	–	Y	Y (Bukauskas et al., 2001)
Cx45	–	–	–	Y

[a] Conflicting literature.
Table summarizes studies of the (homotypic and) heterotypic compatibility between connexins expressed in vascular tissue. Y, channels formed; N, channels not formed.

extracellular loops (E1 and E2), cytoplasmic amino-terminal (NT) and carboxyl-terminal (CT) domains, and a cytoplasmic loop (CL) between M2 and M3 (Evans and Martin, 2002; Kovacs et al., 2007).

The NT is relatively conserved, though its exact length has not been conclusively demonstrated [the NT domain of most α subgroup connexins is ~23 aa (Kyle et al., 2008), but is shorter in Cx45 at ~18 aa (Essner et al., 1996)]; it is predicted to lie within the channel pore (Lin et al., 2006; Purnick et al., 2000) and is an important region involved in channel gating in response to changes in membrane voltage (Kyle et al., 2008).

Disulfide bridge interactions between spatially conserved cysteine residues in the extracellular loops, in E1 that connects M1–M2 and in E2 that connects M3–M4 (Dahl et al., 1992; Yilla et al., 1992), are necessary for the docking process by which oligomerized connexin proteins in each apposing cell form gap junctions.

The extracellular docking forms a tight seal to prevent the loss of cytoplasmic ions and molecules to the extracellular space. The pore itself is formed by one or two of the four hydrophobic transmembrane domains (Maeda et al., 2009), can accommodate molecules of up to ~2 kDa (subjective), while nonuniform pore diameters ranging from ~14 to ~40 Å have been described (Beblo and Veenstra, 1997; Fleishman et al., 2004; Heyman and Burt, 2008; Maeda et al., 2009; Oshima et al., 2007; Unger et al., 1999; Veenstra et al., 1995).

The CL and CT domains, which constitute the majority of the cytoplasmic surface are more divergent in sequence homology [the CL of Cx37 and Cx40 varies in length by 20 aa (Duffy et al., 2002; Seki et al., 2004); there is an unusually elongated CL in Cx45 as compared to the other three vascular connexin isoforms (Kumai et al., 2000; Manthey et al., 1999); the CT domains range in length from 103 aa in Cx37 to 159 aa in Cx43

(Goodenough et al., 1996; Kyle et al., 2008; Stergiopoulos et al., 1999)], are less organized in tertiary structure and, in general, contain sites for intra- and inter-molecular protein–protein binding and for posttranslational modifications, each of which allow for different regulatory mechanisms for fine tuning the permeation pathway.

For example, phosphorylation dynamically modulates Cx43 trafficking to, and internalization from, junctional plaques, the channel open probability and its ion conductance (Solan and Lampe, 2007). Intermolecular interactions between Cx43 and tight junction proteins are implicated in determining the size of the junctional plaque (Hunter et al., 2005). Additionally, intramolecular interactions between CL and CT of Cx43 are responsible for pH-dependent channel gating (Duffy et al., 2002; Sosinsky and Nicholson, 2005). Related intermolecular interactions occur between Cx40 and Cx43 in *hemi*-gap junction channels: the CT of Cx40 can regulate a truncated Cx43 channel and the CT of Cx43 can rescue the pH sensitivity of a truncated Cx40 (Stergiopoulos et al., 1999).

3.2. Hemichannels

Connexins oligomerize in the ER/Golgi, or at a later stage in the *trans*-Golgi network (TGN) (Koval, 2006), to form hexameric ''hemichannels'' (also known as ''connexons''). While most connexins, including Cx37, Cx40 and Cx45, oligomerize in the ER, Cx43 is not assembled into oligomers until the TGN (Maza et al., 2005). The chaperone Erp29 has been implicated in delayed Cx43 oligomerization (Das et al., 2009).

Oligomerization is thought to spontaneously occur through noncovalent interaction (Ahmad and Evans, 2002). The hemichannel structure may be further stabilized through shared sites between neighboring connexins within the same hexamer (Maeda et al., 2009). The NT and M3 regions are implicated in the oligomerization process, with residues within the NT thought to play a prominent role in dictating interaction between members of different phylogenetic subgroups, that is, α:α and β:β interactions are allowed, but α:β interactions are generally not (Beyer et al., 2000; Gemel et al., 2004); of note, Cx45 (γ) is promiscuous.

As such, interactions between connexins in hemichannels are of two described types: *homomeric* hemichannels are composed of six monomers of a single connexin isoform and *heteromeric* hemichannels are composed by at least two different isoforms.

It is becoming apparent that isoform mixing within hemichannels may be a means for fine tuning the permeability character of gap junction channels (Ayad et al., 2006; Bevans and Harris, 1999a,b; Bevans et al., 1998; Brink et al., 1997; He et al., 1999; Locke et al., 2004, 2007; Weber et al., 2004).

3.2.1. Hemichannel trafficking to plasma membrane

At the light microscope level and by biochemical study, there is some evidence for small domains of aggregated nonjunctional hemichannels in plasma membrane. Hemichannels are considered to remain closed until docked with an appositional hemichannel (Evans et al., 2006; Spray et al., 2006), although regulated openings have been suggested (Saez et al., 2005); however, the involvement of connexins as the composition of such functional plasma membrane pores has been brought into question.

Transport of hemichannels to the plasma membrane is largely dependent on an intact microtubule and Golgi network (Falk and Gilula, 1998; Falk et al., 1997; George et al., 1999; Martin et al., 2001; Thomas et al., 2005). The functional significance of interactions between connexins and the actin cytoskeleton are much less clear. There are reports that Cx43 can bypass the Golgi if cells are treated with brefeldin A (BFA) and cotreated with cAMP or low-density lipoprotein (LDL) (Paulson et al., 2000). In part, this suggests that alternative plasma membrane trafficking pathways for hemichannels may exist under certain (patho) physiological conditions; for example, Cx26 may bypass the Golgi en route to the plasma membrane in hepatocytes (Ahmad and Evans, 2002; George et al., 1999; Martin et al., 2001).

Less is known about the trafficking of Cx37, Cx40, and Cx45 hemichannels specifically, though posttranslational modifications, in particular the phosphorylation of the CT domain, may be implicated (Solan and Lampe, 2005, 2007). Many connexins, including Cx37, Cx40 and Cx45, are phosphoproteins as shown by either a phosphatase-sensitive shift in their electrophoretic mobility, direct incorporation of [^{32}P]-phosphate or by mass spectrometry. As analyzed by SDS–PAGE, Cx43 shows multiple electrophoretic isoforms including a faster migrating form that is typically, but not always, nonphosphorylated (termed "P_0"), and at least two phosphorylated, and therefore slower migrating, forms termed "P_1" and "P_2". The Triton X100 detergent solubility of P_0 and P_1 *and* detergent insolubility of P_2 forms (Musil and Goodenough, 1991) have been used extensively to study differences between nonjunctional and junctional pools of Cx43, respectively.

Protein–protein interactions have also been implicated in the trafficking process and the targeting and removal of hemichannels and gap junction channels in the plasma membrane (Giepmans, 2004; Laird, 2006). Most in-depth studies on the binding of connexins to other cell proteins, and the functional consequences of these interactions, have largely focused on Cx43.

In the plasma membrane, gap junction plaques grow, at least in part, by the lateral movement of unpaired hemichannels to the periphery of a gap junction plaque (Gaietta et al., 2002). Interactions between Cx43 and zonula occludens-1 (ZO-1), a tight junction protein, may control the rate of (hemi)channel accretion at the periphery of the plaque and limit the occupied surface area (Hunter et al., 2005).

One emerging mode for plasma membrane localization, and possible regulation of channel activity, exists in the form of lipid raft movement and segregation of hemichannels. Some connexin isoforms are differentially localized to detergent soluble and insoluble lipid rafts and show movement into and out of caveolin-1-based rafts (Langlois et al., 2008; Locke et al., 2005; Simek et al., 2009). There are well-documented lipid rafts unique to EC and VSMC (e.g., extensive caveolin-1 present in EC and absent in VSMC; Callera et al., 2007; Raghu et al., 2007), so it is conceivable that connexin localization or redistribution into different types of lipid raft might alter membrane localization of hemichannels and influence hemichannel/gap junction function in a cell-type-specific manner. There is certainly emerging evidence of an intimate involvement of different phospholipids with different connexins that contributes to modulation of channel structure, form and/or function (Locke and Harris, 2009).

3.2.2. Connexin hemichannels and pannexin channels

As a large membrane pore, even brief opening of unapposed/nonjunctional hemichannels in plasma membranes must be tightly regulated to maintain cellular integrity (Contreras et al., 2003, 2004). Connexin hemichannels (''connexons'') have been implicated in a regulated plasma membrane pathway allowing the uptake and release of large biological and nonbiological molecules. However, the protein composition of this pathway has been of dispute.

The most prominent large molecule nonconnexin pathway is that formed by pannexin channels (''pannexons''). Pannexins (Panx), closely related to innexins, which form gap junctions in invertebrates, share the same transmembrane topology as connexins, but have no primary sequence homology (Baranova et al., 2004; Yen and Saier, 2007). Pannexins do not form intercellular channels because one of their extracellular loops is glycosylated, this modification adding substantial bulk to the extracellular-facing aspect of the protein, preventing the formation of a patent cell–cell channel (insertion of glycosylation sites into the extracellular loop domains of connexins also blocks formation of junctional channels when these sites are glycosylated; Boassa et al., 2007).

Only three pannexin isoforms have been described: Panx1 (47.6 kDa), Panx2 (69.5 kDa) and Panx3 (44.7 kDa). The cellular and tissue expression of pannexins, notably Panx1, overlaps with that of most all connexin isoforms, so it is now believed that many of the phenomena that have been attributed to unpaired plasma membrane connexons may in fact be mediated by pannexons. Pannexin channels are permeable to everything that a connexin hemichannel should be (generally) permeable to, but, in fact, may be wider than the widest connexons (Bao et al., 2007; Locovei et al., 2007). Moreover, pannexin channels are blocked by several of the pharmacological agents commonly used to inhibit connexin hemichannels.

For these reasons, identifying which protein/''hemi''/''channel'' is involved in a particular cellular physiology requires careful evaluation of

the specific experimental conditions and biological requirements in each case (Parthasarathi et al., 2006; Scemes, 2008; Scemes et al., 2007; Spray et al., 2006).

3.3. The gap junction channel

At the plasma membrane, two hexameric hemichannels align across the extracellular space to form a dodecameric intercellular channel. The gap junction plaque is a focal area of membrane containing accreted connexin channels. The composition of the plaque is unique; a requirement for other proteins has not been demonstrated, and the exogenous expression of connexins in a wide variety of model systems is sufficient to result in the formation of membrane structures that are functionally and morphologically indistinguishable from gap junction plaques observed in native tissues.

Interactions between hemichannels when forming junctional channels are of two described types: *homotypic* junctional channels are formed by 12 identical connexin subunits and *heterotypic* channels are formed by two hemichannels that are each homomeric for different isoforms.

As with the oligomerization of connexins into hemichannels, members of the α and β subgroups, for example, Cx43 and Cx26, do not readily form heterotypic channels, despite their extracellular domains being conserved in structure (Oshima et al., 2007). This incompatibility is suspected to result from different hydrogen bonding signatures in E2 (Yeager and Harris, 2007). Again, Cx45 (γ) is rather immoral and can form heterotypic channels with members from α and β subfamilies.

Other connexin domains are also involved in regulating heterotypic compatibility (Maza et al., 2005). In studies of heterotypic Cx37–Cx43 junctions, substitutions of $\sim$12 aa in the NT domain prevented channel formation (Lagree et al., 2003), yet smaller substitutions of between 2 and 8 aa in the same region were sufficient to permit formation of heterotypic gap junctions (Kyle et al., 2008). The intact CL domain is also important; studies looking at heterotypic pairing of hemichannels formed by CL deletion mutants of Cx43 with Cx37, Cx40 and Cx45 showed there was reduced heterotypic gap junction formation with Cx37 and Cx45, and heterotypic Cx40–Cx43 junctions did not form at all (Wang et al., 2005).

4. Gap Junctional Communication Pathways in the Vasculature

Homo- and hetero-cellular contact is commonplace; EC and VSMC connect in all combinations and morphologically distinct gap junctions are observed between both cells *in vivo*. In mouse aortas and arterioles, Cx37, Cx40 and Cx43 are typically expressed in EC, whereas Cx43, and possibly

Cx37, are expressed in VSMC (Haefliger et al., 2004; Isakson et al., 2006a; Johnstone et al., 2009; Li and Simard, 2002; Saitongdee et al., 2004). However, there are conflicting data on the gap junctional connexin content in the MEJ in rat, with claims that both Cx37 and Cx40 are expressed or that only Cx40 is present (Haddock et al., 2006). In mouse, Cx40 and Cx43 are present in the apposed membranes between EC and renin-secreting cells as well as in the mouse cremasteric arterioles (Isakson et al., 2008; Straub et al., 2009). However, as noted above, connexin expression in EC, VSMC, or at the MEJ between EC and VSMC is both vascular bed and species specific (Isakson et al., 2008; van Kempen and Jongsma, 1999).

4.1. Between endothelial cells in large vessels

Immunohistochemistry, transmission and scanning electron microscopy demonstrate that EC of the large vessels are particularly well coupled by gap junctions, with all four vascular connexins expressed to various degrees (Isakson et al., 2006a; Kwak, 2002; Yeh et al., 2000a,b, 2001).

In general, Cx40 and Cx37 are abundantly expressed in elastic (aorta) and muscular (coronary) arteries of various species, while the expression of Cx43 is typically restricted to EC in regions of turbulent flow such as vessel branch regions, particularly in the rat aortic and carotid arteries (Dai et al., 2004; Gabriels and Paul, 1998; Hill et al., 2001; Saitongdee et al., 2004). In other tissues, Cx43 is integral to cell proliferation (Chadjichristos et al., 2006b; Johnstone et al., 2009; Kwak et al., 2003; Liao et al., 2007) and apoptotic control (Kalvelyte et al., 2003), so Cx43 may act to protect EC from improper proliferation or cell death due to elevated sheer stress at these regions (Feaver et al., 2008; Johnson and Nerem, 2007).

Currently, there is no evidence for heterocellular contact between VSMC and EC in large vessels; thus, gap junctional communication in large vessels is likely to be entirely homocellular. However, while immunocytochemistry demonstrates junctional colocalization of Cx37, Cx40 and Cx43 in the EC of mouse aortas, this does not prove that heteromeric or heterotypic channels are present *in vivo* (Yeh et al., 2000a,b); though, functional heterotypic gap junction channels are observed *in vitro* (Isakson and Duling, 2005).

Several studies demonstrate that intracellular signaling/conducted responses within aortic EC occur bidirectionally through gap junctions (Simon and McWhorter, 2003; Wolfle et al., 2007). For example, ablation of Cx40 ($Cx40^{-/-}$) from the mouse genome results in reduced acetylcholine-induced vasodilation (Figueroa and Duling, 2008) and dye transfer between EC (Simon and McWhorter, 2003). That any dye coupling is observed between the EC of $Cx40^{-/-}$ mice shows that some junctional communication remains; upregulation of Cx37 has been demonstrated in this instance (Kruger et al., 2002; Simon and McWhorter, 2003), however, this is disputed. Interestingly, neither Cx37 or Cx45 appears to play significant roles

in the acetylcholine-induced conductive responses in EC, suggesting that they may have other, as yet unestablished, functions (Figueroa and Duling, 2008; Hou et al., 2008; Kumai et al., 2000; Wolfle et al., 2007).

Nonbiological tracer dyes indicate the presence of extensive intercellular communication compartments, and several studies have detected changes in dye transfer pathways in response to different arterial flow patterns across the EC (Ebong et al., 2006), the biological significance of which is also not yet known.

Enhanced gap junctional communication between EC is typically observed as vessel flow rate increases. Using EC in culture, Cx37 and Cx40, but not Cx43, were upregulated in response to elevated flow rates (Ebong et al., 2006). In atheroprone sheer stress models, both Cx37 and Cx43 gap junctions are redistributed to intracellular regions of cultured EC; there is increased plasma membrane organization of gap junctions under atheroprotective flow rates (Dai et al., 2004). As Cx43 is upregulated at sites of turbulent flow *in vivo*, with no alterations to Cx37 or Cx40 expression (Gabriels and Paul, 1998), these studies demonstrate the need for careful consideration of the model system under investigation.

4.2. Between vascular smooth muscle cells

Gap junctions between VSMC are usually between small sections of plasma membrane and do not resemble those between EC, that is, these being large gap junction plaques between tightly sealed opposing EC plasma membranes. As with the EC layers of the large vessels, it is generally accepted that VSMC communication is homocellular, and bidirectional conducted responses by gap junctions may be involved in acetylcholine-induced conducted vasoconstriction (Figueroa and Duling, 2009) or maintaining cell quiescence (Zhang et al., 2003). Following vascular damage through insertion of indwelling catheters in mice, sites distal to the injury in the direction opposite to blood flow showed enhanced cell proliferation (Reidy, 1990). Numerous studies have shown that alterations in VSMC connexin expression are associated with cell proliferation (Brisset et al., 2009).

Only Cx43 and Cx45 are identifiable in the VSMC of healthy aortic and carotid tissues (Haefliger et al., 2004; Isakson et al., 2006a; Li and Simard, 1999; Saitongdee et al., 2004). Heteromeric and heterotypic interactions between Cx43 and Cx45 have been demonstrated *in vitro* (Rackauskas et al., 2007), despite their belonging to different phylogenetic/compatibilty subgroups (α and γ, respectively). This association is mediated, in part, by the binding of Cx43 and Cx45 to the PDZ domains of ZO-1 (Kausalya et al., 2001; Laing et al., 2001). Homotypic Cx43 and Cx45 *versus* heterotypic association of Cx43 and Cx45 hemichannels may be a means by which the permeability characteristics of the VSMC gap junction pathway can be

modulated *in vivo*, as suggested by *in vitro* study (Desplantez et al., 2004; Elenes et al., 2001).

Several studies have also identified expression of Cx37 in VSMC (Kwak, 2002; Simon and McWhorter, 2002, 2003), although it is not normally expressed in healthy adult aortas or carotids (Cai et al., 2004; Saitongdee et al., 2004); this more likely reflects species differences (van Kempen and Jongsma, 1999) or changes occurring in response to the progression of vascular disease (Cai et al., 2004; Kwak, 2002).

4.3. In resistance vessels

As mentioned, connexin expression in resistance vessels is dependent on the vascular bed and species studied. Typically, Cx40 is found in EC, with Cx37, Cx43 and Cx45 being subject to more variable expression both within EC and VSMC (Bruzzone et al., 1993; Cai et al., 2001, 2004; Hakim et al., 2008; Hwan Seul and Beyer, 2000; Isakson, 2008; Isakson and Duling, 2005; Isakson et al., 2006a, 2008; Little et al., 1995a; van Kempen and Jongsma, 1999).

Initial work to address the presence of gap junctions in resistance vessels demonstrated that tracer dyes rapidly moved between EC in hamster cheek pouch arterioles (Segal and Beny, 1992). Anatomical evidence and immunohistochemistry further shows that EC of the resistance vessels are highly coupled, similar to those between EC of large arteries (Bruzzone et al., 1993; Hakim et al., 2008; Isakson et al., 2006a; van Kempen and Jongsma, 1999).

Although *in vivo* morphological verification of gap junction plaques in VSMC is difficult, arteriolar VSMC are electrically coupled (Beny and Connat, 1992). However, experiments to show dye coupling between VSMC within resistance vessels have given mixed results (Beny and Connat, 1992; Little et al., 1995b; Segal and Beny, 1992; Straub et al., 2009).

The unique aspect of resistance vessel physiology is the degree to which EC and VSMC are integrated. While such integration may occur via paracrine mechanisms, gap junctions play important roles at the MEJ in small vessels.

Extensive ultrastructural evidence for MEJ gap junctions has been demonstrated by transmission electron microscopy. Connexin expression is dependent on vessel location and species (Heberlein et al., 2009); recent data have found Cx37 and Cx40 in rat brain arterioles, Cx40 and Cx37 separately or in combination in rat mesentery, Cx40 and Cx43 in mice arterioles and Cx43 in human subcutaneous resistance arteries (Haddock et al., 2006; Isakson and Duling, 2005; Isakson et al., 2006a; Sandow and Garland, 2006; Sandow et al., 2003). Further, Cx37, Cx40 and Cx43 but not Cx45 have been localized at the MEJ sites *in vitro* (Isakson and Duling, 2005) and *in vivo* (Haddock et al., 2006; Isakson et al., 2008; Sandow and

Garland, 2006). However, data from rat studies suggest Cx37 expression at these sites to be more variable than that of Cx40 and Cx43, or absent altogether (Isakson and Duling, 2005; Isakson et al., 2008).

Studies of the "endothelium-derived hyperpolarizing factor" (EDHF) have provided the vast majority of the evidence for functional gap junction signaling from EC to VSMC at the MEJ (de Wit et al., 2006a; Sandow et al., 2009). The EDHF phenomenon is based on observations that stimulation of EC with acetylcholine produces a vascular dilatory "factor" (i.e., EDHF) that moves from EC to VSMC through gap junctions (presumably), even when prostaglandin and nitric oxide (NO) synthase inhibitors are present. This dilatory process is characterized by increases in intracellular Ca^{2+} levels ($[Ca^{2+}]_i$) in EC. As might be expected for a pathway involving gap junctions, VSMC would display a corresponding increase in $[Ca^{2+}]_i$ and respond by constricting. However, the converse has been repeatedly demonstrated; VSMC display a corresponding decrease in $[Ca^{2+}]_i$ and the vessel responds by dilating (Sandow et al., 2009).

Signaling from VSMC to EC through gap junctions at the MEJ has not been studied to the same extent as EDHF. Stimulation of VSMC with phenylephrine produces an increase in $[Ca^{2+}]_i$ via IP_3, which, in isolated vessels and *in vitro*, moves to EC through gap junctions present at the MEJ to produce an increase in EC $[Ca^{2+}]_i$ and subsequent release of NO (Dora et al., 1997; Isakson, 2008; Isakson et al., 2007; Lamboley et al., 2005). This signaling process is highly dependent on the location of the receptor for IP_3 (IP_3-R) at the MEJ; it has been suggested that localization of IP_3-R on the EC side of the MEJ, rather than the VSMC side, is the reason that the Ca^{2+} signal is not observed moving from EC to VSMC (Isakson, 2008).

Evidence has also indicated that gap junctions at the MEJ may not always be functional/open during acetylcholine-induced conduction (Budel et al., 2003). Recent work has suggested that closure may result from posttranslational modification of the CT domain of Cx43 (Isakson et al., 2008). Phosphorylation of serine 368 (Ser368) in the CT domain of Cx43 has been observed in mouse cremaster MEJ, but not rat mesenteric MEJ, correlating with an absence of carboxyfluorescein dye transfer in cremasteric vessels but its abundant transfer in the mesenteric vessels (Isakson et al., 2008; Mather et al., 2005; Siegl et al., 2005; Straub et al., 2009). In fact, if the cAMP analog, pCPT, was applied to mouse cremaster, Ser368 phosphorylation was no longer detected and carboxyfluorescein readily transferred from VSMC to EC (Straub et al., 2009).

4.4. In capillaries and veins

Strikingly, little is known about connexin expression in capillaries and veins, and thus the functional roles remain to be elucidated.

Capillary EC are ionically/electrically coupled (Beach et al., 1998) despite connexins not being readily identified (Looft-Wilson et al., 2004).

This may be a consequence of the relative sensitivity of immunofluorescent and electrophysiological techniques used (Looft-Wilson et al., 2004) or explained by differences in expression levels between vessel beds as determined by signaling requirements of the tissue.

Cx40 and Cx43 have been identified in the EC and VSMC of saphenous veins, with especially high amounts of Cx43 within the VSMC (Deglise et al., 2005). It is thought this may regulate VSMC proliferation, as previously described for VSMC in larger vessels, above.

5. Permeability of Vascular Connexin Channels

Demonstrations of junctional coupling have been established by electrophysiological measurements and observations of the intercellular transfer of small membrane-impermeable fluorescent dyes or cellular metabolites (Tables 2.3 and 2.4). Typically, gap junctions were the only identifiable intimate contact between adjacent cells. Particularly, the observation of intercellular metabolite permeability sparked broad interest in gap junction channels as mediators of intercellular molecular signaling and as key players in the processes of development, physiology and disease (Harris and Locke, 2009).

The most important point to make at the onset is of the large diversity in the permeability and modulatory properties of connexin channels. Homomeric/homotypic and heteromeric/heterotypic channels have all been described, and each is of unique character; additionally, when two connexins are expressed in the same cell, several hemichannel stoichiometries and/or radial connexin arrangements around the central lumen are made possible. Thus, the relevant permeabilities of connexin channels can extend from charge selectivity among atomic ions through the size and charge selectivity among nonbiological tracer molecules (i.e., dyes) to highly specific selectivity among cytoplasmic molecules (i.e., second messengers) (Harris and Locke, 2009).

The properties of junctional channels have so far been reasonably well predicted from those of their component hemichannels. The intercellular channels, behave, for the most part, as if each hemichannel is a functionally independent unit, acting in series with the other docked hemichannel. This does, occasionally, give rise to unexpected permeability character and/or gating behavior (Bukauskas et al., 1995; Oh et al., 1999; Suchyna et al., 1999), not so much reflecting allosteric changes occurring to the pore itself upon hemichannel docking so much as the functional superimposition of hemichannels with different biophysical, regulatory and/or pharmacological properties (Harris, 2001).

Table 2.3 Nonbiological molecular permeants

	Size				
	Mass (Da)	*X* (Å)	*Y* (Å)	*Z* (Å)	Charge
DAPI (Heyman and Burt, 2008)	279	15.4	6.0	NA	+2
PI (Contreras et al., 2003; Retamal et al., 2006; Valiunas, 2002)	661	12.0	9.3	4.5	+2
EB (Contreras et al., 2003; Retamal et al., 2006; Valiunas, 2002)	394	11.6	9.3	4.3	+1
NBD-TMA (Ek-Vitorin et al., 2006; Heyman and Burt, 2008; Simon and McWhorter, 2003)	280	11.7	6.0	3.85	+1
Biocytin (Simon and McWhorter, 2003)	372	NA	NA	NA	0
A350 (Weber et al., 2004)	326	13.0	5.2	3.2	−1
CF	376	12.6	12.7	8.5	−2
LY (Heyman and Burt, 2008)	457	12.6	14.0	5.5	−2
A488 (Heyman and Burt, 2008; Weber et al., 2004)	546	11.3	10.5	9.0	−2
A594 (Heyman and Burt, 2008; Weber et al., 2004)	734	16.6	13.8	9.3	−2
IP_3[a] (Ayad et al., 2006)	414	5.5–10.6	5.4–9.9	3.1–7.9	−6

[a] IP_3 has several structural conformers, so the approximately largest and smallest dimensions are reported (Ayad et al., 2006).

Typical fluorescent probes used to assess the function of gap junctions. NA, not available.

Individual studies bearing directly on the permeability of Cx37, Cx40, Cx43 and Cx45 channels are too numerous to be discussed individually. However, a sampling of the relevant data are integrated, in particular when there is information on the relative permeability to different ions and molecules through each connexin isoform, and when the permeability to a single ion or molecule through the different vascular connexin channels are known, where it is possible to rigorously allow such comparisons to be made. For the latter, differences in the number of functional junctional channels may introduce error [connexin expression can vary greatly

Table 2.4 Relative conductance of vascular gap junctions and hemichannels

	Cx37	Cx40	Cx43	Cx45
Unitary conductance (pS)				
Junction (V_j)	300, 347 (Reed et al., 1993; Veenstra et al., 1994b, 1995)	142–198 (Beblo and Veenstra, 1997; Veenstra et al., 1995)	60–120 (Veenstra et al., 1995; Wang and Veenstra, 1997)	26–37 (Valiunas, 2002; Veenstra et al., 1994a, 1995)
Hemichannel (V_j)	600[a] (Banach et al., 2000; Hu et al., 2006)	300 (Rackauskas et al., 2007)	220 (Contreras et al., 2003)	57 (Valiunas, 2002)
Substate	63 (Veenstra et al., 1994b)	30–36	30–60	23
Relative tracer permeability				
EB or PI	Cx37 = Cx40			
LY	Cx43 ≫ Cx40 > Cx45 = Cx40/Cx45 = Cx43/45[b] > Cx37 (Heyman and Burt, 2008; Rackauskas et al., 2007)			
A350	Cx45 > Cx40 > Cx43 > Cx37 = Cx37/Cx43 (Weber et al., 2004)			
	Cx43 ≫ Cx40 ≫ Cx40/45 = Cx43/Cx45 > Cx37 (Heyman and Burt, 2008; Rackauskas et al., 2007)			
A488	Cx43 > Cx40 > Cx45 ≫ Cx37 = Cx37/Cx43 (Weber et al., 2004)			
A594	Cx43 > Cx45 > Cx40 ≫ Cx37/Cx43 > Cx37(ND) (Weber et al., 2004)			

[a] Predicted hemichannel conductance of Cx37, which has not been demonstrated due to a lack of voltage-dependent saturation (Banach et al., 2000; Veenstra et al., 1994b).
ND, not demonstrated.

between species, tissue studied (i.e., different vascular beds) or cell lines, be affected by posttranslational modifications, as discussed below], as would intracellular distribution, cytoplasmic/nuclear binding, cell volume and concentration of tracer studied (i.e., assay procedure).

5.1. Ion permeability

Channel unitary conductance, in picoSiemens (pS), being the ease or difficulty with which ions pass through single channels when a voltage is imposed across the channel is remarkably different for different connexin isoforms (Beblo and Veenstra, 1997; Hu et al., 2006; Moreno et al., 1994a, b; Puljung et al., 2004; Reed et al., 1993; Valiunas, 2002; Veenstra et al., 1994a,b); thus, the internal pore topography of gap junction channels formed by different connexin isoforms are different. The relative unitary conductance of homotypic channels is in the order: Cx37 (300 pS) > Cx40 (140 pS) > Cx43 (100 pS) > Cx45 (30 pS).

Speaking generally, greater ion selectivity is not observed in channels with smaller conductance, as would be expected for a narrower pore. In fact, connexin channels have a larger pore than the classical ion-selective channels, with more than one ion able to enter the channel at the same time. In most cases, the permeability to current carrying atomic ions is high and the ionic selectivity of connexin channels is unremarkable. However, for Cx43 and Cx40 the ionic selectivity is influenced by interactions between anions and cations within the pore itself (Cottrell and Burt, 2001; Weber et al., 2004); in particular, the electrical conductance of the Cx40 pore is specifically reduced by permeant anions affecting cation permeation.

For Cx37, significant alterations in unitary conductance are also attributed to NT domain truncations (Francis et al., 1999; Kumari et al., 2000). Polymorphic variability in this region increases the susceptibility to atherosclerotic plaque formation, and has been attributed in part to greater nonjunctional hemichannel permeability (Boerma et al., 1999; Derouette et al., 2009).

In the vasculature, gap junctions link EC:EC, VSMC:VSMC and EC:VSMC compartments, and, as there is cell-type-specific expression of Cx37, Cx40, Cx43 and Cx45, there is great potential for the formation of heterotypic junctions (Burt et al., 2001; Cottrell and Burt, 2001; Desplantez et al., 2004).

In vitro systems demonstrate heterotypic Cx37–Cx40 (Rackauskas et al., 2007), Cx37–Cx43 (Brink et al., 1997), Cx43–Cx45 (Elenes et al., 2001; Martinez et al., 2002; Rackauskas et al., 2007) and Cx40–Cx45 junctions (Bukauskas et al., 2006). *In vivo* studies have suggested formation of Cx40–Cx43 heterotypic channels (Cottrell et al., 2002; Valiunas et al., 2000).

The most compelling demonstration for heteromeric channels by electrophysiological means was obtained for Cx37 and Cx43 in transfected cells (Brink et al., 1997), as it was possible to directly compare homotypic and heterotypic single-channel properties. The measured unitary conductances could not be explained solely by the formation of heterotypic or homotypic channels. Similar studies using Cx40 in addition to Cx37 and Cx43, in the same transfected cells, confirmed similar behavior for heteromeric Cx37/Cx43 and Cx40/Cx43 channels (Beyer et al., 2000). The unitary conductances of heterotypic channels, where calculated from conductances of homomeric hemichannels (the conductivity of a homomeric hemichannel is approximately twice that of the homomeric junctional channel) are (shown here as predicted/actual): for Cx40–Cx43, 127/100–150 pS; for Cx43–Cx46, 75/120 pS; for Cx43–Cx45, 51/52 pS.

5.1.1. Electrical coupling

Voltage is generated by the flow of ionic current between two adjacent cells via gap junctions. These electrical connections are typically bidirectional, but may not be symmetrical in their flow (Palacios-Prado and Bukauskas, 2009). Ionic currents resulting from interconnecting cells with different potentials are clearly seen in the heart and nervous system, but are now evident in the ear, lens and in developing embryos.

Conducted responses along vessels require changes of the membrane potential; depolarization results in local and conducted vasoconstriction and hyperpolarization the dilatory conducted response. Although these electrical signals are opposite in their polarity, they both make use of gap junctions, the low-resistance electrical conduction pathway in the vascular wall. Heterotypic junctions formed by Cx37 and Cx40 are rectifying, showing a macroscopic asymmetric voltage–conductance relationship, meaning that junctional currents elicited by hyperpolarization or depolarization of either coupled cell are not identical; ionic flow may thus be unidirectional (Palacios-Prado and Bukauskas, 2009).

5.1.2. Voltage and chemical gating

All intercellular channels are sensitive to "transmembrane" (V_{i-o} or V_m) and "transjunctional" voltage (V_j) differences. These types of voltage gating are intrinsic to hemichannels, so in an intercellular channel each apposed hemichannel contains separate gating structures arranged in series. Evidence for this was shown with Cx37 and/or Cx40 channels; when heterotypic channels were formed from homomeric hemichannels, one polarity of junctional voltage induces a response like that of Cx40 and the other like that of Cx37 (Bruzzone et al., 1993; Hennemann et al., 1992).

The most well-described case of V_m gating is for Cx45, for which there may be species differences; human Cx45 is more sensitive to membrane potential differences than mouse Cx45. Typically, Cx45 channels open upon

depolarization (Barrio et al., 1997), whereas Cx43 channels close (White et al., 1994) and Cx40 channels are unresponsive (White et al., 1994). V_m and V_j sensitivity processes are different, as was shown for Cx43 channels (Revilla et al., 2000), suggesting independent sensors and gating mechanisms.

The molecular determinants and the mechanism of polarity determination of "V_j" or "fast" gating (<1 ms) have been studied extensively for nonvascular connexins, but differences in the gating polarity of different channels result from differences in the charged residues of the NT, which form the entry of the channel pore (Maeda et al., 2009; Oh et al., 2004). Polymorphic variability in the NT region of Cx37 has been implicated in increased susceptibility to altherosclerotic plaque formation (Boerma et al., 1999; Derouette et al., 2009). Data also support involvement of the CT domain in the V_j gating mechanism of Cx43 (Bukauskas et al., 2001).

Some channels also have bipolar V_j/fast gating mechanisms, meaning that the channel may close via intermediate substates (Banach et al., 2000; Oh et al., 2004). This mechanism can involve a proline kink in TM2, an interaction between the CL and CT, posttranslational modification, especially phosphorylation (Cx43 in particular), or result from the movement of a cytoplasmic domain as a gating particle.

Less is known about the molecular determinants and mechanisms of "loop" or "slow" gating (>5 ms), which is also sensitive to V_j and V_{i-o}/V_m. The most defined mechanism for of loop/slow gating is the closure of gap junction channels in response to acidification of the intracellular space, that is, "pH gating" or "chemical gating".

Chemical gating of Cx43 involves pH-dependent intramolecular interactions between specific segments of Cx43 CT and CL, a mechanism that presents itself as a target for chemical or genetic manipulation (Delmar et al., 2004). This mechanism is present and absent in other connexin channels. For example, a functional interaction between Cx40 and Cx43 that modulates the pH sensitivity of junctional channels is almost certainly explained by their presence in the same hemichannels (Gu et al., 2000)—in fact, the Cx43 CT can induce pH sensitivity in CT truncated (i.e., pH insensitive) Cx40 and *vice versa* (Stergiopoulos et al., 1999); however, truncation of the CT of Cx37 or Cx45 has little effect on their pH sensitivity (Stergiopoulos et al., 1999).

In a rare example of a "dominant-positive" effect, "heterotypic" docking of Cx45 with a CT truncation mutant of Cx45 that does not form homotypic junctional channels enables to the truncated Cx45 hemichannel to open (Hulser et al., 2001).

5.2. Molecular permeability

Uncharged and relatively chemically unreactive tracers have been used sparingly to infer the diameter of connexin pore lumens at their narrowest point (the "size-selectivity filter") (Harris, 2001). In only one study, using

sugars as tracers, mannitol (a linear monosaccharide alcohol) and stachyose (a branched tetrasaccharide) were found to be impermeable through Cx40 channels, but mannitol and not raffinose (a branched trisaccharide) or stachyose were permeable through Cx43 channels (Wang and Veenstra, 1997), suggesting that Cx40 channels have a narrower limiting diameter than Cx43 channels.

Connexin channel molecular permeability and the physical size constraints of the pore have been more widely assessed using several types of nonbiological molecules, usually fluorescent dyes of different sizes, charge and chemistry. Dye molecules report the existence and extent of junctional communication pathways, while, at their most basic level, providing some information about the relative abilities of diverse, large permeants to pass through pores formed by different connexins. This literature is vast and, typically, unitary conductance and channel permeability to these larger molecules do not correlate well with each other, meaning the former do not allow easy inferences or extrapolations about the latter (Veenstra et al., 1995).

Dyes are less informative as tools with which to investigate the *biological* nature of the permeability pathway itself. Only a few studies have revealed differences in permeation by different biological molecules through a particular type of connexin channel, or differences in permeation by a particular biological molecule through different types of connexin channels. In large part, the perceived absence of useful data is because these experiments are technically challenging; the pore entrance and exit are cytoplasmic, so (applied, biological) ''permeant'' species cannot typically be altered with impunity.

Introduction of most biologically active compounds into cells can have direct or indirect downstream effects on gap junction channels. Further, biological compounds can be degraded, a factor that does not typically affect assessment of permeability using dyes, and whose rate of degradation can be dependent upon metabolic state and cell type. Critically, the ability to quantitatively detect intercellular transfer is often constrained by available detection methods, such as by chemical modification of the molecules (i.e., adding fluorescent tags) that could affect their permeability. Further, post-translational modifications of connexin may affect biological molecule permeability, either by direct modification of the permeation pathway or by altered voltage gating leading to occupation of conductance substates (this has been demonstrated for Cx43; Qu and Dahl, 2002).

It is easy to believe that the permeation through connexin channels, in part, would depend on the limiting pore width of the channel lumen, that is, its diameter at its narrowest point; historically, a molecular weight limit of ~ 2 kDa and pore diameter of ~ 10 Å had been in place, but permeant charge and chemistry are now known to play important roles, particularly as the channel lumen is not featureless — size, shape and chemical interactions between permeant and pore walls influence molecular permeation.

The few data available do make clear that different connexin channels can have highly distinct and differential permeabilities among cytoplasmic molecules, and that these bear little discernible relation to the channels' ionic charge selectivities, to the permeabilities of nonbiological tracer/dye molecules, or, in part, to permeants' size.

Where possible, available studies with charged and uncharged nonbiological tracers rank the limiting pore diameter of vascular connexins, widest to narrowest (unitary conductance, in pS, is in parentheses): Cx43 (90 pS) $\gg$ Cx40 (180 pS) $\approx$ Cx45 (30 pS) $>$ Cx37 (300 pS). Of note, Cx37 channels are the narrowest pore in spite of having the largest unitary conductance. In fact, for these four connexins, there is almost an inverse correlation in the magnitudes of these channels' conductances and the sizes of the permeants; larger nonbiological tracer molecules permeate channels with low conductances (e.g., Cx45), but are unable to permeate channels with much higher conductances (e.g., Cx37 and Cx40).

To the extent that the limited data also allow comparison between pore width and ionic charge selectivity, the data suggest that the narrower channels (i.e., Cx37, Cx45 and Cx40) are also significantly more charge selective (than Cx43, the widest). Their permeability to large cationic tracers is Cx45 (30 pS) and Cx43 (90 pS) $>$ Cx37 (300 pS), and their permeability to large anionic tracers is Cx43 (90 pS) $>$ Cx40 (180 pS) $>$ Cx45 (30 pS) $\gg$ Cx37 (300 pS) (Bedner et al., 2006; Cottrell and Burt, 2001). One piece of data conflicts with this, that is, the movement of Alexa350 dye (A350), a small anionic dye, through Cx43 channels is specifically reduced by a unique interaction between A350 and the Cx43 pore that does not occur for other connexin channels (Weber et al., 2004).

In fact, while Cx43 channels are equally permeable to large anionic and cationic dyes, Cx43 displays a remarkable and unpredictable divergence with regard to permeation by large anionic biological molecules, thus favoring ADP/ATP over AMP and adenosine (Goldberg et al., 2002). It is difficult to account for this selectivity without invoking some kind of specific affinity between the channel and these permeants.

Remarkable and unexpected findings also involve Cx43 channel permeation by RNA and peptides. Single-stranded interfering RNAs, which one would expect to be physically too large to permeate junctional channels, can do so. This property is connexin specific, with permeability through homotypic Cx43 channels documented (Valiunas et al., 2005). Linear/unstructured peptides of length up to $\sim$10 aa can also permeate homotypic Cx43 junctional channels, which means gap junctions potentially play important roles in cell–cell transfer of peptides in antigen presentation and cross-presentation in the immune system (Neijssen et al., 2005).

5.2.1. Communication compartments

Dye transfer studies establish the presence or absence of gap junctions. The least quantitative studies are the most common; these assess the number of cells to which dye spreads from a ''donor'' cell loaded with tracer. More qualitative clues about relative tracer permeabilities can be inferred if spread is normalized to the number of channels (i.e., ''junctional conductance'' divided by ''unitary conductance''), factors such as ''frictional force'' or various incarnations of ''affinity'' are taken into account, or tracer permeability is normalized to the permeability of a second tracer applied at the same time.

Lucifer yellow (LY, charge − 2) is the most commonly used gap junction-permeable dye. Early studies demonstrated EC:EC transfer of LY, and the absence of EC:VSMC or VSMC:VSMC transfer of LY in cheek pouch arterioles (Segal and Beny, 1992; Welsh and Segal, 1998).

In large vessels, biocytin (charge neutral) and NBD-TMA (charge + 1) transfer between EC in aortas. *Ex vivo*, dye injections of mouse aortic endothelium from $Cx40^{-/-}$ and $Cx37^{-/-}$ mice demonstrated significant reductions in dye transfer compared to wild type (Simon and McWhorter, 2003; Simon et al., 2004). In these studies, wild-type aortic EC were more permeable to biocytin than NBD-TMA, while knockout of Cx40 but not Cx37 in these layers significantly reduced transfer of both biocytin and NBD-TMA compared to control mice (Simon and McWhorter, 2003). Later, it was found that treatment of aortas from Cx37 knockout animals with lipopolysaccharide reduced expression of Cx40 resulting in a decrease in dye transfer (Simon et al., 2004).

5.2.2. Signaling kinetics

The relative junctional permeabilities of different biological molecules are key factors in any coordinated signaling or regulatory system that has a kinetic component, particularly where the rate of change or ''oscillation'' in the levels of a compound are important. Oscillatory changes in signaling molecules (e.g., Ca^{2+}, cAMP, ATP) occur across systems of cells coupled by gap junctions convey information distinct from changes in steady-state levels. Even modest differences or changes in selectivity at cellular junctions have major impact on the strength, character, and location of the intercellular signaling, under both steady-state and kinetic conditions.

Essentially, for two molecules having different junctional permeabilities, it appears as though cells are better coupled with regard to one compound. Whenever there is a difference or a change in synthesis or degradation (e.g., in response to hormone receptor activation or difference/change in connexin channel composition), the profile of concentration of a compound will change with kinetics that also includes their rates of junctional flux. The consequence of having an intercellular pathway is that not only can the

steady-state levels of the compounds be different, but the kinetics of change in those levels are different for each compound in not one, but a population of cells.

5.2.3. Selective permeability

The naive view is that gap junction channels, as large membrane pores, have little selective molecular permeability, so that any permeant biological molecules readily equilibrate within a population of coupled cells. Instead, relative and absolute differences in junctional permeability of different biological molecules are important, and produce profound differences in tissue response, for example, to periodic release of second messengers.

A variety of experimental approaches have been used, some involving direct measurements of molecular flux through unambiguously identified connexin channels and others relying on indirect methods to infer the identity of the transferred compounds or that the transfer is through connexin channels.

The results make clear that different connexin channels can have highly distinct and differential permeabilities among dye molecules, and that these bear little discernible relation to the atomic ion charge selectivities or to the permeabilities to biological tracers (cf., Cx43 permeability of Alexa dyes *versus* adenosine-based molecules).

The vast majority of work documents all-or-none permeability. With only a few exceptions, commonly studied second messengers, that is, ATP, IP_3/Ca^{2+}, cAMP and cGMP, are permeable to some degree through each type of connexin channel studied, and all are important in modulating vessel function (Faigle et al., 2008; Kanaporis et al., 2008). Selectivity has been shown only for cAMP which diffuses more readily through Cx43 than Cx45 (Bedner et al., 2006) or Cx40 junctions (Kanaporis et al., 2008).

In the vasculature, it has been demonstrated that the gap junctions facilitate the movement of IP_3 between EC (Boitano et al., 1992) and heterocellular movement of IP_3 through gap junctions at the MEJ (Isakson et al., 2007), the latter independent of connexin composition (Isakson, 2008). In VSMC, gap junctions facilitate the propagation of oscillatory $[Ca^{2+}]_i$ waves (Christ et al., 1992), and heterocellular movement of Ca^{2+} across the MEJ was demonstrated bidirectionally using *in vitro* vascular cell coculture for EC and VSMC (Isakson et al., 2007). These responses were independent of IP_3 levels, directly indicating Ca^{2+} movement through gap junctions at the MEJ.

Where established to be junctional, as opposed to paracellular, Ca^{2+} signaling is usually considered as evidence that IP_3 permeates junctional channels. However, junctional Ca^{2+} flux may also be involved. In some cases, it is clear that regenerative Ca^{2+} signaling is mediated by IP_3 flux and that the contribution of junctional Ca^{2+} flux is minor (Leybaert et al., 1998). In certain cases, it appears that junctional Ca^{2+} flux is a major factor

and in others that both are involved (Faigle et al., 2008; Isakson, 2001; Isakson et al., 2007; Kanaporis et al., 2008; Saez et al., 1989). Computational modeling has supported each scenario (Iacobas et al., 2006).

5.2.4. Hemichannel-mediated paracrine signaling

Typically, Ca^{2+} wave propagation involves two pathways: direct intercellular flux of IP_3 through gap junction channels and an extracellular pathway involving ATP release and purinergic receptors. In EC, release of ATP through vascular "hemichannels" is thought to propagate oscillatory Ca^{2+} wave conduction in arterioles and capillaries (Bennett et al., 2003; de Wit et al., 2006a,b; Parthasarathi et al., 2006). This promotes vessel contraction and additional Ca^{2+} release from intracellular stores, which regenerates the signal, along the vessel length (Haddock et al., 2006). The paracrine release of ATP may be a compensatory mechanism for reduction in gap junctional permeability of ATP (De Vuyst et al., 2006). However, in vascular disease, the release of ATP is chemoprotective, preventing leukocyte adhesion and accumulation at atherosclerotic regions (Wong et al., 2006a).

A genetic polymorphism in GJA4, the human gene encoding Cx37, is a potential prognostic marker for atherosclerosis. Cx37 expression is altered in mouse and human atherosclerotic lesions; it is absent from the endothelium of advanced plaques but is present in macrophages recruited to the lesions. It is suggested Cx37 hemichannel activity (i.e., release of ATP into the extracellular space) in macrophages inhibits leukocyte adhesion and initiation of the development of atherosclerotic plaques. Macrophages expressing either of the two Cx37 proteins encoded by a polymorphism in the GJA4 gene (Cx37–Ser319, Cx37–Pro319) show differential ATP-dependent adhesion (Wong et al., 2006a).

However, when considering the involvement of "hemichannels" in normal vessel cell physiology and disease, one must be careful; the paracrine/extracellular release of ATP or Ca^{2+} described earlier might occur via any of several connexin and nonconnexin (e.g., pannexin) candidate mechanisms. In many studies, correlation of extracellular release of biological molecules with connexin expression is taken to indicate that the release is through connexin hemichannels.

A large literature documents the multifaceted biological effects of connexin expression. Altered connexin expression has been shown to have dramatic effects on the expression of hundreds of other gene products, which may have downstream effects on nonconnexin plasma membrane proteins and other mechanisms of cell release of signaling molecules. Such changes could alter expression or regulation of the other candidate (ATP or Ca^{2+}) release channels.

Panx1 has been identified in VSMCs of rat cerebral arteries but not in the EC (Chen et al., 2008). Panx2 is expressed in both endothelial and

smooth muscle cell layers, interestingly localizing at regions of gap junctional plaques (Chen et al., 2008).

Pannexin channels can exist alone in membranes, or be activated by purinergic P_2X_7 receptors. Panx1 channels are closed at negative potentials, open at positive potentials and inactivate over time. They are activated at normal resting membrane potentials by mechanical stress or by increases of cytoplasmic Ca^{2+}. Panx1 channels are very permeable to ATP, so much so that current carried through the channel by ATP itself can be recorded. It is, therefore, extremely likely that pannexons are the prime candidates for the ATP release channel and/or the source of paracrine Ca^{2+} wave propagation in the vasculature.

5.3. Posttranslational modifications

Either by direct modification of the permeation pathway, by altered gating leading to occupation of conductance substate(s) or by changing the ability of the connexin to interact with other proteins, posttranslational modifications play an important role in control of gap junction permeability. This has been explicitly demonstrated for Cx43 and, to date, most studies, irrespective of connexin isoform involved, focus on the role of phosphorylation; modification of the CT domain may regulate unapposed hemichannel function (Lampe and Lau, 2004; Zeilinger et al., 2005), and there is differential Cx43 phosphorylation in both healthy and diseased vessels (Isakson et al., 2006a, 2008; Johnstone et al., 2009).

The role of other posttranslational modifications affecting the channel permeability (and of phosphorylation of other connexins) is relatively under explored. For example, NO donors cause nitrosylation of Cx43 and enhance the probability of opening hemichannels (in astrocytes; Retamal et al., 2006), while they lead to reduction in Cx37 junctional coupling (in HUVECs; Kameritsch et al., 2005). In both examples, NO donors were administered at supraphysiological concentrations.

Phosphorylation affects connexin trafficking and the gating properties of the channels in the plasma membrane (Ek-Vitorin et al., 2006; Solan and Lampe, 2008). Phosphorylation in the CT of Ser, Thr and Tyr residues of Cx43 has been described, both predicted and actual, involving, for example, *Src*, MAPK, PKA and PKC, $p34^{cdc}$ and casein kinase 1 (CK-1). Phosphorylation by PKA and CK-1 enhance gap junctional communication by Cx43, whereas PKC, *Src*, and MAPK reduce channel function (Pahujaa et al., 2007; Solan and Lampe, 2005, 2008). Of interest, phosphorylation of Ser368 of Cx43, which is reported to reduce Cx43 involved communication pathways (Solan et al., 2007), has recently been identified in skeletal muscle beds, but not in mesenteric vessels (Isakson et al., 2008; Straub et al., 2009). Additionally, phosphorylation at one site (e.g., Ser365, which enhances communication) inhibits the phosphorylation of others (e.g., of

Ser368, which inhibits communication) (Solan et al., 2007). This suggests that site-specific connexin phosphorylation may be a means to influence both homo- and hetero-cellular communication in the vasculature, although this requires further investigation.

There are also species-specific differences in phosphorylation patterns; one example, rat Cx43 is regulated by PKG, which shifts the channel toward lower conductance states, but human Cx43 is not, as the PKG consensus phosphorylation site (Ser257) is absent from the CT domain (Kwak et al., 1995; Moreno et al., 1994b).

Effects of phosphorylation of other connexins are less well characterized. Phosphorylation of rat Cx45 by PKC has been reported to cause the appearance of a new conductance state (Kwak et al., 1995), but PKC-mediated phosphorylation of mouse Cx45 increases the occupancy time of existing states (van Veen et al., 2000). While Cx37 phosphorylation has not been demonstrated, sequence homology of the Cx43 and Cx37 CT domains suggests the following equivalent binding sites: for MAPK, Cx43–Ser282 and Cx37–Ser275; for PKC, Cx43–Ser368 and Cx37–Ser282 (Burt et al., 2008). The expression of Cx40 is also reportedly altered through signaling pathways involving PKA, implicating a change in the phosphorylation state and site of action (Hoffmann et al., 2003). Phosphorylation by PKA seems to favor the higher conductance states of Cx40 (van Rijen et al., 2000).

5.4. Interaction of connexin with other proteins

While the intercellular communication pathways formed are well defined, to some extent the nonchannel functions of different connexin isoforms are less so. Gap junctions, as part of a larger organization once referred to as the ''nexus'', serve as a network hub for inter- and intra-cellular communication; connexins provide sites for attachment of cytoskeletal proteins, for components involved in multiple intracellular signaling pathways, or other cell junction complexes and membrane channels (Chanson et al., 2007; Giepmans, 2004).

Most studies on the direct binding of connexins to other proteins have focused on Cx43; it interacts with kinases such as *Src*, protein kinases A, C and G, MAPK, cyclin-dependent kinase cdc2, and phosphatases, such as receptor protein tyrosine phosphatase μ, as well as structural proteins such as ZO-1, catenins and cadherins, caveolin, tubulin and drebrin. For example, trafficking of Cx43 (also Cx45) is dependent on CT domain interactions with ZO-1, a tight junction protein (Laing et al., 2001). ZO-1 contains three PDZ domains, the second of which binds to the Cx43 CT domain; most proteins with PDZ domains are membrane-associated and are found at specialized membrane domains such as synapses, junctions, and apical–basolateral interface regions.

While physiological and developmental defects have typically been attributed to defects in the permeation pathway itself, as for most membrane proteins, connexin mutations are more likely to result in trafficking, folding, and/or assembly and regulatory defects to produce a functional knockout. Additionally, ''dominant-negative'' effects are sometimes observed where the expression of one mutant connexin inhibits the functional expression of others, largely via their heteromultimerization with wild-type connexins. In each case, the absence or reduced function of a large multiprotein signaling complex situated at the cell surface can be of just as much importance as the channel activity in influencing cell development and differentiation.

Of further interest, ZO-1 directly regulates gating of Cx43 channels, serving as a scaffold that connects a phospholipase directly to these gap junctions, thereby controlling local phosphatidylinositol levels (van Zeijl et al., 2007). Oxidized phospholipids have also been shown to directly alter Cx43 expression and phosphorylation (Isakson et al., 2006b; Johnstone et al., 2009).

5.5. Pharmacological block

A major problem in the gap junction field is the absence of specific pore blocking reagents for connexin channels, which are necessary for investigating the physiological roles of connexin channels and for structure–function studies of the permeation pathway; a predominance of the known modulators of gap junction communication are lipophilic and/or show some specificity with regard to membrane lipids (Locke and Harris, 2009). Further, the potency and specificity of these reagents are not optimal for long-term studies.

Halothane, an inhalation anesthetic, is widely used to rapidly and reversibly inhibit junctional communication (Spray and Burt, 1990). Halothane is not specific for connexin channels, but appears to be effective on all connexins, though Cx40 and Cx43 have slightly different sensitivities to halothane (He and Burt, 2000); heteromeric channels are significantly less sensitive than the corresponding homomeric channels. Halothane can bind with high affinity to appropriately sized hydrophobic cavities in proteins to stabilize helix–helix configurations, so its action on Cx40 and/or Cx43 channels could indicate structural differences for each connexin in a homo- and hetero-meric configuration.

In addition, peptides targeting the extracellular loop domains have been shown to effectively reduce the formation of gap junction channels (Evans and Leybaert, 2007). The potential utility of these ''mimetic'' peptides is highlighted by the ability to inhibit specific connexin subtypes simply by designing peptides unique to individual connexin isoforms, though there are several drawbacks: first, inhibition of junctional communication typically requires incubation of peptide with cells for several hours and, second,

reasonably high concentrations are needed, though, third, junctional coupling is not reduced completely (Dahl, 2007). In addition to inhibiting gap junctions, mimetic peptides also reduce cellular dye uptake, presumably mediated by connexons—though one cannot rule out their effect on pannexons. For example, in rat mesenteric arteries, connexin mimetic peptides caused a reduction in electrotonic coupling without nonjunctional effects (Matchkov et al., 2006), though a recent report indicates that connexin mimetic peptides strongly reduce membrane currents in *Xenopus* oocytes expressing Panx1 at concentrations similar to those that inhibit connexin channels (Wang et al., 2007).

Peptides targeting the cytoplasmic domains have also emerged as an interesting approach for development of a gap junctional pharmacology; modification of both the chemical and voltage gating behavior of Cx43 can be achieved by a 34 aa peptide (Shibayama et al., 2006) that interferes in the pH-dependent intramolecular interaction between CT and CL. Its application may be useful for maintaining gap junctional communication during acidification of the intracellular space, that is, during cardiac arrhythmia.

Thus, specific inhibitors of connexin channels may have therapeutic utility, and connexin channels are new and promising pharmacological targets for the treatment of many diseases and dysfunctional states, including wound healing, hypertension and atherosclerosis (Herve and Dhein, 2006; Herve and Sarrouilhe, 2005).

6. Involvement of Connexins in Vascular Diseases

6.1. Hypertension

Hypertension, the elevation of blood pressure, is one of the most important risk factors for coronary heart disease and a leading cause of chronic renal failure. Primary (essential) hypertension accounts for nearly all cases worldwide and results from the interaction of genetic and environmental factors that affect cardiac output, peripheral resistance, or both. However, in $\sim 10\%$ of cases (secondary), hypertension is the result of renal disease or atherosclerotic narrowing of the renal artery, both of which affect the renin–angiotensin system and/or Na^+ homeostasis, itself central to blood pressure regulation. It is also clear that unregulated secretion of renin from kidneys is also an important part of the disease process for primary hypertension.

In the kidneys, renin-producing cells are coupled to each other and EC by Cx40, while EC are themselves coupled to each other by Cx43 (Krattinger et al., 2007). Genetic replacement of Cx43 by Cx32 (knock-in, KI) protects Cx43KI32 mice from experimentally induced hypertension as there is decreased renin production (Haefliger et al., 2001, 2006), whereas

knockout of Cx40 makes the animals hypertensive, due in part to excessive stimulation of renin biosynthesis and release, through a defect of conduction along EC leading to increased peripheral resistance cannot be ruled out (Kurtz et al., 2007; Wagner et al., 2007). Thus, renin secretion is likely controlled both by Cx40 signaling in the kidney cells that produce the hormone and by Cx43-dependent signaling that originates in the vascular EC.

Conversely, hypotension has been observed by endothelial-specific knockout of Cx43 using an endothelial TIE-2 promoter; these mice demonstrated a significant decrease in plasma angiotensin II levels (Liao, 2001).

Neither Cx37 nor Cx45 has been implicated in the development of hypertension (Just et al., 2009; Kurtz et al., 2009; Schweda et al., 2009), though genetic polymorphism of Cx37 (C1019T) has been implicated in vessel occlusion and narrowing (''atherosclerosis'') and carotid artery intimal thickening (Collings et al., 2007; Lanfear et al., 2007), all of which may contribute to the progression of the disease.

6.2. Atherosclerosis

Atherosclerosis, a progressive disease of the large arteries, typically leads to myocardial infarction and stroke. Knowledge of the mechanisms underlying atherosclerosis is significant, though many questions about the initiating factors of atherogenesis remain unanswered. Even so, atherogenesis appears to have a robust, connexin-associated pathology as evidenced by studies on human blood vessels and mouse models; in particular, Cx37 has been identified as a major risk factor for development of atherosclerosis, for there are remarkable changes in its expression and function in the endothelium and smooth muscle of the larger arteries (e.g., the abdominal aorta, the coronary arteries, and the carotid arteries), the primary sites of atherogenesis (Derouette et al., 2009; Wong et al., 2006a).

These arteries have two main layers: the ''tunica intima'' lining the lumen of the vessel comprising a single EC layer that is separated from VSMC in the ''tunica media'' by the ECM-rich IEL. In the earliest stages of atherogenesis, EC become more permeable to inflammatory cells, while quiescent VSMC become highly motile and lose their contractile ability. These VSMC accumulate in the tunica intima to form a ''fatty streak'' that eventually forms a ''fibrous cap'', the mature atherosclerotic plaque. In mouse and human aortas and carotids, Cx37, Cx40 and Cx43 are expressed in EC, whereas Cx43 is mainly expressed in VSMC. Expression of Cx37, Cx40 and Cx43 are differentially modified during atherosclerotic plaque development. Mouse models have shown that Cx43 has an atherogenic effect, whereas Cx37 and Cx40 seem to be atheroprotective (Chadjichristos et al., 2006a,b; Chanson and Kwak, 2007; Johnstone et al., 2009; Kwak et al., 2003). Counteracting mechanisms for Cx37 and Cx43 have been shown in the vasculature in aging mice.

The first experimental support for the role of connexins in atherogenesis was obtained by a study of atherosclerotic plaques in human and rabbit carotid arteries, with the observations that Cx43 is downregulated in VSMC underneath the plaque (Kwak, 2002) and that macrophage foam cells in the plaques expressed significant amounts of Cx43 mRNA, even though monocytes and macrophages, from which foam cells arise, did not. It was later found that Cx43 was first upregulated, and then downregulated, in the VSMC of more advanced lesions (Brisset et al., 2009; Chadjichristos et al., 2008; Kwak, 2002). The exact mechanism by which this occurs is unknown, though many studies elucidate a role for Cx43 and its posttranslational phosphorylation in cell proliferation and migration (Sanchez-Alvarez et al., 2006; Tabernero et al., 2006; Xie et al., 1997), key stages in atherogenic development.

While these studies established that connexin expression might be modified during the progression of the disease, they did not establish causality between connexins and atherosclerosis. It was the finding that a single base-pair change in the human Cx37 gene (GJA4), C1019T resulting in the Cx37–Ser319 or Cx37–Pro319 polymorphism, either was a risk factor for atherosclerosis development or limited the extent of atherosclerosis, respectively, which greatly stimulated research into the association (Chanson and Kwak, 2007).

More extensive research has been conducted using mouse models created through interbreeding of specific connexin knockout mice and atherosclerosis-prone LDL receptor-null ($LDLR^{-/-}$) or apolipoprotein E-null ($ApoE^{-/-}$) mice. In mice with both homozygous knockout of LDLR and heterozygous knockout of Cx43, atherosclerotic plaque development was significantly increased (Kwak et al., 2003). Additionally, double knockout of Cx37 and ApoE lead to increased macrophage recruitment and plaque size (Wong et al., 2006b).

Atherosclerosis in coronary arteries results in ischemic heart disease. A common and effective mechanical treatment for coronary atherosclerosis is angioplasty, the disruption of a developing atherosclerotic plaque by balloon-catheter distension. However, renarrowing of the vessels (''restenosis'') typically occurs at the site of intervention in over half of the patients after angioplasty, and up to $\sim 30\%$ of patients after subsequent implantation of a stent, which itself provides mechanical support to the vessel and extends its internal diameter to avoid reocclusion.

Restenosis mechanisms are not fully understood, but parietal trauma induced by the balloon-catheter distension typically triggers platelet aggregation and thrombus formation. In addition, the artery becomes stretched, exaggerating and accelerating the recruitment and infiltration of inflammatory cells. Reendothelialization is necessary to repair the lining of the damaged vasculature and is critical to prevent thrombosis and restenosis.

Both gap junctional and purinergic signaling contribute to reendothelialization of human EC by their effects on both intra- and extra-cellular

Ca^{2+} stores. The release of growth factors and proinflammatory cytokines by platelets, inflammatory cells, and VSMC, in addition to the loss of endothelial antiproliferating agents, such as NO, modulate the phenotype of VSMC, shifting them from a quiescent and ''contractile'' phenotype to one that is ''synthetic'', that is, more proliferating and less differentiated (Bundy et al., 2000). VSMC proliferate shortly after angioplasty and migrate toward the intima. VSCM synthesize ECM and further contribute to intimal hyperplasia. Intimal thickening is greatest after several months, after which ''synthetic'' VSMC dedifferentiate, the wall is remodeled and intimal thickening stops (Brisset et al., 2009).

In the rat carotid artery after balloon-catheter insertion, Cx43 has been shown to be upregulated in intimal and medial VSMC concomitantly to their activation and phenotypic modulation (Chadjichristos et al., 2008). Enhanced Cx43 expression in macrophages of restenotic lesions has also been confirmed in different species (Chadjichristos et al., 2006b). LDL receptor-null mice crossbred to a heterozygous background of Cx43 ($Cx43^{+/-}LDLR^{-/-}$, thus expressing reduced levels of Cx43) display restricted intimal thickening after balloon-catheter distension of the carotid artery, despite marked endothelial denudation and VSMC activation, as compared to control $Cx43^{+/+}LDLR^{-/-}$ littermates (Chadjichristos et al., 2006b). Reduced expression of Cx43 results in decreased macrophage infiltration, VSMC migration, and proliferation, and thus accelerated reendothelialization, suggesting that modulation of Cx43 levels could be a novel therapeutic strategy to prevent restenosis after coronary angioplasty and stent implantation.

7. Concluding Remarks

The highly coordinated behavior of EC in the vascular bed is achieved by gap junctions formed by different connexin isoforms. In addition, gap junctions also couple VSMC, and interconnect EC and VSMC at the MEJ, a short-distance transverse pathway allowing direct and reciprocal communication between the two anatomically distinct vascular cell types.

Significant advances have been made in the understanding of the biophysics of different connexin channels, in particular those found to play prominent roles in the vasculature. Each connexin isoform contributes a particular set of functional or regulatory properties to gap junction channels that appear essential, either intact or as modified by interaction with other connexins and nonconnexin proteins. Approaches using mice with knockout or cell-specific gene disruption for different connexins confirm that Cx37, Cx40, Cx43 and Cx45 serve specific biological functions in the microcirculation.

The function(s) and role(s) of connexins for both maintenance of vascular health and progression of vascular disease states in humans are areas of active and fruitful investigation.

ACKNOWLEDGMENTS

The authors thank Walter Duran, Andrew L. Harris, Brian Duling, Adrian A. Anderson, and Michael J. Rizzo for comments. This work is supported by NIH GM36044 and GM61406 (DL), an American Heart Association Scientist Development Grant, and by NIH HL088554 (both to BEI).

REFERENCES

Ahmad, S., Evans, W.H., 2002. Post-translational integration and oligomerization of connexin 26 in plasma membranes and evidence of formation of membrane pores: implications for the assembly of gap junctions. Biochem. J. 365, 693–699.

Ayad, W.A., Locke, D., Koreen, I.V., Harris, A.L., 2006. Heteromeric, but not homomeric, connexin channels are selectively permeable to inositol phosphates. J. Biol. Chem. 281, 16727–16739.

Banach, K., Ramanan, S.V., Brink, P.R., 2000. The influence of surface charges on the conductance of the human connexin37 gap junction channel. Biophys. J. 78, 752–760.

Bao, L., Samuels, S., Locovei, S., Macagno, E.R., Muller, K.J., Dahl, G., 2007. Innexins form two types of channels. FEBS Lett. 581, 5703–5708.

Baranova, A., Ivanov, D., Petrash, N., Pestova, A., Skoblov, M., Kelmanson, I., et al., 2004. The mammalian pannexin family is homologous to the invertebrate innexin gap junction proteins. Genomics 83, 706–716.

Barrio, L.C., Capel, J., Jarillo, J.A., Castro, C., Revilla, A., 1997. Species-specific voltage-gating properties of connexin45 junctions expressed in *Xenopus* oocytes. Biophys. J. 73, 757–769.

Beach, J.M., McGahren, E.D., Duling, B.R., 1998. Capillaries and arterioles are electrically coupled in hamster cheek pouch. Am. J. Physiol. 275, H1489–H1496.

Beblo, D.A., Veenstra, R.D., 1997. Monovalent cation permeation through the connexin40 gap junction channel. Cs, Rb, K, Na, Li, TEA, TMA, TBA, and effects of anions Br, Cl, F, acetate, aspartate, glutamate, and NO3. J. Gen. Physiol. 109, 509–522.

Bedner, P., Niessen, H., Odermatt, B., Kretz, M., Willecke, K., Harz, H., 2006. Selective permeability of different connexin channels to the second messenger cyclic AMP. J. Biol. Chem. 281, 6673–6681.

Bennett, M.V., Contreras, J.E., Bukauskas, F.F., Saez, J.C., 2003. New roles for astrocytes: gap junction hemichannels have something to communicate. Trend Neurosci. 26, 610–617.

Beny, J.L., Connat, J.L., 1992. An electron-microscopic study of smooth muscle cell dye coupling in the pig coronary arteries. Role of gap junctions. Circ. Res. 70, 49–55.

Beny, J.L., Gribi, F., 1989. Dye and electrical coupling of endothelial cells in situ. Tissue Cell 21, 797–802.

Bevans, C.G., Harris, A.L., 1999a. Direct high affinity modulation of connexin channel activity by cyclic nucleotides. J. Biol. Chem. 274, 3720–3725.

Bevans, C.G., Harris, A.L., 1999b. Regulation of connexin channels by pH. Direct action of the protonated form of taurine and other aminosulfonates. J. Biol. Chem. 274, 3711–3719.

Bevans, C.G., Kordel, M., Rhee, S.K., Harris, A.L., 1998. Isoform composition of connexin channels determines selectivity among second messengers and uncharged molecules. J. Biol. Chem. 273, 2808–2816.

Beyer, E.C., Gemel, J., Seul, K.H., Larson, D.M., Banach, K., Brink, P.R., 2000. Modulation of intercellular communication by differential regulation and heteromeric mixing of co-expressed connexins. Braz. J. Med. Biol. Res. 33, 391–397.

Boassa, D., Ambrosi, C., Qiu, F., Dahl, G., Gaietta, G., Sosinsky, G., 2007. Pannexin1 channels contain a glycosylation site that targets the hexamer to the plasma membrane. J. Biol. Chem. 282, 31733–31743.

Boerma, M., Forsberg, L., Van Zeijl, L., Morgenstern, R., De Faire, U., Lemne, C., et al., 1999. A genetic polymorphism in connexin 37 as a prognostic marker for atherosclerotic plaque development. J. Int. Med. 246, 211–218.

Boitano, S., Dirksen, E.R., Sanderson, M.J., 1992. Intercellular propagation of calcium waves mediated by inositol trisphosphate. Science 258, 292–295.

Brink, P.R., Cronin, K., Banach, K., Peterson, E., Westphale, E.M., Seul, K.H., et al., 1997. Evidence for heteromeric gap junction channels formed from rat connexin43 and human connexin37. Am. J. Physiol. 273, C1386–C1396.

Brisset, A.C., Isakson, B.E., Kwak, B.R., 2009. Connexins in vascular physiology and pathology. Antioxid. Redox Signal. 11, 267–282.

Bruzzone, R., Haefliger, J.A., Gimlich, R.L., Paul, D.L., 1993. Connexin40, a component of gap junctions in vascular endothelium, is restricted in its ability to interact with other connexins. Mol. Biol. Cell 4, 7–20.

Budel, S., Bartlett, I.S., Segal, S.S., 2003. Homocellular conduction along endothelium and smooth muscle of arterioles in hamster cheek pouch: unmasking an NO wave. Circ. Res. 93, 61–68.

Bukauskas, F.F., Elfgang, C., Willecke, K., Weingart, R., 1995. Heterotypic gap junction channels (connexin26–connexin32) violate the paradigm of unitary conductance. Pflugers Arch. 429, 870–872.

Bukauskas, F.F., Bukauskiene, A., Bennett, M.V., Verselis, V.K., 2001. Gating properties of gap junction channels assembled from connexin43 and connexin43 fused with green fluorescent protein. Biophys. J. 81, 137–152.

Bukauskas, F.F., Kreuzberg, M.M., Rackauskas, M., Bukauskiene, A., Bennett, M.V., Verselis, V.K., et al., 2006. Properties of mouse connexin 30.2 and human connexin 31.9 hemichannels: implications for atrioventricular conduction in the heart. Proc. Natl. Acad. Sci. USA 103, 9726–9731.

Bundy, R.E., Marczin, N., Birks, E.F., Chester, A.H., Yacoub, M.H., 2000. Transplant atherosclerosis: role of phenotypic modulation of vascular smooth muscle by nitric oxide. Gen. Pharmacol. 34, 73–84.

Burt, J.M., Fletcher, A.M., Steele, T.D., Wu, Y., Cottrell, G.T., Kurjiaka, D.T., 2001. Alteration of Cx43:Cx40 expression ratio in A7r5 cells. Am. J. Physiol. Cell Physiol. 280, C500–C508.

Burt, J.M., Nelson, T.K., Simon, A.M., Fang, J.S., 2008. Connexin 37 profoundly slows cell cycle progression in rat insulinoma cells. Am. J. Physiol. Cell Physiol. 295, C1103–C1112.

Cai, W.J., Koltai, S., Kocsis, E., Scholz, D., Schaper, W., Schaper, J., 2001. Connexin37, not Cx40 and Cx43, is induced in vascular smooth muscle cells during coronary arteriogenesis. J. Mol. Cell. Cardiol. 33, 957–967.

Cai, W.J., Kocsis, E., Scholz, D., Luo, X., Schaper, W., Schaper, J., 2004. Presence of Cx37 and lack of desmin in smooth muscle cells are early markers for arteriogenesis. Mol. Cell. Biochem. 262, 17–23.

Callera, G.E., Montezano, A.C., Yogi, A., Tostes, R.C., Touyz, R.M., 2007. Vascular signaling through cholesterol-rich domains: implications in hypertension. Curr. Opin. Nephrol. Hypertens. 16, 90–104.

Chadjichristos, C.E., Derouette, J.P., Kwak, B.R., 2006a. Connexins in atherosclerosis. Adv. Cardiol. 42, 255–267.

Chadjichristos, C.E., Matter, C.M., Roth, I., Sutter, E., Pelli, G., Luscher, T.F., et al., 2006b. Reduced connexin43 expression limits neointima formation after balloon distension injury in hypercholesterolemic mice. Circulation 113, 2835–2843.

Chadjichristos, C.E., Morel, S., Derouette, J.P., Sutter, E., Roth, I., Brisset, A.C., et al., 2008. Targeting connexin 43 prevents platelet-derived growth factor-BB-induced phenotypic change in porcine coronary artery smooth muscle cells. Circ. Res. 102, 653–660.

Chanson, M., Kwak, B.R., 2007. Connexin37: a potential modifier gene of inflammatory disease. J. Mol. Med. 85, 787–795.

Chanson, M., Kotsias, B.A., Peracchia, C., O'Grady, S.M., 2007. Interactions of connexins with other membrane channels and transporters. Prog. Biophys. Mol. Biol. 94, 233–244.

Chen, J., Burns, A.R., Phillips, S.C., Sokoya, E.M., 2008. Pannexin protein expression in the rat middle cerebral artery. FASEB J. 22, 1144.

Christ, G.J., Moreno, A.P., Melman, A., Spray, D.C., 1992. Gap junction-mediated intercellular diffusion of Ca^{2+} in cultured human corporal smooth muscle cells. Am. J. Physiol. 263, C373–C383.

Collings, A., Islam, M.S., Juonala, M., Rontu, R., Kahonen, M., Hutri-Kahonen, N., et al., 2007. Associations between connexin37 gene polymorphism and markers of subclinical atherosclerosis: the Cardiovascular Risk in Young Finns study. Atherosclerosis 195, 379–384.

Contreras, J.E., Saez, J.C., Bukauskas, F.F., Bennett, M.V., 2003. Gating and regulation of connexin 43 (Cx43) hemichannels. Proc. Natl. Acad. Sci. USA 100, 11388–11393.

Contreras, J.E., Sanchez, H.A., Veliz, L.P., Bukauskas, F.F., Bennett, M.V., Saez, J.C., 2004. Role of connexin-based gap junction channels and hemichannels in ischemia-induced cell death in nervous tissue. Brain Res. Brain Res. Rev. 47, 290–303.

Cornhill, J.F., Levesque, M.J., Herderick, E.E., Nerem, R.M., Kilman, J.W., Vasko, J.S., 1980. Quantitative study of the rabbit aortic endothelium using vascular casts. Atherosclerosis 35, 321–337.

Cottrell, G.T., Burt, J.M., 2001. Heterotypic gap junction channel formation between heteromeric and homomeric Cx40 and Cx43 connexons. Am. J. Physiol. Cell Physiol. 281, C1559–C1567.

Cottrell, G.T., Wu, Y., Burt, J.M., 2002. Cx40 and Cx43 expression ratio influences heteromeric/heterotypic gap junction channel properties. Am. J. Physiol. Cell Physiol. 282, C1469–C1482.

Coutinho, P., Qiu, C., Frank, S., Tamber, K., Becker, D., 2003. Dynamic changes in connexin expression correlate with key events in the wound healing process. Cell Biol. Int. 27, 525–541.

Dahl, G., 2007. Gap junction-mimetic peptides do work, but in unexpected ways. Cell Commun. Adhes. 14, 259–264.

Dahl, G., Werner, R., Levine, E., Rabadan-Diehl, C., 1992. Mutational analysis of gap junction formation. Biophys. J. 62, 172–180.

Dai, G., Kaazempur-Mofrad, M.R., Natarajan, S., Zhang, Y., Vaughn, S., Blackman, B.R., et al., 2004. Distinct endothelial phenotypes evoked by arterial waveforms derived from atherosclerosis-susceptible and -resistant regions of human vasculature. Proc. Natl. Acad. Sci. USA 101, 14871–14876.

Das, S., Smith, T.D., Sarma, J.D., Ritzenthaler, J.D., Maza, J., Kaplan, B.E., et al., 2009. ERp29 restricts connexin43 oligomerization in the endoplasmic reticulum. Mol. Biol. Cell 20, 2593–2604.

De Vuyst, E., Decrock, E., Cabooter, L., Dubyak, G.R., Naus, C.C., Evans, W.H., et al., 2006. Intracellular calcium changes trigger connexin 32 hemichannel opening. EMBO J. 25, 34–44.

de Wit, C., Hoepfl, B., Wolfle, S.E., 2006a. Endothelial mediators and communication through vascular gap junctions. Biol. Chem. 387, 3–9.

de Wit, C., Wolfle, S.E., Hopfl, B., 2006b. Connexin-dependent communication within the vascular wall: contribution to the control of arteriolar diameter. Adv. Cardiol. 42, 268–283.

Deglise, S., Martin, D., Probst, H., Saucy, F., Hayoz, D., Waeber, G., et al., 2005. Increased connexin43 expression in human saphenous veins in culture is associated with intimal hyperplasia. J. Vasc. Surg. 41, 1043–1052.

Delmar, M., Coombs, W., Sorgen, P., Duffy, H.S., Taffet, S.M., 2004. Structural bases for the chemical regulation of connexin43 channels. Cardiovasc. Res. 62, 268–275.

Derouette, J.P., Desplantez, T., Wong, C.W., Roth, I., Kwak, B.R., Weingart, R., 2009. Functional differences between human Cx37 polymorphic hemichannels. J. Mol. Cell. Cardiol. 46, 499–507.

Desplantez, T., Halliday, D., Dupont, E., Weingart, R., 2004. Cardiac connexins Cx43 and Cx45: formation of diverse gap junction channels with diverse electrical properties. Pflugers Arch. 448, 363–375.

Dewey, M.M., Barr, L., 1964. A study of the structure and distribution of the nexus. J. Cell Biol. 23, 553–585.

Dora, K.A., Doyle, M.P., Duling, B.R., 1997. Elevation of intracellular calcium in smooth muscle causes endothelial cell generation of NO in arterioles. Proc. Natl. Acad. Sci. USA 94, 6529–6534.

Duffy, H.S., Sorgen, P.L., Girvin, M.E., O'Donnell, P., Coombs, W., Taffet, S.M., et al., 2002. pH-dependent intramolecular binding and structure involving Cx43 cytoplasmic domains. J. Biol. Chem. 277, 36706–36714.

Duling, B.R., Day, K.H., Damon, D.N., Paul, D.L., Simon, A., Liao, Y.B., 2003. Connexins 43 and 40 mediate smooth muscle-endothelial cell interactions. FASEB J. 17, A65.

Eastman, S.D., Chen, T.H., Falk, M.M., Mendelson, T.C., Iovine, M.K., 2006. Phylogenetic analysis of three complete gap junction gene families reveals lineage-specific duplications and highly supported gene classes. Genomics 87, 265–274.

Ebong, E.E., Kim, S., DePaola, N., 2006. Flow regulates intercellular communication in HAEC by assembling functional Cx40 and Cx37 gap junctional channels. Am. J. Physiol. Heart Circ. Physiol. 290, H2015–H2023.

Ek-Vitorin, J.F., King, T.J., Heyman, N.S., Lampe, P.D., Burt, J.M., 2006. Selectivity of connexin 43 channels is regulated through protein kinase C-dependent phosphorylation. Circ. Res. 98, 1498–1505.

Elenes, S., Martinez, A.D., Delmar, M., Beyer, E.C., Moreno, A.P., 2001. Heterotypic docking of Cx43 and Cx45 connexons blocks fast voltage gating of Cx43. Biophys. J. 81, 1406–1418.

Elfgang, C., Eckert, R., Lichtenberg-Frate, H., Butterweck, A., Traub, O., Klein, R.A., et al., 1995. Specific permeability and selective formation of gap junction channels in connexin-transfected HeLa cells. J. Cell Biol. 129, 805–817.

Essner, J.J., Laing, J.G., Beyer, E.C., Johnson, R.G., Hackett Jr., P.B., 1996. Expression of zebrafish connexin43.4 in the notochord and tail bud of wild-type and mutant no tail embryos. Dev. Biol. 177, 449–462.

Evans, W.H., Leybaert, L., 2007. Mimetic peptides as blockers of connexin channel-facilitated intercellular communication. Cell Commun. Adhes. 14, 265–273.

Evans, W.H., Martin, P.E., 2002. Gap junctions: structure and function. Mol. Membr. Biol. 19, 121–136.

Evans, W.H., De Vuyst, E., Leybaert, L., 2006. The gap junction cellular internet: connexin hemichannels enter the signalling limelight. Biochem. J. 397, 1–14.

Faigle, M., Seessle, J., Zug, S., El Kasmi, K.C., Eltzschig, H.K., 2008. ATP release from vascular endothelia occurs across Cx43 hemichannels and is attenuated during hypoxia. PLoS ONE 3, e2801.

Falk, M.M., Gilula, N.B., 1998. Connexin membrane protein biosynthesis is influenced by polypeptide positioning within the translocon and signal peptidase access. J. Biol. Chem. 273, 7856–7864.

Falk, M.M., Buehler, L.K., Kumar, N.M., Gilula, N.B., 1997. Cell-free synthesis and assembly of connexins into functional gap junction membrane channels. EMBO J. 16, 2703–2716.

Feaver, R.E., Hastings, N.E., Pryor, A., Blackman, B.R., 2008. GRP78 upregulation by atheroprone shear stress via p38-, alpha2beta1-dependent mechanism in endothelial cells. Arterioscler. Thromb. Vasc. Biol. 28, 1534–1541.

Figueroa, X.F., Duling, B.R., 2008. Dissection of two Cx37-independent conducted vasodilator mechanisms by deletion of Cx40: electrotonic versus regenerative conduction. Am. J. Physiol. Heart Circ. Physiol. 295, H2001–H2007.

Figueroa, X.F., Duling, B.R., 2009. Gap junctions in the control of vascular function. Antioxid. Redox Signal. 11, 251–266.

Figueroa, X.F., Paul, D.L., Simon, A.M., Goodenough, D.A., Day, K.H., Damon, D.N., et al., 2003. Central role of connexin40 in the propagation of electrically activated vasodilation in mouse cremasteric arterioles *in vivo*. Circ. Res. 92, 793–800.

Figueroa, X.F., Isakson, B.E., Duling, B.R., 2004. Connexins: gaps in our knowledge of vascular function. Physiology 19, 277–284.

Fleishman, S.J., Unger, V.M., Yeager, M., Ben-Tal, N., 2004. A Calpha model for the transmembrane alpha helices of gap junction intercellular channels. Mol. Cell 15, 879–888.

Francis, D., Stergiopoulos, K., Ek-Vitorin, J.F., Cao, F.L., Taffet, S.M., Delmar, M., 1999. Connexin diversity and gap junction regulation by pHi. Dev. Genet. 24, 123–136.

Gabriels, J.E., Paul, D.L., 1998. Connexin43 is highly localized to sites of disturbed flow in rat aortic endothelium but connexin37 and connexin40 are more uniformly distributed. Circ. Res. 83, 636–643.

Gaietta, G., Deerinck, T.J., Adams, S.R., Bouwer, J., Tour, O., Laird, D.W., et al., 2002. Multicolor and electron microscopic imaging of connexin trafficking. Science 296, 503–507.

Gemel, J., Valiunas, V., Brink, P., Beyer, E., 2004. Connexin43 and connexin26 form gap junctions, but not heteromeric channels in co-expressing cells. J. Cell Sci. 117, 2469–2490.

George, C.H., Kendall, J.M., Evans, W.H., 1999. Intracellular trafficking pathways in the assembly of connexins into gap junctions. J. Biol. Chem. 274, 8678–8685.

Giepmans, B.N., 2004. Gap junctions and connexin-interacting proteins. Cardiovasc. Res. 62, 233–245.

Goldberg, G.S., Moreno, A.P., Lampe, P.D., 2002. Gap junctions between cells expressing connexin 43 or 32 show inverse permselectivity to adenosine and ATP. J. Biol. Chem. 277, 36725–36730.

Goodenough, D.A., Goliger, J.A., Paul, D.L., 1996. Connexins, connexons, and intercellular communication. Annu. Rev. Biochem. 65, 475–502.

Gu, H., Ek-Vitorin, J.F., Taffet, S.M., Delmar, M., 2000. Coexpression of connexins 40 and 43 enhances the pH sensitivity of gap junctions: a model for synergistic interactions among connexins. Circ. Res. 86, E98–E103.

Haddock, R.E., Grayson, T.H., Brackenbury, T.D., Meaney, K.R., Neylon, C.B., Sandow, S.L., et al., 2006. Endothelial coordination of cerebral vasomotion via

myoendothelial gap junctions containing connexins 37 and 40. Am. J. Physiol. Heart Circ. Physiol. 291, H2047–H2056.
Haefliger, J.A., Demotz, S., Braissant, O., Suter, E., Waeber, B., Nicod, P., et al., 2001. Connexins 40 and 43 are differentially regulated within the kidneys of rats with renovascular hypertension. Kidney Int. 60, 190–201.
Haefliger, J.A., Nicod, P., Meda, P., 2004. Contribution of connexins to the function of the vascular wall. Cardiovasc. Res. 62, 345–356.
Haefliger, J.A., Krattinger, N., Martin, D., Pedrazzini, T., Capponi, A., Doring, B., et al., 2006. Connexin43-dependent mechanism modulates renin secretion and hypertension. J. Clin. Invest. 116, 405–413.
Hakim, C.H., Jackson, W.F., Segal, S.S., 2008. Connexin isoform expression in smooth muscle cells and endothelial cells of hamster cheek pouch arterioles and retractor feed arteries. Microcirculation 15, 503–514.
Harris, A.L., 2001. Emerging issues of connexin channels: biophysics fills the gap. Q. Rev. Biophys. 34, 325–472.
Harris, A.L., Locke, D., 2009. Connexins: A Guide. Springer, New York, NY.
He, D.S., Burt, J.M., 2000. Mechanism and selectivity of the effects of halothane on gap junction channel function. Circ. Res. 86, E104–E109.
He, D.S., Jiang, J.X., Taffet, S.M., Burt, J.M., 1999. Formation of heteromeric gap junction channels by connexins 40 and 43 in vascular smooth muscle cells. Proc. Natl. Acad. Sci. USA 96, 6495–6500.
Heberlein, K.R., Straub, A.C., Isakson, B.E., 2009. The myoendothelial junction: breaking through the matrix? Microcirculation 16, 307–322.
Hennemann, H., Suchyna, T., Lichtenberg-Frate, H., Jungbluth, S., Dahl, E., Schwarz, J., et al., 1992. Molecular cloning and functional expression of mouse connexin40, a second gap junction gene preferentially expressed in lung. J. Cell Biol. 117, 1299–1310.
Herve, J.C., Dhein, S., 2006. Pharmacology of cardiovascular gap junctions. Adv. Cardiol. 42, 107–131.
Herve, J.C., Sarrouilhe, D., 2005. Connexin-made channels as pharmacological targets. Curr. Pharm. Des. 11, 1941–1958.
Heyman, N.S., Burt, J.M., 2008. Hindered diffusion through an aqueous pore describes invariant dye selectivity of Cx43 junctions. Biophys. J. 94, 840–854.
Hill, C.E., Phillips, J.K., Sandow, S.L., 2001. Heterogeneous control of blood flow amongst different vascular beds. Med. Res. Rev. 21, 1–60.
Hirano, E., Knutsen, R.H., Sugitani, H., Ciliberto, C.H., Mecham, R.P., 2007. Functional rescue of elastin insufficiency in mice by the human elastin gene: implications for mouse models of human disease. Circ. Res. 101, 523–531.
Hoffmann, A., Gloe, T., Pohl, U., Zahler, S., 2003. Nitric oxide enhances de novo formation of endothelial gap junctions. Cardiovasc. Res. 60, 421–430.
Holland, W.C., Dunn, C.E., 1954. Role of the cell membrane and mitochondria in the phenomenon of ion transport in cardiac muscle. Am. J. Physiol. 179, 486–490.
Hou, C.J., Tsai, C.H., Su, C.H., Wu, Y.J., Chen, S.J., Chiu, J.J., et al., 2008. Diabetes reduces aortic endothelial gap junctions in ApoE-deficient mice: simvastatin exacerbates the reduction. J. Histochem. Cytochem. 56, 745–752.
Hu, X., Ma, M., Dahl, G., 2006. Conductance of connexin hemichannels segregates with the first transmembrane segment. Biophys. J. 90, 140–150.
Hulser, D.F., Rutz, M.L., Eckert, R., Traub, O., 2001. Functional rescue of defective mutant connexons by pairing with wild-type connexons. Pflugers Arch. Eur. J. Physiol. 441, 521–528.
Hunter, A.W., Barker, R.J., Zhu, C., Gourdie, R.G., 2005. Zonula occludens-1 alters connexin43 gap junction size and organization by influencing channel accretion. Mol. Biol. Cell 16, 5686–5698.

Hwan Seul, K., Beyer, E.C., 2000. Heterogeneous localization of connexin40 in the renal vasculature. Microvasc. Res. 59, 140–148.

Iacobas, D.A., Suadicani, S.O., Spray, D.C., Scemes, E., 2006. A stochastic two-dimensional model of intercellular Ca^{2+} wave spread in glia. Biophys. J. 90, 24–41.

Isakson, B.E., 2001. Intercellular Ca^{2+} signaling in alveolar epithelial cells through gap junctions and by extracellular ATP. Am. J. Physiol. Lung Cell. Mol. Physiol. 280, L221–L228.

Isakson, B.E., 2008. Localized expression of an Ins(1, 4, 5)P3 receptor at the myoendothelial junction selectively regulates heterocellular Ca^{2+} communication. J. Cell Sci. 121, 3664–3673.

Isakson, B.E., Duling, B.R., 2005. Heterocellular contact at the myoendothelial junction influences gap junction organization. Circ. Res. 97, 44–51.

Isakson, B.E., Damon, D.N., Day, K.H., Liao, Y., Duling, B.R., 2006a. Connexin40 and connexin43 in mouse aortic endothelium: evidence for coordinated regulation. Am. J. Physiol. Heart Circ. Physiol. 290, H1199–H1205.

Isakson, B.E., Kronke, G., Kadl, A., Leitinger, N., Duling, B.R., 2006b. Oxidized phospholipids alter vascular connexin expression, phosphorylation, and heterocellular communication. Arterioscler. Thromb. Vasc. Biol. 26, 2216–2221.

Isakson, B.E., Ramos, S.I., Duling, B.R., 2007. Ca^{2+} and inositol 1, 4, 5-trisphosphate-mediated signaling across the myoendothelial junction. Circ. Res. 100, 246–254.

Isakson, B.E., Best, A.K., Duling, B.R., 2008. Incidence of protein on actin bridges between endothelium and smooth muscle in arterioles demonstrates heterogeneous connexin expression and phosphorylation. Am. J. Physiol. Heart Circ. Physiol. 294, H2898–H2904.

Johnson, T.L., Nerem, R.M., 2007. Endothelial connexin 37, connexin 40, and connexin 43 respond uniquely to substrate and shear stress. Endothelium 14, 215–226.

Johnstone, S.R., Ross, J., Rizzo, M.J., Straub, A.C., Lampe, P., Leitinger, N., et al., 2009. Differential Cx43 phosphorylation and smooth muscle cell proliferation, *in vivo*. Am. J. Pathol. 175, 916–924.

Just, A., Kurtz, L., de Wit, C., Wagner, C., Kurtz, A., Arendshorst, W.J., 2009. Connexin 40 mediates the tubuloglomerular feedback contribution to renal blood flow autoregulation. J. Am. Soc. Nephrol. 20, 1577–1585.

Kalvelyte, A., Imbrasaite, A., Bukauskiene, A., Verselis, V.K., Bukauskas, F.F., 2003. Connexins and apoptotic transformation. Biochem. Pharmacol. 66, 1661–1672.

Kameritsch, P., Khandoga, N., Nagel, W., Hundhausen, C., Lidington, D., Pohl, U., 2005. Nitric oxide specifically reduces the permeability of Cx37-containing gap junctions to small molecules. J. Cell. Physiol. 203, 233–242.

Kanaporis, G., Mese, G., Valiuniene, L., White, T.W., Brink, P.R., Valiunas, V., 2008. Gap junction channels exhibit connexin-specific permeability to cyclic nucleotides. J. Gen. Physiol. 131, 293–305.

Kausalya, P.J., Reichert, M., Hunziker, W., 2001. Connexin45 directly binds to ZO-1 and localizes to the tight junction region in epithelial MDCK cells. FEBS Lett. 505, 92–96.

Ko, Y.S., Yeh, H.I., Rothery, S., Dupont, E., Coppen, S.R., Severs, N.J., 1999. Connexin make-up of endothelial gap junctions in the rat pulmonary artery as revealed by immunoconfocal microscopy and triple-label immunogold electron microscopy. J. Histochem. Cytochem. 47, 683–692.

Kovacs, J.A., Baker, K.A., Altenberg, G.A., Abagyan, R., Yeager, M., 2007. Molecular modeling and mutagenesis of gap junction channels. Prog. Biophys. Mol. Biol. 94, 15–28.

Koval, M., 2006. Pathways and control of connexin oligomerization. Trends Cell Biol. 16, 159–166.

Krattinger, N., Capponi, A., Mazzolai, L., Aubert, J.F., Caille, D., Nicod, P., et al., 2007. Connexin40 regulates renin production and blood pressure. Kidney Int. 72, 814–822.

Kruger, O., Beny, J.L., Chabaud, F., Traub, O., Theis, M., Brix, K., et al., 2002. Altered dye diffusion and upregulation of connexin37 in mouse aortic endothelium deficient in connexin40. J. Vasc. Res. 39, 160–172.

Kumai, M., Nishii, K., Nakamura, K., Takeda, N., Suzuki, M., Shibata, Y., 2000. Loss of connexin45 causes a cushion defect in early cardiogenesis. Development 127, 3501–3512.

Kumari, S.S., Varadaraj, K., Valiunas, V., Ramanan, S.V., Christensen, E.A., Beyer, E.C., et al., 2000. Functional expression and biophysical properties of polymorphic variants of the human gap junction protein connexin37. Biochem. Biophys. Res. Commun. 274, 216–224.

Kurtz, L., Schweda, F., de Wit, C., Kriz, W., Witzgall, R., Warth, R., et al., 2007. Lack of connexin 40 causes displacement of renin-producing cells from afferent arterioles to the extraglomerular mesangium. J. Am. Soc. Nephrol. 18, 1103–1111.

Kurtz, L., Gerl, M., Kriz, W., Wagner, C., Kurtz, A., 2009. Replacement of Cx40 by Cx45 causes ectopic localization of renin-producing cells in the kidney but maintains the *in vivo* control of renin gene expression. Am. J. Physiol. Renal Physiol. 297, F403–F409.

Kwak, B.R., 2002. Altered pattern of vascular connexin expression in atherosclerotic plaques. Arterioscler. Thromb. Vasc. Biol. 22, 225–230.

Kwak, B.R., Saez, J.C., Wilders, R., Chanson, M., Fishman, G.I., Hertzberg, E.L., et al., 1995. Effects of cGMP-dependent phosphorylation on rat and human connexin43 gap junction channels. Pflugers Arch. Eur. J. Physiol. 430, 770–778.

Kwak, B.R., Veillard, N., Pelli, G., Mulhaupt, F., James, R.W., Chanson, M., et al., 2003. Reduced connexin43 expression inhibits atherosclerotic lesion formation in low-density lipoprotein receptor-deficient mice. Circulation 107, 1033–1039.

Kyle, J.W., Minogue, P.J., Thomas, B.C., Domowicz, D.A., Berthoud, V.M., Hanck, D.A., et al., 2008. An intact connexin N-terminus is required for function but not gap junction formation. J. Cell Sci. 121, 2744–2750.

Lagree, V., Brunschwig, K., Lopez, P., Gilula, N.B., Richard, G., Falk, M.M., 2003. Specific amino-acid residues in the N-terminus and TM3 implicated in channel function and oligomerization compatibility of connexin43. J. Cell Sci. 116, 3189–3201.

Laing, J.G., Manley-Markowski, R.N., Koval, M., Civitelli, R., Steinberg, T.H., 2001. Connexin45 interacts with zonula occludens-1 and connexin43 in osteoblastic cells. J. Biol. Chem. 276, 23051–23055.

Laird, D.W., 2006. Life cycle of connexins in health and disease. Biochem. J. 394, 527–543.

Lamboley, M., Pittet, P., Koenigsberger, M., Sauser, R., Beny, J.L., Meister, J.J., 2005. Evidence for signaling via gap junctions from smooth muscle to endothelial cells in rat mesenteric arteries: possible implication of a second messenger. Cell Calcium 37, 311–320.

Lampe, P.D., Lau, A.F., 2004. The effects of connexin phosphorylation on gap junctional communication. Int. J. Biochem. Cell Biol. 36, 1171–1186.

Lanfear, D.E., Jones, P.G., Marsh, S., Cresci, S., Spertus, J.A., McLeod, H.L., 2007. Connexin37 (GJA4) genotype predicts survival after an acute coronary syndrome. Am. Heart J. 154, 561–566.

Langlois, S., Cowan, K.N., Shao, Q., Cowan, B.J., Laird, D.W., 2008. Caveolin-1 and -2 interact with connexin43 and regulate gap junctional intercellular communication in keratinocytes. Mol. Biol. Cell 19, 912–928.

Leybaert, L., Paemeleire, K., Strahonja, A., Sanderson, M.J., 1998. Inositol-trisphosphate-dependent intercellular calcium signaling in and between astrocytes and endothelial cells. Glia 24, 398–407.

Li, X., Simard, J.M., 1999. Multiple connexins form gap junction channels in rat basilar artery smooth muscle cells. Circ. Res. 84, 1277–1284.
Li, X., Simard, J.M., 2002. Increase in Cx45 gap junction channels in cerebral smooth muscle cells from SHR. Hypertension 40, 940–946.
Liao, Y., 2001. Endothelial cell-specific knockout of connexin 43 causes hypotension and bradycardia in mice. Proc. Natl. Acad. Sci. USA 98, 9989–9994.
Liao, Y., Regan, C.P., Manabe, I., Owens, G.K., Day, K.H., Damon, D.N., et al., 2007. Smooth muscle-targeted knockout of connexin43 enhances neointimal formation in response to vascular injury. Arterioscler. Thromb. Vasc. Biol. 27, 1037–1042.
Lin, X., Fenn, E., Veenstra, R.D., 2006. An amino-terminal lysine residue of rat connexin40 that is required for spermine block. J. Physiol. 570, 251–269.
Little, T.L., Beyer, E.C., Duling, B.R., 1995a. Connexin 43 and connexin 40 gap junctional proteins are present in arteriolar smooth muscle and endothelium *in vivo*. Am. J. Physiol. 268, H729–H739.
Little, T.L., Xia, J., Duling, B.R., 1995b. Dye tracers define differential endothelial and smooth muscle coupling patterns within the arteriolar wall. Circ. Res. 76, 498–504.
Locke, D., Harris, A.L., 2009. Connexin channels and phospholipids: Association and modulation. BMC Biology 7, 52.
Locke, D., Stein, T., Davies, C., Morris, J., Harris, A.L., Evans, W.H., et al., 2004. Altered permeability and modulatory character of connexin channels during mammary gland development. Exp. Cell Res. 298, 643–660.
Locke, D., Liu, J., Harris, A.L., 2005. Lipid rafts prepared by different methods contain different connexin channels, but gap junctions are not lipid rafts. Biochemistry 44, 13027–13042.
Locke, D., Jamieson, S., Stein, T., Liu, J., Hodgins, M.B., Harris, A.L., et al., 2007. Nature of Cx30-containing channels in the adult mouse mammary gland. Cell Tissue Res. 328, 97–107.
Locovei, S., Scemes, E., Qiu, F., Spray, D.C., Dahl, G., 2007. Pannexin1 is part of the pore forming unit of the P2X(7) receptor death complex. FEBS Lett. 581, 483–488.
Looft-Wilson, R.C., Payne, G.W., Segal, S.S., 2004. Connexin expression and conducted vasodilation along arteriolar endothelium in mouse skeletal muscle. J. Appl. Physiol. 97, 1152–1158.
Maeda, S., Nakagawa, S., Suga, M., Yamashita, E., Oshima, A., Fujiyoshi, Y., et al., 2009. Structure of the connexin 26 gap junction channel at 3.5 Å resolution. Nature 458, 597–602.
Manthey, D., Bukauskas, F., Lee, C.G., Kozak, C.A., Willecke, K., 1999. Molecular cloning and functional expression of the mouse gap junction gene connexin-57 in human HeLa cells. J. Biol. Chem. 274, 14716–14723.
Martin, P.E., Blundell, G., Ahmad, S., Errington, R.J., Evans, W.H., 2001. Multiple pathways in the trafficking and assembly of connexin 26, 32 and 43 into gap junction intercellular communication channels. J. Cell Sci. 114, 3845–3855.
Martinez, A.D., Hayrapetyan, V., Moreno, A.P., Beyer, E.C., 2002. Connexin43 and connexin45 form heteromeric gap junction channels in which individual components determine permeability and regulation. Circ. Res. 90, 1100–1107.
Matchkov, V.V., Rahman, A., Bakker, L.M., Griffith, T.M., Nilsson, H., Aalkjaer, C., 2006. Analysis of effects of connexin-mimetic peptides in rat mesenteric small arteries. Am. J. Physiol. Heart Circ. Physiol. 291, H357–H367.
Mather, S., Dora, K.A., Sandow, S.L., Winter, P., Garland, C.J., 2005. Rapid endothelial cell-selective loading of connexin 40 antibody blocks endothelium-derived hyperpolarizing factor dilation in rat small mesenteric arteries. Circ. Res. 97, 399–407.
Maza, J., Das Sarma, J., Koval, M., 2005. Defining a minimal motif required to prevent connexin oligomerization in the endoplasmic reticulum. J. Biol. Chem. 280, 21115–21121.

Moreno, A.P., Rook, M.B., Fishman, G.I., Spray, D.C., 1994a. Gap junction channels: distinct voltage-sensitive and -insensitive conductance states. Biophys. J. 67, 113–119.

Moreno, A.P., Saez, J.C., Fishman, G.I., Spray, D.C., 1994b. Human connexin43 gap junction channels. Regulation of unitary conductances by phosphorylation. Circ. Res. 74, 1050–1057.

Musil, L.S., Goodenough, D.A., 1991. Biochemical analysis of connexin43 intracellular transport, phosphorylation, and assembly into gap junctional plaques. J. Cell Biol. 115, 1357–1374.

Neijssen, J., Herberts, C., Drijfhout, J.W., Reits, E., Janssen, L., Neefjes, J., 2005. Cross-presentation by intercellular peptide transfer through gap junctions. Nature 434, 83–88.

Oh, S., Rubin, J.B., Bennett, M.V., Verselis, V.K., Bargiello, T.A., 1999. Molecular determinants of electrical rectification of single channel conductance in gap junctions formed by connexins 26 and 32. J. Gen. Physiol. 114, 339–364.

Oh, S., Rivkin, S., Tang, Q., Verselis, V.K., Bargiello, T.A., 2004. Determinants of gating polarity of a connexin 32 hemichannel. Biophys. J. 87, 912–928.

Ohtani, O., Kikuta, A., Ohtsuka, A., Taguchi, T., Murakami, T., 1983. Microvasculature as studied by the microvascular corrosion casting/scanning electron microscope method. I. Endocrine and digestive system. Arch. Histol. Jpn. 46, 1–42.

Oshima, A., Tani, K., Hiroaki, Y., Fujiyoshi, Y., Sosinsky, G.E., 2007. Three-dimensional structure of a human connexin26 gap junction channel reveals a plug in the vestibule. Proc. Natl. Acad. Sci. USA 104, 10034–10039.

Pahujaa, M., Anikin, M., Goldberg, G.S., 2007. Phosphorylation of connexin43 induced by Src: regulation of gap junctional communication between transformed cells. Exp. Cell Res. 313, 4083–4090.

Palacios-Prado, N., Bukauskas. F.F. 2009. Heterotypic gap junction channels as voltage-sensitive valves for intercellular signaling. Proc. Natl. Acad. Sci. USA. (in press).

Parthasarathi, K., Ichimura, H., Monma, E., Lindert, J., Quadri, S., Issekutz, A., et al., 2006. Connexin 43 mediates spread of Ca^{2+}-dependent proinflammatory responses in lung capillaries. J. Clin. Invest. 116, 2193–2200.

Paulson, A.F., Lampe, P.D., Meyer, R.A., TenBroek, E., Atkinson, M.M., Walseth, T.F., et al., 2000. Cyclic AMP and LDL trigger a rapid enhancement in gap junction assembly through a stimulation of connexin trafficking. J. Cell Sci. 113, 3037–3049.

Puljung, M.C., Berthoud, V.M., Beyer, E.C., Hanck, D.A., 2004. Polyvalent cations constitute the voltage gating particle in human connexin37 hemichannels. J. Gen. Physiol. 124, 587–603.

Purnick, P.E., Benjamin, D.C., Verselis, V.K., Bargiello, T.A., Dowd, T.L., 2000. Structure of the amino terminus of a gap junction protein. Arch. Biochem. Biophys. 381, 181–190.

Qu, Y., Dahl, G., 2002. Function of the voltage gate of gap junction channels: selective exclusion of molecules. Proc. Natl. Acad. Sci. USA 99, 697–702.

Rackauskas, M., Kreuzberg, M.M., Pranevicius, M., Willecke, K., Verselis, V.K., Bukauskas, F.F., 2007. Gating properties of heterotypic gap junction channels formed of connexins 40, 43, and 45. Biophys. J. 92, 1952–1965.

Raghu, H., Sharma-Walia, N., Veettil, M.V., Sadagopan, S., Caballero, A., Sivakumar, R., et al., 2007. Lipid rafts of primary endothelial cells are essential for Kaposi's sarcoma-associated herpesvirus/human herpesvirus 8-induced phosphatidylinositol 3-kinase and RhoA-GTPases critical for microtubule dynamics and nuclear delivery of viral DNA but dispensable for binding and entry. J. Virol. 81, 7941–7959.

Reed, K.E., Westphale, E.M., Larson, D.M., Wang, H.Z., Veenstra, R.D., Beyer, E.C., 1993. Molecular cloning and functional expression of human connexin37, an endothelial cell gap junction protein. J. Clin. Invest. 91, 997–1004.

Reidy, M.A., 1990. Proliferation of smooth muscle cells at sites distant from vascular injury. Arteriosclerosis 10, 298–305.

Retamal, M.A., Cortes, C.J., Reuss, L., Bennett, M.V., Saez, J.C., 2006. *S*-nitrosylation and permeation through connexin 43 hemichannels in astrocytes: induction by oxidant stress and reversal by reducing agents. Proc. Natl. Acad. Sci. USA 103, 4475–4480.

Revel, J.P., Karnovsky, M.J., 1967. Hexagonal array of subunits in intercellular junctions of the mouse heart and liver. J. Cell Biol. 33, C7–C12.

Revilla, A., Bennett, M.V., Barrio, L.C., 2000. Molecular determinants of membrane potential dependence in vertebrate gap junction channels. Proc. Natl. Acad. Sci. USA 97, 14760–14765.

Rhodin, J.A., 1967. The ultrastructure of mammalian arterioles and precapillary sphincters. J. Ultrastruct. Res. 18, 181–223.

Rummery, N.M., Hill, C.E., 2004. Vascular gap junctions and implications for hypertension. Clin. Exp. Pharmacol. Physiol. 31, 659–667.

Saez, J.C., Gregory, W.A., Watanabe, T., Dermietzel, R., Hertzberg, E.L., Reid, L., et al., 1989. cAMP delays disappearance of gap junctions between pairs of rat hepatocytes in primary culture. Am. J. Physiol. 257, C1–C11.

Saez, J.C., Berthoud, V.M., Branes, M.C., Martinez, A.D., Beyer, E.C., 2003. Plasma membrane channels formed by connexins: their regulation and functions. Physiol. Rev. 83, 1359–1400.

Saez, J.C., Retamal, M.A., Basilio, D., Bukauskas, F.F., Bennett, M.V., 2005. Connexin-based gap junction hemichannels: gating mechanisms. Biochim. Biophys. Acta 1711, 215–224.

Saitongdee, P., Becker, D.L., Milner, P., Knight, G.E., Burnstock, G., 2004. Levels of gap junction proteins in coronary arterioles and aorta of hamsters exposed to the cold and during hibernation and arousal. J. Histochem. Cytochem. 52, 603–615.

Sanchez-Alvarez, R., Paino, T., Herrero-Gonzalez, S., Medina, J.M., Tabernero, A., 2006. Tolbutamide reduces glioma cell proliferation by increasing connexin43, which promotes the up-regulation of p21 and p27 and subsequent changes in retinoblastoma phosphorylation. Glia 54, 125–134.

Sandow, S.L., Garland, C.J., 2006. Spatial association of K–Ca and gap junction connexins in rat mesenteric artery. FASEB J. 20, A275.

Sandow, S.L., Looft-Wilson, R., Doran, B., Grayson, T.H., Segal, S.S., Hill, C.E., 2003. Expression of homocellular and heterocellular gap junctions in hamster arterioles and feed arteries. Cardiovasc. Res. 60, 643–653.

Sandow, S.L., Haddock, R.E., Hill, C.E., Chadha, P.S., Kerr, P.M., Welsh, D.G., et al., 2009. What's where and why at a vascular myoendothelial microdomain signalling complex. Clin. Exp. Pharmacol. Physiol. 36, 67–76.

Scemes, E., 2008. Modulation of astrocyte P2Y1 receptors by the carboxyl terminal domain of the gap junction protein Cx43. Glia 56, 145–153.

Scemes, E., Suadicani, S.O., Dahl, G., Spray, D.C., 2007. Connexin and pannexin mediated cell–cell communication. Neuron Glia Biol. 3, 199–208.

Schweda, F., Kurtz, L., de Wit, C., Janssen-Bienhold, U., Kurtz, A., Wagner, C., 2009. Substitution of connexin40 with connexin45 prevents hyperreninemia and attenuates hypertension. Kidney Int. 75, 482–489.

Segal, S.S., Beny, J.L., 1992. Intracellular recording and dye transfer in arterioles during blood flow control. Am. J. Physiol. 263, H1–H7.

Segal, S.S., Duling, B.R., 1986. Flow control among microvessels coordinated by intercellular conduction. Science 234, 868–870.

Segal, S.S., Jacobs, T.L., 2001. Role for endothelial cell conduction in ascending vasodilatation and exercise hyperaemia in hamster skeletal muscle. J. Physiol. 536, 937–946.

Seki, A., Duffy, H.S., Coombs, W., Spray, D.C., Taffet, S.M., Delmar, M., 2004. Modifications in the biophysical properties of connexin43 channels by a peptide of the cytoplasmic loop region. Circ. Res. 95, e22–e28.

Severs, N.J., 2001. Immunocytochemical analysis of connexin expression in the healthy and diseased cardiovascular system. Microsc. Res. Tech. 52, 301–322.
Shibayama, J., Lewandowski, R., Kieken, F., Coombs, W., Shah, S., Sorgen, P.L., et al., 2006. Identification of a novel peptide that interferes with the chemical regulation of connexin43. Circ. Res. 98, 1365–1372.
Siegl, D., Koeppen, M., Wölfle, S.E., Pohl, U., de Wit, C., 2005. Myoendothelial coupling is not prominent in arterioles within the mouse cremaster microcirculation *in vivo*. Circ. Res. 97, 781–788.
Simek, J., Churko, J., Shao, Q., Laird, D.W., 2009. Cx43 has distinct mobility within plasma-membrane domains, indicative of progressive formation of gap-junction plaques. J. Cell Sci. 122, 554–562.
Simionescu, M., Simionescu, N., Palade, G.E., 1976. Segmental differentiations of cell junctions in the vascular endothelium. Arteries and veins. J. Cell Biol. 68, 705–723.
Simon, A.M., McWhorter, A.R., 2002. Vascular abnormalities in mice lacking the endothelial gap junction proteins connexin37 and connexin40. Dev. Biol. 251, 206–220.
Simon, A.M., McWhorter, A.R., 2003. Decreased intercellular dye-transfer and down-regulation of non-ablated connexins in aortic endothelium deficient in connexin37 or connexin40. J. Cell Sci. 116, 2223–2236.
Simon, A.M., McWhorter, A.R., Chen, H., Jackson, C.L., Ouellette, Y., 2004. Decreased intercellular communication and connexin expression in mouse aortic endothelium during lipopolysaccharide-induced inflammation. J. Vasc. Res. 41, 323–333.
Sokoya, E.M., Burns, A.R., Marrelli, S.P., Chen, J., 2007. Myoendothelial gap junction frequency does not account for sex differences in EDHF responses in rat MCA. Microvasc. Res. 74, 39–44.
Solan, J.L., Lampe, P.D., 2005. Connexin phosphorylation as a regulatory event linked to gap junction channel assembly. Biochim. Biophys. Acta 1711, 154–163.
Solan, J.L., Lampe, P.D., 2007. Key connexin 43 phosphorylation events regulate the gap junction life cycle. J. Membr. Biol. 217, 35–41.
Solan, J.L., Lampe, P.D., 2008. Connexin 43 in LA-25 cells with active v-src is phosphorylated on Y247, Y265, S262, S279/282, and S368 via multiple signaling pathways. Cell Commun. Adhes. 15, 75–84.
Solan, J.L., Marquez-Rosado, L., Sorgen, P.L., Thornton, P.J., Gafken, P.R., Lampe, P.D., 2007. Phosphorylation at S365 is a gatekeeper event that changes the structure of Cx43 and prevents down-regulation by PKC. J. Cell Biol. 179, 1301–1309.
Sosinsky, G.E., Nicholson, B.J., 2005. Structural organization of gap junction channels. Biochim. Biophys. Acta 1711, 99–125.
Spray, D.C., Burt, J.M., 1990. Structure–activity relations of the cardiac gap junction channel. Am. J. Physiol. 258, C195–C205.
Spray, D.C., Ye, Z.C., Ransom, B.R., 2006. Functional connexin ''hemichannels'': a critical appraisal. Glia 54, 758–773.
Stergiopoulos, K., Alvarado, J.L., Mastroianni, M., Ek-Vitorin, J.F., Taffet, S.M., Delmar, M., 1999. Hetero-domain interactions as a mechanism for the regulation of connexin channels. Circ. Res. 84, 1144–1155.
Straub, A.C., Johnstone, S.R., Rizzo, M.J., Heberlein, K.R., Best, A.K., Boitano, S., Isakson, B.E., 2009. Site specific connexin phosphorylation is associated with reduced heterocellular communication between smooth muscle and endothelium. J. Vasc. Res. (in press).
Suchyna, T.M., Nitsche, J.M., Chilton, M., Harris, A.L., Veenstra, R.D., Nicholson, B.J., 1999. Different ionic selectivities for connexins 26 and 32 produce rectifying gap junction channels. Biophys. J. 77, 2968–2987.

Tabernero, A., Sanchez-Alvarez, R., Medina, J.M., 2006. Increased levels of cyclins D1 and D3 after inhibition of gap junctional communication in astrocytes. J. Neurochem. 96, 973–982.

Thomas, T., Jordan, K., Simek, J., Shao, Q., Jedeszko, C., Walton, P., et al., 2005. Mechanisms of Cx43 and Cx26 transport to the plasma membrane and gap junction regeneration. J. Cell Sci. 118, 4451–4462.

Unger, V.M., Kumar, N.M., Gilula, N.B., Yeager, M., 1999. Three-dimensional structure of a recombinant gap junction membrane channel. Science 283, 1176–1180.

Valiunas, V., 2002. Biophysical properties of connexin-45 gap junction hemichannels studied in vertebrate cells. J. Gen. Physiol. 119, 147–164.

Valiunas, V., Weingart, R., Brink, P.R., 2000. Formation of heterotypic gap junction channels by connexins 40 and 43. Circ. Res. 86, E42–E49.

Valiunas, V., Polosina, Y.Y., Miller, H., Potapova, I.A., Valiuniene, L., Doronin, S., et al., 2005. Connexin-specific cell to cell transfer of short interfering RNA by gap junctions. J. Physiol. 568, 459–468.

van Kempen, M.J., Jongsma, H.J., 1999. Distribution of connexin37, connexin40 and connexin43 in the aorta and coronary artery of several mammals. Histochem. Cell Biol. 112, 479–486.

van Rijen, H.V., van Veen, T.A., Hermans, M.M., Jongsma, H.J., 2000. Human connexin40 gap junction channels are modulated by cAMP. Cardiovasc. Res. 45, 941–951.

van Veen, T.A., van Rijen, H.V., Jongsma, H.J., 2000. Electrical conductance of mouse connexin45 gap junction channels is modulated by phosphorylation. Cardiovasc. Res. 46, 496–510.

van Zeijl, L., Ponsioen, B., Giepmans, B.N., Ariaens, A., Postma, F.R., Varnai, P., et al., 2007. Regulation of connexin43 gap junctional communication by phosphatidylinositol 4, 5-bisphosphate. J. Cell Biol. 177, 881–891.

Veenstra, R.D., Wang, H.Z., Beyer, E.C., Brink, P.R., 1994a. Selective dye and ionic permeability of gap junction channels formed by connexin45. Circ. Res. 75, 483–490.

Veenstra, R.D., Wang, H.Z., Beyer, E.C., Ramanan, S.V., Brink, P.R., 1994b. Connexin37 forms high conductance gap junction channels with subconductance state activity and selective dye and ionic permeabilities. Biophys. J. 66, 1915–1928.

Veenstra, R.D., Wang, H.Z., Beblo, D.A., Chilton, M.G., Harris, A.L., Beyer, E.C., et al., 1995. Selectivity of connexin-specific gap junctions does not correlate with channel conductance. Circ. Res. 77, 1156–1165.

Wagner, C., de Wit, C., Kurtz, L., Grunberger, C., Kurtz, A., Schweda, F., 2007. Connexin40 is essential for the pressure control of renin synthesis and secretion. Circ. Res. 100, 556–563.

Wang, H.Z., Veenstra, R.D., 1997. Monovalent ion selectivity sequences of the rat connexin43 gap junction channel. J. Gen. Physiol. 109, 491–507.

Wang, M., Martinez, A.D., Berthoud, V.M., Seul, K.H., Gemel, J., Valiunas, V., et al., 2005. Connexin43 with a cytoplasmic loop deletion inhibits the function of several connexins. Biochem. Biophys. Res. Commun. 333, 1185–1193.

Wang, J., Ma, M., Locovei, S., Keane, R.W., Dahl, G., 2007. Modulation of membrane channel currents by gap junction protein mimetic peptides: size matters. Am. J. Physiol. Cell Physiol. 293, C1112–C1119.

Weber, P.A., Chang, H.C., Spaeth, K.E., Nitsche, J.M., Nicholson, B.J., 2004. The permeability of gap junction channels to probes of different size is dependent on connexin composition and permeant-pore affinities. Biophys. J. 87, 958–973.

Welsh, D.G., Segal, S.S., 1998. Endothelial and smooth muscle cell conduction in arterioles controlling blood flow. Am. J. Physiol. 274, H178–H186.

White, T.W., Bruzzone, R., Goodenough, D.A., Paul, D.L., 1994. Voltage gating of connexins. Nature 371, 208–209.

Winterhager, E., Pielensticker, N., Freyer, J., Ghanem, A., Schrickel, J.W., Kim, J.S., et al., 2007. Replacement of connexin43 by connexin26 in transgenic mice leads to dysfunctional reproductive organs and slowed ventricular conduction in the heart. BMC Dev. Biol. 7, 26.

Wolfle, S.E., Schmidt, V.J., Hoepfl, B., Gebert, A., Alcolea, S., Gros, D., et al., 2007. Connexin45 cannot replace the function of connexin40 in conducting endothelium-dependent dilations along arterioles. Circ. Res. 101, 1292–1299.

Wolinsky, H., Glagov, S., 1967. A lamellar unit of aortic medial structure and function in mammals. Circ. Res. 20, 99–111.

Wong, C.W., Christen, T., Roth, I., Chadjichristos, C.E., Derouette, J.P., Foglia, B.F., et al., 2006a. Connexin37 protects against atherosclerosis by regulating monocyte adhesion. Nat. Med. 12, 950–954.

Wong, R.C., Dottori, M., Koh, K.L., Nguyen, L.T., Pera, M.F., Pebay, A., 2006b. Gap junctions modulate apoptosis and colony growth of human embryonic stem cells maintained in a serum-free system. Biochem. Biophys. Res. Commun. 344, 181–188.

Xie, H., Laird, D.W., Chang, T.H., Hu, V.W., 1997. A mitosis-specific phosphorylation of the gap junction protein connexin43 in human vascular cells: biochemical characterization and localization. J. Cell Biol. 137, 203–210.

Yeager, M., Harris, A.L., 2007. Gap junction channel structure in the early 21st century: facts and fantasies. Curr. Opin. Cell Biol. 19, 521–528.

Yeh, H.I., Chang, H.M., Lu, W.W., Lee, Y.N., Ko, Y.S., Severs, N.J., et al., 2000a. Age-related alteration of gap junction distribution and connexin expression in rat aortic endothelium. J. Histochem. Cytochem. 48, 1377–1389.

Yeh, H.I., Lai, Y.J., Chang, H.M., Ko, Y.S., Severs, N.J., Tsai, C.H., 2000b. Multiple connexin expression in regenerating arterial endothelial gap junctions. Arterioscler. Thromb. Vasc. Biol. 20, 1753–1762.

Yeh, H.I., Lai, Y.J., Lee, S.H., Lee, Y.N., Ko, Y.S., Chen, S.A., et al., 2001. Heterogeneity of myocardial sleeve morphology and gap junctions in canine superior vena cava. Circulation 104, 3152–3157.

Yen, M.R., Saier Jr., M.H., 2007. Gap junctional proteins of animals: the innexin/pannexin superfamily. Prog. Biophys. Mol. Biol. 94, 5–14.

Yilla, M., Doyle, D., Sawyer, J.T., 1992. Early disulfide bond formation prevents heterotypic aggregation of membrane proteins in a cell-free translation system. J. Cell Biol. 118, 245–252.

Zeilinger, C., Steffens, M., Kolb, H.A., 2005. Length of C-terminus of rCx46 influences oligomerization and hemichannel properties. Biochim. Biophys. Acta 1720, 35–43.

Zhang, W., DeMattia, J.A., Song, H., Couldwell, W.T., 2003. Communication between malignant glioma cells and vascular endothelial cells through gap junctions. J. Neurosurg. 98, 846–853.

Zheng-Fischhofer, Q., Ghanem, A., Kim, J.S., Kibschull, M., Schwarz, G., Schwab, J.O., et al., 2006. Connexin31 cannot functionally replace connexin43 during cardiac morphogenesis in mice. J. Cell Sci. 119, 693–701.

CHAPTER THREE

Genotype–Phenotype Mapping: Developmental Biology Confronts the Toolkit Paradox

Joel Atallah[*,†] *and* Ellen Larsen[*]

Contents

1. Introduction 120
2. Understanding the Genotype–Phenotype Relationship 121
   2.1. The potential and limitations of the GPM analogy 121
   2.2. Internal and external contexts and gene/morphology relationships 123
   2.3. Is the GPM "one-to-many" or "many-to-one?" 124
3. From Sequence to Form 125
   3.1. Sequence conservation amid phenotypic diversity 125
   3.2. Gene regulation 129
   3.3. Signaling cascades 134
4. Beyond Sequence 135
   4.1. Role of developmental dynamics in shaping the phenotype 135
   4.2. Role of genes in molecular and cellular dynamics 136
5. Case Study for Parsing Gene, Cell and Self-Organizing Roles in Morphogenesis 138
6. Conclusion 142
Acknowledgments 142
References 142

Abstract

The quest to understand the relationship between an organism's DNA sequence and three-dimensional form is an interdisciplinary task, integrating diverse fields of the life sciences. The relevance of the metaphor of a genotype–phenotype map is explored from a developmental perspective, in light of the recent concept of a "molecular toolkit" of protein-coding genes, and the widespread view that analyzing the logic and mechanics of gene regulation at multiple levels is key to

* Department of Cell and Systems Biology, University of Toronto, Toronto, Ontario M5S 3G5, Canada
† Current address: Department of Evolution and Ecology, University of California, Davis, California 95616, USA

International Review of Cell and Molecular Biology, Volume 278
ISSN 1937-6448, DOI: 10.1016/S1937-6448(09)78003-7
© 2009 Elsevier Inc.
All rights reserved.

explaining how morphology is genetically encoded. We discuss the challenges of decoding genomes despite variable genetic backgrounds, the dynamically changing physical and molecular contexts of the internal environment during development, and the impact of external forces on morphogenesis.

Key Words: Genotype–phenotype map, Morphogenesis, Gene–morphology relationship, Phenotypic diversity, Gene regulation, Genetic toolkit, Context, Cell dynamics, Self-organization, Emergent properties. © 2009 Elsevier Inc.

1. Introduction

The relationship between inheritance and phenotype has been a subject of inquiry since ancient times. Aristotle believed that both male and female contributed to the development of offspring, the male providing the ''form'' through his semen (which has been interpreted as inherited potential), and the female the ''matter'' (Mayr, 1982). According to his paradigm, a child with a robust father but whose mother was an ill-fed slave, while inheriting the ''form'' of the father, might still lack strength, in much the same way that sowing good seed on an infertile or drought-ridden field would result in low-quality produce. While Aristotle's hypothesis concerning a uniparental genetic contribution to offspring was flawed, we will argue in this review that two issues which Aristotle raised, namely, inheritance and context, are crucial to understanding the relationship between genotype and phenotype, and the paradox of how living forms in all their diversity can be constructed with a limited ''toolkit'' of genes (Carroll, 2005; Section 3.1.1).

Although the terms ''genotype'' and ''phenotype'' were first coined by Johannsen (1911), the relationship between an organism's heredity and physical attributes was an essential component of Darwin's depiction of evolution as ''descent with modification,'' wherein he claimed that different taxa display morphological similarities because they share a common (hereditary) ancestry (Darwin, 1859). He further suggested that differences between organisms are the result of modifications of the heredity influencing development. In today's parlance, descent with modification implies that changes in the DNA of descendants of a common ancestor are responsible for the diversity of form. The process of evolution, therefore, should have provided us with a spectacular natural experiment, allowing researchers to draw a myriad of correlations between genetic data and the panoply of life's phenotypic manifestations. However, for reasons that we will discuss in this review, even in this postgenomic era our understanding of the relationship between DNA sequence and phenotype is still very much in its infancy.

In the first half of the twentieth century, it was commonplace to teach that the phenotype was a result of the interaction of genes and environment. Such a view can be seen as essentially Aristotelean, with both preformed (the ''male contribution,'' according to Aristotle) and environmentally modulated (Aristotle's ''female'') aspects. This perspective was eventually

supplanted by the arguably more limited paradigm of the genome as a computer program encoding a specific developmental outcome. However, the pendulum has started to switch back in recent years to a broader (and less deterministic) focus on the role of both genes and environment in shaping the phenotype. A recent review of gene regulatory networks (GRNs) (Ettensohn, 2009), while beginning with a reference to "how development is encoded in the genome," later discusses the phenomenon of developmental plasticity, highlighting a belated resurgence of interest in the environmental contribution to the phenotype.

The relationship between DNA sequence and form is frequently referred to as the genotype–phenotype map (GPM), a term that is used in quantitative genetics in reference to the effects of specific genomic regions on traits of interest (Alvarez-Castro et al., 2008). Likewise, in medicine, the GPM may refer to the association between mutations at specific loci and a disease or other condition (Concolino et al., 2007; Kamath et al., 2008; Lund et al., 1999; Patterson et al., 1993). Given the complexity of form, researchers have sometimes sought to understand principles of the GPM by looking at specific processes such as RNA folding (Fontana, 2002).

However, since classical genetics has generally taken a forward approach, going from mutation to gene, it can be argued that much of the history of genetics has actually involved determining how the phenotype maps onto the genotype. The present review, while using the terminology of the GPM that is popular today, will remain cognizant of the two-way interaction between genetic information and the developing organism. After a general review of the GPM concept, we will examine how the discovery of surprising similarities at the DNA sequence level influences our view of how genotype maps onto phenotype, and review the current focus on understanding gene regulation, at multiple levels, to explain phenotypic diversity. We will then discuss how an appreciation of the dynamic process of morphogenesis—the interface between sequence and form—must be included in any attempt to bridge the gap between the one-dimensional (1D) molecular genotype and the 3D organism. This will be followed by a case study of a classic attempt to relate genes to morphological structures (bristle patterning in fruit flies) and how this system illustrates the importance of both sequence and morphological dynamics. We will conclude with a short discussion of the reciprocal relationship between genotype and phenotype.

2. Understanding the Genotype–Phenotype Relationship

2.1. The potential and limitations of the GPM analogy

The concept of a GPM can be understood in a variety of ways. In some contexts, a map delineates possible pathways by which to achieve a certain molecular product. In the study of metabolism, for example, the goal might

be to chart how a certain substrate is transformed into a product. A metabolic map would provide possible routes and intermediate stages along the way. Maps relating genes to metabolism have been classically inferred from mutational data in which genetic mutations are correlated with the loss of particular products, a relatively straightforward process (Beadle and Tatum, 1941). With the high-throughput technologies available today coupled to statistical modeling, correlations between quantitative gene expression and a phenotype such as a disease can generate putative GRNs (Rockman, 2008). For many purposes, this kind of mapping may be sufficient.

Often, however, the purpose is to map genes onto processes involved in morphogenesis which may be dynamically nonlinear and involve spatial complexities. In such situations, the physics of the developing tissue may have emergent properties not traceable to the genome in a one-to-one fashion. An interesting example is described by Hilgenfeldt et al. (2008) in which the authors developed a mathematical model of the cone cell arrangement in the ommatidia of fly eyes, which resemble well-studied patterns of soap bubbles. In this case, energy minimization features of soap bubbles were combined with realistic assumptions concerning the mechanical properties of cell adhesion and membrane elasticity. The model was able to predict not only the wild-type morphology of the cone cells, but also the effects of mutational modulation of cell adhesion and cell numbers. A requirement for detailed knowledge of the biophysical context to hypothesize the effects of particular kinds of mutants has important consequences for our conception of a GPM. Between genes and 3D phenotypes lie the self-organizing properties of matter (Section 4), which are not possible to capture from genome sequences.

Perhaps the most pervasive idea about genes is that there are ''genes for'' any given phenotypic trait (Moore, 2003; Weiss, 2003). What is usually meant is that a mutation in a gene will alter the normal phenotype. Where phenotype is measured as a disease state, the recognition of a correlation between mutant genes and particular diseases dates back to at least to the second century A.D., when it was recognized that hemophilia is a hereditary disease generally afflicting males (Rosner, 1995). Currently, the list of known disease causing genes with a Mendelian genetic basis numbers over 12,000, according to the online Mendelian Inheritance in Man® Website http://www.ncbi.nlm.nih.gov/omim/. Nevertheless, many diseases of interest, although having a hereditary component, cannot be predicted on the basis of known allelic variants, although individuals with certain alleles may have a higher predisposition risk (Collins and McKusick, 2001). There has been a shift in focus in human genetics in recent decades from the traditional monogenic diseases to conditions like cancer and diabetes where predisposition may be an outcome of a complex interaction of multiple alleles, in addition to a nongenetic environmental component. It is becoming clearer that in many cases genes do not dictate destiny.

2.2. Internal and external contexts and gene/ morphology relationships

The environmental influence on the phenotype is sometimes referred to in today's parlance as the ''enviromе'' (Butte and Kohane, 2006). More traditionally, it has been regarded as one aspect of ''context,'' a term that includes both external and internal influences on the activity and phenotypic effects of the gene or sequence under consideration. The importance of context for gene expression has been recognized since the beginning of formal genetics. Developmental plasticity studies date back at least to the nineteenth century, when butterfly morphs, originally assigned to species status, were recognized to be different forms of one temperature-sensitive species (Morgan, 1907). In the mid-twentieth century, the black nose, ear, and paw tips on Himalayan rabbits were experimentally determined to depend on temperature (Wagner and Mitchell, 1964). In these cases, the same genotype would respond differently depending on the environment. In the early 1900s, when Mendel's rules of inheritance were rediscovered, the phenomenon of maternal effects was described. The prime example of this type of inheritance is coiling in snails. Genetic control was ascertained to be due to a locus with alternative alleles, with dextral coiling being dominant. Here, the phenotype of the offspring depended not on its genotype but on that of its mother (Sturtevant, 1923). While these examples have not been forgotten, they were not center-stage during the latter part of the twentieth century, a period that saw increased emphasis on genes and genomics. Although most scientists may intellectually agree that context is of basic importance in gene expression, it is still far more common in practice to carry out genetic screens rather than context screens, not only because they are usually easier to implement but also because they give seemingly more clear-cut results and conform to the prevailing expectation of the primacy of genes.

It was inevitable that the pendulum would swing back toward a greater appreciation for the role of context in determining phenotype. The discovery of the toolkit paradox (Section 3.1.1), which became apparent from genome sequencing, and the finding that disease prediction depends not only on genetic predisposition but also lifestyle, undoubtedly played a role in this. Increasingly, authors are addressing the role of context explicitly (Bray and Johnson, 2008).

The genetic background itself, of course, is one of the most important aspects of context, and this was recognized even before our current understanding of gene regulation was formulated. Early in the study of transmission genetics, it was realized that Bar gene eye phenotypes in *Drosophila* resulted from small chromosomal duplications of a particular region of the X chromosome (Bridges, 1936). Both the number of duplications, and whether they occurred tandemly or on separate chromosomes, played a role in determining the phenotype. Another advance involved the

discovery of suppressor genes that silenced mutations. The relevant genetic background is often polygenic in nature, and attempts to understand this aspect of genomes have used quantitative trait locus (QTL) analysis and other techniques (Rockman, 2008).

Yet another aspect of the context is the "competence" of the tissue in which a gene is expressed. The transcription factor *Antennapedia*, when ectopically expressed in the fly antenna imaginal disks, produces leg-like outgrowths instead of antennal structures. This transformation requires a massive change in the spatial coordination of cell behaviors such as proliferation and cell death (Mathi and Larsen, 1988), as well as bristle pattern modification and cell differentiation. A feature of this transformation is that *Antennapedia* can be misexpressed everywhere when expressed in a transgene driven by a heat shock promoter. Interestingly, despite apparently ubiquitous expression, the only region to transform into a leg is the antenna, and the degree of transformation depends on the quantity of Antennapedia and the time of administration (Gibson and Gehring, 1988; Larsen et al., 1996). *Antennapedia*, therefore, can only exercise its influence on morphology when it is produced in tissue that is competent to respond to it temporally and spatially.

Since transcription factors (see also Section 3.2) typically function as part of a multiprotein complex, the function of the transcription factor is often dependant on the type of complex formed in a tissue- and time-dependant fashion. This kind of pleiotropy presents another difficulty in predicting gene function from gene sequence. A case in point is the Hox gene (Section 3.1.1) *fushi tarazu*. Copeland et al. (1996) showed in a *fushi tarazu* mutant fly embryo (*ftz*[−]) that a heat shock promoted transgene lacking a functional Ftz homeodomain could restore much of the gene's functionality. They not only looked at the rescue of segmentation patterns but also at the expression of other genes either repressed or activated by normal Ftz protein (Copeland et al., 1996). They concluded that Ftz DNA-binding functions are mediated by protein–protein interactions which augment the homeodomain-mediated activities. Curiously, one of the important functions of the homeodomain in Ftz appears to be in autoregulation of *ftz* itself.

2.3. Is the GPM "one-to-many" or "many-to-one?"

Monozygotic twins, despite assumed genetic identity (but see Bruder et al., 2008 for evidence of differences in gene copy number), differ in their fingerprints (Arrieta et al., 1992). This can be viewed as a prime illustration of the "one-to-many" nature of the GPM. Environmental effects (such those discussed in the previous section) and stochastic aspects of developmental processes (Ascioti, 2009) may lead to nonidentical morphologies even in the case of individuals with the same genotype. In a more limited sense, the presence of similar genes that pattern different structures

(Section 3.1.1) is another example of a one-to-many relationship between genes and morphology.

The GPM is also many-to-one (Weiss and Terwilliger, 2000). At the most basic level, Mendelian genetics postulates that many hereditary traits are recessive and may not be apparent at the phenotypic level in a given individual, though their existence can be inferred through genetic crosses or DNA sequencing. Even when a population as a whole is considered, however, there is considerable genetic variation that is not reflected in the phenotype. In other words, many genotypes map onto the same phenotype. The robustness of the phenotype to changes at the sequence level is referred to as canalization (Siegal and Bergman, 2002; Waddington, 1961). When a gene is mutated, however, the ability of the organism to buffer the effects of genes at other loci may be compromised (Atallah et al., 2004; Bergman and Siegal, 2003; Dworkin, 2005a,b), leading to a breakdown in canalization. Studies have shown the presence of cryptic genetic variation (Dworkin et al., 2003; Gibson and Dworkin, 2004) for traits that is only revealed in a mutant background. Since models of complex gene networks (Siegal and Bergman, 2002) show that buffering is an emergent property of the process of gene regulation through development, canalization and cryptic genetic variation are to be expected.

The complexity of the GPM, both "one-to-many" and "many-to-one," suggests that a reexamination of the concept is in order. The focus of this review will be largely on the "one-to-many" conundrum, which is of particular relevance to developmental biology (the "many-to-one" paradox is more commonly confronted in population genetics). In the following section, we will look at the absence of a direct correlation between DNA sequences and morphological structures, and examine how the consideration of gene regulation and "motif turnover" provide a partial resolution to this paradox.

3. From Sequence to Form

3.1. Sequence conservation amid phenotypic diversity

In the early years of the molecular revolution, it was sometimes surmised that genetic turnover over millions of years would lead to a situation where most homologous structures were regulated by genes that had diverged to the extent that they were no longer recognizable (Mayr, 1963). Multiple solutions to physiological problems would evolve at the genomic level using unrelated gene sequences. This view may be depicted as an extreme version of the "many-to-one" perspective of the GPM, where so many sequences map to the same phenotype that the search for homologous genes is futile. Later research led to a radical reversal of this paradigm. We now know that

there is strong gene conservation even at the highest taxonomic levels. The genome projects have revealed that even organisms from different kingdoms, such as humans and yeast, share a considerable proportion of genes, despite the striking divergence in their phenotypes. Initially surprising, such findings are now part of the accepted dogma. As far as protein-coding regions are concerned, a genotype–phenotype model that is largely ''one-to-many'' has been imposed by the empirical evidence.

3.1.1. Hox genes and the gene toolkit

The now classic example of a one-to-many map is the Hox genes, named after a shared DNA-binding domain. Probably more than any other discovery, the finding that these transcription factors control anteroposterior patterning in organisms as diverse as nematodes, insects, and vertebrates, representing all three major branches of Bilateria (Gerhart and Kirschner, 1997) has shifted current thinking in biology in a ''genocentric'' direction. No longer is it possible to argue that genes are an incidental by-product of evolution. Indeed, the opposite position—that genes constrain both the phenotype and its evolution—is now being argued with increasing vigor. But it is perhaps telling that after over three decades of research on the Hox genes, we are still no closer to a universally accepted resolution of the fundamental question of why these genes are conserved in body axis specification, despite changes in both their upstream regulators and downstream targets.

In some organisms, the order of the Hox genes along the chromosome was found to be identical to the order of the body regions they specify along the anteroposterior axis (Kmita and Duboule, 2003), a phenomenon that is now referred to as colinearity. Colinearity is particularly obvious in vertebrates, where Hox clusters are compact and contain the full complement of Hox genes. Ironically, the phenomenon was first discovered in *Drosophila melanogaster* (Lewis, 1978), where colinearity is less clear due to the division of the cluster into two complexes in which Hox genes are interspersed with numerous other sequences (Ferrier and Minguillon, 2003). This condition is derived; in more basal insects like *Tribolium*, the cluster is intact (Shippy et al., 2008), and colinearity is more obvious, though the cluster is still replete with far more non-Hox-gene sequences than in vertebrates.

A linear mapping of genes to phenotype is an appealingly simple model of the genotype–phenotype relationship. Once again, however, the significance of these findings is a matter of intense debate (Kmita and Duboule, 2003). Colinearity is not a universal prerequisite for body patterning; there are many known cases, such as *Oikopleura dioica* (Seo et al., 2004) and *Ciona intestinalis* (Ikuta et al., 2004), where Hox genes are dispersed throughout the genome. For fear of being accused of anthropomorphism, and for phylogenetic reasons, most analysts are loathe to suggest that the compact collinear clusters in vertebrates is in any way reflective of the condition of the ancestor of the Bilateria (Duboule, 2007). However, if the vertebrate

condition is derived, the implication is that evolutionary forces can actually lead to a simplification of the genotype–phenotype relationship. Researchers have speculated that such simplification could be a by-product of the vertebrate multiplication of the Hox clusters and the co-option of these genes for additional functions, including the patterning of appendages and genitalia (Duboule, 2007).

Although Hox genes throughout the animal kingdom are considered homologous, sequence differences in their protein-coding regions have occurred, and these may have played a role in evolution. Ronshaugen et al. (2002) provided evidence that the insect body plan, where legs are limited to three thoracic segments, may have evolved through changes in the C-terminus of the Ultrabithorax (Ubx) Hox protein involving the mutation of serine/threonine residues, following the restriction of Ubx expression to the abdominal region. The changes apparently allowed Ubx to repress legs in this part of the organism. While this study suggested that changes in protein structure may be responsible for phenotypic differences between organisms, the trend in recent research has been to consider the proteins that genes code for as ancient and largely unchanged, and to view phenotypic differences as a consequence of changes in gene regulation.

The currently dominant paradigm envisages a gene toolkit (Carroll, 2005), common to a vast number of taxa, along with taxon- and context-specific gene regulation. The latter (see also Section 2.2) implies that even within the same organism, genes (such as those that code for Hox proteins) may be regulated differently, both spatially and temporally, resulting in the use and reuse of the same toolkit to generate nonhomologous structures. The diversity of life is thus mostly a consequence of differences in regulation. The toolkit model could help explain why gene number need not scale to perceived organismal complexity (Hahn and Wray, 2002). The draft sequencing of the human genome (International Human Genome Sequencing Consortium, 2001) initially yielded an estimate of 30–40,000 genes, only about twice that of the far simpler (at least as far as cell number is concerned) nematode *Caenorhabditis elegans*. (A more recent analysis of gene models in the human, based on a more complete sequence, reduced the estimated number of protein-coding genes to 20–25,000; International Human Genome Sequencing Consortium, 2004). Presumably, regulation is key to explaining differences in complexity. Nelson et al. (2004) found evidence in both *D. melanogaster* and *C. elegans* that complexity in gene expression patterns is correlated with mean intergenic distance, a finding consistent with the toolkit model if one grants the authors' hypothesis that most nonrepetitive noncoding DNA is regulatory. Another study showed that among various model species, those believed to be more complex have markedly higher fractions of conserved noncoding sequence (Siepel et al., 2006).

An important caveat, however, is that recent research suggests that the dichotomy between coding and regulatory sequence may be a false one. While it has long been known that *cis*-regulatory sequences, traditionally thought to lie in the flanking regions of genes, may also be located in introns, a handful of studies have found them in exons as well (e.g., Tümpel et al., 2008). A regulatory module in an exon would have a dual function (to code for a protein and to regulate expression) and hence be subject to two levels of constraint. A standard practice in bioinformatic studies looking for regulatory regions is to mask the coding sequence before applying the search algorithm, and when ChIP-on-chip empirical investigations find putative regulatory sites in coding sequence, the tendency is to discard them. The practical result may be that many regulatory regions have been overlooked. From a theoretical point of view, however, it is not yet clear whether these recent findings will have a significant impact on our interpretation of the toolkit model. It is still possible to distinguish between protein coding and its regulation functionally even if the same sequence is used for both.

3.1.2. Ultraconserved sequences

A more recent finding of remarkable molecular conservation was the discovery of nearly 500 ultraconserved sequences (UCSs) of over 200 base pairs in mammalian genomes (Bejerano et al., 2004), with 100% identity between humans and two sequenced rodents (rat and mouse). The vast majority of these sequences (which can overlap with exons but are also commonly found in gene deserts) are also highly conserved (at $\sim$95% identity) with homologous regions in the chicken genome, and about two-thirds align with pufferfish (*Fugu rubripes*) variants at a more modest but still striking identity of about 75%. Equally surprising is the absence of identifiable orthologs for 95% of these sequences in the ascidian *C. intestinalis*, or the model fruit fly or nematode. These findings suggest that the identified UCSs evolved rapidly soon after the split of vertebrates from the basal chordate, but that their molecular evolution all but halted in the lineage leading to birds and mammals.

Such extreme conservation could be a consequence of dramatically reduced mutation in ultraconserved regions, but analysis of the derived allele frequency (DAF) in humans shows that rare alleles strongly predominate among polymorphic sites (Katzman et al., 2007), implicating the activity of purifying selection and hence a functional role for these sequences. Since the majority of UCSs that can act as enhancers drive gene expression in the nervous system, and particularly the forebrain (Pennacchio et al., 2006), it is possible that they are important for cognitive or social functions in birds and mammals. It is still unclear, however, given the diversity in avian and mammalian brains and cognitive processing, why such extreme conservation would be required.

Surprisingly, when four ultraconserved regions were deleted in mice, the animals were viable and fertile and showed no significant signs of impairment relative to a control group (Ahituv et al., 2007). The result was entirely unexpected; the selected sequences had been shown to display enhancer activity when fused to reporter constructs, and were located close to genes which show strong phenotypes when knocked out, suggesting a possible regulatory role. Reconciling these apparently contradictory findings (strong purifying selection on UCSs, but no apparent harm when they are removed from the genome) will be a challenge for future researchers.

If highly conserved regions play a role in gene regulation (Pennacchio et al., 2006; Woolfe et al., 2005), they provide evidence that regulatory regions, in addition to proteins such as the Hox genes (Section 3.1.1), may share homology across diverse species (at least within the vertebrate subphylum). It is not clear how this discovery affects our view of the toolkit model. On the one hand, it lends to support to the importance of regulation. On the other hand, the very purpose of the toolkit model is to explain how species with diverse morphologies can share the same genes—if the regulatory regions are also conserved, we are no closer to a resolution of this paradox. As discussed in the following section, many studies of gene regulation have found that regulatory regions, even among closely related species, show little homology at the sequence level due to the ''turnover'' of binding sites; these findings may suggest that UCSs with a regulatory function are exceptional.

3.2. Gene regulation

3.2.1. The search for a *cis*-regulatory code

The surprising conservation of protein sequence (Section 3.1.1) has led researchers to look at gene regulation to understand how diversity in form is encoded. Transcriptional control has been a primary focus in recent years, and there is increasing evidence for the importance of the role of *cis* effects in transcript-level variation (Genissel et al., 2008). Efforts to find a ''*cis*-regulatory code,'' however, have proved elusive (Siggia, 2005), even in very specific well-described systems such as *Drosophila* embryonic patterning. Most studies have sought to identify *cis*-regulatory modules (CRMs), also known as enhancers, which themselves consist of multiple binding sites for transcription factors. The clustering of binding sites, either homotypic (for the same transcription factor) or heterotypic (for multiple factors), is sometimes a hallmark of a CRM (Berman et al., 2002; Markstein et al., 2002), but because binding sites are typically short, on the order of 6–24 base pairs, this may also occur by chance. Further evidence for a CRM may be gleaned from phylogenetic footprinting, where the conservation of either the primary sequence or the clustering of binding sites in closely related organisms is examined (Grad et al., 2004). However, given evidence

from *Drosophila* that 20–60% of noncoding DNA in this organism may be evolving under positive selection (Andalfatto, 2005), phylogenetic footprinting may fail to find a significant proportion of regulatory regions where the sequence has changed as a consequence of adaptation. To detect adaptive evolution, intraspecific population data about polymorphism, in addition to interspecific divergence, is required (McDonald and Kreitman, 1991). As this becomes more readily available in a variety of organisms, we may increasingly find—if the situation in *Drosophila* is representative—that a greater proportion of noncoding DNA than previously realized has a role in transcriptional regulation.

A key finding in research on transcriptional regulation is that binding site turnover occurs relatively rapidly during evolution, even without changes in the phenotype or the expression pattern of the regulated genes. While one of the earliest demonstrations of turnover was in the comparison of *Drosophila even-skipped* (*eve*) stripe 2 enhancer architecture and function in a handful of closely related fruit fly species (Ludwig et al., 1998, 2000), later research confirmed the generality of turnover in CRMs (Hare et al., 2008; Moses et al., 2006). This discovery may be viewed as an example of the many-to-one nature of the GPM (Section 2.3), where divergent sequences lead to the same phenotype, except that in this case the sequences under consideration are noncoding regulatory regions (proteins are still thought to be highly conserved). While these findings are further evidence that sequence does not encode form directly, it is not yet clear whether the combined output of computational and empirical studies will be able to uncover a regulatory grammar that can explain the variation in CRMs, leading to a model that can relate this variation to changes—or the lack thereof—at the phenotypic level.

3.2.2. Chromatin as a transcriptional gatekeeper

While transcription factor binding to specific nucleotides can initiate transcription of protein-coding genes, there are several potential problems to overcome before this level of decoding is possible. Cellular DNA, if stretched out, is typically on the order of meters in length, and to fit into a microscopic nucleus, considerable folding is required. The folding involves wrapping around histone cores, forming nucleosomes, and then folding the already wrapped DNA. This folding can potentially "hide" sequences from transcription factors even if they are present, thus providing an additional level of control over protein synthesis. In addition to nucleosome proteins, other DNA-binding proteins such as the polycomb and trithorax protein families may function to "close down" or "open up" chromatin to transcription. DNA, plus its associated molecules including proteins and RNA, constitute "chromatin," the multimolecular system being modulated during the course of the development of phenotype as well as by transient physiological changes in response to local environments. Further constraints

on the availability of chromatin to the transcriptional machinery include the chemical modification of DNA by methylation and the modification of histones through the methylation or acetylation of particular amino acids. Another widespread phenomenon is heterochromatinization, in which even large chromosomal regions are compacted (Zacharias, 1995) and unavailable for transcription. These modifications often survive cell replication and become lineage-specific marks for controlling molecular phenotypes (Probst et al., 2009). As a strategy for cell differentiation, this multilayered regulation has the virtue of contributing to the robustness of cell phenotypes, allowing transcription factors to act at low concentration. Without the additional constraints imposed by chromatin-level regulation, the requirements for absolute control of transcription factor numbers/cell might be difficult to achieve.

Chromatin modification can be transmitted not only to the next cell generation through mitosis (Probst et al., 2009) but also even through gamete formation, a notable feature of parent of origin ''imprinting'' in plants (Feil and Berger, 2007). Collectively, chromatin modification phenomena constitute a type of heredity that does not alter DNA sequence, and produce what is often referred to as the epigenome.

Mirroring the diversity of mechanisms involved in chromatin modification is the variety of temporal and spatial phenotypic effects mediated by the epigenome. For example, evidence is accumulating that the enormous differences in morphology, size, behavior, and reproductive capabilities between worker and queen honeybees is modulated by the DNA methylation status of relevant genes in response to nutrition (Kucharski et al., 2008).

The widespread and profound effects of chromatin modification on transcription underscore the general principle that DNA sequence alone cannot easily be translated into phenotype. Chromatin structure is itself often influenced by internal and external environmental conditions (Kucharski et al., 2008). The coordination of development depends on integrating many levels of regulation in response to the local context. Although the regulatory details may be frustratingly convoluted, one suspects that the complexity is the price paid for robust developmental trajectories that respond appropriately to environmental challenges.

3.2.3. Gene regulatory networks

By combining data from numerous studies, networks of interacting genes have been uncovered in an array of diverse organisms, including *Drosophila* (Stathopoulos et al., 2002), echinoderms (Davidson et al., 2002), primitive chordates (Shi et al., 2009), and nematodes (Ririe et al., 2008). These networks can be used to show how interactions between genes can explain differences between organisms at various levels (e.g., transcript-level variation, Nuzhdin et al., 2008). The networks have also demonstrated that the regulatory underpinnings of development of specific tissues or structures can

often be ascribed to discrete, though interconnected, regulatory modules. For example, in the sea urchin GRN, a dedicated network subcircuit underlies specification of sea urchin endoderm (Davidson et al., 2002; Levine and Davidson, 2005). The modular nature of this subcircuit helps to explain why it is highly conserved with the homologous network in starfish (Hinman et al., 2003) despite hundreds of millions of years of evolution and the strikingly different adult morphologies of these echinoderms. The subprogram for generating endoderm can remain unchanged even if the phenotype changes at higher levels of organization, just as a software module that performs a specific function can be reused in multiple computer programs.

Comparison of network architecture in different organisms aims to distill common themes in regulatory control (Davidson and Levine, 2008; Levine and Davidson, 2005). For example, a regulatory control strategy referred to as the "double-negative gate" (Davidson and Levine, 2008), in which a broadly expressed repressor is locally inhibited, is used repeatedly in patterning cascades in the fruit fly embryo (De Renzis et al., 2006; Surkova et al., 2008) and tissue specification in the sea urchin embryo (Revilla-i-Domingo et al., 2007). It is notable that this strategy of using "double-negatives" to constrain the expression of a gene to a specific region is employed widely in GRNs in diverse contexts and organisms, and various explanations for its ubiquity have been proposed (Davidson and Levine, 2008). Understanding the logic of GRNs is akin to learning the syntax of a language: syntax in itself does not convey direct information about the content that is being transmitted (which cannot be known apart from the vocabulary), but it does help to explain the process by which words are logically organized to generate meaning. In a similar way, deducing GRN logic does not yield information about the direct relationship between specific genes and particular phenotypes (information that is derived from functional assays and screens), but they do bring us closer to an appreciation of the nature of the pathways that link sequence to form.

3.2.4. Noncoding RNAs and posttranscriptional regulation

The discovery of microRNAs (miRNAs) in the 1990s, first reported in *C. elegans* (Lee et al., 1993; Wightman et al., 1993), has revolutionized our view of the RNA world and demonstrated that a whole new level of regulation must be considered in any attempt to bridge the gap between sequence and form. Computational techniques for identifying both miRNAs (Lai et al., 2003; Lim et al., 2003) and their targets (Rajewsky, 2006) have been developed. These actors are now being incorporated into the circuit diagrams depicting gene pathways. The analysis of integrated regulatory networks consisting of both transcription factors and miRNAs has uncovered commonalities in the wiring of network modules. There is evidence that specific architectural configurations, such as a feedback loop

consisting of a single miRNA regulating two transcription factors which also regulate each other, are overrepresented in nature, possibly because the miRNA helps to increase the robustness of the feedback loop (Yu et al., 2008). Other evidence suggests that miRNAs, with their selective repression of genes that contain target sites as opposed to those that do not (so-called ''antitargets''), may contribute to developmental robustness by increasing the precision of gene expression patterns (Stark et al., 2005). The regulatory logic in this case appears to be comparable to that of the double-negative gates that commonly feature in transcriptional networks (Section 3.2.3).

It is now recognized that miRNAs are simply one manifestation of a galaxy of silencing noncoding RNAs of various lengths (Brosnan and Voinnet, 2009; Ghildiyal and Zamore, 2009). The widespread occurrence of RNA genes may explain why, for example, genetic studies found at least eight Hox genes in the *Drosophila* bithorax complex (Lewis, 1978), while sequencing has revealed only three that code for proteins (Ronshaugen et al., 2005). Current gene models, therefore, are probably far from complete, and the perceived functional content of the genome is likely to expand with our understanding of posttranscriptional regulation. Whether this will help to explain the previously described absence of a correlation between protein-coding gene number and phenotypic complexity (a conundrum also addressed by the toolkit model discussed earlier) remains to be seen.

3.2.5. Posttranslational control

While transcriptional regulation controls whether a gene is expressed in a given cell, and posttranscriptional processes modify or degrade a transcript prior to translation, posttranslational regulation often determines a protein's subcellular localization. Attempts are now being made to discover how information about this process can be gleaned from the protein sequence. A recent study looked at *CDC14Bretro*, a hominid-specific cell cycle gene generated through retroposition of a splicing variant of the parent gene *CDC14B* (Rosso et al., 2008). While the ancestral gene product, like its parent isoform, colocalized with microtubules, changes in the coding sequence in the ancestor of the African apes apparently enabled it to become associated with the endoplasmic reticulum. These changes show a signature of positive selection on the basis of the ratio of nonsynonymous to synonymous substitutions, although the functional reason for the localization shift is not known.

Rosso et al. (2008) had to use hybrid constructs to show that changes in the core sequence, as opposed to the N- or C-terminus, are responsible for the change in localization. Researchers are still a long way from being able to predict, on the basis of sequence alone, where a protein will be localized. There have been recent attempts, however, to develop computational methods of predicting targets of cyclin-dependent kinases (CDKs) on the

basis of the clustering of phosphorylation consensus motifs (Moses et al., 2007a,b). Turnover of the motifs within a cluster during evolution, without evidence of a functional change, appears to be common. The loss or gain of an entire cluster in a specific lineage, on the other hand, may be associated with adaptive evolution (Moses et al., 2007b). A cluster of CDK consensus sites, therefore, may be a considered a functional unit, analogous to an enhancer at the transcriptional level. In both cases, the regulatory ''grammar'' may allow for considerable variation in sequence without a corresponding change in phenotype, so long as the higher order clusters are preserved. It is evident that the very flexibility in this regulatory strategy constrains predictability and limits the simple application of mapping from gene to phenotype in a comprehensive way.

3.3. Signaling cascades

The context in which genes function also includes signaling cascades. The source of the signal may be either internal (Olivieri et al., 2008) or external. While the bulk of the work on signal transduction has involved chemical signaling, physical signals such as light and heat have also received attention. The stress-induced trimerization of Heat Shock Factors has been understood for several decades as an underlying mechanism for transcriptional upregulation of heat-shock proteins (Morimoto, 1998).

Light has probably been used as a signal since the earliest life forms and therefore has an evolutionary history of billions of years. In addition to its role in photosynthesis, light signaling has been studied extensively in plant morphogenesis (McNellis and Deng, 1995).

Exciting headway is being made on understanding the transduction of mechanical forces into chemical signals. Mechanical forces, such as stress in patterning plant meristems (Hamant et al., 2008), fluid shear stress in vasculogenesis (Tamada et al., 2004), and muscle tension in bone morphogenesis (Muller and Streicher, 1989) have been implicated in the development of form. The details of such processes are beginning to be unraveled at molecular, cellular, and tissue levels of organization. For example, based on decades of work showing that both transcriptional pathways and mechanical forces from extracellular matrix elasticity can influence vascularization, Mammoto et al. (2009) found an inhibitor of Rho activity that both integrates molecular and mechanical signals and regulates the promoter activity of a crucial downstream player in angiogenesis.

But what kinds of mechanisms transduce force so that a biochemical response, such as the one involving the Rho inhibitor, can influence cellular responses? Vogel and Sheetz (2006) reviewed three ways transduction might occur: the regulation of ion channels by tension, the stabilization of weak receptor/ligand binding, and the stretching of proteins to reveal previously hidden binding sites. Recently, this third possibility has been

visualized at the single molecule level. Talin and vinculin are proteins which bind to each other and are involved in attaching the cellular cytoskeleton to the extracellular matrix. Talin was hypothesized to be involved in force transduction because stretching it resulted in vinculin binding and subsequent cytoskeleton reorganization. Using "molecular tweezers" to stretch a single talin molecule, researchers found support for this model by following vinculin binding using fluorescently tagged molecules (del Rio et al., 2009).

The importance of physical signals for our understanding of the relationship between the genotype and phenotype is critical. Our knowledge of the genome and its regulation has centered primarily on the domain of chemistry, and the effects of physical events, be they external or internal, have been hard to incorporate into this view in a seamless way. While the elucidation of how mechanical forces are transduced to chemical signals will not resolve all the problems raised by emergent properties in development, we may yet understand some rules which will allow their consequences to be better predicted.

In the view provided here, signal transduction cascades drive cell processes in response to context and therefore are crucial for coordinating even complicated morphogenesis. DNA provides a source for the structure of molecules needed for both coordination and structure building but does not encode the structure *per se*. It is hard to imagine (from our current perspective) a more evolvable system based on hereditary "information," and indeed, considering the limited genomic toolkit and the enormous variety of organisms around us, it is perhaps the only way that genotypes may be connected to phenotypes. Nevertheless, the very flexibility of the system from an evolutionary perspective is what complicates our efforts to predict phenotype from sequence.

4. Beyond Sequence

4.1. Role of developmental dynamics in shaping the phenotype

The most striking aspect of early development, in which a fertilized egg becomes a multicellular organism, is the precision with which this complex and dynamic process is regulated. During embryogenesis, cells proliferate, change shape and size, die, adhere to one another and separate, secrete molecules, and (in many animals) move. These cell behaviors occur in a repeatable sequence, and, under the same conditions, quite synchronously with other embryos of the same species, to the extent that every model organism used in developmental research has a staging table containing

developmental sequence and timing information. Understanding the relationship of genes to the dynamic changes that occur in the development of adult phenotypes constitutes an explanatory goal for GPMs. Phenotypes, for all their multicellular biodiversity are the result of coordinating changes in only a handful of basic cell behaviors (Larsen, 1992; Larsen and McLaughlin, 1987). Between sequence and phenotype lie dynamics at several levels of organization, leading to the spatial positioning of structures. A complete GPM would include the coordination of cell behavior through time in spatially appropriate domains.

4.2. Role of genes in molecular and cellular dynamics

Genetic studies have provided considerable insight into temporal factors in morphogenesis. Along with morphological change in a defined temporal sequence, there are temporal patterns of gene expression, and when these are interrupted either mutationally or chemically, faulty morphogenesis is often the result. From this information, a correlational map between gene function interruption and phenotypes can be constructed. Such a map, while showing that certain gene products are normally produced in a given place and/or during a certain time period, is far from a real-time depiction of developmental dynamics, although it may be useful for organizing our thinking about genetic cascades and networks. The limitations of this kind of analysis were aptly characterized by Pontecorvo (1951); in a paraphrase of his terminology, we would venture that trying to discover the function of genes by disrupting them is akin to trying to understand ships by firing guns at them.

The importance of considering dynamics has been brought out in studies of DNA synthesis and transcription. On the basis of such studies it has been suggested, for example, that transcript size might play a part in gene pathway regulation. Examining the transcription of a long gene, Ubx, during the rapid ($\sim$8 min) nuclear divisions of early fly embryos, Shermoen and O'Farrell (1991) noted that Ubx transcripts were absent during mitosis. This suggested that nascent transcripts were aborted, since, while they are transcribed at a rate of about 1.4 kb/min, a full-length transcript is about 60 kb, leaving insufficient time to complete a transcript between divisions. Thus, the dynamics of nuclear division and the transcription of long genes leads to a mechanism for regulating transcription during a particular period of development. This regulation is not predicted on the basis of the gene sequence but is a consequence of the dynamics of two processes, mitosis and transcription. At a different scale, heterochronic mutations in *C. elegans* have been described in which whole developmental cascades may be removed or reiterated at a cell division pattern level (Lee et al., 1993). These results show how genes can influence temporal and dynamic events, although nucleotide sequences do not provide a direct readout of the

changing pattern (Moss, 2007). Considering cell behavior generally, it appears that while genes can help determine when a particular behavior occurs, this information is not directly encoded; it arises from their contribution as part of the emergent properties of the system.

On the basis of mutational studies, researchers are now acutely aware of the extent to which both quantitative and timing differences may affect higher level morphologies, and the complex interplay between these variables. In *Drosophila* studies where the Hox gene *Antennapedia* was expressed in different doses and at different times during a larva's life (see also Section 2.2), different degrees of antenna to leg transformation were observed (Gibson and Gehring, 1988; Scanga et al., 1995). In general, there was a distal to proximal transformation of antenna to leg when heat shock was applied at successively later stages. At a given time in development the concentration of *Antennapedia*, controlled by length of heat shock, produced different degrees of transformation. The effects varied from transformation being inversely correlated, insensitive or positively correlated with *Antennapedia* concentration (Larsen et al., 1996).

How do we include dynamic and context-dependant aspects of gene function in a depiction of the relationship between genes and phenotype? One current solution is to use computer modeling in which spatial, temporal, and quantitative gene products can be considered with rules governing their interactions qualitatively and quantitatively (von Dassow and Odell, 2002; von Dassow et al., 2000). These interactions include the unpredictable stochastic interactions of any physical system, as well as the effects of such physical processes as diffusion and convection. By modifying different variables, including reaction kinetics a variety of relationships can be demonstrated which mimic (to some extent) the phenotypes being explored. Analysis of regulatory networks at this level goes beyond circuit diagrams (Section 3.2.3) and is computationally exacting, but the rewards may include a better understanding of network connections. von Dassow et al. (2000), who modeled the parasegmental pattern of gene expression in *Drosophila*, discovered that simulations were remarkably robust in producing the parasegmental pattern despite changes in parameters modifying the dynamics of molecular interactions. These results appear to indicate that it is network properties such as feedback relationships, not the sequences of the genes *per se*, which dictate this type of stability.

Computational approaches of this nature may bring us as close as we will come in the near future to a predictive understanding of how genetic interactions can influence phenotype. They can deal with nonlinear results of interactions at any level of organization, allowing us to better understand emergent properties. In contrast to the narrow preoccupation with gene sequence that is typical of many modern-day studies, these models concentrate on gene properties expressed in relationship to other factors operating in the environment. They can describe the nature of stable gene networks,

or how much variation in components of, for example, a cell cycle, can be tolerated before there are mitotic irregularities. A continuing challenge will be to not only capture the dynamics of molecular changes, but to also incorporate the spatial details and physical parameters of cell and tissue changes during morphogenesis.

It should be noted that the computational work of Van Dassow et al. was based on decades of data on the effects of specific mutations on early fly embryogenesis. Without such a rich source of information, we are left with the problem of mapping genes to phenotype when between the gene and the phenotype there are several different levels of organization and a myriad of emergent properties we cannot predict *a priori*, properties that are often a consequence of self-organization (Kauffman, 1993). An important task is to put network structure and dynamics into the complicated world of the developing organism where physical as well as chemical signals occur at different levels of organization. Since cells and their constituents both create and respond to the physical forces and geometrical conditions they encounter, an increasing number of self-organizing developing systems are being found in both plants and animals. A recent example is that of lateral root distribution in plants. Experiments with *Arabidopsis* have shown that curvature of the root increases cell size which upregulates auxin transporters, leading to locally higher auxin hormone concentrations. It is these higher concentrations which stimulate lateral root outgrowth (Medrano-Soto et al., 2008a,b).

5. Case Study for Parsing Gene, Cell and Self-Organizing Roles in Morphogenesis

Bristle patterns in *Drosophila*, an historically important system for dissecting the relationship between genotype and phenotype, have also been used to examine the role of self-organization in generating form, wherein development itself produces a context which constrains phenotypic patterns. They are considered here as a case study that illustrates many of the themes discussed in this review.

In the early twentieth century, some of the first-identified mutants in the lab of the celebrated *Drosophila* genetics pioneer Morgan removed large conspicuous bristles from the fruit fly thorax (reviewed in Held, 2002). An accurate understanding of the nature of these mutations, however, had to wait until much later. The loss of specific bristles is now known to be a consequence of mutations in particular CRMs of the classic genes controlling bristle development, the proneural *achaete–scute* complex (Gómez-Skarmeta et al., 1995). Changes in these modules can also lead to evolutionary diversification. Although the thoracic bristle arrangement has been largely

conserved in *Drosophila* evolution, some interspecific differences have been observed. For example, while *D. melanogaster* has two dorsocentral bristles, both posterior, another fruit fly species, *Drosophila quadrilineata*, has four, including two anterior bristles. Marcellini and Simpson (2006) analyzed the evolution of the dorsocentral CRM, and showed that the *D. quadrilineata* module drives the expression of *scute* in *D. melanogaster* in more anterior regions than the native enhancer, and—in some cases—can induce a phenotype reminiscent of *D. quadrilineata* (including the anterior bristles) in the model fruit fly. These findings show that the ''natural experiment'' of evolution can be used to probe the relationship of genotype to form, demonstrating how, in confirmation of the toolkit model, regulatory changes are responsible for at least some of the interspecific diversity in phenotypes.

The evolutionary divergence in bristle patterns on the thorax, however, is dwarfed by the diversity on the tarsus (Bock and Wheeler, 1972; Kopp and True, 2002; Fig. 3.1A–C), where the sex comb, a male-specific row of large pigmented bristles, varies strikingly in morphology, even among closely related species. Recent studies have attempted to explain the evolutionary divergence in the number of tarsal segments bearing sex comb teeth (Barmina and Kopp, 2007; Randsholt and Santamaria, 2008), but an understanding of how the sex comb forms within a leg segment has been hampered by the difficulty in identifying sex comb-specific markers. Recently, we have shown, in a variety of species, that a leg-patterning gene, *dachshund*, is strongly reduced in the sex comb despite its heightened expression in the transverse row bristles to which the *D. melanogaster* comb is homologous (Atallah et al., 2009b, and unpublished data), and apparently plays a role in differentiating between these two types of bristles.

The formation of the sex comb—from a cellular perspective—is a complex and dynamic process. In *D. melanogaster*, the comb rotates almost 90° during development (Held et al., 2004; Tokunaga, 1962). An understanding of the mechanics of this process had to wait for live imaging of sex comb development using a fluorescent marker, which has shown that the rotation involves male-specific convergent extension in the cells surrounding the comb (Atallah et al., 2009a; Tanaka et al., 2009). Even without a full knowledge of all of the genetic players, an analysis of the cell dynamics of comb formation (Fig. 3.1D) shows that some aspects of both its development and evolution may be an indirect consequence of the barriers that form when bristles (including those that make up the sex comb) join together into contiguous rows, preventing cells from passing between them (Atallah et al., 2009a). While the initial conditions—the placement of the sex comb teeth and other bristles on the tarsus prior to the rotation—are likely to be genetically determined, the subsequent rearrangement of these bristles may be constrained by cell dynamics on the developing leg

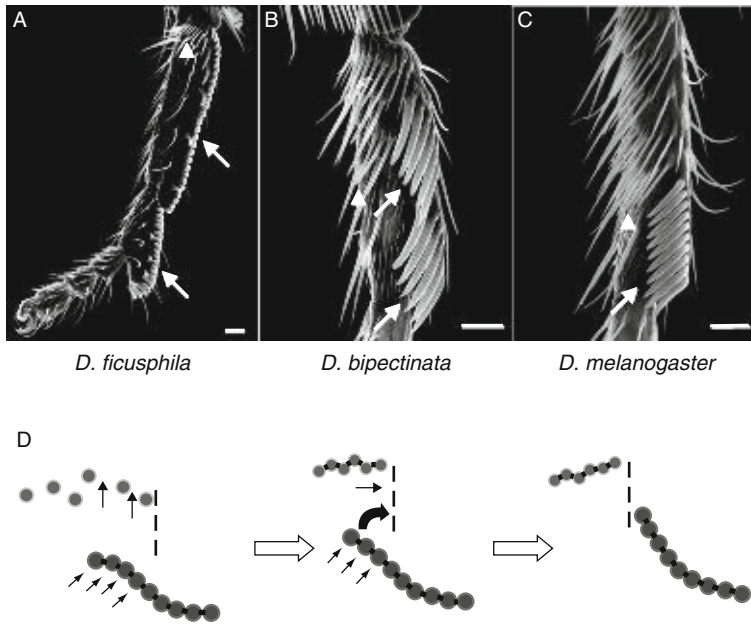

Figure 3.1 The *Drosophila* sex comb. Anterior is to the right and distal is down in all panels. (A–C) Sex comb diversity. The entire tarsus of *Drosophila ficusphila* is shown in (A) while the first tarsal segments of *Drosophila bipectinata* and *D. melanogaster* are shown in (B) and (C). Note that the combs (arrows) are always anterior to (right of) adjacent transverse rows (arrowheads). In some species (e.g., *D. ficusphila*) the sex comb forms in this position. However, in other species, such as *D. melanogaster* (D), many of the sex comb bristles (large dark gray circles) are not anterior to the transverse row bristles (small light gray circles) early in development (these sex comb teeth are marked with small arrows). At this stage, the tissue close to the sex comb is undergoing convergent extension. As the tissue extends, cells just proximal to (above) the comb can initially pass between the transverse row bristles (large arrows depict this process in the left panel), moving proximally (up). When the latter join together into a contiguous row (middle panel), however, these cells can no longer pass between the transverse row bristles (which now act as a barrier) and instead move in an anterior direction (to the right, large straight arrow in the middle panel), leading to a rapid rotation of the proximal (upper) portion of the sex comb and its anterior movement relative to the transverse row just proximal to it. The right panel depicts a later stage where the entire comb is anterior to this row (i.e., right of the dashed line). The cell dynamics in the developing tarsus may thus help to explain the adult position of the sex comb, and why it is anterior to neighboring transverse rows even in species where it does not start out in this location. Scale bars: 20 μm.

(Fig. 3.1D). An examination of these constraints helps to explain why, in the adult fly, despite the dazzling diversity in interspecific sex comb morphology and patterning, combs in diverse species are always found in an anterior position relative to another group of bristles (the transverse rows) to which

they are homologous (Atallah et al., 2009b; Fig. 3.1A–C). Although early in development the comb is not always anterior to these bristles (left panel in Fig. 3.1D), the convergent extension that leads to comb rotation—in the context of the barriers set up by contiguous bristle formations (Fig. 3.1D, middle panel)—leads it move to an anterior position (Fig. 3.1D, right panel).

Drosophila bristle patterns illustrate both the potential and challenge of constructing a GPM. Generations of researchers have dissected this system in an effort to understand how spatial patterning is encoded in the genome. The results have been insightful but in many cases, counterintuitive. Early researchers wanted to understand how prepatterns were set up during development (Stern, 1968), but found that the genes they were aware of did not specify the prepatterns themselves, only the competence to respond to them (Held, 2002). (This was inferred on the basis of the cell-autonomous nature of the mutants they analyzed: a true ''prepattern gene'' that controlled the relative spacing of multiple bristles, would be expected to have a nonautonomous effect when mutated, in contrast to the genes that were known at the time.) Later studies of this competence on the fly notum demonstrated the importance of *cis*-regulation (Gómez-Skarmeta et al., 1995) and the role of enhancer evolution in generating diversity (Marcellini and Simpson, 2006), but much about the upstream regulators that set up the prepatterns is still unknown. The recent and surprising discovery of a second and apparently redundant level of regulation, downstream of *achaete–scute*, that can rescue the pattern in the absence of this complex, shows the limitations on our current model of even this well-studied system (Usui et al., 2008).

The situation on the leg is even more complicated. The initial arrangement of proneural clusters on the tarsus in the male is strikingly similar to that of the female, with transverse rows extending to the tip of the first tarsal segment (Atallah et al., 2009a), but the subsequent modification of the pattern results in an adult phenotype which is surprisingly different. While the activation or repression of specific genes may spur the process of convergent extension which leads to this modification, the effects of convergent extension in a given environment can only be understood by considering local constraints on the cell rearrangement. These constraints are part of the all-important context in which genes act, and it is only through knowledge of the local dynamics that the developmental bias in extant forms—the reason why some patterns exist in nature, and others do not—can be understood. The surprising finding that similar combs can form through remarkably different processes (Atallah et al., 2009b; Tanaka et al., 2009) suggests that external forces (such as selective pressures) may also be guiding comb evolution, although the nature of these forces has yet to be determined.

6. Conclusion

At least since Darwin (1859), the relationship of heredity to the development and evolution of form has been recognized. During the twentieth century, with increasing sophistication, researchers analyzed genetic changes and their impact on morphogenesis. By the early 2000s, the focus had shifted to an effort to understand gene regulation, starting at the transcriptional level and gradually expanding to include the posttranscriptional and posttranslational levels. While there is little evidence that a general regulatory code analogous to the genetic code for amino acid specification will ever be discovered, an effort is being made to understand the regulatory grammar by deriving general principles that describe how regulation operates.

There has been a complementary growth of knowledge in other factors important for morphogenesis, including self-organizing processes (Townes and Holtfreter, 1955) and physical influences (Forgács and Newman, 2005). It is now recognized that feedback from the developing organism to its genome is essential for normal development (Gilbert, 2003; Larsen and Atallah, 2009) a conclusion that jives with the Aristotelian emphasis on the interaction between ''form'' and ''matter''. A major task for the twenty-first century will be to explore the strategies that have evolved for efficiently using relatively few genes to interact with external and internal environments to drive development. From this perspective, the metaphor of ''mapping'' may eventually be viewed as a hindrance in exploring the developmental and evolutionary bases for morphological biodiversity.

ACKNOWLEDGMENTS

E.L is grateful to the Konrad Lorenz Institute for a fellowship supporting this work. Research in the authors' laboratory was funded in part by NSERC (Canada) and by SF approved grants to E.L.

REFERENCES

Ahituv, N., Zhu, Y., Visel, A., Holt, A., Afzal, V., Pennacchio, L.A., et al., 2007. Deletion of ultraconserved elements yields viable mice. PLoS Biol. 5, e234.

Alvarez-Castro, J.M., Le Rouzic, A., Carlborg, O., 2008. How to perform meaningful estimates of genetic effects. PLoS Genet. 2, e1000062.

Andalfatto, P., 2005. Adaptive evolution of non-coding DNA in *Drosophila*. Nature 437, 1149–1152.

Arrieta, M.I., Criado, B., Hauspie, R., Martinez, B., Lobato, N., Lostao, C.M., 1992. Effects of genetic and environmental factors on the a-b, b-c and c-d interdigital ridge counts. Hereditas 117, 189–194.

Ascioti, F.A., 2009. Four twins for a paradox: on "sensitive" twins and the biological counterpart of the "twin paradox". Chaos 19, 013128.
Atallah, J., Dworkin, I., Cheung, U., Greene, A., Ing, B., Leung, L., et al., 2004. The environmental and genetic regulation of *obake* expressivity: morphogenetic fields as evolvable systems. Evol. Dev. 6, 114–122.
Atallah, J., Liu, N.H., Dennis, P., Hon, A., Godt, D., Larsen, E., 2009a. Cell dynamics and developmental bias in the ontogeny of a complex sexually dimorphic trait. Evol. Dev. 11, 191–204.
Atallah, J., Liu, N.H., Dennis, P., Hon, A., Godt, D., Larsen, E., 2009b. Developmental constraints and convergent evolution in *Drosophila* sex comb formation. Evol. Dev. 11, 205–218.
Barmina, O., Kopp, A., 2007. Sex-specific expression of a HOX gene associated with rapid morphological evolution. Dev. Biol. 311, 277–286.
Beadle, G.W., Tatum, E.L., 1941. Genetic control of biochemical reactions in *Neurospora*. Proc. Natl. Acad. Sci. USA 27, 499–506.
Bejerano, G., Pheasant, M., Makunin, I., Stephen, S., Kent, W.J., Mattick, J.S., et al., 2004. Ultraconserved elements in the human genome. Science 304, 1321–1325.
Bergman, A., Siegal, M.L., 2003. Evolutionary capacitance as a general feature of complex gene networks. Nature 424, 549–552.
Berman, B.P., Nibu, Y., Pfeiffer, B.D., Tomancak, P., Celniker, S.E., Levine, M., et al., 2002. Exploiting transcription factor binding site clustering to identify *cis*-regulatory modules involved in pattern formation in the *Drosophila* genome. Proc. Natl. Acad. Sci. USA 99, 757–762.
Bock, I.R., Wheeler, M.R., 1972. The *Drosophila melanogaster* species group. Univ. Tex. Publ. 7213, 1–102.
Bray, S., Johnson, R.S., 2008. Putting the tissue and environmental 'context' into differentiation and gene regulation. Curr. Opin. Genet. Dev. 18, 395–396.
Bridges, C.B., 1936. The Bar "gene" a duplication. Science 83, 210–211.
Brosnan, C.A., Voinnet, O., 2009. The long and the short of noncoding RNAs. Curr. Opin. Cell Biol. 21, 416–425.
Bruder, C.E.G., Piotrowski, A., Gijsbers, A.A.C.J., Andersson, R., Erickson, S., de Stahl, T.D., et al., 2008. Phenotypically concordant and discordant monozygotic twins display different DNA Copy-Number-Variation profiles. Am. J. Hum. Genet. 82, 763–771.
Butte, A.J., Kohane, I.S., 2006. Creation and implications of a phenome–genome network. Nat. Biotechnol. 24, 55–62.
Carroll, S.B., 2005. Endless Forms Most Beautiful. W.W. Norton & Co., New York.
Collins, F.S., McKusick, V.A., 2001. Implications of the Human Genome Project for medical science. JAMA 285, 540–544.
Concolino, D., Rossi, E., Strisciuglio, P., Iembo, M.A., Giorda, R., Ciccone, R., et al., 2007. Deletion of 760 kb region at 4p16 determines the prenatal and postnatal growth retardation characteristic of Wolf–Hirschhorn syndrome. J. Med. Genet. 44, 647–650.
Copeland, J.W., Nasiadka, A., Dietrich, B.H., Krause, H.M., 1996. Patterning of the *Drosophila* embryo by a homeodomain-deleted Ftz polypeptide. Nature 379, 162–165.
Darwin, C., 1859. On the Origin of the Species, first ed. Harvard University Press, Cambridge.
Davidson, E.H., Levine, M.S., 2008. Properties of developmental gene regulatory networks. Proc. Natl. Acad. Sci. USA 105, 20063–20066.
Davidson, E.H., Rast, J.P., Oliveri, P., Ransick, A., Calestani, C., Yuh, C., et al., 2002. A genomic regulatory network for development. Science 295, 1669–1678.
del Rio, A., Perez-Jimenez, R., Liu, R., Roca-Cusachs, P., Fernandez, J.M., Sheetz, M.P., 2009. Stretching single talin rod molecules activates vinculin binding. Science 323, 638–641.

De Renzis, S., Yu, J., Zinzen, R., Wieschaus, E., 2006. Dorsal ventral pattern of Delta trafficking is established by a Snail–Tom–Neuralized pathway. Dev. Cell 10, 257–264.
Duboule, D., 2007. The rise and fall of *Hox* gene clusters. Development 134, 2549–2560.
Dworkin, I., 2005a. Evidence for canalization of *Distal-less* function in the leg of *Drosophila melanogaster*. Evol. Dev. 7, 89–100.
Dworkin, I., 2005b. A study of canalization and developmental stability in the sternopleural bristle system of *Drosophila melanogaster*. Evolution 59, 1500–1509.
Dworkin, I., Palsson, A., Birdsall, K., Gibson, G., 2003. Evidence that *Egfr* contributes to cryptic genetic variation for photoreceptor determination in natural populations of *Drosophila melanogaster*. Curr. Biol. 13, 1888–1893.
Ettensohn, C.A., 2009. Lessons from a gene regulatory network: echinoderm skeletogenesis provides insights into evolution, plasticity and morphogenesis. Development 136, 11–21.
Feil, R., Berger, F., 2007. Convergent evolution of genomic imprinting in plants and mammals. Trends Genet. 23, 192–199.
Ferrier, D.E., Minguillon, C., 2003. Evolution of the Hox/ParaHox gene clusters. Int. J. Dev. Biol. 47, 605–611.
Fontana, W., 2002. Modelling evo-devo with RNA. Bioessays 24, 1164–1177.
Forgács, G., Newman, S.A., 2005. Biological Physics of the Developing Embryo. Cambridge University Press, Cambridge.
Genissel, A., McIntyre, L.M., Wayne, M.L., Nuzhdin, S.V., 2008. *Cis* and *trans* regulatory effects contribute to natural variation in transcriptome of *Drosophila melanogaster*. Mol. Biol. Evol. 25, 101–110.
Gerhart, J., Kirschner, M., 1997. *Cells, Embryos, and Evolution*. Blackwell Science, Malden.
Ghildiyal, M., Zamore, P.D., 2009. Small silencing RNAs: an expanding universe. Nat. Genet. 10, 94–108.
Gibson, G., Dworkin, I., 2004. Uncovering cryptic genetic variation. Nat. Rev. Genet. 5, 681–690.
Gibson, G., Gehring, W., 1988. Head and thoracic transformations caused by ectopic expression of *Antennapedia* during *Drosophila* development. Development 102, 657–675.
Gilbert, S.F., 2003. The reactive genome. In: Muller, G., Newman, S.A. (Eds.), The Origination of Organismal Form. MIT Press, Cambridge, MA, pp. 87–101. Vienna Series in Theoretical Biology.
Gómez-Skarmeta, J.L., Rodríguez, I., Martínez, C., Culí, J., Ferrés-Marcó, D., Beamonte, D., et al., 1995. *Cis*-regulation of *achaete* and *scute*: shared enhancer-like elements drive their coexpression in proneural clusters of the imaginal discs. Genes Dev. 9, 1869–1882.
Grad, Y.H., Roth, F.P., Halfon, M.S., Church, G.M., 2004. Prediction of similarly acting *cis*-regulatory modules by subsequence profiling and comparative genomics in *Drosophila melanogaster* and *D. pseudoobscura*. Bioinformatics 20, 2738–2750.
Hahn, M.W., Wray, G.A., 2002. The g-value paradox. Evol. Dev. 4, 73–75.
Hamant, O., Heisler, M.G., Jönsson, H., Krupinski, P., Uyttewaal, M., Bokov, P., et al., 2008. Developmental patterning by mechanical signals in *Arabidopsis*. Science 322, 1650–1655.
Hare, E.E., Peterson, B.K., Iyer, V.N., Meier, R., Eisen, M.B., 2008. Sepsid *even-skipped* enhancers are functionally conserved in *Drosophila* despite lack of sequence conservation. PLoS Genet. 4, e1000106.
Held Jr., L.I., 2002. Imaginal Discs: The Genetic and Molecular Logic of Pattern Formation. Cambridge University Press, Cambridge.
Held Jr., L.I., Grimson, M.J., Du, Z., 2004. Proving an old prediction: the sex comb rotates at 16 to 24 hours after pupariation. Drosoph. Inf. Serv. 87, 76–78.
Hilgenfeldt, S., Erisken, S., Carthew, R.W., 2008. Physical modeling of cell geometric order in an epithelial tissue. Proc. Natl. Acad. Sci. USA 105, 907–911.

Hinman, V.F., Nguyen, A.T., Cameron, R.A., Davidson, E.H., 2003. Developmental gene regulatory network architecture across 500 million years of echinoderm evolution. Proc. Natl. Acad. Sci. USA 100, 13356–13361.

Ikuta, T., Yoshida, N., Satoh, N., Saiga, H., 2004. *Ciona intestinalis Hox* gene cluster: its dispersed structure and residual collinear expression in development. Proc. Natl. Acad. Sci. USA 101, 15118–15123.

International Human Genome Sequencing Consortium, 2001. Initial sequencing and analysis of the human genome. Nature 409, 860–921.

International Human Genome Sequencing Consortium, 2004. Finishing the euchromatic sequence of the human genome. Nature 431, 931–945.

Johannsen, W., 1911. The genotype conception of heredity. Am. Nat. 45, 129–159.

Kamath, B.M., Thiel, B.D., Gai, X., Conlin, L.K., Munoz, P.S., Glessner, J., et al., 2008. SNP array mapping of chromosome 20p deletions: genotypes, phenotypes, and copy number variation. Hum. Mutat. 30, 371–378.

Katzman, S., Kern, A.D., Bejerano, G., Fewell, G., Fulton, L., Wilson, R.K., et al., 2007. Human genome ultraconserved elements are ultraselected. Science 317, 915.

Kauffman, S.A., 1993. The Origins of Order: Self-Organization and Selection in Evolution. Oxford University Press, Oxford.

Kmita, M., Duboule, D., 2003. Organizing axes in time and space; 25 years of colinear tinkering. Science 301, 331–333.

Kopp, A., True, J.R., 2002. Evolution of male sexual characters in the Oriental *Drosophila melanogaster* species group. Evol. Dev. 4, 278–291.

Kucharski, R., Maleszka, J., Foret, S., Maleszka, R., 2008. Nutritional control of reproductive status in honeybees via DNA methylation. Science 319, 1827–1830.

Lai, E.C., Tomancak, P., Williams, R.W., Rubin, G.M., 2003. Computational identification of *Drosophila* microRNA genes. Genome Biol. 4, R42.

Larsen, E., 1992. Tissue strategies as developmental constraints: implications for animal evolution. Trends Ecol. Evol. 7, 414–417.

Larsen, E., Atallah, J., 2009. Epigenesis, preformation and the Humpty Dumpty problem. In: Hall, B.K., Hallgrimmsson, B. (Eds.), Epigenesis. University of California Press, Berkeley.

Larsen, E., McLaughlin, H., 1987. The morphogenetic alphabet: lessons for simple-minded genes. Bioessays 7, 130–132.

Larsen, E., Lee, T., Glickman, N., 1996. Antenna to leg transformation: dynamics of developmental competence. Dev. Genet. 19, 333–339.

Lee, R.C., Feinbaum, R.L., Ambros, V., 1993. The *C. elegans* heterochronic gene *lin-4* encodes small RNAs with antisense complementarity to *lin-14*. Cell 75, 843–854.

Levine, M., Davidson, E.H., 2005. Gene regulatory networks for development. Proc. Natl. Acad. Sci. USA 102, 4936–4942.

Lewis, E.B., 1978. A gene complex controlling segmentation in *Drosophila*. Nature 276, 565–570.

Lim, L.P., Lau, N.C., Weinstein, E.G., Abdelhakim, A., Yekta, S., Rhoades, M.W., et al., 2003. The micro-RNAs of *Caenorhabditis elegans*. Genes Dev. 17, 991–1008.

Ludwig, M.Z., Patel, N.H., Kreitman, M., 1998. Functional analysis of eve stripe 2 enhancer evolution in *Drosophila*: rules governing conservation and change. Development 125, 949–958.

Ludwig, M.Z., Bergman, C., Patel, N.H., Kreitman, M., 2000. Evidence for stabilizing selection in a eukaryotic enhancer element. Nature 403, 564–567.

Lund, A.M., Aström, E., Söderhäll, S., Schwartz, M., Skovby, F., 1999. Osteogenesis imperfecta: mosaicism and refinement of the genotype–phenotype map in OI type III. Hum Mutat. 13, 503 Mutations in brief no. 242. Online.

Mammoto, A., Connor, K.M., Mammoto, T., Yung, C.W., Huh, D., Aderman, C.M., et al., 2009. A mechanosensitive transcriptional mechanism that controls angiogenesis. Nature 457, 1103–1108.
Marcellini, S., Simpson, P., 2006. Two or four bristles: functional evolution of an enhancer of *scute* in Drosophilidae. PLoS Biol. 4, e386.
Markstein, M., Markstein, P., Markstein, V., Levin, M.S., 2002. Genome-wide analysis of clustered dorsal binding sites identifies putative target genes in the *Drosophila* embryo. Proc. Natl. Acad. Sci. USA 99, 546–548.
Mathi, S.K., Larsen, E., 1988. Patterns of cell division in imaginal discs of *Drosophila*. Tissue Cell 20, 461–472.
Mayr, E., 1963. Animal Species and Evolution. Harvard University Press, Cambridge, MA.
Mayr, E., 1982. The Growth of Biological Thought. Harvard University Press, Cambridge, MA.
McDonald, J.H., Kreitman, M., 1991. Adaptive protein evolution at the *Adh* locus in *Drosophila*. Nature 351, 114–116.
McNellis, T.W., Deng, X.W., 1995. Light control of seedling morphogenetic pattern. Plant Cell 7, 1749–1761.
Medrano-Soto, A., Pal, D., Eisenberg, D., 2008a. Inferring molecular function: contributions from functional linkages. Trends Genet. 24, 587–589.
Medrano-Soto, A., Pal, D., Eisenberg, D., 2008b. Inferring molecular function: contributions from functional linkages. Trends Genet. 12, 587–590.
Moore, D.S., 2003. The Dependent Gene: The Fallacy of 'Nature vs. Nurture. Henry Holt and Company, New York.
Morgan, T.H., 1907. Experimental Zoology. The Macmillan Company, New York.
Morimoto, R., 1998. Regulation of the heat shock transcriptional response: cross talk between a family of heat shock factors, molecular chaperones, and negative regulators. Genes Dev. 12, 3788–3796.
Moses, A.M., Pollard, D., Nix, D.A., Iyer, V.N., Li, X.Y., Biggin, M.D., et al., 2006. Large-scale turnover of functional transcription factor binding sites in *Drosophila*. PLoS Comput. Biol. 2, e130.
Moses, A.M., Hériché, J., Durbin, R., 2007a. Clustering of phosphorylation site recognition motifs can be exploited to predict the targets of cyclin-dependent kinase. Genome Biol. 8, R23.
Moses, A.M., Liku, M.E., Li, J.J., Durbin, R., 2007b. Regulatory evolution in proteins by turnover and lineage-specific changes of cyclin-dependent kinase concensus sites. Proc. Natl. Acad. Sci. USA 104, 17713–17718.
Moss, E.G., 2007. Heterochronic genes and the nature of developmental time. Curr. Biol. 17, R425–R434.
Muller, G.B., Streicher, J., 1989. Ontogeny of the syndesmosis tibiofibularis and the evolution of the bird hindlimb: a caenogenetic feature. Anat. Embryol. (Berl.) 179, 327–339.
Nelson, C.E., Hersh, B.M., Carroll, S.B., 2004. The regulatory content of intergenic DNA shapes genome architecture. Genome Biol. 5, R25.
Nuzhdin, S.V., Tufts, D.M., Hahn, M.W., 2008. Abundant genetic variation in transcript level during early *Drosophila* development. Evol. Dev. 10, 683–689.
Olivieri, P., Tu, Q., Davidson, E.H., 2008. Global regulatory logic for specification of an embryonic cell lineage. Proc. Natl. Acad. Sci. USA 105, 5955–5962.
Patterson, D., Rahmani, Z., Donaldson, D., Gardiner, K., Jones, C., 1993. Physical mapping of chromosome 21. Prog. Clin. Biol. Res. 384, 33–50.
Pennacchio, L.A., Ahituv, N., Moses, A.M., Prabhakar, S., Nobrega, M.A., Shoukry, M., et al., 2006. *In vivo* enhancer analysis of human conserved non-coding sequences. Nature 444, 499–502.
Pontecorvo, G., 1951. Untitled book review. Q. Rev. Biol. 26, 52–53.

Probst, A.V., Dunleavy, E., Almouzni, G., 2009. Epigenetic inheritance during the cell cycle. Nat. Rev. Mol. Cell Biol. 10, 192–206.
Rajewsky, N., 2006. microRNA target predictions in animals. Nat. Genet. 38, 8–13.
Randsholt, N.B., Santamaria, P., 2008. How *Drosophila* change their combs: the Hox gene *Sex combs reduced* and sex comb variation among *Sophophora* species. Evol. Dev. 10, 121–133.
Revilla-i-Domingo, R., Oliveri, P., Davidson, E.H., 2007. A missing link in the sea urchin embryo gene regulatory network: hsC and the double negative specification of micromeres. Proc. Natl. Acad. Sci. USA 104, 12383–12388.
Ririe, T.O., Fernandes, J.S., Sternberg, P.W., 2008. The *Caenorhabditis elegans* vulva: a post-embryonic gene regulatory network controlling organogenesis. Proc. Natl. Acad. Sci. USA 105, 20095–20099.
Rockman, M.V., 2008. Reverse engineering the genotype–phenotype map with natural genetic variation. Nature 456, 738–744.
Ronshaugen, M., McGinnis, N., McGinnis, W., 2002. Hox protein mutation and macroevolution of the insect body plan. Nature 415, 914–917.
Ronshaugen, M., Biemar, F., Piel, J., Levine, M., Lai, E.C., 2005. The *Drosophila* microRNA iab-4 causes a dominant homeotic transformation of halteres to wings. Genes Dev. 19, 2947–2952.
Rosner, F., 1995. Medicine in the Bible and the Talmud. KTAV Publishing House, Inc., Jersey City.
Rosso, L., Marques, A.C., Weier, M., Lambert, N., Lambot, M., Vanderhaeghen, P., et al., 2008. Birth and rapid subcellular adaptation of a hominoid-specific CDC14 protein. PLoS Biol. 6, e140.
Scanga, S., Manoukian, A., Larsen, E., 1995. Time- and concentration-dependent response of the *Drosophila* antenna imaginal disc to *Antennapedia*. Dev. Biol. 169, 673–682.
Seo, H.C., Edvardsen, R.B., Maeland, A.D., Bjordal, M., Jensen, M.F., Hansen, A., et al., 2004. *Hox* cluster disintegration with persistent anteroposterior order of expression in *Oikopleura dioica*. Nature 431, 67–71.
Shermoen, A.W., O'Farrell, P.H., 1991. Progression of the cell cycle through mitosis leads to abortion of nascent transcripts. Cell 67, 303–310.
Shi, W., Levine, M., Davidson, B., 2009. Unraveling genomic regulatory networks in the simple chordate, *Ciona intestinalis*. Genome Res. 15, 1668–1674.
Shippy, T.D., Ronshaugen, M., Cande, J., He, J., Beeman, R.W., Levine, M., et al., 2008. Analysis of the *Tribolium* homeotic complex: insights into mechanisms constraining insect Hox clusters. Dev. Genes Evol. 218, 127–139.
Siegal, M.L., Bergman, A., 2002. Waddington's canalization revisited: developmental stability and evolution. Proc. Natl. Acad. Sci. USA 99, 10528–10532.
Siepel, A., Bejerano, G., Pedersen, J.S., Hinrichs, A.S., Hou, M., Rosenbloom, K., et al., 2006. Evolutionarily conserved elements in vertebrate, insect, worm and yeast genomes. Genome Res. 15, 1034–1050.
Siggia, E., 2005. Computational methods for transcriptional regulation. Curr. Opin. Genet. Dev. 15, 214–221.
Stark, A., Brennecke, J., Bushati, N., Russell, R.B., Cohen, S.M., 2005. Animal microRNAs confer robustness to gene expression and have a significant impact on 3′UTR evolution. Cell 123, 1133–1146.
Stathopoulos, A., Van Drenth, M., Erives, A., Markstein, M., Levine, M., 2002. Whole-genome analysis of dorsal-ventral patterning in the *Drosophila* embryo. Cell 111, 687–701.
Stern, C., 1968. Genetic Mosaics and Other Essays. Harvard University Press, Boston.
Sturtevant, A.H., 1923. Inheritance of direction of coilling in limnaea. Science 58, 269–270.
Surkova, S., et al., 2008. Characterization of the *Drosophila* segment determination morphome. Dev. Biol. 313, 844–862.

Tamada, M., Sheetz, M.P., Sawada, Y., 2004. Activation of a signaling cascade by cytoskeleton stretch. Dev. Cell 7, 709–718.

Tanaka, K., Barmina, O., Kopp, A., 2009. Distinct developmental mechanisms underlie the evolutionary diversification of *Drosophila* sex combs. Proc. Natl. Acad. Sci. USA 106, 4764–4769.

Tokunaga, C., 1962. Cell lineage and differentiation on the male foreleg of *Drosophila melanogaster*. Dev. Biol. 4, 489–516.

Townes, P., Holtfreter, J., 1955. Directed movements and selective adhesions of embryonic amphibian cells. J. Exp. Zool. 128, 53–120.

Tümpel, S., Cambronero, F., Sims, C., Krumlauf, R., Wiedemann, L.M., 2008. A regulatory module embedded in the coding region of *Hoxa2* controls expression in rhombomere 2. Proc. Natl. Acad. Sci. USA 105, 20077–20082.

Usui, K., Goldstone, C., Gilbert, J., Simpson, P., 2008. Redundant mechanisms mediate bristle patterning on the *Drosophila* thorax. Proc. Natl. Acad. Sci. USA 105, 20112–20117.

Vogel, V., Sheetz, M., 2006. Local force and geometry sensing regulate cell functions. Nat. Rev. Mol. Cell Biol. 7, 265–275.

von Dassow, G., Odell, G.M., 2002. Design and constraints of the *Drosophila* segment polarity module: robust spatial patterning emerges from intertwined cell state switches. J. Exp. Zool. (Mol. Dev. Evol.) 294, 179–215.

von Dassow, G., Meir, E., Munro, E.M., Odell, G.M., 2000. The segment polarity network is a robust developmental module. Nature 406, 188–192.

Waddington, C.H., 1961. Genetic assimilation. In: Advances in Genetics, 257–293.

Wagner, R.P., Mitchell, H.K., 1964. Genetics and Metabolism. Wiley, New York.

Weiss, K.M., 2003. Phenotype and genotype. In: Hall, B.K., Olson, W.M. (Eds.), Keywords and Concepts in Evolutionary Developmental Biology. Harvard University Press, Cambridge, USA, pp. 279–288.

Weiss, K.M., Terwilliger, J.D., 2000. How many diseases does it take to map a gene with SNPs? Nat. Genet. 26, 151–157.

Wightman, B., Ha, I., Ruvkun, G., 1993. Posttranscriptional regulation of the heterochronic gene *lin-14* by *lin-4* mediates temporal pattern formation in *C. elegans*. Cell 75, 855–862.

Woolfe, A., Goodson, M., Goode, D.K., Snell, P., McEwen, G.K., Vavouri, T., et al., 2005. Highly conserved non-coding sequences are associated with vertebrate development. PLoS Biol. 3, e7.

Yu, X., Lin, J., Zack, D.J., Mendell, J.T., Qian, J., 2008. Analysis of regulatory network topology reveals functionally distinct classes of microRNAs. Nucleic Acids Res. 36, 6494–6503.

Zacharias, H., 1995. Emil Heitz (1892–1965): chloroplasts, heterochromatin, and polytene chromosomes. Genetics 141, 7–14.

CHAPTER FOUR

Role of Spindle Asymmetry in Cellular Dynamics

Yves Barral* *and* Dimitris Liakopoulos†

Contents

1. Introduction 150
2. Spindle Asymmetry and Control of Cell Cycle 152
   2.1. Spindle asymmetry during mitosis in yeasts 152
   2.2. Spindle asymmetry during budding yeast meiosis 167
   2.3. Models for generation of unequal SPBs 169
   2.4. Centriole control of cytokinesis 171
3. Spindle Asymmetry During Asymmetric Cell Divisions 174
   3.1. SPB inheritance in budding yeast 174
   3.2. Spindle asymmetry during early embryonic development in *Caenorhabditis elegans* 181
   3.3. Spindle asymmetry in *Drosophila* nervous system 189
   3.4. Inheritance of centrosomes in *Drosophila* germline 196
   3.5. Generation of spindle asymmetry in *Annelids* 198
   3.6. Asymmetric segregation of developmental factors in *Ilyanassa obsoleta* 200
4. Concluding Remarks 201
References 203

Abstract

The mitotic spindle is mostly perceived as a symmetric structure. However, in many cell divisions, the two poles of the spindle organize asters with different dynamics, associate with different biomolecules or subcellular domains, and perform different functions. In this chapter, we describe some of the most prominent examples of spindle asymmetry. These are encountered during cell-cycle progression in budding and fission yeast and during asymmetric cell divisions of stem cells and embryos. We analyze the molecular mechanisms that lead to generation of spindle asymmetry and discuss the importance of spindle-pole differentiation for the correct outcome of cell division.

* Institute of Biochemistry, ETH Hönggerberg, HPM, CH-8093 Zurich, Switzerland
† Biochemie Zentrum Heidelberg, Im Neuenheimer Feld 328, D-69120 Heidelberg, Germany

International Review of Cell and Molecular Biology, Volume 278
ISSN 1937-6448, DOI: 10.1016/S1937-6448(09)78004-9
© 2009 Elsevier Inc.
All rights reserved.

Key Words: Spindle asymmetry, Spindle positioning, Centrosomes, Spindle-pole bodies, Mitotic exit, Cell polarity, Cell division. © 2009 Elsevier Inc.

1. Introduction

The mitotic spindle is a tubulin-based structure that serves the task of chromosome segregation. It provides both the pulling forces that separate chromosomes and the positional information that places the plane of cell cleavage between the separated chromosomes. The classical spindle is ideally a highly symmetric structure. The two spindle poles are the sites of tubulin organization and consist of organelles controlling microtubule nucleation that are collectively termed microtubule-organizing centers (MTOCs).

The MTOCs of spindles in animal and green algal cells and those in spermatogenesis cells of basal land plants are called centrosomes (Mineyuki, 2007). Animal centrosomes are comprised of two centrioles connected in an orthogonal orientation to each other and surrounded by a protein matrix, the pericentriolar material (Azimzadeh and Bornens, 2007; Bettencourt-Dias and Glover, 2007; Ou and Rattner, 2004). At the onset of mitosis the preexisting centrosome duplicates. Centrosome duplication is coupled to centriole duplication: the two centrioles separate, and a new daughter centriole is formed orthogonally to each original one. The result is formation of two centrosomes, each containing an old (mother) and a new (daughter) centriole. Mother and daughter centrioles are not equal in morphology, protein composition, and size. A set of proteins localizes only to the mother centriole and forms characteristic structures, the distal and subdistal appendages (Bornens, 2002). In a process called centriole maturation, daughter centrioles acquire new material as the cell cycle proceeds. Therefore, the two centrosomes formed after duplication are not equivalent, because they contain centriole pairs that differ in age and the degree of maturation. One centrosome contains the oldest, mature mother centriole and its daughter, while the other consists of the maturing second oldest centriole and its daughter (Fig. 4.1). After duplication, each of the two centrosomes serves as a MTOC at each pole of the spindle during mitosis. MTOCs of plant cells and meiotic spindles in animal cells do not contain centrioles; microtubules of these spindles are often less focused at the spindle poles and are organized by protein complexes that, however, involve microtubule-associated proteins and γ-tubulin (Mineyuki, 2007; Schmit, 2002), as in their centriole-containing counterparts.

In budding and fission yeast the MTOCs are called spindle-pole bodies (SPBs). The SPBs fulfill functions analogous to the mammalian

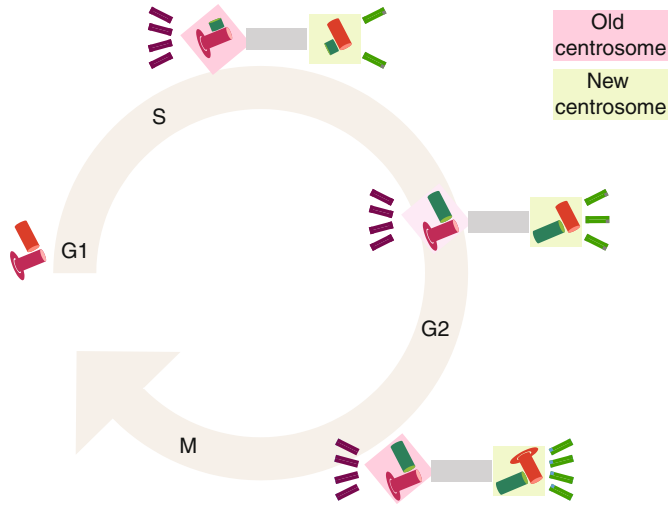

Figure 4.1 The centrosome duplication cycle. A pair of centrioles forms the core of the mammalian centrosome. During centrosome duplication, the centriole pair splits and a new centriole forms orthogonally to each preexisting centriole. Therefore, the centrosomes differ in age, because one contains the oldest centriole and the other its daughter. In addition, they differ in morphology and protein composition, since the younger of the two initial centrioles acquires the full set of proteins gradually during the cell cycle (or possibly only after passage through specific cell-cycle stages), a process called maturation. Thus, the two centrosomes of the mitotic spindle may have different activities regarding MT nucleation (MTs shown as short bars emanating from centrosomes) and, in general, different properties. Proteins that are present only in mature centrioles are depicted as a ring around centrioles.

centrosomes, although they significantly differ from centrosomes in structure and protein composition (Adams and Kilmartin, 2000; Bornens, 2002; Ou and Rattner, 2004). SPBs are laminar structures embedded in the nuclear envelope and lack centriole pairs. SPBs duplicate conservatively (Adams and Kilmartin, 2000; Ding et al., 1997; Grallert et al., 2004; Pereira et al., 2001). A single SPB, the old SPB, is present in interphase. When cells enter mitosis, a second SPB is formed next to the old one. Subsequently, old and new SPBs separate and migrate to opposite sides of the nucleus and form the mitotic spindle. These events occur in a similar fashion both during mitotic and meiotic divisions. The mechanisms of SPB duplication may differ between *Schizosaccharomyces pombe* and *Saccharomyces cerevisiae*, but in both cases new material is incorporated mainly into the newly formed SPB.

MTOCs and SPBs nucleate three distinct sets of microtubules. First, astral microtubules (aMTs) radiate from the poles toward the cytoplasm and the cell cortex. They are required for correct positioning of the spindle within the cell and are part of the machinery that determines the future

plane of cleavage for cytokinesis. Second, interpolar microtubules emanating from the opposite poles interdigitate halfway between the spindle poles and stabilize the spindle. Third, kinetochore microtubules connect spindle poles to kinetochores at the centromeres of chromosomes. Kinetochore and interpolar microtubules generate forces that pull sister chromatids toward opposite directions. In this way, the spindle is organized structurally in two equal halves that mirror each other.

Despite this symmetry, spindles in a variety of biological systems are morphologically asymmetric. For example, in asymmetrically dividing neuroblasts (NBs) in *Drosophila* the anaphase spindle consists of two unequal halves, while in budding yeast one spindle pole nucleates more stable microtubules than the other. In addition to morphological asymmetries, molecular differences are encountered between spindle poles as well. First, as we just mentioned, the two MTOCs of the spindle have different age. Furthermore, in budding and fission yeasts each spindle pole associates with different sets of cell-cycle regulators, and this asymmetry strongly correlates with cell-cycle progression.

Collectively, these asymmetries in spindle morphology and spindle-pole composition or function are summarized here with the term spindle asymmetry. In this chapter, we will review what is known about spindle asymmetry for specific examples of fungi and animal cells and will discuss the mechanisms of asymmetry generation and its possible functions. In the first half, we will describe the role of spindle asymmetry in the control of mitotic progression. In the second half, we will focus on the role of spindle asymmetry in asymmetric cell divisions of embryos and stem cells. Morphological spindle asymmetries have also been reported in plants (Ranganath, 2005 and references therein), but will not be discussed in this chapter.

2. Spindle Asymmetry and Control of Cell Cycle

2.1. Spindle asymmetry during mitosis in yeasts

2.1.1. Mitotic exit and septation initiation networks

Spindle asymmetry in both budding and fission yeasts is observed during anaphase and is thought to ensure in the temporal coordination of cytokinesis with chromosome segregation. In an unperturbed cell cycle, spindle elongation segregates sister chromatids to opposite ends of the cell. Subsequently, the spindle disassembles and cytokinesis cleaves the cell between the separated chromosomes. It is essential that cytokinesis occurs after chromosome segregation. A group of regulatory proteins called the septation initiation network (SIN) in fission yeast and its counterpart, the mitotic exit network (MEN) in budding yeast, form a signal transduction cascade that controls the timing of cytokinesis (Bardin and Amon, 2001;

Krapp et al., 2004b; Simanis, 2003). SIN inactivation leads to successive rounds of nuclear divisions without septation (Fankhauser and Simanis, 1994), while SIN overactivation triggers the formation of several septa already during interphase (Minet et al., 1979; Song et al., 1996). MEN mutant cells arrest with elongated anaphase spindles and do not perform cytokinesis. Thus, despite apparent similarities, SIN triggers cytokinesis but does not regulate spindle disassembly, while MEN activation is required for both spindle disassembly and cytokinesis.

Most SIN and MEN components localize to the SPBs in an asymmetric manner, and MEN and SIN appear to be activated only on one of the two SPBs of the anaphase spindle. How this asymmetry is established is not clear, but involves different mechanisms in fission and budding yeast. Asymmetry of SIN depends on the cell-cycle machinery and the age difference of the SPBs, whereas generation of MEN asymmetry relies most likely on cell polarity (Section 2.1.4).

SIN and MEN are homologous pathways regulated by a small Ras-related GTPase at their top (Bardin and Amon, 2001; Simanis, 2003). This GTPase, called Spg1 in fission yeast and Tem1 in budding yeast, is active in its GTP-bound and inactive in its GDP-bound state. The GTPase-activating protein (GAP) that catalyzes the conversion of Spg1 from the active GTP- to the inactive GDP-form is a heterodimeric protein complex consisting of the proteins Cdc16 and Byr4. Their budding yeast homologs, Bub2 and Bfa1, respectively, form the GAP for Tem1. In both cases, these GAP complexes localize primarily to SPBs throughout the cell cycle. No guanine-nucleotide exchange factor (GEF) is known for Spg1, while the cortical protein Lte1 is proposed to act as a GEF for Tem1 in budding yeast (Shirayama et al., 1994). Both Spg1 and Tem1 are activated during anaphase, yet the exact triggering mechanism is not completely clear. Downstream of the GTPase, a kinase cascade transduces the SIN and MEN signals. These cascades comprise the kinases Cdc7, Sid1, and Sid2 in fission yeast, and Cdc15, and Dbf2 in budding yeast. Cdc7 and Cdc15 are homologous to each other, while Dbf2 is the budding yeast homolog of Sid2. No Sid1 equivalent has been identified in budding yeast. Upon SIN activation, Sid2 and its coactivator Mob1 localizes to a medial ring at the cell cortex and stimulates actomyosin ring assembly and contraction. In budding yeast, Dbf2 and Mob1 also localize to the site of cleavage at the cell cortex in late anaphase and trigger cytokinesis, yet their most critical function is to mediate the release of the phosphatase Cdc14 from the nucleolus. This phosphatase dephosphorylates Cdk substrates and sets off a series of events that essentially lead to the inactivation of Cdk/cyclin B, the disassembly of the spindle and cytokinesis. The corresponding phosphatase Flp1 in *S. pombe* contributes to the robustness of mitotic exit, but unlike Cdc14 in budding yeast, is not essential for this function (Clifford et al., 2008).

2.1.2. Asymmetry of the SIN and age of the SPB

2.1.2.1. SIN asymmetry in metaphase All known SIN components associate with the SPB (Fig. 4.2B). In metaphase, both SPBs seem to bear active Spg1-GTP, since immunofluorescence shows that Spg1 is present on both metaphase SPBs, and no signal is detectable with antibodies specific for Spg1-GDP (Sohrmann et al., 1998). In addition, the kinase Cdc7, which preferentially (but not exclusively) associates with active Spg1-GTP *in vitro* (Sohrmann et al., 1998), and Sid1 (Guertin et al., 2000) are present on both SPBs at this stage. However, SIN activity might be already somewhat asymmetric, since Byr4 associates with only one SPB during metaphase (Cerutti and Simanis, 1999; Li et al., 2000). The partner of Byr4, Cdc16, is

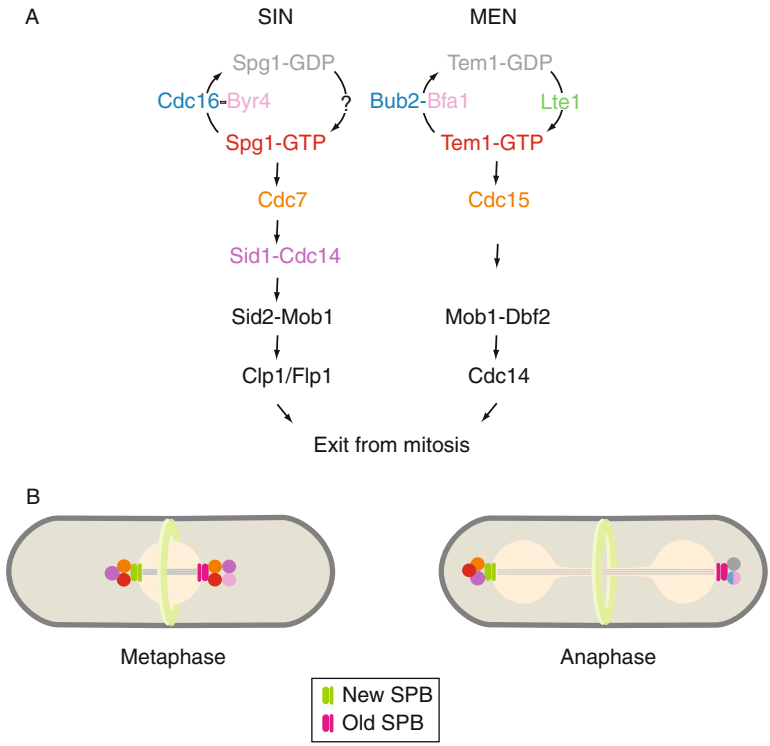

Figure 4.2 (A) The septation initiation network (SIN) and its counterpart in budding yeast, the mitotic exit network (MEN). Homologous proteins are shown in the same order. The cytokinetic apparatus is shown as a ring. (B) SIN asymmetry in fission yeast. Asymmetry may be already present at metaphase, because Byr4 localizes only on one SPB, shown here hypothetically as the old one. In anaphase, active Spg1-GTP components localize at the new SPB, while Spg1 is inactive on the old SPB. Sid2/Mob1 and Clp1/Flp1 localize symmetrically on the SPBs during the entire mitosis.

undetectable on the metaphase spindle (Cerutti and Simanis, 1999; Li et al., 2000). It is not known what keeps Spg1-GTP from activating Cdc7 and triggering septation during metaphase. Possibly, high Cdc2 activity prevents septation (Section 2.1.3).

2.1.2.2. SIN asymmetry in anaphase In anaphase, two remarkable events take place. First, the localization of SIN components becomes highly asymmetric. Second, Spg1 activity now triggers septation. During anaphase B, Spg1 is present on both SPBs, but only one SPB bears the inactive GDP-bound form, as shown using Spg1-GDP-specific antibodies (Sohrmann et al., 1998). Consistent with this, the GAP Byr4-Cdc16 colocalizes to the same SPB and the Spg1-GTP-binding kinase Cdc7 is found on the opposite SPB, together with the downstream kinase Sid1 and its cofactor Cdc14 (Guertin et al., 2000). Thus, during late anaphase SIN activity is asymmetric on the spindle, as judged by the asymmetric presence of Spg1-GTP, Cdc7, and Sid1 on only one SPB.

2.1.2.3. Origin of SIN asymmetry: Integrating SPB age and cell-cycle control Remarkably, in late anaphase the activated SIN components do not localize randomly relative to old and new SPBs, but the new SPB bears the active SIN. Insights into the role of the NIMA-related kinase Fin1 in mitosis allowed an important step toward understanding the origin of SIN asymmetry in *S. pombe* (Grallert et al., 2004). NIMA kinases are downstream effectors of cyclin-dependent kinases (O'Connell et al., 2003). Fin1 functions early in the cell cycle, at the time of SPB duplication, and *fin1* mutations impair the insertion of the SPBs into the nuclear envelope upon SPB duplication. In addition, Fin1 inhibits SIN activity, because Fin1 inactivation after SPB duplication results in Cdc7 localization to both SPBs and to SIN overactivation. Thus, Fin1 acts as an upstream, negative regulator of SIN.

Strikingly, the age and history of the SPBs determine their respective ability to recruit Fin1, revealing that SPBs of fission yeast undergo a maturation process as they pass through subsequent cell cycles (Fig. 4.3A). Indeed, Fin1 localizes to both SPBs in only 50% of growing wild-type cells (Grallert et al., 2004). In the other 50% of the cells, Fin1 localizes only to the old SPB. When present on both SPBs, Fin1 localizes stronger to the old SPB, and is less abundant on the new one. Furthermore, Fin1 recruitment to the new SPB is observed only when its counterpart old SPB has been an old, Fin1-binding SPB in the previous cell cycle (Fig. 4.3A). The mechanism of how this pattern is established is not known yet, but some observations already provide hints. Most importantly, Byr4 binds physically to Fin1 and sequesters the protein to the SPB. Furthermore, Byr4 is absent from the new SPB during all anaphases (Cerutti and Simanis, 1999). This suggests that Fin1 binding to the SPB depends on the interaction with Byr4 and on

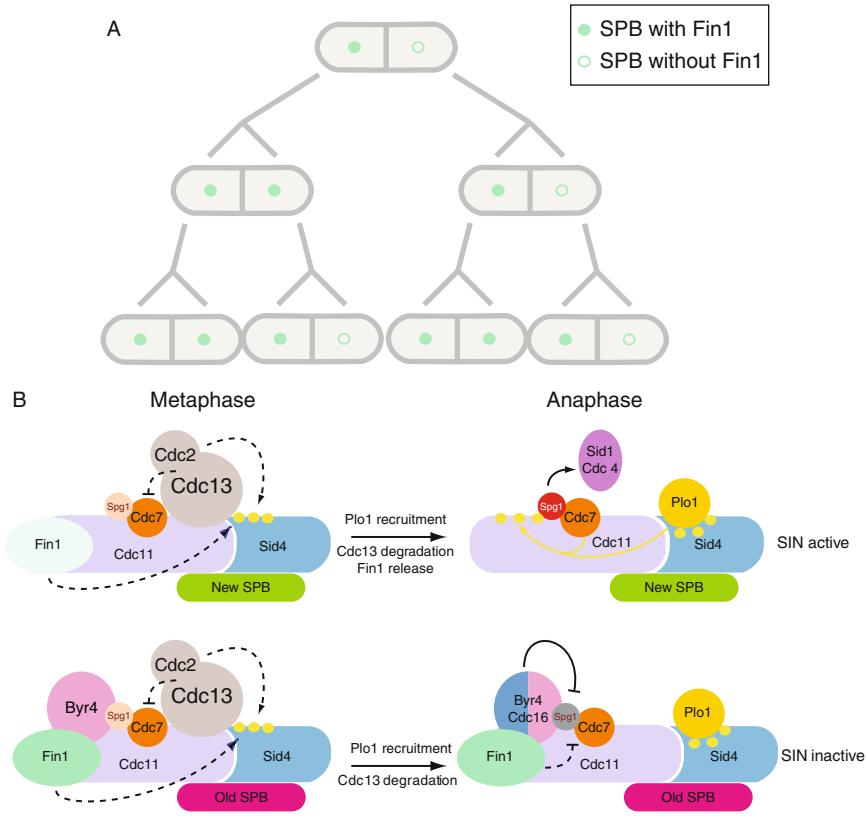

Figure 4.3 (A) Scheme of Fin1 localization based on the history of the SPB. At the end of mitosis Fin1 (solid dot) localizes to the old SPB and only on a new SPB that is produced next to an SPB, that was the old SPB in the previous cell cycle. Fin1 is absent from a new SPB that is assembled next to an SPB that formed just in the previous cell cycle (outlined dot). In this way, half of a cell population displays symmetric Fin1 localization (adapted from Grallert et al., 2004). (B) Hypothetical model for generation of SIN asymmetry based on the presence of Byr4 on the old SPB (adapted from Krapp et al., 2004b; Morrell et al., 2004). Fin1 together with Cdc2–Cdc13 promote the recruitment of Plo1 on the SPB, possibly through Sid4 phosphorylation (grey circles; the exact mechanism involves also Cut12, not shown here). On the new SPB in anaphase, Cdc13 is degraded, possible inhibition of Cdc7 may be thus relieved and Cdc7 together with Plo1 phosphorylate Cdc11. Byr4 binds less efficiently to phosphorylated Cdc11 and it is not recruited on the SPB. Therefore, Spg1 is active on the new SPB. Fin1 is less on the new SPB and/or leaves the new SPB upon SIN activation. On the old SPB, Byr4 recruits Cdc16 and inhibits Spg1 during anaphase. SPB-bound Byr4 may mask the Plo1 phosphorylation sites on Cdc11 and prevent Cdc11 phosphorylation. In addition, Fin1 may inhibit SIN activation.

some additional SPB quality that reflects its history. The nature of this quality is unknown.

On the basis of this data, SIN asymmetry could simply reflect the fact that the old and the new SPB differ in composition and reflect a fundamental asymmetry in spindle make up. This predicts a static situation in terms of SIN signaling, where the new SPB would always be active and the old SPB always silent. The mechanism of SIN asymmetry, however, does not seem to be as simple. First, Cdc7 and Sid1 localize on both SPBs during early mitosis and become asymmetric only during anaphase B (Cerutti and Simanis, 1999). Thus, both SPBs seem to have the potential to initially bind the SIN factors and asymmetry generation appears to be a regulated process and does not simply depend on a fixed SPB property. Consistently, upon ablation of the SIN-active SPB with a laser beam, SIN components relocalize to the old SPB and cells perform septation. Second, localization of most SIN components is dynamic; Spg1 and its downstream effector Sid2 have a high-turnover rate on SPBs, in the order of 1 min (Morrell et al., 2004). Moreover, interfering with SIN activity affects the asymmetric distribution of other SIN components. Overactivation of SIN using a temperature-sensitive *cdc16* mutant leads to the symmetric distribution of Spg1-GTP (Cerutti and Simanis, 1999), Cdc7, and Sid1 to both SPBs (Guertin et al., 2000; Sohrmann et al., 1998), as observed in the *fin1-ts* mutant. Thus, SIN asymmetry relies on feedback control (Cerutti and Simanis, 1999; Guertin et al., 2000; Sohrmann et al., 1998). Taken together, these data suggest that SIN asymmetry relies on age differences between SPBs (Adams and Kilmartin, 2000; Decottignies et al., 2001), and may be amplified through SIN activity.

2.1.3. Role of the Cdc2 kinase in generation of SIN asymmetry

Together with cyclin B (Cdc13), the central cell-cycle regulator of fission yeast, Cdc2, also plays an important role in the regulation of SIN asymmetry. First, downregulation of Cdc2 activity using a chemical inhibitor switched SIN localization from metaphase (symmetric) to the anaphase (asymmetric) configuration (Dischinger et al., 2008). Second, overexpression of a nondegradable form of Cdc13 fails to activate the SIN, and APC null mutants, that are defective in cyclin degradation fail to septate (Chang et al., 2001). In these cells, SIN components remain symmetrically localized to the spindle. Thus, inactivation of Cdc2/Cdc13 at the end of anaphase is required and probably sufficient to activate SIN and establish its asymmetry. There are several scenarios for how Cdc2 may interfere with SIN activity and spatial organization.

First, the Cdc12/Cdc13 complex localizes to the SPB during S-phase and metaphase, already (Morrell et al., 2004). Cdc2/Cdc13 physically interacts with the protein Cdc11 that acts, together with Sid4 and Pcp89, as a platform for the recruitment of SIN proteins on the SPB (Fig. 4.3B).

Cdc11 is the homolog of budding yeast Nud1, the platform for recruitment of the MEN components to the SPB (Section 2.1.4), and of the human centriole-associated protein centriolin, which regulates cytokinesis in mammalian cells (Gromley et al., 2003, 2005). The N-terminus of Cdc11 directly interacts with Byr4 (Krapp et al., 2003, 2004a) and is a phosphorylation substrate of Cdc2/Cdc13 (Morrell et al., 2004). Binding of Byr4 to the SPB depends on Cdc11 and could be regulated by Cdc11 phosphorylation, since Byr4 associates more efficiently with certain phosphorylated forms of Cdc11 (Krapp et al., 2003). Thus, Cdc2-dependent phosphorylation of Cdc11 could regulate the asymmetric localization of Byr4 during metaphase (Cerutti and Simanis, 1999; Krapp et al., 2003, 2004a). However, mutation of all eight Cdc2 consensus phosphorylation sites on Cdc11 could complement *cdc11* null mutants, suggesting that phosphorylation of Cdc11 by Cdc2 is not essential for Cdc11 function (Morrell et al., 2004). Nevertheless, the effect of Cdc2-dependent Cdc11 phosphorylation on SIN asymmetry has not been directly characterized yet.

Second, Cdc2/Cdc13 may regulate SIN activation and asymmetry indirectly through its effector kinases Fin1 and Polo (Plo1). In *cdc2* (and *cdc25*) mutants, Fin1 and Plo1 do not localize to SPBs (Grallert et al., 2004). Polo associates with Cdc11 indirectly through Sid4 and may require phosphorylation of Sid4 by Cdc2 for binding (Morrell et al., 2004). Interestingly, like for Fin1, Cdc2 localization to SPBs might depend on their maturation since accumulation of Cdc2/Cdc13 on the SPBs reaches higher levels in cells arrested in G2, the time of SPB maturation (Adams and Kilmartin, 2000), than in S-phase-arrested cells (Decottignies et al., 2001).

Third, Cdc2–Cdc13 may inhibit SIN activation through phosphorylation of Cdc7, as is the case with its budding yeast ortholog Cdc15 (Jaspersen et al., 2004; Menssen et al., 2001). This would explain why SIN remains inactive during metaphase, when Cdc2/Cdc13 activity is high, despite the accumulation of active Spg1-GTP and Cdc7 on the SPBs. At anaphase onset, Cdc13 becomes degraded and Cdc2/Cdc13 is eliminated from the SPB, relieving Cdc7 inhibition. This may enhance Cdc11 phosphorylation by Plo1, since Polo-dependent hyperphosphorylation of Cdc11 requires Cdc7 activity (Krapp et al., 2003, 2004a). Upon Cdc11 hyperphosphorylation, Byr4, which does not associate with hyperphosphorylated Cdc11, leaves the SPB, leading to activation of Spg1 and further recruitment of Cdc7, resulting in an SIN activation loop (Guertin et al., 2000; Krapp et al., 2004b, 2008; Sohrmann et al., 1998). These events may take place at the new SPB, while somehow delayed on the old SPB by the action of the Fin1 kinase (Grallert and Hagan, 2002). It has been suggested that Cdc11 is hyperphosporylated on the new SPB, which is associated with the active SIN, and hypophosphorylated on the old SPB (Krapp et al., 2003). The PP2A phosphatase is an SIN inhibitor (Le Goff et al., 2001). In mutants of the B′ subunit of the PP2A phosphatase (*par1*) Cdc11 remains

hyperphosphorylated at the end of anaphase and Cdc7 is more symmetric on SPBs, suggesting that PP2A-dependent dephosphorylation of Cdc11 could also be involved in generation of SIN asymmetry.

In summary, the levels of Cdc2 activity on the SPBs may generate SIN asymmetry and couple it to SIN activation. Prior to anaphase, age-dependent differences in association of Cdc2 with the SPBs may initially establish SIN asymmetry. At anaphase, SIN asymmetry may be feedback amplified through activation of the SIN as a result of reduction of Cdc2 activity and/or differences in Cdc2 activity between SPBs.

2.1.4. Linking spindle asymmetry to cell polarity: MEN in budding yeast

Like SIN components, MEN factors localize asymmetrically to SPBs during late anaphase in budding yeast (Fig. 4.4), but unlike in fission yeast, it is not clear with which SPB the activated MEN associates. Furthermore, robust evidence indicates that the cell cortex plays a major role in the establishment of MEN asymmetry.

S. cerevisiae cells are highly polarized. They grow by developing a daughter cell *de novo* in the form of a bud. Bud generation requires polarization of growth toward the forming bud. During this process, a set of septin-dependent diffusion barriers compartmentalize the cell into separated mother and bud domains by preventing the random diffusion of many membrane-associated proteins between these two compartments (Barral et al., 2000; Castillon et al., 2003; Luedeke et al., 2005; Takizawa et al., 2000). Successful anaphases locate one and only one of the two SPBs into the bud, such that the two SPBs are then located in different biochemical environments. Yeast cells utilize this asymmetry to monitor segregation of SPBs and activate mitotic exit only when anaphase has been indeed successful. In case anaphase takes place in the mother cell and the bud does not inherit any SPB, as is the case in spindle positioning-defective *kar9*Δ and *dhc1*Δ mutant cells (Section 3.1), the MEN remains inactive and cells do not exit mitosis (Bardin et al., 2000; Pereira et al., 2000). Therefore, in budding yeast the MEN acts as a checkpoint pathway that allows mitotic progression only when the spindle is properly positioned at the end of anaphase. This checkpoint has been named spindle orientation checkpoint (SPOC).

2.1.4.1. Subcellular distribution of the MEN components As in fission yeast, the MEN components localize asymmetrically to the spindle. Unlike Cdc16 and Byr4 in *S. pombe*, which display different localization patterns during metaphase, both Bub2 and Bfa1 localize together throughout mitosis. Already during metaphase they accumulate in a biased manner onto SPBs, localizing preferentially to the SPB close to the bud (Caydasi and Pereira, 2009; Molk et al., 2004; Monje-Casas and Amon, 2009; Pereira et al., 2000). During anaphase, the Bfa1/Bub2 complex accumulates on the

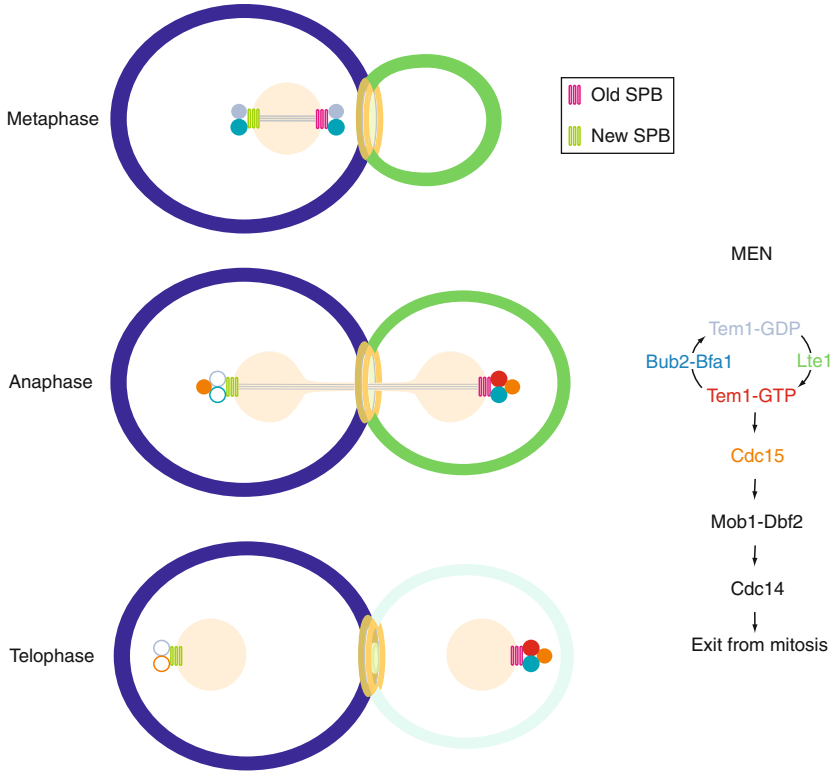

Figure 4.4 Localization of components of the mitotic exit network. Lte1 localizes to the bud cortex. In metaphase, both Bub2/Bfa1 and inactive GDP-Tem1 localize to both SPBs. In anaphase and telophase active GTP-Tem1 is assumed to localize together with Bub2/Bfa1 to the bud-directed SPB, while reduced amounts (outlined circles) of Bub2/Bfa1 and inactive GDP-Tem1 localize to the new SPB. Cdc15 is found on both SPBs during anaphase and accumulates on the bud-directed SPB during telophase. This model assumes that Tem1/MEN activation takes place in the bud; however there are also different models for MEN activation.

SPB that enters the bud, where its levels peak midway in anaphase and diminish through telophase. Localization of Tem1 to SPBs largely depends on the presence of the Bub2/Bfa1 complex, and Tem1 is barely detectable on SPBs in *bub2*Δ and *bfa1*Δ mutant cells (Caydasi and Pereira, 2009; Pereira et al., 2000). Thus, Tem1 localization follows essentially that of Bfa1 and Bub2 in metaphase cells, Tem1 is on both SPBs with a bias toward the bud-directed SPB. During anaphase, both immunofluorescence studies and time-lapse microscopy of cells expressing GFP-tagged Tem1 show that it accumulates essentially on the SPB that has entered the bud (Bardin et al., 2000; Molk et al., 2004). Thus, Tem1, Bfa1, and Bub2 are already asymmetrically distributed at metaphase, and this asymmetry is amplified in anaphase. Reinforcement of MEN asymmetry strongly correlates with

MEN activation. A fusion of the downstream MEN kinase Cdc15 to GFP is absent from the SPBs at metaphase, but accumulates on the bud-directed SPB when MEN is activated during spindle elongation. Subsequently, however, Cdc15-GFP builds up on the mother-directed SPB as well (Molk et al., 2004). Similarly, the kinase Dbf2, which acts downstream of Cdc15, shows the same localization pattern (Visintin and Amon, 2001). Cdc15 localization to the SPBs is abolished in (MEN inactive) *tem1-3* and is symmetric in (MEN overactive) *bub2*Δ mutant cells (Visintin and Amon, 2001). Accordingly, MEN localization is symmetric when MEN is inactive in anaphase: Bub2/Bfa1 and Tem1 localization is symmetric on misoriented anaphase spindles, that is, in *kar9*Δ mutant cells. Furthermore, on these spindles Tem1-GFP and Bfa1-GFP fluorescence intensity on SPBs is reduced (Caydasi and Pereira, 2009). This data strongly suggest that MEN activation and generation of MEN asymmetry are coupled events. Therefore, in order to understand how MEN asymmetry is generated, it is important to understand the molecular mechanism of MEN activation.

2.1.4.2. Molecular mechanism of MEN activation by the bud cortex . . .

According to the most widely accepted model, the bud cortex asymmetrically activates the MEN on the SPB that enters the bud (Bardin et al., 2000). Based on the exclusive localization of Lte1 to the bud cortex and of Tem1 to the bud-directed SPB, this model proposes that Tem1 (and MEN) activation occurs as the bud SPB contacts the bud cortex (Fig. 4.5A). Hence, MEN activation is coupled to the polarized distribution of Lte1.

Localization of Lte1 to the bud cortex depends on the cell polarity determinants Cdc42, a Rho-related GTPase, and its effector, the PAK-related kinase Cla4. It also depends on the yeast ras GTPases Ras1 and Ras2, and on the Kelch domain proteins Kel1/2 (Guerrier, 1970a; Gulli et al., 2000; Hofken and Schiebel, 2002; Jensen et al., 2002; Seshan and Amon, 2005; Seshan et al., 2002; Yoshida et al., 2003). Cdc42 and its GEF Cdc24 are required (together with Cdc28 activity) for establishment but not for maintenance of Lte1 localization, since deactivation of *CDC42* and *CDC24* does not disrupt Lte1 localization after the protein has reached the cortex (Hofken and Schiebel, 2002). The actin cytoskeleton is also not required to direct or maintain Lte1 at the cortex, since actin depolymerization either before or after GFP-Lte1 expression did not abrogate association of GFP-Lte1 with the bud cortex. This suggests that the role of Cdc42/Cdc24 in Lte1 localization is independent of their role in actin organization. The cortical Cla4 kinase phosphorylates and probably activates Lte1; phosphorylated Lte1 remains cortical, whereas dephosphorylated Lte1 is cytoplasmic (Seshan and Amon, 2005; Seshan et al., 2002). Consistently, in *cla4*Δ mutant cells Lte1 is inactive and mislocalizes to both mother and bud (Chiroli et al., 2003; Hofken and Schiebel, 2002; Wild et al., 2004). At lower temperatures, mitotic exit is delayed in these cells. The maintenance

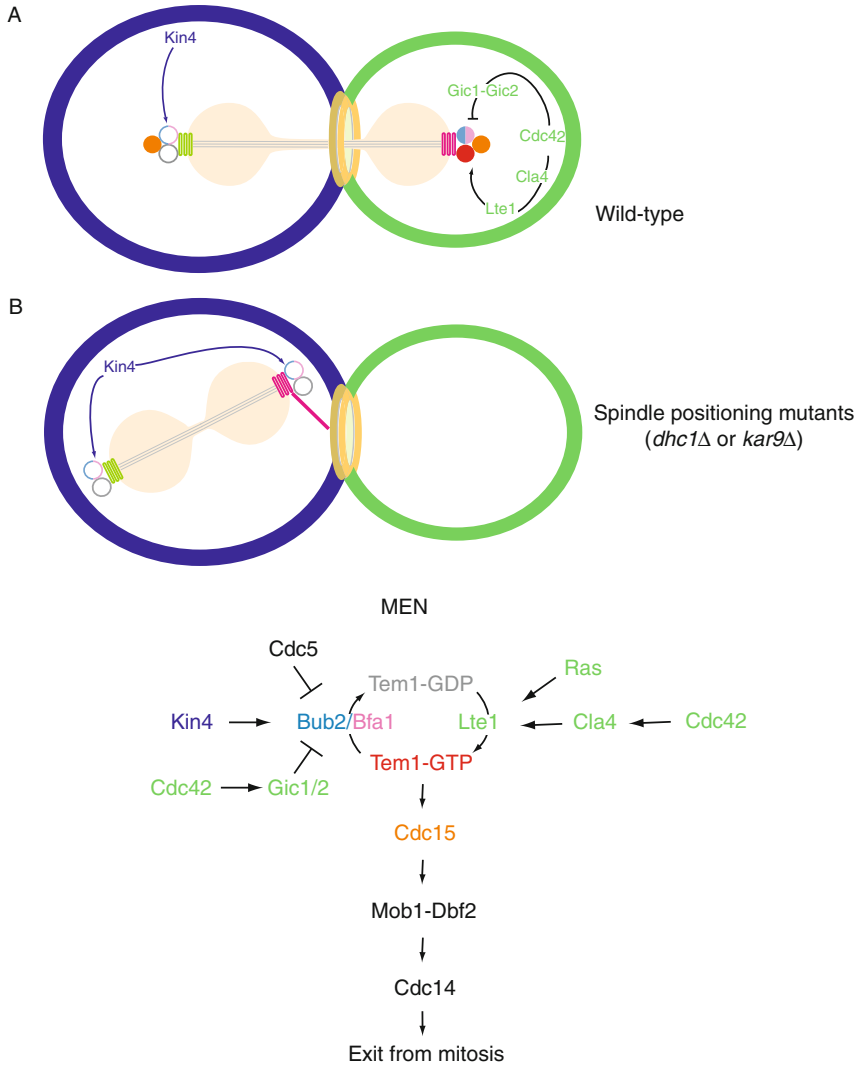

Figure 4.5 The most widely accepted model for MEN regulation. The bud cortex and the mother cortex control MEN activation and asymmetry. Alternative models and the role of the bud neck in MEN control are not depicted here. (A) Lte1 on the bud cortex is thought to activate the MEN. Cdc42 controls Lte1 localization; Lte1 is activated by the Cla4 kinase at the cortex. The Cdc42 effectors Gic1/2 activate Tem1 through Bub2/Bfa1 inhibition. MEN is active on the SPB that enters the bud. (B) In spindle positioning mutants, MEN is inactive and symmetric on SPBs. MEN activation is also controlled on the new SPB. The kinase Kin4 localizes to the mother cortex, phosphorylates Bub2 and Bfa1, and prevents inhibitory phosphorylation of Bub2/Bfa1 by the Cdc5 kinase. Outlined circles depict reduced localization/low protein amounts.

of Lte1 localization to the bud depends also on septins and probably on their barrier function (Hofken and Schiebel, 2002; Jensen et al., 2002; Seshan and Amon, 2005; Seshan et al., 2002; Yoshida et al., 2003). Therefore, septin defects permit inappropriate mitotic exit in cells with misoriented spindles at least partly through Lte1 mislocalization (Castillon et al., 2003).

Cdc42 contributes to MEN activation through a second mechanism that involves Bub2/Bfa1 inhibition by the homologous proteins Gic1 and Gic2, two effectors of the GTPase Cdc42 (Hofken and Schiebel, 2004). Both proteins localize to the bud cortex, but during anaphase Gic1 is partly released and localizes to the cytoplasm and the nucleus. *In vitro* studies show that Gic1 binds to Bub2, Bfa1, and Tem1 and disrupts the binding of the Bub2/Bfa1 complex to Tem1, thus relieving inhibition of Tem1 and activating mitotic exit (Hofken and Schiebel, 2004). Although Gic1 does not accumulate on the SPB, its localization suggests that it may inhibit Bub2/Bfa1 specifically on the SPB that enters the bud. Thus, the cortex may upregulate the MEN asymmetrically on the SPB that enters the bud through both Lte1-dependent activation of Tem1 and inhibition of Bub2/Bfa1 activity (Fig. 4.5A).

2.1.4.3. . . . and the mother cortex In contrast to the bud cortex, which supports MEN activation, the mother cortex seems to act negatively on mitotic exit (Fig. 4.5B). Genetic approaches led to the isolation of the kinase Kin4 as a negative regulator of MEN (D'Aquino et al., 2005; Pereira and Schiebel, 2005). Deletion of the *KIN4* gene leads to suppression of the mitotic exit defect of several MEN mutants and allows cells with mispositioned spindles to exit mitosis. How does Kin4 inhibit MEN activation? Kin4 acts through Bub2 since simultaneous deletion of *KIN4* and *BUB2* does not display any additive effect on MEN activation (Pereira and Schiebel, 2005). Kin4 interferes with phosphorylation of Bub2/Bfa1 by other kinases. Indeed, MEN activation requires hyperphosphorylation and inactivation of Bfa1 by the Polo kinase homolog Cdc5. This hyperphosphorylation of Bfa1 in late mitosis is inhibited upon Kin4 overexpression. Since Kin4 phosphorylates Bfa1 directly, these results suggest that Kin4 acts directly by protecting Bfa1 from being phosphorylated by Cdc5, either physically through binding to Bfa1, or because the Kin4-phosphorylated form of Bfa1 becomes a poor substrate for Cdc5 (Maekawa et al., 2007; Pereira and Schiebel, 2005). The localization of Kin4 is revealing: the kinase is present on the mother cortex, the bud neck and only to the mother SPB during mid-anaphase; it disappears at the end of anaphase. How Kin4 localization is controlled is unclear. In *kar9*Δ and *dhc1*Δ mutant cells with misaligned spindles, Kin4 and Bub2 bind to both SPBs. This suggests that Kin4 inhibits MEN as long as both SPBs are in the mother cell, and might itself become inhibited upon MEN activation.

2.1.4.4. MEN asymmetry, activation, and dynamics Life cell imaging showed that Tem1- and Bub2/Bfa1-GFP rapidly switch localization and become symmetric in response to spindle misorientation (Caydasi and

Pereira, 2009; Molk et al., 2004; Monje-Casas and Amon, 2009). This finding establishes that (1) Tem1 localization and MEN activation are coupled to the position of the SPBs relative to the cell polarity axis, and (2) control of MEN localization and activity is highly dynamic.

It is not possible to simply deduce which SPB associates with active Tem1/MEN during anaphase based on the distribution of MEN activators–inhibitors. On elongated anaphase spindles, the MEN activator Tem1-GFP is found on both SPBs with a biased accumulation on the SPB in the bud, and its effectors Cdc15/Dbf2 are found on both SPBs (although Dbf2 is reported only on the mother SPB in 30–40% of the cells) (Visintin and Amon, 2001). Regarding MEN inhibitors, Bub2/Bfa1 localizes to the bud-directed SPB but Kin4 is found on the mother-directed SPB. At telophase, Tem1 stays on the SPB in the bud and is fainter on the mother SPB, Cdc15/Dbf2 remains on both SPBs and Bub2 disappears from the SPB in the bud. Thus, MEN could be either active on the bud SPB, the mother SPB, or in the cytoplasm.

One study proposes that MEN activation takes place on the SPB in the mother cell, similarly to the activation of SIN in fission yeast (Fraschini et al., 2006). Since Bub2/Bfa1 disappears from the SPB in the mother, Tem1 inhibition could be relieved there first, leading to MEN activation. Accordingly, in *dhc1*Δ and *kar9*Δ mutant cells with mispositioned anaphase spindles, MEN is inactive and Bub2/Bfa1 and Kin4 accumulate on both SPBs, in the mother cell (D'Aquino et al., 2005; Fraschini et al., 2006; Molk et al., 2004; Pereira and Schiebel, 2005). Thus, MEN activation might be associated with elimination of Bub2/Bfa1 from the mother-directed SPB. Elimination of Bub2 from the new SPB (and hence MEN activation) required the activity of bud neck kinases Hsl1, Gin4, and the kinase Swe1, the wee1 kinase homolog in budding yeast (D'Aquino et al., 2005; Fraschini et al., 2006; Pereira and Schiebel, 2005), implying a role of the bud neck in triggering mitotic exit.

Other studies agreed with the role of the bud neck in MEN regulation, but disagree with the view that MEN is active on the mother-directed SPB (Adames et al., 2001; Nelson and Cooper, 2007). Video recordings of living cells showed that interactions of cMTs (the yeast astral microtubules) with the bud neck and not the proximity of the SPB to the neck are important to control mitotic exit. In *tub2-401* and other mutants that cause a reduction of cMT-neck contacts (like *kip2*Δ or *bik1*Δ), an increased proportion of cells undergo mitotic exit, before the bud inherits an SPB. These experiments led to the proposition that the bud neck sends an inhibitory signal to the MEN on the SPB closest to the neck. This signal should depend on Bub2 and on the contacts of cMTs with the bud neck and inhibit Tem1 until anaphase. Once the SPB enters the bud, the cMT-bud neck contacts lessen, Bub2/Bfa1 is inactivated and Tem1 becomes active. This model suggests that inhibition of Bub2/Bfa1 rather than activation through Lte1 plays the major role in MEN activation, and that MEN is active on the bud-directed SPB.

More recent studies support the idea that cMTs are involved in MEN regulation on the bud-directed SPB, but did not detect any role of the bud neck, septins, SDKs, or Swe1 in MEN regulation (Monje-Casas and Amon, 2009). Time-lapse microscopy of living cells showed that Bfa1-GFP accumulates on any of the two SPBs that coincidentally moves close to the bud and diminishes from the one that moves away from the bud upon spindle rotation. Disruption of cell polarity either during actin depolymerization early during the cell cycle or using temperature-sensitive *cdc42* or formin mutants results in association of Bfa1-GFP with both SPBs. Similar effects on Bfa1-GFP distribution were observed upon depolymerization of cMTs using nocodazole, or in cells mutated for a number of factors that affect astral microtubule dynamics and spindle alignment (Monje-Casas and Amon, 2009). In addition, accumulation of Tem1-GTP on the bud-directed SPB is reduced in mutant cells with reduced cMT–cortex interactions, that is, in *kar9*Δ, *dhc1*Δ, or *kip2*Δ mutant cells (Caydasi and Pereira, 2009; Molk et al., 2004). These observations led to the proposition that cMT–cortex interactions are required for the asymmetric localization of Bub2/Bfa1 and hence Tem1 accumulation on the SPB.

However, when the spindle happens to orient correctly in a *kar9*Δ mutant cell (in which cMT–actin interactions are *always* disrupted), Bub2/Bfa1 resumes asymmetric localization and the cell exit mitosis. This suggests that cMT–actin interactions are not required for asymmetric localization of Bub2/Bfa1. It might be that proximity of the SPB to the polarized bud drives asymmetry independent of cMTs, and that the symmetry observed after microtubule disruption reflects SPB mispositioning. Consistent with this idea, cMTs are not required for loading of the Bfa1 onto the SPB, since cMT disruption early in the cell cycle has no effect on Bfa1-GFP recruitment on the SPB. Paradoxically, Tem1 is present on both SPBs in *dhc1*Δ mutant cells even when the spindle is correctly oriented, while Bub2/Bfa1 localization remains asymmetric, as judged by immunofluorescence (D'Aquino et al., 2005). Thus, dynein-dependent (actin-independent) cMT interactions with the cortex may also contribute to MEN asymmetry.

In fact, it is not even clear whether active GTP-bound Tem1 is cytoplasmic or bound to SPBs (Hofken and Schiebel, 2004; Molk et al., 2004). The assumption that active Tem1-GTP resides on the SPB that enters the bud relies on the accumulation of Tem1 on the bud-directed SPB and the localization of Lte1 on the bud cortex (Bardin et al., 2003). Studies on Tem1-GFP dynamics using FRAP showed that one fraction of SPB-bound Tem1-GFP exchanges very fast between SPB and cytoplasm (recovery time of 4.5 s), while a second fraction shows slower turnover in the order of 133 s (Caydasi and Pereira, 2009; Molk et al., 2004; Monje-Casas and Amon, 2009). The rapidly exchanging fraction could represent active, GTP-bound Tem1 that leaves the SPB; thus active Tem1 would not be SPB bound. This

supports the idea that MEN is activated on the SPB in the mother, on which the Tem1 pool is reduced in anaphase. Importantly, immobilization of Bfa1 or Bub2 to the SPB through fusion to the SPB component Cnm67 supported mitotic exit of even misoriented spindles (Caydasi and Pereira, 2009). This data can be interpreted in two ways: either Bfa1/Bub2 needs to leave the SPB to inhibit Tem1 elsewhere, in which case active Tem1 would not be SPB-associated, or MEN is active when Bfa1/Bub2 (and possibly Tem1) accumulate on the SPB.

The asymmetry of Bub2 and Bfa1 does not appear to depend so much on the presence or absence of binding sites, but more on the rate by which the proteins leave the SPBs. Indeed, there is a big difference in Bfa1 dynamics between the two SPBs: Bfa1 is rather stably associated with the SPB close to the bud ($t_{1/2} \sim 40$ s, only 10% of the initial signal intensity can be recovered), while it is much more dynamically associated with the mother-directed SPB ($t_{1/2} = 30$ s and recovery $\sim 70\%$). Immobilization of Bub2/Bfa1 on the bud-directed SPB may be coupled to inhibition of its GAP activity by Cdc5 phosporylation; however, Cdc5 localizes to both SPBs (Pereira and Schiebel, 2005; Shirayama et al., 1998). The Bfa1M423I mutant that is not phosphorylated by Cdc5 localizes to both SPBs during late anaphase (Kim et al., 2008), while the Bub2R85A mutant, which lacks GAP activity *in vitro*, is symmetric on both SPBs during the cell cycle (Fraschini et al., 2006). When the MEN is inactive in *kar9Δ* mutant cells with misoriented spindles localized in the mother cell, Bfa1-GFP is highly dynamic (Caydasi and Pereira, 2009; Monje-Casas and Amon, 2009). Abrogation of Bfa1 phosphorylation by Kin4 decreased the dynamic behavior of Bfa1, suggesting that activation of Bub2/Bfa1 (and MEN inactivation) by Kin4 is coupled to Bfa1 mobilization (Caydasi and Pereira, 2009). From this point of view, a plausible model is that inhibition of Bub2/Bfa1 GAP activity by Cdc5 on the bud-directed SPB leads to immobilization of Bub2/Bfa1 and Tem1 recruitment, while on the mother-directed SPB Kin4 may inhibit this process, leading to Bub2/Bfa1 dissociation and MEN activation. It remains unclear, though, how Tem1 on the bud-directed SPB remains active while associated with Bub2/Bfa1. Generation of antibodies against the specific nucleotide-bound forms of Tem1 would be of great help to clarify which SPB associates with the active MEN as has been done for Spg1 in *S. pombe* cells (Sohrmann et al., 1998), and to determine how MEN asymmetry is generated.

Despite the uncertainties described earlier, it remains clear that cell polarity and cortical compartmentalization are crucial for the generation of MEN asymmetry. On one side, cortical factors that promote MEN activation are confined to the bud through their association with the bud cortex. On the other side, the mother cortex forms a compartment that is inhibitory for the MEN. Cytoplasmic microtubules may play an important role for the communication of the SPBs with the cortex and the regulation

of MEN activity. Up to this point, the mechanism of asymmetry generation is fundamentally different between budding and fission yeast. However, there are also striking similarities in the regulation of SIN and MEN. First, association of SIN and MEN factors with SPBs is directly coupled to activation of the network. Second, it relies on the same types of molecular interactions most MEN proteins associate with the SPB either directly through Nud1 (like Bub2/Bfa1, Kin4, and Cdc5) and/or indirectly through binding of MEN factors that are already at the SPB. Thus, generation of the asymmetric patterns of MEN proteins must occur either through alteration of the interactions between Nud1 and MEN or through regulation of interactions among the MEN proteins. Understanding spindle asymmetry in yeasts will provide the basis to explore the function and mechanisms for generation of spindle asymmetry in higher eukaryotic cells.

2.2. Spindle asymmetry during budding yeast meiosis

Meiosis in budding yeast is initiated upon nutrient starvation. During meiosis, two consecutive rounds of chromosome segregation take place in the cell body and lead to the formation of four spores (Fig. 4.5). The anaphase spindles in meiosis I and II are organized by SPBs. In meiosis I, a new SPB (the second oldest) forms next to the preexisting SPB. After completion of anaphase I and segregation of the homologous chromosome pairs, a second round of SPB duplication occurs giving rise to two new SPBs, one next to the oldest and the other next to the second oldest SPB. These four SPBs in turn organize the two meiosis II spindles. There is a considerable reorganization of the SPB during meiosis II (Fig. 4.5). The cytoplasmic face of the SPB, the outer plaque (OP), nucleates cMTs in meiosis I, but switches to the formation of the prospore membrane (PSM) in meiosis II. This is accompanied by reorganization of the OP. The mitotic components required for cMT anchoring and nucleation, Spc72 and γ-tubulin (Tub4), remain associated with the OP until completion of meiosis I, but are replaced by the meiosis-specific proteins Mpc54p, Mpc70p/Spo21p, Spo74p, and Ady4 during meiosis II (Bajgier et al., 2001; Knop and Strasser, 2000; Nickas et al., 2003). These proteins form the meiotic plaque (MP), and initiate the formation of the PSM that engulfs the meiotic nuclei as a first step toward the formation of meiotic spores.

When the amount of carbon source is adequate, four spores form. However, when carbon source becomes limiting, the cells produce only three or two spores. In this manner, the cell adapts to its nutritional conditions. In dyads, the two spores contain chromosomes of nonsister origin (Davidow et al., 1980) and are hence called nonsister dyads (NSDs). Since the mating type locus is genetically linked with centromeres in yeast, the two spores of NSDs are of opposite mating types. When the environmental conditions become favorable again, these two spores mate

directly after germination, without intervening mitosis. Direct mating of NSD spores is thought to be advantageous because it preserves heterozygocity and protects cells in case of occurrence of recessive mutations in the genome (Taxis et al., 2005).

To form NSDs only two of the four SPBs in meiosis II must build an MP (Fig. 4.6). Formation of an MP occurs with a frequency of 96% only on the two new SPBs, while the older ones remain inactive or are somehow silenced. Therefore, only the new SPBs are able to initiate formation of a PSM and produce viable spores. During meiosis, each SPB is associated with one copy of the genome. Since the two new SPBs always associate one with each of the two meiosis II spindles, they also associate with nonsister

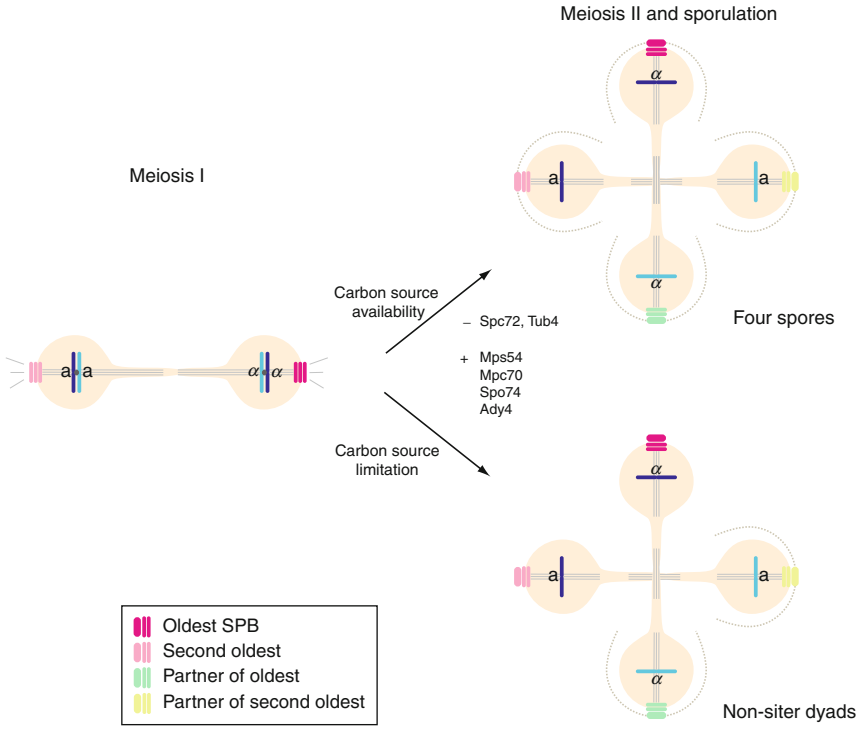

Figure 4.6 Spindle asymmetry during meiosis of budding yeast. Normal meiosis results in production of four haploid spores. Cells can regulate the amount of spores upon nutrient limitation. In case of nonsister dyad (NSD) formation, only the new SPBs organize a prospore membrane. Since the new SPBs belong to different spindles, the dyads contain nonsister chromatids. In addition, they are of opposite mating type, since mating type and centromeres are genetically linked in budding yeast. During the transition from meiosis I to II the outer plaque of the SPB is reorganized, loses the ability to nucleate cMTs, and recruits meiosis-specific components required for prospore membrane formation. Downregulation of the ability of the old SPBs to form a prospore membrane likely occurs at the level of the outer plaque component Nud1.

chromatids; the latter become encapsulated within the PSM formed by the new SPBs, leading to NSD formation.

These observations indicate that SPBs have different capabilities in PSM assembly. How are unequal SPBs generated during meiosis? First, this difference appears to be regulated. All SPBs are capable of producing PSM when the nutritional conditions are favorable, suggesting that the old SPBs are actively silenced upon nutrient limitation. This may involve signaling through an intermediate metabolite, perhaps to regulate the transcription and thus the availability of the MP components (Nickas et al., 2004; Taxis et al., 2005). Second, here again spindle asymmetry is obviously related to the age of the SPB. Third, it also relates to history of the SPB. The probability of the new SPB to form an MP depends not only on its age, but also on the age of its partner SPB. Thus, the partner of the oldest SPB almost never fails to assemble an MP, whereas the partner of the second oldest SPB sometimes does not assemble the MP in favor of its older partner. This is to some extent similar to the pattern of Fin1 localization during fission yeast mitosis (Section 2.1.2.3). Thus, SPB maturation might be a process conserved in fungi.

Analysis of spindle asymmetry during budding yeast meiosis provided new insights to the molecular mechanism of age-related SPB asymmetry. Studies on the localization of proteins of the outer and central plaques of the SPB identified that the MP is assembled on the protein Nud1, which is present symmetrically on all SPBs throughout meiosis (Nud1 also shares homology to the mammalian centriolin involved in asymmetric abscission) (Section 2.4). Mutants of *NUD1* show defects in spore maturation and in asymmetric assembly of the MP. In these mutants, MP assembles in a more random fashion with respect to the age of the SPBs (but not completely randomly). Nud1 physically interacts with components of the MP (Gordon et al., 2006) that specifically assemble on one SPB. During mitosis Nud1 acts as a platform for recruitment of Bub2/Bfa1 and other components of the MEN that are asymmetrically distributed between SPBs. Therefore, Nud1 seems to be at the place where asymmetries are generated both in meiosis and mitosis. It will be interesting to see whether Bub2/Bfa1 and the MEN are required for the asymmetry of MP assembly during meiosis. Regulators of the MEN are required for meiosis in budding yeast (Kamieniecki et al., 2005) and the SIN is also required for spore formation in *S. pombe* (Krapp et al., 2006).

2.3. Models for generation of unequal SPBs

The specific association of proteins with old SPBs suggests that SPBs may undergo a maturation process similar to centrosomes. The new SPB could lack proteins or modifications, which it would gradually acquire during the cell cycle. Although no morphological differences are apparent between the

SPBs in yeasts, the pattern of Fin1 segregation (Fig. 4.3A) suggests that a maturation process may indeed occur in fission yeast. An analogous mechanism could function in *S. cerevisiae* as well.

The key to the generation of unequal SPBs probably lies in the mechanism of SPB duplication. Two models could explain the generation of four different SPBs. The first is based on a quantity shared between old and new SPBs upon duplication, which would be ''diluted'' through subsequent rounds of duplication (Fig. 4.7A). In this model, a new SPB could acquire more of this quantity from an older SPB than from a younger one. Support for this model comes from EM studies showing that, during SPB duplication, some material incorporates also to the old SPB in fission yeast (Ding et al., 1998). However, it is not known what prevents the old SPB from doubling in size, while the new SPB assembles next to it. Thus, spindle asymmetry could be a consequence of the asymmetry in the duplication process. The activity of the cyclin-dependent kinase Cdc2, which is the most upstream regulator of SPB duplication and spindle formation, may play a decisive role in this case. Clearly, the mechanism of SPB duplication is still very unclear to accept or completely rule out such a concept.

The second model proposes that generation of age-dependent differences between the SPBs relies on a specific, cell cycle-dependent modification (Fig. 4.7B). The fact that SPB asymmetry is subject of developmental regulation suggests that SPB maturation might be a regulated process (Nickas et al., 2004). Accelerating the cell cycle using a *wee1* mutant did not influence the pattern of Fin1 localization to the SPBs in fission yeast (Grallert et al., 2004), suggesting that differences are not acquired in a slow maturation process through the cell cycle, but are rather a consequence of the transit from one cell cycle to the next. According to this hypothesis, passage through the cell cycle would leave a mark on the old SPB. This mark could be any kind of covalent modification like phosphorylation or a ubiquitin-like modification. The new SPB does not get modified until the next cell cycle. In the next cell cycle, the old SPB receives a second mark, which can be either of the same or of different nature. Thus, the oldest SPB would be the one most heavily modified and the second oldest ''less'' modified. During budding yeast meiosis, the tag would inhibit MP formation in an additive manner: an SPB with two tags is more inhibited than a single-tagged SPB. This is sufficient to explain the observed distribution of the MP formation. The new SPBs would be identical, but differences would be more pronounced between the new and a double-tagged than a single-tagged SPB. Therefore, MP assembly would occur more frequently on the new SPBs and in rare cases also on the second oldest SPB, as has been observed (Taxis et al., 2005). However, such a model would be inadequate to explain the localization of Fin1 in mitotically dividing *S. pombe*. Only the first model could account for the differences among new SPBs that depend on the age of their counterpart SPB.

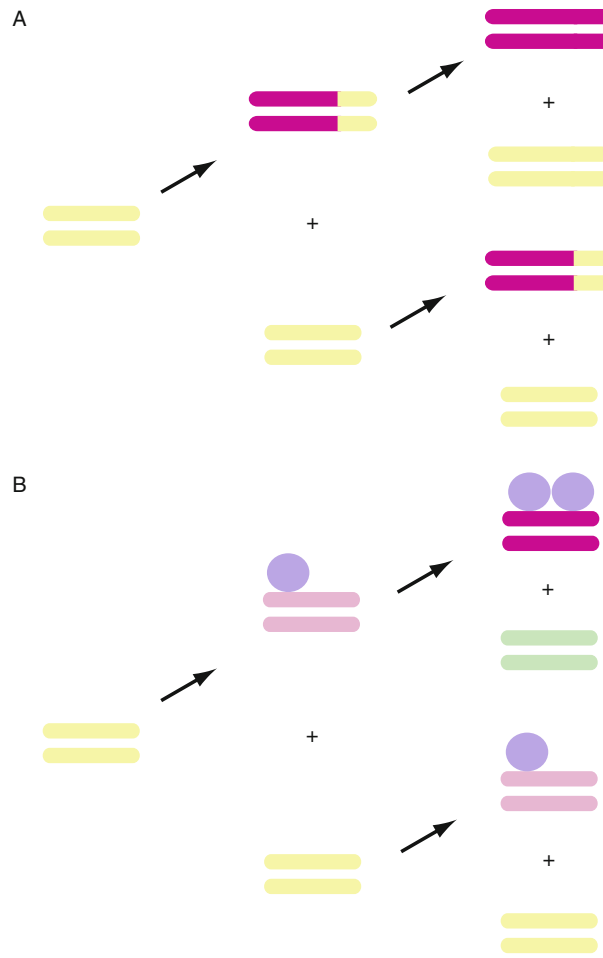

Figure 4.7 Models for SPB asymmetry in yeast. (A) This model is based on the hypothesis that a limiting amount of structural SPB components is available at SPB duplication. In the first cell cycle, the new SPB forms and some new material are used for the maturation of the old one. In the second cell cycle, most available material is incorporated into the new SPB. Therefore, the SPB formed next to an old one is more "mature" and here shown bigger than the (here smaller) SPB formed next to a young one. (B) In the second model, the SPB receives a modification during the passage from each cell cycle to the next. The SPB forming next to an old SPB that has experienced a second cell cycle is somehow more "mature" than its corresponding sister (adapted from Grallert et al., 2004).

2.4. Centriole control of cytokinesis

Like the SPBs in yeasts, centrosomes serve probably as signaling sites to regulate cell-cycle progression. Recent evidence suggests that higher eukaryotic cells coordinate cytokinesis with chromosome segregation

through mechanisms that resemble SIN and MEN (Gromley et al., 2003, 2005). For example, Flp1 (Cdc14) homologs in worms, *Xenopus*, and mammalian cells have a similar function to fission yeast Flp1 and are required for cytokinesis (Gruneberg et al., 2002; Kaiser et al., 2004; Mailand et al., 2002). To this day no GTPase-activated signaling cascade that links centrosomes to mitotic exit and cytokinesis has been identified in mammalian cells. However centriolin, a coiled-coil protein associated with mammalian centrosomes, contains a domain with homology to fission yeast Cdc11 and budding yeast Nud1 and that, like its yeast counterparts, has the ability to bind to the Cdc16/Byr4 (Bub2/Bfa1) complex (Gromley et al., 2005). Overexpression of this domain causes cytokinesis defects in mammalian cells, while microinjection of antibodies in *Xenopus* or siRNA treatment against centriolin in mammalian cells causes failure of cell cleavage (Gromley et al., 2003).

Centriolin is asymmetrically localized in centriole pairs. It is found at the appendages of the old, mature centriole (Gromley et al., 2003). This could point to an asymmetric activity of the centrosome-coordinated pathway that controls cytokinesis analogous to SIN/MEN. Support for this model came from time-lapse microscopic observations of the behavior of centrioles during cytokinesis (Piel et al., 2000, 2001). In these studies, the fate of the centrioles was followed after their segregation to the two daughters. Before cytokinesis, but after ingression of the cytokinetic furrow, the centriole pair split and the mature mother centriole relocalized from the cell center to the midbody, where it somehow regulated cytokinesis. Remarkably, in 70% of the cases only the centriole from one prospective daughter moved to the midbody. This suggests that there is asymmetry in the ability of the two centrosomes to regulate cytokinesis. This asymmetry could relate to the age of the centriole, so that the oldest of the four centrioles is the one that is capable of regulating cytokinesis, although this hypothesis remains to be experimentally tested.

More recent studies shed light on the molecular mechanisms of abscission regulation by the centriole and are consistent with the hypothesis of asymmetric centriole function (Gromley et al., 2005; Pohl and Jentsch, 2008). A structure at the midbody, the midbody ring is required for abscission, the resolving of the plasma membranes at cytokinesis (Fig. 4.8). Movement of the mother centriole to the midbody could not be consistently observed, but the centriole-associated protein centriolin was delivered to the midbody ring. Centriolin was required, to recruit components of the exocytic machinery to the midbody ring, explaining its role in the abscission step in cytokinesis. Abscission occurs through asymmetric delivery of secretory vesicles at one side of the midbody, resulting in separation of the plasma membrane adjacent to the midbody ring. Association of centriolin with the midbody ring depended, among other proteins, on the kinesin

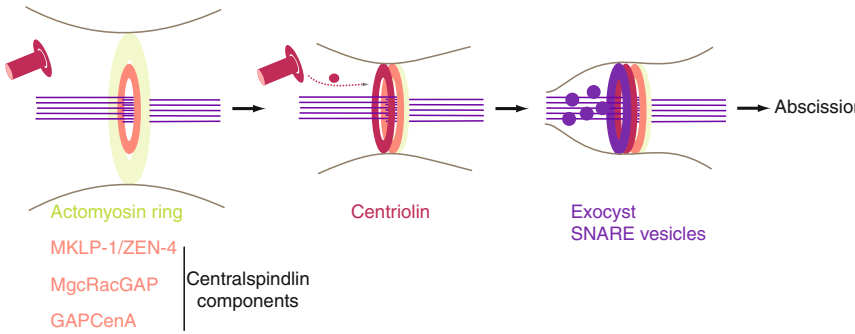

Figure 4.8 Model for organization of abscission. At the time of furrow ingression the centralspindlin complex bundles the microtubules and organizes the midbody. The old centriole moves to the site of cytokinesis, while the new one stays in the cytoplasm. Centriolin is recruited to the centralspindlin complex followed by the exocyst complex and secretory vesicles. Vesicles are delivered asymmetrically on the centriolin ring only from one prospective daughter. Movement of the old centriole to the site of cytokinesis may relate to centriolin recruitment and thus to the asymmetric organization of abscission.

MKLP-1. Interestingly, the GAP GAPCenA, which shares homology to fission yeast Cdc16 and budding yeast Bub2 proteins that regulate MEN/SIN (Cuif et al., 1999), is also part of the midbody ring, but it is not known whether the Cdc11 (Nud1) homology domain of centriolin is required for GAPCenA localization to this structure (Gromley et al., 2005).

In a highly speculative model (Fig. 4.8), the oldest of the four centrioles would regulate cytokinesis. Centriolin and possibly other proteins required for vesicle delivery associate with the old, mature centriole and could be thus transported from the oldest centriole to the midbody. On the midbody centriolin associated with GAPCenA could facilitate membrane delivery and abscission. The asymmetric delivery of secretory vesicles, originating only from one of the adjacent daughter cells, results in abscission on one side of the midbody. Asymmetric abscission around the midbody ring would suggest that vesicle delivery is also regulated asymmetrically by one of the centrosomes. Therefore, it will be interesting to investigate whether asymmetric delivery of exocytic vesicles correlates with the age of the centrosome. However, abscission on both sides of the midbody with concomitant midbody release into the extracellular space has also been observed (Piel et al., 2001). Occasional contribution to cytokinesis by the second oldest centriole could be attributed to the fact that any delay in the duration of the cell cycle due to cell culture conditions would give the second oldest centriole the time to mature too.

3. Spindle Asymmetry During Asymmetric Cell Divisions

3.1. SPB inheritance in budding yeast

S. cerevisiae cells are polarized and divide asymmetrically. The two daughters inherit different sets of proteins and mRNAs, and have different fates similar to asymmetrically dividing cells during development or cell differentiation in multicellular organisms. For example, asymmetric localization in the bud of the mRNA encoding the transcriptional repressor Ash1 prevents mating type switching of the new daughter after mitosis is completed (Bobola et al., 1996). Contrary to most cells, the plane of division is preset from the beginning of the cell cycle in budding yeast. Division takes place at the bud neck and thus correct segregation of sister chromatids between mother and bud during mitosis is strictly dependent on alignment of the anaphase spindle with the polarity (mother/bud) axis.

Mitotic spindle formation starts parallel to bud growth already during S-phase, when a new SPB forms next to the existing old SPB. Prior to anaphase, the two SPBs, while staying embedded in the nuclear envelope, separate and form the intranuclear mitotic spindle. This metaphase spindle migrates along with the entire nucleus toward the mother–bud neck, and aligns with the mother/bud axis. Spindle alignment depends on interactions of cytoplasmic microtubules (cMTs, as astral microtubules are called in budding yeast) with the cell cortex. Apart from tubulin and its chaperones, a number of other genes that function in spindle alignment were genetically identified and classified into two pathways, the "*KAR9*" and the "dynein (*DHC1*) pathway," which partially overlap in function. Inactivation of both pathways is lethal. Inactivation of each pathway individually is not lethal, but causes many spindles to misalign and thus fail to elongate through the narrow opening of the bud neck during anaphase, leading to complete failure of chromosome segregation between mother and bud (Miller and Rose, 1998; Miller et al., 1998).

Importantly, the metaphase spindle in budding yeast not only aligns with the polarity axis but also assumes a specific orientation along this axis, with the old SPB always facing the bud. Thus, in anaphase spindle elongation segregates the old SPB into the bud, while the new SPB remains in the mother cell. The fact that the old SPB is directed to the bud in most divisions shows that spindle orientation is not random, and that the two SPBs display stereotypically different identities and fates. Evidence for this asymmetry comes from cells expressing Spc42—a core SPB component—fused to DsRED. In these cells the old SPB is fluorescent, while the new SPB acquires fluorescence only during the following cell cycle, due to the time required to correctly fold DsRED (Baird et al., 2000; Matz et al., 1999).

Using this trick, Pereira et al. (2001) demonstrated that in 95% of the cases the bud inherits the old SPB. Similarly, most cells transiently overexpressing the protein Spc42-CFP at the time of SPB duplication, while having the old SPB marked with Spc42-YFP, displayed one yellow (old) and one cyan (new) SPB after SPB duplication. These experiments (and others based on FRAP) are consistent with SPB duplication being conservative (at least for the Spc42 protein) and contributing to the functional differentiation of the two spindle poles. How SPB duplication contributes to SPB differentiation is, however, not clear.

Metaphase spindle alignment and SPB inheritance are nearly random in *kar9*Δ cells, showing that the Kar9 pathway acts already during spindle formation to both align and orient the mitotic spindle along the mother–bud axis. Dynein mutants show only a minor perturbation of the bias in SPB inheritance since only approximately 10% of the cells segregate SPBs incorrectly in *dhc1*Δ mutants (Moore et al., 2006). Most of the metaphase spindles are correctly oriented in *dhc1*Δ cells, but often fail to elongate into the bud in anaphase and lose alignment (Adames and Cooper, 2000). In addition, dynein accumulates on cMTs prior to anaphase and is nearly absent from cMTs early in the cell cycle (Shaw et al., 1997). This data indicate that Kar9 functions prior to dynein in spindle alignment and orientation and that dynein is mainly required after Kar9 to sustain correct alignment of the anaphase spindle.

3.1.1. Spindle alignment, spindle orientation, and spindle asymmetry

How does Kar9 facilitate the biased segregation of the old SPB into the bud? The function of Kar9 in spindle orientation is inextricably linked with its function in spindle alignment and its asymmetric loading on the old SPB. Kar9 acts as a linker molecule between cMTs and the bud and bud neck cortices (Korinek et al., 2000; Kusch et al., 2002; Lee et al., 2000). The main cytoskeletal structures at both cortices are formed of actin filaments that are nucleated by formin complexes at the tip of the bud and at the bud neck. All actin cables are oriented with their barbed end pointing toward these nucleation sites. Interaction of Kar9 with the microtubule-associated protein Bim1 (Lansbergen and Akhmanova, 2006) localizes Kar9 to cMTs (Fig. 4.7A; Kusch et al., 2002; Liakopoulos et al., 2003). In addition, Kar9 binds to the type V myosin Myo2, which in turn associates with actin cables (Yin et al., 2000). In this manner, Myo2 travels along the actin cables toward their (+)-end at the bud tip, pulling with it Kar9, the cMTs and the associated SPB (Beach et al., 2000; Lee et al., 2000; Yin et al., 2000). Thus, Kar9 mediates the capture of cMTs by the cortical actin cytoskeleton and their translocation into the bud (Beach et al., 2000; Liakopoulos et al., 2003; Maekawa et al., 2003; Shaw et al., 1997; Yin et al., 2000). Importantly, Kar9 is located exclusively on the cMTs that emanate from only one of the two SPBs, which it directs toward the bud (Liakopoulos et al., 2003;

Maekawa et al., 2003). Since the SPB that segregate into the bud generally corresponds to the old SPB (Pereira et al., 2001), we can conclude that Kar9 preferentially labels the old SPB and the associated cMTs. The bias of Kar9 toward only one SPB is strictly required for its function in alignment of the spindle along the mother/bud axis, while its preference for the old SPB explains the orientation of the spindle along this axis and the pattern of SPB inheritance in yeast (Liakopoulos et al., 2003).

Dynein mediates pulling of the spindle into the bud at the metaphase–anaphase transition and contributes to spindle elongation later in anaphase by pulling both SPBs away from each other (Eshel et al., 1993; Geiser et al., 1997; Li et al., 1993; Saunders et al., 1995; Yeh et al., 1995). Accordingly, dynein localization is asymmetric on the spindle in early anaphase and becomes symmetric as anaphase progresses (Grava et al., 2006). The initial asymmetry of dynein localization contributes to spindle alignment. Already in late metaphase dynein localizes preferentially to cMTs emanating from the SPB closest to the bud neck. In wild-type cells this SPB happens to be the old one due to Kar9-dependent orientation of the metaphase spindle. As cMTs contact the cell cortex, dynein is offloaded from cMT tips and is immobilized at the cortex through its interaction by the cortical protein Num1 (Farkasovsky and Kuntzel, 2001). Cortically anchored dynein is then activated and pulls on cMTs via its (−)-end-directed motor activity, resulting in spindle movement (Adames and Cooper, 2000). Num1 is distributed on the cortex of both mother and bud in preanaphase cells (Cerveny et al., 2007; Farkasovsky and Kuntzel, 2001; Heil-Chapdelaine et al., 2000; Lee et al., 2005). Therefore, asymmetry of dynein localization determines that only one spindle pole is pulled toward the bud and promotes alignment of the spindle with the mother–bud axis (Carvalho et al., 2004; Grava et al., 2006).

Altogether analysis of Kar9 and dynein function in spindle alignment and orientation indicates that both processes strictly depend on the asymmetry of the activity of these components on the spindle. Indeed, mutants with symmetric dynein distribution are unable to grow in the absence of Kar9 and *vice versa* (Grava et al., 2006; Liakopoulos et al., 2003), suggesting that asymmetry of one pathway is required for spindle positioning when the function of the other pathway is compromised. Importantly, Kar9 and dynein asymmetries are not interdependent. Dynein is still asymmetric in *kar9Δ* mutant cells and vice versa (Carvalho et al., 2004; Grava et al., 2006). Accordingly, establishment of Kar9 and dynein asymmetry is also distinct. Asymmetric loading of Kar9 on the spindle is controlled through phosphorylation by specific Cdk/cyclin complexes (Liakopoulos et al., 2003; Moore and Miller, 2007). Dynein asymmetry is controlled through different Cdk/cyclin complexes and, in addition, by signals that are generated at the bud neck (Grava et al., 2006; Fig. 4.9B). Thus, the Kar9 and dynein pathways seem to have mechanistically and temporally distinct but complementary functions to achieve correct spindle positioning in budding yeast.

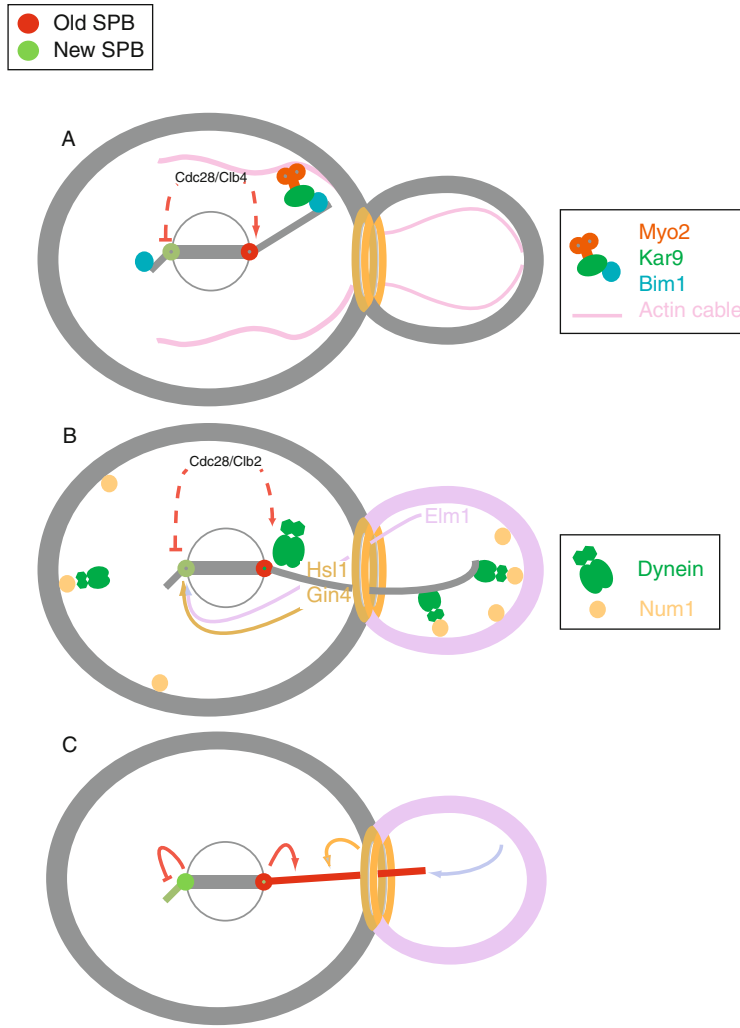

Figure 4.9 Asymmetric SPB inheritance in yeast. The old SPB is always partitioned in the bud at anaphase. Asymmetric inheritance depends on metaphase spindle asymmetry, shown here, in three ways. (A) Asymmetric loading of the Kar9-complex on the old spindle pole. The Kar9 complex pulls the old SPB to the bud. Kar9 asymmetry is regulated by Cdc28. (B) Dynein is asymmetrically loaded on cMTs and is also required for SPB inheritance. Dynein asymmetry is regulated both by Cdc28, by the Elm1 kinase, and by the septin-dependent kinases Hsl1 and Gin4. Septins are depicted as a ring at the bud neck. (C) Microtubules from the old SPB are more stable than cMTs emanating from the new SPB. They could be either stabilized by cortical factors as they reach the bud/bud neck. Alternatively, the old SPB could intrinsically nucleate more stable microtubules than the new one. A third possibility is that the bud/bud neck signals to the SPB which is closest, leading to nucleation of stable cMTs. In this case, the ability of the SPB to nucleate stable cMTs would be independent of SPB age.

3.1.2. Mechanism of spindle asymmetry: Role of Cdks

What prevents the loading of Kar9 and dynein on the mother-bound, new SPB? Since asymmetry of Kar9 and dynein is responsible for spindle orientation, symmetric loading of these proteins on SPBs/cMTs is expected to result in spindle misorientation and guidance of cMTs emanating from both spindle poles into the bud. Earlier studies (Segal et al., 2000) suggested that the spindle behaved in a symmetric manner in cells with reduced Cdc28 activity. According to this observation, both dynein and Kar9 depend on Cdc28 for asymmetry (Grava et al., 2006; Liakopoulos et al., 2003; Maekawa et al., 2003). The complex of Cdc28 with the cyclin Clb4 and possibly Clb5 directly phosphorylates Kar9 (Grava et al., 2006; Liakopoulos et al., 2003; Maekawa et al., 2003; Moore and Miller, 2007). Abrogation of Cdc28/Clb4-dependent Kar9 phosphorylation results in symmetric localization of Kar9 on both old and new SPB and their associated cMTs and in spindle misorientation (Liakopoulos et al., 2003; Moore and Miller, 2007; Moore et al., 2006). This led to the proposition that Cdc28/Clb4 activity could be higher on the new SPB and thus prevent the loading of Kar9 (Liakopoulos et al., 2003). However, later studies showed that Cdc28/Clb4 exists in a complex with Kar9 that is located on the cMTs emanating from the old SPB (Maekawa and Schiebel, 2004). Deletion of *KAR9* abrogates association of Cdc28/Clb4 with the SPB/cMTs suggesting that Kar9 acts as a scaffold for the association of Cdc28/Clb4 complexes with these structures. How Cdc28 activity regulates spindle asymmetry is still not clear. In the face of the Cdc28/Clb4 localization on the old SPB/cMTs, it seems counterintuitive that Cdc28 activity could be higher on the new SPB. Nevertheless, the localization of the Cdc28/Clb4 complex may not reflect its activity. Furthermore, phosphorylation of Kar9 by Cdc28 on the new SPB may inhibit its loading onto cMTs, so that the entire Kar9/Cdc28 complex would rapidly dissociate, and would thus not be detectable through fluorescence microscopy. The situation is even more difficult to untangle due to the fact that Kar9 regulation is in fact achieved through the interplay of numerous modifications: Kar9 is sumoylated independently of phosphorylation and, like phosphorylation, sumoylation contributes to the asymmetric distribution of Kar9 (Leisner et al., 2008; Meednu et al., 2008). Kinetochore defects also affect asymmetric distribution of Kar9, suggesting that spindle positioning is coordinated with chromosome attachment (Leisner et al., 2008). Therefore, establishment and regulation of Kar9 asymmetry is remarkably complex.

There is evidence suggesting that association of Kar9 with the old SPB does not depend on some special intrinsic property of the old SPB. If G1-arrested cells are transiently treated with nocodazole, Kar9 still localizes asymmetrically but is no longer biased toward the old SPB. A caveat of this experiment is that prolonged treatment with nocodazole may interfere with

the function of MT-associated factors that regulate Kar9 asymmetry. Not only Cdc28/Clb4, SUMO, and kinetochore signals, but also the microtubule-associated proteins Bik1 (CLIP-170 homolog) and Stu2 (XMAP215) are involved in the asymmetric distribution of Kar9 (Moore et al., 2006). The function of each of these factors is perturbed in nocodazole treated cells.

Dynein asymmetry is dually regulated by both the Cdc28 kinase (Fig. 4.9B) and cortical factors. In the hypomorphic *cdc28-4* mutant, dynein localizes symmetrically to SPBs and cMTs in 70% of the mitotic spindles, compared to 30% in wild-type cells (Grava et al., 2006). Dynein asymmetry is controlled at the spindle pole but, unlike Kar9, which is controlled by the Cdc28/Clb4 (and Clb3) complexes, dynein asymmetry requires the activity of Cdc28 associated with the later cyclins Clb1 and Clb2. The activity of Cdc28/Clb2 must prevent dynein loading at the new SPB, because deletion of both *CLB1* and *CLB2* results in symmetric distribution of dynein, similar to *cdc28-4* mutants (Grava et al., 2006). How exactly Cdc28/Clb1,2 prevents the loading of dynein on cMTs at the new SPB is not known. Both Clb1 and Clb2 localize symmetrically on the SPBs when fused to YFP (Bailly et al., 2003). Asymmetric Cdc28/Clb2 activity between the old and the new SPBs has not been demonstrated. Mutations in SPB components that abrogate the localization of Clb2 on the SPB result in symmetric distribution of dynein on cMTs during metaphase. A possible mechanism could be the regulation of the interaction of dynein with Kip2, a kinesin-related protein required for the transport of dynein to the cMT (+)-ends (Carvalho et al., 2004; Maekawa et al., 2003). The Kip2 kinesin localizes symmetrically on cMTs (Miller et al., 1998). However, deletion of Kip2 does not affect the distribution of dynein on cMTs (although it affects transport of dynein to the cMT (+)-ends) (Carvalho et al., 2004; Grava et al., 2006). Alternatively, dynein binding on microtubules could be regulated through phosphorylation of its accessory subunits. The development of phosphospecific antibodies against Kar9 and the targets of Cdc28/Clb2 in the dynein pathway will be a powerful tool to elucidate the mechanism of Cdk-dependent spindle asymmetry. The control of dynein asymmetry by the cortex is discussed in Section 3.1.3.

3.1.3. Mechanism of spindle asymmetry: Role of cortex in dynein asymmetry

The role of the cortex in dynein asymmetry (Fig. 4.9B) was revealed through genetic screens (Geiser et al., 1997; Lee et al., 2003). The kinases Elm1, Hsl1, and Gin4 localize to the septin ring at the bud neck (Barral et al., 1999; Bouquin et al., 2000; Longtine et al., 1998). The septin ring acts as a scaffold for the assembly of the cytokinetic apparatus and septin mutants fail to undergo cytokinesis. In null mutants of the bud neck kinases *elm1*Δ, *hsl1*Δ, *gin4*Δ as well as in septin mutants the percentage of cells with symmetric dynein localization doubles.

How exactly the cortex controls dynein asymmetry is not clear. Dynein could first associate with the bud cortex and subsequently be recruited to cMTs. However, mutation of Num1, the cortical anchor for dynein, results in an increased accumulation of dynein at the cMT (+)-ends, suggesting that dynein is offloaded from the cMTs to the cortex rather than the other way around (Sheeman et al., 2003). The offloading model is also supported by experiments showing that transport of dynein to the cortex is mediated by the kinesin Kip2 (Carvalho et al., 2004). The effect of the bud neck kinases is not caused through inhibition of Cdc28. In *elm1*Δ, *hsl1*Δ, and *gin4*Δ mutants the kinase Swe1 is stabilized and inhibits the activity of Cdc28. However, deletion of *SWE1* in these mutants does not reestablish dynein asymmetry. In addition, when cells are genetically manipulated to translocate the whole mitotic spindle into the bud, dynein asymmetry is reversed and dynein is loaded on the cMTs that emanate from the pole which is proximal to the bud neck (Grava et al., 2006). These experiments suggest that the effect of the bud neck kinases on dynein regulation is direct (Grava et al., 2006).

Importantly, simultaneous mutations of the bud neck kinases and the cyclins Clb1, Clb2 have additive effects concerning dynein asymmetry (Grava et al., 2006). This suggests that the mechanism governing dynein asymmetry consists of two branches acting in parallel. One branch uses the bud neck as a spatial cue for spindle positioning. The other depends on Cdc28/Clb2 activity.

3.1.4. Asymmetry of microtubule dynamics and spindle orientation in yeast

Spindle asymmetry in yeast is also evident at the morphological level. During metaphase, cMTs emanating from the old SPB proximal to the bud are stabilized and thus longer compared to the highly dynamic, short cMTs emanating from the new SPB (Grava et al., 2006; Shaw et al., 1997; Vogel et al., 2001). As a result, contacts of the proximal cMTs with the bud cortex and the bud neck are more frequent. Thus, pulling forces by the proximal cMTs provide the main contributions to spindle positioning. The asymmetry in microtubule dynamics can be explained by two models, which do not mutually exclude each other. First, cortical factors in the bud could stabilize cMTs that contact the bud cortex. In this case, the cMTs coming from the old SPB close to the bud would be longer, because they have a higher probability to enter the stabilizing bud compartment. Conversely, microtubules from the new SPB that contact mainly the mother cortex would not be stabilized. Thus, cMT asymmetry would be the result of the polarized distribution of cMT-stabilizing factors that reside in the bud cortex but are absent from the mother cortex, or, vice versa, of cMT-destabilizing factors that localize specifically to the mother cortex.

The second possibility is that cMT asymmetry is regulated at the level of the spindle poles. In this case, asymmetry would depend on the differential loading of regulators onto microtubules in an SPB-dependent manner (Cuschieri et al., 2006; Vogel et al., 2001).

In a third model, which combines the two ideas mentioned earlier, cell polarity would impinge on the SPB that happens to be close to the bud, influencing its cMT-nucleating properties. Thus, the pole close to the bud would become different in terms of cMT-organizing activity, irrespective of whether it would be the old or the new one. This model presumes some kind of communication between the bud and/or the bud neck and the SPB. To this point it is not clear how asymmetry in cMT dynamics is generated at the molecular level.

3.2. Spindle asymmetry during early embryonic development in *Caenorhabditis elegans*

3.2.1. Spindle asymmetry during first embryonic division

The early *C. elegans* embryo is one of the best studied animal systems concerning asymmetric spindle-pole behavior. In the one cell embryo of the nematode, spindle asymmetry is manifested in two ways. First, during metaphase the entire spindle starts shifting toward the posterior due to aMT-dependent forces that pull stronger on the posterior spindle pole. Second, during anaphase the posterior aster oscillates side to side, gradually flattens and finally appears to split at telophase (truncate and flattened morphology, Fig. 4.10A), while the anterior aster keeps its spherical appearance and remains relatively stationary (Albertson, 1984; Keating and White, 1998). Thus, during anaphase/telophase one pole of the spindle is flattened and positioned close to the posterior cortex, while the anterior spindle pole is round-shaped and located near the center of the future anterior cell.

3.2.1.1. Asymmetric spindle displacement and posterior pole oscillations Cell polarity directs spindle asymmetry in the *C. elegans* early embryo. After oocyte fertilization, meiosis II is completed and the embryo polarizes, resulting in the establishment of two distinct domains, a larger anterior (A) and a smaller posterior (P) domains. During mitosis, the embryo cleaves at the border of the two domains into a bigger anterior AB cell and a smaller posterior P1 cell that are the parents of the worm cell lineages (Fig. 4.10B). When establishment of cell polarity is prevented after treatment of embryos with cytochalasin D or latrunculin A, the spindle does not migrate posteriorly and the poles do not flatten (Hill and Strome, 1990). The proteins encoded by the genes *PAR-2* and *PAR-3* (abnormal embryonic PARtitioning of cytoplasm) identified in screens for mutants defective in early cleavage patterning (Kemphues et al., 1988; Morton et al., 1992, 2002; Watts et al., 1996) are the key cortical factors required to polarize the

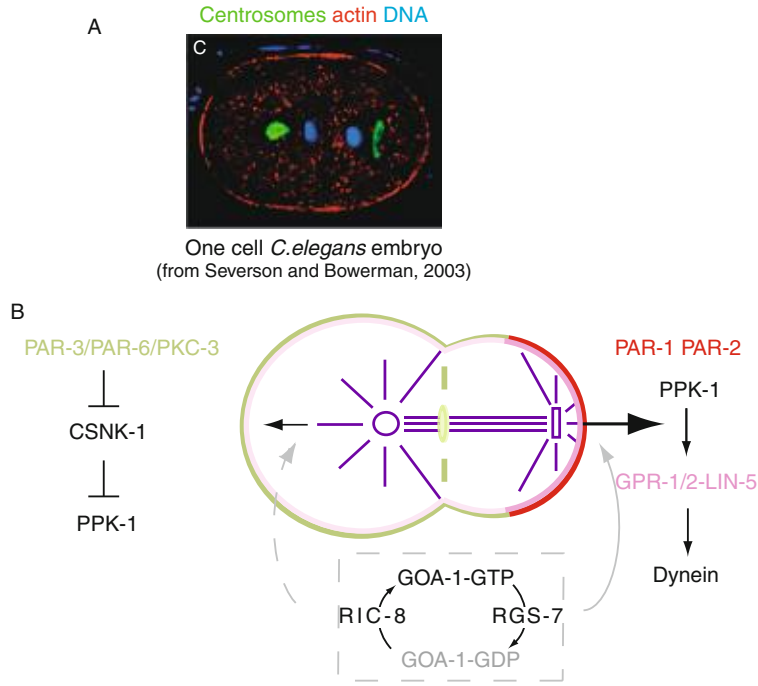

Figure 4.10 Spindle asymmetry during the first embryonic division of *C. elegans*. (A) Asymmetric spindle displacement and morphology. The spindle is displaced posteriorly (right) and the posterior spindle pole is flattened. (B) Spindle displacement and morphology is caused by stronger forces acting on the posterior pole (arrows). Force generation is controlled by the polarized cortex. The PAR-3 complex is localized anteriorly and possibly inhibits the PI(4)P5-kinase PPK-1; the PAR-1 and PAR-2 proteins localize posteriorly. GPR-1/2 localize around the cortex (inner rim; shadowing depicts concentration), but are more concentrated posteriorly, possibly through the action of PPK-1 that may create a membrane domain of specialized lipid composition. Together with the Gα subunits GOA-1/GPA-16, the PAR proteins and GPR-1/2 control microtubule dynamics and the forces that act on the spindle poles via LIN-5/NumA and dynein.

embryo cortex. The A–P axis fails to form and the spindle remains centered in *par-2* and *par-3* mutants. How does polarity drive spindle asymmetry in *C. elegans*?

Spindle displacement toward the posterior part of the embryo and the rocking movements of the posterior aster are thought to rely on the same mechanism (Grill and Hyman, 2005; Grill et al., 2003; Pecreaux et al., 2006; Severson and Bowerman, 2003). As in other systems, forces acting at spindle poles are thought to arise through the interaction of aMTs with cytoskeletal factors beneath the cell membrane (Gonczy et al., 2001; Hyman and White, 1987). Forces could be generated through motor molecules that interact

with astral MTs and/or as aMTs push or pull at the cortex as they grow (Adames and Cooper, 2000; Shaw et al., 1997). Laser severing experiments of the metaphase/anaphase spindle demonstrated that (a) forces pull on aMTs and (b) pulling forces are stronger at the posterior than on the anterior cortex (Colombo et al., 2003a; Grill et al., 2003; Nguyen-Ngoc et al., 2007; Severson and Bowerman, 2003). Mathematical analysis of the displacement of centrosome fragments after centrosome irradiation with a laser beam concluded that the same kind of force generators is active throughout the cortex. These calculations suggested that imbalance in pulling forces can arise as a result of 50% more force generators acting on the posterior than on the anterior pole (Grill and Hyman, 2005; Grill et al., 2003). Further calculations agreed that just one kind of force generator would suffice to provide the force for posterior spindle displacement (Pecreaux et al., 2006). However, these calculations suggested that not the number, but rather the persistence of attachment of the force generator on aMTs (processivity) increases on the posterior cortex as cells proceed through mitosis.

Later studies that utilized live-cell imaging and computer simulations of spindle behavior showed that the average number of aMTs–cortex contacts does not differ between anterior and posterior cortex (Kozlowski et al., 2007). Importantly, these studies suggested that forces are generated when aMTs depolymerize, while retaining cortical attachment. Computer simulations based on this model could indeed reproduce spindle movement and positioning (Kozlowski et al., 2007), when an asymmetry of 50% in cortical forces was imposed in the system. Taken together, mathematical modeling and cell biological studies suggest that forces acting on the spindle are generated as microtubule-associated proteins (MAPs, that may be motors or not) induce aMT catastrophe when aMTs reach the cortex. These MAPs should be processive enough to maintain interaction of the tips of depolymerizing MTs with the cortex (Couwenbergs et al., 2007; Kozlowski et al., 2007). Force imbalance between the two poles may arise when activity/processivity of MAPs is regulated differently between the anterior and posterior cortical domains.

The molecular mechanism of asymmetric force generation at the cortex involves the PAR proteins and heterotrimeric G-protein signaling. The anterior cortex contains the proteins PAR-3, PAR-6, and the atypical protein kinase C (aPKC/PKC-3). It is now apparent that the PAR-3/PAR-6/PKC-3 complex is a universal module that is required together with the polarity GTPase Cdc42 for the establishment and maintenance of cell polarity from worms to mammals. PAR-2 is essential to define the posterior domain (Fig. 4.10) by restricting PAR-3 to the anterior and *vice versa*. In *par-2* and *par-3* mutants the difference in aMT dynamics between the A and P domains is lost (Grill et al., 2003; Labbe et al., 2003, 2004; Severson and Bowerman, 2003), raising the question how the PAR proteins control microtubule dynamics.

It has been proposed that the PAR-3/PAR-6/PKC-3 complex may stabilize aMTs anteriorly, possibly through phosphorylation of microtubule-associated proteins by PKC-3 (Labbe et al., 2003). Likewise, the protein PAR-1 that colocalizes with PAR-2 could directly regulate microtubule dynamics at the posterior pole. PAR-1 is related to microtubule affinity regulatory Ser/Thr kinases (MARK) that control aMT dynamics through phosphorylation of microtubule-associated proteins (Drewes et al., 1997). To this moment, there is no evidence for direct phosphorylation of MAPs by PKC-3 and no major changes in MT dynamics were observed in *par-1* mutants compared to wild-type cells (Labbe et al., 2003). Therefore, the direct involvement of PAR proteins in regulation of aMT dynamics is only hypothetical.

PAR proteins generate force imbalance on the spindle acting most likely through G-protein signaling. Downstream effectors of PAR proteins include heterotrimeric G-proteins (GOA-1 and GPA-16 encode the Gα, GPB-1 the G*β*, and GPC-2 the G*γ*nit), the GEF RIC-8 and the GAP RGS-7, as well as the GoLoCo motif-containing proteins GPR-1/2, that act as G-protein effectors/regulators (Afshar et al., 2004; Colombo et al., 2003b; Couwenbergs et al., 2004; Gotta and Ahringer, 2001; Gotta et al., 2003; Hess et al., 2004; Srinivasan et al., 2003; Tsou et al., 2002, 2003). The signaling molecules are presumably the Gα; their inactivation leads to failure of spindle displacement and absence of pole flattening due to reduction of cortical pulling forces. Consequently, cell division produces two cells of equal size, although PAR cortical polarity remains unaffected (Fig. 4.11A); however, the PAR domains are also equal in size (Colombo et al., 2003a; Gotta and Ahringer, 2001). Similar phenotypes are observed when the function of GPR-1/2 (Colombo et al., 2003a; Gotta et al., 2003; Srinivasan et al., 2003) or RIC-8 is compromised (Afshar et al., 2004; Couwenbergs et al., 2004).

How PAR polarity proteins regulate G-protein signaling is not clear. Both Gα and GPR-1/2 localize on the spindle asters and the cortex. On the cortex, Gα is distributed evenly, while GPR-1/2 is enriched at the posterior PAR-1/PAR-2 domain (Fig. 4.10). This indicates that generation of stronger forces at the posterior cortex may be driven by G-protein signaling through GPR-1/2. Recent evidence suggests that PAR proteins may control GPR-1/2 localization and G-protein signaling through regulation of the lipid composition of the plasma membrane (Panbianco et al., 2008). Polarization by the PAR proteins is required for early accumulation of casein kinase 1 (CSNK-1) at the anterior pole, where it inhibits (probably together with the PAR-3 complex) the accumulation of PI(4)P5-kinase PPK-1. At the posterior pole active PPK-1 enhances GPR-1/2 recruitment and force generation, hypothetically through PIP_2 production. Interestingly, A–P force asymmetry is not fully abrogated in *csnk-1(RNAi)* or *ppk-1(RNAi)* embryos, indicating the existence of parallel acting mechanisms

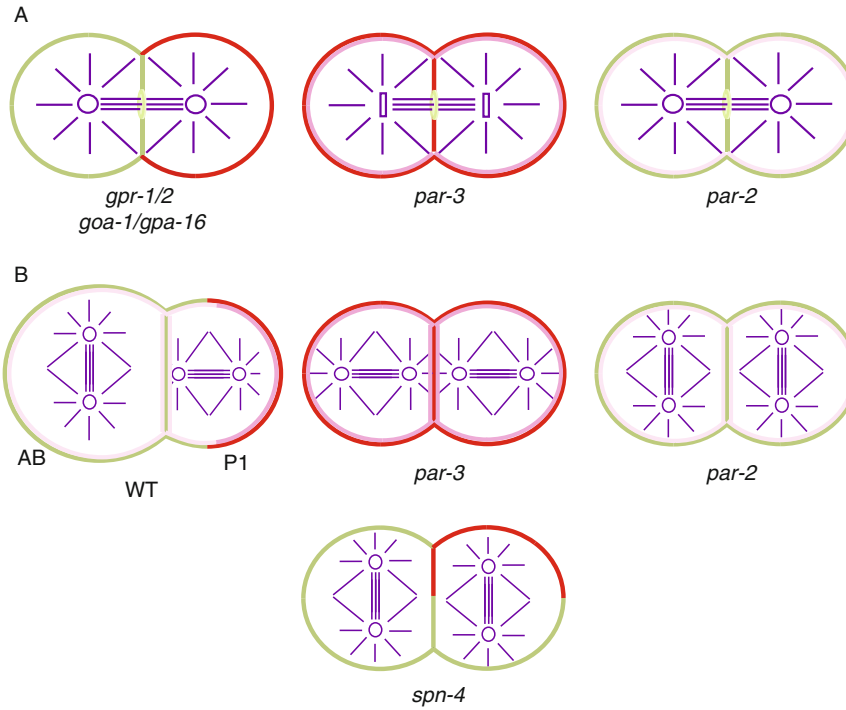

Figure 4.11 (A) In one cell embryos mutant for the Gα subunits (*goa-1/gpa-16*), the spindle is not displaced posteriorly and has a symmetric morphology, but cortical polarity is unaffected. *par-3* embryos display a posterior-like spindle phenotype (both poles flattened), *par-2* embryos an anterior-like phenotype. (B) Second embryonic division. Cortical polarity controls forces on the spindle and spindle orientation. In wild-type embryos the spindle in the posterior P1 cell is displaced anteriorly and its axis aligns with the A–P axis. *par-3* embryos display two symmetrically positioned spindles that are A–P aligned; in *par-3* embryos both spindles align transversely to the A–P axis. The concentrations of GPR-1/2 at the cortex are hypothetical. In the P1 cell of *spn-4* mutant embryos cortical polarity is respecified to align with the mispositioned spindle that has failed to rotate, so that the PAR-2 domain lies over one spindle pole and the PAR-3 domain over the other. Anterior is on the left, posterior on the right. Outer rim: light grey/green: PAR-3, dark grey/red: PAR-2. Inner rim: light grey/pink: GPR-1/2, dark grey/pink: indicates high concentration of GPR-1/2. The cytokinetic ring is depicted as a ring structure.

that control force asymmetry through G-protein signaling downstream of the PAR proteins. Consistent with this idea, PAR proteins are in addition required to confine the protein LET-99 in a cortical band at the border of the A–P domains. LET-99 contains a DEP domain present in regulators of G-protein signaling. It has been proposed that LET-99 opposes G-protein signaling and attenuates aMT-dependent forces, since *let-99* mutants (similar to *cskn-1*(*RNAi*) embryos) display abnormally strong (dynein-dependent) spindle movements and ectopic spindle positioning (Rose and Kemphues,

1998; Tsou et al., 2002, 2003). The exact mechanism of LET-99 action and its relationship to CSNK-1/PPK-1 remain to be clarified.

The link between G-protein signaling and force generation is clear. Gα/GPR-1/2 regulates the dynein motor complex at the cortex (Couwenbergs et al., 2007; Nguyen-Ngoc et al., 2007). Upon downregulation of dynein or GPR-1/2 the asymmetry in the A–P forces is severely reduced. The dynein complex physically interacts with and depends on Gα and GPR-1/2 for its localization at the cortex. Interaction of dynein with Gα/GPR-1/2 requires the protein LIN-5 (Couwenbergs et al., 2007; Gotta et al., 2003; Nguyen-Ngoc et al., 2007; Park and Rose, 2008; Srinivasan et al., 2003). LIN-5 is related to mammalian NuMA, aMT-binding protein required for spindle organization. Thus, cortical dynein fulfills the criteria for a force generator, as it could pull on aMTs via its (−)-end-directed motor activity. This would require anchoring of dynein at the cortex, a task likely mediated by the LIN-5/GPR-1/2/Gα complex, through myristoylation of the Gα subunit (Nguyen-Ngoc et al., 2007). In addition, since GPR-1/2 is enriched posteriorly, more force generating complexes would form on the posterior cortex, explaining why pulling is stronger at this site. This fits very nicely to the predictions of computer modeling (Grill and Hyman, 2005; Grill et al., 2003; Kozlowski et al., 2007). It will be very interesting to see whether force generation by the dynein complex is coupled to modulation of aMT dynamics and/or differences between the anterior/posterior cortical domains in the processivity of the dynein motor, as also suggested by mathematical analysis (Couwenbergs et al., 2007).

Many aspects of the mechanism of force generation have to be clarified still. For example, although both spindle severing experiments and computer modeling concluded that aMT-dependent forces are generated at the cortex, G-protein signaling could regulate activity of factors involved in force generation on the centrosome as well. In this respect, GOA-1, GPA-16, and GPR-1/2 strongly localize on asters (Srinivasan et al., 2003), while the protein LIN-5 primarily associates with spindle poles and may link cortical G-protein signaling to centrosomal control (Du and Macara, 2004; Lorson et al., 2000; Srinivasan et al., 2003). In addition, CSNK-1 moves from the plasma membrane to the asters (Panbianco et al., 2008), while GPR-1/2 seems to asymmetrically localize only on one centrosome in *csnk-1*(*RNAi*) embryos (Panbianco et al., 2008).

The role of actin filaments in force generation is also unclear. It has been reported that microfilaments are not required for spindle displacement after establishment of embryonal polarity (Hill and Strome, 1988, 1990; Strome and Hill, 1988). However, more recent studies show that actin is required for spindle displacement and cortical localization of PAR-2 and PAR-3 even after polarity establishment (Severson and Bowerman, 2003) and microfilament disruption prevented spindle rotation in two-cell embryos (Hyman and White, 1987; Severson and Bowerman, 2003).

Finally, it is also not known whether actin- or MT-dependent motors other than dynein are involved in asymmetric force generation. Modeling predicts that a single kind of motor would suffice to drive spindle movements, but this would be surprising given the redundancy of biological systems.

3.2.1.2. Spindle-pole flattening Flattening of the posterior spindle pole during anaphase of the zygotic division is most likely caused by the strong microtubule-dependent forces acting on this pole. This is consistent with the observation that both asters adopt a flattened morphology in *par-3* mutants, in which the forces pulling on both asters are similar to those applied to the posterior pole in wild-type cells (Cheng et al., 1995; Severson and Bowerman, 2003). In addition, either microfilament disruption, down-regulation of Gα or GPR-1/2, RNAi depletion of dynein and dynactin or disruption of the MT cytoskeleton prevented spindle-pole flattening (Colombo et al., 2003a; Gotta and Ahringer, 2001; Gotta et al., 2003; Severson and Bowerman, 2003). This data strongly suggest that pole flattening and spindle displacement rely on the same mechanism.

Flattening of one spindle pole is a feature of other asymmetric cell divisions as well. For example, morphological differences between the spindle poles are observed during embryonic divisions of the mollusks *Spisula* and *Pholas* (Dan and Tanaka, 1990; Guerrier, 1970b; Kuriyama et al., 1986) and sea urchins (Schroeder, 1987). Spindle asymmetry in sea urchins resembles spindle asymmetry in *C. elegans*: the spindle gets displaced toward one cell end and one pole flattens (Fig. 4.14C). Like in *C. elegans*, the two spindle poles nucleate astral microtubules with different dynamics. The free aster nucleates microtubules that reach a length of 15 μm, while astral MTs from the cortically attached pole only grow to 5 μm. Cortical polarity is also responsible for spindle asymmetry in ascidians (Patalano et al., 2006). The cortically attached spindle pole is attracted by a specialized cortical structure called the centrosome attracting body (CAB). Astral microtubules from the cortically proximal centrosome contact the CAB; centrosome attraction by the cortical CAB complex involves probably activation of microtubule-associated motors or microtubule shortening. However, there are also dissimilarities between worms and ascidians concerning asymmetric spindle morphology. The CAB consists of a mass of endoplasmic reticulum containing asymmetrically segregated mRNAs, an electron dense matrix, and the cortical PAR-3/PAR-6/aPKC complex. Therefore, in the sea urchin aMTs from the flattened spindle pole associate with the PAR-3 domain, whereas in *C. elegans* the flattened spindle pole is associated with the posterior PAR-1/PAR-2 domain (Patalano et al., 2006; Schroeder, 1987). In addition, the difference in morphology between the two poles is already evident during prometaphase in ascidians, but only later (anaphase to cytokinesis) in *C. elegans*. Finally, the spindle pole in ascidians

does not adopt a truncate morphology but rather flattens against and attaches to the adjacent cortex.

3.2.2. Spindle asymmetry during second embryonic division

During the second embryonic division in worms, the smaller posterior cell P1 divides asymmetrically and gives rise to two cells with different sizes and developmental fates. The P1 cell is polarized, similar to the zygote, with cortical PAR-1 and PAR-2 posteriorly and the PAR-3 complex at the anterior cortex (Fig. 4.11B). However, contrary to the first division, the nucleus is displaced toward the anterior PAR-3 domain and the spindle forms transversely to the A–P axis. Subsequently, the spindle rotates 90° and aligns with the A–P axis while remaining anteriorly displaced. The molecular mechanism of spindle rotation remains to be clarified. As in the zygote, cortical polarity is required for spindle displacement and rotation, since both are disrupted in *par* mutants (Fig. 4.11B). One model suggests that rotation of the spindle depends on the interaction of astral microtubules with a cortical site at the border between the AB and the P1 cell, which is a remnant of the previous cytokinesis and contains dynactin (Hyman, 1989). After severing the connection of the one pole to this site with a laser, this cortical site is capable of capturing the opposite pole, suggesting that capturing of the spindle pole is random (Hyman, 1989). Thus, in P1, cortical polarization dictates asymmetric spindle displacement, probably through regulation of dynamics of the aster that happens to be close to this specific cortical site.

However, the phenotype of P1 cells bearing the *spn-4* maternal effect embryonic lethal mutation, suggested that the spindle itself is able to induce polarization of the cell cortex (Gomes et al., 2001). In the P1 cell of *spn-4* embryos the spindle fails to rotate, and the axis of cell polarity is respecified at 90° to the A–P axis of the embryo. The cortex close to one spindle pole contains the PAR-1 and PAR-2 proteins in association with polarized cytoplasm, and the cortex surrounding the other pole bears the PAR-3 complex. As a result, the P1 cell undergoes an asymmetric division but in a 90° angle to a normal P1 division. Based on this phenotype, Gomes et al. proposed that the poles of the spindle become polarized and respecify the axis of cell polarity of the P1 cell in *spn-4* embryos. Indeed, centrosomes are capable to act as cortical ''polarizers.'' For example, the sperm centrosome is responsible for the cortical polarization after fertilization in worms (Cowan and Hyman, 2004; Cuenca et al., 2003) and centrosomes are capable of polarizing the cortex and inducing asymmetric division in cultured NBs (de Anda et al., 2005). In addition, a pathway for microtubule-induced polarity has been identified in *Drosophila* NBs (Siegrist and Doe, 2005), suggesting that a similar pathway may also be active in the *C. elegans* embryo.

It is not known how the decision to form a specific cortical domain over a centrosome is made in *spn-4* mutant cells, and whether it is stochastic or

relates to the age or some other property of the centrosomes. Isolation of other mutants that display the *spn-4* phenotype would help to shed light on the molecular mechanism of cortical polarization by the spindle. Conversely, it is also not clear whether both centrosomes/spindle poles have the same "affinity" for both cortical domains (PAR-1/PAR-2 or PAR-3). During P1 spindle rotation, both centrosomes seem equally capable to drive spindle displacement and associate with the PAR-3 domain, as shown by the laser ablation experiments already described (Hyman, 1989). However, since interaction with the cortex depends on astral microtubules, it is possible that after severing off microtubules of one pole, the opposite pole is captured, because it is the only source of intact aMTs available at this moment.

3.3. Spindle asymmetry in *Drosophila* nervous system

Some of the most well-studied cases of spindle asymmetry are encountered in stem cells of the *Drosophila* central nervous system (CNS) (Gonczy, 2008; Yu et al., 2006). Division of *embryonic* NBs gives rise to two cells: one NB and one ganglion mother cell (GMC). During NB division, a classical spindle forms and aligns with its axis parallel to the neuroepithelial layer. At metaphase, the spindle is placed in the center of the cell and rotates by 90°, aligning with the apical–basal axis of the epithelium (Kaltschmidt et al., 2000). The NB spindle displays three asymmetric characteristics already evident at metaphase and become more pronounced in anaphase and telophase spindles (Fig. 4.12A). (1) The spindle is asymmetrically displaced toward the basal side of the NB. (2) The apical aster grows in size and nucleates a more robust aster than the basal pole that gradually loses its aMT-nucleating activity. (3) The geometry of the spindle is asymmetric at telophase, the midbody lies asymmetrically between the spindle poles and the distance from the midbody to the basal centrosome (basal arm) is shorter compared to the distance from the midbody to the apical centrosome (apical arm). Cell cleavage takes place at the plane of the midbody and thus the cleavage furrow is placed asymmetrically between the spindle poles (a very uncommon feature). The result of asymmetric spindle geometry and spindle translocation to the basal side is a highly asymmetric division: the diameter of the daughter NB is three times the diameter of the GMC. Mutations that abrogate both spindle displacement and asymmetric spindle geometry (like *baz*, *pins* double mutations) lead to high occurrence of symmetric NB divisions that produce equal-sized daughters, while NBs with mutations deactivating only one process display low frequency of symmetric divisions that retain some degree of cell size difference.

Importantly, spindle alignment with cell polarity strongly correlates with spindle displacement and generation of asymmetric spindle geometry: spindles that fail to align with the polarized cortex are always symmetric,

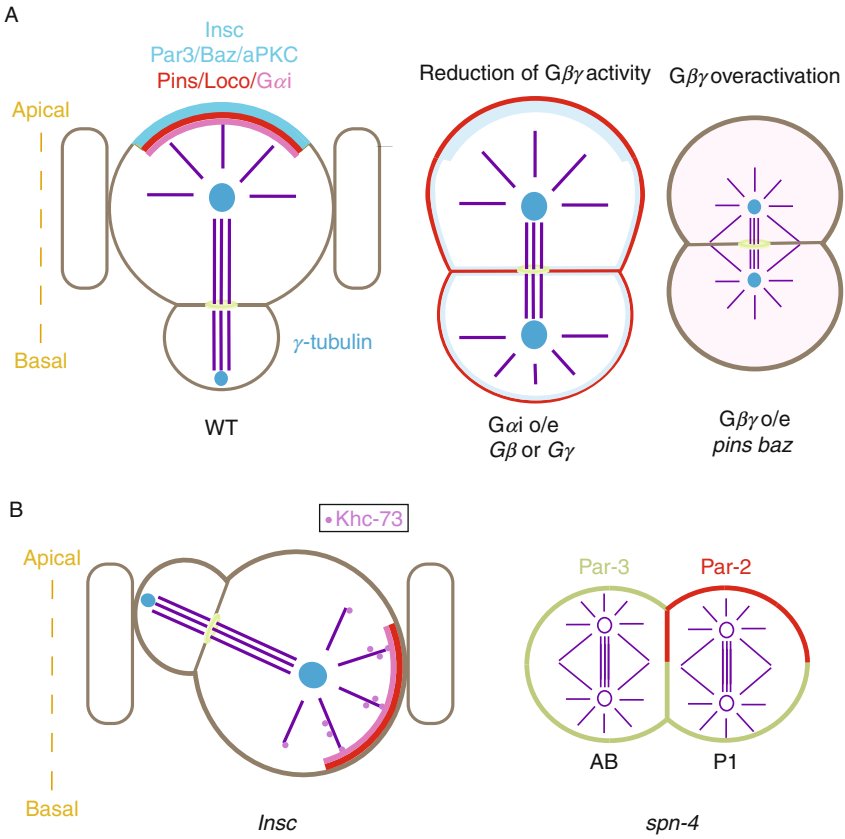

Figure 4.12 Spindle asymmetry during embryonic neuroblast divisions in *Drosophila*. (A) The spindle is displaced basally (bottom), the apical centrosome nucleates a more robust aMT array and contains higher amounts of γ-tubulin than the basal centrosome. The basal arm of the spindle is shorter than the apical arm. The cortex is polarized: the Insc/Par3 complex controls spindle displacement and the Pins/Gαi/Loco complex spindle displacement and spindle morphology; they form an apical cortical crescent above one centrosome. Spindle asymmetry is abrogated when G-protein signaling is perturbed. Gαi overexpression or mutation in Gβ or Gγ causes an apical-like symmetric spindle; mutation of both apical complexes or Gβγ overexpression results in a symmetric spindle with basal characteristics (Pins/Gαi is mislocalized in the cytoplasm). (B) The centrosome is able to polarize the cortex and form a Pins crescent when the spindle forms off the apical–basal axis in *insc* mutants. The kinesin Khc-73 participates in cortical polarization through interaction with the proteins Dlg and Mud (not shown), both of each associate with Pins. Cortical polarization by the centrosome in fly *insc* neuroblasts resembles polarization of the PAR-2 complex over one centrosome of misaligned spindles in the P1 cell in *spn-4* mutant worm embryos. Note that in wild-type worm embryos the spindle aligns horizontally in the P1 cell.

accompanied by symmetric cell divisions (Izumi et al., 2006; Siller et al., 2006). Two cortically polarized complexes with partly redundant functions are involved in generation of spindle asymmetry in *Drosophila* NBs: the Par3 (Baz)/Par6/DaPKC and the Pins/Gαi/Loco complex are both required for the correct outcome of the asymmetric division. Similar to the Par complex in *C. elegans* embryos, the *Drosophila* Par complex, consisting of the Par-3 ortholog Bazooka (Baz), and the proteins Par6 and DaPKC, organizes cortical polarity, since mutations of the Par complex lead to defects in organization of cortical apical–basal polarity and segregation of cell fate determinants (Petronczki and Knoblich, 2001; Wodarz et al., 1999, 2000). Par3/Par6/DaPKC form a cortical crescent over the large apical centrosome from metaphase to telophase.

The Pins/Gαi/Loco complex acts through receptor-independent heterotrimeric G-protein signaling (Bellaiche and Gotta, 2005; Hampoelz and Knoblich, 2004). Key factors are the G-protein complex consisting of (a) the Gαi, Gβ13F, and the Gγ1 subunits and (b) the regulators/effectors of G-protein signaling, the proteins Partner of Inscuteable (Pins) and Locomotion-defective (Loco) (similar to the GPR-1/2 proteins in *C. elegans*), that act as a guanine-nucleotide dissociation inhibitors (GDI) for Gαi (Schaefer et al., 2000; Yu et al., 2005). Like Par3/Par6/DaPKC the Pins/Loco/Gαi complex forms a crescent at the cortex overlying the centrosome on the prospective apical daughter and is linked to the Par complex by the protein Inscuteable (Cai et al., 2003). The protein Gβ13F (and possibly Gγ1) localize mainly uniformly at the cortex (Izumi et al., 2004), and are required for correct localization of both the Par and Pins/Gαi complexes (Fuse et al., 2003; Schaefer et al., 2001).

3.3.1. Asymmetric spindle displacement

The fact that G-protein signaling affects localization of Baz/Par6/DaPKC complicates analysis of the contribution of G-protein signaling in spindle displacement. Downregulation of the Par complex does not affect Pins/Gαi or Gβ13F and Gγ1 localization and DaPKC(*RNAi*) or *baz* mutant NBs show only mild defects in spindle displacement toward the basal axis, while largely retaining asymmetric spindle geometry (Cai et al., 2003; Fuse et al., 2003). This data suggest that the Par complex functions mainly in spindle displacement.

Deactivation of the genes for Gβ13F and Gγ1 that affect both G-protein signaling and largely Par complex localization reduces both asymmetric spindle geometry and spindle displacement (Fuse et al., 2003; Izumi et al., 2004; Yu et al., 2005). Some residual asymmetry in sibling size is contributed by spindle displacement and is abrogated through mutation of *Baz*. Thus, simultaneous deactivation of both G-protein signaling and the Par complexes (like in *pins*, *baz*, or *Gβ13F*, *baz* double mutant NBs) has additive defects and completely abrogates spindle asymmetry and

asymmetric division. Based on this analysis, it was proposed that G-protein signaling affects, in addition to spindle geometry, spindle displacement, similar to *C. elegans* embryos. Indeed, the system coupling cortical G-protein signaling to control of aMT dynamics and generation of asymmetric forces on the spindle is conserved between worms and flies. The proteins Pins and Gαi interact *in vitro* and *in vivo* with mushroom body defect (Mud), the homolog of worm LIN-5 (Section 3.2.1.1) and mammalian NuMA, a protein that organizes MT (−)-ends at the spindle pole (Bowman et al., 2006; Izumi et al., 2006; Siller et al., 2006; Srinivasan et al., 2003). Mud localizes as a crescent to the apical cortex in a Pins/Gαi-dependent fashion. Importantly, in *mud* mutant NBs Par and Pins/Gαi polarity establish normally, but the spindle fails to align with the cortical Par and Pins/Gαi crescent. Therefore, Mud acts downstream of the cortical complexes to couple spindle alignment to cell polarity. Therefore, NuMA/Mud/LIN-5 is a conserved link between Gαi at the cortex and the centrosome. Whether Mud/Pins/Gαi anchors dynein at the cortex (as postulated for the LIN-5/GPR-1/2/Gα complex in worms) and whether dynein is involved, together with Mud, in asymmetric force generation and spindle displacement remains to be investigated. Notably, the situation between worms and flies is not completely analogous. In fly NBs both the Par and Pins/Gαi complexes localize apically and the spindle is displaced toward the basal cortex in NBs opposite to worm embryos, where the spindle displaces toward the GPR-1/2-enriched posterior cortex that is devoid of the Par-3 complex (see Fig. 4.10).

3.3.2. Asymmetric spindle geometry

Heterotrimeric G-protein signaling controls spindle geometry. Mutations in *Gβ13F* and *Gγ1* result in formation of apical-like symmetric spindles with two long arms (Cai et al., 2003; Fuse et al., 2003; Yu et al., 2003). Conversely, simultaneous overexpression of the Gβ13F and Gγ1 subunits leads to basal-like spindles with short arms (Fuse et al., 2003). Based on these observations (and other data), two mechanisms were proposed for generation of asymmetric spindle geometry: either Pins/Loco/Gαi promote the elongation of the spindle arm on the apical side or Gβ13F and Gγ1 act on the basal side to suppress the length of the basal arm. It is not clear whether the Gβ13FGγ1 complex acts directly or whether it indirectly affects spindle asymmetry by modulating localization or activity of Gαi. Downregulation of Gαi has only minor effects on the asymmetry of division (however, other Gα subunits may act redundantly to substitute for Gαi functions), whereas overexpression of a Gαi-GDP-locked form of Gαi as sole cellular Gαi source causes symmetric spindles with two apical-like arms and asters and high frequency of symmetric divisions, resembling *Gβ13F* and *Gγ1* mutant NBs. This is in agreement with the notion that Gαi-GDP sequesters Gβγ. Overexpression of a Gαi-GTP-locked form

causes much milder perturbation in asymmetry of NB divisions (Yu et al., 2005), suggesting that Gαi-GTP is not the active form of Gαi.

How does G-protein signaling control MT dynamics and spindle geometry? The large apical aster of the spindle contains higher amounts of γ-tubulin and components of the γ-TuRC complex than the basal aster (Kaltschmidt et al., 2000). It is possible that G-protein signaling controls γ-tubulin levels and aMT-nucleating activity on centrosomes. However, the role of γ-tubulin level differences between centrosomes in the generation of arm asymmetry is unclear. In *asterless* (*asl*) mutants asters fail to form and γ-tubulin is absent from the spindle poles, yet spindle geometry is not affected. This suggests that γ-tubulin levels on the centrosomes are not the cause of spindle asymmetry (Giansanti et al., 2001). However, it is intriguing that astral microtubules and their interactions with the cortex are dispensable for generation of asymmetric spindle morphology, since spindle alignment, which depends on aMTs, is required for spindle asymmetry. In view of the correlation between centrosome behavior and γ-tubulin/astral microtubule levels in *larval* NB divisions and protostomes (Sections 3.3.4 and 3.5), it would be interesting to closely investigate the correlation between γ-tubulin levels and spindle geometry.

Another possibility is that spindle geometry is controlled by G-protein signaling through Mud/NumA. Mud localizes to the spindle poles and aMTs, functions in centrosome assembly (Izumi et al., 2006), while Mud/NuMA stabilize microtubules *in vitro* (Bowman et al., 2006; Haren and Merdes, 2002). However, Mud localization on the spindle poles does not depend on Pins/Gαi and Mud accumulates over the short basal centrosome at telophase, at a time when the spindle pole is most inactive. This suggests that Mud acts downstream of the cues that dictate aster and arm asymmetry. Therefore, other microtubule-associated proteins must be involved in the generation of asymmetric spindle morphology.

3.3.3. Polarization of cortex by the spindle

As described so far for embryonic NBs, cortical polarity is established first and then acts to induce asymmetric spindle displacement and geometry upon spindle alignment. However, when cortical polarity in NBs is perturbed, a complementary mechanism utilizes signals that originate at the centrosome to polarize the cortex and align the axis of cortical polarity with the axis of the spindle (Siegrist and Doe, 2005). In mitotic *insc* mutants the Insc/Par and the Pins/Gαi complexes are mislocalized until metaphase and the spindles are mispositioned. However, in metaphase a cortical crescent of Pins/Gαi overlying one of the centrosomes is formed, the spindle assumes asymmetric morphology and the cells proceed to divide asymmetrically, but off the apical–basal axis. Polarization of the cortex at metaphase depends on astral microtubules, the kinesin Khc-73, and the cortical protein Dlg. It has been proposed that interaction of the kinesin with Dlg changes the

conformation of Dlg, freeing a domain that binds Pins. Thus, interaction of aMT (+)-tips with cortical Dlg adjacent to the spindle pole/centrosome results in generation of a Dlg population that binds Pins and finally to polarization of Pins/Gαi. Intriguingly, the Pins/Gαi crescent overlies only one spindle pole, suggesting that only one pole of the metaphase spindle has the ability to polarize the cortex. Whether Khc-73 asymmetrically localizes only to aMTs from one spindle pole is unknown. This could mean that the two poles/centrosomes of the spindle are not equal and that the spindle in embryonic NBs is intrinsically asymmetric. Alternatively, once polarization of the cortex by one spindle pole is initiated, the other pole is somehow silenced and loses its polarizing ability. A third possibility is that the spindle does not possess any polarity and that feedback mechanisms amplify any polarization that stochastically starts at the cortical site closest to one spindle pole.

Indications for the existence of intrinsic spindle polarity come from observations of the behavior of centrosomes (Kaltschmidt et al., 2000). Prior to spindle formation in dividing embryonic NBs, centrosomes duplicate next to the basal or the apical cortex. After spindle formation, orientation of the 90° spindle rotation usually correlates with the position of centrosome duplication. Whenever a centrosome duplicates basally, the anterior centrosome moves to the apical site, resulting in anticlockwise spindle rotation; when the centrosome duplicates apically, the posterior centrosome moves apically, and the spindle rotates clockwise. This phenomenon suggests that the two centrosomes may not be equivalent and that their position inside the dividing NB is not random. The origin of centrosome differences is not clear but an obvious possibility is that it depends on centrosome age and maturation.

The ability of centrosomes to polarize the cortex may correlate with the activity of cell-cycle regulatory kinases on centrosomes. Indeed, Cdk1 associates with spindle poles and the activity of Cdk1 is required for correct spindle orientation and to asymmetrically localize Insc and Bazooka to the cortex (Tio et al., 2001). In addition, Polo and Aurora A kinases also localize at the centrosome are required for MT organization and have been shown to directly regulate polarization of aPKC (Wang et al., 2006, 2007). Therefore, the aMT-nucleating and cortex-polarizing activities of the centrosomes may reflect its association with Cdks, Aurora A, and Polo. In addition, E3 ligases or other factors involved in ubiquitin protein degradation may also be involved in cortical polarization by centrosomes. SCF-type ubiquitin ligases control activity of Polo and Cdk kinases on centrosomes (Bettencourt-Dias et al., 2005), while activity of APC/C cyclosome has been shown to promote cortical polarization in worms (Rappleye et al., 2002). Cortical polarization by astral MTs and/or centrosomes may be conserved between flies and worms: spindle-dependent cortical polarization in NBs is highly reminiscent of the spindle ability to redirect polarity in *spn-4* mutant worm embryos (Fig. 4.12B).

3.3.4. Behavior of spindle poles in NB divisions of *Drosophila* larva

Like embryonic NBs, NBs in the larva of *Drosophila* divide asymmetrically, to produce a bigger cell that retains NB potential and a GMC. Larval NBs, however, directly form the mitotic spindle in the final apical–basal orientation (Savoian and Rieder, 2002; Siller et al., 2005) instead of rotating the spindle by 90° like NBs (Fig. 4.13A). In larval NBs, one centrosome stays immobile at the apical cell cortex, while the other centrosome displays very dynamic movements through the cytoplasm (Rebollo et al., 2007; Rusan and Peifer, 2007). These movements pause prior to nuclear envelope breakdown and the migrating centrosome stabilizes its position at the basal cortex. Like in embryonic NBs, the activity of the centrosomes is different in these cells: the apical centrosome nucleates a major aster, while the mobile centrosome has poor MT-nucleating activity that is upregulated only when cells enter mitosis. Moreover, the spindle is asymmetric at late anaphase, with two unequal arms, like in embryonic NBs. The cortex influences the behavior of centrosomes, because in *insc* mutants the apical centrosome dissociates from the cortex and behaves like the basal

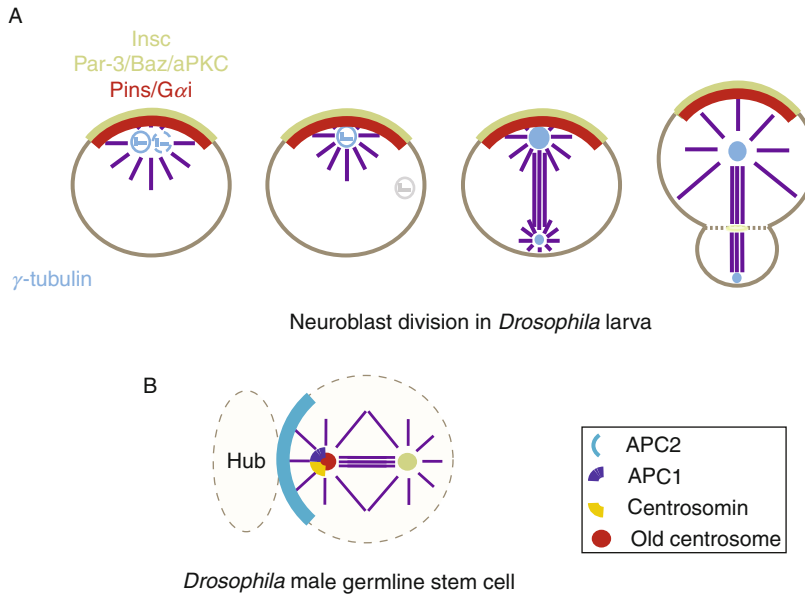

Figure 4.13 (A) Division of *Drosophila* larval neuroblasts. One centrosome remains attached to the apical cortex, while the other moves freely through the cytoplasm and finally reaches the basal side. The mobile centrosome starts to nucleate aMTs only during mitosis. The spindle is otherwise similar to the spindle of embryonic neuroblasts. (B) Age-based spindle asymmetry in *Drosophila* germ line stem cells. The old centrosome stays attached to the Hub through the interactions of aMTs with APC proteins, while the new centrosome is placed distally to the Hub.

centrosome. In addition, in wild-type cells the "dominant" apical centrosome retains factors required for aster nucleation such as γ-tubulin and centrosomin, while the mobile centrosome loses these factors at mitotic exit and regains them in next mitosis. It is not known whether recruitment of γ-tubulin and centrosomin depends solely on association of the centrosome with the cortex or also on centrosomal properties. Similar to embryonic NBs, the ability of the centrosomes to nucleate asters is linked to the activity of the Polo-like kinase (McInnes et al., 2006), raising the possibility that cortical signals and centrosome-based events are integrated at the level of Polo-like kinase. Taken together, this data indicate that asymmetric behavior of the centrosomes in larval NBs depends both on cortical polarity and on intrinsic differences between centrosomes. It is not known whether the asymmetric behavior of the centrosomes relates to their age, but it is very likely that the old centrosome is the one that is anchored at the apical cortex, similar to the division of stem cells of the fly male germ line.

3.4. Inheritance of centrosomes in *Drosophila* germline

A very similar case of spindle asymmetry is encountered during asymmetric divisions in the male germ line of *Drosophila*. These stem cells divide asymmetrically producing one stem cell and one cell that differentiates, first to transit amplifying cells (collectively called spermatogonia), which later differentiate to sperm. Germ line stem cells (GSCs) are maintained in a niche formed by somatic cells at the apical tip of the testes called the Hub. Contact of the stem cells to the Hub is essential for maintenance of the stem cell character, due to signals produced from the Hub that activate the JAK–STAT pathway in the stem cell. During asymmetric division, the daughter that will differentiate must be positioned distant to the Hub to escape signaling from the niche. Therefore, during GSC division the spindle is positioned in such a way that one spindle pole remains in close contact with the Hub, while the other lies in a distant position (Fig. 4.13B). By short transient expression of GFP fused to the pericentrin C-terminus, Yamashita et al. were able to label centrosomes and follow their fate during subsequent divisions. They demonstrated that the old centrosome stays associated with the cortex close to the Hub, much like one centrosome stays associated with the apical cortex in larval NBs. This is achieved by retention of the old centrosome at the Hub-associated cortex upon centrosome duplication (Yamashita and Fuller, 2008; Yamashita et al., 2003, 2007). Anchoring of the old centrosome depends on interactions of astral microtubules with the adherens junction at the cortex adjacent to the Hub. These interactions are mediated by the Apc2 protein, one of the two *Drosophila* homologs of the adenomatous polyposis coli tumor suppressor, resembling association of Kar9 with the old SPB in budding yeast (Section 3.1.1). Similar to what is observed in larval NBs, the mother centrosome nucleates astral

microtubules, while the daughter centrosome lacks nucleating activity until mitosis. Therefore, it seems that lack of astral microtubules allows the daughter centriole to freely move around the cytoplasm until mitosis. Indeed, in centrosomin mutants defective in anchoring of aMTs to the centrosome, the position of mother and daughter centrosomes relative to the Hub is random (Yamashita et al., 2007). It is not known what prevents the daughter centrosome from nucleating aMTs. Nucleating capacity could be acquired gradually, as the centrosome matures. Thus, in *Drosophila* germ line cells spindle asymmetry is based on intrinsic, age-dependent differences between the two centrosomes and on cortical polarity factors, like Insc.

Recent data also indicate the existence of a checkpoint similar to the budding yeast SPOC in male GSCs (Cheng et al., 2008). In *Drosophila* spermatogenesis declines with time, while the number of stem cells remains constant. Decreased spermatogenesis seems to be a result of dedifferentiation of spermatogonia back to GSCs that occurs with age. GSCs arising from dedifferentiated spermatogonia probably cannot initially orient centrosomes relative to the niche, leading to increase of the number of GSCs with Hub-detached, misoriented centrosomes. Importantly, cells with misoriented centrosomes seem to arrest in the cell cycle before spindle formation, until correct centrosome position is restored, whereupon a correctly aligned spindle forms. It is not known whether the old centrosome attaches to the niche in these cells after centrosome alignment. Although the delay of the cell cycle occurs prior to spindle formation in GSCs with misoriented centrosomes, it is reminiscent of the cell-cycle arrest induced by the SPOC in budding yeast cells with misaligned anaphase spindles. A pathway similar to the SPOC may act to delay the cell cycle in *Drosophila* GSCs with misoriented centrosomes, or when the centrosome has not attached to the cortex. Decline in spermatogenesis with age would be then due to delay in stem cell division cycle as a result of centrosome misorientation—essentially as a result of the checkpoint.

Age-dependent asymmetric centrosome inheritance is evident in some but not in all asymmetrically dividing stem cells, even in the same organism. In female *DSas-4* mutant flies that lack centrioles and aMTs, NB division (that requires centrosome function) is affected, while female GSC asymmetric division is unperturbed (Basto et al., 2006). In female *DSas-4* mutant GSCs one pole of the mitotic spindle is still attached to the niche, like in wild-type flies (Stevens et al., 2007). Spindle-pole attachment occurs through the spectrosome, a membrane-rich organelle, that contains cytoskeletal adducin-like proteins, spectrin, and ankyrin (Deng and Lin, 1997). Thus, a polarity-dependent mechanism ensures proper spindle alignment in these cells, suggesting that centrosome age is only one of the factors determining asymmetric behavior of spindle poles in stem cells. An analogous structure, the fusome, connects to one spindle pole and organizes the fixed pattern of the divisions of the GSC descendants. Asymmetric attachment of one spindle pole to the fusome is mediated by cytoplasmic dynein

(McGrail and Hays, 1997). Thus, polarity and centrosome-age based, dynein- or APC-dependent mechanisms may be utilized in parallel to ensure spindle alignment with cell polarity during asymmetric divisions.

3.5. Generation of spindle asymmetry in *Annelids*

An example of extreme spindle asymmetry that depends on regulation of the aMT-nucleating activity of centrosomes is found in the first embryonic division of the freshwater oligochaete *Tubifex* (Fig. 4.14A). In this case, a monastral spindle forms because one centrosome is extruded into the polar body during completion of meiosis and the remaining centrosome does not duplicate before the onset of the first division. As a result, one spindle pole contains a centrosome and nucleates astral microtubules, while the other pole is centrosome-less and is formed by focused microtubules of the interpolar spindle (Ishii and Shimizu, 1997; Shimizu et al., 1998). Importantly, artificial generation of cells that contain a centrosome at each spindle pole (diastral spindle) leads to symmetric division. This suggests that cortical polarity does not play a role in the generation of spindle asymmetry during the first mitotic division in *Tubifex*. However, during the second division, which is also asymmetric, the anaphase spindle adopts an asymmetric configuration with one flat and truncate pole, similar to the *C. elegans* asymmetric spindle. In this case, spindle asymmetry seems to depend on cortical polarity, since it is abrogated after treatment of cells with cytochalasin D (Takahashi and Shimizu, 1997). Thus, *Tubifex* probably utilizes both available mechanisms for the generation of spindle asymmetry: downregulation of centrosomal activity of one spindle pole and transmission of cortical polarity to the spindle.

A variation of the latter theme is encountered during the first embryonic division of the leech *Helobdella robusta* (Fig. 4.14B). In this embryo, a classical symmetric metaphase spindle is formed with one centrosomal aster at each spindle pole. Prior to anaphase, one spindle pole becomes condensed, losing most of its astral microtubules, while the other pole enlarges and adopts the morphology of an aster with a hollow center (Ren and Weisblat, 2006). Importantly, downregulation of one aster is accompanied by transient loss of γ-tubulin, which precedes aster condensation and recovers at anaphase (Ren and Weisblat, 2006). Disruption of microtubule dynamics using taxol or nocodazole leads to spindle symmetrization followed by a symmetric division. The asymmetry of the mitotic spindle does not seem to rely on cortical polarity, since there is no evidence of PAR protein homologs in *Helobdella* (Nelson and Weisblat, 1992). It would be interesting, however, to investigate the effects of depolymerizing the actin cytoskeleton in the first divisions of *Tubifex* and *Helobdella*.

Another feature of spindle asymmetry in *Helobdella* is the asymmetry of the interpolar spindle. In classical preanaphase spindles, the distance of the spindle pole to the kinetochore is the same for both spindle arms. In the case

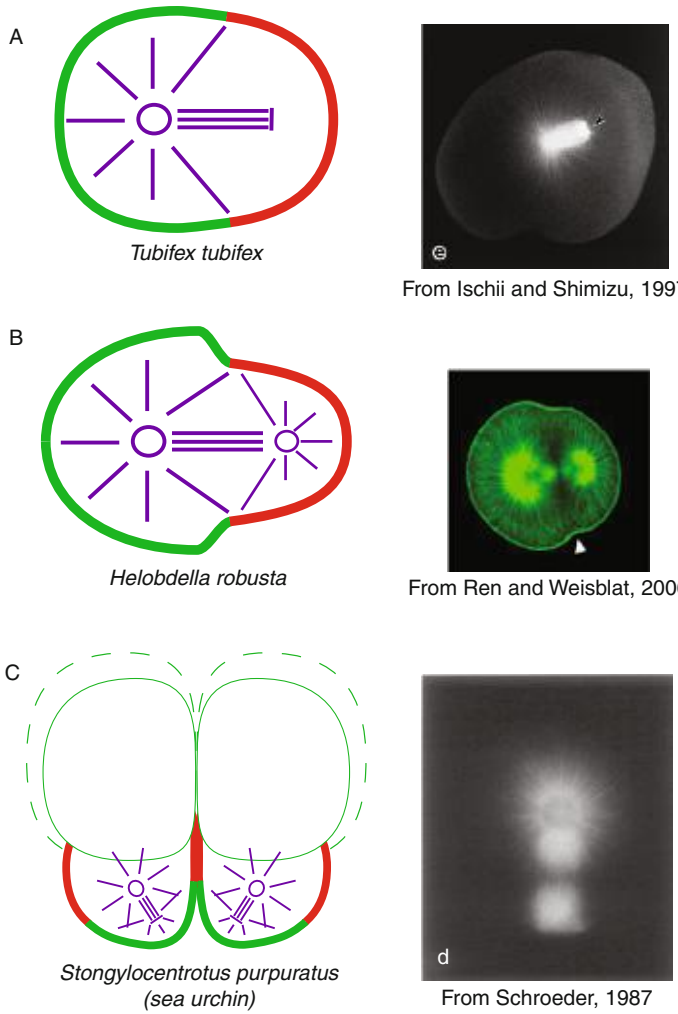

Figure 4.14 Examples of asymmetric spindles with inactivated spindle poles. Different color/grey shading of the cortex indicates the plane of cleavage and the result of the future asymmetric division. (A) In *Tubifex*, the spindle is formed by a MT-nucleating centrosome and an acentrosomal spindle pole. (B) The spindle of *Halobdella* resembles neuroblast spindles in flies: it is displaced asymmetrically toward one cortical site, while the two poles display different MT-nucleating activities and contain different levels of γ-tubulin; the two spindle arms also differ in size. (C) The ascidian spindle is asymmetrically displaced with one flat spindle pole, resembling the spindles in asymmetrically dividing worm embryos.

of *Helobdella*, however, the distance between the anterior aster and the kinetochore is larger than the corresponding distance to the posterior aster (Ren and Weisblat, 2006), which might be the case for *Tubifex* too (Ishii and Shimizu, 1997). In *Helobdella*, spindle arm asymmetry develops in

parallel to the deactivation of one spindle pole (Ren and Weisblat, 2006). It is possible that the differences in levels of MT stability between centrosomes cause the metaphase plate to shift toward the posterior centrosome, due to stabilization of microtubules on the anterior side and vice versa. The asymmetric spindle of *Halobdella* is remarkably reminiscent of the asymmetric spindle during division of *Drosophila* NBs.

Many important questions remain open concerning the role of spindle asymmetry during the divisions of stem cells. For example, the biological significance of the bias in centrosome behavior and segregation is not known. What is the phenotype when centrosome segregation is perturbed and the new centrosome remains in the stem cell? One possibility is that unequal centrosomes serve the asymmetric segregation of cell fate determinants during asymmetric cell divisions, as is the case in the early embryo of the mollusk *Ilyanassa obsoleta*.

3.6. Asymmetric segregation of developmental factors in *Ilyanassa obsoleta*

A special kind of spindle asymmetry has been observed during early embryonic asymmetric cleavages of the mollusc *Ilyanassa obsoleta* and is probably relevant for other related protostomes (Lambert and Nagy, 2002). In this organism, from interphase until prometaphase of the four-cell embryo, one spindle pole associates with specific mRNAs encoding factors for embryonic patterning (Fig. 4.15). At prometaphase the mRNAs are transported from one spindle pole to the adjacent cortical site so that they are inherited exclusively by one daughter cell after cytokinesis. Thus, in a prometaphase spindle of *Ilyanassa* one spindle pole is associated with mRNAs and the other not. Centrosome-based mRNA sorting continues in following divisions and could be followed up to the 24-cell stage. The microtubule cytoskeleton is required for accumulation of the mRNAs on the centrosome, but not for their transport from the centrosome to the cortex, which is actin-dependent. Importantly, when cytokinesis is inhibited by the use of cytochalasin B, generating cells with two centrosomes within the same cytoplasm, one centrosome remains associated with the mRNAs and the other not, suggesting that intrinsic differences between centrosomes result in the asymmetric accumulation of mRNAs. It is not clear what these differences could be and how they are generated. Something must prevent partitioning of specific mRNAs to one centrosome, since these mRNAs are already centrosomally associated at the time of centrosome duplication. Spindle asymmetry is unlikely to rely on cortical polarity in this case, since treatment of the cells with cytochalasin does not disrupt centrosomal mRNA localization. A possible mechanism could rely on age-related differences of centrosomes. In this respect, it would be interesting to investigate whether mRNA would accumulate on one or both centrosomes residing in

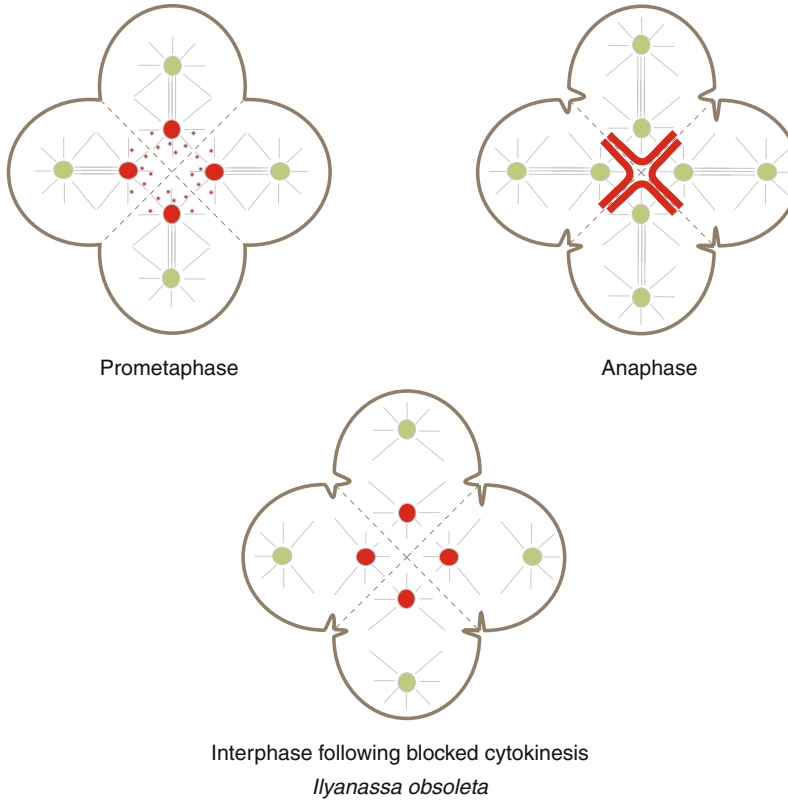

Figure 4.15 Spindle asymmetry utilized for asymmetric segregation of cell fate determinants in *Ilyanassa*. During interphase of the four-cell stage, mRNAs encoding patterning factors (small red/grey dots) associate with one centrosome (shown as a red/dark grey-filled circle, while the other centrosome is shown in green/light grey) in a MT-dependent manner. During mitosis, these mRNAs are transferred to the cortex next to the centrosome (thick red/dark grey lines) by an actin-dependent mechanism and are thus inherited by only one daughter. When cytokinesis is artificially inhibited, mRNAs still associate only with one centrosome during the following interphase.

the same cytoplasm after inhibition of cytokinesis and release of the mRNA from the centrosome using MT depolymerizing agents. At this stage, maturation of the younger centrosome must have been complete, predicting that both centrosomes would be able to associate with mRNA.

4. Concluding Remarks

It is obvious from the cases described in this chapter (which is by far not comprehensive) that many even seemingly symmetric spindles have an asymmetric organization. Asymmetries are mostly manifested in association

of spindle poles with different proteins or subcellular structures. Is it important that the two spindle poles have different compositions or properties and what is the function of this asymmetry? Is there a common theme regarding the mechanism of acquisition of spindle pole identity?

There is a strong correlation between perturbation of spindle asymmetry with malfunctions in cellular processes. In both yeasts, normal cell-cycle progression is liked with asymmetric association of cell-cycle regulators with the spindle poles, while perturbation of asymmetry correlates with defects in the cell cycle. For example, when SIN is overactive leading to formation of ectopic septa, SIN is active on both SPBs. During asymmetric cell divisions, spindle polarity strongly correlates with correct spindle positioning and correct outcome of the cell division. Still, such relationships do not necessarily prove that asymmetry is important for the cellular functions mentioned. Very few experiments have directly addressed the necessity of spindle asymmetry for the regulation of a cellular process. One such experiment was recently performed by Pereira et al., where constitutive targeting of Bfa1 to both SPBs through fusion of the protein to the SPB component Cnm67 rendered MEN active and resulted in spindle disassembly of misoriented spindles in *kar9*Δ mutant cells. From these indications, we can postulate that spindle asymmetry is indeed important to support the functions it is involved in, at least in most cases.

Regarding the function of spindle asymmetry we can make only hypotheses. For the regulation of mitotic exit and cytokinesis in yeasts, it is probably important that the decision to proceed through the cell cycle is made only on one pole and not both, to avoid confusion of the system (in *S. pombe*) and to ensure that mitotic exit occurs only after the bud inherits an SPB in budding yeast. It is clear that the silencing of two SPBs during budding yeast meiosis is used for a developmental decision, similarly to the molusc *Ilyanasa obsoleta*. In contrast, it is not clear why cell abscission is asymmetric. It has been proposed that the accumulation of midbody rings in one cell body can serve as a marker for the number of divisions of the cell and thus as an aging marker. However, since these rings are simultaneously removed by autophagocytosis, it is not clear how such a counting mechanism could work.

The reason why the spindle should be asymmetric during asymmetric cell divisions is more obvious. In these cases, the cells use polarization of the spindle to reinforce spindle alignment with the axis of cell polarity. Like polarization of a compass needle is required for robust alignment with the earth magnetic field, a robust alignment of the spindle with the polarized actin cytoskeleton/cell cortex can be only achieved if the spindle becomes polarized as well. In this way, each spindle pole is committed to a certain cortical compartment, leading to stabilization the position of the spindle in respect to the axis of polarity. In addition, in the case of geometrically asymmetric spindles, the cell uses spindle asymmetry to achieve unequal

positioning of the division plane and a highly asymmetric division. In these cases, differentiation of the spindle poles is utilized to switch the equilibrium in a dynamic cellular process and fix it in a new state. In summary, differentiation of the spindle poles is used to determine and reinforce cellular decisions, regarding cell-cycle progression, developmental processes, or determination of the cleavage plane.

Finally, some common themes arise concerning the mechanisms that generate spindle asymmetry. It seems that an initial, intrinsic asymmetry between spindle poles that may arise stochastically, but often relies on the different age of the MTOCs, is amplified to achieve full pole differentiation. Central in the amplification procedure is the role of Ras-related or heterotrimeric G-protein signaling. We are far from understanding the molecular mechanisms involved in these processes, a goal that promises to be a very exciting future research field.

REFERENCES

Adames, N.R., Cooper, J.A., 2000. Microtubule interactions with the cell cortex causing nuclear movements in *Saccharomyces cerevisiae*. J. Cell Biol. 149, 863–874.

Adames, N.R., Oberle, J.R., Cooper, J.A., 2001. The surveillance mechanism of the spindle position checkpoint in yeast. J. Cell Biol. 153, 159–168.

Adams, I.R., Kilmartin, J.V., 2000. Spindle pole body duplication: a model for centrosome duplication? Trends Cell Biol. 10, 329–335.

Afshar, K., Willard, F.S., Colombo, K., Johnston, C.A., McCudden, C.R., Siderovski, D.P., et al., 2004. RIC-8 is required for GPR-1/2-dependent Galpha function during asymmetric division of *C. elegans* embryos. Cell 119, 219–230.

Albertson, D.G., 1984. Formation of the first cleavage spindle in nematode embryos. Dev. Biol. 101, 61–72.

Azimzadeh, J., Bornens, M., 2007. Structure and duplication of the centrosome. J. Cell Sci. 120, 2139–2142.

Bailly, E., Cabantous, S., Sondaz, D., Bernadac, A., Simon, M.-N., 2003. Differential cellular localization among mitotic cyclins from *Saccharomyces cerevisiae*: a new role for the axial budding protein Bud3 in targeting Clb2 to the mother-bud neck. J. Cell Sci. 116, 4119–4130.

Baird, G.S., Zacharias, D.A., Tsien, R.Y., 2000. Biochemistry, mutagenesis, and oligomerization of DsRed, a red fluorescent protein from coral. PNAS 97, 11984–11989.

Bajgier, B.K., Malzone, M., Nickas, M., Neiman, A.M., 2001. SPO21 is required for meiosis-specific modification of the spindle pole body in yeast. Mol. Biol. Cell 12, 1611–1621.

Bardin, A.J., Amon, A., 2001. MEN and SIN: what's the difference? Nat. Rev. Mol. Cell Biol. 2, 815–826.

Bardin, A.J., Visintin, R., Amon, A., 2000. A mechanism for coupling exit from mitosis to partitioning of the nucleus. Cell 102, 21–31.

Bardin, A.J., Boselli, M.G., Amon, A., 2003. Mitotic exit regulation through distinct domains within the protein kinase Cdc15. Mol. Cell. Biol. 23, 5018–5030.

Barral, Y., Parra, M., Bidlingmaier, S., Snyder, M., 1999. Nim1-related kinases coordinate cell cycle progression with the organization of the peripheral cytoskeleton in yeast. Genes Dev. 13, 176–187.

Barral, Y., Mermall, V., Mooseker, M.S., Snyder, M., 2000. Compartmentalization of the cell cortex by septins is required for maintenance of cell polarity in yeast. Mol. Cell 5, 841–851.

Basto, R., Lau, J., Vinogradova, T., Gardiol, A., Woods, C.G., Khodjakov, A., et al., 2006. Flies without centrioles. Cell 125, 1375–1386.

Beach, D.L., Thibodeaux, J., Maddox, P., Yeh, E., Bloom, K., 2000. The role of the proteins Kar9 and Myo2 in orienting the mitotic spindle of budding yeast. Curr. Biol. 10, 1497–1506.

Bellaiche, Y., Gotta, M., 2005. Heterotrimeric G proteins and regulation of size asymmetry during cell division. Curr. Opin. Cell Biol. 17, 658–663.

Bettencourt-Dias, M., Glover, D.M., 2007. Centrosome biogenesis and function: centrosomics brings new understanding. Nat. Rev. Mol. Cell Biol. 8, 451–463.

Bettencourt-Dias, M., Rodrigues-Martins, A., Carpenter, L., Riparbelli, M., Lehmann, L., Gatt, M.K., et al., 2005. SAK/PLK4 is required for centriole duplication and flagella development. Curr. Biol. 15, 2199–2207.

Bobola, N., Jansen, R.P., Shin, T.H., Nasmyth, K., 1996. Asymmetric accumulation of Ash1p in postanaphase nuclei depends on a myosin and restricts yeast mating-type switching to mother cells. Cell 84, 699–709.

Bornens, M., 2002. Centrosome composition and microtubule anchoring mechanisms. Curr. Opin. Cell Biol. 14, 25–34.

Bouquin, N., Barral, Y., Courbeyrette, R., Blondel, M., Snyder, M., Mann, C., 2000. Regulation of cytokinesis by the Elm1 protein kinase in *Saccharomyces cerevisiae*. J. Cell Sci. 113, 1435–1445.

Bowman, S.K., Neumuller, R.A., Novatchkova, M., Du, Q., Knoblich, J.A., 2006. The *Drosophila* NuMA Homolog Mud regulates spindle orientation in asymmetric cell division. Dev. Cell 10, 731–742.

Cai, Y., Yu, F., Lin, S., Chia, W., Yang, X., 2003. Apical complex genes control mitotic spindle geometry and relative size of daughter cells in *Drosophila* neuroblast and pI asymmetric divisions. Cell 112, 51–62.

Carvalho, P., Gupta Jr., M.L., Hoyt, M.A., Pellman, D., 2004. Cell cycle control of kinesin-mediated transport of Bik1 (CLIP-170) regulates microtubule stability and dynein activation. Dev. Cell 6, 815–829.

Castillon, G.A., Adames, N.R., Rosello, C.H., Seidel, H.S., Longtine, M.S., Cooper, J.A., et al., 2003. Septins have a dual role in controlling mitotic exit in budding yeast. Curr. Biol. 13, 654–658.

Caydasi, A.K., Pereira, G., 2009. Spindle alignment regulates the dynamic association of checkpoint proteins with yeast spindle pole bodies. Dev. Cell 16, 146–156.

Cerutti, L., Simanis, V., 1999. Asymmetry of the spindle pole bodies and spg1p GAP segregation during mitosis in fission yeast. J. Cell Sci. 112, 2313–2321.

Cerveny, K.L., Studer, S.L., Jensen, R.E., Sesaki, H., 2007. Yeast mitochondrial division and distribution require the cortical num1 protein. Dev. Cell 12, 363–375.

Chang, L., Morrell, J.L., Feoktistova, A., Gould, K.L., 2001. Study of cyclin proteolysis in anaphase-promoting complex (APC) mutant cells reveals the requirement for APC function in the final steps of the fission yeast septation initiation network. Mol. Cell. Biol. 21, 6681–6694.

Cheng, N.N., Kirby, C.M., Kemphues, K.J., 1995. Control of cleavage spindle orientation in *Caenorhabditis elegans*: the role of the genes par-2 and par-3. Genetics 139, 549–559.

Cheng, J., Turkel, N., Hemati, N., Fuller, M.T., Hunt, A.J., Yamashita, Y.M., 2008. Centrosome misorientation reduces stem cell division during ageing. Nature 456, 599–604.

Chiroli, E., Fraschini, R., Beretta, A., Tonelli, M., Lucchini, G., Piatti, S., 2003. Budding yeast PAK kinases regulate mitotic exit by two different mechanisms. J. Cell Biol. 160, 857–874.

Clifford, D.M., Wolfe, B.A., Roberts-Galbraith, R.H., McDonald, W.H., Yates III, J.R., Gould, K.L., 2008. The Clp1/Cdc14 phosphatase contributes to the robustness of cytokinesis by association with anillin-related Mid1. J. Cell Biol. 181, 79–88.

Colombo, K., Grill, S.W., Kimple, R.J., Willard, F.S., Siderovski, D.P., Gonczy, P., 2003a. Translation of polarity cues into asymmetric spindle positioning in *Caenorhabditis elegans* embryos. Science 300, 1957–1961.

Colombo, K., Grill, S.W., Kimple, R.J., Willard, F.S., Siderovski, D.P., Gonczy, P., 2003b. Translation of polarity cues into asymmetric spindle positioning in *Caenorhabditis elegans* embryos. Science 300, 1957–1961.

Couwenbergs, C., Spilker, A.C., Gotta, M., 2004. Control of embryonic spindle positioning and Galpha activity by *C. elegans* RIC-8. Curr. Biol. 14, 1871–1876.

Couwenbergs, C., Labbe, J.C., Goulding, M., Marty, T., Bowerman, B., Gotta, M., 2007. Heterotrimeric G protein signaling functions with dynein to promote spindle positioning in *C. elegans*. J. Cell Biol. 179, 15–22.

Cowan, C.R., Hyman, A.A., 2004. Centrosomes direct cell polarity independently of microtubule assembly in *C. elegans* embryos. Nature 431, 92–96.

Cuenca, A.A., Schetter, A., Aceto, D., Kemphues, K., Seydoux, G., 2003. Polarization of the *C. elegans* zygote proceeds via distinct establishment and maintenance phases. Development 130, 1255–1265.

Cuif, M.H., Possmayer, F., Zander, H., Bordes, N., Jollivet, F., Couedel-Courteille, A., et al., 1999. Characterization of GAPCenA, a GTPase activating protein for Rab6, part of which associates with the centrosome. EMBO J. 18, 1772–1782.

Cuschieri, L., Miller, R., Vogel, J., 2006. Gamma-tubulin is required for proper recruitment and assembly of Kar9-Bim1 complexes in budding yeast. Mol. Biol. Cell 17, 4420–4434.

D'Aquino, K.E., Monje-Casas, F., Paulson, J., Reiser, V., Charles, G.M., Lai, L., et al., 2005. The protein kinase Kin4 inhibits exit from mitosis in response to spindle position defects. Mol. Cell 19, 223–234.

Dan, K., Tanaka, Y., 1990. Attachment of one spindle pole to the cortex in unequal cleavage. Ann. NY Acad. Sci. 582, 108–119.

Davidow, L.S., Goetsch, L., Byers, B., 1980. Preferential occurrence of nonsister spores in two-spored asci of *Saccharomyces cerevisiae*: evidence for regulation of spore-wall formation by the spindle pole body. Genetics 94, 581–595.

de Anda, F.C., Pollarolo, G., Da Silva, J.S., Camoletto, P.G., Feiguin, F., Dotti, C.G., 2005. Centrosome localization determines neuronal polarity. Nature 436, 704–708.

Decottignies, A., Zarzov, P., Nurse, P., 2001. *In vivo* localisation of fission yeast cyclin-dependent kinase cdc2p and cyclin B cdc13p during mitosis and meiosis. J. Cell Sci. 114, 2627–2640.

Deng, W., Lin, H., 1997. Spectrosomes and fusomes anchor mitotic spindles during asymmetric germ cell divisions and facilitate the formation of a polarized microtubule array for oocyte specification in *Drosophila*. Dev. Biol. 189, 79–94.

Ding, R., West, R.R., Morphew, D.M., Oakley, B.R., McIntosh, J.R., 1997. The spindle pole body of *Schizosaccharomyces pombe* enters and leaves the nuclear envelope as the cell cycle proceeds. Mol. Biol. Cell 8, 1461–1479.

Ding, D.Q., Chikashige, Y., Haraguchi, T., Hiraoka, Y., 1998. Oscillatory nuclear movement in fission yeast meiotic prophase is driven by astral microtubules, as revealed by continuous observation of chromosomes and microtubules in living cells. J. Cell Sci. 111 (Pt. 6), 701–712.

Dischinger, S., Krapp, A., Xie, L., Paulson, J.R., Simanis, V., 2008. Chemical genetic analysis of the regulatory role of Cdc2p in the *S. pombe* septation initiation network. J. Cell Sci. 121, 843–853.

Drewes, G., Ebneth, A., Preuss, U., Mandelkow, E.M., Mandelkow, E., 1997. MARK, a novel family of protein kinases that phosphorylate microtubule-associated proteins and trigger microtubule disruption. Cell 89, 297–308.

Du, Q., Macara, I.G., 2004. Mammalian pins is a conformational switch that links NuMA to heterotrimeric G proteins. Cell 119, 503–516.

Eshel, D., Urrestarazu, L.A., Vissers, S., Jauniaux, J.C., van Vliet-Reedijk, J.C., Planta, R.J., et al., 1993. Cytoplasmic dynein is required for normal nuclear segregation in yeast. Proc. Natl. Acad. Sci. USA 90, 11172–11176.

Fankhauser, C., Simanis, V., 1994. The cdc7 protein kinase is a dosage dependent regulator of septum formation in fission yeast. EMBO J. 13, 3011–3019.

Farkasovsky, M., Kuntzel, H., 2001. Cortical Num1p interacts with the dynein intermediate chain Pac11p and cytoplasmic microtubules in budding yeast. J. Cell Biol. 152, 251–262.

Fraschini, R., D'Ambrosio, C., Venturetti, M., Lucchini, G., Piatti, S., 2006. Disappearance of the budding yeast Bub2-Bfa1 complex from the mother-bound spindle pole contributes to mitotic exit. J. Cell Biol. 172, 335–346.

Fuse, N., Hisata, K., Katzen, A.L., Matsuzaki, F., 2003. Heterotrimeric G proteins regulate daughter cell size asymmetry in *Drosophila* neuroblast divisions. Curr. Biol. 13, 947–954.

Geiser, J.R., Schott, E.J., Kingsbury, T.J., Cole, N.B., Totis, L.J., Bhattacharyya, G., et al., 1997. *Saccharomyces cerevisiae* genes required in the absence of the CIN8-encoded spindle motor act in functionally diverse mitotic pathways. Mol. Biol. Cell 8, 1035–1050.

Giansanti, M.G., Gatti, M., Bonaccorsi, S., 2001. The role of centrosomes and astral microtubules during asymmetric division of *Drosophila* neuroblasts. Development 128, 1137–1145.

Gomes, J.E., Encalada, S.E., Swan, K.A., Shelton, C.A., Carter, J.C., Bowerman, B., 2001. The maternal gene spn-4 encodes a predicted RRM protein required for mitotic spindle orientation and cell fate patterning in early *C. elegans* embryos. Development 128, 4301–4314.

Gonczy, P., 2008. Mechanisms of asymmetric cell division: flies and worms pave the way. Nat. Rev. Mol. Cell Biol. 9, 355–366.

Gonczy, P., Grill, S., Stelzer, E.H., Kirkham, M., Hyman, A.A., 2001. Spindle positioning during the asymmetric first cell division of *Caenorhabditis elegans* embryos. Novartis Found Symp. 237, 164–175; discussion 176–181.

Gordon, O., Taxis, C., Keller, P.J., Benjak, A., Stelzer, E.H., Simchen, G., et al., 2006. Nud1p, the yeast homolog of centriolin, regulates spindle pole body inheritance in meiosis. EMBO J. 25, 3856–3868.

Gotta, M., Ahringer, J., 2001. Distinct roles for G[alpha] and G[beta][gamma] in regulating spindle position and orientation in *Caenorhabditis elegans* embryos. Nat. Cell Biol. 3, 297–300.

Gotta, M., Dong, Y., Peterson, Y.K., Lanier, S.M., Ahringer, J., 2003. Asymmetrically distributed *C. elegans* homologs of AGS3/PINS control spindle position in the early embryo. Curr. Biol. 13, 1029–1037.

Grallert, A., Hagan, I.M., 2002. *Schizosaccharomyces pombe* NIMA-related kinase, Fin1, regulates spindle formation and an affinity of Polo for the SPB. EMBO J. 21, 3096–3107.

Grallert, A., Krapp, A., Bagley, S., Simanis, V., Hagan, I.M., 2004. Recruitment of NIMA kinase shows that maturation of the *S. pombe* spindle-pole body occurs over consecutive cell cycles and reveals a role for NIMA in modulating SIN activity. Genes Dev. 18, 1007–1021.

Grava, S., Schaerer, F., Faty, M., Philippsen, P., Barral, Y., 2006. Asymmetric recruitment of dynein to spindle poles and microtubules promotes proper spindle orientation in yeast. Dev. Cell 10, 425–439.

Grill, S.W., Hyman, A.A., 2005. Spindle positioning by cortical pulling forces. Dev. Cell 8, 461–465.

Grill, S.W., Howard, J., Schaffer, E., Stelzer, E.H., Hyman, A.A., 2003. The distribution of active force generators controls mitotic spindle position. Science 301, 518–521.

Gromley, A., Jurczyk, A., Sillibourne, J., Halilovic, E., Mogensen, M., Groisman, I., et al., 2003. A novel human protein of the maternal centriole is required for the final stages of cytokinesis and entry into S phase. J. Cell Biol. 161, 535–545.

Gromley, A., Yeaman, C., Rosa, J., Redick, S., Chen, C.-T., Mirabelle, S., et al., 2005. Centriolin anchoring of exocyst and SNARE complexes at the midbody is required for secretory-vesicle-mediated abscission. Cell 123, 75–87.

Gruneberg, U., Glotzer, M., Gartner, A., Nigg, E.A., 2002. The CeCDC-14 phosphatase is required for cytokinesis in the *Caenorhabditis elegans* embryo. J. Cell Biol. 158, 901–914.

Guerrier, P., 1970a. Characteristics of segmentation and determination of dorsoventral polarity in the development of Spiralia. 3. *Pholas dactylus* and *Spisula subtruncata* (lamellibranch molluscs). J. Embryol. Exp. Morphol. 23, 667–692.

Guerrier, P., 1970b. Characteristics of segmentation and determination of dorsoventral polarity in the development of Spiralia. I. The form of the first equal cleavage division. J. Embryol. Exp. Morphol. 23, 611–637.

Guertin, D.A., Chang, L., Irshad, F., Gould, K.L., McCollum, D., 2000. The role of the sid1p kinase and cdc14p in regulating the onset of cytokinesis in fission yeast. EMBO J. 19, 1803–1815.

Gulli, M.P., Jaquenoud, M., Shimada, Y., Niederhauser, G., Wiget, P., Peter, M., 2000. Phosphorylation of the Cdc42 exchange factor Cdc24 by the PAK-like kinase Cla4 may regulate polarized growth in yeast. Mol. Cell 6, 1155–1167.

Hampoelz, B., Knoblich, J.A., 2004. Heterotrimeric G proteins: new tricks for an old dog. Cell 119, 453–456.

Haren, L., Merdes, A., 2002. Direct binding of NuMA to tubulin is mediated by a novel sequence motif in the tail domain that bundles and stabilizes microtubules. J. Cell Sci. 115, 1815–1824.

Heil-Chapdelaine, R.A., Tran, N.K., Cooper, J.A., 2000. Dynein-dependent movements of the mitotic spindle in *Saccharomyces cerevisiae*. Do not require filamentous actin. Mol. Biol. Cell 11, 863–872.

Hess, H.A., Roper, J.-C., Grill, S.W., Koelle, M.R., 2004. RGS-7 completes a receptor-independent heterotrimeric G protein cycle to asymmetrically regulate mitotic spindle positioning in *C. elegans*. Cell 119, 209–218.

Hill, D.P., Strome, S., 1988. An analysis of the role of microfilaments in the establishment and maintenance of asymmetry in *Caenorhabditis elegans* zygotes. Dev. Biol. 125, 75–84.

Hill, D.P., Strome, S., 1990. Brief cytochalasin-induced disruption of microfilaments during a critical interval in 1-cell *C. elegans* embryos alters the partitioning of developmental instructions to the 2-cell embryo. Development 108, 159–172.

Hofken, T., Schiebel, E., 2002. A role for cell polarity proteins in mitotic exit. EMBO J. 21, 4851–4862.

Hofken, T., Schiebel, E., 2004. Novel regulation of mitotic exit by the Cdc42 effectors Gic1 and Gic2. J. Cell Biol. 164, 219–231.

Hyman, A.A., 1989. Centrosome movement in the early divisions of *Caenorhabditis elegans*: a cortical site determining centrosome position. J. Cell Biol. 109, 1185–1193.

Hyman, A.A., White, J.G., 1987. Determination of cell division axes in the early embryogenesis of *Caenorhabditis elegans*. J. Cell Biol. 105, 2123–2135.

Ishii, R., Shimizu, T., 1997. Equalization of unequal first cleavage in the Tubifex egg by introduction of an additional centrosome: implications for the absence of cortical mechanisms for mitotic spindle asymmetry. Dev. Biol. 189, 49–56.

Izumi, Y., Ohta, N., Itoh-Furuya, A., Fuse, N., Matsuzaki, F., 2004. Differential functions of G protein and Baz-aPKC signaling pathways in *Drosophila* neuroblast asymmetric division. J. Cell Biol. 164, 729–738.

Izumi, Y., Ohta, N., Hisata, K., Raabe, T., Matsuzaki, F., 2006. *Drosophila* pins-binding protein Mud regulates spindle-polarity coupling and centrosome organization. Nat. Cell Biol. 8, 586–593.

Jaspersen, S.L., Huneycutt, B.J., Giddings Jr., T.H., Resing, K.A., Ahn, N.G., Winey, M., 2004. Cdc28/Cdk1 regulates spindle pole body duplication through phosphorylation of Spc42 and Mps1. Dev. Cell 7, 263–274.

Jensen, S., Geymonat, M., Johnson, A.L., Segal, M., Johnston, L.H., 2002. Spatial regulation of the guanine nucleotide exchange factor Lte1 in *Saccharomyces cerevisiae*. J. Cell Sci. 115, 4977–4991.

Kaiser, B.K., Nachury, M.V., Gardner, B.E., Jackson, P.K., 2004. *Xenopus* Cdc14 alpha/beta are localized to the nucleolus and centrosome and are required for embryonic cell division. BMC Cell Biol. 5, 27.

Kaltschmidt, J.A., Davidson, C.M., Brown, N.H., Brand, A.H., 2000. Rotation and asymmetry of the mitotic spindle direct asymmetric cell division in the developing central nervous system. Nat. Cell Biol. 2, 7–12.

Kamieniecki, R.J., Liu, L., Dawson, D.S., 2005. FEAR but not MEN genes are required for exit from meiosis I. Cell Cycle 4, 1093–1098.

Keating, H.H., White, J.G., 1998. Centrosome dynamics in early embryos of *Caenorhabditis elegans*. J. Cell Sci. 111, 3027–3033.

Kemphues, K.J., Priess, J.R., Morton, D.G., Cheng, N.S., 1988. Identification of genes required for cytoplasmic localization in early *C. elegans* embryos. Cell 52, 311–320.

Kim, J., Jang, S.S., Song, K., 2008. Different levels of Bfa1/Bub2 GAP activity are required to prevent mitotic exit of budding yeast depending on the type of perturbations. Mol. Biol. Cell 19, 4328–4340.

Knop, M., Strasser, K., 2000. Role of the spindle pole body of yeast in mediating assembly of the prospore membrane during meiosis. EMBO J. 19, 3657–3667.

Korinek, W.S., Copeland, M.J., Chaudhuri, A., Chant, J., 2000. Molecular linkage underlying microtubule orientation toward cortical sites in yeast. Science 287, 2257–2259.

Kozlowski, C., Srayko, M., Nedelec, F., 2007. Cortical microtubule contacts position the spindle in *C. elegans* embryos. Cell 129, 499–510.

Krapp, A., Cano, E., Simanis, V., 2003. Mitotic hyperphosphorylation of the fission yeast SIN scaffold protein cdc11p is regulated by the protein kinase cdc7p. Curr. Biol. 13, 168–172.

Krapp, A., Cano, E., Simanis, V., 2004a. Analysis of the *S. pombe* signalling scaffold protein Cdc11p reveals an essential role for the N-terminal domain in SIN signalling. FEBS Lett. 565, 176–180.

Krapp, A., Gulli, M.P., Simanis, V., 2004b. SIN and the art of splitting the fission yeast cell. Curr. Biol. 14, R722–R730.

Krapp, A., Collin, P., Cokoja, A., Dischinger, S., Cano, E., Simanis, V., 2006. The *Schizosaccharomyces pombe* septation initiation network (SIN) is required for spore formation in meiosis. J. Cell Sci. 119, 2882–2891.

Krapp, A., Collin, P., Cano Del Rosario, E., Simanis, V., 2008. Homoeostasis between the GTPase Spg1p and its GAP in the regulation of cytokinesis in *S. pombe*. J. Cell Sci. 121, 601–608.

Kuriyama, R., Borisy, G.G., Masui, Y., 1986. Microtubule cycles in oocytes of the surf clam, *Spisula solidissima*: an immunofluorescence study. Dev. Biol. 114, 151–160.

Kusch, J., Meyer, A., Snyder, M.P., Barral, Y., 2002. Microtubule capture by the cleavage apparatus is required for proper spindle positioning in yeast. Genes Dev. 16, 1627–1639.

Labbe, J.-C., Maddox, P.S., Salmon, E.D., Goldstein, B., 2003. PAR proteins regulate microtubule dynamics at the cell cortex in *C. elegans*. Curr. Biol. 13, 707–714.

Labbe, J.-C., McCarthy, E.K., Goldstein, B., 2004. The forces that position a mitotic spindle asymmetrically are tethered until after the time of spindle assembly. J. Cell Biol. 167, 245–256.

Lambert, J.D., Nagy, L.M., 2002. Asymmetric inheritance of centrosomally localized mRNAs during embryonic cleavages. Nature 420, 682–686.

Lansbergen, G., Akhmanova, A., 2006. Microtubule plus end: a hub of cellular activities. Traffic 7, 499–507.

Le Goff, X., Buvelot, S., Salimova, E., Guerry, F., Schmidt, S., Cueille, N., et al., 2001. The protein phosphatase 2A B′-regulatory subunit par1p is implicated in regulation of the *S. pombe* septation initiation network. FEBS Lett. 508, 136–142.

Lee, L., Tirnauer, J.S., Li, J., Schuyler, S.C., Liu, J.Y., Pellman, D., 2000. Positioning of the mitotic spindle by a cortical-microtubule capture mechanism. Science 287, 2260–2262.

Lee, W.L., Oberle, J.R., Cooper, J.A., 2003. The role of the lissencephaly protein Pac1 during nuclear migration in budding yeast. J. Cell Biol. 160, 355–364.

Lee, W.L., Kaiser, M.A., Cooper, J.A., 2005. The offloading model for dynein function: differential function of motor subunits. J. Cell Biol. 168, 201–207.

Leisner, C., Kammerer, D., Denoth, A., Britschi, M., Barral, Y., Liakopoulos, D., 2008. Regulation of mitotic spindle asymmetry by SUMO and the spindle-assembly checkpoint in yeast. Curr. Biol. 18, 1249–1255.

Li, Y.Y., Yeh, E., Hays, T., Bloom, K., 1993. Disruption of mitotic spindle orientation in a yeast dynein mutant. Proc. Natl. Acad. Sci. USA 90, 10096–100100.

Li, C., Furge, K.A., Cheng, Q.-C., Albright, C.F., 2000. Byr4 localizes to spindle-pole bodies in a cell cycle-regulated manner to control Cdc7 localization and septation in fission yeast. J. Biol. Chem. 275, 14381–14387.

Liakopoulos, D., Kusch, J., Grava, S., Vogel, J., Barral, Y., 2003. Asymmetric loading of Kar9 onto spindle poles and microtubules ensures proper spindle alignment. Cell 112, 561–574.

Longtine, M.S., Fares, H., Pringle, J.R., 1998. Role of the yeast Gin4p protein kinase in septin assembly and the relationship between septin assembly and septin function. J. Cell Biol. 143, 719–736.

Lorson, M.A., Horvitz, H.R., van den Heuvel, S., 2000. LIN-5 is a novel component of the spindle apparatus required for chromosome segregation and cleavage plane specification in *Caenorhabditis elegans*. J. Cell Biol. 148, 73–86.

Luedeke, C., Frei, S.B., Sbalzarini, I., Schwarz, H., Spang, A., Barral, Y., 2005. Septin-dependent compartmentalization of the endoplasmic reticulum during yeast polarized growth. J. Cell Biol. 169, 897–908.

Maekawa, H., Schiebel, E., 2004. Cdk1-Clb4 controls the interaction of astral microtubule plus ends with subdomains of the daughter cell cortex. Genes Dev. 18, 1709–1724.

Maekawa, H., Usui, T., Knop, M., Schiebel, E., 2003. Yeast Cdk1 translocates to the plus end of cytoplasmic microtubules to regulate bud cortex interactions. EMBO J. 22, 438–449.

Maekawa, H., Priest, C., Lechner, J., Pereira, G., Schiebel, E., 2007. The yeast centrosome translates the positional information of the anaphase spindle into a cell cycle signal. J. Cell Biol. 179, 423–436.

Mailand, N., Lukas, C., Kaiser, B.K., Jackson, P.K., Bartek, J., Lukas, J., 2002. Deregulated human Cdc14A phosphatase disrupts centrosome separation and chromosome segregation. Nat. Cell Biol. 4, 317–322.

Matz, M.V., Fradkov, A.F., Labas, Y.A., Savitsky, A.P., Zaraisky, A.G., Markelov, M.L., et al., 1999. Fluorescent proteins from nonbioluminescent *Anthozoa* species 17, 969–973.

McGrail, M., Hays, T.S., 1997. The microtubule motor cytoplasmic dynein is required for spindle orientation during germline cell divisions and oocyte differentiation in *Drosophila*. Development 124, 2409–2419.

McInnes, C., Mazumdar, A., Mezna, M., Meades, C., Midgley, C., Scaerou, F., et al., 2006. Inhibitors of Polo-like kinase reveal roles in spindle-pole maintenance. Nat. Chem. Biol. 2, 608–617.

Meednu, N., Hoops, H., D'Silva, S., Pogorzala, L., Wood, S., Farkas, D., et al., 2008. The spindle positioning protein Kar9p interacts with the sumoylation machinery in *Saccharomyces cerevisiae*. Genetics 180, 2033–2055.

Menssen, R., Neutzner, A., Seufert, W., 2001. Asymmetric spindle pole localization of yeast Cdc15 kinase links mitotic exit and cytokinesis. Curr. Biol. 11, 345–350.
Miller, R.K., Rose, M.D., 1998. Kar9p is a novel cortical protein required for cytoplasmic microtubule orientation in yeast. J. Cell Biol. 140, 377–390.
Miller, R.K., Heller, K.K., Frisen, L., Wallack, D.L., Loayza, D., Gammie, A.E., et al., 1998. The kinesin-related proteins, Kip2p and Kip3p, function differently in nuclear migration in yeast. Mol. Biol. Cell 9, 2051–2068.
Minet, M., Nurse, P., Thuriaux, P., Mitchison, J.M., 1979. Uncontrolled septation in a cell division cycle mutant of the fission yeast *Schizosaccharomyces pombe*. J. Bacteriol. 137, 440–446.
Mineyuki, Y., 2007. Plant microtubule studies: past and present. J. Plant Res. 120, 45–51.
Molk, J.N., Schuyler, S.C., Liu, J.Y., Evans, J.G., Salmon, E.D., Pellman, D., et al., 2004. The differential roles of budding yeast Tem1p, Cdc15p, and Bub2p protein dynamics in mitotic exit. Mol. Biol. Cell 15, 1519–1532.
Monje-Casas, F., Amon, A., 2009. Cell polarity determinants establish asymmetry in MEN signaling. Dev. Cell 16, 132–145.
Moore, J.K., Miller, R.K., 2007. The cyclin-dependent kinase Cdc28p regulates multiple aspects of Kar9p function in yeast. Mol. Biol. Cell 18, 1187–1202.
Moore, J.K., D'Silva, S., Miller, R.K., 2006. The CLIP-170 homologue Bik1p promotes the phosphorylation and asymmetric localization of Kar9p. Mol. Biol. Cell 17, 178–191.
Morrell, J.L., Tomlin, G.C., Rajagopalan, S., Venkatram, S., Feoktistova, A.S., Tasto, J.J., et al., 2004. Sid4p-Cdc11p assembles the septation initiation network and its regulators at the *S. pombe* SPB. Curr. Biol. 14, 579–584.
Morton, D.G., Roos, J.M., Kemphues, K.J., 1992. par-4, a gene required for cytoplasmic localization and determination of specific cell types in *Caenorhabditis elegans* embryogenesis. Genetics 130, 771–790.
Morton, D.G., Shakes, D.C., Nugent, S., Dichoso, D., Wang, W., Golden, A., et al., 2002. The *Caenorhabditis elegans* par-5 gene encodes a 14-3-3 protein required for cellular asymmetry in the early embryo. Dev. Biol. 241, 47–58.
Nelson, S.A., Cooper, J.A., 2007. A novel pathway that coordinates mitotic exit with spindle position. Mol. Biol. Cell 18, 3440–3450.
Nelson, B.H., Weisblat, D.A., 1992. Cytoplasmic and cortical determinants interact to specify ectoderm and mesoderm in the leech embryo. Development 115, 103–115.
Nguyen-Ngoc, T., Afshar, K., Gonczy, P., 2007. Coupling of cortical dynein and G alpha proteins mediates spindle positioning in *Caenorhabditis elegans*. Nat. Cell Biol. 9, 1294–1302.
Nickas, M.E., Schwartz, C., Neiman, A.M., 2003. Ady4p and Spo74p are components of the meiotic spindle pole body that promote growth of the prospore membrane in *Saccharomyces cerevisiae*. Eukaryot. Cell 2, 431–445.
Nickas, M.E., Diamond, A.E., Yang, M.-J., Neiman, A., 2004. Regulation of spindle pole function by an intermediary metabolite. Mol. Biol. Cell 15, 2606-2616.
O'Connell, M.J., Krien, M.J., Hunter, T., 2003. Never say never. The NIMA-related protein kinases in mitotic control. Trends Cell Biol. 13, 221–228.
Ou, Y., Rattner, J.B., 2004. The centrosome in higher organisms: structure, composition, and duplication. Int. Rev. Cytol. 238, 119–182.
Panbianco, C., Weinkove, D., Zanin, E., Jones, D., Divecha, N., Gotta, M., et al., 2008. A casein kinase 1 and PAR proteins regulate asymmetry of a PIP(2) synthesis enzyme for asymmetric spindle positioning. Dev. Cell 15, 198–208.
Park, D.H., Rose, L.S., 2008. Dynamic localization of LIN-5 and GPR-1/2 to cortical force generation domains during spindle positioning. Dev. Biol. 315, 42–54.
Patalano, S., Pruliere, G., Prodon, F., Paix, A., Dru, P., Sardet, C., et al., 2006. The aPKC-PAR-6-PAR-3 cell polarity complex localizes to the centrosome attracting body, a macroscopic cortical structure responsible for asymmetric divisions in the early ascidian embryo. J. Cell Sci. 119, 1592–1603.

Pecreaux, J., Roper, J.C., Kruse, K., Julicher, F., Hyman, A.A., Grill, S.W., et al., 2006. Spindle oscillations during asymmetric cell division require a threshold number of active cortical force generators. Curr. Biol. 16, 2111–2122.

Pereira, G., Schiebel, E., 2005. Kin4 kinase delays mitotic exit in response to spindle alignment defects. Mol. Cell 19, 209–221.

Pereira, G., Hofken, T., Grindlay, J., Manson, C., Schiebel, E., 2000. The Bub2p spindle checkpoint links nuclear migration with mitotic exit. Mol. Cell 6, 1–10.

Pereira, G., Tanaka, T.U., Nasmyth, K., Schiebel, E., 2001. Modes of spindle pole body inheritance and segregation of the Bfa1p- Bub2p checkpoint protein complex. EMBO J. 20, 6359–6370.

Petronczki, M., Knoblich, J.A., 2001. DmPAR-6 directs epithelial polarity and asymmetric cell division of neuroblasts in *Drosophila*. Nat. Cell Biol. 3, 43–49.

Piel, M., Meyer, P., Khodjakov, A., Rieder, C.L., Bornens, M., 2000. The respective contributions of the mother and daughter centrioles to centrosome activity and behavior in vertebrate cells. J. Cell Biol. 149, 317–330.

Piel, M., Nordberg, J., Euteneuer, U., Bornens, M., 2001. Centrosome-dependent exit of cytokinesis in animal cells. Science 291, 1550–1553.

Pohl, C., Jentsch, S., 2008. Final stages of cytokinesis and midbody ring formation are controlled by BRUCE. Cell 132, 832–845.

Ranganath, R.M., 2005. Asymmetric cell divisions in flowering plants—one mother, ''two-many'' daughters. Plant Biol. (Stuttg) 7, 425–448.

Rappleye, C.A., Tagawa, A., Lyczak, R., Bowerman, B., Aroian, R.V., 2002. The anaphase-promoting complex and separin are required for embryonic anterior–posterior axis formation. Dev. Cell 2, 195–206.

Rebollo, E., Sampaio, P., Januschke, J., Llamazares, S., Varmark, H., Gonzalez, C., 2007. Functionally unequal centrosomes drive spindle orientation in asymmetrically dividing *Drosophila* neural stem cells. Dev. Cell 12, 467–474.

Ren, X., Weisblat, D.A., 2006. Asymmetrization of first cleavage by transient disassembly of one spindle pole aster in the leech *Helobdella robusta*. Dev. Biol. 292, 103–115.

Rose, L.S., Kemphues, K., 1998. The let-99 gene is required for proper spindle orientation during cleavage of the *C. elegans* embryo. Development 125, 1337–1346.

Rusan, N.M., Peifer, M., 2007. A role for a novel centrosome cycle in asymmetric cell division. J. Cell Biol. 177, 13–20.

Saunders, W.S., Koshland, D., Eshel, D., Gibbons, I.R., Hoyt, M.A., 1995. *Saccharomyces cerevisiae* kinesin- and dynein-related proteins required for anaphase chromosome segregation. J. Cell Biol. 128, 617–624.

Savoian, M.S., Rieder, C.L., 2002. Mitosis in primary cultures of *Drosophila melanogaster* larval neuroblasts. J. Cell Sci. 115, 3061–3072.

Schaefer, M., Shevchenko, A., Knoblich, J.A., 2000. A protein complex containing Inscuteable and the Galpha-binding protein Pins orients asymmetric cell divisions in *Drosophila*. Curr. Biol. 10, 353–362.

Schaefer, M., Petronczki, M., Dorner, D., Forte, M., Knoblich, J.A., 2001. Heterotrimeric G proteins direct two modes of asymmetric cell division in the *Drosophila* nervous system. Cell 107, 183–194.

Schmit, A.C., 2002. Acentrosomal microtubule nucleation in higher plants. Int. Rev. Cytol. 220, 257–289.

Schroeder, T.E., 1987. Fourth cleavage of sea urchin blastomeres: microtubule patterns and myosin localization in equal and unequal cell divisions. Dev. Biol. 124, 9–22.

Segal, M., Clarke, D.J., Maddox, P., Salmon, E.D., Bloom, K., Reed, S.I., 2000. Coordinated spindle assembly and orientation requires Clb5p-dependent kinase in budding yeast. J. Cell Biol. 148, 441–452.

Seshan, A., Amon, A., 2005. Ras and the Rho effector Cla4 collaborate to target and anchor Lte1 at the bud cortex. Cell Cycle 4, 940–946.
Seshan, A., Bardin, A.J., Amon, A., 2002. Control of Lte1 localization by cell polarity determinants and Cdc14. Curr. Biol. 12, 2098–2110.
Severson, A.F., Bowerman, B., 2003. Myosin and the PAR proteins polarize microfilament-dependent forces that shape and position mitotic spindles in *Caenorhabditis elegans*. J. Cell Biol. 161, 21–26.
Shaw, S.L., Yeh, E., Maddox, P., Salmon, E.D., Bloom, K., 1997. Astral microtubule dynamics in yeast: a microtubule-based searching mechanism for spindle orientation and nuclear migration into the bud. J. Cell Biol. 139, 985–994.
Sheeman, B., Carvalho, P., Sagot, I., Geiser, J., Kho, D., Hoyt, M.A., et al., 2003. Determinants of *S. cerevisiae* dynein localization and activation: implications for the mechanism of spindle positioning. Curr. Biol. 13, 364–372.
Shimizu, T., Ishii, R., Takahashi, H., 1998. Unequal cleavage in the early Tubifex embryo. Dev. Growth Differ. 40, 257–266.
Shirayama, M., Matsui, Y., Toh, E.A., 1994. The yeast TEM1 gene, which encodes a GTP-binding protein, is involved in termination of M phase. Mol. Cell. Biol. 14, 7476–7482.
Shirayama, M., Zachariae, W., Ciosk, R., Nasmyth, K., 1998. The Polo-like kinase Cdc5p and the WD-repeat protein Cdc20p/fizzy are regulators and substrates of the anaphase promoting complex in *Saccharomyces cerevisiae*. EMBO J. 17, 1336–1349.
Siegrist, S.E., Doe, C.Q., 2005. Microtubule-induced Pins/Galphai cortical polarity in *Drosophila* neuroblasts. Cell 123, 1323–1335.
Siller, K.H., Serr, M., Steward, R., Hays, T.S., Doe, C.Q., 2005. Live imaging of *Drosophila* brain neuroblasts reveals a role for Lis1/dynactin in spindle assembly and mitotic checkpoint control. Mol. Biol. Cell 16, 5127–5140.
Siller, K.H., Cabernard, C., Doe, C.Q., 2006. The NuMA-related Mud protein binds pins and regulates spindle orientation in *Drosophila* neuroblasts. Nat. Cell Biol. 8, 594–600.
Simanis, V., 2003. Events at the end of mitosis in the budding and fission yeasts. J. Cell Sci. 116, 4263–4275.
Sohrmann, M., Schmidt, S., Hagan, I., Simanis, V., 1998. Asymmetric segregation on spindle poles of the *Schizosaccharomyces pombe* septum-inducing protein kinase Cdc7p. Genes Dev. 12, 84–94.
Song, K., Mach, K.E., Chen, C.Y., Reynolds, T., Albright, C.F., 1996. A novel suppressor of ras1 in fission yeast, byr4, is a dosage-dependent inhibitor of cytokinesis. J. Cell Biol. 133, 1307–1319.
Srinivasan, D.G., Fisk, R.M., Xu, H., van den Heuvel, S., 2003. A complex of LIN-5 and GPR proteins regulates G protein signaling and spindle function in *C. elegans*. Genes Dev. 17, 1225–1239.
Stevens, N.R., Raposo, A.A., Basto, R., St Johnston, D., Raff, J.W., 2007. From stem cell to embryo without centrioles. Curr. Biol. 17, 1498–1503.
Strome, S., Hill, D.P., 1988. Early embryogenesis in *Caenorhabditis elegans*: the cytoskeleton and spatial organization of the zygote. Bioessays 8, 145–149.
Takahashi, H., Shimizu, T., 1997. Role of intercellular contacts in generating an asymmetric mitotic apparatus in the Tubifex embryo. Dev. Growth Differ. 39, 351–362.
Takizawa, P.A., DeRisi, J.L., Wilhelm, J.E., Vale, R.D., 2000. Plasma membrane compartmentalization in yeast by messenger RNA transport and a septin diffusion barrier. Science 290, 341–344.
Taxis, C., Keller, P., Kavagiou, Z., Jensen, L.J., Colombelli, J., Bork, P., et al., 2005. Spore number control and breeding in *Saccharomyces cerevisiae*: a key role for a self-organizing system. J. Cell Biol. 171, 627–640.
Tio, M., Udolph, G., Yang, X., Chia, W., 2001. cdc2 links the *Drosophila* cell cycle and asymmetric division machineries. Nature 409, 1063–1067.

Tsou, M.F., Hayashi, A., DeBella, L.R., McGrath, G., Rose, L.S., 2002. LET-99 determines spindle position and is asymmetrically enriched in response to PAR polarity cues in *C. elegans* embryos. Development 129, 4469–4481.

Tsou, M.F., Hayashi, A., Rose, L.S., 2003. LET-99 opposes Galpha/GPR signaling to generate asymmetry for spindle positioning in response to PAR and MES-1/SRC-1 signaling. Development 130, 5717–5730.

Visintin, R., Amon, A., 2001. Regulation of the mitotic exit protein kinases Cdc15 and Dbf2. Mol. Biol. Cell 12, 2961–2974.

Vogel, J., Drapkin, B., Oomen, J., Beach, D., Bloom, K., Snyder, M., 2001. Phosphorylation of gamma-tubulin regulates microtubule organization in budding yeast. Dev. Cell 1, 621–631.

Wang, H., Somers, G.W., Bashirullah, A., Heberlein, U., Yu, F., Chia, W., 2006. Aurora-A acts as a tumor suppressor and regulates self-renewal of *Drosophila* neuroblasts. Genes Dev. 20, 3453–3463.

Wang, H., Ouyang, Y., Somers, W.G., Chia, W., Lu, B., 2007. Polo inhibits progenitor self-renewal and regulates Numb asymmetry by phosphorylating Pon. Nature 449, 96–100.

Watts, J.L., Etemad-Moghadam, B., Guo, S., Boyd, L., Draper, B.W., Mello, C.C., et al., 1996. par-6, a gene involved in the establishment of asymmetry in early *C. elegans* embryos, mediates the asymmetric localization of PAR-3. Development 122, 3133–3140.

Wild, A.C., Yu, J.W., Lemmon, M.A., Blumer, K.J., 2004. The p21-activated protein kinase-related kinase Cla4 is a coincidence detector of signaling by Cdc42 and phosphatidylinositol 4-phosphate. J. Biol. Chem. 279, 17101–17110.

Wodarz, A., Ramrath, A., Kuchinke, U., Knust, E., 1999. Bazooka provides an apical cue for inscuteable localization in *Drosophila* neuroblasts. Nature 402, 544–547.

Wodarz, A., Ramrath, A., Grimm, A., Knust, E., 2000. *Drosophila* atypical protein kinase C associates with Bazooka and controls polarity of epithelia and neuroblasts. J. Cell Biol. 150, 1361–1374.

Yamashita, Y.M., Fuller, M.T., 2008. Asymmetric centrosome behavior and the mechanisms of stem cell division. J. Cell Biol. 180, 261–266.

Yamashita, Y.M., Jones, D.L., Fuller, M.T., 2003. Orientation of asymmetric stem cell division by the APC tumor suppressor and centrosome. Science 301, 1547–1550.

Yamashita, Y.M., Mahowald, A.P., Perlin, J.R., Fuller, M.T., 2007. Asymmetric inheritance of mother versus daughter centrosome in stem cell division. Science 315, 518–521.

Yeh, E., Skibbens, R., Cheng, J., Salmon, E., Bloom, K., 1995. Spindle dynamics and cell cycle regulation of dynein in the budding yeast, *Saccharomyces cerevisiae*. J. Cell Biol. 130, 687–700.

Yin, H., Pruyne, D., Huffaker, T.C., Bretscher, A., 2000. Myosin V orientates the mitotic spindle in yeast. Nature 406, 1013–1015.

Yoshida, S., Ichihashi, R., Toh-e, A., 2003. Ras recruits mitotic exit regulator Lte1 to the bud cortex in budding yeast. J. Cell Biol. 161, 889–897.

Yu, F., Cai, Y., Kaushik, R., Yang, X., Chia, W., 2003. Distinct roles of Galphai and Gbeta13F subunits of the heterotrimeric G protein complex in the mediation of *Drosophila* neuroblast asymmetric divisions. J. Cell Biol. 162, 623–633.

Yu, F., Wang, H., Qian, H., Kaushik, R., Bownes, M., Yang, X., et al., 2005. Locomotion defects, together with pins, regulates heterotrimeric G-protein signaling during *Drosophila* neuroblast asymmetric divisions. Genes Dev. 19, 1341–1353.

Yu, F., Kuo, C.T., Jan, Y.N., 2006. *Drosophila* neuroblast asymmetric cell division: recent advances and implications for stem cell biology. Neuron 51, 13–20.

CHAPTER FIVE

Cell Adhesion in Amphibian Gastrulation

Rudolf Winklbauer

Contents

1. Introduction 216
2. Characteristics of Amphibian Gastrulation 217
   2.1. Multilayered structure of the amphibian blastula and gastrula 217
   2.2. Gastrulation movements 220
   2.3. Preview: Two classes of morphogenetic forces in the amphibian gastrula 222
3. Gastrula Tissue as a Liquid: Cell Adhesion, Cell Sorting, Boundary Formation, and Tissue Positioning 223
   3.1. Liquid-like properties of tissues 223
   3.2. Differential adhesion, cell sorting, and tissue positioning in the blastula and gastrula 227
   3.3. The molecular basis of cell–cell adhesion in the amphibian embryo 231
   3.4. Tissue separation: Beyond differential adhesion 243
   3.5. Function of differential adhesion and tissue separation in the embryo 246
4. Collective Cell Migration, Cell Rearrangement, and Intercellular Migration 249
   4.1. Basic features of cell rearrangement and intercellular migration 250
   4.2. Cadherin adhesion and intercellular migration in the amphibian gastrula 252
   4.3. Collective and intercellular migration of the anterior mesendoderm 253
   4.4. Intercellular migration-related aspects of mesodermal convergent extension 256
5. Conclusion 260
Acknowledgments 261
References 261

Department of Cell and Systems Biology, University of Toronto, Toronto, Ontario M5S 3G5, Canada

International Review of Cell and Molecular Biology, Volume 278
ISSN 1937-6448, DOI: 10.1016/S1937-6448(09)78005-0
© 2009 Elsevier Inc.
All rights reserved.

Abstract

The amphibian gastrula can be regarded as a single coherent tissue which folds and distorts itself in a reproducible pattern to establish the embryonic germ layers. It is held together by cadherins which provide the flexible adhesion required for the massive cell rearrangements that accompany gastrulation. Cadherin expression and adhesiveness increase as one goes from the vegetal cell mass through the anterior mesendoderm to the chordamesoderm, and then decrease again slightly in the ectoderm. Together with a basic random component of cell motility, this flexible, differentially expressed adhesiveness generates surface and interfacial tension effects which, in principle, can exert strong forces. However, conclusive evidence for an *in vivo* role of differential adhesion-related effects in gastrula morphogenesis is still lacking. The most important morphogenetic process in the amphibian gastrula seems to be intercellular migration, where cells crawl actively across each other's surface. The crucial aspect of this process is that cell motility is globally oriented, leading for example to mediolateral intercalation of bipolar cells during convergent extension of the chordamesoderm or to the directional migration of unipolar cells during translocation of the anterior mesendoderm on the ectodermal blastocoel roof. During these movements, the boundary between ectoderm and mesoderm is maintained by a tissue separation process.

Key Words: *Xenopus*, Gastrulation, Cadherin, Convergent extension, Cell migration, Differential adhesion. © 2009 Elsevier Inc.

1. Introduction

It is remarkable that after more than half a billion years of evolution, the basic body plan of almost all multicellular animals is formed by a process so similar at its core that we are compelled to denote it with a common term, gastrulation. It consists of the establishment of the germ layers by a rearrangement of embryonic parts in which the future endoderm, and mesoderm if present, move from the surface to the interior, leaving the ectoderm to cover the embryo. Despite its basic conservation, gastrulation can be strongly modified, which is obvious within the vertebrates. Amphibians, together with lampreys, sturgeons, and lungfishes, most likely represent the primitive mode of vertebrate gastrulation. Here, holoblastic cleavage divides the whole egg into cells, and the blastula forms as a hollow sphere. In groups with meroblastic cleavage, such as teleosts, reptiles, or birds, an uncleaved vegetal yolk cell is retained which can be extremely large and whose presence requires a substantial modification of gastrulation (Arendt and Nubler-Jung, 1999; Collazo et al., 1994; Shook and Keller, 2008).

Amphibian gastrulation has been studied descriptively and comparatively since the early nineteenth century (Beetschen, 2001). This research culminated in the work of Vogt, who used vital dyes to follow the various regions of the embryo through gastrulation. In his landmark paper (Vogt, 1929), he depicted gastrulation as composed of a number of distinct, yet integrated "gastrulation movements," such as epiboly, invagination, convergence, or extension. Shortly afterwards, Holtfreter had begun to analyze the mechanism of amphibian gastrulation, by examining its cellular basis and attempting to reduce tissue movements to the behavior of cells. His notion of tissue affinity and selective cell adhesion as morphogenetic mechanisms (Holtfreter, 1939, 1944; Townes and Holtfreter, 1955) had a profound impact far beyond the field of amphibian development.

This classical work had been performed mostly on urodele amphibians. When research on amphibian gastrulation was revived in the 1970s by Keller, it concentrated on an anuran species, the frog, *Xenopus laevis*. *Xenopus* had become the model of choice for the molecular analysis of early vertebrate development, and invaluable molecular and cell biological tools and concepts were becoming available. This allowed Holtfreter's research program to be revisited at a more sophisticated technical level, yet essentially on the same conceptual basis: region-specific cell behaviors drive the canonical, regionally expressed gastrulation movements, which together bring about gastrulation (Keller, 1986). The combination of new techniques to study gene function with classical "cut-and-paste" microsurgery, used in a background of extensive research on embryonic patterning and regional specification, has made *Xenopus* gastrulation the best understood paradigm for this process in vertebrates. This review focuses on the mechanisms and roles of cell adhesion, and the generation and function of regional differences of adhesion during amphibian, and in particular *Xenopus*, gastrulation.

2. Characteristics of Amphibian Gastrulation

2.1. Multilayered structure of the amphibian blastula and gastrula

A typical invertebrate embryo is built from a single-layered epithelium. Epithelial cells possess distinct apical and basolateral membrane domains, and are linked by subapical junctional complexes to form stable sheets. By changing the shape or arrangement of cells, epithelia fold, stretch, or contract to generate complex structures (Schock and Perrimon, 2002), and these morphogenetic mechanisms play important roles in invertebrate gastrulation. It is a distinguishing feature of the vertebrate blastula that its wall is initially several cell layers thick, although part of it can secondarily

become single layered. The morphogenetic movements of vertebrate gastrulation occur within this characteristic context (Shook and Keller, 2008) (Figs. 5.1A and B and 5.2A).

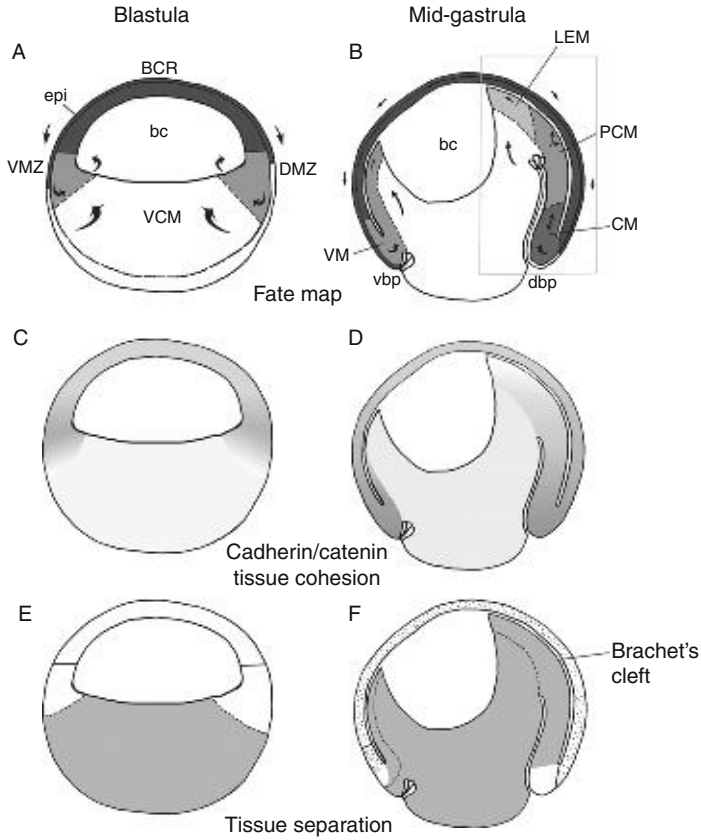

Figure 5.1 Blastula and mid-gastrula regions of *Xenopus*. (A, B) Prospective germ layers. Dark, ectoderm of blastocoel roof (BCR); white, endoderm of vegetal cell mass (VCM); intermediate, mesoderm of dorsal (DMZ) or ventral marginal zone (VMZ) of blastula or of gastrula (VM, ventral mesoderm; CM, chordamesoderm; PCM, prechordal mesoderm; LEM, leading edge mesendoderm). epi, epithelial layer; bc, blastocoel cavity; vbp, dbp, ventral and dorsal blastopore, respectively. Arrows indicate directions of tissue movements. Boxed region in (B) is shown in Fig. 5.2. (C, D) Cadherin/catenin expression. Higher cadherin membrane density is symbolized by darker shading. Tissue cohesiveness essentially conforms to this pattern. (E, F) Tissue separation. In the blastula, the vegetal cell mass shows separation behavior (gray), the remaining tissue indiscriminate behavior (white). In the gastrula, separation behavior has spread into the mesoderm, the BCR developed repulsion behavior (dotted), small regions in the dorsal and ventral blastopore lips remain indifferent. In all figures, animal is to the top, dorsal to the right.

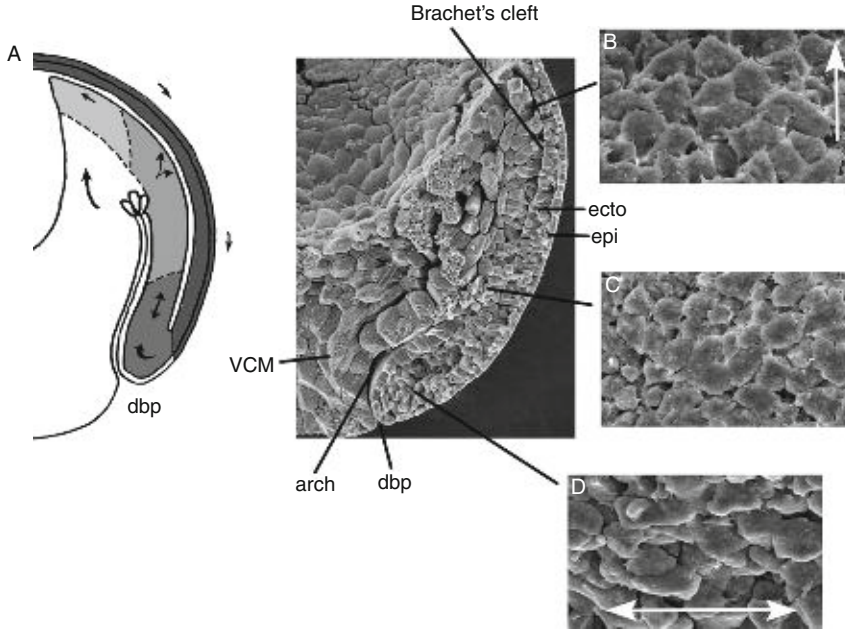

Figure 5.2 Scanning electron micrographs of dorsal regions of mid-gastrula. (A) The boxed region from Fig. 5.1B is shown (right). For mesoderm regions, refer to drawing (right, and Fig. 5.1B). ecto, ectoderm; epi, epithelial layer of ectoderm; dbp, dorsal blastopore; arch, archenteron; VCM, vegetal cell mass. (B–D) Cell orientation in different dorsal mesoderm regions. Mesoderm is shown from substrate side, after removal of the ectoderm. (B) Shingle arrangement of leading edge mesendoderm; cells are oriented animally (arrow). (C) Prechordal plate mesoderm. (D) Chordamesoderm, mediolateral cell orientation (double arrow).

The generation of the multilayered blastula wall has been studied in *Xenopus*. During early cleavage divisions, blastomeres become separated by newly inserted membranes, while their exterior surface is inherited from the egg surface. This apical membrane is nonadhesive, whereas the basolateral membranes mediate mutual blastomere attachment (Byers and Armstrong, 1986; Muller and Hausen, 1995; Roberts et al., 1992; reviewed by Müller, 2001). As cleavage progresses, division planes become oriented either perpendicular or parallel to the embryo surface; the latter mode generates a population of nonpolarized inner blastomeres (Chalmers et al., 2003; Muller and Hausen, 1995; Strauss et al., 2006).

In the outer layer of blastomeres, junctional complexes comprising tight junctions, adherens junctions, and desmosomes develop (Muller and Hausen, 1995; Regen and Steinhardt, 1986). Tight junctions seal the blastocoel from the exterior (Muller and Hausen, 1995), and expansion of the fluid- and matrix-filled blastocoel spans the surface layer of blastomeres

into a sphere. The inner blastomeres are attached to this outer layer to form the multilayered blastocoel wall. Due to its apico-basolateral polarity and the presence of junctional complexes, the outer layer is often referred to as an epithelium that covers the inner, "mesenchymal" layers. However, the cells of both the apical and the inner layers are tightly packed, express the same cadherins, and contain epithelial, but not mesenchymal intermediate filaments (Klymkowsky et al., 1992). Moreover, apical and deep layers are intimately attached to each other without an intervening basal lamina. Thus, the blastocoel wall may be considered a multilayered epithelium, such as are characteristic of vertebrates (discussed in Shook and Keller, 2003).

In *Xenopus*, the blastula wall remains multilayered in all regions, but varies in thickness. Its thin, small-celled animal part, the blastocoel roof (BCR), is distinct from the massive vegetal part. The latter consists of the vegetal mass of large, yolk-rich cells, and of an equatorial ring of intermediate-sized cells, the marginal zone (Fig. 5.1A; Keller, 1976; Keller and Schoenwolf, 1977; Nakatsuji, 1975; Nieuwkoop and Florschutz, 1950). In most urodeles, the BCR has become single layered by the time of gastrulation (Shook and Keller, 2008), but the vegetal cell mass remains multilayered in all amphibians. Overall, the amphibian early embryo consists essentially of a single coherent tissue held together by cell–cell adhesion (Fig. 5.2A).

2.2. Gastrulation movements

Mapping the prospective germ layers onto the amphibian blastula reveals that the marginal zone between BCR and vegetal cell mass contains the prospective mesoderm, the vegetal cell mass will become included in the endoderm, and most of the BCR will form ectoderm (Fig. 5.1A; Dale and Slack, 1987; Keller, 1975, 1976; Moody, 1987). Gastrulation consists of the movement of the prospective mesoderm and endoderm to the interior of the embryo, and in the proper positioning of the different mesodermal and endodermal tissue precursors along the future dorsoventral and anteroposterior axes. Due to the multilayered histology of the gastrula, these movements involve massive cell rearrangements, for example, the directed, active intercalation of cells. Such intercellular migration (Gumbiner, 2005) of cells across the surface of neighboring cells plays a fundamental role in amphibian gastrulation.

Gastrulation movements are best described for *Xenopus*. Here, two intercellular migration processes cooperate to drive mesoderm and endoderm internalization. Above the blastopore, the mesoderm of the blastopore lip moves inward by involution (Fig. 5.1B). The force driving this poorly understood process seems to be generated in the mesodermal cells deep to the epithelial layer (Keller, 1981), and the movement is associated with a rearrangement of blastopore lip cells (Ibrahim and Winklbauer, 2001;

Winklbauer and Schürfeld, 1999). The vegetal cell mass also contributes to internalization. Its cells surge animally toward the blastocoel floor, and outward, in a movement termed vegetal rotation (Fig. 5.1A and B) (Winklbauer and Schürfeld, 1999). In its course, the peripheral blastocoel floor is applied against the BCR. Together with involution, vegetal rotation generates a vortex pattern of cell movement in the equatorial region: involution contributes a downward and inward flow of material, and vegetal rotation a complementary upward and outward translocation of cells (Fig. 5.1A). Both involution and vegetal rotation begin dorsally and spread ventrally.

Once internalized, mesoderm and endoderm advance animally across the BCR (Fig. 5.1B). This process is most vigorous on the prospective dorsal side, such that the leading tissue, after having reached the future anterior end of the embryo, continues to advance by moving posteriorly for some distance on the ventral side (Bauer et al., 1994; Tracey et al., 1998). In part, this movement is due to anterior mesoderm and endoderm translocating as a whole on the BCR substratum (Davidson et al., 2002; Keller and Schoenwolf, 1977; Nakatsuji, 1975; Winklbauer, 1990; Winklbauer and Nagel, 1991). In addition, vegetal cell mass is constantly inserted at the BCR-apposed leading edge (Bauer et al., 1994), in an apparent continuation of vegetal rotation (Fig. 5.1B) (Ibrahim and Winklbauer, 2001).

The antero-posterior axis of a vertebrate body becomes distinctly elongated, and in some amphibians, the initial phase of this elongation is an integral part of gastrulation, as for example, in *Xenopus*. Here, cells of the somitic and chordamesoderm (Fig. 5.1B) rearrange by mediolateral and radial intercalation to narrow and lengthen the tissue. This convergent extension movement starts during involution, and continues into tailbud stages (Keller and Danilchik, 1988; Keller and Tibbetts, 1989; Lane and Keller, 1997; Shih and Keller, 1992a,b; Wilson and Keller, 1991; Wilson et al., 1989; for review see Keller et al., 2000, 2003). In the BCR, a similar convergent extension takes place in the future central nervous system. In this way, neuroectodermal and chordamesodermal/somitic tissue elongate in register (Keller et al., 1992a,b). In many amphibian species, however, convergent extension is a postgastrular event (del Pino et al., 2007). Convergent extension is a prime example of intercellular migration, as intercalating cells extend locomotory protrusions across the surface of their neighbors, and move relative to them (Elul and Keller, 2000; Keller et al., 1989; Shih and Keller, 1992a,b).

Towards the end of gastrulation, the blastopore closes below the vegetal cell mass. Inside the embryo, the blastopore deepens to form the archenteron (Figs. 5.1B and 5.2A), first by involution, then dorsally by the posterior addition of mesoderm and neuroectoderm through convergent extension, and furthermore by an expansion of the apical surface of formerly contracted bottle cells. The initially slit-like archenteron is inflated dorsally,

its cavity replacing the collapsing blastocoel (Ewald et al., 2004; Keller, 1981; Nieuwkoop and Florschutz, 1950). Laterally and ventrally, the archenteron remains unconspicuous. As mesoderm and endoderm move to the interior, the ectodermal BCR spreads to cover the embryo in the process of epiboly (Fig. 5.1A and B). The respective increase in area is due to the flattening and expansion of the cells of the outer BCR layer, and to a rearrangement of inner cells (Fig. 5.2A) which reduces the number of BCR layers (Keller, 1978, 1980; Marsden and DeSimone, 2001).

Compared to intercellular and collective migration, epithelial shape change is of minor importance in amphibians such as *Xenopus*. In this species, its most prominent expression is the establishment of the blastopore (Fig. 5.1B) by bottle cell formation at the onset of gastrulation. The epithelial cells at the vegetal boundary of the dorsal marginal zone constrict their apical surfaces to generate the blastoporal indentation. Above it, the bulging marginal zone forms the blastopore lip. Later in gastrulation, respreading of these bottle cells contributes to archenteron elongation (Hardin and Keller, 1988; Keller, 1978, 1981). In urodeles, epithelial morphogenesis is more prominent. In Cynops, explanted epithelial layer from the vegetal half of the gastrula invaginates *in vitro* to form a well-developed archenteron (Komazaki, 1993), implying that epithelial folding contributes significantly to internalization and performs at least part of the function ascribed to involution in *Xenopus*. *Xenopus* is also atypical with respect to the minor role that ingression plays. In other anurans, and most notably in urodeles, internalization involves the massive ingression of prospective mesodermal cells at the blastopore lip or the archenteron roof, that is, an epithelial–mesenchymal transition that is also commonly observed in invertebrate gastrulation (Minsuk and Keller, 1997; Shook and Keller, 2003; Shook et al., 2002, 2004).

2.3. Preview: Two classes of morphogenetic forces in the amphibian gastrula

The multilayered tissue that builds the amphibian gastrula shows behavior resembling that of a liquid. Although held together by mutual adhesion, cells are motile in various ways, and a random component of this motility seems to produce effects known from liquids, such as surface tension, or phase separation of different components. These consequences of the combination of flexible adhesion with random motility could in principle drive morphogenesis or stabilize gastrula structures. Through spatial differences in adhesiveness, boundaries could be established between regions, and tissue positions be determined.

Another class of morphogenetic mechanisms is based not on random, but on oriented cell motility. Living tissue is an unusual fluid, in that it can generate forces to drive predetermined flow patterns endogenously, by the expenditure of metabolic energy: active cell movements lead to cell

rearrangement and to intercellular migration. However, it is not the presence of active movement itself which is relevant in this respect, but the fact that cell behavior is organized: cells are oriented and aligned according to a global pattern. This leads to nonrandom exchanges of neighbors, and orderly, programmed tissue deformations. In the context of intercellular migration, cell adhesion enters in connection with the substratum for migration, which is provided by the surface of adjacent cells. The forces produced by random and by oriented cell movement are similar in magnitude, and the former, if not employed directly for morphogenetic purposes, will have to be properly controlled to prevent adverse effects on gastrula structure or movements.

3. Gastrula Tissue as a Liquid: Cell Adhesion, Cell Sorting, Boundary Formation, and Tissue Positioning

When Holtfreter experimented with the dissociation and reaggregation of amphibian embryonic tissues, he noted that different cell types could be incorporated into a common aggregate, indicating a basal adhesive mechanism. However, cells would eventually sort out into discrete populations according to their origins, suggesting an additional, selective component. Moreover, tissues assumed specific spatial configurations when combined experimentally, for example, by engulfing or repelling each other, and these "tissue affinities" changed dynamically during development. Holtfreter realized that these principles could potentially explain not only the stability of embryonic structures, but also many morphogenetic movements (Holtfreter, 1939, 1944; Townes and Holtfreter, 1955). Later, Steinberg proposed in his Differential Adhesion Hypothesis (DAH) that a quantitative difference in the strength of adhesion between cell types would be sufficient to promote cell sorting and the reproducible spatial arrangement of tissues (Steinberg, 1963, 1970).

After discussing liquid-like properties of tissues in general, the application of the concept to the amphibian gastrula will be examined. Results from cell sorting and related experiments suggest that a pattern of regional differences of adhesiveness exists, and molecular data provide insights into the mechanisms and modulations of gastrula tissue cohesion. In discussing possible functions of differential adhesion, it will be found that despite the undoubted presence of respective effects in gastrula tissue, it is still to be demonstrated unambiguously that they play a constructive role in the early amphibian embryo.

3.1. Liquid-like properties of tissues

Adhesion between aggregated cells is usually flexible and allows for cell rearrangement. In aggregates, cells show spontaneous random motility (Mombach and Glazier, 1996; Rieu and Sawada, 2002; Rieu et al., 2000),

but move also in response to external, tissue-deforming forces (Phillips et al., 1977; Rieu and Sawada, 2002). In both cases, cells have to make and break contacts to exchange neighbors. The combination of tight cohesion with the ability of elements to move freely relative to each other is a generic property of liquids, and its occurrence in cell aggregates is the basis for the analogy between tissues and liquids.

In a body of liquid, surface tension minimizes the surface area, for example, by shaping a drop. Cell aggregates show similar behavior, and by analogy, a surface minimizing tension has been defined for tissues (Beysen et al., 2000; Foty et al., 1994; Graner, 1993; Jakab et al., 2008; Steinberg, 1978). Tissue cohesion is essentially mediated by membrane-inserted adhesion molecules which engage in specific binding. To peel the interacting surfaces of two cells apart requires mechanical work, which is defined as surface adhesive free energy. In an aggregate, it tends to be minimized by maximizing cell contacts—that is, adhesion molecule engagement—through an appropriate rearrangement of cells. Overall, this leads to the minimization of the surface area of an aggregate, and the corresponding driving force is expressed as a surface tension. In other words, an aggregate assumes the shape with the least external surface, as on this surface, adhesion molecules can find no binding partners on opposite cells.

A simple microscopic interpretation of tissue surface tension (Fig. 5.3A) can be based on principles that apply when a cell is peeled off its substratum (Ward et al., 1994). Near the aggregate surface, neighboring cells tend to increase their lateral contacts by zippering up. Membrane fluctuations above the contact area bring free adhesion molecules into close proximity, and their binding drives the extension of the contact zone at the expense of free outer surface. This increases tension in the plane of the free surface. Above a critical value, the tension would peel off the cells from each other. The critical tension where zippering and peeling are in equilibrium corresponds to the global surface tension (Fig. 5.3A).

Both zippering up and peeling off can be complex processes. For example, the dynamics of endo- and exocytosis may affect the membrane flow between contacting and free cell surfaces (Delva and Kowalczyk, 2009; Yap et al., 2007). Also, cadherin-mediated contact formation in cultured cells involves small GTPases such as Rac and RhoA which regulate the dynamics of the actin cortex (e.g., Braga et al., 1997; Kovacs et al., 2002; Noren et al., 2001; Yamada and Nelson, 2007). Nevertheless, an equilibrium between peeling off and zippering up would eventually have to be reached. Although the value of this critical tension will be determined not only by the affinities and densities of adhesion molecules, but also by their clustering and mobility, by the stiffness of the membrane and the cell cortex, and so forth (Ward et al., 1994), adhesion strength will still be constantly sampled by the establishment and breaking of bonds, and be a major determinant of surface tension.

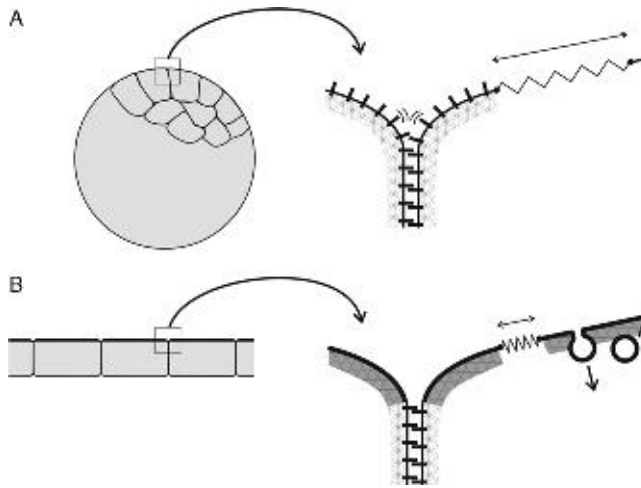

Figure 5.3 Effects of adhesiveness on surface of tissues. (A) In mesenchymal aggregates (left), cells maximize contacts by zippering up lateral membranes (right), driven by the binding of adhesion molecules (small bars). At equilibrium, surface is under tension (expanded spring, double arrow). (B) In epithelia (left), the apical surface (right; thick line) is nonadhesive, therefore zippering up of lateral membranes is limited, and tension in surface remains low (spring, double arrow).

Liquid-like behavior is also observed when cells from different tissues are mixed: cells typically sort out according to their origins. It has been proposed that quantitative differences in the strength of adhesion are sufficient to explain sorting by thermodynamic principles. This concept was introduced as the DAH (Steinberg, 1963, 1970), whose application has then been extended to explain all liquid-like behaviors of tissues. The DAH holds that in a mixed aggregate, adhesion molecule engagement would be maximized when the strongly adhesive cells were contacting each other. This state of minimum free energy would be stable once attained by random movements of cells. In this view, sorting would be analogous to the demixing of immiscible fluids (Beysen et al., 2000).

When mixed cells from two tissues segregate from each other, the two domains that form assume a characteristic spatial configuration. Moreover, the same configuration is attained when the two tissues are combined directly as explants. For example, one cell type can become completely engulfed by the other, leading to an inside-outside arrangement of tissues. Partial engulfment of one population by the other generates a serially arranged, elongated structure. If adhesion between populations is negligible, they separate completely. These tissue positioning effects can also be explained within the framework of the DAH. It is argued that the final configurations represent equilibrium states, whereby the relative strengths of the surface tensions of the two tissues, and that of the interfacial tension at

their common boundary, determine the tissue arrangement (Foty et al., 1996; Graner, 1993; Phillips and Davis, 1978; Steinberg, 1970; Steinberg and Takeichi, 1994).

In the simple case where two cell types express the same homophilic adhesion molecule, though at different densities, and where surface tension is proportional to this density (Foty and Steinberg, 2005; Hegedüs et al., 2006; Jia et al., 2007), interfacial tension should be directly related to the surface tensions of the two populations. By assuming a simple mass action kinetics of adhesive bond formation, Steinberg estimated that interfacial tension would always be in a range consistent with a pattern of complete engulfment. In particular, the more cohesive tissue would be enclosed by the less cohesive one (Steinberg, 1978). In zebrafish embryonic cells, adhesive strength between two different cell types amounts to the strength of adhesion between cells of the less adhesive type, which is also consistent with complete engulfment (Krieg et al., 2008). When cadherin expression is experimentally varied in a cell line, a 50% difference in cadherin levels is sufficient for the induction of sorting and complete engulfment (Duguay et al., 2003; Foty and Steinberg, 2005).

Although this proposed mechanism relies on special assumptions about the molecular basis of interfacial tension, complete engulfment of more cohesive by less cohesive tissue has become a core tenet of the DAH, probably because most tissue combinations do indeed conform to this pattern (Foty et al., 1996). Given the possible complexity of tissue–tissue adhesion, this surprising empirical finding has no obvious molecular explanation, but it is not a necessary consequence of the DAH. It implies, first, that adhesion mechanisms are shared by most cell types, to allow formation of a common aggregate; and second, that any qualitative variation in their molecular basis is such that adhesion varies merely quantitatively. An explanation for this phenomenon could include: tissues use more than one adhesion systems in parallel, with overlaps between tissues; if a specific adhesion molecule is present on both interacting tissues, it will likely be independently expressed, and thus at different concentrations; adhesion molecules often interact nonspecifically—cadherins, for example, exist in multiple isoforms, but binding is promiscuous, allowing for the interaction of cells expressing different cadherins (Niessen and Gumbiner, 2002; Prakasam et al., 2006). Such mechanisms taken together could make quantitative adhesion differences a common feature, thus explaining the abundance of the respective tissue positioning pattern.

Mechanisms have been proposed that could influence surface tension and cell sorting in addition to differential adhesion. In particular, a contribution of cell cortex contractility has been suggested (Brodland, 2002; Harris, 1976; Krieg et al., 2008), but this may depend on special assumptions, for example, about how cells move in aggregates. Brodland (2002) considers cell rearrangements that occur by the expansion or shrinking of

existing cell–cell boundaries, with adhesiveness per boundary area remaining constant. This implies specific mechanisms of adhesion molecule dynamics, for example, regulated exo- and endocytosis, which may not occur generally. To explain cell sorting in the zebrafish gastrula, an induced stiffening of the cell cortex in areas exposed to the culture medium has been invoked (Krieg et al., 2008). Altogether, the DAH may underestimate the complexity of cell sorting in specific cases. However, patterns of complete engulfment are obtained with cell types from widely different sources, suggesting a common basic determinant for which differential adhesion seems to be the most likely candidate.

The DAH is usually applied to mesenchymal aggregates, but not to epithelia. In epithelia, a stable, often nonadhesive apical membrane domain and firm lateral linkage of cells precludes formation of a compact, multilayered mass (Fig. 5.3B). Instead, isolated epithelia can self-interact with their adhesive basal side to form folded structures which preserve their apical surface area. With their basal surface, they can also attach to and spread over a mesenchymal aggregate, and by transferring to it their ability to resist surface minimization (Fig. 5.3B), they reduce its usually strong surface tension and facilitate the generation of nonspherical shapes (Ninomiya and Winklbauer, 2008).

3.2. Differential adhesion, cell sorting, and tissue positioning in the blastula and gastrula

Explants from the amphibian gastrula show liquid-like behavior in the sense discussed earlier (Davis, 1984; Phillips, 1984; Phillips and Davis, 1978), and their surface tension can be measured (Davis et al., 1997; Kalantarian et al., 2009). Tissue surface tension differs between regions of the gastrula. In *Rana*, average surface tension is lowest in the endoderm, intermediate in lateral mesoderm, higher in epidermal ectoderm of the BCR, and highest in prospective neural ectoderm (Davis et al., 1997) (Table 5.1). In *Xenopus*, surface tension is also lowest in the endodermal vegetal cell mass (Ninomiya, David, and Winklbauer, unpublished results), intermediate in the prechordal mesoderm, and high in the ectodermal BCR. Chordamesoderm, which had not been examined in *Rana*, is similar to the ectoderm (Kalantarian et al., 2009; Ninomiya and Winklbauer, 2008) (Table 5.1). In *Rana*, the difference between the lowest and the highest tissue average, respectively, is about fourfold. The respective values for zebrafish gastrula ectoderm and artificially induced mesoderm are similar to those of *Rana* (Schotz et al., 2008) (Table 5.1).

Differences between regions are also obvious from cell sorting experiments. Sorting out of mid-blastula animal and vegetal cells, and of late blastula marginal zone cells has been shown for *Xenopus*, at the earliest stages when such experiments are feasible (Turner et al., 1989). At later stages,

Table 5.1 Tissue surface tension values (in mJ/m^2) in amphibian and fish gastrulae

Rana pipiens[a]		*Xenopus laevis*[b]		*Danio rerio*[c]	
Endoderm	0.4				
Mesoderm (lateral)	0.6	Mesoderm (prechordal)	~1	Mesoderm	0.4
		Chordamesoderm	3		
Ectoderm (BCR)	0.8	Ectoderm (BCR)	3.4	Ectoderm	0.8
Ectoderm (neural)	1.6				
Ranges of surface tension values within tissue (in mJ/m^2)					
Rana ectoderm (BCR)	0.3–1.6				
Xenopus ectoderm (BCR)	1.1–7.7				
Danio mesoderm	0.1–0.8				

[a] Davis et al. (1997).
[b] Ninomiya and Winklbauer (2008), Kalantarian et al. (2009).
[c] Schotz et al. (2008).

differences between germ layers are observed. In the experiments of Townes and Holtfreter (1955), differential sorting of ectodermal, mesodermal, and endodermal cells from the urodele neurula has been demonstrated. Similarly, when *Xenopus* prospective ectoderm is induced by activin treatment to form chordamesoderm or endoderm, respectively, these two cell types sort from each other, and from ectodermal cells during gastrula stages (Kuroda et al., 1999).

Differences exist also within germ layers. Prospective neural cells sort from epidermal cells of the urodele neurula (Townes and Holtfreter, 1955), in agreement with measured surface tension differences between the neural and epidermal moieties of the frog gastrula ectoderm (Davis et al., 1997). In *Xenopus*, cells from anterior and posterior parts of the chordamesoderm sort from each other when mixed at the early gastrula stage (Ninomiya et al., 2004). Similarly, when ectoderm cells are induced by different doses of activin to form specific mesoderm regions—prechordal mesoderm, anterior chordamesoderm, and posterior chordamesoderm—and then mixed with uninduced ectoderm, all four cell types segregate from each other (Ninomiya and Winklbauer, 2008). Apparently, a detailed pattern of cell affinities becomes established in early development.

Tissue positioning effects are generally as expected from embryonic tissue surface tensions and from the rule that less cohesive tissues engulf more cohesive ones. When combined with endoderm and mesoderm, inner

ectoderm cells of the frog, *Rana pipiens*, form the innermost tissue, to be surrounded by mesoderm, which in turn is enclosed by endoderm (Fig. 5.4A and B) (Phillips and Davis, 1978). A corresponding pattern is seen with other amphibians: when mesoderm is placed with endoderm, it becomes engulfed (Holtfreter, 1944; Townes and Holtfreter, 1955), and when inner ectodermal cells, without the epithelial layer, are combined with endoderm, they move to the center of the explant (Holtfreter, 1944). In *Xenopus*, chordamesoderm positions itself at the center of an aggregate when combined with anterior mesoderm or ectoderm, as expected from its cohesiveness (Kuroda et al., 1999; Ninomiya and Winklbauer, 2008). However, ectoderm is not engulfed by artificially induced endoderm (Kuroda et al., 1999).

It is striking that in these *in vitro* experiments, the order of germ layers is the inverse of the normal sequence, implying that the inverse arrangement corresponds to an equilibrium state. How is this reconciled with the topology of germ layers in the embryo? The clue lies in a special property of the epithelial layer of the ectoderm: since its apical surface is nonadhesive, it is excluded from any aggregate and always comes to reside on the outside (Holtfreter, 1939; Phillips and Davis, 1978). Thus, when whole ectoderm, not only its inner layers, is combined with endoderm or mesoderm

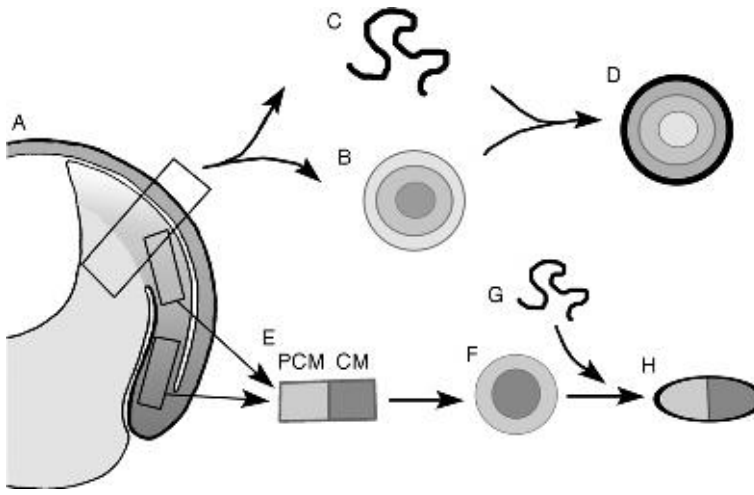

Figure 5.4 Tissue positioning effects in gastrula explants. When endoderm, mesoderm, and ectoderm is explanted (upper box in (A)), and the epithelial layer is removed (C), the tissues arrange in the inverse order, with ectoderm being in the center, endoderm on the surface, and mesoderm in between (B). When epithelium is added, the normal arrangement is attained, with endoderm in the center (D). When prechordal (PCM) and chordamesoderm (CM) are combined (lower boxes in (A), E), chordamesoderm becomes engulfed (F). Addition of epithelial layer (G) restores the normal serial arrangement (H).

(Fig. 5.4B–D), it moves to the exterior (Holtfreter, 1939; Phillips and Davis, 1978; Townes and Holtfreter, 1955). Together with the tendency of mesoderm to intercalate between ectoderm and endoderm (Holtfreter, 1939; Phillips and Davis, 1978; Townes and Holtfreter, 1955), this leads to a normal germ layer arrangement (Fig. 5.4B–D).

Although mesoderm segregates from endoderm as well as from ectoderm, it nevertheless attaches firmly to each. In fact, it serves as a glue between the two. Thus, when gastrula ectoderm is placed on an endodermal explant, it spreads first, but soon reverses its movement to completely detach itself from the endoderm. This separation is prevented if mesoderm is included (Holtfreter, 1939; Townes and Holtfreter, 1955). Proper positioning of the mesoderm peripherally to the endoderm depends in turn on the presence of the ectoderm. This shows dramatically when the ectoderm is removed from a whole neurula: then the mesoderm breaks up into patches which sink into the underlying endoderm, to eventually reverse the normal order of these germ layers, in agreement with the *in vitro* pattern of positioning (Holtfreter, 1944; Townes and Holtfreter, 1955). The axial mesoderm of a BCR-less *Xenopus* gastrula also sinks into the endodermal vegetal cell mass (Keller and Jansa, 1992). Ultimately, it is the coating of the inner ectodermal cells by an epithelial layer which drives the ectoderm to the explant surface and thus establishes the normal configuration of germ layers (Fig. 5.4B–D) (Phillips and Davis, 1978). A similar effect is generated by the enveloping layer of the zebrafish gastrula (Krieg et al., 2008).

This phenomenon, that epithelial coating determines tissue configurations, is also encountered during positioning of axial mesoderm regions (Ninomiya and Winklbauer, 2008). When explanted without the covering epithelium, anterior mesoderm engulfs the chordamesoderm posterior to it (Fig. 5.4A, E, and F). Adding back an epithelial layer prevents engulfment and preserves a linear array of regions (Fig. 5.4G and H). The same effect is seen when anterior and posterior cells are mixed and allowed to sort out in the presence or absence of an epithelial layer. Furthermore, when cells from prechordal mesoderm, anterior and posterior chordamesoderm, and ectoderm are mixed, sorting occurs, but tissues are arranged according to their normal sequence only when the aggregate is coated by an epithelial layer (Ninomiya and Winklbauer, 2008; Ninomiya et al., 2004). Thus, the basal surface of an epithelium cannot only sequester a preferred cell type, to determine the inside-out sequence of tissues, but it can also induce a linear array where all tissues are in contact with the covering layer (Fig. 5.4).

An explanation for this effect considers that tissue positioning through differential adhesion is strongly context sensitive. A tissue will normally border on several neighbors, and the stability of each edge where tissues meet will depend on the mutual adhesion between any two of these. In other words, a whole series of adhesive interactions will specify its

equilibrium position, and tissues will readily change their configuration when removed from their normal context, especially when low, balanced interfacial tensions are replaced by high, newly introduced surface tensions as a consequence of explantation (Ninomiya and Winklbauer, 2008). In the tissue positioning experiments involving prechordal mesoderm and chordamesoderm, a serial pattern was changed into a radial inside-out arrangement by explantation, which in turn was reverted to a serial pattern by epithelial coating (Fig. 5.4A, E–H). Apparently, the radial pattern is an artifact induced by removing the tissues from their normal context. Radial patterns are most frequent *in vitro*, but serial patterns abound in intact organisms. This suggests that similar *in vitro* effects may be responsible for many of the tissue patterns observed at cell sorting.

In summary, a pattern of correlated cell sorting, surface tension, and tissue positioning domains is present during blastula and gastrula stages, which seems to be similar in the few amphibian species examined. Generally, the tissue cohesiveness that can tentatively be inferred from these data increases from the vegetal endoderm to the anterior and lateral mesoderm, to reach a high point in the chordamesoderm and neural ectoderm, and to decrease again slightly in the remaining ectodermal BCR (Fig. 5.1C and D). This pattern, its development and function will be discussed in detail after its putative molecular basis has been described.

3.3. The molecular basis of cell–cell adhesion in the amphibian embryo

A number of molecular factors have been described which are involved in the mediation or control of cell–cell adhesion in the early amphibian embryo. Most of these are ubiquitously present in the blastula and gastrula, but their expression or function is often modulated regionally. A few adhesion-related genes are expressed in the prospective ectoderm only, and others in all of the mesoderm, or in mesodermal subregions such as the anterior or the posterior dorsal mesoderm.

3.3.1. The cadherin/catenin complex

Cadherins are centrally involved in holding the early amphibian embryo together. The vertebrate classic cadherins contain five extracellular cadherin repeats (EC domains) and a conserved cytoplasmic domain which binds the armadillo-repeat proteins β-catenin, plakoglobin, and p120-catenins, and other factors. β-catenin interacts with α-catenin to dynamically link cadherins to the actin cytoskeleton, whereas an important function of p120-catenins is to regulate cadherin stability at the cell membrane (Gumbiner, 2005; Halbleib and Nelson, 2006; Nelson, 2008; Tepass et al., 2000).

3.3.1.1. Components In *Xenopus*, maternal cadherins provide for the cohesion of cleavage and blastula stage embryos. The independently isolated EP- and C-cadherin (Choi et al., 1990; Ginsberg et al., 1991) are putative allelic variants, and the same holds for the XB- and U-cadherin pair (Angres et al., 1991; Herzberg et al., 1991). EP/C- and XB/U-cadherins in turn are very similar to each other, and are probably pseudoalleles generated during a tetraploidization event in the *Xenopus* lineage (Kuhl and Wedlich, 1996). They are most closely related to mammalian P-cadherin (Gallin, 1998). From the first cleavage divisions onwards, EP/C- and XB/U-cadherins are expressed on the basolateral membranes of all blastomeres (Angres et al., 1991; Herzberg et al., 1991; Levi et al., 1991), with XB/U-cadherin being a minor component (Muller et al., 1994). After the onset of zygotic transcription at the mid-blastula stage, and throughout gastrulation, EP/C- and XB/U-cadherins continue to be expressed, and there is only limited, region-specific expression of additional adhesion molecules.

In most vertebrate gastrulae, E-cadherin holds the place taken by EP/C- and XB/U-cadherin in *Xenopus*. In amniotes such as chicken and mouse, but also in *Drosophila*, the mesoderm switches from E- to N-cadherin expression as it moves to the interior of the gastrula as a migratory mesenchymal tissue (Hatta and Takeichi, 1986; Oda et al., 1998; Radice et al., 1997). In the zebrafish, however, E-cadherin remains expressed in post-involution mesoderm (Babb and Marrs, 2004; Montero et al., 2005). In *Xenopus*, the mesoderm and endoderm internalize as a coherent cell mass. As this mass engages in intercellular and substrate-dependent migration, it continues to express EP/C- and XB/U-cadherin.

The maternal cadherins are essential for blastomere adhesion (Angres et al., 1991; Heasman et al., 1994; Kurth et al., 1999; Muller et al., 1994). Reducing the maternal expression of EP/C-cadherin, or of both EP/C- and XB/U-cadherin, by antisense oligonucleotides diminishes the adhesion of inner blastomeres, but leaves the epithelial layer of the blastula intact (Heasman et al., 1994; Kurth et al., 1999), probably due to the adhesive functions of tight junction components such as claudin (Brizuela et al., 2001). However, overexpressed cytoplasmic domain of *Xenopus* N-cadherin, which inhibits endogenous cadherins in a dominant-negative fashion, affects the epithelial layer at high doses; at lower doses, only inner cells are dissociated (Kintner, 1992). XmN-cadherin is also expressed maternally, but is soon downregulated (Hojyo et al., 1998).

In the *Xenopus* embryo, β- and α-catenin are also maternally expressed. β-catenin associates with cadherin before the complex reaches the cell membrane. Most of the β-catenin present in a cell is associated with EP/C- and XB/U-cadherin, and its distribution closely mimics that of the cadherins (DeMarais and Moon, 1992; Fagotto and Gumbiner, 1994; Schneider et al., 1993). When EP/C-cadherin is overexpressed, β-catenin membrane density increases proportionally, whereas depletion of both maternal cadherins leads to a corresponding decrease (Kurth et al., 1999).

In contrast, α-catenin associates with the cadherin/β-catenin complex only at the cell membrane. Although an excess of cytoplasmic α-catenin is normally present, it does not associate significantly with additional, overexpressed EP/C-cadherin. However, depletion of cadherins reduces α-catenin membrane association (Kurth et al., 1999; Schneider et al., 1993). Interestingly, whereas β-catenin colocalizes with cadherin in cell–cell contacts, but also on free cell membranes, α-catenin is restricted to areas of contact. Unlike β-catenin, it is absent from the surface of BCR cells that faces the blastocoel cavity (Schneider et al., 1993). This suggests that α-catenin is not a constitutive component of the cadherin/catenin complex, but correlated with actual cell contact formation. Inhibiting α-catenin function diminishes blastomere adhesion at the blastula stage (Kofron et al., 1997; Sehgal et al., 1997).

Plakoglobin, an armadillo-repeat protein closely related to β-catenin, associates preferentially with desmosomal cadherins, but is also found in adherens junctions (Chitaev et al., 1998). It is maternally expressed in *Xenopus* (Fouquet et al., 1992; Kofron et al., 1997), forming dots along gastrula cell membranes which do not colocalize with overexpressed cadherin, however (Kurth et al., 1999). In plakoglobin-depleted blastulae, cell adhesion is reduced in particular in the vegetal cell mass, the maintenance of the cortical actin cytoskeleton is impaired, and gastrulation is delayed. These effects are not rescued by α- or β-catenin mRNA injection, suggesting nonoverlapping functions (Kofron et al., 1997, 2002).

Members of the p120 catenin subfamily of Arm domain proteins bind to the cytoplasmic domain of classic cadherins at a juxtamembrane site, different from that of β-catenin binding. This interaction stabilizes cadherin at the cell membrane by attenuating its endocytosis (Reynolds and Carnahan, 2004). Moreover, p120 catenins affect the function of Rho GTPases, potentially activating Rac and inhibiting RhoA (Grosheva et al., 2001; Noren et al., 2000; Yanagisawa and Anastasiadis, 2006), and they are involved in the lateral clustering of cadherins (Yap et al., 1998). In the *Xenopus* early embryo, the family members p120-catenin, ARVCF, and δ-catenin are expressed (McCrea and Park, 2007), and depletion of p120 catenin or ARVCF diminishes C-cadherin protein expression, whereas their overexpression increases it (Fang et al., 2004; Tao et al., 2007). However, no concomitant effect on cell adhesion was detected (Fang et al., 2004). ARVCF and perhaps p120 catenin are able to also diminish adhesion independently of cadherin membrane expression, which is revealed when membrane-tethered ARVCF is overexpressed in ectodermal cells of the gastrula. Adhesion is rescued by activated Rac, implying an inhibition of this GTPase by exogenous ARVCF (Reintsch et al., 2008).

3.3.1.2. Spatio-temporal expression Membrane expression of the cadherin/catenin complex is spatially patterned (Fig. 5.1C and D). In the gastrula, cadherin and β-catenin density increases from a relatively high

level in the ectodermal BCR to its strongest expression in the dorsal chordamesoderm, becomes lower again in anterior mesoderm, and is weakest in the endodermal vegetal mass (Fig. 5.1D; Angres et al., 1991; Fagotto and Gumbiner, 1994). Density varies in a graded fashion between regions, except where tissues become secondarily apposed at Brachet's cleft. Thus dorsally and ventrally, β-catenin staining is strongest in the blastopore lip and decreases toward the anterior mesoderm, which leads to the apposition of less intensely stained anterior mesoderm and strongly labeled BCR (Fig. 5.1D Fagotto and Gumbiner, 1994), a pattern which is confirmed by C-cadherin staining (Ogata et al., 2007). In the late gastrula, dorsal blastopore lip and adjacent chordamesoderm and neural ectoderm are still the most intensely labeled tissues (Fagotto and Gumbiner, 1994), and it is these which are engaged in active convergent extension. At this stage, β-catenin staining increases in the outer layer of the ectoderm, probably reflecting the onset of E-cadherin expression. A similar overall pattern is seen with α-catenin staining (Schneider et al., 1993).

The pattern of regional cadherin/catenin intensity differences is already observed at the earliest cleavage stages. XB/U-cadherin, β-catenin, and α-catenin are most strongly expressed on marginal zone blastomere membranes, at slightly lower levels animally, and most weakly vegetally (Fagotto and Gumbiner, 1994; Herzberg et al., 1991; Schneider et al., 1993), suggesting that these differences are established in the egg cytoplasm under maternal control. Maternal cadherin and catenin proteins are indeed prelocalized in the egg, and enriched in its animal half to be segregated into animal blastomeres (Ginsberg et al., 1991; Herzberg et al., 1991; Schneider et al., 1993). A maternal mechanism must also be responsible for the further increased density at marginal zone membranes that is established before the onset of transcription in the mid-blastula (Fig. 5.1C).

The pattern of cadherin/catenin membrane density reflects strikingly well the pattern of tissue cohesiveness deduced from cell sorting or tissue positioning effects, or from measurements of tissue surface tension (Fig. 5.1C and D). During gastrulation, this pattern is distorted in the course of tissue rearrangements, but beyond that, it is not very dynamic. It seems as if the single, multilayered tissue which forms the *Xenopus* blastula is "folded back" on itself without much change in local cadherin/catenin membrane expression (Fig. 5.1C and D). The question then arises how this pattern is maintained throughout early development, that is, through the transition from maternal control to zygotic transcription, the induction and patterning of mesoderm and neural tissue, and the execution of gastrulation movements.

3.3.1.3. Control of expression If blastula-stage BCR is experimentally induced to form mesoderm of different anterior–posterior positions, cell adhesiveness changes accordingly. The antero-posterior sequence of dorsal

mesodermal tissue identities as well as the adhesion differences that determine their sorting properties can simultaneously be induced by graded activin signaling. This suggests that in the embryo, a gradient of nodal-related factors that patterns the axis also regulates tissue cohesiveness (Kuroda et al., 1999; Ninomiya and Winklbauer, 2008; Ninomiya et al., 2004). It implies that the cadherin/catenin pattern is actively maintained after the mid-blastula transition.

This could be achieved by ubiquitous factors responding to a graded activin-like signal to regulate cadherin expression. A constitutively active Gαq, a component of trimeric G-proteins, is able to downregulate C-cadherin transcription and to decrease adhesion if expressed in ectoderm cells (Rizzoti et al., 1998), but the effect has only been demonstrated for postgastrula stages, and it is unclear whether it plays a role in normal development. At the level of mRNA stability, *Xenopus* cold-inducible RNA binding protein (XCIRP) has been proposed to regulate the expression of C- and E-cadherin, but also that of α- and β-catenin, and of N-CAM and paraxial protocadherin (PAPC) (Peng et al., 2006). However, no *in vivo* role or region-specific effects have been demonstrated. ARVCF and p120-catenin can affect cadherin expression of gastrula cells (Fang et al., 2004; Tao et al., 2007). Also, two G-protein-coupled receptors, the LPA receptor and a receptor for an unknown ligand, Xflop, are expressed in the early embryo, and overexpression of either receptor increases cadherin membrane density in the late blastula, whereas depletion diminishes it (Tao et al., 2007). However, a role for any of these factors in determining the endogenous pattern of cadherin/catenin complex expression has not yet been demonstrated.

Zygotic patterning of cadherin/catenin density could also be achieved in a mosaic fashion by regional mechanisms. In fact, the best characterized modulator of normal cadherin membrane expression in *Xenopus* is the FLRT3/Rnd1 pathway, which reduces expression in the anterior mesoderm (Ogata et al., 2007). It depends on the interaction of a fibronectin-leucine-rich transmembrane (FLRT) protein with a small GTPase-like factor, Rnd1. FLRTs contain a series of leucine-rich repeats and a fibronectin type III domain in their extracellular part, a transmembrane domain, and a cytoplasmic tail. In the embryo, ectopic expression of cytoplasmically truncated FLRT3 is sufficient to drive cell sorting, suggesting a role in the modulation of adhesion (Karaulanov et al., 2006). Similarly, overexpression of Rnd1, which differs from other Rho-like GTPases by lacking intrinsic GTPase activity, disrupts cell adhesion in the *Xenopus* embryo (Wunnenberg-Stapleton et al., 1999).

In the early gastrula, FLRT3 and Rnd1 expression overlap in the involuted, prospective anterior mesoderm at all dorsoventral levels. Moreover, both proteins interact physically and functionally, with FLRT3 acting upstream of Rnd1 to upregulate the dynamin-mediated endocytosis of

C-cadherin. This leads to the apposition of tissues with low (anterior mesoderm) and high levels (ectodermal BCR) of membrane-expressed cadherin. Knockdown of FLRT or Rnd expresssion increases cadherin density in the mesoderm. Although this is associated with gastrulation defects, Brachet's cleft is not affected (Ogata et al., 2007). Since RhoA overexpression rescues adhesion in Rnd1 overexpressing cells (Wunnenberg-Stapleton et al., 1999), it may act downstream of the FLRT/Rnd pathway. If similar modulators of cadherin membrane expression should exist for other regions, like the chordamesoderm or endoderm, to locally control the elements of the global cadherin/catenin pattern in a mosaic fashion, they have not yet been identified.

3.3.2. Nonprotein membrane components that affect adhesion

Nonprotein membrane constituents are also essential for blastomere adhesion. A monoclonal antibody against neutral glycolipids from blastulae detects the antigen in an animal-to-vegetal gradient in the blastula and gastrula. The antibody interferes with the reaggregation of animal, but not vegetal blastomeres, suggesting an early, maternally determined mechanism of differential adhesion (Turner et al., 1992). Ganglioside GM1 is also present in the animal cytoplasm of oocytes, eggs, and cleavage stage embryos. Its distribution shows a sharp boundary which runs through the animal part of marginal blastomeres at the 32-cell stage. In the blastula, cells of the animal hemisphere and the marginal zone show membrane and cytoplasmic staining with anti-GM1 antibody, and this pattern is maintained during gastrulation (Kubo et al., 1995). A similar localization of GM1 is seen in *Bufo arenarum*. Inhibition of its function attenuates gastrulation movements and cell–extracellular matrix interaction (Aybar et al., 2000). In contrast, sulfated galactosylceramide is localized to the vegetal cytoplasm of the *Xenopus* egg, and becomes incorporated into vegetal blastomeres of the blastula and gastrula (Kubo et al., 1995). Adhesion between *Xenopus* blastomeres is also inhibited upon interference with blood-group B trisaccharide-bearing membrane molecules, including glycosphingolipids and GPI-anchored glycoproteins (Nomura et al., 1998).

The relationship between these factors and the cadherin/catenin complex is not known. Ca^{2+}-dependent cell–cell adhesion can be mediated by direct carbohyrate–carbohydrate interaction (Bucior and Burger, 2004), allowing for an independent, parallel adhesion mechanism. Indeed, in animal blastomeres, neutral glycolipids and cadherins seem to act additively (Heasman et al., 1994). In the medaka gastrula, on the other hand, glycolipids and glycoproteins are colocalized with cadherins in membrane microdomains and contribute to cell adhesion in a nonadditive, cooperative fashion (Adachi et al., 2008). This would be compatible with both the cadherin/catenin complex and the glycolipids/glycoproteins being essential

for cell–cell adhesion. Both mechanisms would tend to increase adhesiveness in the animal half of the embryo relative to the vegetal cell mass.

3.3.3. Cytoskeletal modulators at the cadherin/catenin complex

Cell adhesion depends on the cortical actin cytoskeleton. Although the extracellular domains of isolated cadherin proteins can mediate binding (Leckband and Prakasam, 2006), interaction of the cytoplasmic domains of cadherins with actin filaments is essential for strong cell–cell adhesion, and changes in cortical actin can modulate adhesiveness (Cavey et al., 2008; Gumbiner, 2005; Nelson, 2008; Pokutta and Weis, 2007). In turn, the cadherin/catenin complex is implicated in the control of the actin cytoskeleton at the membrane (Nandadasa et al., 2009). For example, p120 catenins can activate Rac through the guanidine exchange factor Vav2, and inhibit RhoA to affect the cytoskeleton (Grosheva et al., 2001; Noren et al., 2000; Yanagisawa and Anastasiadis, 2006). This feedback loop between cortical cytoskeletal dynamics and cadherin-mediated adhesiveness adds to the complexity of adhesion regulation. It can explain how changes in the cytoskeleton that seem not immediately related to adhesion nevertheless have an impact on tissue cohesiveness. For example, depletion of myosin II in *Xenopus* gastrula cells reduces adhesiveness, through a loss of actin cytoskeleton integrity (Skoglund et al., 2008).

In *Xenopus*, dominant-negative or constitutively active Rac1 both lower blastula cell adhesiveness (Bisson et al., 2007; Hens et al., 2002), and RhoA has been involved in various local mechanisms of adhesion modulation. A Cdc42 function in adhesion will be discussed in relation to its role in the mesoderm, but the GTPase is expressed ubiquitously in an animal-to-vegetal gradient similar to the cadherin/catenin complex (Choi and Han, 2002). A possible link to this complex is provided by IQGAPs. These proteins contain several interaction motifs, including binding sites for Cdc42 and Rac, actin, E-cadherin, and β-catenin, and regulate the cytoskeleton and cell adhesion (Fukata et al., 1999; Kuroda et al., 1998). Two isoforms, IQGAP1 and IQGAP2, are expressed in the *Xenopus* embryo (Yamashiro et al., 2003). Overexpression of IQGAP1 lowers embryonic cell adhesiveness, an effect which is abolished by coexpression of dominant-negative Cdc42 (Sokol et al., 2001). This would be consistent with Cdc42 acting through IQGAP1 to lower cell adhesion.

However, IQGAP1 overexpression by itself raises the level of active Cdc42, which blurs the upstream/downstream relationship and suggests a more sophisticated mechanism of action of the Cdc42–IQGAP complex (Sokol et al., 2001). Moreover, diminishing the levels of both IQGAP1 and the nuclear-localized IQGAP2 simultaneously also reduces cell–cell adhesion in the late gastrula or neurula ectoderm. Although the total amount of C-cadherin or β-catenin protein is not changed when IQGAP2 is inhibited, β-catenin and IQGAP1 localization at sites of cell contact are reduced,

adhesion is decreased, and the cortical actin cytoskeleton is less dense (Yamashiro et al., 2007). In contrast to the overexpression results, this suggests a positive regulation of adhesion by Cdc42 and IQGAP, perhaps at later stages of development. Knockdown of another RhoGTPase effector, the Cdc42 effector protein 2 (XCEP2), lowers cell–cell adhesion as well. The effect is seen late, however, in postgastrula stage ectodermal explants (Nelson and Nelson, 2004).

3.3.4. Components of signal transduction mechanisms that affect cell adhesion

Several components of signaling pathways which affect adhesion are ubiquitously expressed in the blastula and gastrula. Since the expression patterns of the respective ligands are not known, it is unclear whether these factors modulate adhesion globally or locally. ErbB receptor tyrosine kinases mediate signaling from EGF-like ligands, and in mammalian cells, a member of the family, the EGF receptor, affects cell adhesion by binding to cadherins and catenins and by regulating assembly of the complex (Hoschuetzky et al., 1994; Kanai et al., 1995). In *Xenopus*, all four ErbBs are expressed at gastrula stages (Nie and Chang, 2006). Inhibiting ErbB function in the dorsal mesoderm decreases adhesion in a dissociation-reaggregation assay (Nie and Chang, 2007), consistent with a requirement for ErbB signaling for normal adhesion.

Eph receptor tyrosine kinases and their ephrin ligands are also widely expressed in the embryo. EphrinA-type ligands are tethered to the cell membrane via GPI anchors, while ephrinBs are transmembrane proteins. The receptors are subdivided correspondingly into EphA and EphB subclasses, although EphA4 can bind both ephrinA and -B ligands. Within subclasses, binding is promiscuous. Eph receptor ligation and clustering leads to ''forward signaling,'' but receptor–ligand interaction also stimulates ''reverse signaling'' downstream of the ephrin ligand. A main target of Eph/ephrin signaling is the cytoskeleton, whose modulation indirectly affects cell adhesion. Eph/ephrin signaling is often involved in boundary formation and cell repulsion, in situations where receptor and ligand are expressed in complementary patterns (Blits-Huizinga et al., 2004; Kullander and Klein, 2002; Murai and Pasquale, 2003; Pasquale, 2005; Poliakov et al., 2004; Tepass et al., 2002). However, it also can trigger adhesive responses and modulate tissue cohesion when receptor and ligand are coexpressed (Cooke et al., 2005; Dravis et al., 2004; Hornberger et al., 1999).

In the *Xenopus* blastula and gastrula, expression of several Eph receptors and ephrins has been described, including the receptors EphA2 (G42/50/XE10) (Brandli and Kirschner, 1995; Helbling et al., 1998; Weinstein et al., 1996), EphA4 (Sek-1/Pagliaccio) (Winning and Sargent, 1994), EphB1 (Xelk/Xek) (Jones et al., 1995; Scales et al., 1995), EphB2 (Tanaka et al., 1998), EphB3 (TCK, Pl7a) (Scales et al., 1995), and EphB4 (Helbling

et al., 1999); and the ligands ephrinA1 (Elf-a, Elf-a') (Weinstein et al., 1996), ephrinB1 (Xlerk) (Jones et al., 1997), ephrinB2 (Smith et al., 1997), and ephrinB3 (Helbling et al., 1999). Many of these factors may be present ubiquitously, although detailed descriptions of expression patterns are still lacking. Also, no *in vivo* function during gastrulation for any of these factors has yet been established, despite their potential importance in the regulation of cell interaction. However, putative roles have been deduced from gain-of-function experiments.

Overexpression of ephrinB1 or of an extracellularly deleted construct induces blastomere deadhesion in the blastula. Although this effect is not associated with decreased C-cadherin expression or cadherin–catenin binding, it can be rescued by C-cadherin overexpression (Jones et al., 1998). Moreover, when BCR cells are mixed which ectopically express either ephrinB1 or its receptor, EphB2, they sort out from each other. Importantly, sorting depends on the interaction of both ephrinB1 and EphB2 with the scaffold protein, Dishevelled (Dsh) (Tanaka et al., 2003). Through Dsh, ephrinB1 is able to activate the Wnt planar cell polarity (PCP) pathway (Lee et al., 2006). These findings indicate that ephrinB signaling has the potential to affect cell adhesion and sorting in the early *Xenopus* embryo, although a role in the normal control of adhesiveness has not yet been established.

Intracellular signaling factors have also been identified as modulators of cell adhesion. p21-activated kinases are prominent regulators of the cytoskeleton (Bokoch, 2003), and Pak1 has been implicated in EphA4-induced deadhesion. Group I Paks (Pak1–3) are activated by Cdc42 or Rac binding, whereas group II Paks (Pak4–6) lack the respective GTPase binding site (Bokoch, 2003; Jaffer and Chernoff, 2002). Pak5 is expressed in prospective ectoderm and mesoderm of the *Xenopus* blastula and gastrula, and localizes to cell–cell contacts. Constitutively active Pak5 diminishes cell adhesion in the mesoderm, whereas dominant-negative Pak5 increases it (Faure et al., 2005), suggesting that Pak5 downregulates tissue cohesion. In *Drosophila*, a group II Pak is recruited to adherens junctions by Cdc42, indicating the possibility that Pak5 functions downstream of Cdc42 in the *Xenopus* embryo. Another intracellular factor is integrin-linked kinase (ILK). It was isolated as an integrinβ1-binding scaffold protein involved in cell–ECM adhesion. In *Xenopus*, its knockdown decreases cell–cell adhesion in later development by an unknown mechanism (Yasunaga et al., 2005).

3.3.5. Modulators of cell adhesion in the mesoderm

Activin treatment changes the fate of ectodermal BCR cells, to form mesodermal and endodermal derivatives. At the same time, it can diminish cell–cell adhesion (Brieher and Gumbiner, 1994). Since FLRT3 is a direct target of activin signaling, its ability to reduce cadherin membrane expression could explain this activin-induced attenuation of adhesiveness (Ogata et al., 2007). Another proposed mechanism involves the downregulation

not of membrane expression, but of the adhesive function of C-cadherin, by activin-induced PAPC (Chen and Gumbiner, 2006).

Protocadherins contain six or more extracellular EC domains, and their cytoplasmic domains lack the conserved catenin binding motifs of classical cadherins (Frank and Kemler, 2002). Three protocadherins are known to be expressed in gastrula mesoderm: paraxial protocadherin (PAPC), axial protocadherin (AXPC), and protocadherin in neural crest and somites (PCNS). During gastrulation, PAPC is initially expressed in the early involuting, dorsal anterior mesoderm, under the control of activin and Wnt signaling, and the transcription factor Xlim1 (Hukriede et al., 2003; Kim et al., 1998; Medina et al., 2004; Schambony and Wedlich, 2007). Later, expression spreads laterally and ventrally, and after the mid-gastrula stages, it ceases in the dorsal anterior mesoderm, but increases in the paraxial, somitic mesoderm (Hukriede et al., 2003; Kim et al., 1998). PCNS is closely related to PAPC. It is expressed from mid-gastrula stages onward, in the dorsal mesoderm from which PAPC expression begins to disappear, but also in lateral and ventral postinvolution mesoderm (Rangarajan et al., 2006).

In *Xenopus* blastomeres, as in various lines of cultured cells, PAPC does not act as an adhesion molecule that would mediate, for example, attachment to a substratum of purified PAPC (Chen and Gumbiner, 2006). However, ectopic expression in the embryo promotes cell sorting (Chen and Gumbiner, 2006; Kim et al., 1998), suggesting that it modulates adhesion. Indeed, activin-induced expression of PAPC decreases C-cadherin-dependent adhesion. The extracellular domain of PAPC is sufficient for this effect. Its mechanism is not known, but seems not to involve a physical interaction between C-cadherin and PAPC (Chen and Gumbiner, 2006). Knockdown of PAPC increases the adhesiveness of activin-induced or endogenous dorsal mesoderm cells, as does treatment with an activating, affinity-increasing cadherin antibody (Chen and Gumbiner, 2006; Zhong et al., 1999). In a different role, PAPC employs its cytoplasmic domain to stimulate RhoA activation, which in turn is required for the separation of prospective ectoderm and mesoderm (Medina et al., 2004). In contrast to PAPC, ectopic expression of the related protocadherin, PCNS, does not induce cell sorting, and no effects of its knockdown on gastrulation were described (Rangarajan et al., 2006).

The multiple pathways that regulate PAPC expression include noncanonical Wnt signaling (Schambony and Wedlich, 2007). It had been known that overexpression of Wnt5A diminishes adhesion, and that mesoderm cohesion can be rescued by coexpression of N-cadherin or dominant-negative Cdc42. This was taken to suggest that noncanonical Wnt signaling through Cdc42 induced the downregulation of cadherin-mediated adhesion (Choi and Han, 2002; Torres et al., 1996). A more detailed analysis revealed that Wnt5A acts through the receptor tyrosine kinase Ror2, an unconventional Wnt receptor, to activate via PI3K and Cdc42 the JNK signaling cascade, and eventually the transcription of PAPC (Schambony

and Wedlich, 2007). Thus, the effects of Wnt5A on cell adhesion can be explained at least partially by the antiadhesive effects of PAPC (Chen and Gumbiner, 2006).

The only adhesion-related factor known to be specifically expressed in chordamesoderm is AXPC. After the onset of gastrulation, it is localized to the dorsal marginal zone, most likely to the prospective notochord region, and it remains expressed in the notochord of the neurula (Kim et al., 1998; Kuroda et al., 2002). In this way, AXPC expression is complementary to that of PAPC: the latter initially occupies the prechordal mesoderm, which abuts the AXPC-expressing chordamesoderm anteriorly; later, the border between the two expression domains corresponds to the notochord–somite boundary. Ectopic AXPC expression stimulates cell sorting, and it partially mediates effects of activin induction on sorting (Kim et al., 1998; Kuroda et al., 2002). Interestingly, in these experiments, the sorting pattern induced by both activin and AXPC is consistent with increased adhesion in the chordamesoderm. This would be the only instance where a mesoderm-specific factor strengthens adhesion, instead of reducing it. Morpholino knockdown of AXPC does not affect sorting, suggesting that another AXPC-like factor may act redundantly (Kuroda et al., 2002).

The ephrin receptor, EphA4, is expressed in the *Xenopus* mesoderm. Its ectopic activation in BCR cells of the blastula diminishes adhesion and leads to lesions in the blastula wall. Like with ephrinB1 overexpression, C-cadherin expression or its linkage to the cytoskeleton via α- and β-catenin are not affected, but cadherin overexpression rescues adhesion (Winning and Sargent, 1994; Winning et al., 1996, 2001). The antiadhesive signal downstream of EphA4 involves inhibition of RhoA: EphA4 activation leads to the Nck-mediated recruitment of Pak1, and Pak1 in turn prevents activated Cdc42 and/or Rac1 from activating RhoA (Bisson et al., 2007; Winning et al., 2002). A role of this mechanism in the normal control of mesoderm cell adhesion has not been demonstrated so far.

The exact role in gastrula cell adhesion of *Xenopus Camello* (*Xcml*) is also not clear. The protein contains an *N*-acetyltransferase motif and is associated with the secretory pathway, consistent with a role in protein modification in the Golgi complex. It is first expressed in the internalized mesoderm of the gastrula. Overexpression diminishes cell contacts, and attenuates the reaggregation of dissociated blastomeres (Popsueva et al., 2001). This is consistent with a role in the constitutive downregulation of adhesiveness in Xcml expressing cells, that is, in the mesoderm, but the effect of a loss of Xcml function is not known.

3.3.6. Ectodermal factors

The region-specific expression of different adhesion molecules, as a mechanism to establish differential adhesion, seems to be rare in the *Xenopus* gastrula. Examples are restricted to the gastrula ectoderm. Thus, E-cadherin

appears at mid-gastrula stages in a subregion of the ectoderm, that is, in its outer, epithelial layer (Angres et al., 1991; Choi and Gumbiner, 1989; Nandadasa et al., 2009; Schneider et al., 1993), and N-cadherin on prospective neural plate cells in the dorsal ectoderm of late gastrulae (Detrick et al., 1990; Nandadasa et al., 2009). Ectopic expression of N-cadherin in ectoderm cells increases their adhesiveness and induces their segregation from nonexpressing cells (Detrick et al., 1990). In the prospective neural plate, the Ig-family adhesion molecule N-CAM also becomes expressed toward the end of gastrulation (Balak et al., 1987; Kintner and Melton, 1987). In the newt, Pleurodeles, N-CAM is expressed already in the early gastrula, and not restricted to prospective neural tissue, but detected in the ectoderm, chordamesoderm, and endoderm (Saint-Jeannet et al., 1989).

Putative modulators of adhesion are also found in the ectoderm. The protocadherin NFPC is expressed maternally and throughout gastrulation, initially in all of the ectoderm, but later only on the ventral side. However, effects of NFPC overexpression or of dominant-negative NFPC are only seen after gastrulation, in the embryonic epidermis (Bradley et al., 1998). The animally expressed transcription factor Foxl1e regulates adhesion in the prospective ectoderm of the blastula and gastrula. As Foxl1e promotes ectoderm formation, it may act far upstream of the actual adhesion mechanism (Mir et al., 2007).

In the late gastrula, E-cadherin (Angres et al., 1991; Choi and Gumbiner, 1989) and the tetraspanin xTspan-1 (Yamamoto et al., 2007), a four-pass transmembrane protein that is involved in the formation of membrane rafts (Hemler, 2003), are restricted to the epithelial layer of the ventral and dorsal ectoderm, respectively. Expression of cytoplasmically truncated E-cadherin affects the integrity of the epithelial layer, and this defect can be rescued by full-length E-cadherin, but not C-cadherin (Levine et al., 1994; Nandadasa et al., 2009). An adhesion-lowering effect of xTspan1 has also been observed, but only upon ectopic expression in deep ectodermal cells (Yamamoto et al., 2007).

3.3.7. Summary: The molecular basis for gastrula tissue cohesion and regional differences of adhesion

For the cohesion of the multilayered tissue which forms the *Xenopus* blastula and gastrula, ubiquitously expressed cadherins are essential, with EP/C-cadherin being the major, and the closely related XB/U- as well as XmN-cadherins being minor factors. Regional expression of other cadherins or other adhesion molecules such as N-CAM is only seen in the ectoderm at late gastrula stages. However, cadherin expression varies quantitatively between regions, mimicking the independently inferred cohesion differences of tissues (Fig. 5.1C and D). Glycolipids and the carbohydrate moieties of not well-characterized glycoproteins are also essential for adhesion; it is not known whether these act in parallel or in cooperation with

cadherin. They show quantitative or qualitative animal–vegetal differences in expression, such that adhesion differences between regions would presumably be accentuated.

It is tempting to assume that the regional density differences of the cadherin/catenin complex would determine the differential adhesiveness of early embryonic tissues. However, direct evidence for this is yet lacking. In fact, several observations seem to disagree with this notion. Thus, modulation of cadherin density by p120 catenin or ARVCF is not associated with adhesion differences detectable in a reaggregation assay (Fang et al., 2004), and localized C-cadherin overexpression does not induce sorting of early blastomeres (Kurth et al., 1999) or chordamesoderm cells (Reintsch et al., 2005). This suggests that cadherin/catenin density may be uncoupled from adhesiveness, at least experimentally. Moreover, clones of gastrula cells expressing dominant-negative cadherins do not segregate from surrounding cells, but appear to disperse normally (Broders and Thiery, 1995; Lee and Gumbiner, 1995), although lowering of tissue surface tension and thus cohesion by 50% has been shown for moderately high doses of cytoplasmically deleted C-cadherin (Kalantarian et al., 2009). This suggests that in the embryo, moderate differences in cadherin-mediated adhesiveness do not necessarily translate into sorting.

A number of additional mechanisms have been identified that could establish adhesion differences, whether or not cadherin/catenin complex expression is a main determinant. For example, protocadherins have been proposed not to act as adhesion molecules, but to modulate cadherin adhesiveness. Moreover, factors that affect the cortical actin cytoskeleton will almost inevitably have an impact on adhesiveness, due to the complex link between adhesion and cortex structure and dynamics. This raises the theoretical possibility that at least some of the differential adhesion seen in the early embryo is an inadvertant by-product of other processes, for example, the regulation of cell shape and motility.

3.4. Tissue separation: Beyond differential adhesion

3.4.1. Ecto-mesodermal boundary

Sorting boundaries between nonmixing cell populations are not necessarily visible histologically, but betray themselves by the fact that motile cells on either side do not cross them. In contrast, ectoderm and mesoderm of the amphibian gastrula are separated by a visible boundary termed Brachet's cleft (Figs. 5.1F and 5.2A). In *Xenopus*, Brachet's cleft forms as mesoderm and endoderm of the blastocoel floor are applied against the ectodermal BCR by vegetal rotation (Winklbauer and Schürfeld, 1999): instead of fusing, the tissues remain separated. Correspondingly, in *an vitro* assay, mesodermal or endodermal cell aggregates remain on the surface of explanted BCR, whereas small BCR explants soon sink in, demonstrating

that no physical obstacle, such as a basal lamina, prevents reintegration of cells (Wacker et al., 2000; Winklbauer and Keller, 1996). In agreement with this, electron microscopic examination shows that ectodermal and mesodermal cells are at least over part of their surface in direct, close contact (Nakatsuji, 1976; Nakatsuji and Johnson, 1983). This apparently paradoxical situation of tissue adhesion across a histologically visible border points to a more complex mechanism of boundary formation.

The above-mentioned *in vitro* assay was used to analyze the development of tissue separation at Brachet's cleft (Ibrahim and Winklbauer, 2001; Wacker et al., 2000). Two complementary tissue behaviors were identified: a repulsion behavior of the BCR, and separation behavior of the mesoderm and endoderm (Fig. 5.1E and F). On mid-blastula stage BCR, explants from all regions of the embryo and from all stages sink in, but at the beginning of gastrulation, the BCR acquires the ability to repell tissue. Repulsion is selective toward tissues showing separation behavior, which at the blastula stage is restricted to the vegetal cell mass (Fig. 5.1E). Dorsally, separation behavior then spreads into the marginal zone at the onset of gastrulation, first into the anterior and then the posterior mesoderm. At all times, the blastopore lip exhibits neither separation nor repulsion behavior. Having a buffer zone with such indiscriminate behavior at the junction between internalized mesendoderm and ectodermal BCR is essential for the continuity of tissue in the blastopore lip region (Fig. 5.1F) (Wacker et al., 2000). On the ventral side, tissue separation shows similar changes. A notable difference is that the ventral mesoderm extends beyond the blastopore lip into the BCR (Fig. 5.1B), and this BCR mesoderm behaves initially like ectodermal BCR with respect to repulsion behavior (Fig. 5.1F). As involution progresses and the BCR mesoderm moves into the lip region, it adopts indiscriminate behavior (Ibrahim and Winklbauer, 2001).

Separation behavior seems not to be based on cell sorting by differential adhesion. Vegetal cells integrate into an explanted mid-blastula BCR layer (Wacker et al., 2000), but segregate from these cells in a sorting assay (Turner et al., 1989). Moreover, posterior mesoderm from the blastopore lip permits anterior, internalized mesoderm to sink in (Wacker et al., 2000), but it is engulfed by the latter in sorting experiments (Ninomiya and Winklbauer, 2008). Probably, other mechanisms act instead of or in parallel to adhesion differences to ensure tissue separation.

Cadherins are expressed at different densities on either side of Brachet's cleft (Fig. 5.1D), but the cleft forms even if cadherin density is rendered similar on both sides (Ogata et al., 2007). However, overexpression of either EP/C- or XB/U-cadherin in the mesoderm interferes with separation behavior in the BCR assay and forces explants to integrate into the BCR (Wacker et al., 2000). Apparently, cadherin-mediated adhesion must normally be modulated to allow for the separation of ectoderm and

mesoderm, and this mechanism can be overwhelmed by an excess of cadherin. The putative mechanism is not known, but its control by upstream factors has been studied in the prechordal mesoderm (Fig. 5.1B).

In this region, the transcription factors Mix.1 and Goosecoid (Gsc) are coexpressed, and act as transcriptional repressors to control separation behavior (Wacker et al., 2000). In the same region, the Wnt receptor Xfz7 is required. If its expression is blocked by morpholino antisense oligonucleotides, Brachet's cleft is absent between prechordal mesoderm and ectoderm. Downstream of Xfz7, noncanonical Wnt signaling including the activation of PKC is necessary for separation behavior (Winklbauer et al., 2001). It requires also the interaction of Xfz7 with the protocadherin PAPC, and activation of RhoA and Rho kinase. The ankyrin repeat domain protein 5 (xANR5) functions synergistically with PAPC (Chung et al., 2007; Hukriede et al., 2003; Medina et al., 2004). PAPC reduces the strength of C-cadherin-mediated adhesion, and a cytoplasmically deleted mutant form is sufficient for this effect (Chen and Gumbiner, 2006). However, this truncated PAPC does not promote tissue separation (Medina et al., 2004), suggesting that it is not the direct attenuation of cadherin adhesion by PAPC that underlies the formation of Brachet's cleft. This agrees with the notion that a mechanism independent of differential adhesion establishes the cleft.

Circumstantial evidence suggests that other factors may also affect tissue separation. Bves is a member of a small family of integral membrane proteins with three transmembrane domains. *In vitro*, it accumulates at cell–cell contacts and mediates adhesiveness, and its knockdown disrupts epithelial sheet formation (Ripley et al., 2004; Wada et al., 2001). Similar *in vitro* behavior is seen for Xenopus Bves (Xbves) (Ripley et al., 2006). Xbves is expressed throughout early development, preferentially in the ectoderm and mesoderm. Disruption of its function impairs gastrulation movements, and most strikingly, it results in the dispersal of Xbves-deficient cells across germ layers (Ripley et al., 2006). This is contrary to the expected effect of altered adhesiveness in part of a tissue, namely the sorting out of cells from their normal neighbors, and could indicate that the primary function of Xbves is not in adhesion *per se*, but in the maintenance of tissue separation.

The animally expressed transcription factor Xlim5 regulates cell adhesion in prospective ectoderm of the late blastula and the gastrula without affecting cell fate (Houston and Wylie, 2003). Loss of Xlim5 function reduces adhesiveness in the ectoderm. When Xlim5 is ectopically expressed in vegetal cells, their sorting from ectoderm cells is prevented, although they still mix with normal vegetal cells. Moreover, after gastrulation, vegetal Xlim5 expressing cells are found scattered in other germ layers. Again, such behavior is not consistent with Xlim5 regulating differential adhesion, and points to a role in tissue separation processes.

3.4.2. Notochord–somite boundary

A second example of tissue separation in the gastrula is the segregation of notochord and somitic tissue. In the second half of gastrulation, a fissure forms on either side of the dorsal midline to separate the formerly continuous tissues. Fissure formation spreads from anterior to posterior in the internalized mesoderm (Keller et al., 1989; Shih and Keller, 1992a,b) where cells are engaged in the intercalation movements of convergent extension. However, when a cell reaches the notochord–somite boundary, it neither crosses it nor does it retract into the interior of the respective tissue, a phenomenon referred to as "boundary capture" (Keller et al., 2000).

When individual cells within the notochord domain are forced to assume a somitic fate by ectopically activating canonical Wnt signaling, these cells cross the established boundary to join endogenous somitic tissue (Reintsch et al., 2005). This indicates that the early notochord–somite boundary, like Brachet's cleft, does not form an absolute physical barrier to cell movement. Interestingly, expression of a dominant-negative cadherin construct does not interfere with sorting across the boundary in either direction, suggesting that simple differential adhesion may not be sufficient to explain tissue separation. Direct observation of cell motility indicated that while cells of like fate are able to form stable, oriented protrusions on each other's surface to engage in intercalation movements, somitic cells extend only short-lived random processes when surrounded by notochord cells. This can explain why cells of different fate do not normally interdigitate at the boundary, thus contributing to the formation of a fissure (Reintsch et al., 2005).

In summary, tissue separation involving the establishment of a visible cleft is a special case of boundary formation. It may be required when adjacent tissues move past each other, such as when mesoderm and endoderm translocate across the BCR, or the notochord elongates at a rate different from that of the adjacent somitic mesoderm (Keller et al., 1989). Both at Brachet's cleft and at the notochord–somite boundary, differential cell adhesion seems not sufficient to implement separation of tissues, but the nature of the additional mechanisms is not known. Induced retraction of cells upon contact, as mediated, for example, by ephrin/Eph signaling, is a possible mechanism. Absence of interdigitating protrusive activity and cell motility at the boundary, as observed at the notochord–somite interface (Keller et al., 1989), can have a similar effect. In both cases, cell properties would only be altered upon contact at the tissue boundary, and the mechanisms could work independently of overall differences in cell adhesiveness between adjacent cell populations.

3.5. Function of differential adhesion and tissue separation in the embryo

The tissues of the early amphibian embryo are formed by the partitioning of coherent cell masses, and not from dispersed, individually specified cells that would need to congregate by sorting out. Thus, the question arises as to the

in vivo function of cell adhesion differences which lead to cell sorting under experimental conditions. Within the framework of the DAH, three features are directly linked to differential adhesion: cohesion differences between tissues; the formation of sorting boundaries; and the positioning of the respective tissues relative to each other. Changing cell adhesion and thus cohesiveness in part of a previously homogeneous tissue will establish a sorting boundary that delimits this part, and the two subregions thus defined will eventually assume positions that correspond to a thermodynamic equilibrium configuration. In principle, each of these three features could be the primary function of adhesion differences in the embryo, with the other two being accidental, yet unavoidable consequences that introduce constraints on morphogenesis. As a fourth option, all three of these features could be nonfunctional, for example, be side effects of yet another change in cellular properties such as motility, that indirectly influences cell adhesion.

(1) Boundary formation by differential adhesion is a commonly discussed mechanism in various developmental systems, but it is not clear how important it is in amphibian gastrulation. Labeling small patches of tissue shows that random dispersal of cells occurs in many regions of the early embryo (e.g., Bauer et al., 1994; Dale and Slack, 1987; Kim et al., 1998). Ectopic PAPC expression restricts this scattering of cells (Kim et al., 1998), but PAPC-depleted embryos have not been examined for an increased dispersal of anterior mesoderm (Chen and Gumbiner, 2006). In experiments where extensive cell scattering did indeed occur, it involved crossing of Brachet's cleft, suggesting that tissue separation was affected (Houston and Wylie, 2003; Ripley et al., 2006).

Mechanisms other than differential adhesion can establish mixing boundaries without imposing a link between cohesion, boundary formation, and tissue positioning. Tissue separation processes involve a reaction of cells at the boundary between two tissues, leaving their internal cohesiveness at least in principle unaffected. Eph/ephrin signaling is an instructive paradigm for such a mechanism. Eph receptors and their ephrin ligands are often expressed in complementary patterns in adjacent tissues. Consequently, they can interact only at the common boundary, where they induce mutual repulsion between cells and establish a mixing boundary (Tepass et al., 2002). Tissue separation at Brachet's cleft and between the forming notochord and somites points at mechanisms which are beyond simple differential adhesion. Other boundaries, for example, between prechordal mesoderm and chordamesoderm, or mesoderm and endoderm, are not associated with cleft formation, and remain candidates for differential adhesion-based mechanisms.

(2) Adjusting tissue cohesiveness, for example, in order to facilitate cell movements, could be the primary cause of differential adhesion. If for such a reason, cohesion would be changed in part of a tissue, this part would secondarily be prevented from mixing with the remaining cell population, and it would show a tendency to either be engulfed by, or engulf,

neighboring tissue. This raises the question why the pattern of tissue cohesiveness should remain relatively stable throughout gastrulation, as observed, while the pattern of cell movements changes. Also, absolute values of cohesion vary strongly between embryos, such that variation within a given tissue is larger than the average differences between tissues (Table 5.1). Moreover, cohesion can be reduced experimentally to a point near complete tissue disintegration, yet gastrulation still proceeds (Heasman et al., 1994). These observations suggest that gastrulation movements are compatible with a wide range of tissue cohesiveness.

(3) The tissue positioning effect of differential adhesion could be its primary function. In fact, Holtfreter proposed that his ''tissue affinities'' are among the actual driving forces of gastrulation. He observed that affinities seemed to change over time, leading to tissue movements *in vitro* as new equilibrium configurations were approached. These *in vitro* movements were interpreted to correspond to morphogenetic processes in the gastrula or neurula (Holtfreter, 1939, 1944; Townes and Holtfreter, 1955). As a general mechanism, such a dynamic role for differential adhesion seems unlikely, at least for *Xenopus*, where the overall pattern of regional adhesion differences does not change conspicuously during gastrulation. But also for other amphibians, the examples for affinity changes are in fact mostly related to the neurula. This does not preclude, however, that differential adhesion facilitates some gastrulation movements. Also, instances of dynamic changes in tissue cohesion at a smaller scale may have gone unnoticed, and could drive local movements. For the zebrafish gastrula, it has been estimated that increased cohesion of the internalized mesoderm contributes to mesoderm spreading between epiblast and yolk cell in the direction of the animal pole, but that it is not sufficient to drive this movement (Schotz et al., 2008).

If not the formation, but the stability of embryonic structure is considered, one finds, first, that a very similar overall pattern of differential adhesion is as well compatible with the simple layout of the blastula as with the highly folded structure of the gastrula. This seems to limit the role that differential adhesion may have in stabilizing early embryonic anatomy. Second, removing the ectoderm from the embryo causes a dramatic inversion of the remaining germ layers (Holtfreter, 1944; Keller and Jansa, 1992; Townes and Holtfreter, 1955). At first sight, this appears to suggest that differential adhesion is a strong determinant of gastrula structure. But in fact, it only illustrates the principle that removing components from a tissue array necessarily changes equilibrium conditions and thus affects tissue positions. In the present case, the removal of the ectoderm replaces the lower meso–ectodermal interfacial tension with the stronger surface tension of the mesoderm (Phillips and Davis, 1978), changing drastically the equilibrium of tensions. An explanation of how the inverse pattern of tissue positioning tendencies could nevertheless contribute to the stability of the germ layer arrangement in the intact embryo is yet lacking.

Whether differential adhesion contributes to structural stability at a smaller scale has not been explicitly addressed, but it seems that in experiments where the pattern of adhesion differences has been changed, tissue mispositioning is not a striking, easily noticed effect. For example, preventing the normal reduction of adhesiveness in anterior mesoderm affects gastrulation, but not the relative positioning of this tissue, as seen from the expression of marker genes (Chen and Gumbiner, 2006; Ogata et al., 2007). The same is observed after manipulating cadherin function in parts of the gastrula (Broders and Thiery, 1995).

(4) Spatial differences of cohesion could be nonfunctional. For example, they could follow from region-specific cellular properties that indirectly affect adhesion, or be due to arbitrary differences in the control of adhesion molecule expression in different cellular contexts. Initial differences could be stabilized by compensatory changes in adjacent tissue, and a nonfunctional, yet stable pattern of differential adhesiveness could then be conserved. For example, the inverse pattern of germ layer stability, after having been initially established in response to unknown circumstances, could continue to be conserved because any major changes would have adverse positioning effects. The basic inverse pattern was indeed found in all urodele and anuran amphibians examined to date. However, the chordamesoderm of *Xenopus* (Kubota et al., 1999; Ninomiya and Winklbauer, 2008) and mesoderm of the zebrafish gastrula (Schotz et al., 2008) do not conform to this pattern. By being more cohesive than ectoderm, their position relative to the ectoderm fits the canonical pattern proposed by the DAH.

In conclusion, it appears that the role of differential adhesion in the amphibian gastrula is not yet known. This may seem surprising. Differential adhesion effects leading to cell sorting and tissue positioning *in vitro* have been well documented for the early embryo, and a number of molecular mechanisms than modulate adhesiveness have been described. Nevertheless, unambiguous, specific functions for differential adhesion have yet to be identified. On the other hand, there is ample evidence for the role of region-specific, oriented cell motility in gastrulation. Therefore, as a ''null-hypothesis,'' one might propose that the observed adhesion differences between gastrula regions are largely non-functional.

4. Collective Cell Migration, Cell Rearrangement, and Intercellular Migration

Studying cells that move individually on a planar substratum *in vitro* has led to a basic understanding of cell migration. It involves the extension and attachment of cytoplasmic protrusions at the cell's leading edge, and the

detachment and retraction of the cell body at the trailing edge. Localized actin polymerization, cell–substrate interaction, and acto-myosin contractility are molecular counterparts of such cellular processes (Rafelski and Theriot, 2004; Revenu et al., 2004). Although cells can migrate individually *in vivo*, they often move as whole coherent masses or clusters on external substrata, showing *collective migration* (Friedl et al., 2004). Examples include epidermal wound healing (Martin and Parkhurst, 2004) or border cell migration in the *Drosophila* ovary (Niewiadomska et al., 1999).

In coherent cell masses, *cell rearrangement* is also an important mode of movement. In models of rearrangement inspired by epithelial morphogenesis, it is often assumed that polygonal cells are tightly packed, and instead of moving with the aid of cytoplasmic protrusions, preexisting cell contact areas grow by the parallel expansion of the mutually attached membranes of two neighboring cells, and shrink by parallel contraction (e.g., Brodland, 2002; Weliky et al., 1991). However, in the amphibian gastrula, active cell rearrangement seems to be associated with a regulated protrusive activity of less densely packed cells. Such crawling of cells over each other's surface, or *intercellular migration* (Gumbiner, 2005), is the focus of this section. Migration across the surface of cells has been studied in several systems (Keller et al., 2003; Letourneau et al., 1990; Li et al., 2001; Niewiadomska et al., 1999), but despite its frequent occurrence, little is known about its mechanism.

A special case of rearrangement is *cell intercalation*, where cells interdigitate in a regular, oriented fashion with their neighbors, such as in mediolateral and radial intercalation during convergent extension of the axial mesoderm (Keller et al., 2003). Cell rearrangement can also be driven by external forces. For example, when an aggregate is centrifuged, its cells are first deformed in accord with the flattening of the aggregate, but after a while, they resume their normal polyhedral shape, which necessitates an exchange of neighbors (Phillips and Davis, 1978; Phillips et al., 1977). However, this process can also involve the stress-induced formation of locomotory protrusions, and thus an active component, as suggested for amphibian embryonic tissues (Beloussov et al., 2000).

4.1. Basic features of cell rearrangement and intercellular migration

When cells move in multicellular aggregates, adhesion molecules play a dual role, providing both tissue cohesiveness and the molecular substratum for migration. The latter function implies that adhesion has to be compatible with repeated cell attachment and detachment, and the exertion of traction forces. It has been shown that cadherins can serve as a substratum for migration. Border cell migration depends on cadherin-mediated adhesion (Niewiadomska et al., 1999; Pacquelet and Rorth, 2005), and neurites can extend on isolated N-cadherin extracellular domain (Bixby and Zhang, 1990).

If movement is driven by the advance of locomotory processes on neighboring cell surface, cell detachment to create free substratum surface must be crucial for intercellular migration. Although the binding of two cadherin molecules from opposite cell membranes is reversible, adhesion at the level of the two respective cells is not. The off-rate of cadherin binding is relatively low (Leckband and Prakasam, 2006), and if the density of cadherin molecules on the membrane is large enough (Chen et al., 2005), cells remain firmly attached to each other and do not spontaneously detach. Moreover, adhesion effects are rather strong as compared to other forces generated by the cell. The force required to break a bond between two C-cadherin molecules is about 50×10^{-12} N (Leckband and Prakasam, 2006), whereas a single myosin II molecule or a polymerizing actin filament generate a force of the order of 1×10^{-12} N, respectively (Fukui, 1993). The forces generated by locomoting cells are typically in the 10^{-8} N range (e.g., Delanoe-Ayari et al., 2008; du Roure et al., 2005; Thoumine and Ott, 1997), corresponding to the rupture force for a few hundred of the tens of thousands cadherin bonds of a cell.

Despite this firm binding, cells can pull away from each other. A possibility is to rupture bonds sequentially, not all at once, thus peeling a cell off its substratum. This process has been analyzed by using *Dictyostelium* amoeboid cells. When moderate forces were applied, cells rolled across the substratum by peeling off at one end and attaching at the other at velocities typical for migrating cells. Moreover, peeling rate and thus velocity increased with the magnitude of applied force (Decave et al., 2002).

Rolling across the substratum as a whole is not possible for cells moving in an aggregate, where they are attached to cells on all sides. To pass between lateral neighbors, a cell would have to peel off from all simultaneously, which precludes cell rotation. A possible mechanism combines peeling with the endocytosis of cell membrane at the cell's rear end, and the insertion of new membrane at the front (Umeda and Inouye, 1999). Instead of peeling, endocytosis of adhesion molecules could also be directly responsible for the shrinkage of cell–cell contact zones, providing the force required to break adhesive bonds (de Beco et al., 2009; Troyanovsky et al., 2006), although this would not generate free surfaces for the attachment of migrating cells.

When adherent cells are separated experimentally not by peeling, but by pulling them apart such that force is applied to all adhesion bonds simultaneously, it is not these bonds that break, but the cell's cytoplasm is fragmented. Thin membrane tethers are drawn out from the cell bodies, and only when these eventually rupture, cells are completely separated (Benoit and Gaub, 2002; Puech et al., 2006). This can serve as a model process for other, active detachment mechanisms which involve a disruption of cytoplasmic integrity. Thus, many cells migrating *in vitro* remain attached at their rear ends by slender strands of cytoplasm. These eventually break, leaving a trail of cytoplasmic fragments behind (Lauffenburger and Horwitz, 1996).

Similarly, cell–cell adhesion can be disrupted by an induced collapse of the cortical cytoskeleton. When ephrin/Eph receptor signaling induces the repulsion of cells, it promotes membrane tether formation and eventually the endocytosis of contact sites (Poliakov et al., 2004; Zimmer et al., 2003). Another way to disrupt adhesion is the proteolytic cleavage of the cadherin extracellular domain, that is, cadherin shedding (Dello Sbarba and Rovida, 2002). No conclusive evidence is available yet for a downregulation of cadherin affinity by inside-out signaling (Gumbiner, 2005).

4.2. Cadherin adhesion and intercellular migration in the amphibian gastrula

To study cadherin function in the *Xenopus* gastrula, extracellularly or cytoplasmically truncated constructs have been used which seem to inhibit endogenous cadherins in a dominant-negative fashion, although their effects on adhesion are not clearly understood. The cytoplasmic domain of cadherins whose extracellular moiety has been deleted is thought to compete with endogenous cadherins for interacting components such as catenins (Kintner, 1992). Its dominant-negative effect on adhesion probably involves a modulation of the cytoskeleton (Reintsch et al., 2008). Expression of membrane-anchored cadherin extracellular domain also diminishes adhesion. High doses cause the disintegration of the BCR (Lee and Gumbiner, 1995), and moderate doses reduce tissue surface tension of explants (Kalantarian et al., 2009). However, the construct is still able to mediate cell binding to immobilized cadherin (Brieher et al., 1996).

In *Xenopus*, expression of C-cadherin extracellular domain at levels just short of interfering with tissue cohesion impedes mesoderm involution, blastopore closure, and convergent extension at the dorsal side, but has no obvious effects in other regions of the gastrula. A similar phenotype is obtained with an analogous XB-cadherin construct (Kalantarian et al., 2009; Kuhl et al., 1996; Lee and Gumbiner, 1995). Expression of the C-cadherin cytoplasmic domain also leads to an arrest of gastrulation and eventually to a loss of tissue integrity (Lee and Gumbiner, 1995). When this construct is expressed in only a small region of the embryo, a relatively normal blastula forms. During gastrulation, involution and convergent extension are impeded when the affected cells are included in the dorsal posterior mesoderm and ectoderm. If present in the anterior, migrating mesoderm, gastrulation movements are only weakly compromised (Broders and Thiery, 1995).

When the amount of C-cadherin protein is reduced by antisense oligonucleotide inhibition of the maternal mRNA, cell adhesion is strongly affected in the blastula. However, adhesion recovers with time, and gastrulation is completed although probably at reduced tissue cohesion (Heasman et al., 1994). In contrast, when the maternally expressed XmN-cadherin is

similarly inhibited, cleavage and blastula stage adhesion is normal, but gastrulation is arrested shortly after its initiation (Hojyo et al., 1998), as if XmN-cadherin were specifically involved in intercellular movements, and not in tissue cohesion. Knockdown of maternal α-catenin or plakoglobin, or expression of dominant-negative α-catenin, also interferes with blastomere adhesion and gastrulation (Kofron et al., 1997; Sehgal et al., 1997).

Overexpression of full-length C-cadherin affects gastrulation only weakly. Involution and convergent extension progress, although at the end of gastrulation, a yolk plug protrudes from the blastopore (Lee and Gumbiner, 1995), consistent with an effect on the vegetal cell mass. No gastrulation defects were seen with XB-cadherin overexpression (Kuhl et al., 1996). Coexpression of dominant-negative and full-length cadherins rescues gastrulation movements, but only to a moderate extent (Kuhl et al., 1996; Lee and Gumbiner, 1995).

In summary, these findings indicate that gastrulation is surprisingly robust in the face of variations of tissue cohesion. Certainly, movements cannot take place when tissue integrity is disrupted, but above that critical level of cell adhesion, embryos complete gastrulation. The large individual differences in normal tissue cohesiveness also indicate that gastrulation tolerates well the variations in cohesiveness. However, the rate of some gastrulation movements differs strongly between batches of embryos, leading to a disparity between movements, and to a variable gastrula morphology (Ewald et al., 2004; Winklbauer and Schürfeld, 1999) which could be an expression of this variability in mechanical tissue properties. Interestingly, only a subset of gastrulation movements is directly affected to a noticeable degree, those at the dorsal blastopore lip and the chordamesoderm where cadherin expression and tissue cohesion are highest. This implies that increased adhesiveness in this region may be functionally significant.

4.3. Collective and intercellular migration of the anterior mesendoderm

All the complexity of migration in cell aggregates is displayed in the movement of the anterior mesendoderm of *Xenopus* (Fig. 5.2A). First, this multicellular mass translocates as a whole across the BCR substratum, exemplifying collective migration. Second, the substratum consists mainly of the surface of ectodermal cells, and the movement of the mesendoderm relative to the BCR can be considered a special case of intercellular migration. Lastly, cells within the translocating mesendoderm mass show also intercellular migration.

Despite its multicellular character, mesoderm migration has mostly been studied with single cells moving *in vitro* on an artificial FN substratum. Under these conditions, cells translocate by repeatedly extending, dividing, and retracting lamellipodia which pull the yolk-laden cell body forward.

At their rear ends, cells detach, often by leaving cytoplasmic strands behind. On their natural substratum, the BCR, single mesendoderm cells move likewise by extending lamelliform protrusions (Howard and Smith, 1993; Nakatsuji, 1986; Nakatsuji and Johnson, 1982; Ramos and DeSimone, 1996; Selchow and Winklbauer, 1997; Smith et al., 1990; Winklbauer and Keller, 1996; Winklbauer and Selchow, 1992).

When two migrating dorsal mesendoderm cells collide head-on with their leading lamellipodia, these protrusions immediately collapse, and the cells move apart, being pulled by other lamellipodia which now become dominant. Such contact inhibition of movement is not observed when a lamellipodium encounters the cell body of another cell. Then, the lamellipodium is able to extend between the FN substratum and the cell body. Eventually, the underlapping cell will come to a halt as it is unable to completely lift the obstacle off the substratum, and the cells will start to move away from each other. Apparently, this contact is not sufficient to establish stable cell–cell adhesion. When cell density is high, however, attempts to move apart are mechanically restrained, and cell aggregates form in a cadherin-dependent process (Winklbauer et al., 1992). Contact behavior is different in ventral mesendoderm: cells attach to each other readily upon contact, and aggregates form faster (Reintsch and Hausen, 2001).

Aggregates continue to migrate on FN. Whereas isolated cells frequently change direction and velocity, translocation becomes more persistent and continuous in aggregates, where cells show only limited movement relative to each other (Winklbauer et al., 1992). Only cells at the aggregate margin extend lamellipodia, a phenomenon known from the migration of epithelial patches (Kolega, 1981). Thus, the ability of isolated cells to underlap neighboring cells with their protrusions is suppressed in larger, permanent aggregates. However, when placed on a more natural substratum consisting of the secreted extracellular matrix of the BCR, inhibition of protrusion formation is overcome, and internal cells underlap each other with lamelliform processes (Winklbauer et al., 1991, 1992).

The *in vivo* substratum for mesendoderm migration consists of the FN fibril-based BCR extracellular matrix and the cadherin-expressing membrane of the BCR cells. The FN fibril network is rather sparse, and the main contact of mesendoderm cells is with the surface of BCR cells (Nakatsuji et al., 1982). Close contacts, consistent with cadherin-mediated adhesion, can be observed between mesendoderm and BCR cells (Nakatsuji, 1976). In agreement with this, mesendoderm cells attach to the BCR surface even when interaction with FN is inhibited. However, cells are then round and do not spread or extend cytoplasmic protrusions along the BCR surface, nor do they migrate (Winklbauer, 1990; Winklbauer and Keller, 1996; Winklbauer et al., 1991). Thus, the FN matrix is essential for protrusion formation and locomotion, but not for substrate adhesion of mesendoderm cells.

How adhesion to and detachment from the BCR cell surface are achieved in this instance of intercellular migration is not understood, but further analysis of the tissue separation mechanisms discussed earlier should shed light on this problem. Compared to the *in vitro* conditioned substratum, the endogenous BCR substratum has an additional effect on the mesendoderm. It induces small, but distinct gaps between individual cells, suggesting that direct contact to the BCR induces local cell detachment in the mesendoderm (Fig. 5.2B and C) (Winklbauer et al., 1991). Also, tiny stubs can be seen on the surface of migrating mesendoderm cells in contact with the BCR, possibly ruptured membrane tethers (Winklbauer and Nagel, 1991).

As the mesendoderm moves toward the animal pole, its cells rearrange to accommodate to the changing shape of this tissue (Bauer et al., 1994; Davidson et al., 2002). At least part of the rearrangement is probably due to intercellular migration, as cells deep within the mesendodermal mass also extend filiform or lamelliform protrusions, without being in contact with the FN matrix (Fig. 5.2A) (Davidson et al., 2002; Komazaki, 1991; Nakatsuji, 1976). Although mesendoderm cell protrusions attach preferentially and rapidly to FN-coated substrates, they also bind to cell surfaces. They distinguish between mesendoderm and BCR cells, and attach more readily to the former, consistent with the use of each other's surface as substratum for migration. Moreover, protrusions always adhere more rapidly than the cell bodies to the same substratum, supporting a mechanism where the cell body is pulled forward by a protrusion firmly attached to the substratum (Winklbauer and Selchow, 1992).

In *Xenopus*, the protrusions of BCR-attached anterior mesendoderm cells are oriented toward the animal pole, in the direction of mesendoderm translocation, leading to a characteristic shingle arrangement of cells (Fig. 5.2B) (Davidson et al., 2002; Nagel et al., 2004; Winklbauer and Nagel, 1991). A similar orientation is observed in urodeles (Boucaut et al., 1991; Kubota and Durston, 1978; Nakatsuji et al., 1982). Moreover, when placed on BCR extracellular matrix that has been deposited *in vitro*, mesendoderm aggregates move in the direction of the animal pole (Nakatsuji and Johnson, 1983; Winklbauer and Nagel, 1991). This indicates that the BCR matrix contains guidance cues that orient mesendoderm cells and determine their direction of migration.

Guidance by the BCR matrix depends on PDGF signaling. In the *Xenopus* gastrula, a matrix-binding form of PDGF-A is synthesized by BCR cells, whereas its receptor, PDGFR-α, is expressed in a complementary pattern in the migrating mesendoderm (Ataliotis et al., 1995). Directional migration, as well as the animally directed orientation of cells, is abolished when PDGF signaling is inhibited, but also when PDGF-A is overexpressed, consistent with an instructive role for this factor (Nagel et al., 2004). The chemokine SDF-1α and its receptor, CXCR4, are also

expressed in a complementary pattern, very similar to that of PDGF-A and its receptor. Moreover, SDF-1α overexpressing BCR explants attract mesendoderm aggregates *in vitro* (Fukui et al., 2007). The *in vivo* function of this chemotactic system is not yet understood.

Mesoderm cells of the toad, Bufo, often extend cytoplasmic blebs instead of lamellipodia (Komazaki, 1991). Locomotion in the absence of lamellipodia or filopodia has been documented for gastrula cells of a newt, *Cynops*. Its vegetal cells glide over an *in vitro* substratum by internalizing membrane at the rear end, and adding it at the front end, while the membrane of the middle part of the elongated cell body remains stationary relative to the substratum (Kubota, 1981). Such a mode of translocation would be well suited for intercellular migration.

Although more densely packed than the mesoderm of amniotes, which undergo an epithelial–mesenchymal transition (Shook and Keller, 2008), amphibian mesoderm exhibits distinct gaps between cells (Fig. 5.2). Instead of the triple cell junctions which are usually assumed in simulation models of cell rearrangement, cells meet typically at small triangular gaps, such that only two cells are in contact instead of three. Some of these gaps are large enough to be detectable in the light microscope. But even where cells seem apposed to each other, stretches of close contact alternate with regions where membranes are separated by considerable space (Johnson, 1970, 1972, 1977a). These gaps are filled with extracellular material, very likely proteoglycans or hyaluronic acid (Johnson, 1977a,b,c). The effect of this intercellular matrix on tissue cohesion and intercellular migration is not known. It is tempting to view it as a lubricant which reduces the degree of cadherin-mediated adhesion.

4.4. Intercellular migration-related aspects of mesodermal convergent extension

Convergent extension of the dorsal, axis-forming mesoderm is a major paradigm for active cell rearrangement during embryonic morphogenesis, but the spatial and temporal complexity of the process is sometimes underestimated. In *Xenopus*, convergent extension starts at the early-to-middle gastrula stage in the mesoderm of the dorsal blastopore lip, and continues into the tailbud stages. During this time, the region partaking in the movement involutes, and then becomes subdivided by a tissue separation process into the notochord precursor and the presomitic mesoderm. Each of these subregions continue to converge and extend, while the notochord differentiates, and the somites segment and then differentiate as well (Keller and Danilchik, 1988; Keller and Tibbetts, 1989; Keller et al., 1989; Shih and Keller, 1992a,b; Wilson and Keller, 1991; Wilson et al., 1989).

In accordance with this complexity, the whole of convergent extension is composed of a number of different cellular processes that act in parallel or

sequentially. However, two basic tendencies are expressed throughout. First, intercalation of cells in the mediolateral direction is an essential feature that leads to the narrowing of the axial mesoderm. Second, to translate this movement into a lengthening, and not into a thickening of the tissue, it has to express a radial component, that is, radial intercalation. At different phases, one or the other tendency seems to dominate (e.g., Wilson and Keller, 1991; Wilson et al., 1989). In addition to these basic mechanisms, other processes participate. For example, at the notochord–somite interface, a boundary-capture mechanism contributes to convergent extension: intercalating notochord cells become trapped and accumulate at the boundary, thereby lengthening it (Keller et al., 1989, 2000). Further, in the postgastrulation presomitic mesoderm, cells become columnar, and this shape change contributes to the contraction of the paraxial mesoderm toward the midline, and therefore to convergence (Wilson et al., 1989). Thus, although convergent extension is at a superficial level a single, continuous, far-reaching movement at the dorsal side of the embryo, it is composed of a number of cellular processes that have probably been co-opted to contribute at different times and in different regions to the overarching task of generating an elongated dorsal body axis.

Molecular and cellular analyses of convergent extension focus almost exclusively on the intercalation of mediolaterally elongated cells which extend protrusions at both ends, in a bipolar, oriented fashion (Keller, 2002; Shih and Keller, 1992a,b; Wallingford et al., 2000, 2002). Such cells are first found in the involuting mesoderm of the dorsal blastopore lip (Fig. 5.2D) (Lane and Keller, 1997). In explants, mediolateral intercalation by bipolar cells spreads from anterior to posterior, perhaps paralleling the process of mesoderm involution (Shih and Keller, 1992a,b). At postgastrula stages, it is seen at the blastopore, in the notochord, and in segmenting somitic mesoderm (Keller et al., 1989; Wilson et al., 1989).

The protrusions at the ends of the bipolar cells move across the surface of neighboring cells, presumably pulling cells past one another. This notion is based on the correlation between the presence of these dynamic, oriented processes, and actual cell intercalation (Keller et al., 2008). In the chordamesoderm, an antero-posterior gradient of activin/nodal signaling intensity is sufficient to induce the mediolateral alignment of cells (Ninomiya et al., 2004). Moreover, signaling through the noncanonical Wnt pathway is a necessary condition for orientation (Keller, 2002; Wallingford et al., 2002). Once orientation has been initiated, alignment of cells may have a self-propagating component. In dissociated and reaggregated axial mesoderm cells *in vitro*, alignment occurs in a self-organization process along the periphery of the aggregate (Green et al., 2004).

In vitro, live imaging of mesoderm cell motility is confined to the outermost layer of an explant, and under these artificial conditions, lamellipodia seem to extend in the surface plane of the mesodermal layer

(Davidson et al., 2006; Shih and Keller, 1992a,b; Tahinci and Symes, 2003; Wallingford et al., 2000). If this were normally the case for protrusions in all layers, it would tend to produce convergent thickening instead of an anteroposterior elongation. One would therefore expect that in the embryo, protrusions extend between the anterior and posterior sides of neighboring cells. However, postinvolution mesoderm supposedly engaged in convergent extension often consists of columnar cells, with no obvious mediolateral orientation (Keller and Schoenwolf, 1977), whereas at the blastopore lip, cells seem indeed to overlap with their protrusions in the plane of the tissue surface (Keller et al., 1992b). Clearly, more observations on the arrangement of protrusions in the embryo are needed to understand their role in convergent extension.

This role also depends on how cell adhesion is regulated during tissue rearrangement. For example, protrusions might actively wedge between cells, breaking cell–cell adhesion, or they could invade free membrane surface generated by the prior detachment of cells. Of the different possibilities for cell deadhesion discussed earlier, it seems that peeling is least likely, since these bipolar cells have no trailing edge where peeling could occur. In a simulation of notochord cell intercalation, Weliky et al. (1991) assumed that differential cortical tension would lead to the shrinkage or expansion of existing cell–cell boundaries, but this model disregards the role of lamellipodia. Morphological evidence seems to favor active detachment as being responsible for the dynamic regulation of cell contacts. In the scanning electron microscope, lateral contacts between aligned cells are often characterized by fine, threadlike extensions reminiscent of membrane tethers (Keller et al., 1992a,b), and similar processes can be seen in live images of cells undergoing convergent extension in explants (Tahinci and Symes, 2003).

A molecular mechanism regulating adhesion/deadhesion cycles during convergent extension has also been proposed (Faure et al., 2005). Membrane-localized Pak5 diminishes adhesion when activated, and promotes it when inactive. Further, addition of Ca^{2+} to cells dissociated in Ca^{2+}-free buffer downregulates Pak5 activity and thus promotes adhesion; after aggregation, activity returns to normal. These findings can be synthesized into a conceptual model where Pak5 activation leads to cell detachment, followed by the downregulation of its activity and a consequent increase in adhesiveness, which in turn leads to the reattachment of cells (Faure et al., 2005). If such cycles were asynchronously expressed in different cells, strong adhesion between cells could be combined with flexibility of cell attachment. It would explain why both the inhibition and the activation of Pak5 inhibit convergent extension: in the first case, cells would be locked in the strongly adhesive state, unable to rapidly exchange neighbors and to intercalate; in the second case, cell attachment would be permanently downregulated, preventing the exertion of traction necessary for movement.

A similar interpretation based on cyclic changes of adhesion states could be applied to other findings. For example, convergent extension is attenuated when adhesion is increased by incubation with an antibody that augments C-cadherin binding (Zhong et al., 1999), but not by overexpression of C-cadherin (Lee and Gumbiner, 1995). Possibly, the dynamics of adhesion and detachment is affected in the first instance, and cells are locked in a permanent adhesive state, whereas overexpression is still compatible with active detachment.

According to its sorting behavior, surface tension, and strength of cadherin expression, chordamesoderm is the most cohesive tissue in the gastrula. This could be required, for example, if convergent extension were to move adjacent, passive tissues, and intercalating cells would need to develop strong traction forces. On the other hand, it has been argued that activin-induced convergent extension in BCR explants correlates with diminished cell adhesion, and the factors that downregulate adhesiveness, for example, PAPC and FLRT3/Rnd1, are necessary for convergent extension (Chen and Gumbiner, 2006; Lee and Gumbiner, 1995; Ogata et al., 2007). Even more confusing, both these factors are expressed anterior to the chordamesoderm in the early gastrula, in prechordal mesoderm not engaged in convergent extension (Medina et al., 2004; Ogata et al., 2007; Schambony and Wedlich, 2007). Thus, as far as activin-induced lowering of adhesiveness is mediated by FLRT3/Rnd1 (Ogata et al., 2007) and PAPC (Chen and Gumbiner, 2006), it occurs outside the converging–extending tissue. Since interfering with these factors inhibits convergent extension (Chen and Gumbiner, 2006; Kim et al., 1998; Ogata et al., 2007; Schambony and Wedlich, 2007; Unterseher et al., 2004; Zhong et al., 1999), nonautonomous effects seem plausible.

PAPC is expressed at later gastrula stages in the paraxial, somite-forming mesoderm, and its inhibition affects convergent extension of dorsal mesoderm at these stages as well. However, when chordamesoderm and PAPC-expressing paraxial mesoderm are tested separately, no inhibition is observed in the latter (Unterseher et al., 2004). This would again suggest a nonautonomous effect. To complicate matters even more, PAPC knockdown in blastopore lips prevents convergence, but not lengthening of respective explants (Unterseher et al., 2004), whereas the whole of convergent extension is compromised by PAPC inhibition in activin-induced animal caps (Chen and Gumbiner, 2006; Kim et al., 1998). Lastly, PAPC inhibition affects mediolateral cell orientation and alignment, which alone should compromise the mediolateral intercalation essential for convergence (Unterseher et al., 2004). It is not clear how the function of PAPC in adhesion (Chen and Gumbiner, 2006) and in cell orientation (Unterseher et al., 2004) is related to each other.

Convergent extension exemplifies that in an important regard, embryonic tissues do not behave like ordinary fluids: active, oriented cell

movements generate internal forces not normally encountered with fluids, leading to nonrandom exchanges of cell neighbors, and orderly, programmed tissue deformations. In the case of convergent extension, the force generated in this way has been measured (Moore et al., 1995), and can be compared to forces produced by random motility, that is, to tissue surface tension. In chordamesoderm explants from which the epithelial layer has been removed, surface tension generates enough hydrostatic pressure to offset the force resulting from active, directed cell intercalation (Ninomiya and Winklbauer, 2008), showing that the two mechanisms produce forces of similar magnitude.

5. Conclusion

Amphibian gastrulation takes place in the context of multilayered coherent cell masses and consequently, cell rearrangement is the main process in the gastrula. Typically, it is driven by active intercellular migration. It combines the translocation of cells over each others' surface with a coordinated, programmed spatial orientation of the cells' locomotory activities. This global orientation of motility is essential for the generation of the tissue shape changes characteristic of gastrulation. Two instances of cell orientation have been studied in detail in the *Xenopus* gastrula. In anterior mesoderm, PDGF signaling is necessary for the orientation of unipolar cells in the direction of tissue movement. In the chordamesoderm, anteroposterior tissue polarity that is induced by a graded activin/nodal signal, and Wnt/PCP signaling cooperate to align bipolar cells along the mediolateral axis, perpendicular to the direction of chordamesoderm extension. Coordinated, directional cell movement is also seen during vegetal rotation of the endodermal cell mass or during epibolic thinning of the inner layers of the BCR, and is expected to play a role in mesoderm involution.

These oriented cell movements are superimposed on basic random motility whose expression ranges from membrane fluctuations to stochastic cell translocation due to inaccuracies in oriented motility. This random component of motility allows cells, by constantly probing the adhesiveness of their environment, to approach spatial configurations that correspond to minima of free energy. In this sense, gastrula tissue shows liquid-like behavior. In particular, at free surfaces, this mechanism generates tissue surface tension, and when cells differ in adhesiveness, it leads to cell sorting and to interfacial tensions between sorted populations. These surface and interfacial tensions produce forces that are of similar magnitute as those generated by oriented cell motility, and they could in principle drive morphogenetic processes and determine tissue positioning. However, direct evidence for such positive *in vivo* roles is lacking; strong effects of these

tensions on tissue shapes and movements are all observed *in vitro*, in gastrula tissue explants. The generation of artificial, new surface area and the consequent introduction of surface tensions that disturb the normal equilibrium of tissue arrays in the embryo may be the main reason for these experimentally induced effects. Differential adhesion could also underlie boundary formation, but again, conclusive evidence for such an *in vivo* role in the gastrula is lacking. The best studied example, formation of Brachet's cleft, consists of a tissue separation process involving mechanisms beyond differential adhesion.

ACKNOWLEDGMENTS

I thank Ashley Bruce, Erich Damm, Robert David, Tony Harris, and Martina Nagel for critical reading of the manuscript; Olivia Luu, Erich Damm, and Hiromasa Ninomiya for help with the figures; and Martina Nagel for editing references. My research is supported by grants from the Canadian Institutes of Health Research and from the National Cancer Institute of Canada.

Notes added in proof: Tissues as ''active fluids'' have been discussed in Bittig et al. (2008) New Journal of Physics 10, 063001. C-cadherin shedding and an adhesion independent, aPKC-dependent signaling function has been shown for the Xenopus gastrula (Seifert et al. (2009), J. Cell Sci. 122, 2514-2523).

REFERENCES

Adachi, T., Sato, C., Kishi, Y., Totani, K., Murata, T., Usui, T., et al., 2008. Membrane microdomains from early gastrula embryos of medaka, *Oryzias latipes*, are a platform of E-cadherin- and carbohydrate-mediated cell-cell interaction during epiboly. Glycoconj. J. 26, 285–299.

Angres, B., Müller, A.H.J., Kellermann, J., Hausen, P., 1991. Differential expression of two cadherins in *Xenopus laevis*. Development 111, 8229–8244.

Arendt, D., Nubler-Jung, K., 1999. Rearranging gastrulation in the name of yolk: evolution of gastrulation in yolk-rich amniote eggs. Mech. Dev. 81, 3–22.

Ataliotis, P., Symes, K., Chou, M.M., Ho, L., Mercola, M., 1995. PDGF signaling is required for gastrulation of *Xenopus laevis*. Development 121, 3099–3110.

Aybar, M.J., Genta, S.B., Sanchez Riera, A.N., Sanchez, S.S., 2000. Participation of the GM1 ganglioside in the gastrulation of anuran amphibian *Bufo arenarum*. J. Exp. Zool. 286, 457–472.

Babb, S.G., Marrs, J.A., 2004. E-cadherin regulates cell movements and tissue formation in early zebrafish embryos. Dev. Dyn. 230, 263–277.

Balak, K., Jacobson, M., Sunshine, J., Rutishauser, U., 1987. Neural cell adhesion molecule expression in *Xenopus* embryos. Dev. Biol. 119, 540–550.

Bauer, D.V., Huang, S., Moody, S.A., 1994. The cleavage stage origin of Spemann's organizer: analysis of the movements of blastomere clones before and during gastrulation. Development 120, 1179–1189.

Beetschen, J.-C., 2001. Amphibian gastrulation: history and evolution of a 125 year-old concept. Int. J. Dev. Biol. 45, 771–795.

Beloussov, L.V., Louchinskaia, N.N., Stein, A.A., 2000. Tension-dependent collective cell movements in the early gastrula ectoderm of *Xenopus laevis* embryos. Dev. Genes Evol. 210, 92–104.

Benoit, M., Gaub, H.E., 2002. Measuring cell adhesion forces with the atomic force microscope at the molecular level. Cells Tissues Organs 172, 174–189.

Beysen, D.A., Forgacs, G., Glazier, J.A., 2000. Cell sorting is analogous to phase ordering in fluids. Proc. Natl. Acad. Sci. USA 97, 9467–9471.

Bisson, N., Poitras, L., Mikryukov, A., Temblay, M., Moss, T., 2007. EphA4 signaling regulates blastomere adhesion in the *Xenopus* embryo by recruiting Pak 1 to suppress Cdc42 function. Mol. Biol. Cell 18 (3), 1030–1043.

Bixby, J.L., Zhang, R., 1990. Purified N-Cadherin is a potent substrate for the rapid induction of neurite outgrowth. J. Cell Biol. 110, 1253–1260.

Blits-Huizinga, C.T., Nelersa, C.M., Malhotra, A., Liebl, D.J., 2004. Ephrins and their receptors: binding versus biology. IUBMB Life 56, 257–265.

Bokoch, G.M., 2003. Biology of the p21-activated kinases. Ann. Rev. Biochem. 72, 743–781.

Boucaut, J.C., Darribere, T., Shi, D.L., Riou, J.F., Delarue, M., Johnson, K.E., 1991. The amphibian embryo: an experimental model for the *in vivo* analysis of interactions between embryonic cells and extracellular matrix molecules. *In Vivo* 5, 473–481.

Bradley, R.S., Espeseth, A., Kintern, C., 1998. NF-protocadherin, a novel member of the cadherin superfamily, is required for *Xenopus* ectodermal differentiation. Curr. Biol. 8, 325–334.

Braga, V.M.M., Machesky, L.M., Hall, A., Hotchin, N.A., 1997. The small GTPases Rho and Rac are required for the establishment of cadherin-dependent cell–cell contacts. J. Cell Biol. 137, 1421–1431.

Brandli, A.W., Kirschner, M.W., 1995. Molecular cloning of tyrosine kinases in the early *Xenopus* embryo: identification of Eck-related genes expressed in cranial neural crest cells of the second (hyoid) arch. Dev. Dyn. 203, 119–140.

Brieher, W.M., Gumbiner, B.M., 1994. Regulation of C-cadherin function during activin induced morphogenesis of *Xenopus* animal caps. J. Cell Biol. 126, 519–527.

Brieher, W.M., Yap, A.S., Gumbiner, B.M., 1996. Lateral dimerization is required for the homophilic binding activity of C-cadherin. J. Cell Biol. 135, 487–496.

Brizuela, B.J., Wessely, O., De Robertis, E.M., 2001. Overexpression of the *Xenopus* tight-junction protein claudin causes randomization of the left-right body axis. Dev. Biol. 230, 217–229.

Broders, F., Thiery, J.-P., 1995. Contribution of cadherins to directional cell migration and histogenesis in *Xenopus* embryos. Cell Adhes. Commun. 3, 419–440.

Brodland, G.W., 2002. The Differential Interfacial Tension Hypothesis (DITH): a comprehensive theory for the self-rearrangement of embryonic cells and tissues. J. Biomech. Eng. 124, 188–197.

Bucior, I., Burger, M.M., 2004. Carbohydrate–carbohydrate interactions in cell recognition. Curr. Opin. Struct. Biol. 14, 631–637.

Byers, T.J., Armstrong, P.B., 1986. Membrane protein redistribution during *Xenopus* first cleavage. J. Cell Biol. 102, 2176–2184.

Cavey, M., Rauzi, M., Lenne, P.-F., Lecuit, T., 2008. A two-tiered mechanism for stabilization and immobilization of E-cadherin. Nature 453 (7196), 751–756.

Chalmers, A.D., Strauss, B., Papalopulu, N., 2003. Oriented cell divisions asymmetrically segregate aPKC and generate cell fate diversity in the early *Xenopus* embryo. Development 130, 2657–2668.

Chen, X., Gumbiner, B.M., 2006. Paraxial protocadherin mediates cell sorting and tissue morphogenesis by regulating C-cadherin adhesion activity. J. Cell Biol. 174, 301–313.

Chen, C.P., Posy, S., Ben-Shaul, A., Shapiro, L., Honig, B.H., 2005. Specificity of cell–cell adhesion by classical cadherins: critical role for low-affinity dimerization through beta-strand swapping. Proc. Natl. Acad. Sci. USA 102, 8531–8536.

Chitaev, N.A., Averbakh, A.Z., Troyanovsky, R.B., Troyanovsky, S.M., 1998. Molecular organization of the desmoglein-plakoglobin complex. J Cell Sci. 111, 1941–1949.

Choi, Y.S., Gumbiner, B., 1989. Expression of cell adhesion molecule E-cadherin in *Xenopus* embryos begins at gastrulation and predominates in the ectoderm. J Cell Biol. 108, 2449–2458.

Choi, S.-C., Han, J.-K., 2002. *Xenopus* Cdc42 regulates convergent extension movements during gastrulation through Wnt/Ca^{2+} signaling pathway. Dev. Biol. 244, 342–357.

Choi, Y.S., Seghal, R., McCrea, P., Gumbiner, B., 1990. A cadherin-like protein in eggs and cleaving embryos of *Xenopus laevis* is expressed in oocytes in response to progesterone. J. Cell Biol. 110, 1575–1582.

Chung, H.A., Yamamoto, T.S., Ueno, N., 2007. ANR5, an FGF target gene product, regulates gastrulation in *Xenopus*. Curr. Biol. 17, 932–939.

Collazo, A., Bolker, J.A., Keller, R., 1994. A phylogenetic perspective on teleost gastrulation. Am. Nat. 144, 133–152.

Cooke, J.E., Kemp, H.A., Moens, C.B., 2005. EphA4 is required for cell adhesion and rhombomere-boundary formation in the zebrafish. Curr. Biol. 15, 536–542.

Dale, L., Slack, J.M.W., 1987. Fate map for the 32-cell stage of *Xenopus laevis*. Development 99, 527–551.

Davidson, L.A., Hoffstrom, B.G., Keller, R., DeSimone, D.W., 2002. Mesendoderm extension and mantle closure in *Xenopus laevis* gastrulation: combined roles for integrin aa, fibronectin, and tissue geometry. Dev. Biol. 242, 109–129.

Davidson, L.A., Marsden, M., Keller, R., Desimone, D.W., 2006. Integrin alpha5beta1 and fibronectin regulate polarized cell protrusions required for *Xenopus* convergence and extension. Curr. Biol. 16, 833–844.

Davis, G.S., 1984. Migration-directing liquid properties of embryonic amphibian tissues. Am. Zool. 24, 649–655.

Davis, G.S., Phillips, H.M., Steinberg, M.S., 1997. Germ-layer surface tensions and ''tissue affinities'' in *Rana pipiens* gastrulae: quantitative measurements. Dev. Biol. 192, 630–644.

De Beco, S., Gueudry, C., Amblard, F., Coscoy, S., 2009. Endocytosis is required for E-cadherin redistribution at mature adherens junctions. Proc. Natl. Acad. Sci. USA 106, 7010–7015.

Decave, E., Garrivier, D., Brechet, Y., Bruckert, F., Fourcade, B., 2002. Peeling process in living cell movement under shear flow. Phys. Rev. Lett. 89, 108101.

del Pino, E.M., Venegas-Ferrin, M., Romero-Carvajal, A., Montenegro-Larrea, P., Saenz-Ponce, I.M., Moya, I.M., et al., 2007. A comparative analysis of frog early development. Proc. Natl. Acad. Sci. USA.

Delanoe-Ayari, H., Iwaya, S., Maeda, Y.T., Inose, J., Riviere, C., Sano, M., et al., 2008. Changes in the magnitude and distribution of forces at different *Dictyostelium* developmental stages. Cell Motil. Cytoskeleton 65, 314–331.

Dello Sbarba, P., Rovida, E., 2002. Transmodulation of cell surface regulatory molecules via ectodomain shedding. Biol. Chem. 383, 69–83.

Delva, E., Kowalczyk, A.P., 2009. Regulation of cadherin trafficking. Traffic 10, 259–267.

DeMarais, A.A., Moon, R.T., 1992. The armadillo homologs β-catenin and plakoglobin are differentially expressed during early development of *Xenopus laevis*. Dev. Biol. 153, 337–346.

Detrick, R.J., Dickey, D., Kintern, C.R., 1990. The effects of N-cadherin misexpression on morphogenesis in *Xenopus* embryos. Neuron 4, 493–506.

Dravis, C., Yokoyama, N., Chumley, M.J., Cowan, C.A., Silvany, R.E., Shay, J., et al., 2004. Bidirectional signaling mediated by ephrin-B2 and EphB2 controls urorectal development. Dev. Biol. 271, 272–290.

du Roure, O., Saez, A., Buguin, A., Austin, R.H., Chavrier, P., Silberzan, P., et al., 2005. Force mapping in epithelial cell migration. Proc. Natl. Acad. Sci. USA 102, 2390–2395.

Duguay, D., Foty, R.A., Steinberg, M.S., 2003. Cadherin-mediated cell adhesion and tissue segregation: qualitative and quantitative determinants. Dev. Biol. 253, 309–323.

Elul, T., Keller, R., 2000. Monopolar protrusive activity: a new morphogenetic cell behavior in the neural plate dependent on vertical interactions with the mesoderm in *Xenopus*. Dev. Biol. 224, 3–19.

Ewald, A.J., Peyrot, S.M., Tyszka, J.M., Fraser, S.E., Wallingford, J.B., 2004. Regional requirements for dishevelled signaling during *Xenopus* gastrulation: separable effects on blastopore closure, mesendoderm internalization and archenteron formation. Development 131, 6195–6209.

Fagotto, F., Gumbiner, B.M., 1994. Beta-catenin localization during *Xenopus* embryogenesis: accumulation at tissue and somite boundaries. Development 120, 3667–3679.

Fang, X., Ji, H., Kim, S.W., Park, J.I., Vaught, T.G., Anastasiadis, P.Z., et al., 2004. Vertebrate development requires ARVCF and p120 catenins and their interplay with RhoA and Rac. J. Cell Biol. 165, 87–98.

Faure, S., Cau, J., de Santa Barbara, P., Bigou, S., Ge, Q., Delsert, C., et al., 2005. *Xenopus* p21-activated kinase 5 regulates blastomere adhesive properties during convergent extension movements. Dev. Biol. 277, 472–492.

Foty, R.A., Steinberg, M.S., 2005. The differential adhesion hypothesis: a direct evaluation. Dev. Biol. 278, 255–263.

Foty, R.A., Forgacs, G., Pfleger, C.M., Steinberg, M.S., 1994. Liquid properties of embryonic tissues: measurement of interfacial tensions. Phys. Rev. Lett. 72, 2298–2301.

Foty, R.A., Pfleger, C.M., Forgacs, G., Steinberg, M.S., 1996. Surface tensions of embryonic tissues predict their mutual envelopment behavior. Development 122, 1611–1620.

Fouquet, B., Zimbelmann, R., Franke, W.W., 1992. Identification of plakoglobin in oocytes and early embryos of *Xenopus laevis*: maternal expression of a gene encoding a junctional plaque protein. Differentiation 51, 187–194.

Frank, M., Kemler, R., 2002. Protocadherins. Curr. Opin. Cell Biol. 14, 557–562.

Friedl, P., Hegerfeldt, Y., Tusch, M., 2004. Collective cell migration in morphogenesis and cancer. Int. J. Dev. Biol. 48, 441–449.

Fukata, M., Nakagawa, M., Kuroda, S., Kaibuchi, K., 1999. Cell adhesion and Rho small GTPases. J. Cell Sci. 112, 4491–4500.

Fukui, Y., 1993. Toward a new concept of cell motility: cytoskeletal dynamics in amoeboid movement and cell division. Int. Rev. Cytol. 144, 85–125.

Fukui, A., Goto, T., Kitamoto, J., Homma, M., Asashima, M., 2007. SDF-1α regulates mesendodermal cell migration during frog gastrulation. Biochem. Biophys. Res. Commun. 354, 472–477.

Gallin, W.J., 1998. Evolution of the "classical" cadherin family of cell adhesion molecules in vertebrates. Mol. Biol. Evol. 15, 1099–1107.

Ginsberg, D., DeSimone, D., Geiger, B., 1991. Expression of a novel cadherin (EP-cadherin) in unfertilized eggs and early *Xenopus* embryos. Development 111, 315–325.

Graner, F., 1993. Can surface adhesion drive cell-rearrangement? Part I: Biological cell-sorting. J. Theor. Biol. 164, 445–476.

Green, J.B.A., Dominguez, I., Davidson, L.A., 2004. Self-organization of vertebrate mesoderm based on simple boundary conditions. Dev. Dyn. 231, 576–581.

Grosheva, I., Shtutman, M., Elbaum, M., Bershadsky, A.D., 2001. P120 catenin affects cell motility via modulation of activity of Rho-family GTPases: a link between cell-cell contact formation and regulation of cell locomotion. J. Cell Sci. 114, 695–707.

Gumbiner, B.M., 2005. Regulation of cadherin-mediated adhesion in morphogenesis. Nat. Rev. Mol. Cell. Biol. 6, 622–634.
Halbleib, J.M., Nelson, W.J., 2006. Cadherins in development: cell adhesion, sorting, and tissue morphogenesis. Genes Dev. 20, 3199–3214.
Hardin, J., Keller, R., 1988. The behavior and function of bottle cells during gastrulation of *Xenopus laevis*. Development 103, 211–230.
Harris, A.K., 1976. Is cell sorting caused by differences in the work of intercellular adhesion? A critique of the Steinberg hypothesis. J. Theor. Biol. 61, 267–285.
Hatta, K., Takeichi, M., 1986. Expression of N-cadherin adhesion molecules associated with early morphogenetic events in chick development. Nature 320, 447–449.
Heasman, J., Ginsberg, D., Geiger, B., Goldstone, K., Pratt, T., Yoshida-Noro, C., et al., 1994. A functional test for maternally inherited cadherin in *Xenopus* shows its importance in cell adhesion at the blastula stage. Development 120, 49–57.
Hegedüs, B., Marga, F., Jakab, K., Sharpe-Timms, K.L., Forgacs, G., 2006. The interplay of cell–cell and cell–matrix interactions in the invasive properties of brain tumors. Biophys. J. 91, 2708–2716.
Helbling, P.M., Tran, C.T., Brändli, A.W., 1998. Requirement for EphA receptor signaling in the segregation of *Xenopus* third and fourth arch neural crest cells. Mech. Dev. 78, 63–79.
Helbling, P.M., Saulnier, D.M., Robinson, V., Christiansen, J.H., Wilkinson, D.G., Brändli, A.W., 1999. Comparative analysis of embryonic gene expression defines potential interaction sites for *Xenopus* EphB4 receptors with ephrin-B ligands. Dev. Dyn. 216, 361–373.
Hemler, M.E., 2003. Tetraspanin proteins mediate cellular penetration, invasion, and fusion events and define a novel type of membrane microdomain. Ann. Rev. Cell Dev. Biol. 19, 397–422.
Hens, M.D., Nikolic, I., Woolcock, C.M., 2002. Regulation of *Xenopus* embryonic cell adhesion by the small GTPase, rac. Biochem. Biophys. Res. Commun. 298, 363–370.
Herzberg, F., Wildermuth, V., Wedlich, D., 1991. Expression of XB-cad, a novel cadherin, during oogenesis and early development of *Xenopus*. Mech. Dev. 35, 33–42.
Hojyo, T., Tooi, O., Tashiro, K., Shiokawa, K., 1998. Exogastrula formation in *Xenopus laevis* embryos depleted with maternal XmN-cadherin mRNA by antisense S-oligo DNA. Biochem. Biophys. Res. Commun. 242, 170–175.
Holtfreter, J., 1939. Gewebeaffinitat, ein Mittel der embryonalen Formbildung. Arch. Exp. Zellforsch. 23, 169–209.
Holtfreter, J., 1944. A study of the mechanics of gastrulation; Part II. J. Exp. Zool. 95, 171–212.
Hornberger, M.R., Dütting, D., Ciossek, T., Yamada, T., Handwerker, C., Lang, S., et al., 1999. Modulation of EphA receptor function by coexpressed ephrinA ligands on retinal ganglion cell axons. Neuron 22, 731–742.
Hoschuetzky, H., Aberle, H., Kemler, R., 1994. β-catenin mediates the interaction of the cadherin–catenin complex with epidermal growth factor receptor. J. Cell Biol. 127, 1375–1380.
Houston, D.W., Wylie, C., 2003. The *Xenopus* LIM-homeodomain protein Xlim5 regulates the differential adhesion properties of early ectoderm cells. Development 130, 2695–2704.
Howard, J.E., Smith, J.C., 1993. Analysis of gastrulation: different types of gastrulation movement are induced by different mesoderm-inducing factors in *Xenopus laevis*. Mech. Dev. 43, 37–48.
Hukriede, N.A., Tsang, T.E., Habas, R., Khoo, P.L., Steiner, K., Weeks, D.L., et al., 2003. Conserved requirement of Lim1 function for cell movements during gastrulation. Dev. Cell 4, 83–94.

Ibrahim, H., Winklbauer, R., 2001. Mechanisms of mesendoderm internalization in the *Xenopus* gastrula: lessons from the ventral side. Dev. Biol. 240, 108–122.
Jaffer, Z.M., Chernoff, J., 2002. p21-activated kinases: three more join the Pak. Int. J. Biochem. Cell Biol. 34, 713–717.
Jakab, K., Damon, B., Marga, F., Doaga, O., Mironov, V., Kosztin, I., et al., 2008. Relating cell and tissue mechanics: implications and applications. Dev. Dyn. 237, 2438–2449.
Jia, D., Dajusta, D., Foty, R.A., 2007. Tissue surface tensions guide *in vitro* self-assembly of rodent pancreatic islet cells. Dev. Dyn. 236, 2039–2049.
Johnson, K.E., 1970. The role of changes in cell contact behavior in amphibian gastrulation. J. Exp. Zool. 175, 391–428.
Johnson, K.E., 1972. The extent of cell contact and the relative frequency of small and large gaps between presumptive mesodermal cells in normal gastrulae of *Rana pipiens* and the arrested gastrulae of the *Rana pipiens*×*Rana catesbeiana* hybrid. J. Exp. Zool. 179, 227–237.
Johnson, K.E., 1977a. Extracellular matrix synthesis in blastula and gastrula stages of normal and hybrid frog embryos. I. Autoradiographic observations. J. Cell Sci. 25, 323–334.
Johnson, K.E., 1977b. Extracellular matrix synthesis in blastula and gastrula stages of normal and hybrid frog embryos. I. Toluidine blue and lanthanum staining. J. Cell Sci. 25, 313–322.
Johnson, K.E., 1977c. Changes in the cell coat at the onset of gastrulation in *Xenopus laevis* embryos. J. Exp. Zool. 199, 137–142.
Jones, T.L., Karavanova, I., Maéno, M., Ong, R.C., Kung, H.F., Daar, I.O., 1995. Expression of an amphibian homolog of the Eph family of receptor tyrosine kinases is developmentally regulated. Oncogene 10, 1111–1117.
Jones, T.L., Karavanova, I., Chong, L., Zhou, R.P., Daar, I.O., 1997. Identification of XLerk, an Eph family ligand regulated during mesoderm induction and neurogenesis in *Xenopus laevis*. Oncogene 14, 2159–2166.
Jones, T.L., Chong, L.D., Kim, J., Xu, R.H., Kung, H.F., Daar, I.O., 1998. Loss of cell adhesion in *Xenopus laevis* embryos mediated by the cytoplasmic domain of XLerk, an erythropoietin-producing hepatocellular ligand. Proc. Natl. Acad. Sci. USA 95, 576–581.
Kalantarian, A., Ninomiya, H., Saad, S.M., David, R., Winklbauer, R., Neumann, A.W., 2009. Axisymmetric drop shape analysis for estimating the surface tension of cell aggregates by centrifugation. Biophys. J. 96, 1606–1616.
Kanai, Y., Ochiai, A., Shibata, T., Oyama, T., Ushijima, S., Akimoto, S., et al., 1995. c-erb-2 gene product directly associates with β-catenin and plakoglobin. Biochem. Biophys. Res. Commun. 208, 1067–1072.
Karaulanov, E.E., Bottcher, R.T., Niehrs, C., 2006. A role for fibronectin-leucin-rich transmembrane cell-surface proteins in homotypic cell adhesion. EMBO Rep. 7, 283–290.
Keller, R.E., 1975. Vital dye mapping of the gastrula and neurula of *Xenopus laevis*.I. Prospective areas and morphogenetic movements of the superficial layer. Dev. Biol. 42, 222–241.
Keller, R.E., 1976. Vital dye mapping of the gastrula and neurula of *Xenopus laevis*. II. Prospective areas and morphogenetic movements of the deep layer. Dev. Biol. 51, 118–137.
Keller, R.E., 1978. Time-lapse cinemicrographic analysis of superficial cell behavior during and prior to gastrulation in *Xenopus laevis*. J. Morphol. 157, 223–248.
Keller, R.E., 1980. The cellular basis of epiboly: an SEM study of deep-cell rearrangement during gastrulation in *Xenopus laevis*. J. Embryol. Exp. Morphol. 60, 201–234.
Keller, R., 1981. An experimental analysis of the role of bottle cells and the deep marginal zone in gastrulation of *Xenopus laevis*. J. Exp. Zool. 216, 81–101.

Keller, R., 1986. The cellular basis of amphibian gastrulation. In: Browder, L. (Ed.), Developmental Biology: A Comprehensive Synthesis. Vol. 2: The Cellular Basis of Morphogenesis. Plenum, New York, pp. 241–327.
Keller, R., 2002. Shaping the vertebrate body plan by polarized embryonic cell movements. Science 298, 1950–1954.
Keller, R., Danilchik, M., 1988. Regional expression, pattern and timing of convergence and extension during gastrulation of *Xenopus laevis*. Development 103, 193–209.
Keller, R., Jansa, S., 1992. *Xenopus* gastrulation without a blastocoel roof. Dev. Dyn. 195, 162–176.
Keller, R.E., Schoenwolf, G.C., 1977. An SEM study of cellular morphology, contact, and arrangement, as related to gastrulation in *Xenopus laevis*. W. Roux's Arch. 182, 165–186.
Keller, R., Tibbetts, P., 1989. Mediolateral cell intercalation in the dorsal, axial mesoderm of *Xenopus laevis*. Dev. Biol. 131, 539–549.
Keller, R., Cooper, M.S., Danilchik, M., Tibbetts, P., Wilson, P.A., 1989. Cell intercalation during notochord development in *Xenopus laevis*. J. Exp. Zool. 251, 134–154.
Keller, R., Shih, J., Sater, A., 1992a. The cellular basis of the convergence and extension of the *Xenopus* neural plate. Dev. Dyn. 193, 199–217.
Keller, R., Shih, J., Sater, A., Moreno, C., 1992b. The patterning and functioning of protrusive activity during convergence and extension of the *Xenopus* organizer. Development 1992 (Suppl.), 81–91.
Keller, R., Davidson, R., Edlund, A., Elul, T., Ezin, M., Shook, D., et al., 2000. Mechanisms of convergence and extension by cell intercalation. Philos. Trans. R. Soc. Lond. B 355, 897–922.
Keller, R., Davidson, L.A., Shook, D.R., 2003. How we are shaped: the biomechanics of gastrulation. Differentiation 71, 171–205.
Keller, R., Shook, D., Skoglund, P., 2008. The forces that shape embryos: physical aspects of convergent extension by cell intercalation. Phys. Biol. 5, 015007 (23pp).
Kim, S.-H., Yamamoto, A., Bouwmeester, T., Agius, E., De Robertis, E.M., 1998. The role of paraxial protocadherin in selective adhesion and cell movements of the mesoderm during *Xenopus* gastrulation. Development 125, 4681–4691.
Kintner, C.R., 1992. Regulation of embryonic cell adhesion by the cadherin cytoplasmic domain. Cell 69, 225–236.
Kintner, C.R., Melton, D.A., 1987. Expression of *Xenopus* N-CAM RNA in ectoderm is an early response to neural induction. Development 99, 311–325.
Klymkowsky, M.W., Shook, D.R., Maynell, L.A., 1992. Evidence that the deep keratin filament systems of the *Xenopus* embryo act to ensure normal gastrulation. Proc. Natl. Acad. Sci. USA 89, 8736–8740.
Kofron, M., Spagnuolo, A., Klymkowsky, M., Wylie, C., Heasman, J., 1997. The roles of maternal α-catenin and plakoglobin in the early *Xenopus* embryo. Development 124, 1553–1560.
Kofron, M., Heasman, J., Lang, S.A., Wylie, C.C., 2002. Plakoglobin is required for maintenance of the cortical actin skeleton in early *Xenopus* embryos and for cdc42-mediated wound healing. J. Cell Biol. 158, 695–708.
Kolega, J., 1981. The movement of cell clusters *in vitro*: morphology and directionality. J. Cell Sci. 49, 15–32.
Komazaki, S., 1991. Changes in intercellular contacts, motility, and adhesiveness of the presumptive mesodermal cells of Bufo vulgaris embryos before and during gastrulation. J. Exp. Zool. 258, 327–335.
Komazaki, S., 1993. Movement of an epithelial layer isolated from early embryos of the newt, *Cynops pyrrhogaster*. II. Formation of a blastoporal groove and archenteron in a superficial epithelial layer isolated from initial gastrula. Dev. Growth Differ. 35, 471–478.

Kovacs, E.M., Ali, R.G., McCormack, A.J., Yap, A.S., 2002. E-cadherin homophilic ligation directly signals through Rac and phosphatidylinositol 3-kinase to regulate adhesive contacts. J. Biol. Chem. 277, 6708–6718.

Krieg, M., Arboleda-Estudillo, Y., Puech, P.-H., Kafer, J., Graner, F., Muller, D.J., et al., 2008. Tensile forces govern germ-layer organization in zebrafish. Nat. Cell Biol. 10, 429–436.

Kubo, H., Kotani, M., Ozawa, H., Kawashima, I., Tai, T., Suzuki, A., 1995. Differential distribution of ganglioside GM1 and sulfatide during the development of *Xenopus* embryos. Dev. Growth Differ. 37, 243–255.

Kubota, H.Y., 1981. Creeping locomotion of the endodermal cells dissociated from gastrulae of the Japanese newt, *Cynops pyrrhogaster*. Exp. Cell Res. 133, 137–148.

Kubota, H.Y., Durston, A.J., 1978. Cinematographical study of cell migration in the opened gastrula of *Ambystoma mexicanum*. J. Embryol. Exp. Morphol. 44, 71–80.

Kuhl, M., Wedlich, D., 1996. *Xenopus* cadherins: sorting out types and functions in embryogenesis. Dev. Dyn. 207, 121–134.

Kuhl, M., Finnemann, S., Binder, O., Wedlich, D., 1996. Dominant-negative expression of a cytoplasmatically deleted mutant of XB/U-cadherin disturbs mesoderm migration during gastrulation in *Xenopus laevis*. Mech. Dev. 54, 71–82.

Kullander, K., Klein, R., 2002. Mechanisms and functions of Eph and ephrin signaling. Nat. Rev. Mol. Cell Biol. 3, 475–486.

Kuroda, S., Fukata, M., Nakagawa, M., Fuji, K., Nakamura, T., Ookubo, T., Izawa, I., Nagase, T., Nomura, N., Tani, H., Shoji, I., Matsuura, Y., et al., 1998. Role of IQGAP1, a target of small GTPases Cdc42 and Rac1, in regulation of E-cadherin-mediated cell-cell adhesion. Science 281, 832–835.

Kuroda, H., Sakumoto, H., Kinoshita, K., Asashima, M., 1999. Changes in the adhesive properties of dissociated and reaggregated *Xenopus laevis* embryo cells. Dev. Growth Differ. 41, 283–291.

Kuroda, H., Inui, M., Sugimoto, K., Hayata, T., Asashima, M., 2002. Axial protocadherin is a mediator of prenotochord cell sorting in *Xenopus*. Dev. Biol. 244, 267–277.

Kurth, T., Fesenko, I.V., Schneider, S., Munchberg, F.E., Joos, T.E., Spieker, T.P., et al., 1999. Immunocytochemical studies of the interactions of cadherins and catenins in the early *Xenopus* embryo. Dev. Dyn. 215, 155–169.

Lane, M.C., Keller, R., 1997. Microtubule disruption reveals that Spemann's organizer is subdivided into two domains by the vegetal alignment zone. Development 124, 895–906.

Lauffenburger, D.A., Horwitz, A.F., 1996. Cell migration: a physically integrated molecular process. Cell 84, 359–369.

Leckband, D., Prakasam, A., 2006. Mechanism and dynamics of cadherin adhesion. Annu. Rev. Biomed. Eng. 8, 259–287.

Lee, C.-H., Gumbiner, B., 1995. Disruption of gastrulation movements in *Xenopus* by a dominant-negative mutant for C-cadherin. Dev. Biol. 171, 363–373.

Lee, H.S., Bong, Y.S., Moore, K.B., Soria, K., Moody, S.A., Daar, I.O., 2006. Dishevelled mediates ephrinB1 signalling in the eye field through the planar cell polarity pathway. Nat. Cell Biol. 8, 55–63.

Letourneau, P.C., Shattuck, T.A., Roche, F.K., Takeichi, M., Lemmon, V., 1990. Nerve growth cone migration onto Schwann cells involves the calcium-dependent adhesion molecule, N-cadherin. Dev. Biol. 138, 430–442.

Levi, G., Ginsberg, D., Girault, J.-M., Sabanay, I., Thiery, J.-P., Geiger, B., 1991. EP-cadherin in muscles and epithelia of *Xenopus laevis* embryos. Development 113, 1335–1344.

Levine, E., Lee, C.H., Kintner, C., Gumbiner, B.M., 1994. Selective disruption of E-cadherin function in early *Xenopus* embryos by a dominant negative mutant. Development 120, 901–909.

Li, G., Satyamoorthy, K., Herlyn, M., 2001. N-cadherin-mediated intercellular interactions promote survival and migration of melanoma cells. Cancer Res. 61, 3819–3825.
Marsden, M., DeSimone, D.W., 2001. Regulation of cell polarity, radial intercalation and epiboly in *Xenopus*: novel roles for integrin and fibronectin. Development 128, 3635–3647.
Martin, P., Parkhurst, S.M., 2004. Parallels between tissue repair and embryo morphogenesis. Development 131, 3021–3034.
McCrea, P.D., Park, J.I., 2007. Developmental functions of the P120-catenin sub-family. Biochim. Biophys. Acta 1773, 17–33.
Medina, A., Swain, R.K., Kuerner, K.-M., Steinbeisser, H., 2004. *Xenopus* paraxial protocadherin has signaling functions and is involved in tissue separation. EMBO J. 23, 3249–3258.
Minsuk, S.B., Keller, R.E., 1997. Surface mesoderm in *Xenopus*: a revision of the stage 10 fate map. Dev. Genes Evol. 207, 389–401.
Mir, A., Kofron, M., Zorn, A.M., Bajzer, M., Haque, M., Heasman, J., et al., 2007. FoxI1e activates ectoderm formation and controls cell position in the *Xenopus* blastula. Development 134, 779–788.
Mombach, J.C., Glazier, J.A., 1996. Single cell motion in aggregates of embryonic cells. Phys. Rev. Lett. 76, 3032–3035.
Montero, J.A., Carvalho, L., Wilsch-Bräuninger, M., Kilian, B., Mustafa, C., Heisenberg, C.P., 2005. Shield formation at the onset of zebrafish gastrulation. Development 132, 1187–1198.
Moody, S.A., 1987. Fates of the blastomeres of the 32-cell-stage *Xenopus* embryo. Dev. Biol. 122, 300–319.
Moore, S.W., Keller, R.E., Koehl, M.A.R., 1995. The dorsal involuting marginal zone stiffens anisotropically during its convergent extension in the gastrula of *Xenopus laevis*. Development 121, 3131–3140.
Müller, H.A., 2001. Of mice, frogs and flies: generation of membrane asymmetries in early development. Dev. Growth Differ. 43, 327–342.
Muller, H.-A.J., Hausen, P., 1995. Epithelial cell polarity in early *Xenopus* development. Dev. Dyn. 202, 405–420.
Muller, H.-A.J., Kuhl, M., Finnemann, S., Schneider, S., van der Poel, S.Z., Hausen, P., et al., 1994. *Xenopus* cadherins: the maternal pool comprises distinguishable members of the family. Mech. Dev. 47, 213–223.
Murai, K.K., Pasquale, E.B., 2003. Eph'ective signaling: forward, reverse and crosstalk. J. Cell Sci. 116, 2823–2832.
Nagel, M., Tahinci, E., Symes, K., Winklbauer, R., 2004. Guidance of mesoderm cell migration in the *Xenopus* gastrula requires PDGF signaling. Development 131, 2727–2736.
Nakatsuji, N., 1975. Studies on the gastrulation of amphibian embryos: cell movement during gastrulation in *Xenopus laevis* embryos. W. Roux Arch. 178, 1–14.
Nakatsuji, N., 1976. Studies on the gastrulation of amphibian embryos: ultrastructure of the migrating cells of anurans. W. Roux's Arch. 180, 229–240.
Nakatsuji, N., 1986. Presumptive mesoderm cells from *Xenopus laevis* gastrulae attach to and migrate on substrata coated with fibronectin or laminin. J. Cell Sci. 86, 109–118.
Nakatsuji, N., Johnson, K.E., 1982. Cell locomotion *in vitro* by *Xenopus laevis* gastrula mesodermal cells. Cell Motil. 2, 149–161.
Nakatsuji, N., Johnson, K.E., 1983. Conditioning of a culture substratum by the ectodermal layer promotes attachment and oriented locomotion by amphibian gastrula mesodermal cells. J. Cell Sci. 59, 43–60.
Nakatsuji, N., Gould, A.C., Johnson, K.E., 1982. Movement and guidance of migrating mesoderm cells in *Ambystoma maculatum* gastrulae. J. Cell Sci. 56, 207–222.

Nandadasa, S., Tao, Q., Menon, N.R., Heasman, J., Wylie, C., 2009. N- and E-cadherins in *Xenopus* are specifically required in the neural and non-neural ectoderm, respectively, for F-actin assembly and morphogenetic movements. Development 136, 1327–1338.

Nelson, W.J., 2008. Regulation of cell–cell adhesion by the cadherin–catenin complex. Biochem. Soc. Trans. 36, 149–155.

Nelson, K.K., Nelson, R.W., 2004. Cdc42 effector protein 2 (XCEP2) is required for normal gastrulation and contributes to cellular adhesion in *Xenopus laevis*. BMC Dev. Biol. 4, 13.

Nie, S., Chang, C., 2006. Regulation of early *Xenopus* development by ErbB signaling. Dev. Dyn. 235, 301–314.

Nie, S., Chang, C., 2007. Regulation of *Xenopus* gastrulation by ErbB signaling. Dev. Biol. 303, 93–107.

Niessen, C.M., Gumbiner, B.M., 2002. Cadherin-mediated cell sorting not determined by binding or adhesion specificity. J. Cell Biol. 156, 389–399.

Nieuwkoop, P.D., Florschutz, P.A., 1950. Quelques caracteres speciaux de la gastrulation et de la neurulation de l'oeuf de *Xenopus laevis*, Daud. Et de quelques autres Anoures. 1ere partie. Etude descriptive. Arch. Biol. 61, 113–150.

Niewiadomska, P., Godt, D., Tepass, U., 1999. DE-cadherin is required for intercellular motility during *Drosophila* oogenesis. J. Cell Biol. 144, 533–547.

Ninomiya, H., Winklbauer, R., 2008. Epithelial coating controls mesenchymal shape change through tissue-positioning effects and reduction of surface-minimizing tension. Nat. Cell Biol. 10, 61–69.

Ninomiya, H., Elinson, R.P., Winklbauer, R., 2004. Antero-posterior tissue polarity links mesoderm convergent extension to axial patterning. Nature 430, 364–367.

Nomura, K.H., Kobayashi, R., Hirabayashi, Y., Fujisue-Sakai, M., Mizuguchi, S., Nomura, K., 1998. Involvement of blood-group-B-active trisaccharides in Ca^{2+}-dependent cell–cell adhesion in the *Xenopus* blastula. Dev. Genes Evol. 208, 9–18.

Noren, N.K., Liu, B.P., Burridge, K., Kreft, B., 2000. P120 catenin regulates the actin cytoskeleton via Rho family GTPases. J. Cell Biol. 150, 567–580.

Noren, N.K., Niessen, C.M., Gumbiner, B.M., Burridge, K., 2001. Cadherin engagement regulates Rho family GTPases. J. Biol. Chem. 276, 33305–33308.

Oda, H., Tsukita, S., Takeichi, M., 1998. Dynamic behavior of the cadherin-based cell–cell adhesion system during *Drosophila* gastrulation. Dev. Biol. 203, 435–450.

Ogata, S., Morokuma, J., Hayata, T., Kolle, G., Niehrs, C., Ueno, N., et al., 2007. TGF-beta signaling-mediated morphogenesis: modulation of cell adhesion via cadherin endocytosis. Genes Dev. 21, 1817–1831.

Pacquelet, A., Rorth, P., 2005. Regulatory mechanisms required for DE-cadherin function in cell migration and other types of adhesion. J. Cell Biol. 170, 803–812.

Pasquale, E.B., 2005. Eph receptor signalling casts a wide net on cell behaviour. Nat. Rev. Mol. Cell Biol. 6, 462–475.

Peng, Y., Yang, P.-H., Tanner, J.A., Huang, J.-D., Li, M., Lee, H.F., et al., 2006. Cold-inducible RNA binding protein is required for the expression of adhesion molecules and embryonic cell movement in *Xenopus laevis*. Biochem. Biophys. Res. Commun. 344, 416–424.

Phillips, H.M., 1984. Physical analysis of tissue mechanics in amphibian gastrulation. Am. Zool. 24, 657–672.

Phillips, H.M., Davis, G.S., 1978. Liquid-tissue mechanics in amphibian gastrulation: germ layer assembly in *Rana pipiens*. Am. Zool. 18, 81–93.

Phillips, H.M., Steinberg, M.S., Lipton, B.H., 1977. Embryonic tissues as elasticoviscous liquids. II. Direct evidence for cell slippage in centrifuged aggregates. Dev. Biol. 59, 124–134.

Pokutta, S., Weis, W.I., 2007. Structure and mechanism of cadherins and catenins in cell–cell contacts. Ann. Rev. Cell Dev. Biol. 23, 237–261.

Poliakov, A., Cotrina, M., Wilkinson, D.G., 2004. Diverse roles of Eph receptors and ephrins in the regulation of cell migration and tissue assembly. Dev. Cell 7, 465–480.

Popsueva, A.E., Luchinskaya, N.N., Ludwig, A.V., Zinovjeva, O.Y., Poterayev, D.A., Feigelman, M.M., Ponomarev, M.B., Berekelya, L., Belyavsky, A.V., 2001. Overexpression of camello, a member of a novel protein family, reduces blastomere adhesion and inhibits gastrulation in *Xenopus laevis*. Dev. Biol. 234, 483–496.

Prakasam, A.K., Maruthamuthu, V., Leckband, D.E., 2006. Similarities between heterophilic and homophilic cadherin adhesion. Proc. Natl. Acad. Sci. USA 103, 15434–15439.

Puech, P.H., Poole, K., Knebel, D., Muller, D.J., 2006. A new technical approach to quantifying cell–cell adhesion forces by AFM. Ultramicroscopy 106, 637–644.

Radice, G.L., Rayburn, H., Matsunami, H., Knudsen, K.A., Takeichi, M., Hynes, R.O., 1997. Developmental defects in mouse embryos lacking N-cadherin. Dev. Biol. 181, 64–78.

Rafelski, S.M., Theriot, J.A., 2004. Crawling towards a unified model of cell mobility: spatial and temporal regulation of actin dynamics. Ann. Rev. Biochem. 73, 209–239.

Ramos, J.W., DeSimone, D.W., 1996. *Xenopus* embryonic cell adhesion to fibronectin: position-specific activation of RGD/synergy site-dependent migratory behavior at gastrulation. J. Cell Biol. 134, 227–240.

Rangarajan, J., Luo, T., Sargent, T.D., 2006. PCNS: a novel protocadherin required for cranial neural crest migration and somite morphogenesis in *Xenopus*. Dev. Biol. 295, 206–218.

Regen, C.M., Steinhardt, R.A., 1986. Global properties of the *Xenopus* blastula are mediated by a high-resistance epithelial seal. Dev. Biol. 113, 147–154.

Reintsch, W.E., Hausen, P., 2001. Dorsoventral differences in cell–cell interactions modulate the motile behaviour of cells from the *Xenopus* gastrula. Dev. Biol. 240, 387–403.

Reintsch, W.E., Habring-Mueller, A., Wang, R.W., Schohl, A., Fagotto, F., 2005. β-catenin controls cell sorting at the notochord-somite boundary independently of cadherin-mediated adhesion. J. Cell Biol. 170, 675–686.

Reintsch, W.E., Mandato, C.A., McCrea, P.D., Fagotto, F., 2008. Inhibition of cell adhesion by xARVCF indicates a regulatory function at the plasma membrane. Dev. Dyn. 237, 2328–2341.

Revenu, C., Athman, R., Robine, S., Louvard, D., 2004. The co-workers of actin filaments: from cell structures to signals. Nat. Rev. Mol. Cell Biol. 5, 1–12.

Reynolds, A.B., Carnahan, R.H., 2004. Regulation of cadherin stability and turnover by p120ctn: implications in disease and cancer. Semin. Cell Dev. Biol. 15, 657–663.

Rieu, J.-P., Sawada, Y., 2002. Hydrodynamics and cell motion during the rounding of two dimensional hydra cell aggregates. Eur. Phys. J. B 27, 167–172.

Rieu, J.-P., Upadhyaya, A., Glazier, J.A., Ouchi, N.B., Sawada, Y., 2000. Diffusion and deformations of single Hydra cells in cellular aggregates. Biophys. J. 79, 1903–1914.

Ripley, A.N., Chang, M.S., Bader, D.M., 2004. Bves is expressed in the epithelial components of the retina, lens, and cornea. Invest. Ophthalmol. Vis. Sci. 45, 2475–2483.

Ripley, A.N., Osler, M.E., Wright, C.V.E., Bader, D., 2006. Xbves is a regulator of epithelial movement during early *Xenopus laevis* development. Proc. Natl. Acad. Sci. USA 103, 614–619.

Rizzoti, K., Paquereau, L., Shaw, A., Knibiehler, B., Audigier, Y., 1998. A constitutively activated mutant of Gαq downregulates EP-cadherin expression and decreases adhesion between ectodermal cells at gastrulation. Mech. Dev. 76, 19–31.

Roberts, S.J., Leaf, D.S., Moore, H.-P., Gerhart, J.C., 1992. The establishment of polarized membrane traffic in *Xenopus laevis* embryos. J. Cell Biol. 118, 1359–1369.

Saint-Jeannet, J.-P., Foulquier, F., Goridis, C., Duprat, A.-M., 1989. Expression of N-CAM precedes neural induction in *Pleurodeles waltl* (Urodele, amphibian). Development 106, 675–683.

Scales, J.B., Winning, R.S., Renaud, C.S., Shea, L.J., Sargent, T.D., 1995. Novel members of the eph receptor tyrosine kinase subfamily expressed during *Xenopus* development. Oncogene 11, 1745–1752.

Schambony, A., Wedlich, D., 2007. Wnt-5a/Ror2 regulate expression of XPAPC through an alternative noncanonical signaling pathway. Dev. Cell 12, 779–792.

Schneider, S., Herrenknecht, K., Butz, S., Kemler, R., Hausen, P., 1993. Catenins in *Xenopus* embryogenesis and their relation to the cadherin-mediated cell–cell adhesion system. Development 118, 629–640.

Schock, F., Perrimon, N., 2002. Molecular mechanisms of epithelial morphogenesis. Ann. Rev. Cell Dev. Biol. 18, 463–493.

Schotz, E.-M., Burdine, R.D., Julicher, F., Steinberg, M.S., Heisenberg, C.-P., Foty, R.A., 2008. Quantitative differences in tissue surface tension influence zebrafish germ layer positioning. HFSP J. 2, 42–56.

Sehgal, R.N.M., Gumbiner, B.M., Reichardt, L.F., 1997. Antagonism of cell adhesion by an α-catenin mutant, and of the Wnt signaling pathway by α-catenin in *Xenopus* embryos. J. Cell Biol. 139, 1033–1046.

Selchow, A., Winklbauer, R., 1997. Structure and cytoskeletal organization of migratory mesoderm cells from the *Xenopus* gastrula. Cell Motil. Cytoskelet. 36, 12–29.

Shih, J., Keller, R., 1992a. Cell motility driving mediolateral intercalation in explants of *Xenopus laevis*. Development 116, 901–914.

Shih, J., Keller, R., 1992b. Patterns of cell motility in the organizer and dorsal mesoderm of *Xenopus laevis*. Development 116, 915–930.

Shook, D., Keller, R., 2003. Mechanisms, mechanics and function of epithelial-mesenchymal transitions in early development. Mech. Dev. 120, 1351–1383.

Shook, D., Keller, R., 2008. Epithelial type, ingression, blastopore architecture and the evolution of chordate mesoderm morphogenesis. J. Exp. Zool. 310B, 85–110.

Shook, D.R., Majer, C., Keller, R., 2002. Urodeles remove mesoderm from the superficial layer by subduction through a bilateral primitive streak. Dev. Biol. 248, 220–239.

Shook, D.R., Majer, C., Keller, R., 2004. Patterns and morphogenesis of presumptive superficial mesoderm in two closely related species, *Xenopus laevis* and *Xenopus tropicalis*. Dev. Biol. 270, 163–185.

Skoglund, P., Rolo, A., Chen, X., Gumbiner, B.M., Keller, R., 2008. Convergence and extension at gastrulation require a myosin IIB-dependent cortical actin network. Development 135, 2435–2445.

Smith, J.C., Symes, K., Hynes, R.O., DeSimone, D.D., 1990. Mesoderm induction and control of gastrulation in *Xenopus laevis*: the role of fibronectin and integrins. Development 135, 2435–2445.

Smith, A., Robinson, V., Patel, K., Wilkinson, D.G., 1997. The EphA4 and EphB1 receptor tyrosine kinases and ephrin-B2 ligand regulate targeted migration of branchial neural crest cells. Curr. Biol. 7, 561–570.

Sokol, S.Y., Li, Z., Sacks, D.B., 2001. The effect of IQGAP1 on *Xenopus* embryonic ectoderm requires Cdc42. J. Biol. Chem. 276, 48425–48430.

Steinberg, M.S., 1963. Reconstruction of tissues by dissociated cells. Science 141, 401–408.

Steinberg, M.S., 1970. Does differential adhesion govern self-assembly processes in histogenesis? Equilibrium configurations and the emergence of a hierarchy among populations of embryonic cells. J. Exp. Zool. 173, 395–434.

Steinberg, M.S., 1978. Specific cell ligands and the differential adhesion hypothesis: how do they fit together? In: Garrod, D.R. (Ed.), Specificity of Embryological Interactions. Chapman & Hall, London (Receptors and Recognition, Series B, Vol.4).

Steinberg, M.S., Takeichi, M., 1994. Experimental specification of cell sorting, tissue spreading, and specific spatial patterning by quantitative differences in cadherin expression. Proc. Natl. Acad. Sci. USA 91, 206–209.

Strauss, B., Adams, R.J., Papalopulu, N., 2006. A default mechanism of spindle orientation based on cell shape is sufficient to generate cell fate diversity in polarised *Xenopus* blastomeres. Development 133, 3883–3893.

Tahinci, E., Symes, K., 2003. Distinct functions of Rho and Rac are required for convergent extension during *Xenopus* gastrulation. Dev. Biol. 259, 318–335.

Tanaka, M., Wang, D.Y., Kamo, T., Igarashi, H., Wang, Y., Xiang, Y.Y., et al., 1998. Interaction of EphB2-tyrosine kinase receptor and its ligand conveys dorsalization signal in *Xenopus laevis* development. Oncogene 17, 1509–1516.

Tanaka, M., Kamo, T., Ota, S., Sugimura, H., 2003. Association of dishevelled with Eph tyrosine kinase receptor and ephrin mediates cell repulsion. EMBO J. 22, 847–858.

Tao, Q., Nandadasa, S., McCrea, P.D., Heasman, J., Wylie, C., 2007. G-protein-coupled signals control cortical actin assembly by controlling cadherin expression in the early *Xenopus* embryo. Development 134, 2651–2661.

Tepass, U., Truong, K., Godt, D., Ikura, M., Peifer, M., 2000. Cadherins in embryonic and neural morphogenesis. Nat. Rev. Mol. Cell Biol. 1, 91–100.

Tepass, U., Godt, D., Winklbauer, R., 2002. Cell sorting in animal development: signaling and adhesive mechanisms in the formation of tissue boundaries. Curr. Opin. Gen. Dev. 12, 572–582.

Thoumine, O., Ott, A., 1997. Time scale dependent viscoelastic and contractile regimes in fibroblasts probed by microplate manipulation. J. Cell Sci. 110, 2109–2116.

Torres, M.A., Yang-Snyder, J.A., Purcell, S.M., DeMarais, A.A., McGrew, L.L., Moon, R.T., 1996. Activities of the Wnt-1 class of secreted signaling factors are antagonized by the Wnt-5A class and by a dominant negative cadherin in early Xenopus development. J. Cell Biol. 133, 1123–1137.

Townes, P.L., Holtfreter, J., 1955. Directed movements and selective adhesion of embryonic amphibian cells. J. Exp. Zool. 128, 53–120.

Tracey, W.D., Pepling, M.E., Horb, M.E., Thomsen, G.H., Gergen, J.P., 1998. A *Xenopus* homologue of aml-1 reveals unexpected patterning mechanisms leading to the formation of embryonic blood. Development 125, 1371–1380.

Troyanovsky, R.B., Sokolov, E.P., Troyanovsky, S.M., 2006. Endocytosis of cadherin from intracellular junctions is the driving force for cadherin adhesive dimer disassembly. Mol. Biol. Cell 17, 3484–3493.

Turner, A., Snape, A.M., Wylie, C.C., Heasman, J., 1989. Regional identity is established before gastrulation in the *Xenopus* embryo. J. Exp. Zool. 251, 245–252.

Turner, A.P., Brown, D., Heasman, J., Cook, G.M., Evans, J., Vickers, L., et al., 1992. Involvement of a neutral glycolipid in differential cell adhesion in the *Xenopus* blastula. EMBO J. 11, 3845–3855.

Umeda, T., Inouye, K., 1999. Theoretical model for morphogenesis and cell sorting in *Dictyostelium discoideum*. Phys. D 126, 189–200.

Unterseher, F., Hefele, J.A., Giehl, K., De Robertis, E.M., Wedlich, D., Schambony, A., 2004. Paraxial protochadherin coordinates cell polarity during convergent extension via RhoA and JNK. EMBO J. 23, 3259–3269.

Vogt, W., 1929. Gestaltungsanalyse am Amphibiankeim mit ortlicher Vitalfarbung. II Teil. Gastrulation und Mesodermbildung bei Urodelen und Anuren. Arch. Entw. Mech. 120, 384–706.

Wacker, S., Grimm, K., Joos, T., Winklbauer, R., 2000. Development and control of tissue separation at gastrulation in *Xenopus*. Dev. Biol. 224, 428–439.

Wada, A.M., Reese, D.E., Bader, D.M., 2001. Bves: prototype of a new class of cell adhesion molecules expressed during coronary artery development. Development 128, 2085–2093.

Wallingford, J.B., Rowing, B.A., Vogeli, K.M., Rothbacher, U., Fraser, S.E., Harland, R.M., 2000. Dishevelled controls cell polarity during *Xenopus* gastrulation. Nature 405, 81–85.
Wallingford, J.B., Fraser, S.E., Harland, R.M., 2002. Convergent extension: the molecular control of polarized cell movement during embryonic development. Dev. Cell 2, 695–706.
Ward, M.D., Dembo, M., Hammer, D.A., 1994. Kinetics of cell detachment: peeling of discrete receptor clusters. Biophys. J. 67, 2522–2534.
Weinstein, D.C., Rahman, S.M., Ruiz, J.C., Hemmati-Brivanlou, A., 1996. Embryonic expression of eph signalling factors in *Xenopus*. Mech. Dev. 57, 133–144.
Weliky, M., Minsuk, S., Keller, R., Oster, G., 1991. Notochord morphogenesis in *Xenopus laevis*: simulation of cell behavior underlying tissue convergence and extension. Development 113, 1231–1244.
Wilson, P., Keller, R., 1991. Cell rearrangement during gastrulation of *Xenopus*: direct observation of cultured explants. Development 112, 289–300.
Wilson, P.A., Oster, G., Keller, R., 1989. Cell rearrangement and segmentation in *Xenopus*: direct observation of cultured explants. Development 105, 155–166.
Winklbauer, R., 1990. Mesodermal cell migration during *Xenopus* gastrulation. Dev. Biol. 142, 155–168.
Winklbauer, R., Keller, R.E., 1996. Fibronectin, mesoderm migration and gastrulation in *Xenopus*. Dev. Biol. 177, 413–426.
Winklbauer, R., Nagel, M., 1991. Directional mesoderm cell migration in the *Xenopus* gastrula. Dev. Biol. 148, 573–589.
Winklbauer, R., Schürfeld, M., 1999. Vegetal rotation, a new gastrulation movement involved in the internalization of the mesoderm and endoderm in *Xenopus*. Development 126, 3703–3713.
Winklbauer, R., Selchow, A., 1992. Motile behavior and protrusive activity of migratory mesoderm cells from the *Xenopus* gastrula. Dev. Biol. 150, 335–351.
Winklbauer, R., Selchow, A., Nagel, M., Stoltz, C., Angres, B., 1991. Mesoderm cell migration in the *Xenopus* gastrula. In: Keller, R. (Ed.), Gastrulation. Plenum Press, New York, pp. 147–168.
Winklbauer, R., Selchow, A., Nagel, M., Angres, B., 1992. Cell interaction and its role in mesoderm cell migration during *Xenopus* gastrulation. Dev. Dyn. 195, 290–302.
Winklbauer, R., Median, A., Swain, R.K., Steinbeisser, H., 2001. Frizzled-7 signaling controls tissue separation during *Xenopus* gastrulation. Nature 413, 856–860.
Winning, R.S., Sargent, T.D., 1994. Pagliaccio, a member of the Eph family of receptor tyrosine kinase genes, has localized expression in a subset of neural crest and neural tissues in *Xenopus laevis* embryos. Mech. Dev. 46, 219–229.
Winning, R.S., Scales, J.B., Sargent, T.D., 1996. Disruption of cell adhesion in *Xenopus* embryos by Pagliaccio, an Eph-class receptor tyrosine kinase. Dev. Biol. 179, 309–319.
Winning, R.S., Wyman, T.L., Walker, G.K., 2001. EphA4 activity causes cell shape change and a loss of cell polarity in *Xenopus laevis* embryos. Differentiation 68, 126–132.
Winning, R.S., Ward, E.K., Scales, J.B., Walker, G.K., 2002. EphA4 catalytic activity causes inhibition of RhoA GTPase in *Xenopus laevis* embryos. Differentiation 70, 46–55.
Wunnenberg-Stapleton, K., Blitz, I.L., Hashimoto, C., Cho, K.W., 1999. Involvement of the small GTPases XrhoA and XRnd1 in cell adhesion and head formation in early *Xenopus* development. Development 126, 5339–5351.
Yamada, S., Nelson, W.J., 2007. Localized zones of Rho and Rac activities drive initiation and expansion of epithelial cell–cell adhesion. J. Cell Biol. 178, 517–527.
Yamamoto, Y., Grubisic, K., Oelgeschlaeger, M., 2007. *Xenopus* tetraspanin-1 regulates gastrulation movements and neural differentiation in the early *Xenopus* embryo. Differentiation 75, 235–245.

Yamashiro, S., Noguchi, T., Mabuchi, I., 2003. Localization of two IQGAPs in cultured cells and early embryos of *Xenopus laevis*. Cell Motil. Cytoskelet. 55, 36–50.

Yamashiro, S., Abe, H., Mabuchi, I., 2007. IQGAP2 is required for the cadherin-mediated cell-to-cell adhesion in *Xenopus laevis* embryos. Dev. Biol. 308, 485–493.

Yanagisawa, M., Anastasiadis, P.Z., 2006. P120 catenin is essential for mesenchymal cadherin-mediated regulation of cell motility and invasiveness. J. Cell Biol. 174, 1087–1096.

Yap, A.S., Niessen, C.M., Gumbiner, B.M., 1998. The juxtamembrane region of the cadherin cytoplasmic tail supports lateral clustering, adhesive strengthening, and interaction with p120ctn. J. Cell Biol. 141, 779–789.

Yap, A.S., Crampton, M.S., Hardin, J., 2007. Making and breaking contacts: the cellular biology of cadherin regulation. Curr. Opin. Cell Biol. 19, 508–514.

Yasunaga, T., Kusakabe, M., Yamanaka, H., Hanafusa, H., Masuyama, N., Nishida, E., 2005. *Xenopus* ILK (integrin-linked kinase) is required for morphogenetic movements during gastrulation. Genes Cells 10, 369–379.

Zhong, Y., Brieher, W.M., Gumbiner, B.M., 1999. Analysis of C-cadherin regulation during tissue morphogenesis with an activating antibody. J. Cell Biol. 144, 351–359.

Zimmer, M., Palmer, A., Kohler, J., Klein, R., 2003. EphB-ephrinB bi-directional endocytosis terminates adhesion allowing contact mediated repulsion. Nat. Cell Biol. 5, 869–878.

CHAPTER SIX

Molecular and Cell Biology of Testicular Germ Cell Tumors

Paolo Chieffi,* Renato Franco,† *and* Giuseppe Portella‡

Contents

1. Introduction 278
2. Epidemiology and Risk Factors 279
3. Histopathology 280
   3.1. Origin and development 280
   3.2. Classification 282
   3.3. Staging of testicular tumors 286
   3.4. ITGCN, Unclassified 287
   3.5. Seminomatous–TGCTs 287
   3.6. NSE tumors 289
   3.7. Somatic malignancies arising in testicular GCT 293
   3.8. Regression of primitive GCTs 293
4. Prognostic and Diagnostic Markers 294
   4.1. Serum tumor markers 294
   4.2. New discovered markers for TGCTs 295
5. Therapy 297
   5.1. Traditional treatment 297
   5.2. Aurora-kinase inhibitors 298
   5.3. Receptor and nonreceptor tyrosine kinases inhibitors 299
   5.4. Angiogenesis inhibitors 300
6. Conclusions and Perspectives 301
Acknowledgments 301
References 302

Abstract

Although testicular germ cell tumors (TGCTs) are relatively uncommon, they are particularly important as they tend to affect children and young men, representing the most common tumor in male aged from 20 to 40 years. TGCTs are a

* Dipartimento di Medicina Sperimentale, II Università di Napoli, 80138 Naples, Italy
† Area Funzionale di Anatomia Patologica, Istituto Nazionale dei Tumori "Fondazione G. Pascale," 80131 Naples, Italy
‡ Dipartimento di Biologia e Patologia Cellulare e Molecolare, Università di Napoli "Federico II," 80131 Naples, Italy

International Review of Cell and Molecular Biology, Volume 278
ISSN 1937-6448, DOI: 10.1016/S1937-6448(09)78006-2
© 2009 Elsevier Inc.
All rights reserved.

heterogeneous group of tumors, with specific peculiarities reflecting on epidemiologic distribution and clinic-pathological features. TGCTs show a high-cure rates in both seminomas and nonseminomas and represent the model of a curable neoplasia: sensitive serum tumor markers, accurate prognostic classification, contribute to a high effectiveness of cancer therapy. However, up to 30% of patients diagnosed with metastatic nonseminomas do not achieve a durable remission, and in metastatic teratomas cisplatin-based treatment resistance has been observed. These different prognostic and therapeutic features of TGCTs highlight the need for a better understanding of the molecular biology of TGCT, that could help to improve disease management and to tailor aggressiveness of treatment to the severity of the prognosis.

Key Words: Testis, Testicular cancer, Gonocytes, Testicular germ cells, Kinase inhibitors. © 2009 Elsevier Inc.

1. Introduction

Testicular germ cell tumors (TGCTs) of the testis are a heterogeneous group of neoplasms seen mainly in children and young men (Chieffi, 2007; Oosterhuis and Looijenga, 2005). They are classified as seminomatous (SE-TGCT) and nonseminomatous (NSE-TGCT) tumors. Distinction of prebuberal TGCTs, exclusively represented by yolk sac tumor (YST) and teratoma, and postpuberal TGCTs, invariably arising from intratubular germ cell neoplasias (ITGCNs) seems to have a great prognostic relevance (Chaganti and Houldsworth, 2000; Ulbright, 1993).

Postpuberal TCGTs are the most frequent solid malignant tumor in men between 20 and 40 years of age, accounting for up to 60% of all malignancies diagnosed at this age. Despite a high-cure rate, they represent the most frequent cause of death from solid tumors in this age group (Oosterhuis and Looijenga, 2005; Pottern, 1998). Seminomas are radio- and chemo-sensitive tumors, virtually completely curable (Jones and Vasey, 2003). NSE tumors are usually treated with surgery and chemotherapy, with different cure rates depending on the disease stage (Shelley et al., 2002). The cure rate reaches up to 99% in the early stages of NSE tumors, although in advanced disease decreases from 90% in patients with good prognostic category to 50% in patients with poor prognostic features (Shelley et al., 2002).

The rapid growth and progression of postpuberal TGCTs cause early lymph node metastases and/or distant metastases. At the time of diagnosis about 25% of seminoma patients and up to 60% of the nonseminoma patients suffers from metastatic disease (Al Ghamdi and Jewett, 2005; Classen et al., 2001; Peckham, 1988; Perrotti et al., 2004; Porcaro et al., 2002), posing a therapeutic problem since in metastatic disease the

treatment achieves modest results. Thus, despite the general success of postpuberal TGCTs treatment, 10–20% of patients diagnosed with metastatic disease will not achieve a durable complete remission after initial treatment, either due to incomplete response or a tumors relapse.

The review will focus on the molecular alterations identified in postpuberal TGCTs and on novel targeted antineoplastic strategies that could contribute to the cure of chemotherapy resistant TGCTs.

2. Epidemiology and Risk Factors

TGCTs have significantly increased in the past 50 years; this increase is probably due to changes in environmental factors contributing to the development of these lesions. A number of environmental factors have been investigated to explain the possible links. Some evidence suggests association of increased TGCTs risk and maternal smoking during pregnancy, adult height, body mass index, diet rich in cheese, and others (Bonner et al., 2002; Dieckmann and Pichlmeier, 2002; Dieckmann et al., 2008, 2009; García-Rodríguez et al., 1996; Garner et al., 2003), however, the biological mechanisms remain to be elucidated.

Hypothesized environmental agents involved in the development of TGCTs, include pesticides (McGlynn et al., 2008) and nonsteroidal estrogens, such as diethylstilbestrol (DES) (Martin et al., 2008). It has been proposed that increased levels of estrogen exposure *in utero* to increase the risk of TGCTs (Garner et al., 2008) and the exposure of women to the nonsteroidal estrogen DES during pregnancy increases the risk of TGCTs (Strohsnitter et al., 2001). However, other studies have not confirmed a role for estrogen in TGCTs development (Dieckmann et al., 2001). Despite the contrasting results reported in the literature a clear role for environmental factors in the etiology of TGCTs is suggested by population migration studies. Sweden has an incidence of TGCTs about twice that of Finland and although first generation migrants from Finland to Sweden show no increased risk (Ekbom et al., 2003), second generation males born to the migrant parents in Sweden have a tendency to an increased frequency (Montgomery et al., 2005).

Familial predisposition to TGCTs, ethnic variations in incidence, and an association with certain chromosome abnormality syndromes strongly suggest that inherited factors, also, play a role in disease development. The familial predisposition is one of the strongest for any tumor type, since the increased relative risk of TGCTs development associated with fathers and sons of TGCTs patients is fourfold (Forman et al., 1992). However, gene(s) involved in familial TGCTs have not been identified so far (Krausz and Looijenga, 2008). Genome-wide linkage analysis of affected families has

provided evidence for two susceptibility loci, one at Xq27 locus for undescended testis probably playing an indirect role and another at 12q which results in hyperexpression of the product of the CCND2 gene (Lutke Holzik et al., 2004). It is probable that both genetic and environmental factors produce the high familial risk seen in TGCTs and that the interplay between these two factors, along with genetic heterogeneity, may make familial associated susceptibility loci difficult to determine.

3. Histopathology

3.1. Origin and development

The origin and biology of TGCTs are currently distinct on whether they occur in pre- and postpuberal age, being pure teratomas and YSTs with a substantially benign prognosis the most common hystotypes of prepuberal testis and seminoma, pure NSE tumors and mixed germ cell tumors (GCTs) with a relative more aggressive behavior typical of adult testis (Looijenga and Oosterhuis, 1999).

It has been suggested that the initiating event in the pathogenesis of TGCT occurs during embryonal development (Chieffi, 2007). The most widely accepted model of postpuberal TGCTs development proposes an initial tumorigenic event *in utero* and the development of a precursor lesion known as intratubular germ cell neoplasia undifferentiated (ITGCNU), also known as carcinoma *in situ* (CIS) (Skakkebaek, 1972). This is followed by a period of dormancy until after puberty when postpuberal TGCTs emerge. This prepubertal dormancy suggests that the TGCTs development is hormone dependent.

Recently, it has been proposed that tumors originate from neoplastic cells that retain stem cell properties such as self-renewal (Wicha, et al., 2006), and this novel hypothesis has fundamental implications for the pathogenesis of TGCTs. According with stem cells hypothesis, tumors originate from tissue stem cells or from their immediate progeny. This cellular subcomponent drives tumorigenesis and aberrant differentiation, contributing to cellular heterogeneity of the tumor and also to the resistance to antineoplastic treatments.

ITGCNU cells are generally accepted as the common preinvasive precursor cells that gives rise to postpuberal TGCTs (Oosterhuis and Looijenga, 2005; Ulbright, 1999). ITGCNU almost found invariably in the periphery of overt postpuberal TGCTs and is estimated that it is present in approximately 5% of the contralateral testis of patients with postpuberal TGCTs (Berthelsen et al., 1982). Preinvasive ITGCNU cells are supposed to be able to develop in different germinal and somatic tissues and are regarded as pluripotent or totipotent cells and therefore can be considered as TGCTs stem cells.

ITGCNU cells share morphological similarities with gonocytes and it has been proposed that ITGCNU cells could be remnants of undifferentiated embryonic/fetal cells (Nielsen et al., 1974; Skakkebaek et al., 1987). Their fetal origin is also supported by immunohistochemical studies of proteins present in ITGCNU, also shown to be present in primordial germ cells (PGCs) and gonocytes. The identification of ITGCNU cells in prepubertal patients, who later developed TGCTs, indicated that the cells had originated prior to puberty (Müller et al., 1984).

Therefore, ITGCNU cell represents an interesting variant of cancer stem cell since it originates before the tissue that it propagates in is fully differentiated and functional. The observation that two transcription factors, *POU5F1* (OCT3/4) and *NANOG,* known to be associated with pluripotency in ES cells are expressed in ITGCNU has further contributed to assess the embryonic origin of these cells. A link between ITGCNU cells and embryonic cells has been further supported by a substantial overlap between human ES cells and ITGCNU cells gene expression profiles, as shown by Almstrup et al. (2004). All hystotypes could be present in postpuberal TGCTs, because of its totipontent profile, even seminoma can switch to nonseminoma hystotype through *reprogramming* phenomenon (Fig. 6.1) (Hoei-Hansen et al., 2005; Looijenga, 2009; Rajpert-De Meyts et al., 2003). The role of these factors will be discussed in more detail in the next sections.

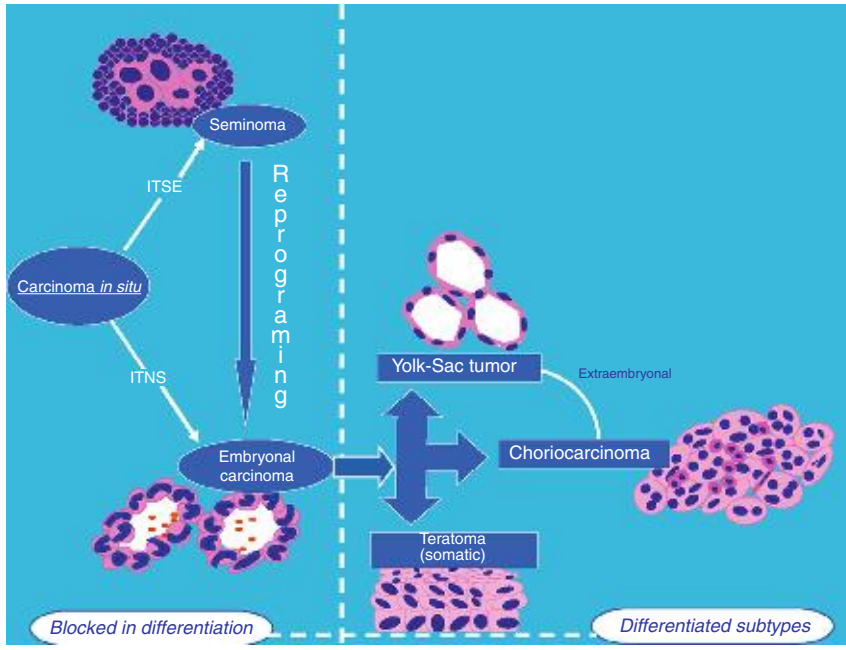

Figure 6.1 Differentiative relations between TGCT histotypes.

Seminoma consists of transformed germ cells, that closely resemble the PGC/gonocyte, apparently blocked in their differentiation. Nonseminoma could be constituted by cells with typical pluripotency of PGC/gonocyte. In particular, embryonal carcinoma reflect undifferentiated stem cells, Teratoma represent somatic differentiation, while choriocarcinoma and YST extraembryonal differentiation. Genetic studies have shown that postpubertal testis tumors are often aneuploid with a consistent chromosomal abnormality composed of a gain of short arm of chromosome 12, usually in the form of an isochromosome, i(12p). In contrast tumors arising in prepubertal gonads are typically unassociated with 12p amplification and tend to be diploid. The most consistent structural chromosomal abnormality is an isochromosome 12p. Tumors lacking i(12p) have other structural abnormalities of 12p, among them the amplification of 12p11.2–p12.1. Gain of 12p sequences may be related to invasive growth. Chaganti and Houldsworth (2000) suggested that cyclin D2 (mapped to 12p13) is the most likely candidate gene of pathogenetic relevance (Table 6.1).

3.2. Classification

The main classification systems commonly used are those of British Classification System (BCS) and World Health Organization (WHO) classification (Tables 6.1 and 6.2) (Theakera and Meadb, 2004). WHO classification recapitulates the classical histological entities, that is, seminoma and

Table 6.1 Chromosomal aberration in TGCTs

Age	Histology	Incidence (per 100,000 population)	Genetic abnormalities	Ploidy
Prepubertal	Teratoma/ YST	0.12	− 1p, 6q	Teratoma: diploid, YST: aneuploid
Postpubertal	Seminoma/ nonseminoma	6.0	IGCNU: ± i(12p), Seminoma: i(12p), Nonseminoma: i(12p)	IGCNU: hipertriploid, Seminoma: hipertriploid, Nonseninoma: hipertriploid
Older (>40 years)	Spermatocytic seminoma	0.2	+ 9	Tetraploid/ diploid

Table 6.2 WHO classification of TGCTs

Tumors of one histological type	Tumors of more than one histological type
• Seminoma Seminoma with syncytiotrophoblastic cells • Spermatocytic seminoma Spermatocytic seminoma with sarcoma • Embryonal carcinoma • Trophoblastic tumors Choriocarcinoma Trophoblastic neoplasms other than choriocarcinoma – Monophasic choriocarcinoma – Placental site trophoblastic tumor • Teratoma Dermoid cyst Monodermal teratoma Teratoma with somatic type malignancies	• Mixed embryonal carcinoma and teratoma • Mixed teratoma and seminoma • Choriocarcinoma and teratoma/embryonal carcinoma • Others

nonseminoma hystotypes, encouraging the recognition of specific pattern for each one entity (Table 6.2). BCS is rarely used and difficult to apply. It recognizes all nonseminoma hystotypes as teratoma at different stage of differentiation (Theakera and Meadb, 2004) (Table 6.3).

An alternative classification system for human GCTs has recently been developed (Looijenga and Oosterhuis, 1999; Van de Geijn et al., 2009). Five entities have been recognized, based on various parameters, including cell of origin, histology, genomic imprinting status, age at and location of clinical presentation, and chromosomal constitution. This classification points mainly on pathogenetic mechanisms, with purpose to improve clinical diagnosis and treatment response prediction. Type I GCTs groups teratomas and YSTs of prepubertal age. The type II GCTs are postpuberal SE and NSE GCTs. The type III GCTs is represented by spermatocytic seminomas (SSs), typically seen in males more than 50 years of age. Finally the last two groups are not present in testis: type IV GCTs is represented by dermoid cysts of ovary, whereas the type V is the hydatiform mole that develops from an empty egg and a spermatozoa (Tables 6.3 and 6.4) (Looijenga and Oosterhuis, 1999; Van de Geijn et al., 2009).

Tumor pattern could be confirmed, then immunohistochemical staining are performed in order to clearly define histotype component of tumors and correct percentage of each one histotype in mixed tumor (Table 6.5).

Table 6.3 Comparison of British (TTP & R) and WHO classification in the TGCTs

British	WHO
Seminoma	Seminoma
Spermatocytic seminoma	Spermatocytic seminoma
Teratoma	Non seminomatous germ cell tumor
• Teratoma differentiated (TD)	• Mature teratoma
• Malignant teratoma intermediate (MTI)	• Embryonal carcinoma with teratoma (teratocarcinoma)
• Malignant teratoma undifferentiated (MTU)	• Embryonal carcinoma
• YST	• Yolk sac tumor
• Malignant teratoma trophoblastic	• Choriocarcinoma

A panel of immunohistochemical markers are useful to these tools. Moreover, immunohistochemical stainings are widely used in diagnosis of metastatic disease of uncertain origin (Emerson and Ulbright, 2007; Theakera and Meadb, 2004; Van de Geijn et al., 2009).

Since therapy modalities largely relies on pathologic findings of TGCTs, pathology reports should include factors that are prognostically significant or have implications for therapeutic decision. The increased interest in surveillance-only management of non-high-risk patients with stage I disease necessitates accurate identification of high-risk patients in whom surveillance is not recommended. Vascular invasion and the proportion of embryonal carcinoma component in a mixed TGCT, which are both reliable prognosticators for identification of high-risk patients, can be best evaluated through careful examination of an appropriately sampled testicular neoplasm (Theakera and Meadb, 2004; Van de Geijn et al., 2009).

Among postpubertal testicular GCTs, diagnostic challenges could be offered mainly when unusual features are encountered (Emerson and Ulbright, 2007; Hammerich et al., 2008; Looijenga and Oosterhuis, 1999; Theakera and Meadb, 2004; Ulbright, 2005; Van de Geijn et al., 2009; Young, 2008). As therapy is based upon accurate histopathological diagnosis, thus misclassification of tumor types could impact on treatment choice with associated risk. Thus postpuberal TGCTs should be addressed to expert pathologist, in fact, in a published British audit, tumors reviewed between 1992 and 1997, a discrepancy rate of 6% in tumor classification between the referring and central units has been recorded, with treatment changes in over half of these patients. Moreover, discrepancies in the interpretation of vascular invasion has been recorded in 20% of cases, with a further impact on treatment, as patients with stage I NSE GCT with vascular invasion are generally sent to adjuvant chemotherapy (Theakera and Meadb, 2004; Young, 2008).

Table 6.4 Classification of TGCTs in five entities (Looijenga and Oosterhuis, 1999)

Type	Anatomical site	Phenotype	Age	Originating cell	Genomic imprinting	Genotype
I	Testis, ovary, sacral region, retroperitoneum, mediastinum, neck, midline brain	(Immature) Teratoma/ yolk-sac tumour	Neonates and children	Early PGC/ gonocytes	Biparental, partially erased	Diploid (Teratoma). Aneuploid (yolk-sac tumour): + of 1q, 12(p13) and 20q, and loss of 1p, 4, and 6q
II	Testis	Seminoma/ nonseminoma	>15 years (median age 35 and 25 years)	PGC/gonocyte	Erased	Aneuploid (± triploid): + of X, 7, 8, 12p, and 21; loss of Y, 1p, 11, 13, and 18
	Ovary	Dysgerminoma/ nonseminoma	>4 years	PGC/gonocyte	Erased	Aneuploid
	Dysgenetic gonad	Dysgerminoma/ nonseminoma	Congenital	PGC/gonocyte	Erased	Diploid/tetraploid
	Anterior mediastinum	Seminoma/ nonseminoma	Adolescent	PGC/gonocyte	Erased	Diploid/tri-tetraploid
	Midline brain	Germinoma/ nonseminoma	Children (median age 13 years)	PGC/gonocyte	Erased	Diploid/tri-tetraploid
III	Testis	Spermatocytic seminoma	Children/Adults	Spermatogonium/ spermatocyte	Partially complete paternal	Aneuploid: + of 9
IV	Ovary	Dermoid cyst	>50 years	Oogonia/oocite	Partially complete maternal	(Near) Diploid, diploid/ tetraploid, peritriploid (+ of X, 7, 12, and 15)
V	Placenta, uterus	Hydatiform mole	Fertile period	Empty ovum/ spermatozoa	Completely paternal	Diploid (XX and XY)

Note: The classification of TGCTs is based on Looijenga and Oosterhuis (1999).

Table 6.5 Main immunohistochemical markers useful for diagnosis of TGCTs subtypes

Immunohistochemistry in testicular tumors										
	PLAP	c-Kit	OCT4	CD30	AFP	AE1/AE3	CK7	EMA	HMGA1	HMGA2
Seminoma	+	+	+	−	−	v	v	−	+	−
SS	−	v	−	−	−	−	ND	−	ND	ND
Embryonal carcinoma	+	−	+	+	v	+	+	−	+	+
YST	+	−	−	v	v	+	−		−	+

Notes: +, expressed; −, not expressed; ND, not determined; v, variable.

In this section we will discuss histopathological entities of postpuberal TGCTs, pointing mainly on differential diagnosis problems and solution proposed by use of specific immunohistochemical stainings. Management and sampling are surgical samples represent two important phases of diagnostic procedures. In particular in TGCTs diagnosis accuracy should be required, due to different histotypes composing a TGCTs, with specific implications in choicing therapeutic strategies (Emerson and Ulbright, 2007; Hammerich et al., 2008; Looijenga and Oosterhuis, 1999; Theakera and Meadb, 2004; Ulbright, 2005; Van de Geijn et al., 2009; Young, 2008). Thus observation of tumoral areas with differing appearances should be sampled, garantueeing at least 1 section per 1 cm tumor diameter. Tumor sections should include, when possible, tonaca albuginea in order to evidence eventual infiltration. Normal parenchyma, when present, should be included in sample proceeding in order to evidence ITGCNU areas. Moreover rete testis, epididim, and spermatic funicle, sectioned at more levels, should be documented (Young, 2008).

3.3. Staging of testicular tumors

Pathologic staging based on the TNM system is largely applicable to localized disease, and to retroperitoneal lymph node dissections, it really cannot be applied to nonsurgical metastatic disease. Metastasis evidence is detected through strumental exams, as computed tomography/magnetic resonance imaging size of the metastatic lymph nodes in the retroperitoneum. Thus, adjuvant therapy is stated according clinical staging based on the radiographic findings. In 1997, an internationally agreed-on prognostic factor-based staging classification, applicable to TGCTs was proposed. Staging of testis tumors considers TNM classification associated to levels of prognostically important serum tumoral markers, as human chorionic

gonadotropin (hCG), α-fetoprotein (AFP), and lactate dehydrogenase (LD), reflecting tumoral turnover (Tables 6.4 and 6.5).

3.4. ITGCN, Unclassified

ITGCNU is the precursor of all invasive TGCTs, excluding SS and prepubertal TGCTs, and it is identified adjacent in about 90% of cases. The ITGCNU cells are similar to seminoma cells, suggesting that seminoma is the invasive component of ITGCNU cells. Without intervention, about 50% of ITGCNU cases will progress to an invasive GCT within 5 years of the diagnosis of ITGCNU, but on long-term follow-up almost all patients will develop an invasive GCT. Cytogenetic studies underline similar chromosomal status between ITGCNU cells and the adjacent invasive component, with the gain of 12p found in the invasive part respect to IGCCNU. Thus acquisition of excess genetic material on the short arm of chromosome 12 could be critical genetic event leading to invasion (Bahrami et al., 2006).

Pathological findings. Grossly areas with ITGCNU are similar to normal testis parenchyma. Histologically, ITGCNU cell are large primitive atypical elements, twice the size of normal germ cells. These cells lie along the thickened basement membrane of atrophic seminiferous tubules or replace the entire tubules. The neoplastic cells have large nuclei with prominent nucleoli and large clear cytoplasm enriched of glycogen. Immunohistochemical neoplastic cells stain for placental-like alkaline phosphatase (PLAP), for c-Kit (CD117), OCT3/4, also known as POU5F1, but are negative for cytokeratins, hCG, or AFP. D2-40, an antibody raised against a transmembrane mucoprotein called podoplanin, stains ITGCNU cells (Bahrami et al., 2006; Eble et al., 2004; Ulbright, 2005; Young, 2008).

3.5. Seminomatous–TGCTs

Two types of SE-TGCTs are described: (a) classical seminoma and its variants; (b) SS.

3.5.1. Seminoma

Seminoma is the most common TGCT , representing 50% of the cases (Table 6.6). Moreover seminoma component is recognizable in a large proportion of mixed GCTs. The peak incidence is between 34 and 45 years, which is about one decade later than that of most other GCTs. Painless testicular enlargement is its clinical. More rarely symptoms are linked to metastasis onset (Ulbright, 2004). In localized disease, extension to the spermatic cord or epididymis is recorded seen in less than 10% of patients, and in 2% of cases both testes are involved (Ro et al., 2000).

Pathologic features. Grossly, seminomas are firm with homogenous appearance, organized in single or multiple nodules. Necrosis and

Table 6.6 Relative proportions of histological types of GCTs

Histologic type	Proportion in the testis (%)
Teratoma	4
Dysgerminoma/seminoma	50
Yolk sac tumor	1
Embryonal carcinoma	10
Choriocarcinoma	0.3
Polyembryoma	<1
Mixed germ cell tumor	33

hemorrhage are rarely observed and generally are signs of a mixed GCTs (Ulbright, 2004). Microscopic findings in classical seminoma are nested neoplastic cells separated by thin fibrovascular trabeculae infiltrate by reactive T cell lymphocytes. It is associated to IGCN. Neoplastic cells are large, uniform, round to polygonal with distinct cell membrane. The nuclei contain one or more prominent nucleoli and mitotic rate is variable. Granulomatous reactions are frequently observed, resulting sometimes in obscuring neoplastic component, even in metastasis sites. A variant recognized by WHO is seminoma with syncytiotrophoblastic giant cells (Eble et al., 2004). Syncytiotrophoblasts stained positively with hCG are seen in approximately 20% of seminomas. The presence of these cells does not impart an adverse prognosis but does correlate with mild elevation of serum human chorionic gonadotropin (S-hCG) (Weissbach et al., 1999).

Seminoma could be characterized by different pattern of growth with respect to nested one in a fibro-inflammatory background. The histological variant of pattern of growth are cribriform/microcystic, tubular, and intertubular (Emerson and Ulbright, 2007). In these cases problematic diagnostic procedure could be presented. Interubular variant is characterized by neoplastic growth sparing integrity of seminiferous tubules. Neoplastic cells retain cytological features of classic seminoma cells, but they could escape to recognition of not expert pathologist. Cribriform/microcystic variants due to edema present in neoplasia could simulate YSTs; in these cases, specific immunohistochemical staining specific for seminoma, that is, OCT3/4 and HMGA1 positivity and AFP negativity could exclude the presence of yolk sac component. Moreover tubular pattern of growth has to be distinguished by Sertoli cell tumors, using inhibin staining as diagnostic for Sertoli cells originated tumors (Emerson and Ulbright, 2007; Franco et al., 2008; Looijenga and Oosterhuis, 1999; Theakera and Meadb, 2004; Young, 2008).

Finally seminoma cells could show atypical features, such as a mitotic rate higher than 6/HPF, some years ago popularized as ''anaplastic seminoma'' entity, potentially indicative of poorer prognosis. Nowadays, this

characteristics and others retained not typical in seminoma, that is, pleomorphism, nuclear overlapping, lack or paucity of lymphocytes infiltrate, lack or paucity of clear cytoplasms seems not related to worse prognosis, above all for unreproducibility of such morphological observation. But not conventional features observed in some seminoma could represent a problem in differential diagnosis with respect to solid growth of embryonal carcinoma. Combined seminoma embryonal carcinoma is difficult to recognize when small foci of embryonal carcinoma are situated within the main bulk of the seminoma. CD30 positivity could help in identifying such foci and to classify as mixed GCTs (Theakera and Meadb, 2004; Young, 2008).

3.5.2. Spermatocytic seminoma

SS accounts for 1–2% of all testicular neoplasm (Talerman, 1980). Although it frequently occur in patients older than 50 years, about one-third of SS is seen in the usual age of classical seminoma age range (Young, 2008). The cell of origin of SS are more differentiated than that of classical seminoma, with cytogenetic loss of chromosome 9, rather than isochromosome 12p (Bahrami et al., 2006; Verdorfer et al., 2004). Moreover, it is not associated to cryptorchidism, ITGCNU, or other GCTs subtypes (Talerman, 1980). It has an indolent natural history, with a very low risk of metastasis. However, sarcomatous dedifferentiation with a very poor prognosis because of hematogenous spreading has been recorded in 6% of cases (Burke and Mostofi, 1993).

Pathological findings. Grossly SS is an homogeneous yellow-gray mass; when sarcomatous dedifferentiation is encountered a more heterogeneous cut surface is described. Histologically, SS consists of diffuse proliferation of polymorphic cells, small, intermediate, and large sized. Intermediate cells are more represented and they are characteristically with ''spiralized'' chromatin, as it is seen in spermatocytes. Large cells are generally uninucleated and sometimes multinucleated. Sarcomatous differentiation can occur with undifferentiated or differentiated patterns, such as chondrosarcoma and rhabdomysarcoma. All immunohistochemical markers commonly described in other GCT subtypes are negative in SS, with the exception of c-Kit. Moreover, cytoplasmic positivity of CAM 5.2 in SS cells has been described (Bahrami et al., 2006; Eble et al., 2004; Ulbright, 2005; Young, 2008).

3.6. NSE tumors

According to classical classification nonseminoumatous tumors consists of pure teratoma, embryonal carcinoma, YST, choriocarcinoma, and mixed TGCTs. The pure form of each one histotype is relatively rare with respect to combination of different components in mixed TGCTs.

3.6.1. Embryonal carcinoma

Embryonal carcinoma is present as component in 80% of mixed TGCTs, while as pure is relatively uncommon. Embryonal carcinoma occurs most frequently between 25 and 35 years of age. It is rare in elderly and unknown in prebural age. Two-thirds of cases occur with distant metastasis (Mostofi et al., 1988; Rodriguez et al., 1986). Differently from seminoma, embryonal carcinoma occurs as a poorly demarcated mass with large foci of hemorrhage and necrosis. Different microscopic pattern of growth has been described, including solid, syncytial, acinar, tubular, or papillary. The neoplastic cells are polygonal, undifferentiated, and epithelioid with marked atypia. Nuclei are vesicular with evident nuclear membrane. High mitotic rate is present. Also in this case ITGN is present in testicular parenchyma near tumor (Ulbright, 2005; Young, 2008). Vascular invasion is a critical feature commonly described, because of worsening prognosis. It should be documented in final report, but it has to be distinguished from artifactual intravascular implants, even through help of immunohistochemical markers of endothelium (Bahrami et al., 2006).

Embryonal carcinoma cells express, cytokeratin, but not epithelial membrane antigen. As seminoma, they express also PLAP and OCT3/4 (Jones et al., 2004). Moreover, typically CD30 is also a sensitive marker for primitive embryonal carcinoma, but it is frequently lost in metastasis after chemotherapy (Ferreiro, 1994). The embryonal carcinoma cells are usually negative for carcinoembryonic antigen, hCG, and CD117 (c-Kit) (Leroy et al., 2002). Sometimes EC should be differentiated from seminoma, as yet discussed (Leroy et al., 2002). Another differential diagnosis occur in metastatic sites, in order to exclude somatic adenocarcinoma. Its typical profile in absence of EMA expression could be helpful in this aim (Emerson and Ulbright, 2007).

3.6.2. Yolk sac tumor

Among GCTs, YST differentiates toward embryonic yolk sac, allantois, and extraembryonic mesenchyme. Pure form is the most frequent GCT in prepuberal population, where it not associated to ITGCNU (Bahrami et al., 2006). YST is extremely rare as pure tumors in postpuberal testis, while it represents a frequent component of mixed GCTs in adult. Pure YST in children is observed in range of age from some days to 11 years and it is generally recorded as stage I disease. Elevated serum α-fetoprotein (S-AFP) is almost always observed.

Pathologic features. Grossly it characterized by solid lobulated mass with a gelatinous to mucinous cut surface. Hemorrhage, necrosis, and cystic change may be present.

Microscopically, YST is haracterized by different pattern of growth, as reticular, endodermal sinus, papillary, solid, glandular-alveolar, myxoid,

sarcomatoid, hepatoid, and parietal patterns. Generally more pattern are observed in a single YST, being reticular-mycocistic patter the most common feature. Schiller–Duval bodies is the most characteristic features and is constituted by central fibrovascular core surrounded by malignant cuboidal to columnar cells. Moreover, PAS positive hyaline globules are frequently observed. AFP immunostaining is commonly observed in YST. Staining for cytokeratin, PLAP, and α1-antitrypsin are always observed, while neoplasm is generally negative for CD30, hCG, and OCT3/4. Recently, Glypican 3, a membrane-bound heparin sulfate proteoglycan, seems to be specifically expressed in YST and choriocarcinoma with respect to seminoma, embryonal carcinoma, and teratoma (Emerson and Ulbright, 2007).

3.6.3. Trophoblastic tumors

Among trophoblastic tumors, choriocarcinoma is absolutely the most frequent. Pure choriocarcinoma is extremely rare. Choriocarcinoma foci are observed in 8% of mixed GCTs. Both as pure and as component in a mixed GCTs, choriocarcinoma is responsible of an aggressive outcome, because of rapid hematogenous dissemination (Ulbright, 2005). Patients are diagnosed in an advanced stage and sometimes testis neoplasia is regressed. Very high value of hCG (>100,000 mIU/ml) in serum are recorded and it proportionally related to worse prognosis (Ulbright, 2005).

Pathologic features. Choriocarcinoma appears as an hemorrhagic nodule, when it is pure and as multiple hemorrhagic areas in an heterogeneous mass, when a component of a mixed GCTs is present.

Histologically, choriocarcinoma consisted of variable amounts of 2 cell components, syncytiotrophoblast and cytotrophoblasts. Syncytiotrophoblasts are multinucleated cells and cytotrophoblasts are uniform, polygonal cells (Bahrami et al., 2006; Ulbright, 2005; Young, 2008). Syncytiotrophoblasts are positive to hCG and cytothrophoblasts are positive to inhibin. Glypican 3 is expressed by all choriocarcinoma, particularly by syncytrophoblasts, PLAP staining is observed in 50% of choriocarcinoma (Emerson and Ulbright, 2007).

3.6.4. Teratoma

Teratomas are composed of different tissue deriving from one or more germinal endodermal, mesodermal, and ectodermal layers. Classically mature teratomas is defined when composed of differentiated tissues, while immature teratoma consisted of embryonic or fetal-like tissues, associated to differentiated elements. Monodermal teratoma is composed of tissues derived from one of the three germ layers (Ulbright, 2005).

Teratoma characteristics has not great prognostic relevance in testicular teratoma. In fact, the behavior of testis teratomas, but less so for ovary teratomas, depends on patient age, being prepuberal testis pure teratoma invariably benign and postpuberal pure teratoma invariably malignant. Pure

teratoma in prepuberal testis is the second most frequent GCTs (Bahrami et al., 2006). It is generally composed of mature tissues, however, variable amount of immature elements could be present; nevertheless, presence of immature histology is not an indicator of poor prognosis (Bahrami et al., 2006; Ulbright, 2005). Pure teratoma in postpuberal testis is rare, while teratomatous elements occur as component of 50% of mixed tumors. In this age, even when with mature histology, pure teratoma are at risk of metastasis. Moreover prepuberal teratomas are diploid; postpuberal teratomas are aneuploid and have isochromosome 12p (Bahrami et al., 2006). Prepuberal teratomas are generally diagnosed in children younger than 4 years with mean age of 20 months. Thirty-seven percent of postpuberal pure teratoma are seen in young patients with metastasis symptoms (Leibovitch et al., 1995).

Pathologic findings. Grossly pure teratomas has heterogeneous cut surface, generally with cystic areas, filled by serous, fluid, mucinous, or keratinic materials.

Histologically, tumors are composed of variable amounts of endodermal, ectodermal, and mesodermal tissues. Different types of specialized epithelium, neural tissue and cartlage, and other mature tissue are represented. Cytologic atypia is frequently seen in postpuberal teratomas (Ro et al., 2000). Immature histology is defined when some elements are not attributable to any adult tissue or when embryonic or fetal tissue are recognized. Generally, immature elements are mesenchymal spindle cells, rarely neural and epithelial elements are observed.

Vascular invasion could be seen in postpuberal teratomas and is represented by mature or immature elements, having capacity to differentiate into various cell lineage. Therefore, metastasis could have morphology different from primary site (Bahrami et al., 2006).

ITGCNU is observed in 90% of the cases of postpuberal teratomas, while it is nonpresent in prepuberal teratoma. Orchiectomy is absolutely curative in prepuberal cases. Dermoid cyst is considered as a specialized form of mature teratoma, occurring in postpuberal testis. It consists of keratinizing epithelium with cutaneous appendages; sometimes noncutaneous mature elements are observed. In contrast to postpuberal teratomas, it is not associated to ITGCNU and does not have malignant potential. Thus orchiectomy could be curative for dermoid cyst, if diagnosis is rendered when extensive sampling excludes the presence of any other teratoma elements and/or adjacent ITGCNU (Ro et al., 2000).

3.6.5. Mixed GCTs

Mixed GCTs of testis is the second most frequent GCT, following seminoma. It comprises 30–50% of cases. It is associated to serum elevation of markers, such as hCG and AFP, generally related to YST and syncytiotrophoblastic components, respectively, in this tumor (Ulbright, 2004).

Pathological findings. Grossly mixed GCTs have a variegate cute surface, reflecting different histological subtypes. In order of frequency embryonal carcinoma, teratoma, YST, seminoma, choriocarcinoma, and polyembrioma are described (Mosharafa et al., 2004). The most common associations are embryonal carcinoma/teratoma and embryonal carcinoma/seminona, the latter generally composed of distinct entities, suggesting multicentric origin rather than initial differentiation of seminoma in embryonal carcinoma. All subtypes have to be reported with approximate proportions (R.o et al., 2000). The significance of embryonal carcinoma proportion is particularly relevant for therapeutic management of patients.

Polyembrioma is considered a distinct form of mixed GCT. It consists of embryoid bodies that recapitulate amnion cavity and yolk sac and result of a mixture of embryonal carcinoma and YST. Embryoid bodies are dispersed in a myxoid stroma. It is generally associated to other tumoral components in mixed GCTs and according to some authors, because of its association to immature teratoma, it could represent the most immature form of teratoma, resembling early embryo (Ulbright, 2004).

3.7. Somatic malignancies arising in testicular GCT

Somatic malignancies generally arise from teratoma components and rarely from YST components and SS. It is described in primary site or in metastasis. Primary site somatic malignancies in primary site generally do not affect prognosis, while extratesticular somatic malignancies worsen significantly prognosis, above all when it is represented by rhabdomyosarcoma or primitive neuroectodermal tumor. In 3–6% of cases, somatic malignancies occur in patients with metastasis treated with chemotherapy, probably due to destruction of chemosensitive GCTs, allowing over-growth of preexisting somatic malignancies (Comiter et al., 1998).

3.8. Regression of primitive GCTs

Primitive GCT of testis could undergo spontaneous regression, resulting in hyaline scarring. This phenomenon has been referred as "burnout" GCTs. On microscopic examination hyaline scarring can be associated to scanty residual invasive neoplasm and to ITGCNU of adjacent tubules. Sometimes, hemosiderin deposits chronic inflammatory infiltrate and prominent vessels. Intratubular calcification are considered expression of burnout embryonal carcinoma (Balzer and Ulbright, 2006; Young, 2008). Clinical diagnosis of regressed GCTs are very difficult to diagnose, but ultrasound could individuate testis abnormality, above all when GCT metastasis has been previously diagnosed.

4. Prognostic and Diagnostic Markers

Research is ongoing to identify specific biomarkers that can improve diagnosis, surveillance of tumor progression, and prediction of patient prognosis. The identification of biomarkers that may predict response to specific therapies also will be useful in stratifying patients for treatment selection. The clinical use of serum markers has been established during the years and are a valid tool for prognostic purpose and the follow-up of patients. In recent years, an intense activity toward identifying novel biomarkers has been performed and many proteins are described as ''potential biomarkers'' for any cancer. Most of these novel markers are not been validated and require expensive and time-consuming molecular techniques; markers with a well assessed clinical role will be discussed in Section 4.1.

4.1. Serum tumor markers

Three serum tumor markers, serum lactate dehydrogenase (S-LD) catalytic, S-AFP concentration, and S-hCG concentration, are currently used for prognostic and follow-up purposes. The majority of patients present with elevated serum markers and their prechemotherapy levels have been integrated into the International Germ Cell Cancer Consensus Group consensus prognostic index for NSE GCT classification. Patients are stratified into good-, intermediate-, and poor-prognosis subgroups based on the primary tumor site, levels of serum tumor markers, and whether extrapulmonary visceral metastases are present (von Eyben, 2003).

AFP is an embryonic protein of molecular weight 70,000 dalton. AFP is normally produced by the fetal yolk sac, the fetal gastrointestinal tract, and eventually by the fetal liver. Levels of AFP in fetal serum rise until the end of the first trimester of gestation and then fall. The normal range of AFP for adults and children is variously reported as under 50, under 10, and under 5 ng/mL. At birth, normal infants have high AFP levels, decreasing to normal levels within the second years of life. AFP is the main tumor marker used to monitor testicular cancer, although it is not produced by pure seminomas (Horwich et al., 2006).

S-hCG levels are essential in both the diagnosis and follow-up of hCG-producing TGCTs. After orchiectomy, an increased level of hCG indicates persistent disease, whereas after chemotherapy-induced complete remission of metastatic disease, reappearance of hCG indicates the presence of a relapse.

Although it is indicated that S-LD is a useful marker, studies have shown that total S-LD levels are not specific. Isoenzyme fraction 1 is the more sensitive and specific for TGCTs patients with seminoma have a raised

LD-1 more often than a raised AFP and hCG, whereas patients with nonseminoma have a raised AFP more often than a raised LD-1 and hCG. LD-1 is related to the characteristic chromosomal abnormality in all types of TGCT, a high copy number of chromosome 12p. In contrast, AFP and hCG are found mainly in NSE GCTs and they related to the histologic differentiation of the tumors (von Eyben, 2003).

4.2. New discovered markers for TGCTs

A number of markers has been reported over time that can be used to discriminate CIS, seminoma, embryonal carcinoma, teratoma, and yolk sac. The most common are HMGA1, HMGA2, PATZ1, Aurora-B, Nek2, OCT3/4, c-Kit, PLAP, NANOG, SOX2, and others. For example, HMGA1 and HMGA2 are differently expressed with respect to the state of differentiation of TGCTs, with overexpression of both proteins in pluripotential embryonal carcinoma cells and loss of expression of HMGA1 in YSTs and of both proteins in mature adult tissue of teratoma areas. Therefore, the different profile of HMGA1 and HMGA2 protein expression could represent a valuable diagnostic tool in some cases of problematic histological differential diagnosis (Franco et al., 2008).

PATZ1 is a recently discovered zinc finger protein that acts as a transcriptional repressor. Although expression of PATZ1 protein was increased in TGCTs, it was delocalized in the cytoplasm, suggesting an impaired function (Fedele et al., 2008). Another marker that could be used to discriminate the different tumor histotype is Aurora-B expression; in fact, it was detected in all CIS, seminomas and embryonal carcinomas analyzed but not in teratomas and yolk sac carcinomas (Chieffi et al., 2004; Esposito et al., 2009). Aurora-B will be discussed in more detail later.

It is shown that Nek2 protein, a centrosomal kinase required for centrosome disjunction and formation of the mitotic spindle, is upregulated and localized in the nucleus of neoplastic cells of seminomas. Such nuclear localization and the upregulation of Nek2 protein were also observed in the Tcam-2 seminoma cell line. In addition, the nuclear localization of Nek2 is a feature of the more undifferentiated germ cells of mouse testis and correlates with expression of the stemness markers OCT4 and PLZF (Barbagallo et al., 2009). OCT3/4 is a well-characterized marker for PGCs. It is positive in all cases of CIS, seminoma, and embryonal carcinoma (de Jong et al., 2005; Looijenga et al., 2003a). There has been a various amount of reports over the years that OCT3/4 is also expressed in normal adult stem cells and nongerm cell-derived cancers. However, recent data indicate that these observations are likely related to the use of nonspecific antibodies, the latter also recognizing pseudogenes (Atlasi et al., 2008; Ledford, 2007; Lengner et al., 2007; Liedtke et al., 2007). OCT3/4 is a transcription factor of the family of octamer-binding proteins (also known

as the POU homeodomain proteins) and is regarded as one of the key regulators of pluripotency (de Jong and Looijenga, 2006). In addition to OCT3/4, several other embryonic stem-cell-specific proteins are important for maintaining the so-called ''stemness'' of pluripotent cells, such as NANOG and SOX2 (Avilion et al., 2003; Boiani and Scholer, 2005; Yamaguchi et al., 2005; Yates and Chambers, 2005).

NANOG protein was detected in germline stem cells (gonocytes) within the developing testis. In addition, NANOG is highly and specifically expressed in CIS, embryonal carcinoma, and seminomas, but not in teratoma and YSTs revealing a molecular and developmental link between GCTs and the embryonic cells from which they arise (Hart et al., 2005).

SOX2 is a member of the SOX protein family, transcription factors that regulate development from the early embryonal stage to differentiated lineages of specialized cells. SOX proteins are known to cooperate with POU proteins. The best characterized SOX–POU cooperation is that between SOX2 and OCT3/4. SOX2 is not detected in human germ cells regardless of their developmental age, in contrast to data in mouse embryos (de Jong et al., 2008; Perrett et al., 2008). SOX2 is expressed in embryonal carcinoma, the undifferentiated part of nonseminomas, but it is absent in seminomas, YSTs, and normal spermatogenesis (de Jong et al., 2008; Perrett et al., 2008). CIS cells are indeed negative for SOX2, although SOX2 positive Sertoli cells can be present in seminiferous tubules lacking germ cells or in the presence of CIS (de Jong et al., 2008).

Expression analysis of SOX family members in TGCTs revealed that is specifically expressed in CIS and seminoma but not in embryonal carcinoma (de Jong et al., 2008). In addition, SOX17 maps to the chromosomal region 8p23, which is gained in seminoma (Korkola et al., 2008). This indicates that SOX17 is a candidate SOX protein for cooperation with OCT3/4 in CIS and seminoma. These data also illustrate that SOX17 is a new marker to discriminate CIS and seminoma from embryonal carcinoma. Of interest is that SOX17 distinguishes embryonic from adult hematopoietic stem cells (Kim et al., 2007). Current research focuses on the processes that may regulate the differential expression of SOX2 versus SOX17 and on the role of these SOX proteins in the different histologies of the TGCT subtypes involved. Analysis of expression patterns in microarray studies revealed additional markers, MCFD2, BOB1, and PROM1, for seminoma compared to normal testis (Gashaw et al., 2005). Studies demonstrated indeed increased expression levels of these three proteins in seminoma cells compared to normal adult testes (Gashaw et al., 2007). Because all three of these markers are also expressed at low levels in normal adult testicular tissue, their suitability as practical additional diagnostic markers remains to be proven.

In recent years, the role of miRNAs in carcinogenesis of human testicular cancer and germ cell development has emerged (Bernstein et al., 2003).

It was demonstrated that knockout mice for Dicer suffered from an early decrease in germ cell number and an impaired ability to differentiate, indicating that Dicer1 and miRNAs are important for both survival and proper differentiation of male germ cells (Maatouk et al., 2008). Subsequently, it was demonstrated that miRNAs 372 and 373 can overcome cell cycle arrest mediated by p53 (Voorhoeve et al., 2006). In contrast, in TGCT cell lines with mutated p53 or expressing low levels of p53 were shown to be negative for these miRNAs and it can be assumed that miRNAs 372 and 373 can bypass the p53 checkpoint allowing the growth of TGCT. Further research into the functional mechanisms of miRNAs and the role of DND in TGCT are likely to give more interesting clues.

5. Therapy

5.1. Traditional treatment

A substantial increase in cure rates of the medical treatment of advanced testicular cancer has raised from approximately 25% in the mid-1970s to nearly 80% today. This is the highest cure rate in solid tumor. Improved survival is primarily due to effective chemotherapy (Einhorn and Donohue, 1977). A great advance in chemotherapy for TGCT was the introduction of cisplatin in association with vinblastine, and bleomycin. The response rate increased to more than 80% with the use of this regimen in combination with surgery (Einhorn and Donohue, 1977). In the late 1980s, investigators observed that clinical and tumor features could predict the likelihood of patient response to standard chemotherapy regimens. Algorithms were developed to stratify patients into ''good'' or ''poor'' prognostic groups. The International Germ Cell Cancer Collaborative Group (IGCCG) was formed and a universal classification scheme was developed. In this stratification system, patients are separated into good-, intermediate-, and poor-prognostic groups according to predicted outcome to cisplatin-combination chemotherapy, based mainly on histology, but also on primary site, sites of metastasis, and serum tumor marker elevation.

Traditional treatment of classic seminoma with clinical stage I (localized disease), after orchiectomy, is low-dose radiation to the regional lymph nodes, that guarantee a cure rate of more than 90%. Alternatively surveillance and adjuvant chemotherapy could be apply. However, with surveillance alone, 15–20% of such cases may relapse. In pooled analysis high tumor sizes and rete testis invasion in stage I worsen significantly survival when surveillance is adopted. (Chung et al., 2002; Porcaro et al., 2002). On the other hand for SS, because of its indolent natural history, orchiectomy is generally curative. Cases with sarcomatous dedifferentiation requires aggressive chemotherapeutic treatment, although without a significant

improvement of prognosis (Burke and Mostofi, 1993). For pediatric TGCTs, orchiectomy is generally curative. Chemotherapy is reserved to rare advanced stage cases of prepuberal YSTs.

Because of frequent retroperitoneal lymph node metastasis in NSE-TGCTs, the standard management for a localized disease (stage I) is retroperitoneal lymph node dissection and/or surveillance. But surveillance requires at least 2 years of follow-up, because of frequent late relapse after orchiectomy. Overall, the cure rate for patients with NSE GCTs in clinical stage I exceeds 95% (Bahrami et al., 2006). Approximately 70–80% of patients with metastatic germ cell cancer can be cured with cisplatin (CDDP)-based combination chemotherapy (Feldman et al., 2008); however, resistance to CDDP treatment may arise. Two types of resistance are observed: CDDP-refractory disease, characterized by disease stabilization during treatment followed by disease progression and absolute CDDP-refractory disease with progression even during treatment (Beyer et al., 1996). Both groups have poor prognosis and the identification of new treatment alternatives for patients with refractory disease is a priority and novel molecular targets are being explored, the results of some of the studies currently performed are summarized in the next sections of this review.

5.2. Aurora-kinase inhibitors

Errors in mitosis can provide a source of the genomic instability that is typically associated with tumorigenesis. Many mitotic regulators are aberrantly expressed in tumor cells. The kinases Aurora-A, -B, and -C represent a family of protein well conserved throughout eukaryotic evolution and members of this family have been extensively studied in a range of different model organisms (Carmena, and Earnshaw, 2003; Katayama, et al., 2003; Vader et al., 2006). All three mammalian members of this family are overexpressed in human cancer cells (Chieffi et al., 2004; Li et al., 2003; Sakakura et al., 2001; Sen et al., 2002). Although the catalytic domains of the Auroras are highly conserved, these proteins show different subcellular localizations. Aurora-A (STK-15) localizes to the duplicated centrosomes and to the spindle poles in mitosis. It has been implicated in several processes required for building a bipolar spindle apparatus, including centrosome maturation and separation. Aurora-A has been found to be overexpressed in the meiotic testicular cells (Mayer et al., 2003). It is interesting to note the aneuploidy of human TGCTs is associated with amplification of centrosomes (Mayer et al., 2003). Aurora-B (AIM-1) is a chromosomal passenger protein. Aurora-B binds three other chromosome passenger proteins-inner-centromere protein (INCENP), survivin, and borealin (Carmena and Earnshaw, 2006; Gassmann et al., 2004). During mitosis, Aurora-B is required for phosphorylation of histone H3 on serine 10, and this might be important for chromosome condensation (Ota et al., 2002). Aurora-B

clearly regulates kinetochore function, as it is required for correct chromosome alignment and segregation. Aurora-B is also required for spindle-checkpoint function and cytokinesis (Terada et al., 1998).

Aurora-A and -B are overexpressed in primary breast and colon tumor samples (Katayama et al., 1999; Miyoshi et al., 2001; Tanaka et al., 1999). Aurora-A is localized (20q13) to an amplicon associated with poor prognosis in patients with breast and colon tumors (Katayama et al., 1999). Many studies have identified other tumor types, in which Aurora-A was amplified or overexpressed (Tatsuka et al., 1998; Zhou et al., 1998). Aurora-C (STK-13) is also overexpressed in colorectal cancers (Takahashi et al., 2000). The distribution and the expression of Aurora-B were investigated in neoplasms derived from germ cells showing that the expression of Aurora-B is a consistent feature of human seminomas and embryonal carcinomas suggesting that Aurora-B is a potential target in the therapy of TGCTs (Chieffi et al., 2004; Esposito et al., 2009). Three Aurora-kinase inhibitors have recently been described targeting the enzymatic activity of the Aurora kinase and in particular blocking Aurora-B activity: ZM447439, Hesperadin 8 and VX-680 (Harrington et al., 2004; Hauf et al., 2003; Keen and Taylor, 2004). AZD1152, is a reversible ATP-competitive Aurora inhibitor, AZD1152 is 1000-fold more selective for Aurora kinase B than for Aurora kinase A, being the Ki values of 0.36 versus 1300 nM, respectively (Wilkinson et al., 2007). AZD1152 has shown highly significant tumor growth inhibition in a diverse panel of solid human cancer tumor xenograft models, including lung and colorectal cancers and his good solubility makes it suitable for clinical use. AZD1152 and other Aurora inhibitor are currently in early clinical evaluation, showing reversible neutropenia as major side effect. All these molecules act by inhibiting phosphorylation of histone H3 on serine 10 and consequently blocking cell division (Ota et al., 2002; Terada et al., 1998). Although germinal cell tumors are highly responsive to commonly used chemotherapeutic treatment, cases of acute toxicity and chronic collateral effects, such as sterility, are recorded. Therefore, the availability of novel drugs such as Aurora-B inhibitor(s) could represent an escape from chemotherapy early and late effects.

5.3. Receptor and nonreceptor tyrosine kinases inhibitors

Protein phosphorylation plays key roles in many physiological processes and is often deregulated in neoplastic lesions. Current understanding of how protein kinases and phosphatases orchestrate the phosphorylation changes that control cellular functions, has made these enzymes potential drug targets for the treatment of different types of cancer. Recently, receptor and nonreceptor tyrosine kinases (TKs) have emerged as clinically useful drug target molecules for treating cancer (Krause and Van Etten, 2005).

Imatinib mesilate (STI-571) was primarily designed to inhibit bcr-abl TK activity and to treat chronic myeloid leukemia. STI-571 is also an inhibitor of c-Kit receptor TK, and is currently the drug of choice for the therapy of metastatic gastrointestinal stromal tumors (GISTs), which frequently express constitutively activated forms of the c-Kit-receptor (Krause and Van Etten, 2005). Platelet-derived growth factor receptor-α (PDGFR-α), and c-Kit are expressed at high levels in TGCTs (Kemmer et al., 2004; Palumbo et al., 2002; Rapley et al., 2004; Shamblott et al., 1998).

The c-Kit/stem cell factor system is a signaling pathway for migration and survival of PGCs (Manova et al., 1990). c-Kit is a tyrosine kinase receptor for the stem cell factor, ligand binding leads to the c-Kit receptor heterodimerization and tyrosine kinase activity and the downstream signal involves both apoptosis and cell cycle progression (Rossi et al., 2000). Activating mutations of c-Kit have recently been found in 93% of bilateral TGCTs, albeit in less of 2% of unilateral TGCTs (Looijenga et al., 2003b). These mutations affect codon 816 of *c-Kit* gene resulting in a constitutional kinase active, in a manner similar to other receptorial tyrosine kinase activating mutations (Looijenga et al., 2003b). However, the mutation in exon 17 is not inhibited by the tyrosine kinase inhibitor imatinib mesylate (Heinrich et al., 2002; Madani et al., 2003).

The success of the tyrosine kinase inhibitors in the treatment of some cancers has invigorated the development of kinase inhibitors as anticancer drugs and a large number of these compounds are currently undergoing clinical trials and it is likely that molecules capable to inhibit exon 17 *c-Kit* activating mutations will be identified contributing to the development of molecular targeted therapies.

5.4. Angiogenesis inhibitors

Tumors require access to blood vessels for the supply of oxygen and to maintain growth. The development and the growth of new vessels (angiogenesis) are essential for tumor growth and progression. Judah Folkman in the early 1970s proposed the inhibition of tumor blood vessel as a therapeutic approach for treating cancer patients (Folkman, 1996). The blood vessel growth in normal tissues is regulated through a balance between the action of proangiogenic factors, such as vascular endothelial growth factor (i.e., VEGF) (Ferrara, 2004) and the action of angiogenic inhibitors (i.e., thrombospondin-1) (Gasparini et al., 2005; Nieder et al., 2006). In neoplastic lesions the angiogenic balance is shifted toward the proangiogenic factors, and irregular and uncoordinated tumor vessel growth is the result. VEGFR tyrosine kinase, p53, cyclooxygenase-2 (COX-2), and matrix metalloproteinases (MMPs) all directly and/or indirectly influence the proangiogenic switch (Gasparini et al., 2005; Nieder et al., 2006). More than five inhibitors of the VEGF pathway have entered clinical phases I–III trials.

Bevacizumab (Avastin(TM)), an antibody against VEGF, was shown to prolong survival in a phase III clinical trial in renal cell cancer and was efficient in two randomized clinical trials investigating the treatment of metastatic colorectal cancer (Midgley and Kerr, 2005; Ranieri et al., 2006).

ZD6474 is an orally bioavailable inhibitor of VEGF receptor-2 tyrosine kinase activity that in preclinical studies has been shown to inhibit both VEGF-induced signaling in endothelial cells and tumor-induced angiogenesis. ZD6474 produced significant broad-spectrum antitumor activity in a panel of human tumor xenografts (Lee, 2005; Zakarija and Soff, 2005). The results obtained so far with inhibitors of angiogenesis suggest that these are novel molecules, currently in development could be useful for the treatment of chemoteraputic resistant TGCTs and to increase patients survival.

6. Conclusions and Perspectives

Both environmental and genetic factors play an important role in the development of TGCTs. These factor cause the deregulation of the normal differentiation processes of PGC. The incidence of TGCTs has been increasing over the last decades. Remarkably, differences in incidence between adjacent countries such as Sweden and Finland are still largely unexplained, calling for further studies. Diagnosis is usually based on identification of histological subgroups. In recent years, immunohistochemistry with a panel of suitable markers, including OCT3/4, SOX2, SOX17, HMGA1, and HMGA 2 and others has given further advantages to discriminate between subgroups.

A unique characteristic of TGCTs is their sensitivity to treatment. Although the better responses of seminomas versus nonseminomas is well reported, as the frequent recurrence of mature teratomas in residual treatment-resistant tumors highlighting the need for more effective therapies in these resistant forms A deeper understanding of the molecular mechanisms underlying the development of TGCTs may provide new tools to specifically target neoplastic cells and could contribute to overcome acquired and intrinsic chemotherapy resistance. Promising molecules capable to selectively target neoplastic cells, that is, the Aurora-B serine–threonine kinases, TKs, and proangiogenic factors inhibitors, already under clinical evaluation will open a new scenario for TGCTs treatment.

ACKNOWLEDGMENTS

This work was supported by grants to Paolo Chieffi from Italian Ministry of Education (MIUR-PRIN 2007), and to Giuseppe Portella from Associazione Italiana per la Ricerca sul Cancro (AIRC).

REFERENCES

Al Ghamdi, A.M., Jewett, M.A., 2005. Stage I nonseminomatous germ cell tumours: the case for management by risk stratification. Can. J. Urol. 12, 62–65.

Almstrup, K., Hoei-Hansen, C.E., Wirkner, U., Blake, J., Schwager, C., Ansorge, W., et al., 2004. Embryonic stem cell-like features of testicular carcinoma *in situ* revealed by genome-wide gene expression profiling. Cancer Res. 64, 4736–4743.

Atlasi, Y., Mowla, S.J., Ziaee, S.A., Gokhale, P.J., Andrews, P.W., 2008. OCT4 spliced variants are differentially expressed in human pluripotent and non-pluripotent cells. Stem Cells 26, 3068–3074.

Avilion, A.A., Nicolis, S.K., Pevny, L.H., Perez, L., Vivian, N., Lovell Badge, R., 2003. Multipotent cell lineages in early mouse development depend on SOX2 function. Genes Dev. 17, 126–140.

Bahrami, A., Ro, J.Y., Ayala, A.G., 2006. An overview of testicular germ cell tumors. Arch. Pathol. Lab. Med. 131, 1267–1280.

Balzer, B.L., Ulbright, T.M., 2006. Spontaneous regression of testicular germ cell tumors: an analysis of 42 cases. Am. J. Surg. Pathol. 30, 858–865.

Barbagallo, F., Baronetto, M.P., Franco, R., Chieffi, P., Dolci, S., Fry, A.M., et al., 2009. Increased expression and nuclear localization of the centrosomal kinase Nek2 in human testicular seminomas. J. Pathol. 217, 431–441.

Bernstein, E., Kim, S.Y., Carmell, M.A., Murchison, E.P., Alcorn, H., Li, M.Z., et al., 2003. Dicer is essential for mouse development. Nat. Genet. 35, 215–217.

Berthelsen, J.G., Skakkebaek, N.E., von der Maase, H., Sorensen, B.L., Mogensen, P., 1982. Screening for carcinoma *in situ* of the contralateral testis in patients with germinal testicular cancer. Br. Med. J. 285, 1683–1686.

Beyer, J., Kramar, A., Mandanas, R., Linkesch, W., Greinix, A., Droz, J.P., et al., 1996. High-dose chemotherapy as salvage treatment in germ cell tumors: a multivariate analysis of prognostic variables. J. Clin. Oncol. 14, 2638–2645.

Boiani, M., Scholer, H.R., 2005. Regulatory networks in embryo-derived pluripotent stem cells. Nat. Rev. Mol. Cell Biol. 6, 872–884.

Bonner, M.R., McCann, S.E., Moysich, K.B., 2002. Dietary factors and the risk of testicular cancer. Nutr. Cancer 44, 35–43.

Burke, A.P., Mostofi, F.K., 1993. Spermatocytic seminoma: a clinicopathologic study of 79 cases. J. Urol. Pathol. 1, 21–32.

Carmena, M., Earnshaw, W.C., 2003. The cellular geography of aurora kinases. Nat. Rev. Mol. Cell Biol. 4, 842–854.

Carmena, M., Earnshaw, W.C., 2006. INCENP at the kinase crossroads. Nat. Rev. Cell Biol. 8, 110–111.

Chaganti, R.S., Houldsworth, J., 2000. Genetics and biology of adult human male germ cell tumors. Cancer Res. 60, 1474–1482.

Chieffi, P., 2007. Molecular targets for the treatment of testicular germ cell tumors. Mini Rev. Med. Chem. 7, 755–759.

Chieffi, P., Troncone, G., Caleo, A., Libertini, S., Linardopoulos, S., Tramontano, D., et al., 2004. Aurora B expression in normal testis and seminomas. J. Endocrinol. 181, 263–270.

Chung, P., Parker, C., Panzarella, T., Gospodarowicz, M.K., Jewett, S., Milosevic, M.F., et al., 2002. Surveillance in stage I testicular seminoma. Can. J. Urol. 9, 1637–1640.

Classen, J., Souchon, R., Hehr, T., Bamberg, M., 2001. Treatment of early stage testicular seminoma. J. Cancer Res. Clin. Oncol. 127, 475–481.

Comiter, C.V., Kibel, A.S., Richie, J.P., Nucci, M.R., Renshaw, A.A., 1998. Prognostic features of teratomas with malignant transformation: a clinicopathological study of 21 cases. J. Urol. 159, 59–863.

de Jong, J., Looijenga, L.H., 2006. Stem cell marker OCT3/4 in tumor biology and germ cell tumor diagnostics: history and future. Crit. Rev. Oncog. 12, 171–203.
de Jong, J., Stoop, H., Dohle, G.R., Bangma, C.H., Kliffen, M., van Esser, J.W., et al., 2005. 4/4 for pre-invasive and invasive testicular germ cell tumours. J. Pathol. 206, 242–249.
de Jong, J., Stoop, H., Gillis, A.J., van Gurp, R.J., van de Geijn, G.J., Boer, M., et al., 2008. Differential expression of SOX17 and SOX2 in germ cells and stem cells has biological and clinical implications. J. Pathol. 215, 21–30.
Dieckmann, K.P., Pichlmeier, U., 2002. Is risk of testicular cancer related to body size? Eur. Urol. 42, 564–569.
Dieckmann, K.P., Endsin, G., Pichlmeier, U., 2001. How valid is the prenatal estrogen excess hypothesis of testicular germ cell cancer? A case control study on hormone-related factors. Eur. Urol. 40, 677–683.
Dieckmann, K.P., Hartmann, J.T., Classen, J., Lüdde, R., Diederichs, M., Pichlmeier, U., 2008. Tallness is associated with risk of testicular cancer: evidence for the nutrition hypothesis. Br. J. Cancer 99, 1517–1521.
Dieckmann, K.P., Hartmann, J.T., Classen, J., Diederichs, M., Pichlmeier, U., 2009. Is increased body mass index associated with the incidence of testicular germ cell cancer? J. Cancer Res. Clin. Oncol. 135, 731–738.
Eble, J.N., Sauter, G., Epstein, J.I., Sesterhenn, I.A., 2004. System and male genital organs. IARC Press, Lyon, France pp. 218–249.
Einhorn, L.H., Donohue, J., 1977. Cis-diamminedichloroplatinum, vinblastine, and bleomycin combination chemotherapy in disseminated testicular cancer. Ann. Intern. Med. 87, 293–298.
Ekbom, A., Richiardi, L., Akre, O., Montgomery, S.M., Sparén, P., 2003. Age at immigration and duration of stay in relation to risk for testicular cancer among Finnish immigrants in Sweden. J. Natl. Cancer Inst. 95, 1238–1240.
Emerson, R.E., Ulbright, T.M., 2007. Morphological approach to tumours of the testis and paratestis. J. Clin. Pathol. 60, 866–880.
Esposito, F., Libertini, S., Franco, R., Abagnale, A., Marra, L., Portella, G., et al., 2009. Aurora B expression in post-puberal testicular germ cell tumours. J. Cell. Physiol. 221, 435–439.
Fedele, M., Franco, R., Salvatore, G., Baronetto, M.P., Barbagallo, F., Pero, R., et al., 2008. *PATZ1* gene has a critical role in the spermatogenesis and testicular tumours. J. Pathol. 215, 39–47.
Feldman, D.R., Bosl, G.J., Sheinfeld, J., Motzer, R.J., 2008. Medical treatment of advanced testicular cancer. JAMA 299, 672–684.
Ferrara, N., 2004. Vascular endothelial growth factor: basic science and clinical progress. Endocr. Rev. 25, 581–611.
Ferreiro, J.A., 1994. Ber-H2 expression in testicular germ cell tumors. Hum. Pathol. 25, 522–524.
Folkman, J., 1996. New perspectives in clinical oncology from angiogenesis research. Eur. J. Cancer 32, 2534–2539.
Forman, D., Oliver, R.T., Brett, A.R., Marsh, S.G., Moses, J.H., Bodmer, J.G., et al., 1992. Familial testicular cancer: a report of the UK family register, estimation of risk and an HLA class 1 sib-pair analysis. Br. J. Cancer 65, 255–262.
Franco, R., Esposito, F., Fedele, M., Liguori, G., Pierantoni, G., Botti, G., et al., 2008. Detection of high mobility group proteins A1 and A2 represents a valid diagnostic marker in post-puberal testicular germ cell tumours. J. Pathol. 214, 58–64.
García-Rodríguez, J., García-Martín, M., Nogueras-Ocaña, M., de Dios Luna-del-Castillo, M., Espigares García, M., Olea, N., et al., 1996. Exposure to pesticides and cryptorchidism: geographical evidence of a possible association. Environ. Health Perspect. 104, 1090–1095.

Garner, M.J., Birkett, N.J., Johnson, K.C., Shatenstein, B., Ghadirian, P., Krewski, D., Canadian Cancer Registries Epidemiology Research Group, 2003. Dietary risk factors for testicular carcinoma. Int. J. Cancer 106, 934–941.

Garner, M., Turner, M.C., Ghadirian, P., Krewski, D., Wade, M., 2008. Testicular cancer and hormonally active agents. J. Toxicol. Environ. Health B Crit. Rev. 11, 260–275.

Gashaw, I., Grummer, R., Klein-Hitpass, L., Dushaj, O., Bergmann, M., Brehm, R., et al., 2005. Gene signatures of testicular seminoma with emphasis on expression of ets variant gene 4. Cell. Mol. Life Sci. 62, 2359–2368.

Gashaw, I., Dushaj, O., Behr, R., Biermann, K., Brehm, R., Rübben, H., et al., 2007. Novel germ cell markers characterize testicular seminoma and fetal testis. Mol. Hum. Reprod. 13, 721–727.

Gasparini, G., Longo, R., Toi, M., Ferrara, N., 2005. Angiogenic inhibitors: a new therapeutic strategy in oncology. Nat. Clin. Pract. Oncol. 2, 562–577.

Gassmann, R., Carvalho, A., Henzing, A.J., Ruchaud, S., Hudson, D.F., Nigg, E.A., et al., 2004. Borealin: a novel chromosomal passenger required for stability of the bipolar mitotic spindle. J. Cell Biol. 166, 179–191.

Hammerich, K.A., Ayala, G.E., Wheele, T., 2008. Application of immunohistochemistry to the genitourinary system (Prostate, Urinary Bladder, Testis, and Kidney). Arch. Pathol. Lab. Med. 132, 432–440.

Harrington, E.A., Bebbington, D., Moore, J., Rasmussen, R.K., Ajose-Adeogun, A.O., Nakayama, T., et al., 2004. VX-680, a potent and selective small-molecule inhibitor of the Aurora kinases, suppresses tumor growth *in vivo*. Nat. Med. 10, 262–267.

Hart, A.H., Hartley, L., Parker, K., Ibrahim, M., Looijenga, L.H., Pauchnik, M., et al., 2005. The pluripotency homeobox gene NANOG is expressed in human germ cell tumors. Cancer 104, 2092–2098.

Hauf, S., Cole, R.W., LaTerra, S., Zimmer, C., Schnapp, G., Walter, L., et al., 2003. The small molecule Hesperadin reveals a role for Aurora B in correcting kinetochore-microtubule attachment and in maintaining the spindle assembly checkpoint. J. Cell Biol. 161, 281–294.

Heinrich, M.C., Blanke, C.D., Druker, B.J., Corless, C.L., 2002. Inhibition of KIT tyrosine kinase activity: a novel molecular approach to the treatment of KIT-positive malignancies. J. Clin. Oncol. 20, 1692–1703.

Hoei-Hansen, C.E., Almstrup, K., Nielsen, J.E., Brask Sonne, S., Graem, N., Skakkebaek, N.E., et al., 2005. Stem cell pluripotency factor NANOG is expressed in human fetal gonocytes, testicular carcinoma *in situ* and germ cell tumours. Histopathology 47, 48–56.

Horwich, A., Shipley, J., Huddart, R., 2006. Testicular germ-cell cancer. Lancet 367, 754–765.

Jones, R.H., Vasey, P.A., 2003. Part II: testicular cancer—management of advanced disease. Lancet Oncol. 4, 738–747.

Jones, T.D., Ulbright, T.M., Eble, J.N., Baldridge, L.A., Cheng, L., 2004. OCT4 staining in testicular tumors: a sensitive and specific marker for seminoma and embryonal carcinoma. Am. J. Surg. Pathol. 28, 935–940.

Katayama, H., Ota, T., Jisaki, F., Ueda, Y., Tanaka, T., Odashima, S., Suzuki, F., et al., 1999. Mitotic kinase expression and colorectal cancer progression. J. Natl. Cancer Inst. 91, 1160–1162.

Katayama, H., Brinkley, W.R., Sen, S., 2003. The Aurora kinases: role in cell transformation and tumorigenesis. Cancer Metastasis Rev. 22, 451–464.

Keen, N., Taylor, S., 2004. Aurora-kinase inhibitors as anticancer agents. Nat. Rev. Cancer 4, 927–936.

Kemmer, K., Corless, C.L., Fletcher, J.A., McGreevey, L., Haley, A., Griffith, D., et al., 2004. KIT mutations are common in testicular seminomas. Am. J. Pathol. 164, 305–313.

Kim, I., Saunders, T.L., Morrison, S.J., 2007. Sox17 dependence distinguishes the transcriptional regulation of fetal from adult hematopoietic stem cells. Cell 130, 470–483.
Korkola, J.E., Heck, S., Olshen, A.B., Reuter, V.E., Bosl, G.J., Houldsworth, J., et al., 2008. *In vivo* differentiation and genomic evolution in adult male germ cell tumors. Genes Chromosomes Cancer 47, 43–55.
Krause, D.S., Van Etten, R.A., 2005. Tyrosine kinases as targets for cancer therapy. N. Engl. J. Med. 353, 172–187.
Krausz, C., Looijenga, L.H., 2008. Genetic aspects of testicular germ cell tumors. Cell Cycle 7, 3519–3524.
Ledford, H., 2007. Doubts raised over stem-cell marker. Nature (London) 449, 647.
Lee, D., 2005. Phase II data with ZD6474, a small-molecule kinase inhibitor of epidermal growth factor receptor and vascular endothelial growth factor receptor, in previously treated advanced non-small-cell lung cancer. Clin. Lung Cancer 7, 89–91.
Leibovitch, I., Foster, R.S., Ulbright, T.M., Donohue, J.P., 1995. Adult primary pure teratoma of the testis: the Indiana experience. Cancer 75, 244–2250.
Lengner, C.J., Camargo, F.D., Hochedlinger, K., Welstead, G.G., Zaidi, S., Gokhale, S., 2007. Oct4 expression is not required for mouse somatic stem cell self-renewal. Cell Stem Cell 1, 403–415.
Leroy, X., Augusto, D., Leteurtre, E., Gosselin, B., 2002. CD30 and CD117 (c-kit) used in combination are useful for distinguishing embryonal carcinoma from seminoma. J. Histochem. Cytochem. 50, 283–285.
Li, D., Zhu, J., Firozi, P.F., Abruzzese, J.L., Evans, D.B., Cleary, K., et al., 2003. Overexpression of oncogenic STK15/BTAK/Aurora A kinase in human pancreatic cancer. Clin. Cancer Res. 9, 991–997.
Liedtke, S., Enczmann, J., Waclawczyk, S., Wernet, P., Kögler, G., 2007. Oct4 and its pseudogenes confuse stem cell research. Cell Stem Cell 1, 364–366.
Looijenga, L.H., 2009. Human testicular (non)seminomatous germ cell tumours: the clinical implications of recent pathobiological insights. J. Pathol. 218, 146–162.
Looijenga, L.H., Oosterhuis, J.W., 1999. Pathogenesis of testicular germ cell tumours. Rev. Reprod. 4, 90–100.
Looijenga, L.H., Stoop, H., de Leeuw, H.P., de Gouveia Brazao, C.A., Gillis, A.J., van Roozendaal, K.E., et al., 2003a. POU5F1 (OCT3/4) identifies cells with pluripotent potential in human germ cell tumors. Cancer Res. 63, 2244–2250.
Looijenga, L.H., de Leeuw, H., van Oorschot, M., van Gurp, R.J., Stoop, H., Gillis, A.J., et al., 2003b. Stem cell factor receptor (c-KIT) codon 816 mutations predict development of bilateral testicular germ-cell tumors. Cancer Res. 63, 7674–7678.
Lutke Holzik, M.F., Rapley, E.A., Hoekstra, H.J., Sleijfer, D.T., Nolte, I.M., Sijmons, R.H., 2004. Genetic predisposition to testicular germ-cell tumours. Lancet Oncol. 5, 363–371.
Maatouk, D.M., Loveland, K.L., McManus, M.T., Moore, K., Harfe, B.D., 2008. Dicer1 is required for differentiation of the mouse male germline. Biol. Reprod. 79, 696–703.
Madani, A., Kemmer, K., Sweeney, C., Corless, C., Ulbright, T., Heinrich, M., et al., 2003. Expression of KIT and epidermal growth factor receptor in chemotherapy refractory non-seminomatous germ-cell tumors. Ann. Oncol. 14, 873–880.
Manova, K., Nocka, K., Besmer, P., Bachvarova, R.F., 1990. Gonadal expression of c-kit encoded at the W locus of the mouse. Development 110, 1057–1069.
Martin, O.V., Shialis, T., Lester, J.N., Scrimshaw, M.D., Boobis, A.R., Voulvoulis, N., 2008. Testicular dysgenesis syndrome and the estrogen hypothesis: a quantitative meta-analysis. Environ. Health Perspect 116, 149–157.
Mayer, F., Stoop, H., Sen, S., Bokemeyer, C., Oosterhuis, J.W., Looijenga, L.H.J., 2003. Aneuploidy of human testicular germ cell tumors is associated with amplification of centrosomes. Oncogene 22, 3859–3866.

McGlynn, K.A., Quraishi, S.M., Graubard, B.I., Weber, J.P., Rubertone, M.V., Erickson, R.L., 2008. Persistent organochlorine pesticides and risk of testicular germ cell tumors. J. Natl. Cancer Inst. 100, 663–671.

Midgley, R., Kerr, D., 2005. Bevacizumab—current status and future directions. Ann. Oncol. 16, 999–1004.

Miyoshi, Y., Iwao, K., Egawa, C., Noguchi, S., 2001. Association of centrosomal kinase STK15/BTAK mRNA expression with chromosomal instability in human breast cancers. Int. J. Cancer 92, 370–373.

Montgomery, S.M., Granath, F., Ehlin, A., Sparén, P., Ekbom, A., 2005. Germ-cell testicular cancer in offspring of Finnish immigrants to Sweden. Cancer Epidemiol. Biomarkers Prev. 14, 280–282.

Mosharafa, A.A., Foster, R.S., Leibovich, B.C., Ulbright, T.M., Bihrle, R., Einhorn, L.H., 2004. Histology in mixed germ cell tumors: is there a favorite pairing? J. Urol. 171, 471–1473.

Mostofi, F.K., Sesterhenn, I.A., Davis Jr., C.J., 1988. Developments in histopathology of testicular germ cell tumors. Semin. Urol. 6, 171–188.

Müller, J., Skakkebaek, N.E., Nielsen, O.H., Graem, N., 1984. Cryptorchidism and testis cancer. Atypical infantile germ cells followed by carcinoma *in situ* and invasive carcinoma in adulthood. Cancer 54, 629–634.

Nieder, C., Wiedenmann, N., Andratschke, N., Molls, M., 2006. Current status of angiogenesis inhibitors combined with radiation therapy. Cancer Treat. Rev. 32, 348–364.

Nielsen, H., Nielsen, M., Skakkebaek, N.E., 1974. The fine structure of possible carcinoma-in-situ in the seminiferous tubules in the testis of four infertile men. Acta Pathol. Microbiol. Scand. A. 82, 235–248.

Oosterhuis, J.W., Looijenga, L.H., 2005. Testicular germ-cell tumors in a broader perspective. Nat. Rev. Cancer 5, 210–222.

Ota, T., Suto, S., Katayama, H., Han, Z.B., Suzuki, F., Maeda, M., et al., 2002. Increased mitotic phosphorylation of histone H3 attributable to AIM-1/Aurora-B overexpression contributes to chromosome number instability. Cancer Res. 62, 5168–5177.

Palumbo, C., van Roozendaal, K., Gillis, A.J., van Gurp, R.H., de Munnik, H., Oosterhuis, J.W., et al., 2002. Expression of the PDGF alpha-receptor 1.5 kb transcript, OCT-4, and c-KIT in human normal and malignant tissues Implications for the early diagnosis of testicular germ cell tumours and for our understanding of regulatory mechanisms. J. Pathol. 196, 467–477.

Peckham, M., 1988. Testicular cancer. Acta Oncol. 27, 439–453.

Perrett, R.M., Turnpenny, L., Eckert, J.J., O'Shea, M., Sonne, S.B., Cameron, I.T., et al., 2008. The early human germ cell lineage does not express SOX2 during *in vivo* development or upon *in vitro* culture. Biol. Reprod. 78, 852–858.

Perrotti, M., Ankem, M., Bancilla, A., deCarvalho, V., Amenta, P., Weiss, R., 2004. Prospective metastatic risk assignment in clinical stage I nonseminomatous germ cell testis cancer: a single institution pilot study. Urol. Oncol. 22, 174–177.

Porcaro, A.B., Antoniolli, S.Z., Maffei, N., Beltrami, P., Bassetto, M.A., Curti, P., 2002. Management of testicular seminoma advanced disease: report on 14 cases and review of the literature. Arch. Ital. Urol. Androl. 74, 81–85.

Pottern, A., 1998. Testicular and penile cancer. In: Ernstoff Heaney Peschel. Blackwell Science, Oxford, UK.

Rajpert-De Meyts, E., Bartkova, J., Samson, M., Hoei-Hansen, C.E., Frydelund-Larsen, L., Bartek, N.E., Skakkebaek, N.E., 2003. The emerging phenotype of the testicular carcinoma *in situ* germ cell. APMIS 111, 267–278.

Ranieri, G., Patruno, R., Ruggirei, E., Montemurro, S., Valerio, P., Ribatti, D., 2006. Vascular endothelial growth factor (VEGF) as a target of bevacizumab in cancer: from the biology to the clinic. Curr. Med. Chem. 1, 1845–1847.

Rapley, E.A., Hockley, S., Warren, W., Johnson, L., Huddart, R., Crockford, G., et al., 2004. Somatic mutations of KIT in familial testicular germ cell tumours. Br. J. Cancer 90, 2397–2401.

Ro, J.Y., Amin, M.B., Sahin, A.A., Ayala, A.G., 2000. Tumors and tumorous conditions of the male genital tract. In: Fletcher, C.D.M. (Ed.), Diagnostic Histopathology of Tumors. 2nd ed. Churchill Livingstone, London, England, pp. 733–838.

Rodriguez, P.N., Hafez, G.R., Messing, E.M., 1986. Nonseminomatous germ cell tumor of the testicle: does extensive staging of the primary tumor predict the likelihood of metastatic disease? J. Urol. 136, 604–608.

Rossi, P., Sette, C., Dolci, S., Geremia, R., 2000. Role of c-kit in mammalian spermatogenesis. J. Endocrinol. Invest. 64, 1153–1159.

Sakakura, C., Hagiwara, A., Yasuoka, R., Fujita, Y., Nakanishi, M., Masuda, K., et al., 2001. Tumour-amplified kinase BTAK is amplified and overexpressed in gastric cancers with possible involvement in aneuploid formation. Br. J. Cancer 84, 824–831.

Sen, S., Zhou, H., Zhang, R.D., Yoon, D.S., Vakar-Lopez, F., Ito, S., et al., 2002. Amplification/overexpression of a mitotic kinase gene in human bladder cancer. J. Natl. Cancer Inst. 94, 1320–1329.

Shamblott, M.J., Axelman, J., Wang, S., Bugg, E.M., Littlefield, J.W., Donovan, P.J., et al., 1998. Derivation of pluripotent stem cells from cultured human primordial germ cells. Proc. Natl. Acad. Sci. USA 95, 13726–13731.

Shelley, M.D., Burgon, K., Mason, M.D., 2002. Treatment of testicular germ-cell cancer: a cochrane evidence-based systematic review. Cancer Treat. Rev. 28, 237–253.

Skakkebaek, N.E., 1972. Possible carcinoma-in-situ of the testis. Lancet 2, 516–517.

Skakkebaek, N.E., Berthelsen, J.G., Giwercman, A., Müller, J., 1987. Carcinoma-in-situ of the testis: possible origin from gonocytes and precursor of all types of germ cell tumours except spermatocytoma. Int. J. Androl. 10, 19–28.

Strohsnitter, W.C., Noller, K.L., Hoover, R.N., Robboy, S.J., Palmer, J.R., Titus-Ernstoff, L., et al., 2001. Cancer risk in men exposed *in utero* to diethylstilbestrol. J. Natl. Cancer Inst. 93, 545–551.

Takahashi, T., Futamura, M., Yoshimi, N., Sano, J., Katada, M., Takagi, Y., et al., 2000. Centrosomal kinases, HsAIRK1 and HsAIRK3, are overexpressed in primary colorectal cancers. Jap. J. Cancer Res. 91, 1007–1014.

Talerman, A., 1980. Spermatocytic seminoma: clinicopathological study of 22 cases. Cancer 45, 2169–2176.

Tanaka, T., Kimura, M., Matsunaga, K., Fukada, D., Mori, H., Okano, Y., 1999. Centrosomal kinase AIK1 is overexpressed in invasive ductal carcinoma of the breast. Cancer Res. 59, 2041–2044.

Tatsuka, M., Katayama, H., Ota, T., Tanaka, T., Odashima, S., Suzuki, F., et al., 1998. Multinuclearity and increased ploidy caused by overexpression of the aurora- and Ipl1-like midbody-associated protein mitotic kinase in human cancer cells. Cancer Res. 58, 4811–4816.

Terada, Y., Tatsuka, M., Suzuki, F., Yasuda, Y., Fujita, S., Otsu, M.A., 1998. AIM-1: a mammalian midbody-associated protein required for cytokinesis. EMBO J. 17, 667–676.

Theakera, J.M., Meadb, G.M., 2004. Diagnostic pitfalls in the histopathological diagnosis of testicular germ cell tumours. Curr. Diagnostic Pathol. 10, 220–228.

Ulbright, T.M., 1993. Germ cell neoplasm of the testis. Am. J. Surg. Pathol. 17, 1075–1091.

Ulbright, T.M., 1999. Protocol for the examination of specimens from patients with malignant germ cell and sex cord-stromal tumors of the testis, exclusive of paratesticular malignancies: a basis for checklists. Arch. Pathol. Lab. Med. 123, 14–19.

Ulbright, T.M., 2004. Testicular and paratesticular tumors. In: Mills, S.E. (Ed.), Sternberg's Diagnostic Surgical Pathology. 14th ed. Lippincott Williams & Wilkins, Philadelphia, PA, pp. 2173–2176.

Ulbright, T.M., 2005. Germ cell tumors of the gonads: a selective review emphasizing problems in differential diagnosis, newly appreciated, and controversial issues. Modern Pathol. 18, S61–S79.

Vader, G., Medema, R.H., Lens, S.M., 2006. The chromosomal passenger complex: guiding Aurora-B through mitosis. J. Cell Biol. 173, 833–837.

Van de Geijn, G.J.M., Hersmus, R., Looijejnga, L.H., 2009. Recent developments in testicular germ cell tumor research. Birth Defects Res. (Part C) 87, 96–113.

Verdorfer, I., Rogatsch, H., Tzankov, A., Steiner, H., Mikuz, G., 2004. Molecular cytogenetic analysis of human spermatocytic seminomas. J. Pathol. 204, 277–281.

von Eyben, F.E., 2003. Laboratory markers and germ cell tumors. Crit. Rev. Clin. Lab. Sci. 40, 377–427.

Voorhoeve, P.M., le Sage, C., Schrier, M., Gillis, A.J., Stoop, H., Nagel, R., et al., 2006. A genetic screen implicates miRNA-372 and miRNA-373 as oncogenes in testicular germ cell tumors. Cell 12, 1169–1181.

Weissbach, L., Bussar-Maatz, R., Lohrs, U., Schubert, G.E., Mann, K., Hartmann, M., et al., 1999. Prognostic factors in seminomas with special respect to HCG: results of a prospective multicenter study: Seminoma Study Group. Eur. Urol. 36, 601–608.

Wicha, M.S., Liu, S., Dontu, G., 2006. Cancer stem cells: an old idea—a paradigm shift. Cancer Res. 66, 1883–1890.

Wilkinson, R.W., Odedra, R., Heaton, S.P., Wedge, S.R., Keen, N.J., Crafter, C., et al., 2007. AZD1152, a selective inhibitor of Aurora B kinase, inhibits human tumor xenograft growth by inducing apoptosis. Clin. Cancer Res. 1, 3682–3688.

Yamaguchi, S., Kimura, H., Tada, M., Nakatsuji, N., Tada, T., 2005. Nanog expression in mouse germ cell development. Gene Expr. Patterns 5, 639–646.

Yates, A., Chambers, I., 2005. The homeodomain protein Nanog and pluripotency in mouse embryonic stem cells. Biochem. Soc. Trans. 33 (Part 6), 1518–1521.

Young, R.H., 2008. Testicular tumors—some new and a few perennial problems. Arch. Pathol. Lab. Med. 132, 548–564.

Zakarija, A., Soff, G., 2005. Update on angiogenesis inhibitors. Curr. Opin. Oncol. 6, 578–583.

Zhou, H., Kuang, J., Zhong, L., Kuo, W.L., Gray, J.W., Sahin, A., et al., 1998. Tumour amplified kinase STK15/BTAK induces centrosome amplification, aneploidy and transformation. Nat. Genet. 20, 189–193.

CHAPTER SEVEN

Polarity Proteins and Cell–Cell Interactions in the Testis

Elissa W.P. Wong *and* C. Yan Cheng

Contents

1. Introduction 310
2. Rho GTPases and Cell–Cell Interactions in the Testis: Cdc42 315
   2.1. Mediating the action of transforming growth factor-βs (e.g., TGF-β3) in the seminiferous epithelium of adult rat testes 319
   2.2. Regulation of filopodia formation 321
   2.3. Cdc42 in protein trafficking 322
   2.4. Effects on actin cytoskeleton 325
   2.5. Ubiquitination of junction proteins 326
   2.6. Assembly and maintenance of epithelial apico-basal cell polarity 327
3. Polarity Proteins and Cell–Cell Interactions in the Testis 327
   3.1. The Crumbs (CRB) protein complex 328
   3.2. The partitioning-defective (Par) protein complex 330
   3.3. The Scribble protein complex 331
   3.4. 14-3-3 proteins 332
4. The Apical ES-BTB-Basement Membrane Functional Axis in the Seminiferous Epithelium that Coordinates the Cellular Events of Spermiation and BTB Restructuring During the Seminiferous Epithelial Cycle of Spermatogenesis: The Role of Polarity Proteins in Mediating the Apical ES-BTB-Basement Membrane Axis 335
5. Roles of Polarity Proteins in Coordinating the Opposing Effects of Cytokines and Testosterone in Primary Preleptotene Spermatocyte Transit at the BTB 339
6. Concluding Remarks and Future Perspectives 341

Acknowledgment 342
References 342

Mary M. Wohlford Laboratory for Male Contraceptive Research, Center for Biomedical Research, Population Council, New York, New York 10065, USA

International Review of Cell and Molecular Biology, Volume 278
ISSN 1937-6448, DOI: 10.1016/S1937-6448(09)78007-4
© 2009 Elsevier Inc.
All rights reserved.

Abstract

In mammalian testes, extensive junction restructuring takes place in the seminiferous epithelium at the Sertoli–Sertoli and Sertoli–germ cell interface to facilitate the different cellular events of spermatogenesis, such as mitosis, meiosis, spermiogenesis, and spermiation. Recent studies in the field have shown that Rho GTPases and polarity proteins play significant roles in the events of cell–cell interactions. Furthermore, Rho GTPases, such as Cdc42, are working in concert with polarity proteins in regulating cell polarization and cell adhesion at both the blood–testis barrier (BTB) and apical ectoplasmic specialization (apical ES) in the testis of adult rats. In this chapter, we briefly summarize recent findings on the latest status of research and development regarding Cdc42 and polarity proteins and how they affect cell–cell interactions in the testis and other epithelia. More importantly, we provide a new model in which how Cdc42 and components of the polarity protein complexes work in concert with laminin fragments, cytokines, and testosterone to regulate the events of cell–cell interactions in the seminiferous epithelium via a local autocrine-based regulatory loop known as the apical ES—BTB—basement membrane axis. This new functional axis coordinates various cellular events during different stages of the seminiferous epithelium cycle of spermatogenesis.

Key Words: Testis, Spermatogenesis, Sertoli cells, Germ cells, Blood–testis barrier, Adherens junction, Tight junction, Ectoplasmic specialization, Seminiferous epithelial cycle. © 2009 Elsevier Inc.

1. Introduction

In mammalian testes, spermatogenesis takes place in the seminiferous tubule, which is the functional unit that produces spermatozoa (haploid, 1n) from spermatogonia (diploid, 2n) under the influence of the pituitary hormone follicle stimulating hormone (FSH) (Cheng and Mruk, 2002; de Kretser and Kerr, 1988; Sharpe, 1994; Walker and Cheng, 2005). The process of spermatogenesis, however, is also supported by Leydig cells in the interstitium, which produce testosterone to maintain Sertoli and germ cell function and to regulate germ cell maturation (Page et al., 2008; Walker and Cheng, 2005), such as cell-cycle progression (Lie et al., 2009), under the influence of pituitary hormone lutenizing hormone (LH). Additionally, estrogen (e.g., estradiol-17β) produced by Leydig cells in the interstitium, and Sertoli and germ cells in the seminiferous epithelium, is also critical to germ cell development such as apoptosis as demonstrated by studies reported in recent years (Carreau et al., 2008; Hess, 2003; Shaha, 2008).

Morphologically, the seminiferous epithelium is segregated into the basal and the apical (or adluminal) compartments by the blood–testis barrier

(BTB) which is a testis-specific ultrastructure between adjacent Sertoli cells located near to the basement membrane (Fig. 7.1). Besides conferring cell polarity, the BTB also provides the "gate" function so that water, electrolytes, nutrients, and biomolecules cannot freely diffuse paracellularly from the interstitium and basal compartment to the apical compartments (Mruk and Cheng, 2008; Mruk et al., 2008). Also, the BTB confers the immunological barrier in the testis (Mruk et al., 2008), which restricts the access of drugs, environmental toxicants, and ions to the developing spermatids behind the BTB. In turn, drugs and ions utilize different drug transporters and ion channels to enter the apical compartment (Mruk and Cheng, 2008).

Spermatogenesis is a highly complex biochemical process which is composed of several discrete cellular events that take place in the seminiferous epithelium of the testis, namely *mitosis*, *meiosis*, *spermiogenesis*, and *spermiation*, during the seminiferous epithelial cycle (Fig. 7.2). In adult rat testes, the seminiferous epithelial cycle can be divided into 14 stages (12 stages in mice and 6 stages in humans) (de Kretser and Kerr, 1988), which is typified by the unique association between Sertoli cells and the developing spermatids in the seminiferous epithelium (Hess and de Franca, 2008; Leblond and Clermont, 1952; Parvinen, 1982) as shown in Fig. 7.2. During the initial

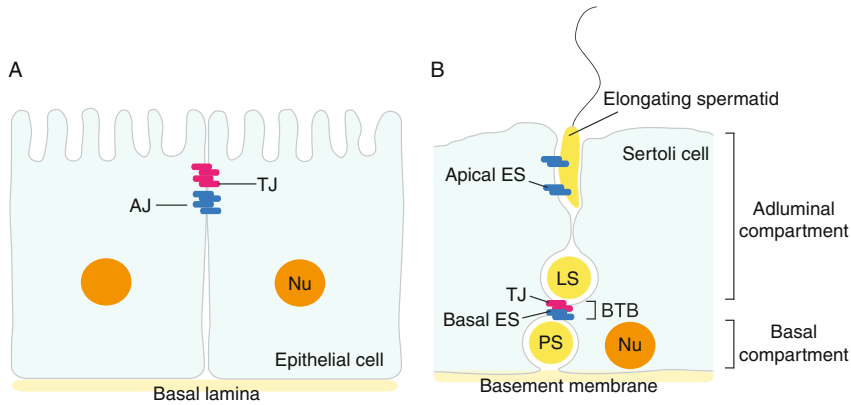

Figure 7.1 Differences in the spatial arrangement of tight junction (TJ) and adherens junction (AJ) in epithelia versus the seminiferous epithelium in adult mammalian testes. (A) In most epithelia, TJ is restricted to the apical region of adjacent epithelial cells, underneath of which lies AJ, a cell–cell actin-based anchoring junction type. Furthest away from TJ is the basal lamina, a form of extracellular matrix (ECM). In other blood–tissue barrier, the TJ alone confers the barrier function, such as in the blood–brain barrier and the blood–retina barrier. (B) In mammalian testes, such as rats, the blood–testis barrier (BTB) is closest to the basement membrane (a modified form of ECM) instead of the apical region of the Sertoli cell. Also, the BTB is composed of coexisting TJ and basal ES (an atypical AJ type in the testis). The apical ES, however, is restricted to the Sertoli cell–elongating spermatid interface. The presence of the BTB also segregates the seminiferous epithelium into the basal and adluminal compartments.

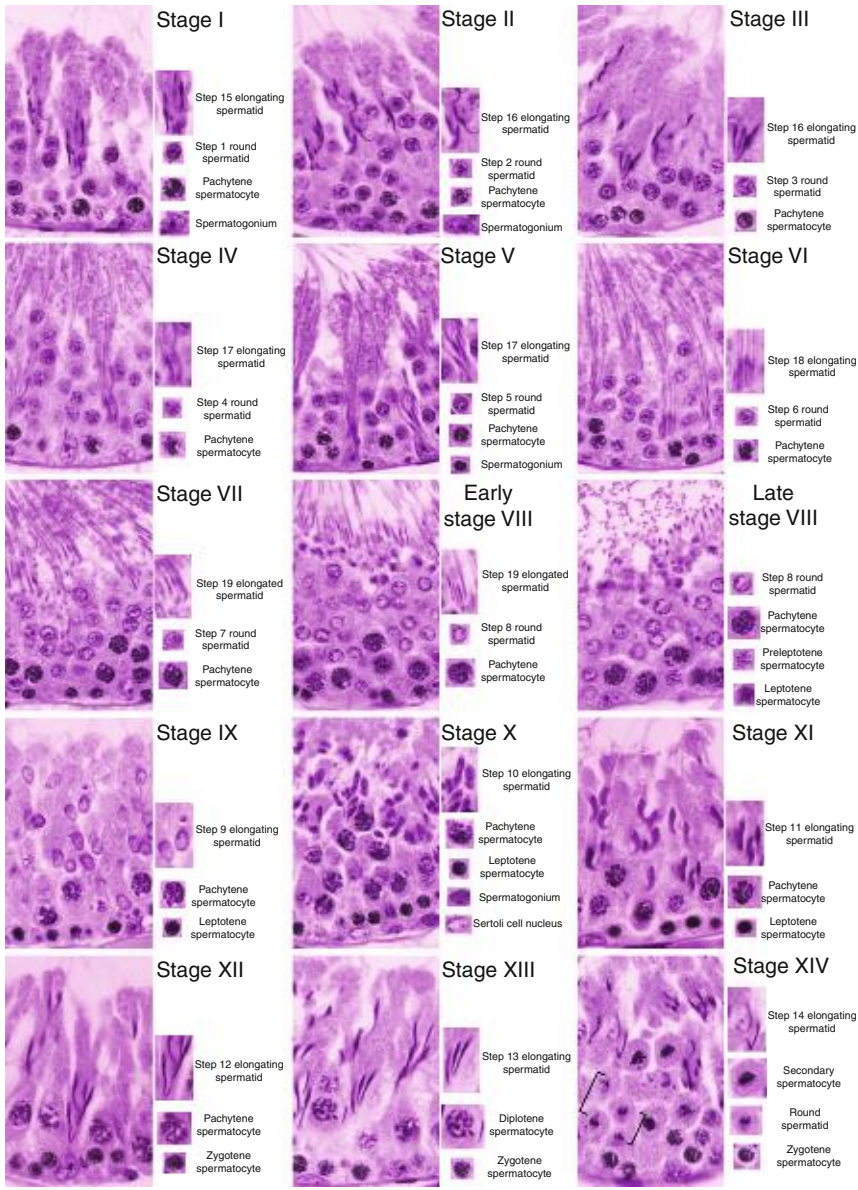

Figure 7.2 Different stages of the seminiferous epithelial cycle of spermatogenesis in adult rat testes. Stages I through XIV of the epithelial cycle in adult rat testes are shown. The typical germ cells at different stages of their development that are found in specific stage of the epithelial cycle are shown on the right panel of the corresponding micrographs. For instance, both meiosis I and II take place in Stage XIV in rat testes, so that secondary spermatocytes following meiosis I and round spermatids (step 1) from meiosis II following telephase II (see square brackets) are clearly visible.

phase of spermatogenesis, spermatogonia undergo *mitosis* to replenish the most primitive germ cells such as type A spermatogonia, some of which will differentiate into type B spermatogonia. It is noted that some type B spermatogonia, regulated by a yet-to-be-defined mechanism(s), commit to differentiate into primary spermatocytes. These are the germ cells that will enter the cell-cycle progression events and differentiate into preleptotene spermatocytes. Once formed, preleptotene spermatocytes begin to traverse the BTB at stages VIII–IX of the epithelial cycle while differentiating into leptotene and zygotene spermatocytes (Russell, 1977). Concomitant with these events, condensation and replication of the chromatin materials take place during the transit of primary spermatocytes at the BTB, so that diplotene spermatocytes (tetraploid, 4n) can undergo diakinesis, to be followed by *meiosis* I and then *meiosis* II that take place at stage XIV of the epithelial cycle in rat testes to generate round spermatids (or step 1 spermatid) (haploid, 1n) (Lie et al., 2009) (Fig. 7.2). Recent studies have shown that the transit of primary spermatocytes at the BTB that takes place at stages VIII–IX of the epithelial cycle is modulated, at least in part, by mitogen-activated protein kinase (MAPK) (e.g., p38 MAPK and extracellular signal-regulated kinase 1/2, ERK1/2) (Li et al., 2006; Lui et al., 2003d; Wong et al., 2004; Xia et al., 2006), which also regulates the "opening" and "closing" of the BTB downstream of cytokines (e.g., TGF-β3 and TNFα) by determining the steady-state level of integral membrane proteins at the BTB (Lui et al., 2001; Siu et al., 2003). ERK1/2 that found in pachytene spermatocytes were also shown to regulate chromatin condensation (Di Agostino et al., 2002; Inselman and Handel, 2004). Collectively, these findings illustrate that the events of primary spermatocytes in transit at the BTB and the preparation of spermatocytes for cell-cycle progression (e.g., chromatin condensation) can be coordinated by MAPK found in Sertoli and germ cells in the microenvironment of the seminiferous epithelium at or near the BTB. These findings also suggest that the cellular events that take place locally in the seminiferous epithelium are highly coordinated, such as by MAPK.

Once meiosis completes, spermatids (haploid, 1n) undergo a series of well-defined morphological changes from step 1 through step 19 spermatids in rat testes in a process known as *spermiogenesis*, which is typified by the condensation of the genetic material into spermatid nucleus in the head region, development of the acrosome above the sperm head, packaging of the mitochondria into the mitochondrial sheath that constitutes the spermatid midpiece and elongation of the tail, as well as formation of the residual body to be phagocytosed by the Sertoli cell at *spermiation* (Mruk et al., 2008). At present, the biochemical and/or molecular mechanism(s) that regulate *spermiogenesis* and/or *spermiation* remain obscure. Recent studies, however, have shown that gonadotropins (e.g., FSH) are involved in spermiation in men (Matthiesson et al., 2006). Once the fully developed elongated spermatids (step 19) line up at the adluminal edge of the

epithelium at stage VIII of the epithelial cycle, *spermiation* takes place in which the adhesion protein complex between step 19 spermatids and the Sertoli cell is disrupted, so that spermatozoa can enter the seminiferous tubule lumen and be transported to the epididymis for their subsequent maturation. During spermiogenesis and spermiation, a cellular phenomenon pertinent to these events that takes place in the seminiferous epithelium has been largely unexplored for decades: the proper orientation of developing spermatids. It is noted that the heads of developing spermatids are pointing toward the basement membrane in all stages of the epithelial cycle from steps 1 through 19 spermatids. It has been postulated that apical ectoplasmic specialization (ES), a testis-specific atypical adherens junction (AJ) type, confers spermatid orientation during spermiogenesis (Vogl et al., 1993, 2008; Wong et al., 2008a). However, other studies have shown that tight junction (TJ) is the cell junction type that confers cell polarity and/or orientation in epithelial cells (Cereijido et al., 2004, 2008). Thus, it is not known how ES confers spermatid polarity in the testis since apical ES at the Sertoli–spermatid interface is a putative anchoring junction type and the only anchoring device between Sertoli cells and spermatids (step 8 through step 19 spermatids). Furthermore, spermiation that takes place at stage VIII of the epithelial cycle is concomitant with the event of BTB restructuring to facilitate the transit of primary spermatocytes across the BTB and the preparation of these germ cells for metaphase I. Interestingly, these three cellular events, namely (i) spermiation, (ii) BTB restructuring, and (iii) germ cell-cycle progression, take place at the opposite ends of the Sertoli cell epithelium. Thus, it seems logical to speculate that there is a local regulatory loop in the seminiferous epithelium to coordinate these cellular events during the epithelial cycle.

In this chapter, we discuss recent findings in the field regarding the role of polarity proteins, such as partitioning-defective3/partitioning-defective6/atypical protein kinase C (Par3/Par6/aPKC) protein complex, which are the integrated components of the apical ES in conferring spermatid polarity during spermiogenesis besides its involvement in regulating spermatid adhesion. In addition, the small Rho GTPase Cdc42 (Cell division cycle 42), which was first identified as an essential gene for the asymmetric cell division in budding yeast, is found to interact with the Par3/Par6/aPKC protein complex to regulate polarity in mammalian cells. Besides its regulation via the Par6-based protein complex, Cdc42 regulates cell adhesion and junction function through regulating filopodia formation, protein trafficking, and actin cytoskeleton. Furthermore, some of the polarity proteins that are integrated components of the BTB were shown to regulate Sertoli cell adhesion at the BTB via their effects on the kinetics of endocytic vesicle-mediated protein endocytosis, and served as molecular switches to coordinate spermiation and BTB restructuring. Additionally, there are recent findings in the field that illustrate proteins in the basement

membrane, such as at the Sertoli cell–extracellular matrix (ECM) interface (e.g., integrins at the hemidesmosome), can also provide a feedback regulatory mechanism to modulate the BTB integrity. In addition, it is apparent that proteins released at spermiation (such as fragments of the laminin–integrin-based adhesion complex at the apical ES) are working in concert with polarity proteins to regulate BTB directly and indirectly via hemidesmosome. In short, based on recently published findings in the field, we report herein the presence of a local apical ES-BTB-basement membrane functional axis that is mediated by polarity proteins to coordinate the events of junction restructuring in the seminiferous epithelium during spermatogenesis. While much work is needed to design functional experiments to tackle the precise roles of this functional axis, we provide a working biochemical model for investigators in the field which serves as a framework for future investigation in the next decade.

2. Rho GTPases and Cell–Cell Interactions in the Testis: Cdc42

Cdc42 (~22 kDa) is one of the best characterized members of the Rho GTPases which belong to the Ras-related small GTPases superfamily (Boureux et al., 2007; Jaffe and Hall, 2005; Wennerberg and Der, 2004). Rho GTPases comprise a family of at least 25 members (Wennerberg and Der, 2004) which are known to regulate a diverse array of cellular processes including cell adhesion and cell movement in epithelia and/or endothelia including the seminiferous epithelium (Huveneers and Danen, 2009; Lui et al., 2003a; Samarin and Nusrat, 2009; Takai et al., 2001). While there are studies in the literature illustrating the role of other Ras superfamily members such as Rab GTPases (e.g., Rab4A, Rab8B) in regulating protein–protein interactions in the testis (Lau and Mruk, 2003; Mruk et al., 2007), most functional studies were performed on Rho GTPases (Hall et al., 1993; Leung et al., 1993; Lui et al., 2003b, 2005; Toure et al., 1998, 2001) in particular Cdc42 which was shown to control multiple cellular functions in different epithelial cells as illustrated in Table 7.1. Thus, we focus our discussion on Cdc42 herein since a survey on other GTPases pertinent to cell–cell interactions in the testis can be found in recent reviews in the field (Mruk and Cheng, 2004; Mruk et al., 2008).

Classical Rho GTPases such as RhoA, Rac1, and Cdc42 contain a Rho-type GTPase-like domain which allows them to shuttle between an active GTP-bound state and inactive GDP-bound state (Jaffe and Hall, 2005; Valencia et al., 1991; Wennerberg and Der, 2004) (Fig. 7.3). Three classes of proteins are present to regulate the activity of classical Rho GTPases including Cdc42: (1) guanine nucleotide exchange factors (GEFs) which

Table 7.1 Phenotypes of altering Cdc42 activity in different cell and model systems

Cell/model system	Method of altering Cdc42 activity[a]	Phenotypes	References
MDCK[b]	CA	↑ Actin, E-cadherin, and β-catenin at cell–cell adhesion site Cells are tightly contacted with each other at the lateral surface Protects cells from hepatocyte growth factor (HGF) and 12-*O*-tetradecanoylphorbol-13-acetate (TPA)-induced junction disruption	Kodama et al. (1999)
Caco-2	DN	Disrupts E-cadherin and F-actin after calcium switch	Otani et al. (2006)
MDCK	NWASP–CRIB is overexpressed to inhibit Cdc42	↓ Afadin, E-cadherin, and claudin-1 at the cell–cell adhesion sites after calcium switch ↑ Afadin, E-cadherin, and claudin-1 at the cell–cell adhesion sites after calcium switch	Fukuhara et al. (2003)
	CA	Induces formation of filopodia	
HeLa	CA	Induces cell–cell contact rich in actin, β-catenin, and N-cadherin	Stoffler et al. (1998)
MDCK	DA, DN	Apical localization of transmembrane basolateral markers vesicular stomatitis virus G protein (VSVG) and low-density lipoprotein receptor (LDLR)	Cohen et al. (2001)
	DA	Basolateral membrane protein NaK-ATPase found at the apical surface	
MDCK	CA, DN	↑ Exit of p75 (apical) from *trans*-Golgi network (TGN) ↓ Exit of LDLR and neuronal-cell adhesion molecule (NCAM) (basolateral)	Musch et al. (2001)
	CA	↓ Perinuclear/cytoplasmic actin but ↑ cortical actin	
MDCK	CA	↓ Endocytic and biosynthetic traffic Occludin found at lateral membrane Extended distribution of junctions ↑ Cortical actin	Rojas et al. (2001)

		↓ Transepithelial electrical resistance (TER) ↑ Paracellular diffusion of radiolabeled inulin, IgA, and transferrin	
	DN	↑ Cortical actin ↓ TER ↓ Apical endocytosis and transcytosis ↑ Biosynthetic traffic	
MDCK	DN	Mistargeting of basolateral proteins VSVG and gp58 Disrupts recycling of gp58	Kroschewski et al. (1999)
	CA	Disrupts ZO-1 distribution at cell–cell interface	
Cell free endocytosis assay system	Addition of recombinant Rho GDI to inactivate Cdc42	↑ Endocytosis of E-cadherin	Izumi et al. (2004)
CHO	DN	Disrupts perinuclear clustering of endocytic recyling compartment	Balklava et al. (2007)
HeLa	DN	↓ Recycling of clathrin-independent cargo ↓ Endocytosis of clathrin-dependent cargo	
MCF-7	CA	↑ Ubiquitination and degradation of E-cadherin after depletion of calcium ↑ Filopodia formation	Shen et al. (2008b)
	Cdc42 si	Blocks E-cadherin degradation induced by the removal of calcium	
Sertoli cells	DN	Inhibits TGF-β3-mediated enhancement in protein endocytosis	Wong et al. (2009b)

[a] Overexpression of constitutively active (CA) or dominant negative (DN) mutant of Cdc42 is commonly used to manipulate Cdc42 activity. In addition, overexpression of Cdc42 and Rac interactive binding (CRIB) domain of neural Wiskott–Aldrich syndrome protein (NWASP) or silencing of Cdc42 (Cdc42 si) is also being used to study the function of Cdc42. ↑, stimulation; ↓, inhibition.

[b] MDCK cells, Madin-Darby Canine Kidney epithelial cells; CHO cells, Chinese Hamster Ovary cells; HeLa cells, cervical cancer cells derived from Henrietta Lacks.

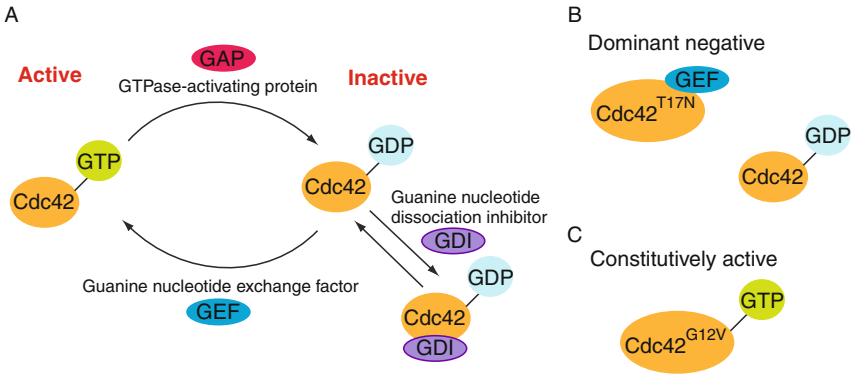

Figure 7.3 The cycling of Cdc42 GTPase between GTP- (active) and GDP-bound (inactive) state. (A) The activation of Cdc42 GTPase involves the exchange of GDP for GTP via phosphorylation, which is stimulated by GEF (guanine nucleotide exchange factor), leading to an increase in affinity of activated Cdc42 for its effector to stimulate downstream signaling functions. Activated Cdc42 GTPase can be inactivated by its binding with GTPase-activating protein (GAP), leading to dephosphorylation, and a shutdown of the signaling function. The release of GDP from the Cdc42 GTPase is blocked by guanine nucleotide dissociation inhibitor (GDI). The GDI-bound Cdc42 GTPase is sequestered in the cytosol. (B) This illustrates a dominant-negative form of Cdc42 in which the threonine (Thr, T) in residue 17 from the N-terminus is mutated to asparagine (Asn, N), which allows binding of GEF but not effectors. Thus, GEF is sequestered by the dominant-negative form and this prevents endogenous Cdc42 from activating by GEF (Bollag and McCormick, 1991; Heasman and Ridley, 2008). (C) This is the constitutively active form of Cdc42 wherein the glycine (Gly, G) in residue 12 from the N-terminus is mutated to valine (Val, V), which is defective in GTPase activity, thus it cannot be dephosphorylated (i.e., inactivated) but remains phosphorylated (activated). Other common constitutively active mutants include mutation at residue 18 from phenylalanine (Phe, F) to leucine (Leu, L) and mutation at residue 61 from glutamine (Gln, Q) to leucine (Leu, L) (Bollag and McCormick, 1991; Heasman and Ridley, 2008).

promote the exchange of GDP for GTP to activate Rho GTPases (Garcia-Mata and Burridge, 2007; Rossman et al., 2005); (2) GTPase-activating proteins (GAPs) which enhance the intrinsic GTPase activity of Rho GTPases to inactivate them (Moon and Zheng, 2003; Tcherkezian and Lamarche-Vane, 2007); and (3) guanine nucleotide dissociation inhibitors (GDIs) which functions to prevent the dissociation of GDP from Rho GTPases and sequester them from effector targets (DerMardirossian and Bokoch, 2005) (Fig. 7.3). Upon activation, Rho GTPases undergo conformational changes resulting in an increased affinity for downstream effector proteins which stimulate various cellular processes such as actin dynamics, gene expression, cell-cycle progression, cell migration, and cell adhesion (Heasman and Ridley, 2008; Jaffe and Hall, 2005; Vetter and Wittinghofer, 2001). For instance, it was illustrated that the dynamic interactions between Cdc42, its effector IQ motif containing GTPase activating protein 1

(IQGAP1) and β-catenin played a crucial role in conferring the N-cadherin-based cell adhesion function between Sertoli and germ cells in the testis (Lui et al., 2005). In Sertoli–germ cell cocultures, it was shown that the assembly of stable anchoring junctions between these cells was associated with an increase in Cdc42–IQGAP1 interaction. However, a loss of Sertoli–germ cell anchoring junction adhesion induced by the depletion of calcium in the culture media was shown to cause a loss of Cdc42–IQGAP1 association. Instead, IQGAP1 associates more with catenins, decreasing the pool of catenins associating with the actin-based cell-cell AJ. Thus, this leads to a loss of cadherin-based germ cell adhesion to Sertoli cells (Lui et al., 2005).

Besides switching between GTP- and GDP-bound forms, Rho GTPases can also be regulated by ubiquitination (Asanuma et al., 2006) and phosphorylation (Loirand et al., 2006; Tu et al., 2003). On the other hand, nonclassical/atypical Rho GTPases such as RhoH is constitutively bound to GTP but lacking GTPase activity (Chardin, 2006; Jaffe and Hall, 2005; Wennerberg and Der, 2004). Thus, this subgroup of Rho GTPases is not regulated by GAPs, GEFs, or GDIs. Instead, they are regulated through gene expression, phosphorylation, and ubiquitin/proteasome-mediated degradation (Chardin, 2006). The roles of these atypical Rho GTPases in cell–cell interactions in the testis remain to be investigated. In the following sections, we discuss some of the biological effects of Cdc42 on regulating cell–cell interaction and adhesion, in the seminiferous epithelium and other epithelia, highlighting areas of research that deserve attention in future studies.

2.1. Mediating the action of transforming growth factor-βs (e.g., TGF-β3) in the seminiferous epithelium of adult rat testes

Recent studies have illustrated the crucial role of Cdc42 in mediating the action of transforming growth factor-β (TGF-β) in the testis regarding its effects on junction dynamics in the seminiferous epithelium during spermatogenesis via cross talk with other signaling molecules (Fig. 7.4). Figure 7.4 depicts the three signaling pathways downstream of TGF-βs following the activation of TGF-β2 or TGF-β3 with their receptors at the Sertoli cell membrane. For instance, using the cadmium model to study cell-cell interactions in the testis which is known to induce cell adhesion disruption in the seminiferous epithelium in particular at the Sertoli-Sertoli (e.g., the BTB) and Sertoli-germ cell (e.g., the apical ES) interface (Wong et al., 2004); it has been shown that treatment of rats with cadmium chloride can induce TGF-β3 (Wong et al., 2005). It also activates the Cdc42/JNK pathway downstream of TGF-β3 which leads to an increase in the steady-state level of α_2-macroglobulin (a non-specific protease inhibitor) in the seminiferous epithelium, limiting unwanted proteolysis following a surge of protease activities (e.g., cathepsin L)

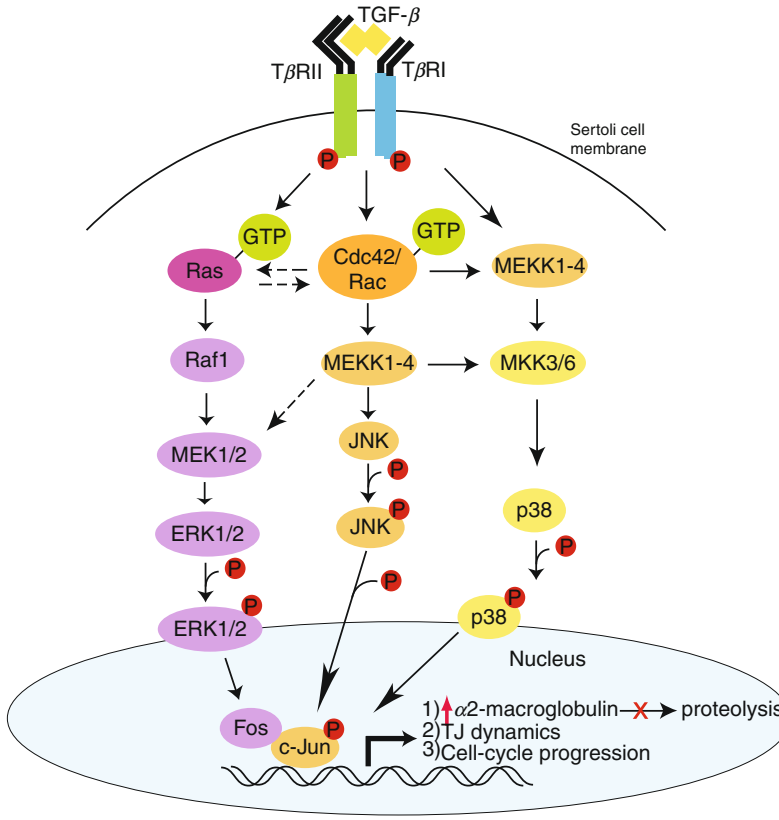

Figure 7.4 The TGF-β-mediated signaling function in epithelia including the seminiferous epithelium of adult rat testes. Based on recent studies in the field, TGF-βs are known to regulate different cellular functions in the testis following activation of their receptors via ligand-receptor binding, such as for cell cycle progression in germ cells, TJ dynamics, and α2-macroglobulin production, via ERK, p38 MAP or JNK (black arrows). This schematic diagram illustrates the significance of Cdc42 in TGF-βs-mediated signaling function since this GTPase regulates not only the JNK signaling pathway downstream, also the ERK1/2 and p38 MAPK pathways via its cross talk with Ras and MEK1/2 (hatched arrows) or its direct effects on MEKK1-4 and MKK3/6 (black arrows).

(Wong et al., 2005). This pathway perhaps is also needed to regulate phagocytosis of residual bodies and/or apoptotic germ cells by the Sertoli cell to limit unwanted proteolysis in the seminiferous epithelium, illustrating the significance of Cdc42 in these events. It was also reported that an activation of ERK1/2 via the action of TGF-β3 would limit the anchoring junction restructuring at the Sertoli–germ cell interface, inducing changes in Sertoli–germ cell interactions, without affecting the BTB integrity (Xia and Cheng, 2005; Xia et al., 2006). But since there is cross talk between Cdc42 and Ras

(Fig. 7.4) (for a review, see Boutros et al., 2008), Cdc42 can thus mediate the TGF-β3-induced ERK1/2 activation to affect germ cell adhesion in the seminiferous epithelium. Additionally, TGF-β3 was also shown to regulate BTB dynamics and germ cell adhesion via an activation of p38 MAPK (Fig. 7.4) and via the cross talk between Cdc42/Rac, Ras, and MEKK1-4 (Boutros et al., 2008) (Fig. 7.4), Cdc42 thus also plays a role in regulating BTB and anchoring junction dynamics (Lui et al., 2003c; Xia et al., 2006). Taken collectively, the findings summarized in Fig. 7.4 illustrate the critical role of Cdc42 in mediating TGF-β-based actions and other cellular events in the testis via its direct effects on JNK and/or indirect effects on ERK1/2 and p38 MAPK via cross talk with upstream MEKK1–4, MEK1/2, and MKK3/6 (Fig. 7.4) (Boutros et al., 2008).

2.2. Regulation of filopodia formation

Among the numerous cellular processes that Cdc42 regulates, actin cytoskeleton dynamic and filopodia formation are the best documented. Filopodia are thin, finger-like cytoplasmic protrusions which contain parallel bundles of filamentous-(F-) actin. They are found at the leading edge of migrating cells such as fibroblasts and tumor cells and have important implication in wound healing and formation of cell–cell contact (Chhabra and Higgs, 2007; Gupton and Gertler, 2007; Mattila and Lappalainen, 2008). Activated Cdc42 stimulates the initiation and elongation of actin filament and causes the extension of filopodia. These protruded filopodia, in turn, align opposing cells and adhere them together, leading to the formation of cell junctions (Chhabra and Higgs, 2007; Gupton and Gertler, 2007; Mattila and Lappalainen, 2008; Vasioukhin et al., 2000). This suggests that activation of Cdc42 might enhance cell–cell adhesion via increasing the number of filopodia. Consistent with this postulation, several studies have shown that overexpression of a constitutively active mutant of Cdc42 induces cell–cell contact and strengthens cell–cell adhesion (Kodama et al., 1999; Rojas et al., 2001; Stoffler et al., 1998). In addition, by using electron microscopy, these cells have been shown to have extended cell junctions with the cell membrane fused along the lateral borders (Kodama et al., 1999; Rojas et al., 2001). It has been suggested that Cdc42 affects the rate of AJ and TJ formation based on studies using the calcium switch model (Fukuhara et al., 2003). Induced activation of Cdc42 increases the velocities of junction formation after calcium switch. Conversely, specific inhibition of Cdc42 by overexpressing the Cdc42 and Rac interactive binding (CRIB) domain of neural Wiskott–Aldrich syndrome protein (NWASP) (NWASP–CRIB) (Takenawa and Miki, 2001) delays AJ and TJ formation (Fukuhara et al., 2003). Besides, activation of Cdc42 protects cells from hepatocyte growth factor (HGF) and 12-*O*-tetradecanoylphorbol-13-acetate (TPA)-induced junction disruption (Kodama et al., 1999). Collectively, these

results show that activation of Cdc42 facilitates the formation of cell–cell adhesion. Interestingly, it has been reported that higher amount of activated Cdc42 is required for the assembly of claudin-based TJ than that of E-cadherin-based AJ (Fukuhara et al., 2003). A possible explanation is that low level of activated Cdc42 is able to recruit AJ effectors, which has a lower affinity for activated Cdc42 (Garrard et al., 2003). Subsequently, as mature AJ forms, more Cdc42 is activated by AJ proteins such as nectins (Honda et al., 2003; Kawakatsu et al., 2002) which is required to recruit TJ effectors for TJ assembly (Fukuhara et al., 2003). In the seminiferous epithelium of rat testes, filopodia *per se* are not visible in Sertoli cells even though isolated Sertoli cells in culture are highly motile cells and are capable of migrating across the pores of the bicameral units (Mruk et al., 1997, 2003). They also have "finger-like" structures which resemble filopodia when Sertoli cells are cultured *in vitro* (Lee and Cheng, 2003; Siu et al., 2005). Nevertheless, Sertoli cells *in vivo* form "finger-like" cytoplasmic processes and/or structures which "hold" up to 30–50 germ cells to support their development at various stages (Weber et al., 1983). It is highly likely that Cdc42 regulates the formation of these "finger-like" structures in the seminiferous epithelium *in vivo* which are similar to filopodia in other epithelia. This postulation is supported by recent studies using immunohistochemistry which shows that Cdc42 is localized in the entire seminiferous epithelium illustrating its possible involvement in new junction assembly between Sertoli cells and developing germ cells (Wong et al., 2009b). However, Cdc42 is predominantly localized at the BTB in virtually all stages of the epithelial cycle except at stage VIII when BTB undergoes restructuring to facilitate the transit of primary preleptotene spermatocytes (Wong et al., 2009b). Work is needed in future studies to assess if component proteins of the filopodia, such as enabled/vasodilator-stimulated phosphoprotein (ENA/VASP) family proteins (Mattila and Lappalainen, 2008), are found in the seminiferous epithelium, and if Cdc42 regulates their function.

2.3. Cdc42 in protein trafficking

Epithelial cells, including Sertoli cells in the testes, are polarized cells with a differential distribution of plasma membrane proteins and macromolecules, which, in turn, are separated into the apical and basolateral domains by the TJs. The presence of TJs acts as a barrier to prevent the free diffusion of the plasma membrane components between the apical and basolateral domains (Shin et al., 2006). Therefore, the establishment and maintenance of cell polarity and cell junctions are intimately related. On the other hand, polarized distribution of plasma membrane components is highly regulated by the biosynthetic, endocytic, recycling, and transcytotic mechanisms in cells (Duffield et al., 2008; Mellman and Nelson, 2008; Zahraoui et al., 2000).

The involvement of Cdc42 in cell polarity and protein trafficking was initially reported in yeast. For instance, Cdc42 mutants are defective in budding. Instead, they continue to grow into large spherical cells which failed to display polarized protein secretion and asymmetric distribution of actin cytoskeleton which are necessary for budding (Adams et al., 1990). Subsequent studies in mammalian cells revealed that Cdc42 also plays a central role in establishing cell polarity and directed protein trafficking (Cerione, 2004; Etienne-Manneville, 2004; Jaffe and Hall, 2005). Membranous or secretory proteins are budded into secretory vesicles from the *trans*-Golgi network (TGN). Initial protein sorting is carried out in the TGN and common recycling endosomes (Ang et al., 2004; Rodriguez-Boulan et al., 2005). Proteins which are targeted to the apical or basolateral domains are exocytosed to the cell surface. Exocyst complex, which is composed of eight evolutionarily conserved proteins, is present to tether, dock, and fuse the post-Golgi secretory vesicles at the specific sites in the plasma membrane (Wu et al., 2008). Transcytosis also plays a significant role in mediating the transport of proteins between different compartments of the cell (Leyt et al., 2007; Polishchuk et al., 2004; Tuma and Hubbard, 2003). At the same time, proteins are continuously endocytosed and recycled back to the plasma membrane (Doherty and McMahon, 2009).

In 1999, Mellman and colleagues reported that Cdc42 is functionally linked to protein trafficking in mammalian epithelia cells. In particular, it is essential to target newly synthesized proteins to the basolateral region of cells. At the same time, recycling of basolateral proteins is also controlled by Cdc42 (Kroschewski et al., 1999). Subsequent studies confirmed Cdc42's role in regulating the basolateral protein trafficking. It was found that constitutive activation or inactivation of Cdc42 leads to the mislocalization of basolateral membrane markers vesicular stomatitis virus G protein (VSVG) and low-density lipoprotein receptor (LDLR) to the apical membrane. However, the apical distribution of p75 membrane marker remains unchanged. Interestingly, activation state of Cdc42 seems to have no effect on the targeting of secretory proteins to apical (gp80/glucosaminoglycans) or basolateral (laminin/heparan sulfate proteoglycan) domains (Cohen et al., 2001). Further investigation demonstrates that Cdc42 differentially affects the rate of release of apical and basolateral proteins from the TGN. For instance, exit of apical protein p75 from the TGN is increased while the release of basolateral proteins LDLR or neuronal-cell adhesion molecule (N-CAM) is inhibited after the overexpression of dominant-active or -inactive Cdc42. These observations are possibly due to the reorganization of perinuclear/cytoplasmic actin to the cortical region of the cells, mediated by the activation of Cdc42 (Musch et al., 2001). Cdc42 is also involved in spatiotemporal activation of the exocyst complex which is required for the docking and fusion of vesicles to the plasma membrane (Wu et al., 2008). It was shown that GTP-bound Cdc42 together with phosphatidylinositol

4,5-bisphosphate recruited Sec3, one of the protein subunits of the exocyst complex, to the site of polarized growth in yeast. Recruitment of Sec3 to the bud site, in turn, activates the exocyst complex to increase the rate of polarized secretion of proteins for budding (Zhang et al., 2001, 2008). A recent paper by Sakurai-Yageta et al. (2008) demonstrates that activation of Cdc42 induces the interaction between its downstream effector IQGAP1 and Sec3/Sec8 exocyst subunits in breast adenocarcinoma cells. This interaction is necessary for the exocytosis of membrane type 1-metalloproteinase (MT1-MMP) to degrade ECM which promotes the invasive characteristic of tumor cells.

Endocytosis is another event of vesicular trafficking which is tightly regulated by Cdc42. In *Drosophila* neuroectodermal epithelium, Cdc42 regulates vesicular trafficking by inhibiting the endocytosis of apical proteins from the plasma membrane. Overexpression of dominant-negative Cdc42 results in an enhanced endocytic uptake of AJ proteins such as *Drosophila* epithelial-cadherin (DE-cadherin) and Armadillo (*Drosophila* β-catenin, Arm) as well as apical polarity proteins such as Crumbs (Crb). The endocytosed apical proteins are found accumulated in enlarged endosomal compartments, illustrating that inhibition of Cdc42 activity also blocks the transport of apical proteins from early to late endosomes (Harris and Tepass, 2008). Interestingly, regulation of endocytosis by Cdc42 is reversed in the *Drosophila* dorsal thorax epithelium where Cdc42 promotes endocytosis (Georgiou et al., 2008; Leibfried et al., 2008). Both studies show that deletion of Cdc42 blocks endocytosis. Disruption in the localization of E-cadherin and Arm was observed (Georgiou et al., 2008; Leibfried et al., 2008) but not basolateral marker lethal giant larvae (Lgl) (Leibfried et al., 2008). Studies by electron and fluorescent microscopy revealed the presence of elongated tubular extensions from the plasma membrane. Furthermore, when stained with an antibody against the extracellular domain of E-cadherin in fixed but nonpermeabilized cells, these tubular structures were shown to contain cell surface E-cadherin, indicating a defect in vesicle scission from the plasma membrane during endocytosis (Georgiou et al., 2008; Leibfried et al., 2008). The observed discrepancies in endocytosis regulation might be ascribed to the fact that Cdc42 works together with Bazooka (*Drosophila* Par3) to regulate endocytosis in neuroectoderm (Harris and Tepass, 2008) while this regulation is independent of Bazooka in dorsal thorax epithelium (Georgiou et al., 2008; Leibfried et al., 2008).

In a genome-wide search for genes regulating endocytosis, Cdc42 as well as Par6 are found to be two conserved endocytic regulators in *Caenorhabditis elegans* and mammalian cells. Further analysis shows that the blockade in endocytosis by expressing dominant-negative mutants of Par6 or Cdc42 is likely due to the disruption of recycling endosomes. In addition, Par6 and Cdc42 differentially regulate the uptake and recycling of clathrin-independent or clathrin-dependent cargo proteins, illustrating that clathrin

also actively participates in this Par6/Cdc42-mediated endocytosis (Balklava et al., 2007). By using a cell-free endocytosis assay system, it has been reported that trans-interaction of E-cadherin activates Cdc42 which, in turn, inhibits the endocytosis of trans-interacting E-cadherin via the F-actin linking activity of IQGAP1 (Izumi et al., 2004). AJ-enriched membrane fraction from liver is used in the cell-free assay system to study endocytosis, instead of the traditionally used biotinylation of cell surface proteins (Le et al., 1999) or labeling of cell surface protein by using antibody which targets the extracellular domain of protein (Georgiou et al., 2008). Although it was found that TJ proteins such as claudin-1 and occludin are not endocytosed in the cell-free assay system, which is in contrast to recently published reports which show that TJ proteins are continuously endocytosed (Matsuda et al., 2004; Shen et al., 2008a), this assay still is a valuable tool which provides easy manipulation to characterize individual factors which are involved in endocytosis. A recent report has also demonstrated the role of Cdc42 in mediating cytokine-induced acceleration in protein endocytosis at the Sertoli cell BTB (Wong et al., 2009b). For instance, overexpression of dominant-negative Cdc42 in Sertoli cells with an established TJ-permeability barrier was shown to abolish the TGF-β3-mediated acceleration of protein endocytosis, such as occludin (Wong et al., 2009b).

2.4. Effects on actin cytoskeleton

Cdc42 is a well-known actin regulator. Cdc42 regulates actin polymerization via: (i) WASPs/actin-related protein2/3(Arp2/3), (ii) formins/mammalian diaphanous (mDia), and (iii) LIM kinase (LIMK)/Rho kinase (ROCK)/cofilin (Jaffe and Hall, 2005; Ridley, 2006). Since several recent reviews and/or reports are in the literature including studies in the testes which discuss the regulation of actin by Cdc42 via these protein complexes (Heasman and Ridley, 2008; Jaffe and Hall, 2005; Lui et al., 2003a,b; Ridley, 2006; Witte and Bradke, 2008), we focus on highlighting how Cdc42 affects cell junctions and vesicular trafficking via its effects on actin dynamics.

Actin cytoskeleton is involved in regulating multiple events in vesicular formation and transport. It is involved in the budding and scission of vesicles from both the TGN (exocytic vesicles) and plasma membrane (endocytic vesicles) (Merrifield et al., 2002). It also facilitates the docking and fusion of secretory vesicles to the plasma membrane, especially to the basolateral membrane (Rodriguez-Boulan et al., 2005). Consistent with this functional role, Cdc42 is known to regulate exocytosis to the basolateral region (Cohen et al., 2001; Kroschewski et al., 1999). Finally, it also serves as the track for myosin-driven vesicles to move within the cell. In addition, it is known that Cdc42 regulates endocytosis in the dorsal thorax epithelium of *Drosophila* pupae via the WASP/Arp2/3 and dynamin (Georgiou et al., 2008; Leibfried

et al., 2008). Collectively, these studies illustrate how Cdc42 regulates vesicle scission and trafficking via its effects on actin dynamics.

Interestingly, it was found that Cdc42 regulates cell tension and cell shape by altering the distribution of actin (Musch et al., 2001; Otani et al., 2006) and E-cadherin (Otani et al., 2006). Activation of Cdc42 causes redistribution of actin from the perinuclear/cytoplasmic region to the cortical region, leading to the rounding of cells (Musch et al., 2001). Similarly, Tuba, a Cdc42-specific GEF, also helps in maintaining the normal tension in cells by activating Cdc42 which, in turn, regulates N-WASP to control the distribution of actin and E-cadherin (Otani et al., 2006).

2.5. Ubiquitination of junction proteins

Ubiquitination is an important mechanism to control the homeostasis of transmembrane proteins in epithelia by regulating protein endocytosis and degradation in the lysosomes (d'Azzo et al., 2005; Lui and Cheng, 2007; Reyes-Turcu et al., 2009). Through a three-step enzymatic reaction, which is carried out by (1) ubiquitin-activating enzyme (E1), (2) ubiquitin-conjugating enzyme (E2), and (3) ubiquitin ligase (E3), ubiquitin, a small globular protein is added onto the target protein (monoubiquitination). More ubiquitin proteins can be conjugated onto existing ubiquitin to form a polyubiquitin chains on the target protein (polyubiquitination). Apart from degradation of misfolded proteins, recent studies have shown that ubiquitination, particularly monoubiquitination, is also involved in regulating the homeostasis of normal cellular proteins via protein trafficking of endocytosed proteins since ubiquitinated proteins can be recycled back to cell surface via the endosome-mediated sorting mechanism (Berthouze et al., 2009; d'Azzo et al., 2005; Haugsten et al., 2008; Huang et al., 2009). Ubiquitinated proteins can be recognized by downstream effector proteins containing ubiquitin-binding domains which, in turn, activate protein endocytosis and degradation (Chen and Sun, 2009; Hicke and Dunn, 2003; Pickart and Fushman, 2004). For instance, it is known that Hakai, a c-Cbl like E3 ubiquitin ligase, ubiquitinates E-cadherin and leads to its endocytosis and degradation (Fujita et al., 2002). Subsequent study in MDCK cells reveals that Cdc42 is one of the upstream signaling molecules regulating the ubiquitination of E-cadherin via Hakai (Shen et al., 2008b). By depleting the calcium level in the culture environment, it causes the endocytosis and degradation of E-cadherin. It was found that Cdc42 was first activated after calcium depletion. Cdc42 activation, in turn, stimulated the epidermal growth factor receptor (EGFR) signaling pathway, which phosphorylated Src kinase and E-cadherin, leading to the binding of Hakai. Instead of recycling back to cell surface, E-cadherin was shown to be targeted to the lysosomes for degradation (Shen et al., 2008b). Since recent studies have shown that cytokine-induced transient BTB disruption, such as by TGF-β2, TGF-β3, and TNFα, is mediated via enhanced

endocytosis of integral membrane proteins at the BTB (Xia et al., 2009; Yan et al., 2008a), it remains to be determined if these endocytosed proteins are ubiquitinated, perhaps mediated by Cdc42, so that they can be targeted to late endosome for intracellular degradation, thereby compromising the BTB integrity.

2.6. Assembly and maintenance of epithelial apico-basal cell polarity

The roles of Rho GTPases, in particular Cdc42, in the formation and maintenance of apico-basal cell polarity in epithelia by working in concert with the Par-based polarity protein complex has been intensively investigated in recent years (Iden and Collard, 2008; Yamada and Nelson, 2007). Mammalian Par3/Par6/aPKC complex binds to activated Cdc42 via the semi-CRIB domain in Par6 (Joberty et al., 2000; Lin et al., 2000). Binding of activated Cdc42 to Par6 induces a conformational change in the C-terminal postsynaptic density-95/disks large/zonula occludens-1 (PDZ) domain of Par6, increasing its affinity for downstream mediators (Garrard et al., 2003; Peterson et al., 2004). For instance, binding of GTP-bound Cdc42 to Par6 enhances the kinase activity of aPKC (Yamanaka et al., 2001). This event can activate the Crumbs- and Scribble-based polarity complexes, recruiting them to the TJ site and also phosphorylating downstream target proteins, whose identities remain unknown to date (Iden and Collard, 2008). This process, however, leads to polarization and maturation of the epithelium into fully polarized epithelium. It remains to be determined the target proteins downstream of the Cdc42/Par3/Par6/aPKC protein complex in the Sertoli cell that help to cause cell polarization in the seminiferous epithelium. However, recent studies have shown that JAMs and Src kinases are likely involved in this event (Wong et al., 2008b).

3. Polarity Proteins and Cell–Cell Interactions in the Testis

In epithelia, including the seminiferous epithelium of adult mammalian testes, the differential distribution of cellular proteins and macromolecules along the apical and basolateral membrane domains, which is maintained by the ''fence function'' conferred by TJ, causes the establishment of the apical and basal polarity between adjacent epithelial cells (Mruk and Cheng, 2004; Shin et al., 2006; Yeaman et al., 1999). Earlier genetic and biochemical analyses based on studies in *Drosophila melanogaster* and *C. elegans* have identified three protein complexes that are known to be involved in determining cell polarity (Assemat et al., 2008), and subsequent

studies have also confirmed the roles of these highly conserved proteins in conferring polarity in mammalian cells: (1) the Crumbs (CRB) protein complex (Bazellieres et al., 2009; Makarova et al., 2003; Wong et al., 2008a), (2) the partitioning-defective (Par) protein complex (Assemat et al., 2008; Goldstein and Macara, 2007; Wong et al., 2008a), and (3) the Scribble complex (Nakagawa and Huibregtse, 2000; Santoni et al., 2002) (Fig. 7.5) (Table 7.2).

3.1. The Crumbs (CRB) protein complex

The CRB3/protein associated with Lin-7 1 (Pals1)/Pals1 associated tight junction protein (PATJ) polarity protein complex in mammalian cells, including Sertoli and germ cells in the testis, is the homologue of the *Drosophila* CRB/Stardust/DmPATJ complex (Wong et al., 2008a) (Table 7.2). There are three isoforms of integral membrane protein CRB in mammals, known as CRB1, CRB2, and CRB3, with CRB3 expressed predominantly in epithelial cells (Makarova et al., 2003). Interestingly, the expression of CRB3 in germ cells is higher than that in Sertoli cells in rat testes (Wong et al., 2008b). Pals1 is a membrane-associated guanylate kinase (MAGUK) protein. Similar to zonula occludens-1 (ZO-1, an adaptor at

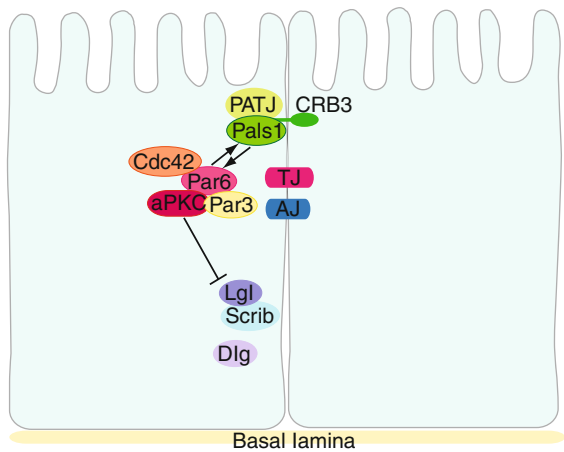

Figure 7.5 The three highly conserved polarity protein complexes: the partitioning defective (PAR), Crumbs (CRB) and Scribble complexes, that are found in multiple epithelia including the seminiferous epithelium in rat testes. Many components of these proteins are also found in germ cells in the seminiferous epithelium. Interaction between Par6 and Pals1 provides cross talk between the CRB and Par complexes (black arrows). aPKC is a crucial component in the polarity protein complexes which provides cross talk between the three conserved polarity complexes. Phosphorylation of Lgl by aPKC maintains the Scribble complex at the basolateral domain (solid line bars).

Table 7.2 Components of the Crumbs (CRB), partitioning-defective (PAR), and Scribble complexes in mammalian cells

Polarity complex	Component proteins	Protein type	Apparent molecular weight (kDa)[a]	References
CRB	CRB3[b]	Transmembrane	24	Makarova et al. (2003), Wong et al. (2008b)
	Pals1	Cytoplasmic	77	Wong et al. (2008b)
	PATJ	Cytoplasmic	55, 100	Wong et al. (2008b)
Par	Par3	Cytoplasmic	100, 150, 180	Fujita et al. (2007), Lin et al. (2000), Wong et al. (2008b)
	Par6	Cytoplasmic	37, 45, 60	Cline and Nelson (2007), Wong et al. (2008b), Yamanaka et al. (2003)
	aPKC	Cytoplasmic	80	Wong et al. (2008b)
	Cdc42	Cytoplasmic	22	Gliki et al. (2004), Lui et al. (2003b, 2005)
	14-3-3	Cytoplasmic	30	Chaudhary and Skinner (2000), Perego and Berruti (1997), Wong et al. (2009a)
Scribble	Scrib	Cytoplasmic	175	Assemat et al. (2008)
	Lgl1/2	Cytoplasmic	113, 115	Assemat et al. (2008)
	Dlg1-4	Cytoplasmic	80–200	Assemat et al. (2008)

[a] Apparent molecular weight denoted here is mostly based on studies in the testis (Wong et al., 2008b, 2009a). It was found that the molecular weight of PATJ is different from some of the published results which is 75–230 kDa (Lemmers et al., 2002). However, it should be noted that in the testis, a smaller mRNA transcript of 4.1 kb is detected besides the 7 kb transcript which is detected in other tissues such as small intestine and heart (Lemmers et al., 2002). Thus, it is possible that PATJ protein of smaller molecular weight is detected in the testis. Molecular weight of components of the Scribble complex is based on studies in other epithelia since not much research has been carried out in the testis.

[b] CRB3, Crumbs3; Pals1, protein associated with Lin-7 1; PATJ, Pals1 associated tight junction protein; Par3, partitioning-defective3; Par6, partitioning-defective6; aPKC, atypical protein kinase C; Cdc42, cell cycle division 42; Scrib, Scribble; Lgl1/2, lethal giant larvae1/2; Dlg1-5, discs large1-5.

TJ), Pals1 possesses a guanylate kinase (GUK) domain but it has no intrinsic catalytic activity; however, it interacts with a number of peripheral proteins via its PDZ domain, including CRB3 and Par6 (Makarova et al., 2003; Roh et al., 2002b). The interaction between Pals1 and Par6 also provides cross talk between the Par and CRB complexes (Hurd et al., 2003b; Wang et al., 2004). PATJ is a scaffolding protein with multiple PDZ domains, as such it is capable of interacting with several proteins at the TJ, including claudin-1 and ZO-3 (Roh et al., 2002a). Both Pals1 and PATJ are found in Sertoli and germ cells in rat testes with their expression more predominant in germ cells than Sertoli cells, analogous to CRB3 (Wong et al., 2008b). These findings illustrate that the CRB polarity protein complex is present in the seminiferous epithelium and it is an integrated complex of both Sertoli and germ cells (Fig. 7.5). In addition, cross talk between the CRB and Par complexes is crucial in regulating the adhesion of germ cells onto the Sertoli cell in the seminiferous epithelium (Wong et al., 2008b). Similar to Par6 and Cdc42, members of the CRB complex have been implicated in the protein trafficking process. Knockdown of Pals1 leads to defect in AJ formation, seemingly due to a disruption in E-cadherin exocytosis after the depletion of Pals1 (Wang et al., 2007). Furthermore, Pals1 and PATJ are found interacting with Rich1/angiomotin complex, a complex which was thought to be important in targeting membrane proteins to TJ sites (Wells et al., 2006).

3.2. The partitioning-defective (Par) protein complex

The Par3/Par6 proteins were first identified in *C. elegans* which regulates anterior–posterior polarity in zygote (Kemphues et al., 1988). The Par3/Par6 proteins form a conserved complex with GTP-Cdc42 and atypical protein kinase C (aPKC) (Assemat et al., 2008; Wong et al., 2008a) (Fig. 7.5) and several other protein components (Table 7.2). In mammals, Par6 serves as a crucial adaptor, recruiting Par3, active Cdc42/Rac1 and aPKC to facilitate TJ assembly (Joberty et al., 2000; Lin et al., 2000). aPKC, besides activating Par3 via phosphorylation, also activates CRB3 in the CRB protein complex and Scribble in the Scribble complex, illustrating that it plays a crucial role to maintain cross talk between the three polarity protein complexes in different epithelia (Iden and Collard, 2008). In the testis, Par3, Par6, Cdc42, and aPKC have been identified in Sertoli and germ cells (Fujita et al., 2007; Gliki et al., 2004; Lui et al., 2003b; Wong et al., 2008b). Using immunohistochemistry and dual-labeled immunofluorescence analysis, Par6 is localized both at the basal ES/TJ at the BTB and apical ES at the spermatid–Sertoli cell interface, colocalizing with occludin, N-cadherin, and γ-catenin at the BTB and with nectin-3 at the apical ES. Besides, its expression is greatly diminished at both BTB and apical ES at stage VIII of the epithelial cycle during BTB restructuring and spermiation

(Wong et al., 2008b). More importantly, the loss of Par6 at the apical ES was shown to associate with a loss of orientation of the elongating spermatids in the seminiferous epithelium (Wong et al., 2008b). A study by coimmunoprecipitation has demonstrated that the Par6-based polarity complex plays a crucial role to regulate adhesion of elongating/elongated spermatids to the Sertoli cell in the seminiferous epithelium via a novel mechanism. Par6/Pals1 forms a complex with JAM-C in both Sertoli cells and spermatids to allow the homotypic interaction between JAM-C to confer adhesion of spermatids in the seminiferous epithelium in all epithelial stages except at stage VIII (Wong et al., 2008b). At the late stage VIII or when spermatids are induced to leave the seminiferous epithelium by adjudin [1-(2,4-dichlorobenzyl)-1H-indazole-3-carbohydrazide], the Par6/Pals1 complex becomes tightly associated with Src kinase, "pulling" the Par6/Pals1 complex away from JAM-C, thus destabilizing the JAM-C-based adhesion function. This, in turn, disrupts the apical ES to facilitate spermiation (Wong et al., 2008b). Additionally, the knockdown of Par6 or Par3 leads to a redistribution of JAM-A and α-catenin at the Sertoli—Sertoli cell interface, destabilizing the TJ-permeability barrier function, leading to transient disruption of the BTB integrity (Wong et al., 2008b). These findings thus demonstrate unequivocally the significance of Par6 in conferring adhesion and polarity function at the BTB and apical ES. Furthermore, these data also illustrate that the Par6-based polarity complex serves as the molecular "switch" which coordinates the events of spermiation and BTB restructuring at stage VIII of the epithelial cycle (see Section 4).

3.3. The Scribble protein complex

The mammalian Scribble complex, which consists of Scribble (Scrib, also known as Vartul), disks large (Dlg1-5) and lethal giant larvae (Lgl1/2), are localized at the basolateral domain of epithelial cells (Assemat et al., 2008; Yamanaka and Ohno, 2008) (Table 7.2) (Fig. 7.5). Initial studies in *D. melanogaster* revealed that they are tumor suppressor genes as their deletions lead to overproliferation and outgrowth of tissue. Subsequent studies in mammalian cells showed that the Scribble complex is associated with tumorigenesis in mammals, possibly via their interaction with tumor suppressor genes such as adenomatous polyposis coli (APC) (Etienne-Manneville et al., 2005; Matsumine et al., 1996). Binding of Lgl and Par3 to Par6/aPKC complex is mutually exclusive. Phosphorylation of Lgl by aPKC segregates it from Par6/aPKC complex, thus allowing the binding of Par3 and localization of Par3/Par6/aPKC at the apical domain; at the same time, basolateral localization of Lgl is also maintained. Thus, kinase activity of aPKC plays an essential role in establishing and maintaining the antagonistic interactions between the apical Par complex and basolateral Scribble complex (Yamanaka et al., 2003). In MDCK cells, Scrib was shown to be involved in regulating E-cadherin-mediated cell–cell adhesion,

via stabilizing interaction between E-cadherin and α-catenin (Qin et al., 2005). While members of the Scribble complex are shown to express in the testis, such as Lgl2 (Assemat et al., 2008), however, their functional roles in spermatogenesis remain to be clarified.

3.4. 14-3-3 proteins

As briefly discussed earlier, there are three major polarity protein complexes in epithelia, two of which, namely the CRB- and Par-based polarity complexes, have been identified and functionally studied in mammalian testes (Fujita et al., 2007; Gliki et al., 2004; Lui et al., 2003b; Wong et al., 2008b). Furthermore, recent functional studies have illustrated the significance of some of their component proteins in cell adhesion and BTB function in the testis (Wong et al., 2008a,b). Herein, we switch our focus on 14-3-3 proteins, which are the homologues of *C. elegans* Par5 in mammalian cells (Morton et al., 2002), since recent studies have illustrated the importance of 14-3-3 proteins in spermatogenesis (Wong et al., 2009a).

14-3-3 proteins are a family of small (~ 30 kDa) acidic proteins which are expressed in all eukaryotic cells (Aitken, 2006; Morrison, 2009; Sun et al., 2009) including Sertoli and germ cells (Chaudhary and Skinner, 2000; Perego and Berruti, 1997; Wong et al., 2009a). The name "14-3-3" is used to describe the elution and migration pattern of this group of proteins on two-dimensional DEAE-cellulose chromatography and starch gel electrophoresis from which they were initially isolated from mammalian brain (Aitken, 2006; Morrison, 2009; Sun et al., 2009). To date, seven isoforms of 14-3-3 are found in mammals namely β, ε, η, γ, τ/θ, ζ, and σ (Aitken, 2006; Bridges and Moorhead, 2005; Muslin and Lau, 2005). Binding of 14-3-3s to target proteins is mostly phosphorylation dependent, where they recognize conserved phosphoserine/phosphothreonine containing motifs in target proteins (Aitken, 2006; Bridges and Moorhead, 2005). However, 14-3-3s can also bind to unphosphorylated domains in target proteins (Waterman et al., 1998).

Through binding to over 200 target proteins, 14-3-3s are involved in diverse cellular processes such as cell-cycle control, protein transcription, protein trafficking, and DNA repair (Jin et al., 2004; Pozuelo Rubio et al., 2004). 14-3-3s are thought to be regulated by phosphorylation to form homo- or heterodimers (Aitken, 2006; Woodcock et al., 2003). They function as scaffolding proteins to colocalize target proteins in close proximity to facilitate phosphorylation or enzymatic activity to occur. Functional domains on target proteins can be masked upon 14-3-3s binding to prevent interaction with other effector proteins. The binding of 14-3-3s onto their target proteins can also induce changes in protein conformation, thereby modulating their activities (Bridges and Moorhead, 2005).

Besides binding to the conserved phosphoserine/phosphothreonine containing motifs, 14-3-3s were found to recognize a dibasic motif in

several cell surface channel proteins (Mrowiec and Schwappach, 2006; Shikano et al., 2006). For instance, KCNK3 (potassium channel, subfamily K, member 3 which is a member of the superfamily of potassium channel proteins) was found to contain two trafficking signals: one for β-COP, a component of coat protein complex I (COPI) and one for 14-3-3β. Binding of β-COP and 14-3-3β to KCNK3 is mutually exclusive. Phosphorylation of KCNK3 favors the binding of 14-3-3β which overwrites the retention signal of β-COP to maintain channel in endoplasmic reticulum (ER). As a result, KCNK3 are transported to the plasma membrane (O'Kelly et al., 2002). This mechanism also helps to ensure multimeric membrane proteins are fully assembled before they are transported to the cell surface (Heusser et al., 2006; Yuan et al., 2003). Along with this line of evidence, recent studies have shown that 14-3-3 regulates the kinetics of protein trafficking in Sertoli cells with an established TJ-permeability barrier (Wong et al., 2009a). It was shown that multiple isoforms of 14-3-3 are found in both Sertoli and germ cells including 14-3-3 α, β, θ, γ, δ, and ζ (Chaudhary and Skinner, 2000; Perego and Berruti, 1997; Wong et al., 2009a), with germ cells express relatively more 14-3-3 than Sertoli cells (Wong et al., 2009a). Knockdown of 14-3-3θ by RNAi leads to a loss of cell adhesion function at the Sertoli cell BTB, which is resulted from a mislocalization of N-cadherin and ZO-1, but not α- and β-catenins, at the Sertoli–Sertoli cell interface. Such changes in protein localization were shown to be mediated via changes in the kinetics of protein endocytosis by enhancing the internalization of JAM-A and N-cadherin in Sertoli cells with an established TJ-permeability barrier (Wong et al., 2009a). Studies by immunohistochemistry and dual-labeled immunofluorescence analysis have demonstrated the localization of 14-3-3θ at the apical ES and BTB in adult rat testes (Wong et al., 2009a). Furthermore, a considerable loss of 14-3-3θ at the apical ES was detected prior to spermiation, illustrating that 14-3-3θ is likely to be involved in the maintenance of the apical ES function (Wong et al., 2009a). In short, these findings illustrate the crucial regulatory role of 14-3-3 in the testis during spermatogenesis at both the apical ES and BTB. Thus we speculate that similar to Par6, 14-3-3 perhaps also serves as a molecular "switch" to coordinate the events of spermiation and BTB restructuring that take place simultaneously at the opposite ends of the seminiferous epithelium at stage VIII of the epithelial cycle.

Phosphorylation of integral membrane proteins and their peripheral adaptors is an important biochemical process to control TJ and AJ functions, such as by regulating the subcellular localization of TJ and AJ proteins (Gonzalez-Mariscal et al., 2008; Nelson, 2008; Sallee et al., 2006). 14-3-3s are involved in this process by interacting with Raf, the central downstream effector of Ras GTPases (Hekman et al., 2004; Light et al., 2002). Activation of Ras by growth factors such as epidermal growth factor (EGF) phosphorylates C-Raf, causing its translocation from cytosol to the plasma membrane. Binding of 14-3-3 to

C-Raf counteracts this activation, eventually leading to the concentration of cadherins and β-catenin at the cell–cell interface (Rajalingam and Rudel, 2005; Rajalingam et al., 2005). Apart from regulating the localization of TJ and AJ proteins, 14-3-3 also regulates cell junction function by controlling the degradation of junction proteins by the proteasome. Human immunodeficiency virus-1 (HIV-1) crosses the blood–brain barrier (BBB) by downregulating the levels of TJ proteins of endothelial cells that constitute the BBB via neurotoxic viral proteins gp120 and Tat (Andras et al., 2003; Kanmogne et al., 2005). Further investigation shows that HIV-1 gp120 enhances the degradation of TJ proteins mediated by the proteasome pathway. Interestingly, silencing of 14-3-3τ (also termed θ) accelerates the gp120-mediated TJ proteins degradation, indicating that the presence of 14-3-3τ protects the endothelial cells by maintaining the integrity of the TJ (Nakamuta et al., 2008). To this end, it is not known if the disappearance of 14-3-3θ at the apical ES prior to spermiation or when 14-3-3θ is knocked down in Sertoli cells by RNAi affects the degradation of TJ or AJ proteins besides protein endocytosis. Further analysis will be needed to resolve this issue.

Several studies suggest that 14-3-3s are central mediators involved in integrin-regulated cell adhesion/migration and cytoskeleton dynamics. In a yeast two-hybrid screen, 14-3-3β was found to bind to the β subunit of integrin in a phosphorylation-independent manner (Han et al., 2001). On the other hand, 14-3-3s also bind to phosphorylated cytoplasmic domain of β2-integrin (Fagerholm et al., 2002). Overexpression of 14-3-3β increases integrin-mediated cell spreading and migration when cells were plated on fibronectin (Han et al., 2001). Conversely, by making use of the interaction between 14-3-3 and another adhesion receptor glycoprotein Ib to sequester endogenous 14-3-3ζ (Du et al., 1994, 1996), it was found that integrin-mediated cell spreading was delayed. Inhibition in cell spreading is due to a block in integrin-induced Cdc42 and Rac activation, indicating that 14-3-3 may serve as mediator to transduce signal downstream of integrin (Bialkowska et al., 2003). 14-3-3 may also help to localize activated Rac to membrane ruffles (Chahdi and Sorokin, 2008; Somanath and Byzova, 2009). An interesting question raised is that overexpression of 14-3-3β does not result in tyrosine phosphorylation of focal adhesion kinase (FAK), p130cas and paxillin, three downstream signaling molecules of integrin (Han et al., 2001), despite 14-3-3ζ is known to bind to phosphorylated p130cas (Garcia-Guzman et al., 1999). It is likely that 14-3-3 acts downstream of p130cas. Furthermore, different isoforms of 14-3-3 may exhibit a distinct binding pattern and hence cellular activities. Since α6β1-integrin–laminin-333 is the major cell adhesion protein complex at the apical ES at the elongating/elongated spermatid–Sertoli cell interface in the seminiferous epithelium (Mulholland et al., 2001; Palombi et al., 1992; Salanova et al., 1995; Siu and Cheng, 2004; Yan and Cheng, 2006), and β1-integrin is also a component of the hemidesmosome in the testis (Yan et al., 2008b),

it remains to be determined if 14-3-3 plays a critical role in mediating the integrin-based signaling function at these sites during spermatogenesis, such as the breakdown of the integrin–laminin protein complex at the apical ES during spermiation, and the cross talk between hemidesmosome and BTB during BTB restructuring at stages VIII–XI of the epithelial cycle. While 14-3-3 regulates cell adhesion and spreading via integrin, it also exhibits a direct effect on actin cytoskeleton which affects the formation of membrane protrusion. 14-3-3 specifically binds to phosphorylated cofilin at Ser-3, a phosphorylation site that inactivates cofilin activity and hence actin severing and depolymerization. Binding of 14-3-3 protects phosphorylated cofilin from dephosphorylation and maintains a pool of inactive cofilin in the cells (Gohla and Bokoch, 2002).

As mentioned earlier, *C. elegans* Par5 was identified as a 14-3-3 protein. In addition, Par5/14-3-3 is thought to control the asymmetric localization of other Par proteins (Morton et al., 2002). Similar to its role in *C. elegans*, 14-3-3 is found to work together with Par proteins, which, in turn, controls cell polarity and cell adhesion in mammalian cells. 14-3-3 regulates the activity of the Par3/Par6/aPKC on cell polarity via a phosphorylation-dependent interaction with Par3. Interestingly, the interaction between 14-3-3 and Par3 does not depend on the phosphorylation of Par3 by aPKC (Hurd et al., 2003a). This result is strengthened by the observation that Par3β or Par3L, a splice variant of Par3 which lacks aPKC binding domain (Gao et al., 2002; Kohjima et al., 2002), interacts with 14-3-3 (Izaki et al., 2005). On the other hand, protein phosphatase 1α (PP1α) dephosphorylates Par3, in turn, controlling the binding between 14-3-3, Par3, and aPKC, which subsequently regulates TJ assembly (Traweger et al., 2008).

4. The Apical ES-BTB-Basement Membrane Functional Axis in the Seminiferous Epithelium that Coordinates the Cellular Events of Spermiation and BTB Restructuring During the Seminiferous Epithelial Cycle of Spermatogenesis: The Role of Polarity Proteins in Mediating the Apical ES-BTB-Basement Membrane Axis

The apical ES, once formed between step 8 spermatids and Sertoli cells, is the only anchorage device that persists through step 19 spermatids in the rat testis until spermiation (Mruk et al., 2008; Russell, 1993). Recent studies have shown that the Par polarity proteins, such as Par6 and 14-3-3θ (Par5) are found at the apical ES, likely to be used to confer spermatid orientation (Wong et al., 2008b, 2009a) even though this is a putative anchoring

junction type. This conclusion was reached based on the observations that a loss of spermatid orientation, such as by treatment of rats with adjudin to induce spermatid loss from the epithelium, is associated with a significant decline in the expression of Par6 and 14-3-3θ at the apical ES (Wong et al., 2008b, 2009a). The loss of Par6 is also associated with defragmentation of actin filament bundles at the apical ES and the loss of adhesion function at the site, illustrating polarity proteins are integrated components of the apical ES and may take part in conferring cell adhesion (Wong et al., 2008b).

A recent study has shown that biologically active laminin β3 and/or γ3 chains formed at the apical ES at spermiation can destabilize the BTB (Yan et al., 2008b). In this context, it is of interest to note that matrix metalloprotease-2 (MMP-2) (Siu and Cheng, 2004), a protease that is able to cleave laminin and is activated by membrane type 1-matrix metalloprotease (MT1-MMP), is a putative component of the apical ES that appears in $\sim$stage VI–VIII of the epithelial cycle (but considerably diminished in late stage VIII when spermiation takes place), colocalizing with the laminin γ3 chain (Siu and Cheng, 2004). We speculate that the presence of Par6 protein (Wong et al., 2008b, 2009a) or 14-3-3 is involved in targeting MT1-MMP to the apical ES, similar to the role ascribed to Cdc42 (Sakurai-Yageta et al., 2008), to activate and increase the secretion of MMP-2 such as at stage VIII of the seminiferous epithelial cycle just before spermiation to facilitate the cleavage of the laminin chains. Besides disrupting BTB integrity, it was shown that the biologically active laminin fragments generated at the apical ES also modulated BTB integrity indirectly via their effects on the hemidesmosome by reducing the steady-state level of β1-integrin at the hemidesmosome (Yan et al., 2008b). Thus, Par-based polarity proteins may play a role in coordinating these events at the apical ES, hemidesmosome, and the BTB.

On the other hand, polarity proteins such as 14-3-3 (Par5) are known to regulate protein endocytosis since a loss of 14-3-3 protein function by RNAi leads to a redistribution of TJ and basal ES proteins from the Sertoli–Sertoli cell interface, thereby destabilizing the BTB integrity (Wong et al., 2008b). However, it remains to be determined if Par6 and/or 14-3-3θ also regulate protein endocytosis at the apical ES since ultrastructurally, apical ES and basal ES are almost identical except that ultrastructures pertinent to apical ES are found on both sides of the Sertoli cells in basal ES (Wong et al., 2008b, 2009a).

Collectively, these findings have prompted us to propose a biochemical model shown in Fig. 7.6 regarding the presence of a functional apical ES-BTB-basement membrane functional axis that coordinates the events of spermiation and BTB restructuring that occur simultaneously at stage VIII of the epithelial cycle. It is likely that the biologically active laminin fragments are working in concert with the Par-based polarity complexes and perhaps other protein kinases (e.g., FAK and Src) that transmit signals

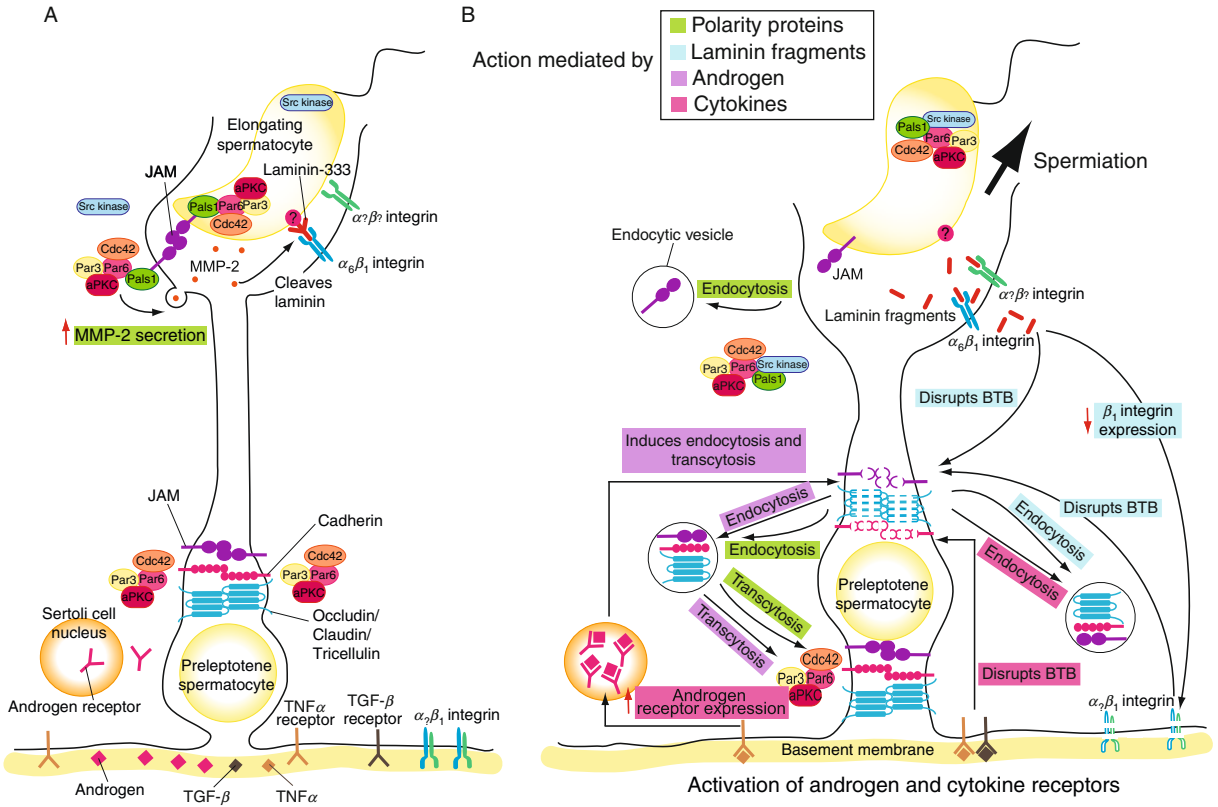

Figure 7.6 (continued)

between these sites to coordinate these events during spermatogenesis. For instance, recent studies have shown that FAK and/or Src is an integrated component of the apical ES and BTB in rat testes (Siu et al., 2003; Yan and Cheng, 2006). In short, Par-based polarity proteins serve as molecular switches whereas laminin fragments act as autocrine factors to coordinate the events of apical ES and BTB restructuring that occur at the opposite ends of the seminiferous epithelium at stage VIII of the epithelial cycle.

Figure 7.6 Schematic drawing illustrating the involvement of cytokines, testosterone, biologically active fragments of laminin chains, hemidesmosome, and polarity proteins in regulating spermiation and BTB restructuring during the seminiferous epithelial cycle of spermatogenesis. This schematic drawing was prepared based on recent findings in the field as detailed in the text. (A) In this panel, the known protein complexes at the apical ES, namely the JAM-C-based protein complex and the α6-β1-integrin/laminin-333-based protein complex are shown. The cell adhesion at the BTB is conferred by the JAM-A-based, cadherin-based, and the occludin-, claudin-, and tricellulin-based protein complexes. Just prior to spermiation, the polarity protein complex, Cdc42/Par3/Par6/Pals1/aPKC, remains associated with JAM-C. The presence of the polarity complex is likely involved in targeting and activating MMP-2 at the apical ES, which apparently is being used to cleave the laminin chains to generate the biologically active fragments. (B) During spermiation at the apical ES, Src kinase was shown to associate more tightly with Par6 and Pals1, causing the dissociation of the Par-based polarity complex from the JAM-C-based protein complex. JAM-C may also be internalized via endocytosis due to the absence of Par6 at the apical ES at spermiation, further destabilizing the JAM-C-based adhesion and facilitating spermiation at stage VIII of the epithelial cycle. Laminin fragments generated at the apical ES site were shown to perturb the BTB integrity *directly* or *indirectly*, acting as autocrine factors, via their effects on a yet-to-be identified integrin receptor at the BTB, and β1-integrin at the hemidesmosome. At the BTB, the biologically active laminin fragments apparently accelerate endocytic-vesicle-mediated endocytosis of integral membrane proteins, destabilizing the ''old'' TJ-fibrils above a primary preleptotene spermatocyte in transit at the BTB at stage VIII of the epithelial cycle. Cytokines, such as TGF-β2 and TGF-β3, are also likely to be involved in ''destabilizing'' the ''old'' BTB by accelerating endocytosis of BTB integral membrane proteins above the primary spermatocytes in transit. However, the combined effects of testosterone and TNFα-induced androgen receptor expression may accelerate the production (e.g., *de novo* synthesis of occludin, claudins, and JAMs) and assembly of ''new'' TJ-fibrils behind a primary spermatocyte in transit, and by transcytosing junction proteins from the ''old'' barrier to new site behind the spermatocyte. The processes of protein endocytosis and recycling, and perhaps transcytosis, are facilitated by polarity protein components, such as Par3, Par6, and 14-3-3. The polarity protein complex may serve as initial spatial cue to direct endocytosed proteins for forming ''new'' barrier behind the primary spermatocyte. Through the combined and concerted efforts of cytokines, testosterone, and biologically active laminin fragments, and with the participation of polarity proteins via their actions on protein endocytosis, recycling, and transcytosis, ''new'' TJ-fibrils can be formed behind a primary spermatocyte in transit prior to the dissolution of the ''old'' TJ-fibrils. Thus, the BTB is being restructured to facilitate the transit of spermatocytes while the immunological barrier can be maintained during spermatogenesis.

5. Roles of Polarity Proteins in Coordinating the Opposing Effects of Cytokines and Testosterone in Primary Preleptotene Spermatocyte Transit at the BTB

Cytokines are known regulators of TJ-permeability barrier in many epithelia, such as in small intestine and kidney, in studies using different cell lines (Al-Sadi et al., 2009; Walsh et al., 2000). The initial reports describing the disruptive effects of cytokines (e.g., TGF-β3 and TNFα) on the Sertoli cell TJ-permeability function appeared only in the early 2000s (Lui et al., 2001, 2003c; Siu et al., 2003). Since then, however, much progress has been made in the field, which includes the identification of the p38 MAPK and ERK1/2 as the two putative signaling pathways utilized by TGF-β3 in the testis to regulate BTB dynamics *in vivo* either alone or in combination with anchoring junction restructuring in the seminiferous epithelium (Li et al., 2006; Lui et al., 2003d; Wong et al., 2004; Xia et al., 2006; Yan et al., 2008b). These findings are important because they illustrate that the BTB permeability function can be manipulated by using specific inhibitors against these two MAPKs (Lui et al., 2003c,d; Xia and Cheng, 2005) (for a review, see Li et al., 2009). For instance, the cadmium-induced BTB disruption can be delayed by blocking the activation of p38 MAPK (Lui et al., 2003d; Wong et al., 2004), illustrating the environmental toxicant-induced BTB damage can possibly be therapeutically "protected" via the use of specific inhibitors against p38 MAPK (Siu et al., 2009; Li et al., 2009). On the other hand, it is of interest that testosterone promotes the integrity of the BTB (Meng et al., 2005) and maintains the junctional complex integrity in the seminiferous epithelium (Wang et al., 2006) via classical (i.e., involving androgen receptor) and perhaps nonclassical androgen action (i.e., involving ERK1/2 and c-Src nonreceptor protein kinases) (Walker, 2009). These opposing effects of cytokines (e.g., TGF-β3 and TNFα) and testosterone that disrupt and promotes the BTB integrity, respectively, seemingly suggest that if these molecules are working in concert, they can provide a novel mechanism to facilitate the migration of primary spermatocytes across the BTB while maintaining the immunological barrier. For instance, testosterone can promote the assembly of "new" TJ-fibrils below a primary preleptotene spermatocyte in transit while cytokines promote the dissolution of "old" TJ-fibrils above the spermatocyte in transit. Recent findings seem to support this novel mechanism in the testis. It was shown that both cytokines (e.g., TGF-β2, TGF-β3) (Xia et al., 2009; Yan et al., 2008a) and testosterone (Yan et al., 2008a) enhance endocytosis of integrated proteins at the BTB utilizing the clathrin-dependent pathway. However, endocytosed proteins following treatment of Sertoli cells with cytokines were shown to be targeted for degradation, whereas testosterone promoted

recycling, perhaps transcytosis, of the endocytosed proteins back to the cell surface (Yan et al., 2008a). In this context, it is of interest to note that TNFα was shown to stimulate androgen receptor expression by Sertoli cells (Chuang et al., 2007) via upregulation of NFκB, which binds to several enhancer motifs in the androgen receptor promoter, thereby promoting androgen receptor expression (Delfino et al., 2003). Thus, TNFα can have a dual-effect on the Sertoli cell TJ-barrier by promoting the assembly of "new" TJ-fibrils behind a primary spermatocyte in transit while disrupting the "old" TJ-fibrils above the migrating spermatocyte. As such, the immunological barrier can be maintained during the transit of spermatocytes (Fig. 7.6). Nonetheless, this postulate must be further validated in future functional studies to examine the opposing effects of cytokines and testosterone on junction restructuring.

How can the endocytosed proteins be transcytosed from the apical to the basal region of a primary preleptotene spermatocyte in transit? Indeed a recent study shed light on such possibility. Coureuil et al. (2009) found that *Neisseria meningitides*, the bacteria that cause cerebrospinal meningitis in humans, forms an "ectopic early junction-like domain" between their adhesion sites on microvascular endothelial cells. Through activating Cdc42, Par3/Par6/aPKC complex is recruited to the ectopic early junction-like domain which subsequently targets TJ (e.g., claudin-5) and AJ (VE-cadherin) proteins to the site. Interestingly, immunofluorescence microcopy shows that TJ and AJ proteins found at the ectopic early junction-like domain are recruited from the intercellular junctions of microvascular endothelial cells, leading to an increase in permeability of the endothelial cell layer to facilitate the entry of *N. meningitides*. It is likely that primary preleptotene spermatocytes utilize the Cdc42/Par3/Par6/aPKC complex to transcytosed junction proteins between two Sertoli cells, from the apical to the basal region of the migrating preleptotene spermatocyte. In this way, AJ and TJ are disrupted to allow the entry of preleptotene spermatocytes into the adluminal compartment of the seminiferous epithelium. At the same time, BTB integrity is maintained as new junctions are formed at the base of the migrating cells. This speculation is supported by several recent reports. First, we demonstrated that the silencing of Par3 or Par6 perturbed the Sertoli cell BTB by causing mislocalization of integral membrane proteins and/or their adaptors at the BTB site, such as JAM-A, N-cadherin, α-catenin, and/or ZO-1, thereby disrupting the BTB integrity (Wong et al., 2008b). This shows that, similar to other epithelial cells, Par polarity complex is necessary to target and maintain junction proteins at the cell–cell interface. Second, it is increasingly clear regarding the role of 14-3-3 and Cdc42 in regulating protein endocytosis in Sertoli cells with an established TJ-permeability barrier that mimics the BTB *in vivo* (Wong et al., 2009a,b). More importantly, recent findings have demonstrated unequivocally that Cdc42, besides facilitating protein endocytosis at the Sertoli cell BTB, is also crucial to the TGF-β3-mediated

acceleration of protein endocytosis (Wong et al., 2009b). For instance, overexpression of a dominant negative Cdc42 renders the loss of responsiveness of the Sertoli cells to TGF-β3-induced enhancement in protein endocytosis (Wong et al., 2009b). These findings are important since they illustrate that Cdc42 is working in concert with the Par3/Par6-based polarity complex to regulate cytokine-mediated Sertoli cell BTB integrity via protein endocytosis. However, several important questions will be needed to address in future studies: What are the possible extrinsic or intrinsic cues that activate and localize the Cdc42/Par3/Par6/aPKC polarity complex to the basal region of a migrating preleptotene spermatocyte? How are these extrinsic or intrinsic cues be asymmetrical initiated? We speculate that cytokines, such as TGF-β-3, are likely one of the extrinsic cues that regulates junction dynamics via Par proteins (Bose and Wrana, 2006; Ozdamar et al., 2005; Wang et al., 2008a). Recent studies have found that Wnt family proteins, which are involved in regulating planar cell polarity (Seifert and Mlodzik, 2007), are also involved in activating downstream Par polarity complex (Schlessinger et al., 2007; Zhang et al., 2007). Lastly, what is the role of Cdc42, Par3 or Par6 in the clathrin-mediated endocytosis? Does Hrs also play a role in cytokine-mediated endocytic trafficking in light of its function in early endosome sorting mechanism (Huang et al., 2009).

6. Concluding Remarks and Future Perspectives

Herein we provide an updated discussion based on the latest findings in the field on the role of Rho GTPases (e.g., Cdc42) and components of the mammalian polarity protein complexes (e.g., Par6, Par3, and 14-3-3) on cell–cell interactions in the testis at the Sertoli–Sertoli cell interface (e.g., the BTB) and the Sertoli–germ cell interface (e.g., the apical ES). More importantly, we have provided an integrated model as depicted in Fig. 7.6 on how the different cellular events pertinent to cell–cell interactions in the seminiferous epithelium of adult rat testes are coordinated via the crucial actions of polarity proteins, biologically active laminin fragments, and hemidesmosome on BTB dynamics and spermiation. Figure 7.6 also illustrates the concerted effects of cytokines (e.g., TNFα), androgens (e.g., testosterone), and polarity proteins (e.g., Par6) to regulate the transit of primary preleptotene spermatocytes at the BTB during stage VIII of the seminiferous epithelial cycle of spermatogenesis. However, there are many open questions remain to be addressed in future studies. For instance, are the components of the Scribble protein complex present in the seminiferous epithelium? If they are, how does this protein complex interact with the CRB- and Par-based polarity protein complexes to affect cell adhesion and cell polarity at the BTB and apical ES in the testis?

What are the target proteins downstream following activation of aPKC by Cdc42 in the Par3/Par6 protein complex that elicit the assembly of cell polarity, such as spermatid orientation and Sertoli cell polarity, in the seminiferous epithelium? Many of these questions can now be tackled based on the model depicted in Fig. 7.6.

ACKNOWLEDGMENT

This work was supported by grants from the National Institutes of Health (NICHD, R01 HD056034; R03 HD051512; U54 HD029990, Project 5) to CYC.

REFERENCES

Adams, A.E., Johnson, D.I., Longnecker, R.M., Sloat, B.F., Pringle, J.R., 1990. CDC42 and CDC43, two additional genes involved in budding and the establishment of cell polarity in the yeast *Saccharomyces cerevisiae*. J. Cell Biol. 111, 131–142.

Aitken, A., 2006. 14-3-3 proteins: a historic overview. Semin. Cancer Biol. 16, 162–172.

Al-Sadi, R., Boivin, M., Ma, T., 2009. Mechanism of cytokine modulation of epithelial tight junction barrier. Front Biosci. 14, 2765–2778.

Andras, I.E., Pu, H., Deli, M.A., Nath, A., Hennig, B., Toborek, M., 2003. HIV-1 Tat protein alters tight junction protein expression and distribution in cultured brain endothelial cells. J. Neurosci. Res. 74, 255–265.

Ang, A.L., Taguchi, T., Francis, S., Folsch, H., Murrells, L.J., Pypaert, M., et al., 2004. Recycling endosomes can serve as intermediates during transport from the Golgi to the plasma membrane of MDCK cells. J. Cell Biol. 167, 531–543.

Asanuma, K., Yanagida-Asanuma, E., Faul, C., Tomino, Y., Kim, K., Mundel, P., 2006. Synaptopodin orchestrates actin organization and cell motility via regulation of RhoA signalling. Nat. Cell Biol. 8, 485–491.

Assemat, E., Bazellieres, E., Pallesi-Pocachard, E., Le Bivic, A., Massey-Harroche, D., 2008. Polarity complex proteins. Biochim. Biophys. Acta 1778, 614–630.

Balklava, Z., Pant, S., Fares, H., Grant, B.D., 2007. Genome-wide analysis identifies a general requirement for polarity proteins in endocytic traffic. Nat. Cell Biol. 9, 1066–1073.

Bazellieres, E., Assemat, E., Arsanto, J.P., Le Bivic, A., Massey-Harroche, D., 2009. Crumbs proteins in epithelial morphogenesis. Front Biosci. 14, 2149–2169.

Berthouze, M., Venkataramanan, V., Li, Y., Shenoy, S.K., 2009. The deubiquitinases USP33 and USP20 coordinate beta2 adrenergic receptor recycling and resensitization. EMBO J. 28, 1684–1696.

Bialkowska, K., Zaffran, Y., Meyer, S.C., Fox, J.E., 2003. 14-3-3 zeta mediates integrin-induced activation of Cdc42 and Rac. Platelet glycoprotein Ib-IX regulates integrin-induced signaling by sequestering 14-3-3 zeta. J. Biol. Chem. 278, 33342–33350.

Bollag, G., McCormick, F., 1991. Regulators and effectors of Ras proteins. Annu. Rev. Cell Biol. 7, 601–632.

Bose, R., Wrana, J.L., 2006. Regulation of Par6 by extracellular signals. Curr. Opin. Cell Biol. 18, 206–212.

Boureux, A., Vignal, E., Faure, S., Fort, P., 2007. Evolution of the Rho family of Ras-like GTPases in eukaryotes. Mol. Biol. Evol. 24, 203–216.

Boutros, T., Chevet, E., Metrakos, P., 2008. Mitogen-activated protein (MAP) kinase/MAP kinase phosphatase regulation: roles in cell growth, death, and cancer. Pharmacol. Rev. 60, 261–310.

Bridges, D., Moorhead, G.B., 2005. 14-3-3 proteins: a number of functions for a numbered protein. Sci. STKE 2005 re10.

Carreau, S., de Vienne, C., Galeraud-Denis, I., 2008. Aromatase and estrogens in man reproduction: a review and latest advances. Adv. Med. Sci. 53, 139–144.

Cereijido, M., Contreras, R.G., Shoshani, L., 2004. Cell adhesion, polarity, and epithelia in the dawn of metazoans. Physiol. Rev. 84, 1229–1262.

Cereijido, M., Contreras, R.G., Shoshani, L., Flores-Benitez, D., Larre, I., 2008. Tight junction and polarity interaction in the transporting epithelial phenotype. Biochim. Biophys. Acta 1778, 770–793.

Cerione, R.A., 2004. Cdc42: new roads to travel. Trends Cell. Biol. 14, 127–132.

Chahdi, A., Sorokin, A., 2008. Protein kinase A-dependent phosphorylation modulates beta1Pix guanine nucleotide exchange factor activity through 14-3-3beta binding. Mol. Cell. Biol. 28, 1679–1687.

Chardin, P., 2006. Function and regulation of Rnd proteins. Nat. Rev. Mol. Cell Biol. 7, 54–62.

Chaudhary, J., Skinner, M.K., 2000. Characterization of a novel transcript of 14-3-3 theta in Sertoli cells. J. Androl. 21, 730–738.

Chen, Z.J., Sun, L.J., 2009. Nonproteolytic functions of ubiquitin in cell signaling. Mol. Cell 33, 275–286.

Cheng, C.Y., Mruk, D.D., 2002. Cell junction dynamics in the testis: Sertoli–germ cell interactions and male contraceptive development. Physiol. Rev. 82, 825–874.

Chhabra, E.S., Higgs, H.N., 2007. The many faces of actin: matching assembly factors with cellular structures. Nat. Cell Biol. 9, 1110–1121.

Chuang, C.K., Lee, K.H., Fan, C.T., Su, Y.S., 2007. FSH-sensitive murine Sertoli cell lines immortalized by human telomerase gene hTERT express the androgen receptor in response to TNF-alpha stimulation. Biosci. Rep. 27, 403–411.

Cline, E.G., Nelson, W.J., 2007. Characterization of mammalian Par 6 as a dual-location protein. Mol. Cell. Biol. 27, 4431–4443.

Cohen, D., Musch, A., Rodriguez-Boulan, E., 2001. Selective control of basolateral membrane protein polarity by cdc42. Traffic 2, 556–564.

Coureuil, M., Mikaty, G., Miller, F., Lecuyer, H., Bernard, C., Bourdoulous, S., et al., 2009. Meningococcal type IV pili recruit the polarity complex to cross the brain endothelium. Science 325, 83–87.

d'Azzo, A., Bongiovanni, A., Nastasi, T., 2005. E3 ubiquitin ligases as regulators of membrane protein trafficking and degradation. Traffic 6, 429–441.

de Kretser, D., Kerr, J., 1988. The cytology of the testis. In: Knobil, E., Neill, J., Ewing, L., Greenwald, C., Markert, C., Pfaff, D. (Eds.), The Physiology of Reproduction. Raven Press, New York, pp. 837–932.

Delfino, F.J., Boustead, J.N., Fix, C., Walker, W.H., 2003. NF-kappaB and TNF-alpha stimulate androgen receptor expression in Sertoli cells. Mol. Cell. Endocrinol. 201, 1–12.

DerMardirossian, C., Bokoch, G.M., 2005. GDIs: central regulatory molecules in Rho GTPase activation. Trends Cell Biol. 15, 356–363.

Di Agostino, S., Rossi, P., Geremia, R., Sette, C., 2002. The MAPK pathway triggers activation of Nek2 during chromosome condensation in mouse spermatocytes. Development 129, 1715–1727.

Doherty, G.J., McMahon, H.T., 2009. Mechanisms of endocytosis. Annu. Rev. Biochem. 78, 857–902.

Du, X., Harris, S.J., Tetaz, T.J., Ginsberg, M.H., Berndt, M.C., 1994. Association of a phospholipase A2 (14-3-3 protein) with the platelet glycoprotein Ib-IX complex. J. Biol. Chem. 269, 18287–18290.

Du, X., Fox, J.E., Pei, S., 1996. Identification of a binding sequence for the 14-3-3 protein within the cytoplasmic domain of the adhesion receptor, platelet glycoprotein Ib alpha. J. Biol. Chem. 271, 7362–7367.

Duffield, A., Caplan, M.J., Muth, T.R., 2008. Protein trafficking in polarized cells. Int. Rev. Cell Mol. Biol. 270, 145–179.

Etienne-Manneville, S., 2004. Cdc42—the centre of polarity. J. Cell Sci. 117, 1291–1300.

Etienne-Manneville, S., Manneville, J.B., Nicholls, S., Ferenczi, M.A., Hall, A., 2005. Cdc42 and Par6-PKCzeta regulate the spatially localized association of Dlg1 and APC to control cell polarization. J. Cell Biol. 170, 895–901.

Fagerholm, S., Morrice, N., Gahmberg, C.G., Cohen, P., 2002. Phosphorylation of the cytoplasmic domain of the integrin CD18 chain by protein kinase C isoforms in leukocytes. J. Biol. Chem. 277, 1728–1738.

Fujita, Y., Krause, G., Scheffner, M., Zechner, D., Leddy, H.E., Behrens, J., et al., 2002. Hakai, a c-Cbl-like protein, ubiquitinates and induces endocytosis of the E-cadherin complex. Nat. Cell Biol. 4, 222–231.

Fujita, E., Tanabe, Y., Hirose, T., Aurrand-Lions, M., Kasahara, T., Imhof, B.A., et al., 2007. Loss of partitioning-defective-3/isotype-specific interacting protein (par-3/ASIP) in the elongating spermatid of RA175 (IGSF4A/SynCAM)-deficient mice. Am. J. Pathol. 171, 1800–1810.

Fukuhara, A., Shimizu, K., Kawakatsu, T., Fukuhara, T., Takai, Y., 2003. Involvement of nectin-activated Cdc42 small G protein in organization of adherens and tight junctions in Madin-Darby canine kidney cells. J. Biol. Chem. 278, 51885–51893.

Gao, L., Macara, I.G., Joberty, G., 2002. Multiple splice variants of Par3 and of a novel related gene, Par3L, produce proteins with different binding properties. Gene 294, 99–107.

Garcia-Guzman, M., Dolfi, F., Russello, M., Vuori, K., 1999. Cell adhesion regulates the interaction between the docking protein p130(Cas) and the 14-3-3 proteins. J. Biol. Chem. 274, 5762–5768.

Garcia-Mata, R., Burridge, K., 2007. Catching a GEF by its tail. Trends Cell Biol. 17, 36–43.

Garrard, S.M., Capaldo, C.T., Gao, L., Rosen, M.K., Macara, I.G., Tomchick, D.R., 2003. Structure of Cdc42 in a complex with the GTPase-binding domain of the cell polarity protein, Par6. EMBO J. 22, 1125–1133.

Georgiou, M., Marinari, E., Burden, J., Baum, B., 2008. Cdc42, Par6, and aPKC regulate Arp2/3-mediated endocytosis to control local adherens junction stability. Curr. Biol. 18, 1631–1638.

Gliki, G., Ebnet, K., Aurrand-Lions, M., Imhof, B.A., Adams, R.H., 2004. Spermatid differentiation requires the assembly of a cell polarity complex downstream of junctional adhesion molecule-C. Nature 431, 320–324.

Gohla, A., Bokoch, G.M., 2002. 14-3-3 regulates actin dynamics by stabilizing phosphorylated cofilin. Curr. Biol. 12, 1704–1710.

Goldstein, B., Macara, I.G., 2007. The PAR proteins: fundamental players in animal cell polarization. Dev. Cell 13, 609–622.

Gonzalez-Mariscal, L., Tapia, R., Chamorro, D., 2008. Crosstalk of tight junction components with signaling pathways. Biochim. Biophys. Acta 1778, 729–756.

Gupton, S.L., Gertler, F.B., 2007. Filopodia: the fingers that do the walking. Sci. STKE 2007 re5.

Hall, C., Sin, W.C., Teo, M., Michael, G.J., Smith, P., Dong, J.M., et al., 1993. α2-chimerin, an SH2-containing GTPase-activating protein for the Ras-related protein p21rac derived by alternate splicing of the human n-chimerin gene, is selectively expressed in brain regions and testes. Mol. Cell. Biol. 13, 4986–4998.

Han, D.C., Rodriguez, L.G., Guan, J.L., 2001. Identification of a novel interaction between integrin beta1 and 14-3-3beta. Oncogene 20, 346–357.
Harris, K.P., Tepass, U., 2008. Cdc42 and Par proteins stabilize dynamic adherens junctions in the *Drosophila neuroectoderm* through regulation of apical endocytosis. J. Cell Biol. 183, 1129–1143.
Haugsten, E.M., Malecki, J., Bjorklund, S.M., Olsnes, S., Wesche, J., 2008. Ubiquitination of fibroblast growth factor receptor 1 is required for its intracellular sorting but not for its endocytosis. Mol. Biol. Cell 19, 3390–3403.
Heasman, S.J., Ridley, A.J., 2008. Mammalian Rho GTPases: new insights into their functions from *in vivo* studies. Nat. Rev. Mol. Cell Biol. 9, 690–701.
Hekman, M., Wiese, S., Metz, R., Albert, S., Troppmair, J., Nickel, J., et al., 2004. Dynamic changes in C-Raf phosphorylation and 14-3-3 protein binding in response to growth factor stimulation: differential roles of 14-3-3 protein binding sites. J. Biol. Chem. 279, 14074–14086.
Hess, R.A., 2003. Estrogen in the adult male reproductive tract: a review. Reprod. Biol. Endocrinol. 1, 52.
Hess, R.A., de Franca, L.R., 2008. Spermatogenesis and cycle of the seminiferous epithelium. In: Cheng, C.Y. (Ed.), Molecular Mechanisms in Spermatogenesis. Landes Bioscience/Springer Science+Business Media, LLC, Austin, TX, pp. 1–15.
Heusser, K., Yuan, H., Neagoe, I., Tarasov, A.I., Ashcroft, F.M., Schwappach, B., 2006. Scavenging of 14-3-3 proteins reveals their involvement in the cell-surface transport of ATP-sensitive K+ channels. J. Cell Sci. 119, 4353–4363.
Hicke, L., Dunn, R., 2003. Regulation of membrane protein transport by ubiquitin and ubiquitin-binding proteins. Annu. Rev. Cell Dev. Biol. 19, 141–172.
Honda, T., Shimizu, K., Kawakatsu, T., Fukuhara, A., Irie, K., Nakamura, T., et al., 2003. Cdc42 and Rac small G proteins activated by trans-interactions of nectins are involved in activation of c-Jun N-terminal kinase, but not in association of nectins and cadherin to form adherens junctions, in fibroblasts. Genes Cells 8, 481–491.
Huang, S.H., Zhao, L., Sun, Z.P., Li, X.Z., Geng, Z., Zhang, K.D., et al., 2009. Essential role of Hrs in endocytic recycling of full-length TrkB receptor but not its isoform TrkB.T1. J. Biol. Chem. 284, 15126–15136.
Hurd, T.W., Fan, S., Liu, C.J., Kweon, H.K., Hakansson, K., Margolis, B., 2003a. Phosphorylation-dependent binding of 14-3-3 to the polarity protein Par3 regulates cell polarity in mammalian epithelia. Curr. Biol. 13, 2082–2090.
Hurd, T.W., Gao, L., Roh, M.H., Macara, I.G., Margolis, B., 2003b. Direct interaction of two polarity complexes implicated in epithelial tight junction assembly. Nat. Cell Biol. 5, 137–142.
Huveneers, S., Danen, E.H., 2009. Adhesion signaling—crosstalk between integrins, Src and Rho. J. Cell Sci. 122, 1059–1069.
Iden, S., Collard, J.G., 2008. Crosstalk between small GTPases and polarity proteins in cell polarization. Nat. Rev. Mol. Cell Biol. 9, 846–859.
Inselman, A., Handel, M.A., 2004. Mitogen-activated protein kinase dynamics during the meiotic G2/MI transition of mouse spermatocytes. Biol. Reprod. 71, 570–578.
Izaki, T., Kamakura, S., Kohjima, M., Sumimoto, H., 2005. Phosphorylation-dependent binding of 14-3-3 to Par3beta, a human Par3-related cell polarity protein. Biochem. Biophys. Res. Commun. 329, 211–218.
Izumi, G., Sakisaka, T., Baba, T., Tanaka, S., Morimoto, K., Takai, Y., 2004. Endocytosis of E-cadherin regulated by Rac and Cdc42 small G proteins through IQGAP1 and actin filaments. J. Cell Biol. 166, 237–248.
Jaffe, A.B., Hall, A., 2005. Rho GTPases: biochemistry and biology. Annu. Rev. Cell Dev. Biol. 21, 247–269.

Jin, J., Smith, F.D., Stark, C., Wells, C.D., Fawcett, J.P., Kulkarni, S., et al., 2004. Proteomic, functional, and domain-based analysis of *in vivo* 14-3-3 binding proteins involved in cytoskeletal regulation and cellular organization. Curr. Biol. 14, 1436–1450.

Joberty, G., Petersen, C., Gao, L., Macara, I.G., 2000. The cell-polarity protein Par6 links Par3 and atypical protein kinase C to Cdc42. Nat. Cell Biol. 2, 531–539.

Kanmogne, G.D., Primeaux, C., Grammas, P., 2005. HIV-1 gp120 proteins alter tight junction protein expression and brain endothelial cell permeability: implications for the pathogenesis of HIV-associated dementia. J. Neuropathol. Exp. Neurol. 64, 498–505.

Kawakatsu, T., Shimizu, K., Honda, T., Fukuhara, T., Hoshino, T., Takai, Y., 2002. Trans-interactions of nectins induce formation of filopodia and lamellipodia through the respective activation of Cdc42 and Rac small G proteins. J. Biol. Chem. 277, 50749–50755.

Kemphues, K.J., Priess, J.R., Morton, D.G., Cheng, N.S., 1988. Identification of genes required for cytoplasmic localization in early *C. elegans* embryos. Cell 52, 311–320.

Kodama, A., Takaishi, K., Nakano, K., Nishioka, H., Takai, Y., 1999. Involvement of Cdc42 small G protein in cell–cell adhesion, migration, and morphology of MDCK cells. Oncogene 18, 3996–4006.

Kohjima, M., Noda, Y., Takeya, R., Saito, N., Takeuchi, K., Sumimoto, H., 2002. PAR3beta, a novel homologue of the cell polarity protein PAR3, localizes to tight junctions. Biochem. Biophys. Res. Commun. 299, 641–646.

Kroschewski, R., Hall, A., Mellman, I., 1999. Cdc42 controls secretory and endocytic transport to the basolateral plasma membrane of MDCK cells. Nat. Cell Biol. 1, 8–13.

Lau, A.S., Mruk, D.D., 2003. Rab8B GTPase and junction dynamics in the testis. Endocrinology 144, 1549–1563.

Le, T.L., Yap, A.S., Stow, J.L., 1999. Recycling of E-cadherin: a potential mechanism for regulating cadherin dynamics. J. Cell Biol. 146, 219–232.

Leblond, C.P., Clermont, Y., 1952. Definition of the stages of the cycle of the seminiferous epithelium in the rat. Ann. N. Y. Acad. Sci. 55, 548–573.

Lee, N.P., Cheng, C.Y., 2003. Regulation of Sertoli cell tight junction dynamics in the rat testis via the nitric oxide synthase/soluble guanylate cyclase/3′, 5′-cyclic guanosine monophosphate/protein kinase G signaling pathway: an *in vitro* study. Endocrinology 144, 3114–3129.

Leibfried, A., Fricke, R., Morgan, M.J., Bogdan, S., Bellaiche, Y., 2008. *Drosophila* Cip4 and WASp define a branch of the Cdc42-Par6-aPKC pathway regulating E-cadherin endocytosis. Curr. Biol. 18, 1639–1648.

Lemmers, C., Medina, E., Delgrossi, M.H., Michel, D., Arsanto, J.P., Le Bivic, A., 2002. hINADl/PATJ, a homolog of discs lost, interacts with crumbs and localizes to tight junctions in human epithelial cells. J. Biol. Chem. 277, 25408–25415.

Leung, T., How, B.E., Manser, E., Lim, L., 1993. Germ cell beta-chimaerin, a new GTPase-activating protein for p21rac, is specifically expressed during the acrosomal assembly stage in rat testis. J. Biol. Chem. 268, 3813–3816.

Leyt, J., Melamed-Book, N., Vaerman, J.P., Cohen, S., Weiss, A.M., Aroeti, B., 2007. Cholesterol-sensitive modulation of transcytosis. Mol. Biol. Cell 18, 2057–2071.

Li, M.W., Xia, W., Mruk, D.D., Wang, C.Q., Yan, H.H., Siu, M.K., et al., 2006. Tumor necrosis factor α reversibly disrupts the blood–testis barrier and impairs Sertoli–germ cell adhesion in the seminiferous epithelium of adult rat testes. J. Endocrinol. 190, 313–329.

Li, M.W., Mruk, D.D., Cheng, C.Y., 2009. Mitogen-activated protein kinases in male reproductive function. Trends Mol. Med. 15, 159–168.

Lie, P.P., Cheng, C.Y., Mruk, D.D., 2009. Coordinating cellular events during spermatogenesis: a biochemical model. Trends Biochem. Sci. 34, 366–373.

Light, Y., Paterson, H., Marais, R., 2002. 14-3-3 antagonizes Ras-mediated Raf-1 recruitment to the plasma membrane to maintain signaling fidelity. Mol. Cell. Biol. 22, 4984–4996.

Lin, D., Edwards, A.S., Fawcett, J.P., Mbamalu, G., Scott, J.D., Pawson, T., 2000. A mammalian PAR-3–PAR-6 complex implicated in Cdc42/Rac1 and aPKC signalling and cell polarity. Nat. Cell Biol. 2, 540–547.

Loirand, G., Guilluy, C., Pacaud, P., 2006. Regulation of Rho proteins by phosphorylation in the cardiovascular system. Trends Cardiovasc. Med. 16, 199–204.

Lui, W.Y., Cheng, C.Y., 2007. Regulation of cell junction dynamics by cytokines in the testis: a molecular and biochemical perspective. Cytokine Growth Factor Rev. 18, 299–311.

Lui, W.Y., Lee, W.M., Cheng, C.Y., 2001. Transforming growth factor-β3 perturbs the inter-Sertoli tight junction permeability barrier *in vitro* possibly mediated via its effects on occludin, zonula occludens-1, and claudin-11. Endocrinology 142, 1865–1877.

Lui, W.Y., Lee, W.M., Cheng, C.Y., 2003a. Rho GTPases and spermatogenesis. Biochim. Biophys. Acta 1593, 121–129.

Lui, W.Y., Lee, W.M., Cheng, C.Y., 2003b. Sertoli–germ cell adherens junction dynamics in the testis are regulated by RhoB GTPase via the ROCK/LIMK signaling pathway. Biol. Reprod. 68, 2189–2206.

Lui, W.Y., Lee, W.M., Cheng, C.Y., 2003c. Transforming growth factor β-3 regulates the dynamics of Sertoli cell tight junctions via the p38 mitogen-activated protein kinase pathway. Biol. Reprod. 68, 1597–1612.

Lui, W.Y., Wong, C.H., Mruk, D.D., Cheng, C.Y., 2003d. TGF-β3 regulates the blood–testis barrier dynamics via the p38 mitogen activated protein (MAP) kinase pathway: an *in vivo* study. Endocrinology 144, 1139–1142.

Lui, W.Y., Mruk, D.D., Cheng, C.Y., 2005. Interactions among IQGAP1, Cdc42, and the cadherin/catenin protein complex regulate Sertoli–germ cell adherens junction dynamics in the testis. J. Cell Physiol. 202, 49–66.

Makarova, O., Roh, M.H., Liu, C.J., Laurinec, S., Margolis, B., 2003. Mammalian crumbs3 is a small transmembrane protein linked to protein associated with Lin-7 (Pals1). Gene 302, 21–29.

Matsuda, M., Kubo, A., Furuse, M., Tsukita, S., 2004. A peculiar internalization of claudins, tight junction-specific adhesion molecules, during the intercellular movement of epithelial cells. J. Cell Sci. 117, 1247–1257.

Matsumine, A., Ogai, A., Senda, T., Okumura, N., Satoh, K., Baeg, G.H., et al., 1996. Binding of APC to the human homolog of the *Drosophila* discs large tumor suppressor protein. Science 272, 1020–1023.

Matthiesson, K.L., McLachlan, R.I., O'Donnell, L., Frydenberg, M., Robertson, D.M., Stanton, P.G., et al., 2006. The relative roles of follicle-stimulating hormone and luteinizing hormone in maintaining spermatogonial maturation and spermiation in normal men. J. Clin. Endocrinol. Metab. 91, 3962–3969.

Mattila, P.K., Lappalainen, P., 2008. Filopodia: molecular architecture and cellular functions. Nat. Rev. Mol. Cell Biol. 9, 446–454.

Mellman, I., Nelson, W.J., 2008. Coordinated protein sorting, targeting, and distribution in polarized cells. Nat. Rev. Mol. Cell Biol. 9, 833–845.

Meng, J., Holdcraft, R.W., Shima, J.E., Griswold, M.D., Braun, R.E., 2005. Androgens regulate the permeability of the blood–testis barrier. Proc. Natl. Acad. Sci. USA 102, 16696–16700.

Merrifield, C.J., Feldman, M.E., Wan, L., Almers, W., 2002. Imaging actin and dynamin recruitment during invagination of single clathrin-coated pits. Nat. Cell Biol. 4, 691–698.

Moon, S.Y., Zheng, Y., 2003. Rho GTPase-activating proteins in cell regulation. Trends Cell. Biol. 13, 13–22.

Morrison, D.K., 2009. The 14-3-3 proteins: integrators of diverse signaling cues that impact cell fate and cancer development. Trends Cell Biol. 19, 16–23.

Morton, D.G., Shakes, D.C., Nugent, S., Dichoso, D., Wang, W., Golden, A., et al., 2002. The *Caenorhabditis elegans* par-5 gene encodes a 14-3-3 protein required for cellular asymmetry in the early embryo. Dev. Biol. 241, 47–58.

Mrowiec, T., Schwappach, B., 2006. 14-3-3 proteins in membrane protein transport. Biol. Chem. 387, 1227–1236.

Mruk, D.D., Cheng, C.Y., 2004. Sertoli–Sertoli and Sertoli–germ cell interactions and their significance in germ cell movement in the seminiferous epithelium during spermatogenesis. Endocr. Rev. 25, 747–806.

Mruk, D.D., Cheng, C.Y., 2008. Delivering non-hormonal contraceptives to men: advances and obstacles. Trends Biotechnol. 26, 90–99.

Mruk, D., Zhu, L.J., Silvestrini, B., Lee, W.M., Cheng, C.Y., 1997. Interactions of proteases and protease inhibitors in Sertoli–germ cell cocultures preceding the formation of specialized Sertoli–germ cell junctions *in vitro*. J. Androl. 18, 612–622.

Mruk, D.D., Siu, M.K., Conway, A.M., Lee, N.P., Lau, A.S., Cheng, C.Y., 2003. Role of tissue inhibitor of metalloproteases-1 in junction dynamics in the testis. J. Androl. 24, 510–523.

Mruk, D.D., Lau, A.S., Sarkar, O., Xia, W., 2007. Rab4A GTPase catenin interactions are involved in cell junction dynamics in the testis. J. Androl. 28, 742–754.

Mruk, D.D., Silvestrini, B., Cheng, C.Y., 2008. Anchoring junctions as drug targets: role in contraceptive development. Pharmacol. Rev. 60, 146–180.

Mulholland, D.J., Dedhar, S., Vogl, A.W., 2001. Rat seminiferous epithelium contains a unique junction (ectoplasmic specialization) with signaling properties both of cell/cell and cell/matrix junctions. Biol. Reprod. 64, 396–407.

Musch, A., Cohen, D., Kreitzer, G., Rodriguez-Boulan, E., 2001. cdc42 regulates the exit of apical and basolateral proteins from the trans-Golgi network. EMBO J. 20, 2171–2179.

Muslin, A.J., Lau, J.M., 2005. Differential functions of 14-3-3 isoforms in vertebrate development. Curr. Top. Dev. Biol. 65, 211–228.

Nakagawa, S., Huibregtse, J.M., 2000. Human scribble (Vartul) is targeted for ubiquitin-mediated degradation by the high-risk papillomavirus E6 proteins and the E6AP ubiquitin-protein ligase. Mol. Cell. Biol. 20, 8244–8253.

Nakamuta, S., Endo, H., Higashi, Y., Kousaka, A., Yamada, H., Yano, M., et al., 2008. Human immunodeficiency virus type 1 gp120-mediated disruption of tight junction proteins by induction of proteasome-mediated degradation of zonula occludens-1 and -2 in human brain microvascular endothelial cells. J. Neurovirol. 14, 186–195.

Nelson, W.J., 2008. Regulation of cell–cell adhesion by the cadherin–catenin complex. Biochem. Soc. Trans. 36, 149–155.

O'Kelly, I., Butler, M.H., Zilberberg, N., Goldstein, S.A., 2002. Forward transport. 14-3-3 binding overcomes retention in endoplasmic reticulum by dibasic signals. Cell 111, 577–588.

Otani, T., Ichii, T., Aono, S., Takeichi, M., 2006. Cdc42 GEF Tuba regulates the junctional configuration of simple epithelial cells. J. Cell Biol. 175, 135–146.

Ozdamar, B., Bose, R., Barrios-Rodiles, M., Wang, H.R., Zhang, Y., Wrana, J.L., 2005. Regulation of the polarity protein Par6 by TGFbeta receptors controls epithelial cell plasticity. Science 307, 1603–1609.

Page, S.T., Amory, J.K., Bremner, W.J., 2008. Advances in male contraception. Endocr. Rev. 29, 465–493.

Palombi, F., Salanova, M., Tarone, G., Farini, D., Stefanini, M., 1992. Distribution of beta 1 integrin subunit in rat seminiferous epithelium. Biol. Reprod. 47, 1173–1182.

Parvinen, M., 1982. Regulation of the seminiferous epithelium. Endocr. Rev. 3, 404–417.

Perego, L., Berruti, G., 1997. Molecular cloning and tissue-specific expression of the mouse homologue of the rat brain 14-3-3 theta protein: characterization of its cellular and

developmental pattern of expression in the male germ line. Mol. Reprod. Dev. 47, 370–379.
Peterson, F.C., Penkert, R.R., Volkman, B.F., Prehoda, K.E., 2004. Cdc42 regulates the Par-6 PDZ domain through an allosteric CRIB-PDZ transition. Mol. Cell 13, 665–676.
Pickart, C.M., Fushman, D., 2004. Polyubiquitin chains: polymeric protein signals. Curr. Opin. Chem. Biol. 8, 610–616.
Polishchuk, R., Di Pentima, A., Lippincott-Schwartz, J., 2004. Delivery of raft-associated, GPI-anchored proteins to the apical surface of polarized MDCK cells by a transcytotic pathway. Nat. Cell Biol. 6, 297–307.
Pozuelo Rubio, M., Geraghty, K.M., Wong, B.H., Wood, N.T., Campbell, D.G., Morrice, N., et al., 2004. 14-3-3-affinity purification of over 200 human phosphoproteins reveals new links to regulation of cellular metabolism, proliferation, and trafficking. Biochem. J. 379, 395–408.
Qin, Y., Capaldo, C., Gumbiner, B.M., Macara, I.G., 2005. The mammalian scribble polarity protein regulates epithelial cell adhesion and migration through E-cadherin. J. Cell Biol. 171, 1061–1071.
Rajalingam, K., Rudel, T., 2005. Ras–Raf signaling needs prohibitin. Cell Cycle 4, 1503–1505.
Rajalingam, K., Wunder, C., Brinkmann, V., Churin, Y., Hekman, M., Sievers, C., et al., 2005. Prohibitin is required for Ras-induced Raf-MEK-ERK activation and epithelial cell migration. Nat. Cell Biol. 7, 837–843.
Reyes-Turcu, F.E., Ventii, K.H., Wilkinson, K.D., 2009. Regulation and cellular roles of ubiquitin-specific deubiquitinating enzymes. Annu. Rev. Biochem. 78, 363–397.
Ridley, A.J., 2006. Rho GTPases and actin dynamics in membrane protrusions and vesicle trafficking. Trends Cell Biol. 16, 522–529.
Rodriguez-Boulan, E., Kreitzer, G., Musch, A., 2005. Organization of vesicular trafficking in epithelia. Nat. Rev. Mol. Cell Biol. 6, 233–247.
Roh, M.H., Liu, C.J., Laurinec, S., Margolis, B., 2002a. The carboxyl terminus of zona occludens-3 binds and recruits a mammalian homologue of discs lost to tight junctions. J. Biol. Chem. 277, 27501–27509.
Roh, M.H., Makarova, O., Liu, C.J., Shin, K., Lee, S., Laurinec, S., et al., 2002b. The Maguk protein, Pals1, functions as an adapter, linking mammalian homologues of Crumbs and Discs Lost. J. Cell Biol. 157, 161–172.
Rojas, R., Ruiz, W.G., Leung, S.M., Jou, T.S., Apodaca, G., 2001. Cdc42-dependent modulation of tight junctions and membrane protein traffic in polarized Madin-Darby canine kidney cells. Mol. Biol. Cell 12, 2257–2274.
Rossman, K.L., Der, C.J., Sondek, J., 2005. GEF means go: turning on RHO GTPases with guanine nucleotide-exchange factors. Nat. Rev. Mol. Cell Biol. 6, 167–180.
Russell, L., 1977. Movement of spermatocytes from the basal to the adluminal compartment of the rat testis. Am. J. Anat. 148, 313–328.
Russell, L.D., 1993. Morphological and functional evidence for Sertoli–germ cell relationships. In: Russell, L.D., Griswold, M.D. (Eds.), The Sertoli Cell. Cache River Press, Clearwater, pp. 365–390.
Sakurai-Yageta, M., Recchi, C., Le Dez, G., Sibarita, J.B., Daviet, L., Camonis, J., et al., 2008. The interaction of IQGAP1 with the exocyst complex is required for tumor cell invasion downstream of Cdc42 and RhoA. J. Cell Biol. 181, 985–998.
Salanova, M., Stefanini, M., De Curtis, I., Palombi, F., 1995. Integrin receptor alpha 6 beta 1 is localized at specific sites of cell-to-cell contact in rat seminiferous epithelium. Biol. Reprod. 52, 79–87.
Sallee, J.L., Wittchen, E.S., Burridge, K., 2006. Regulation of cell adhesion by protein-tyrosine phosphatases: II. Cell–cell adhesion. J. Biol. Chem. 281, 16189–16192.
Samarin, S., Nusrat, A., 2009. Regulation of epithelial apical junctional complex by Rho family GTPases. Front Biosci. 14, 1129–1142.

Santoni, M.J., Pontarotti, P., Birnbaum, D., Borg, J.P., 2002. The LAP family: a phylogenetic point of view. Trends Genet. 18, 494–497.

Schlessinger, K., McManus, E.J., Hall, A., 2007. Cdc42 and noncanonical Wnt signal transduction pathways cooperate to promote cell polarity. J. Cell Biol. 178, 355–361.

Seifert, J.R., Mlodzik, M., 2007. Frizzled/PCP signalling: a conserved mechanism regulating cell polarity and directed motility. Nat. Rev. Genet. 8, 126–138.

Shaha, C., 2008. Estrogens and spermatogenesis. In: Cheng, C.Y. (Ed.), Molecular Mechanisms in Spermatogenesis. Landes Bioscience/Springer Science+Business Media, LLC, Austin, TX, pp. 42–64.

Sharpe, R.M., 1994. Regulation of spermatogenesis. In: Knobil, E., Neil, J.D. (Eds.), The Physiology of Reproduction. Raven Press, New York, pp. 1363–1434.

Shen, L., Weber, C.R., Turner, J.R., 2008a. The tight junction protein complex undergoes rapid and continuous molecular remodeling at steady state. J. Cell Biol. 181, 683–695.

Shen, Y., Hirsch, D.S., Sasiela, C.A., Wu, W.J., 2008b. Cdc42 regulates E-cadherin ubiquitination and degradation through an epidermal growth factor receptor to Src-mediated pathway. J. Biol. Chem. 283, 5127–5137.

Shikano, S., Coblitz, B., Wu, M., Li, M., 2006. 14-3-3 proteins: regulation of endoplasmic reticulum localization and surface expression of membrane proteins. Trends Cell Biol. 16, 370–375.

Shin, K., Fogg, V.C., Margolis, B., 2006. Tight junctions and cell polarity. Annu. Rev. Cell Dev. Biol. 22, 207–235.

Siu, M.K., Cheng, C.Y., 2004. Interactions of proteases, protease inhibitors, and the β1 integrin/laminin γ3 protein complex in the regulation of ectoplasmic specialization dynamics in the rat testis. Biol. Reprod. 70, 945–964.

Siu, M.K., Lee, W.M., Cheng, C.Y., 2003. The interplay of collagen IV, tumor necrosis factor-α, gelatinase B (matrix metalloprotease-9), and tissue inhibitor of metalloproteases-1 in the basal lamina regulates Sertoli cell-tight junction dynamics in the rat testis. Endocrinology 144, 371–387.

Siu, M.K., Wong, C.H., Lee, W.M., Cheng, C.Y., 2005. Sertoli–germ cell anchoring junction dynamics in the testis are regulated by an interplay of lipid and protein kinases. J. Biol. Chem. 280, 25029–25047.

Siu, E.R., Mruk, D.D., Porto, C.S., Cheng, C.Y., 2009. Cadmium-induced testicular injury. Toxicol. Appl. Pharmacol. 238, 240–249.

Somanath, P.R., Byzova, T.V., 2009. 14-3-3β-Rac1–p21 activated kinase signaling regulates Akt1-mediated cytoskeletal organization, lamellipodia formation, and fibronectin matrix assembly. J. Cell Physiol. 218, 394–404.

Stoffler, H.E., Honnert, U., Bauer, C.A., Hofer, D., Schwarz, H., Muller, R.T., Drenckhahn, M., Bahler, M., 1998. Targeting of the myosin-I myr 3 to intercellular adherens type junctions induced by dominant active Cdc42 in HeLa cells. J. Cell Sci. 111, 2779–2788.

Sun, I., Wong, E., Li, M., Lee, W., Cheng, C.Y., 2009. 14-3-3 and its binding partners are regulators of protein–protein interactions during spermatogenesis. J. Endocrinol. 202, 327–336.

Takai, Y., Sasaki, T., Matozaki, T., 2001. Small GTP-binding proteins. Physiol. Rev. 81, 153–208.

Takenawa, T., Miki, H., 2001. WASP and WAVE family proteins: key molecules for rapid rearrangement of cortical actin filaments and cell movement. J. Cell Sci. 114, 1801–1809.

Tcherkezian, J., Lamarche-Vane, N., 2007. Current knowledge of the large RhoGAP family of proteins. Biol. Cell 99, 67–86.

Toure, A., Dorseuil, O., Morin, L., Timmons, P., Jegou, B., Reibel, L., et al., 1998. MgcRacGAP, a new human GTPase-activating protein for Rac and Cdc42 similar to *Drosophila* rotundRacGAP gene product, is expressed in male germ cells. J. Biol. Chem. 273, 6019–6023.

Toure, A., Morin, L., Pineau, C., Becq, F., Dorseuil, O., Gacon, G., 2001. Tat1, a novel sulfate transporter specifically expressed in human male germ cells and potentially linked to rhogtpase signaling. J. Biol. Chem. 276, 20309–20315.

Traweger, A., Wiggin, G., Taylor, L., Tate, S.A., Metalnikov, P., Pawson, T., 2008. Protein phosphatase 1 regulates the phosphorylation state of the polarity scaffold Par-3. Proc. Natl. Acad. Sci. USA 105, 10402–10407.

Tu, S., Wu, W.J., Wang, J., Cerione, R.A., 2003. Epidermal growth factor-dependent regulation of Cdc42 is mediated by the Src tyrosine kinase. J. Biol. Chem. 278, 49293–49300.

Tuma, P.L., Hubbard, A.L., 2003. Transcytosis: crossing cellular barriers. Physiol. Rev. 83, 871–932.

Valencia, A., Chardin, P., Wittinghofer, A., Sander, C., 1991. The Ras protein family: evolutionary tree and role of conserved amino acids. Biochemistry 30, 4637–4648.

Vasioukhin, V., Bauer, C., Yin, M., Fuchs, E., 2000. Directed actin polymerization is the driving force for epithelial cell–cell adhesion. Cell 100, 209–219.

Vetter, I.R., Wittinghofer, A., 2001. The guanine nucleotide-binding switch in three dimensions. Science 294, 1299–1304.

Vogl, A.W., Pfeiffer, D.C., Redenbach, D.M., Grove, B., 1993. Sertoli cell cytoskeleton. In: Russell, L.D., Griswold, M.D. (Eds.), The Sertoli Cell. Cache River Press, Clearwater, pp. 39–86.

Vogl, A.W., Vaid, K.S., Guttman, J.A., 2008. The Sertoli cell cytoskeleton. In: Cheng, C.Y. (Ed.), Molecular Mechanisms in Spermatogenesis. Landes Bioscience/Springer Science, Austin, TX, pp. 186–211.

Walker, W.H., 2009. Molecular mechanisms of testosterone action in spermatogenesis. Steroids 74, 602–607.

Walker, W.H., Cheng, J., 2005. FSH and testosterone signaling in Sertoli cells. Reproduction 130, 15–28.

Walsh, S.V., Hopkins, A.M., Nusrat, A., 2000. Modulation of tight junction structure and function by cytokines. Adv. Drug Deliv. Rev. 41, 303–313.

Wang, Q., Hurd, T.W., Margolis, B., 2004. Tight junction protein Par6 interacts with an evolutionarily conserved region in the amino terminus of PALS1/stardust. J. Biol. Chem. 279, 30715–30721.

Wang, R.S., Yeh, S., Chen, L.M., Lin, H.Y., Zhang, C., Ni, J., et al., 2006. Androgen receptor in Sertoli cell is essential for germ cell nursery and junctional complex formation in mouse testes. Endocrinology 147, 5624–5633.

Wang, Q., Chen, X.W., Margolis, B., 2007. PALS1 regulates E-cadherin trafficking in mammalian epithelial cells. Mol. Biol. Cell 18, 874–885.

Wang, X., Nie, J., Zhou, Q., Liu, W., Zhu, F., Chen, W., et al., 2008. Downregulation of Par-3 expression and disruption of Par complex integrity by TGF-beta during the process of epithelial to mesenchymal transition in rat proximal epithelial cells. Biochim. Biophys. Acta 1782, 51–59.

Waterman, M.J., Stavridi, E.S., Waterman, J.L., Halazonetis, T.D., 1998. ATM-dependent activation of p53 involves dephosphorylation and association with 14-3-3 proteins. Nat. Genet. 19, 175–178.

Weber, J.E., Russell, L.D., Wong, V., Peterson, R.N., 1983. Three-dimensional reconstruction of a rat stage V Sertoli cell: II. Morphometry of Sertoli–Sertoli and Sertoli–germ-cell relationships. Am. J. Anat. 167, 163–179.

Wells, C.D., Fawcett, J.P., Traweger, A., Yamanaka, Y., Goudreault, M., Elder, K., et al., 2006. A Rich1/Amot complex regulates the Cdc42 GTPase and apical-polarity proteins in epithelial cells. Cell 125, 535–548.

Wennerberg, K., Der, C.J., 2004. Rho-family GTPases: it's not only Rac and Rho (and I like it). J. Cell Sci. 117, 1301–1312.

Witte, H., Bradke, F., 2008. The role of the cytoskeleton during neuronal polarization. Curr. Opin. Neurobiol. 18, 479–487.

Wong, C.H., Mruk, D.D., Lui, W.Y., Cheng, C.Y., 2004. Regulation of blood–testis barrier dynamics: an *in vivo* study. J. Cell Sci. 117, 783–798.

Wong, C.H., Mruk, D.D., Siu, M.K., Cheng, C.Y., 2005. Blood–testis barrier dynamics are regulated by α_2-macroglobulin via the c-Jun N-terminal protein kinase pathway. Endocrinology 146, 1893–1908.

Wong, E.W., Mruk, D.D., Cheng, C.Y., 2008a. Biology and regulation of ectoplasmic specialization, an atypical adherens junction type, in the testis. Biochim. Biophys. Acta 1778, 692–708.

Wong, E.W., Mruk, D.D., Lee, W.M., Cheng, C.Y., 2008b. Par3/Par6 polarity complex coordinates apical ectoplasmic specialization and blood–testis barrier restructuring during spermatogenesis. Proc. Natl. Acad. Sci. USA 105, 9657–9662.

Wong, E.W., Sun, S., Li, M.W., Lee, W.M., Cheng, C.Y., 2009a. 14-3-3 protein regulates cell adhesion in the seminiferous epithelium of rat testes. Endocrinology doi:10.1210/en.2009-0427.

Wong, E.W.P., Mruk, D.D., Lee, W.M., Cheng, C.Y., 2009b. Cdc42 regulates Sertoli cell blood–testis barrier dynamics via its effects on the events of cytokine-induced protein endocytosis (submitted).

Woodcock, J.M., Murphy, J., Stomski, F.C., Berndt, M.C., Lopez, A.F., 2003. The dimeric versus monomeric status of 14-3-3zeta is controlled by phosphorylation of Ser58 at the dimer interface. J. Biol. Chem. 278, 36323–36327.

Wu, H., Rossi, G., Brennwald, P., 2008. The ghost in the machine: small GTPases as spatial regulators of exocytosis. Trends Cell Biol. 18, 397–404.

Xia, W., Cheng, C.Y., 2005. TGF-β3 regulates anchoring junction dynamics in the seminiferous epithelium of the rat testis via the Ras/ERK signaling pathway: an *in vivo* study. Dev. Biol. 280, 321–343.

Xia, W., Mruk, D.D., Lee, W.M., Cheng, C.Y., 2006. Differential interactions between transforming growth factor-β3/TβR1, TAB1, and CD2AP disrupt blood–testis barrier and Sertoli–germ cell adhesion. J. Biol. Chem. 281, 16799–16813.

Xia, W., Wong, E.W., Mruk, D.D., Cheng, C.Y., 2009. TGF-β3 and TNFα perturb blood–testis barrier (BTB) dynamics by accelerating the clathrin-mediated endocytosis of integral membrane proteins: a new concept of BTB regulation during spermatogenesis. Dev. Biol. 327, 48–61.

Yamada, S., Nelson, W.J., 2007. Synapses: sites of cell recognition, adhesion, and functional specification. Annu. Rev. Biochem. 76, 267–294.

Yamanaka, T., Ohno, S., 2008. Role of Lgl/Dlg/Scribble in the regulation of epithelial junction, polarity, and growth. Front Biosci. 13, 6693–6707.

Yamanaka, T., Horikoshi, Y., Suzuki, A., Sugiyama, Y., Kitamura, K., Maniwa, R., et al., 2001. PAR-6 regulates aPKC activity in a novel way and mediates cell–cell contact-induced formation of the epithelial junctional complex. Genes Cells 6, 721–731.

Yamanaka, T., Horikoshi, Y., Sugiyama, Y., Ishiyama, C., Suzuki, A., Hirose, T., et al., 2003. Mammalian Lgl forms a protein complex with PAR-6 and aPKC independently of PAR-3 to regulate epithelial cell polarity. Curr. Biol. 13, 734–743.

Yan, H.H., Cheng, C.Y., 2006. Laminin α3 forms a complex with β3 and γ3 chains that serves as the ligand for $\alpha6\beta1$-integrin at the apical ectoplasmic specialization in adult rat testes. J. Biol. Chem. 281, 17286–17303.

Yan, H.H., Mruk, D.D., Lee, W.M., Cheng, C.Y., 2008a. Blood–testis barrier dynamics are regulated by testosterone and cytokines via their differential effects on the kinetics of protein endocytosis and recycling in Sertoli cells. FASEB J. 22, 1945–1959.

Yan, H.H., Mruk, D.D., Wong, E.W., Lee, W.M., Cheng, C.Y., 2008b. An autocrine axis in the testis that coordinates spermiation and blood–testis barrier restructuring during spermatogenesis. Proc. Natl. Acad. Sci. USA 105, 8950–8955.

Yeaman, C., Grindstaff, K.K., Nelson, W.J., 1999. New perspectives on mechanisms involved in generating epithelial cell polarity. Physiol. Rev. 79, 73–98.

Yuan, H., Michelsen, K., Schwappach, B., 2003. 14-3-3 dimers probe the assembly status of multimeric membrane proteins. Curr. Biol. 13, 638–646.

Zahraoui, A., Louvard, D., Galli, T., 2000. Tight junction, a platform for trafficking and signaling protein complexes. J. Cell Biol. 151, F31–F36.

Zhang, X., Bi, E., Novick, P., Du, L., Kozminski, K.G., Lipschutz, J.H., et al., 2001. Cdc42 interacts with the exocyst and regulates polarized secretion. J. Biol. Chem. 276, 46745–46750.

Zhang, X., Zhu, J., Yang, G.Y., Wang, Q.J., Qian, L., Chen, Y.M., et al., 2007. Dishevelled promotes axon differentiation by regulating atypical protein kinase C. Nat. Cell Biol. 9, 743–754.

Zhang, X., Orlando, K., He, B., Xi, F., Zhang, J., Zajac, A., et al., 2008. Membrane association and functional regulation of Sec3 by phospholipids and Cdc42. J. Cell Biol. 180, 145–158.

Index

A

Actin cytoskeleton, 325–326
African trypanosomes, *Trypanosoma brucei*
  endocytic and lysosomal targeting signals, 29–30
  endocytic pathways
    cargo adaptors and sorting, 18–20
    CME, 16–18
    cytoskeleton involvement, 24–25
    early and recycling endocytic compartments, 20–21
    endsomal sorting complexity, 25
    lysosome, 22–24
    multivesicular bodies and late endocytosis, 21–22
    surface receptors, 25–27
  endomembrane sorting, posttranslational modification, 30
  ER-associated degradation (ERAD), 37–38
  flagellum, sorting, 30–31
  glycosome, sorting, 31
  Golgi apparatus
    binary fission, Golgi replication, 39–40
    cell-cycle and life-cycle coordination, 41
    cytoskeleton, 40–41
    retrograde transport, 42
  immune evasion mechanisms
    cellular immune responses, 11–12
    innate immunity, 13–16
    membrane dynamics and antibody clearance, 7–11
    VSG and antigenic variation, 5–7
  membrane protein biosynthesis, 32
  polypeptide delivery
    data mining, 34
    Leishmania lipophosphoglycan (LPG), 33
    N-terminal signal peptide (SP), 32
    Saccharomyces cerevisiae, 32
    signal recognition particle (SRP), 32
    trypanosomastids, 34
  polypeptide folding and maturation
    calnexin (CNX) and calreticulin (CRT), 35–37
    GRP94, 35
    oligosaccharyltransferase (OST), 35–36
    PDI knockdown, 37
  remodeling and signaling, 27–28
  trans-membrane domain proteins
    ISGs, 44–45
    late endocytosis and multivesicular body, 45–46
    ubiquitylation and endocytosis, 43
    VSG sorting problem, 42–43
  trypanosome endomembrane system
    comparative genomics, 47
    convergent evolution, 49
    flagellar pocket, evolutionary exploitation, 49–50
    G-protein signaling complexity, 48–49
    life eukaryotic tree, 46–47
  trypanosome life cycle
    epimastigotes, 5
    lymphatic system, 3
    nondividing metacyclic stage, 4
    parasite life cycle, 3
    stumpy induction factor (SIF), 4
    trypanosome metabolism, 5
    tsetse fly, 3–5
    variant surface glycoprotein (VSG), 4
    Winterbottom's sign, 4
Alexa350 dye (A350), 94
Amphibian gastrulation
  cell–cell adhesion, molecular factors
    cadherin/catenin complex, 231–236
    cell adhesion modulators, 241–243
    cytoskeletal modulators, 237–238
    ecto-mesodermal boundary, 243–245
    nonprotein membrane components, 236–237
    notochord-somite boundary, 246
    signal transduction mechanisms, 238–239
  cell sorting, 226–227
  differential adhesion and tissue separation
    adjusting tissue cohesiveness, 247–248
    boundary formation, 247
    spatial differences of cohesion, 249
    tissue positioning effect, 248–249
  gastrulation movements
    apical surface, 221–222
    convergent extension, 221
    intercellular and collective migration, 222
    intercellular migration processes, 220–221
  intracellular migration
    cadherin adhesion, 252–253

Amphibian gastrulation (*cont.*)
and cell rearrangement, 250–252
and collective migration, 253–256
mesodermal convergent extension, 256–260
liquid-like properties of tissues
differential adhesion hypothesis (DAH), 225–226
interfacial tension, 226–227
surface tension, 224
morphogenetic forces, 222–223
multilayered structure
apical *vs*. basolateral membranes, 219
epithelial cells, 217
invertebrate gastrulation *vs*. vertebrate blastula, 217–218
multilayered blastocoel wall, 219–220
tissue positioning effects, 228–229
Angiogenesis inhibitors, 300–301
Antennapedia, 124, 137
Astral microtubules (aMTs), 151
Atherosclerosis
balloon-catheter distension, 103–104
Cx37, 102–103
Cx43, 103–104
fibrous cap, 102
intima and media, 102, 104
myocardial infarction and stroke, 102
Aurora-kinase inhibitors, 298–299

C

CDC14Bretro, 133
Cell–cell adhesion, molecular factors
cadherin/catenin complex
components, 232–233
control of expression, 234–236
spatio-temporal expression, 233–234
cell adhesion modulators
ectodermal factors, 241–242
gastrula tissue cohesion, 242–243
cytoskeletal modulators, 237–238
ectodermal factors, 241–242
gastrula tissue cohesion, 242–243
nonprotein membrane components, 236–237
signal transduction mechanisms, 238–239
Cell division cycle 42 (Cdc42)
location of, 314
polarity proteins and cell-cell interactions
Crumbs (CRB) protein complex, 328–330
partitioning-defective (Par) protein complex, 330–331
14-3-3 proteins, 332–335
Scribble protein complex, 331–332
Rho GTPases and cell–cell interactions
actin cytoskeleton, 325–326
classifications, 315, 318
dynamic interactions, 318–319
epithelial apico-basal cell polarity, 327
filopodia formation, 321–322
protein trafficking, 322–325
transforming growth factor β (TGF-β), 319–321
ubiquitination, 326–327
Cell intercalation, 250
Cell rearrangement, 250
Centriolin
abscission regulation, 172–173
structure of, 172
Centrosome attracting body (CAB), 187
Clathrin-mediated endocytosis (CME), 16–18
Connexin37 (Cx37), 102–103
Connexin40 (Cx40), 79, 90
Connexin43 (Cx43), 75, 79, 103–104
Connexin45 (Cx45), 78
Crumbs (CRB) protein, 328–330
Cytoplasmic microtubules, 174

D

DAH. *See* Differential adhesion hypothesis
Differential adhesion
adjusting tissue cohesiveness, 247–248
boundary formation, 247
spatial differences of cohesion, 249
tissue positioning effect, 248–249
Differential adhesion hypothesis (DAH)
mesenchymal aggregates, 227
tissue positioning effects, 225, 248–249
tissue separation
ecto-mesodermal boundary, 243–245
notochord-somite boundary, 246

E

E-cadherin, 324
EDHF. *See* Endothelium-derived hyperpolarizing factor
Endocytic pathways, African trypanosomes
cargo adaptors and sorting, 18–20
CME, 16–18
cytoskeleton involvement, 24–25
early and recycling endocytic compartments, 20–21
endsomal sorting complexity, 25
lysosome, 22–24
multivesicular bodies and late endocytosis, 21–22
surface receptors, 25–27
Endothelium-derived hyperpolarizing factor (EDHF), 86
Expression site associated genes (ESAGs), 7

F

Fibronectin-leucine-rich transmembrane (FLRT), 235
Filopodia, 321–322

G

Gap junctional communication pathways, connexin channels
  capillaries and veins, 86–87
  endothelial cells, large vessels, 83–84
  resistance vessels, 85–86
  vascular smooth muscle cells, 84–85
Gap junction channel, 82
Gene regulation
  chromatin, transcriptional gatekeeper, 130–131
  cis-regulatory code, 129–130
  gene regulatory networks, 131–132
  noncoding RNAs and posttranscriptional regulation, 132–133
  posttranslational control, 133–134
Genotype–phenotype map (GPM)
  Aristotle's hypothesis, 120
  contexts and gene/morphology relationships
    Antennapedia, 124
    envirome, 123
    fushi tarazu, 124
    genetic control and maternal effects, 123
    quantitative trait locus (QTL) analysis, 124
  Darwin's depiction, 120
  developmental dynamics, phenotype shaping, 135–136
  gene regulation
    chromatin, transcriptional gatekeeper, 130–131
    cis-regulatory code, 129–130
    gene regulatory networks, 131–132
    noncoding RNAs and posttranscriptional regulation, 132–133
    posttranslational control, 133–134
  molecular and cellular dynamics, genes
    Arabidopsis, 138
    C. elegans, 136
    Hox gene *Antennapedia*, 137
  morphogenesis
    bristle patterns, *Drosophila*, 141
    comb formation cell dynamics, 139
    dachshund, 139
    Drosophila genetics, 138–139
    Drosophila sex comb, 140
    proneural achaete–scute complex, 138
  one-to-many conundrum, 125
  potential and limitations, 121–122
  sequence conservation amid phenotypic diversity
    Hox genes and gene toolkit, 126–128
    ultraconserved sequences, 128–129
  signaling cascades
    light, 134
    molecular tweezers, 135
    Rho activity, 134
    talin and vinculin, 135
Glucose-regulated protein 94 (GRP94), 35
Glycosylphosphatidylinositol (GPI) anchor, 6
Golgi apparatus
  binary fission, Golgi replication, 39–40
  cell-cycle and life-cycle coordination, 41
  cytoskeleton, 40–41
  retrograde transport, 42
GPM. *See* Genotype–phenotype map

H

Hemichannels, vascular connexin channels
  oligomerization, 79
  pannexin channels, 81–82
  plasma membrane, 80–81
  trans-Golgi network (TGN), 79
Hepatic Kupffer cells, 11
Histopathology, testicular germ cell tumors
  classification, 282–286
  ITGCN, 287
  NSE tumors, 289–293
    embryonal carcinoma, 290
    mixed GCTs, 292–293
    teratoma, 291–292
    trophoblastic tumors, 291
    yolk sac tumor, 290–291
  origin and development, 280–282
  regression of primitive GCTs, 293
  seminoma, 287–289
  somatic malignancies, testicular GCT, 293
  spermatocytic seminoma, 289
  testicular tumors staging, 286–287

I

Imatinib mesilate (STI-571), 300
Immune evasion mechanisms, African trypanosomes
  cellular immune responses, 11–12
  innate immunity, 13–16
  membrane dynamics and antibody clearance, 7–11
  VSG and antigenic variation, 5–7
Interpolar microtubules, 152
Intracellular migration
  cadherin adhesion, 252–253
  and cell rearrangement, 250–252
  and collective migration, 253–256
  mesodermal convergent extension, 256–260
Intratubular germ cell neoplasias (ITGCNs), 287
Invariant surface glycoproteins (ISGs), 44–45
Ion permeability
  channel unitary conductance, 90–91
  electrical conductance, Cx40 pore, 90
  electrical coupling, 91
  gap junctions, 90
  voltage and chemical gating, 91–92
ITGCNs. *See* Intratubular germ cell neoplasias

K

Kinetochore microtubules, 152

L

Last common eukaryotic ancestor (LCEA), 46–47
Leishmania lipophosphoglycan (LPG), 33

M

Microtubule-organizing centers (MTOCs)
  definition, 150
  microtubules, 151–152
Mitotic exit network (MEN)
  in budding yeast
    activation and dynamics, 163–167
    molecular mechanism, 161–163
    mother cortex, 163
    subcellular distribution, 159–161
  and septation initiation networks (SIN) asymmetry, 152–153
Molecular permeability
  communication compartments, 95
  dye molecules, 93
  hemichannel-mediated paracrine signaling, 97–98
  selective permeability, 96–97
  signaling kinetics, 95–96
MTOCs. *See* Microtubule-organizing centers

N

Nonseminomatous (NSE) tumors
  embryonal carcinoma, 290
  mixed GCTs, 292–293
  teratoma, 291–292
  trophoblastic tumors, 291
  yolk sac tumor, 290–291
Nonsister dyads (NSDs), 167

O

Oligosaccharyltransferase (OST), 35–36

P

Panx1, 97–98
Partitioning-defective (Par) protein, 330–331
PDI. *See* Protein disulfide isomerase
Permeability, vascular connexin channels
  interaction, other proteins, 99–100
  ion permeability
    channel unitary conductance, 90–91
    electrical conductance, Cx40 pore, 90
    electrical coupling, 91
    gap junctions, 90
    voltage and chemical gating, 91–92
  molecular permeability
    communication compartments, 95
    dye molecules, 93
    hemichannel-mediated paracrine signaling, 97–98
    selective permeability, 96–97
    signaling kinetics, 95–96
  nonbiological molecular permeants, 88
  pharmacological block, 100–101
  posttranslational modifications, 98–99
  vascular gap junctions and hemichannels, conductance, 89
Polarity proteins
  apical ES-BTB-basement membrane axis, 335–339
  and cell–cell interactions
    Crumbs (CRB) protein complex, 328–330
    partitioning-defective (Par) protein complex, 330–331
    14–3–3 proteins, 332–335
    Scribble protein complex, 331–332
  in primary preleptotene spermatocyte, 339–341
Polypeptide delivery, African trypanosomes
  data mining, 34
  Leishmania lipophosphoglycan (LPG), 33
  N-terminal signal peptide, 32
  Saccharomyces cerevisiae, 32
  signal recognition particle (SRP), 32
  trypanosomastids, 34
Polypeptide folding and maturation, African trypanosomes
  calnexin (CNX) and calreticulin (CRT), 35–37
  GRP94, 35
  oligosaccharyltransferase (OST), 35–36
  PDI knockdown, 37
Protein disulfide isomerase (PDI), 28–29
Protein trafficking, Cdc42
  in budding yeast, 323
  endocytosis, 324–325
  mammalian epithelial cells, 323–324
  tight junctions (TJs), 322
Protocadherins, 240

R

Rho GTPases and cell–cell interactions
  actin cytoskeleton, 325–326
  classifications, 315, 318
  dynamic interactions, 318–319
  epithelial apico-basal cell polarity, 327
  filopodia formation, 321–322
  protein trafficking
    in budding yeast, 323
    endocytosis, 324–325
    mammalian epithelial cells, 323–324
    tight junctions (TJs), 322
  transforming growth factor β (TGF-β), 319–321
  ubiquitination, 326–327

S

Scribble protein, 331–332
Seminoma, 282, 287–289
Septation initiation networks (SIN) asymmetry
  and mitotic exit network (MEN), 152–153
  role of Cdc2 kinase, 157–159
  and spindle-pole bodies (SPBs)
    anaphase, 155
    metaphase, 154–155
    origin of, 155–157
Signal recognition particle (SRP), 32
SPBs. *See* Spindle-pole bodies
Spermatocytic seminoma, 289
Spermatogenesis
  biochemical process, 311
  in mammalian testes, 310
  seminiferous epithelial cycle, 311–313
Spindle asymmetric cell cycle
  budding yeast meiosis
    analysis of, 169
    nonsister dyads formation, 167–169
  centrilsole control of cytokinesis, 171–173
  mitosis in yeasts
    MEN in budding yeast, 159–167
    mitotic exit network (MEN) and septation initiation networks (SIN), 152–153
    role of Cdc2 kinase, 157–159
    septation initiation networks (SIN) asymmetry, 154–157
  models for unequal SPBs, 169–171
Spindle asymmetric cell divisions
  in *Annelids*
    Helobdella, 198–200
    Tubifex, 198
  in *Drosophila* central nervous system
    asymmetric characteristics, 189
    asymmetric spindle displacement, 191–192
    cortex polarization, 193–194
    spindle geometry, 192–193
    spindle poles, 195–196
  in *Drosophila* germline
    age-dependent centrosome inheritance, 197–198
    germ line stem cells (GSCs), 196–197
  early embryonic development in *Caenorhabditis elegans*
    embryonic division, 188–189
    spindle displacement and posterior pole oscillations, 181–187
    spindle-pole flattening, 187–188
  segregation in *Ilyanassa obsolete*, 200–201
  SPB inheritance in budding yeast
    microtubule dynamics and spindle orientation, 180–181
    role of Cdks, 178–179
    role of cortex in dynein asymmetry, 179–180
    spindle alignment orientation and symmetry, 174–177
Spindle orientation checkpoint (SPOC), 159
Spindle-pole bodies (SPBs)
  definition, 150
  microtubules, 151–152
Spindle-pole flattening, 187–188
Stumpy induction factor (SIF), 4

T

Testicular germ cell tumors (TGCTs)
  classification, 278
  cure rate, 278
  epidemiology and risk factors, 279–280
  histopathology
    classification, 282–286
    ITGCN, 287
    NSE tumors, 289–293
    origin and development, 280–282
    regression of primitive GCTs, 293
    seminoma, 287–289
    somatic malignancies, testicular GCT, 293
    spermatocytic seminoma, 289
    testicular tumors staging, 286–287
  lymph node/distant metastases, 278
  prognostic and diagnostic markers
    new discovered markers, 295–297
    serum tumor markers, 294–295
  therapy
    angiogenesis inhibitors, 300–301
    aurora-kinase inhibitors, 298–299
    traditional treatment, 297–298
    tyrosine kinase inhibitors, 299–300
Testis
  polarity proteins and cell−cell interactions
    Crumbs (CRB) protein complex, 328–330
    partitioning-defective (Par) protein complex, 330–331
    14-3-3 proteins, 332–335
    Scribble protein complex, 331–332
  Rho GTPases and cell−cell interactions
    actin cytoskeleton, 325–326
    classifications, 315, 318
    dynamic interactions, 318–319
    epithelial apico-basal cell polarity, 327
    filopodia formation, 321–322
    protein trafficking, 322–325
    transforming growth factor β (TGF-β), 319–321
    ubiquitination, 326–327
TGCTs. *See* Testicular germ cell tumors
Tight junctions (TJs), protein trafficking, 322
Transferring receptor (TfR), 8
Transforming growth factor β (TGF-β), 319–321
Trans-Golgi network (TGN), 79
Trans-membrane domain proteins
  ISGs, 44–45

Trans-membrane domain proteins (*cont.*)
late endocytosis and multivesicular body, 45–46
ubiquitylation and endocytosis, 43
VSG sorting problem, 42–43
Trypanosome endomembrane system
comparative genomics, 47
convergent evolution, 49
flagellar pocket, evolutionary exploitation, 49–50
G-protein signaling complexity, 48–49
life eukaryotic tree, 46–47
Trypanosome life cycle
epimastigotes, 5
lymphatic system, 3
nondividing metacyclic stage, 4
parasite life cycle, 3
stumpy induction factor (SIF), 4
trypanosome metabolism, 5
tsetse fly, 3–5
Winterbottom's sign, 4
Tyrosine kinase inhibitors, 299–300

U

Ubiquitination mechanism, 326–327

V

Variant surface glycoprotein (VSG), 4–9
Vascular connexin channels
Cx40, 79
Cx43, 75, 79
Cx45, 78
disulfide bridge interactions, 78
gap junctional communication pathways
capillaries and veins, 86–87
endothelial cells, large vessels, 83–84
resistance vessels, 85–86
vascular smooth muscle cells, 84–85
gap junctions, 75–78
hemichannels
oligomerization, 79
pannexin channels, 81–82
plasma membrane, 80–81
trans-Golgi network (TGN), 79
permeability
interaction, other proteins, 99–100
ion permeability, 90–92
molecular permeability, 92–98
nonbiological molecular permeants, 88
pharmacological block, 100–101
posttranslational modifications, 98–99
vascular gap junctions and hemichannels, conductance, 89
phosphorylation, 79
SDS–PAGE, 75
vascular diseases
atherosclerosis, 102–104
hypertension, 101–102
vasculature
heterocellular gap junctions, 74–75
homocellular gap junctions, 74
internal elastic lamina (IEL), 73
lamellar units, 74
myoendothelial junction (MEJ), 72
vessel composition and functional interactions, 73
Vascular diseases, connexin channels
atherosclerosis
balloon-catheter distension, 103–104
Cx37, 102–103
Cx43, 103–104
fibrous cap, 102
intima and media, 102, 104
myocardial infarction and stroke, 102
hypertension, 101–102
VSG. *See* Variant surface glycoprotein

X

Xlim5, transcription factor, 245